THE DEVELOPMENT OF AN
ASYMMETRIC PALLADIUM-CATALYZED
CONJUGATE ADDITION AND ITS
APPLICATION TOWARD THE TOTAL
SYNTHESES OF TAIWANIAQUINOID
NATURAL PRODUCTS

Thesis by

Jeffrey Clinton Holder

In Partial Fulfillment of the Requirements for the degree

of

Doctor of Philosophy

CALIFORNIA INSTITUTE OF TECHNOLOGY

Pasadena, California

2014

(Defended 5 May 2014)

To my mother, Joanne Beaudet, for her constant and unwavering support

ACKNOWLEDGEMENTS

ABSTRACT

The asymmetric synthesis of quaternary stereocenters remains a challenging problem in organic synthesis. Past work from the Stoltz laboratory has resulted in methodology to install quaternary stereocenters α- or γ- to carbonyl compounds. Thus, the asymmetric synthesis of β-quaternary stereocenters was a desirable objective, and was accomplished by engineering the palladium-catalyzed addition of arylmetal organometallic reagents to α,β-unsaturated conjugate acceptors.

Herein, we described the rational design of a palladium-catalyzed conjugate addition reactions utilizing a catalyst derived from palladium(II) trifluoroacetate and pyridinooxazole ligands. This reaction is highly tolerant of protic solvents and oxygen atmosphere, making it a practical and operationally simple reaction. The mild conditions facilitate a remarkably high functional group tolerance, including carbonyls, halogens, and fluorinated functional groups. Furthermore, the reaction catalyzed conjugate additions with high enantioselectivity with conjugate acceptors of 5-, 6-, and 7-membered ring sizes. Extension of the methodology toward the asymmetric synthesis of flavanone products is presented, as well.

A computational and experimental investigation into the reaction mechanism provided a stereochemical model for enantioinduction, whereby the α-methylene protons adjacent the enone carbonyl clashes with the *tert*-butyl groups of the chiral ligand. Additionally, it was found that the addition of water and ammonium hexafluorophosphate significantly increases the reaction rate without sacrificing enantioselectivity. The synergistic effects of these additives allowed for the reaction to proceed at a lower temperature, and thus facilitated expansion of the substrate scope to sensitive functional groups such as protic amides and aryl bromides. Investigations into a scale-up synthesis of the chiral ligand (*S*)-*tert*-butylPyOx are also presented. This three-step synthetic route allowed for synthesis of the target compound of greater than 10 g scale.

Finally, the application of the newly developed conjugate addition reaction toward the synthesis of the taiwaniaquinoid class of terpenoid natural products is discussed. The conjugate addition reaction formed the key benzylic quaternary stereocenter in high enantioselectivity, joining together the majority of the carbons in the taiwaniaquinoid scaffold. Efforts toward the synthesis of the B-ring are presented.

TABLE OF CONTENTS

CHAPTER 1

CHAPTER 2

APPENDIX 1

CHAPTER 3

APPENDIX 11

APPENDIX 12

LIST OF FIGURES

APPENDIX 2

Spectra relevant to Chapter 3: Palladium-catalyzed asymmetric conjugate addition of arylboronic acids to heterocyclic acceptors

CHAPTER 4

Mechanism and enantioselectivity in palladium-catalyzed conjugate addition of arylboronic acids to β-substituted cyclic enones: Insights from computation and experiment

APPENDIX 3

Spectra relevant to Chapter 4: Mechanism and enantioselectivity in palladium-catalyzed conjugate addition of arylboronic acids to β-substituted cyclic enones: Insights from computation and experiment

APPENDIX 4

X-ray structures relevant to Chapter 4: Mechanism and enantioselectivity in palladium- catalyzed conjugate addition of arylboronic acids to β-substituted cyclic enones: Insights from computation and experiment

CHAPTER 5

Development of a Scalable Synthesis of the (S)-4-(tert-butyl)-2-(pyridin-2-yl)-4,5-dihydrooxazole ((S)–t-BuPyOx) Ligand

APPENDIX 5

Spectra relevant to Chapter 5: Development of a Scalable Synthesis of the (S)-4-(tert-butyl)-2-(pyridin-2-yl)-4,5-dihydrooxazole ((S)–t-BuPyOx) Ligand

CHAPTER 6
Progress toward the catalytic asymmetric total synthesis of (+)-taiwaniaquinone H and other taiwaniaquinoid natural products

APPENDIX 6
Spectra relevant to Chapter 6: Progress toward the catalytic asymmetric totaly synthesis of (+)-taiwaniaquinone H and other taiwaniaquinoid natural products

APPENDIX 7
X-ray structures relevant to Chapter 6: Progress toward the catalytic asymmetric totaly synthesis of (+)-taiwaniaquinone H and other taiwaniaquinoid natural products

APPENDIX 9
Progress toward the total synthesis of yuccaol natural products

APPENDIX 10
The development of novel NHC-based ligand scaffolds for use in heteroaromatic conjugate addition reactions

APPENDIX 11
Progress toward the development of a novel reductive Heck reaction

LIST OF SCHEMES

CHAPTER 5
Development of a Scalable Synthesis of the (S)-4-(tert-butyl)-2-(pyridin-2-yl)-4,5-dihydrooxazole ((S)–t-BuPyOx) Ligand

CHAPTER 6
Progress toward the catalytic asymmetric total synthesis of (+)-taiwaniaquinone H and other taiwaniaquinoid natural products

APPENDIX 8
Progress toward the total synthesis of nanolobatolide

APPENDIX 9
Progress toward the total synthesis of yuccaol natural products

APPENDIX 10
The development of novel NHC-based ligand scaffolds for use in heteroaromatic conjugate addition reactions

APPENDIX 11
Progress toward the development of a novel reductive Heck reaction

LIST OF TABLES

CHAPTER 4
Mechanism and enantioselectivity in palladium-catalyzed conjugate addition of arylboronic acids to β-substituted cyclic enones: Insights from computation and experiment

APPENDIX 4
X-ray structures relevant to Chapter 4: Mechanism and enantioselectivity in palladium-catalyzed conjugate addition of arylboronic acids to β-substituted cyclic enones: Insights from computation and experiment

CHAPTER 6
Progress toward the catalytic asymmetric total synthesis of (+)-taiwaniaquinone H and other taiwaniaquinoid natural products

APPENDIX 7
X-ray structures relevant to Chapter 6: Progress toward the catalytic asymmetric total synthesis of (+)-taiwaniaquinone H and other taiwaniaquinoid natural products

APPENDIX 8
Progress toward the total synthesis of nanolobatolide

APPENDIX 9
Progress toward the total synthesis of yuccaol natural products

APPENDIX 10
The development of novel NHC-based ligand scaffolds for use in heteroaromatic conjugate addition reactions

APPENDIX 11

Progress toward the development of a novel reductive Heck reaction

APPENDIX 12

Notebook cross-reference for new compounds

LIST OF ABBREVIATIONS

Å	Ångstrom
$[\alpha]_D$	specific rotation at wavelength of sodium D line
Ac	acetyl
Anal.	combustion elemental analysis
APCI	atmospheric pressure chemical ionization
app	apparent
aq	aqueous
AIBN	2,2'-azobisisobutyronitrile
Ar	aryl
atm	atmosphere
BBN	borabicyclononane
Bn	benzyl
Boc	*tert*-butyloxycarbonyl
bp	boiling point
br	broad
Bu	butyl
i-Bu	*iso*-butyl
n-Bu	butyl
t-Bu	*tert*-Butyl
Bz	benzoyl
c	concentration for specific rotation measurements
°C	degrees Celsius
ca.	about (Latin circa)
calc'd	calculated
CAN	ceric ammonium nitrate

cat	catalytic
Cbz	carbobenzyloxy
CCDC	Cambridge Crystallographic Data Centre
CDI	1,1'-carbonyldiimidazole
cf.	compare (Latin confer)
CI	chemical ionization
CID	collision-induced dissociation
cm^{-1}	wavenumber(s)
comp	complex
Cy	cyclohexyl
d	doublet
D	deuterium
dba	dibenzylideneacetone
DBU	1,8-diazabicyclo[5.4.0]undec-7-ene
DCE	dichloroethane
dec	decomposition
DIAD	diisopropyl azodicarboxylate
DMA	*N*,*N*-dimethylacetamide
DMAP	4-dimethylaminopyridine
dmdba	bis(3,5-dimethoxybenzylidene)acetone
DMF	*N*,*N*-dimethylformamide
DMSO	dimethyl sulfoxide
DNA	(deoxy)ribonucleic acid
dppb	1,4-bis(diphenylphosphino)butane
dppf	1,1'-bis(diphenylphosphino)ferrocene
dr	diastereomeric ratio
E_A	activation energy

EC_{50}	median effective concentration (50%)
EDC	N-(3-dimethylaminopropyl)-N'-ethylcarbodiimide
ee	enantiomeric excess
EI	electron impact
e.g.	for example (Latin exempli gratia)
equiv	equivalent
ESI	electrospray ionization
Et	ethyl
FAB	fast atom bombardment
FID	flame ionization detector
g	gram(s)
GC	gas chromatography
gCOSY	gradient-selected correlation spectroscopy
GlyPHOX	2-(2-(diphenylphosphino)phenyl)oxazoline
h	hour(s)
HIV	human immunodeficiency virus
HMDS	1,1,1,3,3,3-hexamethyldisilazane
HMPA	hexamethylphosphoramide
HOBt	1-hydroxybenzotriazole
HPLC	high-performance liquid chromatography
HRMS	high-resolution mass spectroscopy
HSV	herpes simplex virus
$h\nu$	light
Hz	hertz
IC_{50}	median inhibition concentration (50%)
i.e.	that is (Latin id est)
IR	infrared (spectroscopy)

J	coupling constant
kcal	kilocalorie
KDA	potassium diisopropylamide
KHMDS	potassium hexamethyldisilazide
λ	wavelength
L	liter
LDA	lithium diisopropylamide
lit.	literature value
LTQ	linear trap quadrupole
m	multiplet; milli
m	meta
m/z	mass to charge ratio
M	metal; molar; molecular ion
Me	methyl
MHz	megahertz
μ	micro
μwaves	microwave irradiation
min	minute(s)
MM	mixed method
mol	mole(s)
MOM	methoxymethyl
mp	melting point
Ms	methanesulfonyl (mesyl)
MS	molecular sieves
n	nano
N	normal
nbd	norbornadiene

NBS	*N*-bromosuccinimide
NIST	National Institute of Standards and Technology
NMO	*N*-methylmorpholine *N*-oxide
NMR	nuclear magnetic resonance
NOE	nuclear Overhauser effect
NOESY	nuclear Overhauser enhancement spectroscopy
Nu	nucleophile
[O]	oxidation
o	ortho
p	para
PA	proton affinity
PCC	pyridinium chlorochromate
PDC	pyridinium dichromate
Ph	phenyl
pH	hydrogen ion concentration in aqueous solution
PhH	benzene
PhMe	toluene
PHOX	phosphinooxazoline
Piv	pivaloyl
p*Ka*	p*K* for association of an acid
PMB	*p*-methoxybenzyl
pmdba	bis(4-methoxybenzylidene)acetone
ppm	parts per million
PPTS	pyridinium *p*-toluenesulfonate
Pr	propyl
i-Pr	isopropyl
Py	pyridine

q	quartet
ref	reference
R	generic for any atom or functional group
R_f	retention factor
rt	room temperature
s	singlet or strong or selectivity factor
sat.	saturated
SET	single electron transfer
S_N2	second-order nucleophilic substitution
sp.	species
t	triplet
TBAF	tetrabutylammonium fluoride
TBHP	*tert*-butyl hydroperoxide
TBS	*tert*-butyldimethylsilyl
TCDI	1,1'-thiocarbonyldiimidazole
TCNE	tetracyanoethylene
Tf	trifluoromethanesulfonyl (trifyl)
TFA	trifluoroacetic acid
TFE	2,2,2-trifluoroethanol
THF	tetrahydrofuran
TIPS	triisopropylsilyl
TLC	thin-layer chromatography
TMEDA	*N,N,N',N'*-tetramethylethylenediamine
TMS	trimethylsilyl
TOF	time-of-flight
Tol	tolyl
TON	turnover number

t_R	retention time
Ts	p-toluenesulfonyl (tosyl)
UV	ultraviolet
v/v	volume to volume
w	weak
w/v	weight to volume
X	anionic ligand or halide

CHAPTER 1

A brief history of palladium-catalyzed conjugate addition
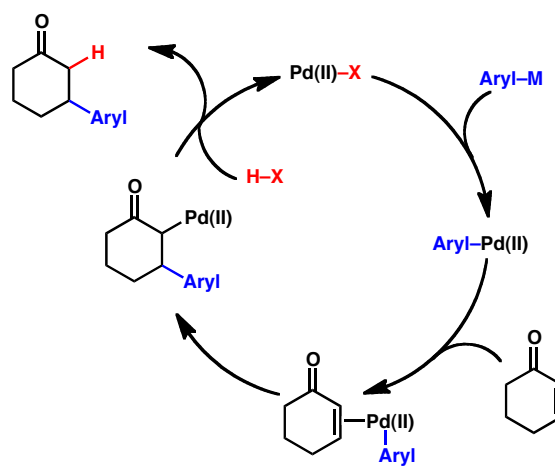
Abstract
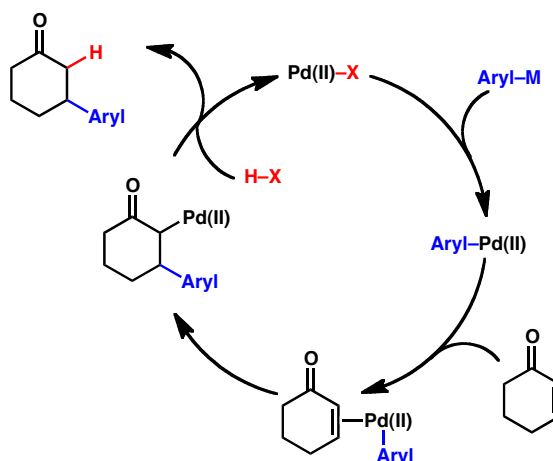
Palladium-catalyzed conjugate addition constitutes a diverse array of reactions designed to insert the olefin of a conjugate acceptor into an aryl-palladium bond, followed by hydrolytic turnover of the palladium enolate. The study of these reactions has led to the disclosure of a number of catalytic systems for the synthesis and asymmetric synthesis of benzylic stereocenters. This review briefly covers the chronological development of these catalytic reactions, specifically discussing the mechanistic hypotheses and studies underlying the key developments. These systems are compared and contrasted with the conjugate addition manifolds operating with copper and rhodium catalysts, and a discussion of both advantages and disadvantages of palladium systems are presented.

1.1 Motivations for palladium-catalyzed conjugate addition

β-substituted ketones are important intermediates in synthetic organic chemistry. Historically, these compounds were accessed by Michael addition, the 1,4-addition of malonate-derived nucleophiles to appropriate α,β-unsaturated acceptor compounds. Since the discovery of the Michael reaction, a number of metal-based reagents have been developed as conjugate addition nucleophiles. More recently, many of these processes have been rendered enantioselective by employing chiral ligands and transition metal catalysts.[1] Asymmetric conjugate additions are well-established from copper[2] and rhodium[3] catalysts, and have seen expansion to the formation of quaternary stereocenters.[4] However, each metal system has its drawbacks. Use of copper catalysts typically requires highly reactive stoichiometric organomagnesium, organozinc, or organoaluminum reagents. These reagents are incompatible with many functional groups, and the conditions required to successfully add these reagents to conjugate acceptors typically require rigorously dry, deoxygenated solvents and extended reaction times at cryogenic temperatures. Rhodium-catalyzed reactions typically employ less reactive (and thus highly functional group tolerant) boron-based reagents, however, the expensive rhodium precatalysts are often oxygen sensitive and thermally unstable rhodium(I) dimers. While not as sensitive to water as the copper-catalyzed conditions, the rhodium-catalyzed reactions are highly oxygen sensitive.

Palladium-catalyzed conjugate additions combine the most favorable characteristics of the copper and rhodium systems. They often utilize easily-handled boron (or sometimes silicon) reagents, which do not require rigorously anhydrous reaction conditions or cryogenic reaction temperatures, and react *via* palladium(II)-catalyzed cycles that are not prohibitively sensitive to oxygen. Additionally, many of these reactions employ common palladium sources, ligands, and solvents. Combined, these advantages convey a simple reaction procedure that does not employ excessively expensive or sensitive reagents. However, palladium-catalyzed conjugate addition is

significantly less explored than the copper or rhodium systems, and room for future development

exists.

   This review will briefly describe the recent advances in the synthesis of β-arylketones *via*

palladium-catalyzed 1,4-addition of aryl organometal reagents to enones, including the recent

development of asymmetric processes.

1.1.1   Oxidative Heck reaction of allylic alcohols

   Early methods for the palladium-catalyzed synthesis of β-aryl compounds did not involve

arylmetal insertion into enone olefins directly, but rather utilized Heck reactions on rigged

substrates designed to afford 1,4-addition products. Larock and coworkers describe a strategy for

the arylation of cyclic allylic alcohols based on the Heck reaction whereby β-hydride elimination

affords an enol that tautomerizers to give the formal 1,4-addition product (Scheme 1.1).[5]

Palladium-catalyzed Heck addition of aryliodides **1** to cyclopentenol **2** cleanly furnished β-

arylated ketone **3** (Scheme 1.1a), however analogous reaction with cyclohexenol **4** furnished two

arylated products **5** and **6**, indicating divergent reaction mechanisms (Scheme 1.1b).

Scheme 1.1 Divergent reactivity of five- and six-membered cyclic allylic alcohols.
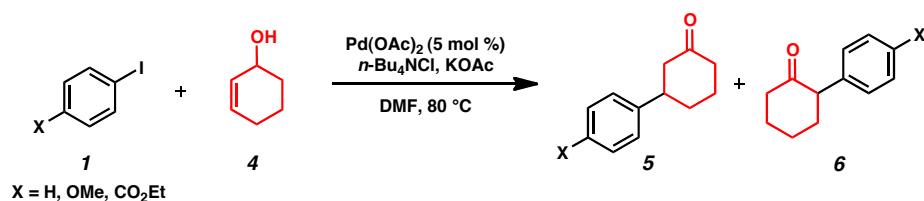
Larock and coworkers rationalized the divergent outcomes by suggesting two possible

isomeric olefin insertion pathways by which the arylpalladium species could react. Phenylation of

the olefin carbon distal to the alcohol would generate alkylpalladium **5**, which would furnish

desired enol **6** upon β-hydride elimination (Figure 1.1). This enol tautomerizes readily to β-

arylated ketone **7**, the expected product. However, isomeric olefin insertion would generate

alkylpalladium **8**. β-hydride elimination of this species generates homoallylic alcohol **9**, which

cannot itself tautomerize to observed ketone product **11**, but can undergo a series of migratory

insertion/β-hydride elimination events to "chain walk" to enol **10**, which can tautomerize to

observed α-arylated ketone **7.**

Figure 1.1 Mechanistic rationale for reaction products
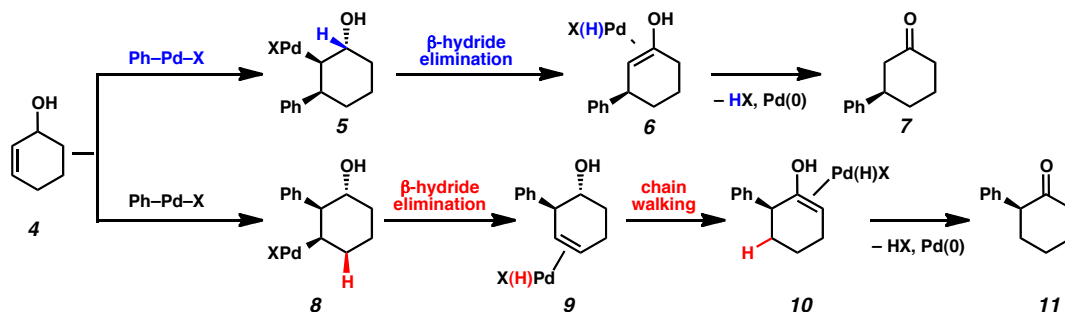
A direct, palladium-catalyzed 1,4-addition to an enone system would require a different

mechanism for turning over the metal catalyst. This mechanism necessarily differs from the Heck

reaction in two of the elementary steps of the catalytic cycle: formation of the arylpalladium

species and turnover of the alkylpalladium species.[6] The currently accepted mechanism is very

similar to the analogous mechanism put forth by Hayashi for rhodium-catalyzed conjugate

addition reactions.[3] The first key difference between direct conjugate addition reactions and the

Heck reaction is that the catalyst is a palladium(II) species (**12**) and no redox reactions occur at

the metal center (Figure 1.2). This redox neutral catalytic cycle is a direct result of the mechanism

of catalyst turnover. Thus, oxidative addition is not a suitable step to form arylpalladium **13**, and

this aryl moiety must be introduced by transmetallation. Insertion of enone **14** into the

arylpalladium bond furnishes alkylpalladium **15**, an intermediate common to both catalytic

cycles. Here, a possible side reaction of the catalytic cycles forms if alkylpalladium **15** undergoes

β-hydride elimination to furnish Heck-type product **16** and a palladium hydride, which is readily

reduced by loss of HX to palladium(0), a species that is off the productive catalytic cycle. In the

conjugate addition catalytic cycle, enolate **15**, or as its tautomer palladium enolate **17**, undergoes

protonolysis to furnish β-arylated product **18**. Water-mediated hydrolysis likely forms a

palladium hydroxide species, and the active catalyst for conjugate addition reactions (**12**) is often

believed to be a palladium(II) hydroxide due to the species' ability to undergo transmetallation

rapidly with arylboron reagents. Thus, a closed catalytic cycle is completed when hydrolysis of

palladium enolate **17** regenerates palladium(II) **12**.

Figure 1.2 Mechanistic discrepancy between 1,4-addition and Heck reaction catalytic cycles
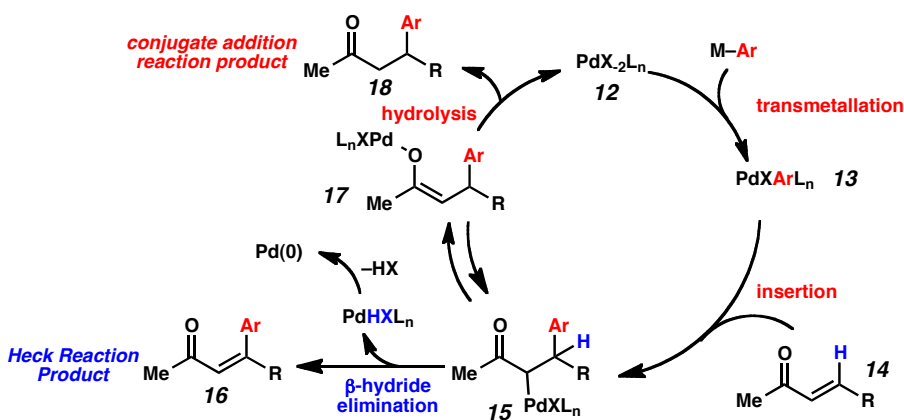
1.2 Palladium-catalyzed reactions using Brønsted or Lewis acid additives

A number of groups have reported the use palladium catalysts to promote the conjugate addition of arylmetal species to conjugate acceptors utilizing Brønsted or Lewis acid additives or solvents. The first reports from the early-1980s employ ArHgCl or Ar_4Sn reagents in conjunction with tetrabutylammonium chloride additives and Brønsted acid reaction solvents to facilitate the 1,4-addition.[7] However, it was not until the mid-1990s that widespread investigation of palladium-catalyzed conjugate addition began to manifest.

1.2.1 Antimony salts as stoichiometric additives

Uemura and coworkers first reported the use of antimony(III) chloride as a stoichiometric Lewis acid to promote the palladium-catalyzed addition of tetraphenylborates to conjugate acceptors (Scheme 1.2).[8] They hypothesize that protonolysis of a B–Ph bond is catalyzed by the acetic acid solvent, and that triphenylborane is the active reagent. Phenylenone **18** is successfully transformed to diphenyl ketone **19**. Later works suggest a mechanism implicating palladium(0) oxidative addition of one of the aryl–B bonds to form the active arylpalladium complex. Turnover is hypothesized to be accomplished by antimony-coordination of the carbonyl (**20**) and subsequent intramolecular chlorodepalladation (i.e., **21**). Hydrolysis of the enolate is accomplished with acetic acid to yield diaryl ketone **19**. The author of this review suggests that the known decomposition products of triphenylborane- phenylboroxine or phenylboronic acid- are likely to be the active reagents. Additionally, it follows that this reaction may follow a palladium(II), redox neutral, catalytic cycle by invoking transmetallation from these arylboron reagents as opposed to direct oxidative addition of a B–aryl bond. Work from Uemura demonstrating arylboronic acids as competent arylation reagents supports this view,[8d] as does a preponderance of subsequent palladium/arylboron reagent work to be discussed herein.

Scheme 1.2 SbCl₃-mediated conjugate addition and mechanistic rationale

a. SbCl₃-catalyzed addition of aryltetrafluoroborate
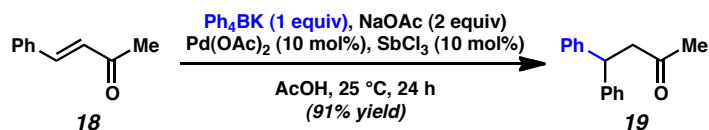
b. Mechanistic proposal for catalyst turnover
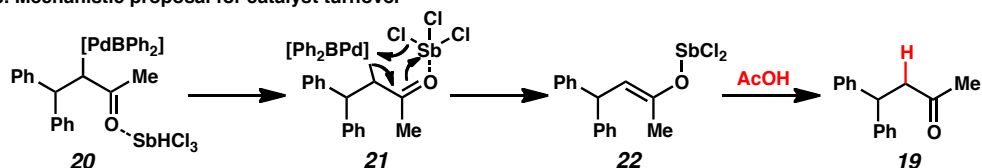
Demark and coworkers reported an analogous transformation utilizing organosiloxanes as the aryl source.[9] Here, a fluoride additive was required to promote the transmetallation between relatively unreactive organosiloxane reagents and the palladium catalyst, presumably by formation of hypervalent silicon. Cyclohexenone **23** reacts with arylsiloxane **24** to furnish conjugate addition adduct **25** with minimal Heck reaction side product **26** (Scheme 1.3a). Adapting mechanistic insights from rhodium-catalyzed conjugate addition reactions developed by Hayashi and Miyaura, Denmark suggested a redox-neutral palladium(II) based catalytic cycle, and shows catalyst turnover *via* palladium enolate hydrolysis (Scheme 1.3b). Denmark shows the antimony-assisted turnover mechanism suggested by Uemura, with alkylpalladium **30** undergoing intramolecular depalladation to furnish the antimony enolate **31**, but suggests that invoking protonation of oxo-π-allyl enolate **28** to afford enol **29** is also a plausible mechanism of turnover.

Scheme 1.3 Palladium-catalyzed conjugate addition of organosiloxanes and hypothesized

mechanisms of turnover

a. SbCl₃-catalyzed addition of organosiloxanes

b. Mechanistic proposals for catalyst turnover
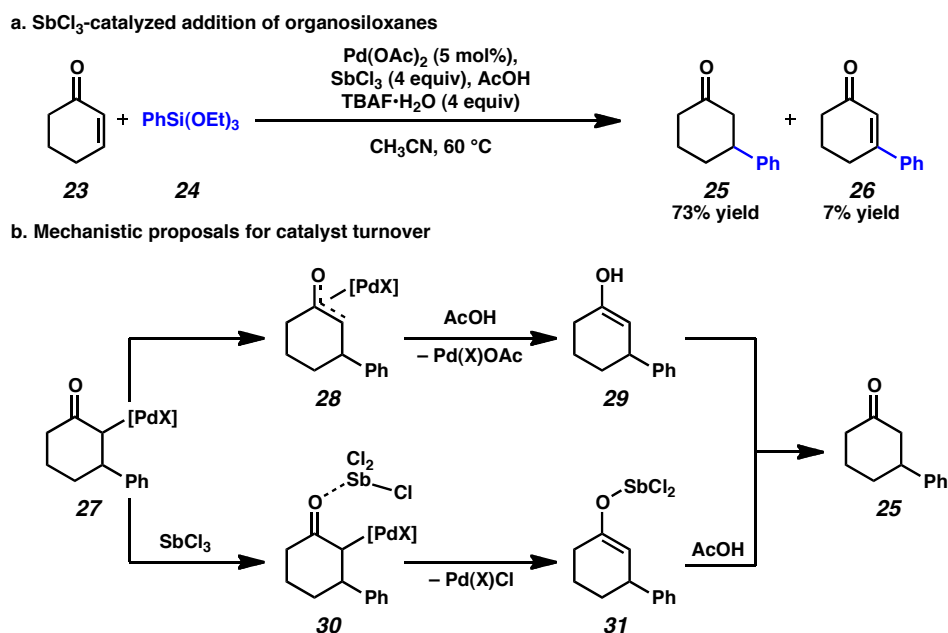
1.2.2   *Addition of sulfinic acids to conjugate acceptors*

In 2012, Duan and Li brought the use of acidic reaction medium as a way to promote palladium-catalyzed conjugate addition to its logical conclusion, actually utilizing aryl sulfinic acids as the phenyl donor source.[10] They demonstrate the arylation of a number of conjugate acceptors (**32**) using phenylsulfinic acid (**33**), and generate a wide array of products (Table 1.1). Cyclic ketones bearing aryl tertiary (**25**) or quaternary (**35**) stereocenters could be furnished, as well as tertiary stereocenters for acyclic ketones (**19**) and esters (**36**)

Table 1.1 Substrate scope of aryl sulfinic acid conjugate addition
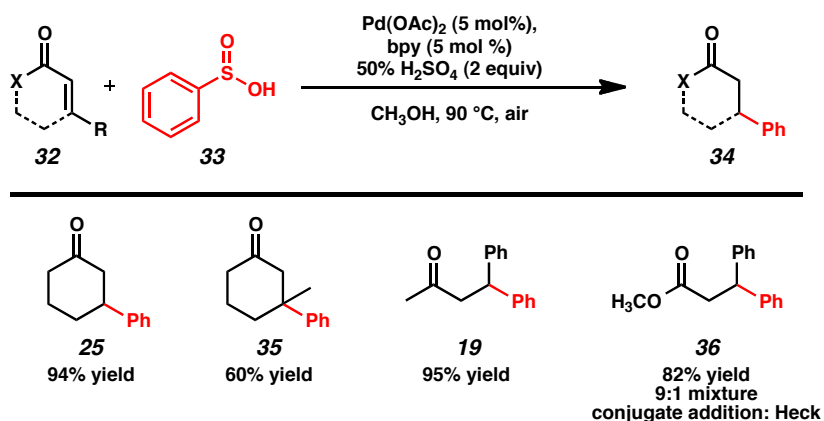
The mechanistic explanation for the formation of the active arylpalladium species involves expulsion of SO_2 gas (Figure 1.3). Invoking the sulfinic acid to coordinate the metal center via Pd–O bonded intermediate **37**, they suggest formation of arylpalladium **38** by β–carbon elimination, effectively releasing SO_2 while transferring the aryl moiety to the metal center. This process is isoelectronic to the more commonly encountered β–hydride elimination. Arylpalladium **38** undergoes conjugate addition reaction to afford the observed array of products, suggesting that β–carbon elimination is a viable entry into the conjugate addition reaction manifold beyond the typical transmetallation sequence. Though conjugate *arylations* have not been disclosed with C–C bond cleavage *via* β–carbon elimination, this mechanism of conjugate addition has been demonstrated with β–carbon elimination of alkynes and their subsequent Rh-catalyzed asymmetric conjugate addition. [11]

Figure 1.3 Mechanistic hypothesis for generation of arylpalladium species
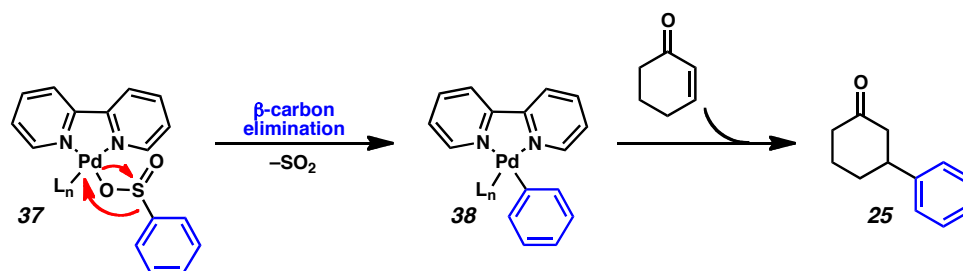
1.3 Palladium-catalyzed conjugate addition of arylboronic acids

In the early 21st century, the popularity of palladium-catalyzed conjugate addition reactions of arylboron reagents has risen. Unlike some early examples of palladium-catalyzed conjugate addition, they utilized arylboronic acids as the aryl reagent instead of more reactive and highly toxic tin and mercury reagents. These reactions often depend on the protic, Brønsted acid solvents to assist in turnover of the palladium catalyst *via* protonolysis of the latent alkylpalladium species furnished by the C–C bond forming phenylpalladation step.

1.3.1 *Triphenylphosphine as ligands for conjugate addition*

Arylboron reagents are a highly desirable class of aryl reagent for organotransition metal catalyzed reactions, as demonstrated by the ubiquitous Suzuki-Miyaura cross coupling reaction. They are bench-stable, easily-handled, relatively non-toxic and their byproducts are easily removed from reactions. Uemura's application of these reagents to 1,4-addition reactions ushered in a similar rapid expansion of palladium-catalyzed conjugate addition reactions. Ohta and coworkers disclosed palladium-catalyzed 1,4-addition to cyclic and acyclic enones by a catalyst derived from palladium(0) and chloroform (Scheme 1.4).[12] They hypothesized that the reactive species was palladium(II) species **39**, generated from oxidative addition to the chloroform additive. More recently, similar conditions have been adapted for conjugate additions employing palladium(II) acetate with microwave catalysis while avoiding the need to oxidize palladium(0) with chloroform.[13]

Scheme 1.4 Palladium(0) and chloroform catalyst system for conjugate addition of arylboronic acids
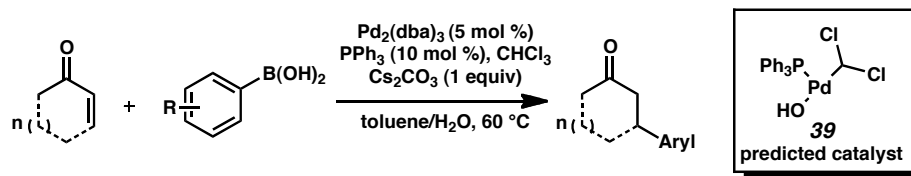
Supporting Ohta's hypothesized catalyst structure (**39**), Hartwig and corworkers proposed

that analogous palladium hydroxide complexes are the active catalysts in Suzuki coupling

reactions, and demonstrated that palladium(II) hydroxides are kinetically competent catalysts for

transmetallation with arylboronic acids while the corresponding palladium(II) halides were not.[14]

These result suggests that palladium(II) hydroxides are the active catalysts for reactions involving

transmetallation of boronic acids in aqueous media, even in reactions where the palladium(II)

halides are formed directly (as in Suzuki couplings *via* oxidative addition) or otherwise are

present in higher concentrations. Ohta proposes a similar ligand exchange, where oxidative

addition of phosphine-palladium(0) **40** to chloroform yields palladium chloride **41** (Scheme 1.5).

Ligand exchange with hydroxide in the basic reaction medium generates 16-electron complex **42**,

which likely undergoes ligand dissociation to form the active, 14-electron catalyst (**39**).

Scheme 1.5 Proposed mechanism for formation of the active catalyst
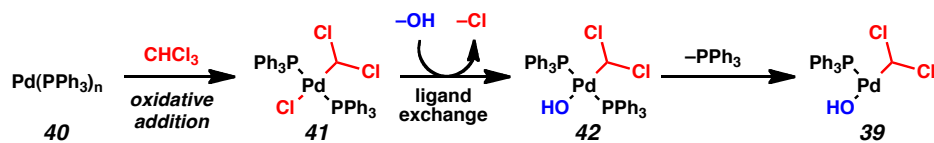
1.3.2 *Bisphosphine ligands in palladium-catalyzed conjugate addition*

Miyaura, having pioneered some early work in rhodium-catalyzed conjugate addition,

reported the first dicationic palladium(II) precatalyst (**43**) for conjugate addition utilizing 1,2-

bis(diphenylphosphino)ethane as the ligand (Scheme 1.6).[15] Cationic arylpalladium(II) species are

known to coordinate and insert olefins significantly faster than their neutral counterparts; this

phenomenon has been applied to the copolymerization of carbon monoxide and olefins utilizing

cationic palladium catalysts and triarylboron reagents.[16] Additionally, cationic palladium(II)

species are known to transmetallate rapidly with arylboron reagents, while neutral palladium(II)

is slow or inert in the same transmetallation.[17] Notably, these reactions proceed at ambient temperature in aqueous tetrahydrofuran. Miyaura's work tolerated a wide array of cyclic (e.g., **25**) and acyclic (e.g., **44**) enone substrates.

Scheme 1.6 Dicationic palladium(II)-catalyzed conjugate addition of arylboronic acids
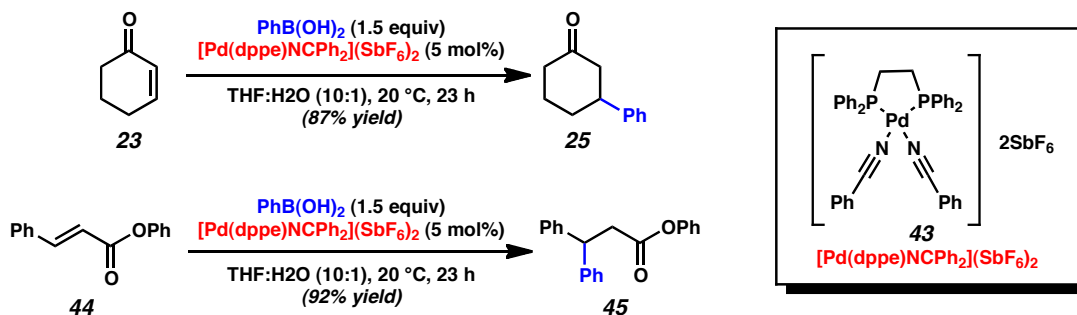
The tendency for the catalyst in Miyaura's reactions to turn over *via* hydrolysis as opposed to β–hydride elimination is rooted in the fact that cationic palladium(II) enolates undergo facile hydrolysis.[18] This phenomenon may be attributed to the increased Lewis acidity of the palladium(II) cation, which may shift the enolate tautomer equilibrium such that it exists primarily as the oxygen-bound enolate. Typically, carbon-bound enolates are observed for intermediates in other palladium(II) catalytic cycles, such as α-arylations of ketone enolates.[19] Oxygen-bound palladium(II) enolates cannot undergo β–hydride elimination, and must therefore undergo hydrolysis to liberate the catalyst. Additionally, perhaps the cationic palladium(II) is less nucleophilic than its neutral analog, and is slower to abstract β–hydrogens. Thus, the carbon-bound enolate tautomer isomerizes on a time scale significantly fast enough to prevent competitive β–hydride elimination from occurring.

Miyaura also demonstrated explicit transmetallation of arylboronic acids with precatalyst **43** (Scheme 1.7).[20] A Hammett plot generated by varying the electronic nature of the *para*-X substituent gave a negative ρ value, and supports the Wheland-type transmetallation intermediate

46. This correlates with the observation that electron-rich arylboronic acids react readily under these conditions. Isolated complex **47** proved to be chemically competent in 1,4-addition reactions, though the stabilizing presence of triphenylphosphine required elevated reaction temperatures, and suggests that the arylpalladium(II) species is the key intermediate in the C–C bond forming conjugate addition catalytic cycle.

Scheme 1.7 Isolation of arylpalladium(II) cationic complexes
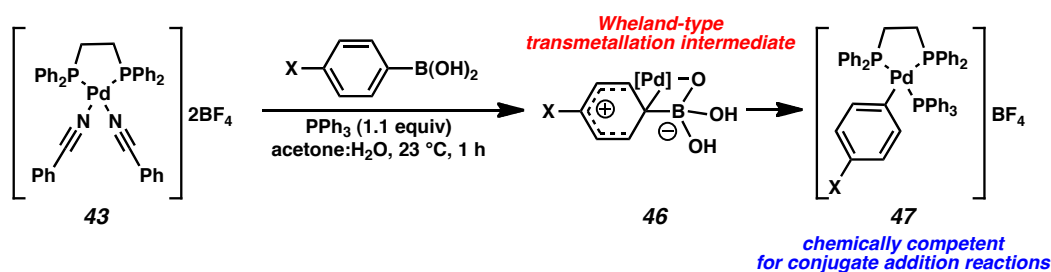
1.3.3 *Diamine ligands in conjugate addition*

Diamine ligands have seen extensive use in palladium-catalyzed conjugate addition reactions. Unlike bulkier di- or triarylphosphine ligands, diamines have been employed in catalysts that synthesize both tertiary and quaternary centers. Lu and coworkers reported a bipyridine-based system that successfully catalyzed conjugate addition to cyclic and acyclic enones (Scheme 1.8).[21] Of a number of diamine ligands screened, bipyridine significantly outperformed other diamines; a result consistent throughout much of the palladium-catalyzed 1,4-addition literature entailing diamine ligands. Though a wide variety of cyclic (**25**) and acyclic (**49**) β-aryl ketones could be synthesized, a large excess of arylboronic acid was required to drive the reaction to full conversion. Furthermore, the large excess of bipyridine relative to palladium was found to suppress formation of Heck products and biaryl homocoupling products. A follow-up report detailed the use of phase transfer additives to facilitate the same reaction in aqueous reaction media.[22]

Scheme 1.8 Diamine ligands for palladium-catalyzed 1,4-addition
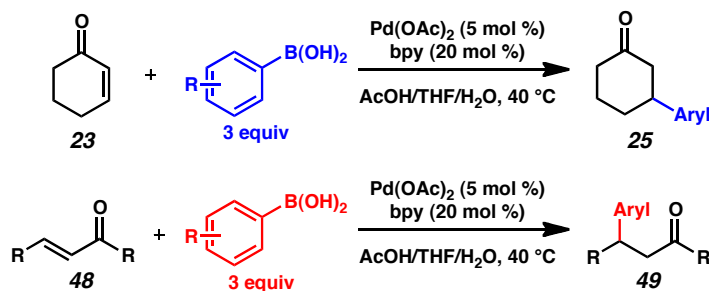
Itami and coworkers employed unique diamine palladium complex **50**, perhaps the first unsymmetric diamine ligand to be employed in palladium-catalyzed 1,4-additions.[23] Lu had explored several unsymmetric ligands, including a number of chiral diamines, but found none to be efficacious. Though Itami's work is functional on both cyclic and acyclic enone substrates, it is most notable for its ability to functionalize fullerenes *via* palladium-catalyzed hydroarylation (Scheme 1.9).

Scheme 1.9 Hydroarylation of fullerenes
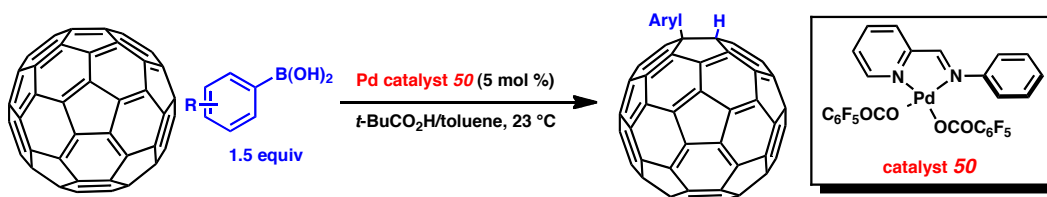
In 2010, Lu and coworkers described the first reported palladium-catalyzed conjugate addition forming quaternary stereocenters by using dimeric [(bpy)Pd(OH)]₂ (**51**) as the precatalyst.[24] This catalyst system builds off the success of their Pd/bpy results, and employs some of the observations made my Miyaura and others concerning the increased efficacy of cationic palladium(II) hydroxide in transmetallation with arylboron reagents and the facile hydrolysis of cationic palladium(II) enolates. Moving to the cationic diamine complex facilitated

milder reaction conditions that do not require acetic acid as a cosolvent to assist in enolate hydrolysis. This system tolerates a variety of cyclic enone ring sizes, including five- (**52**) and six-membered (**35**) rings (Table 1.2), as well as acyclic ketones (**53**). β-aryl enones (**54**) are unreactive, however electron-rich (**55**) and electron-poor (**56**) arylboronic acids are competent in the reaction manifold. Minnaard detailed a similar system in 2013, however, they employed a catalyst derived *in situ* from palladium(II) trifluoroacetate and bpy.[25]

Table 1.2 Cationic palladium(II)-bypridine catalysts forming quaternary stereocenters by 1,4-addition
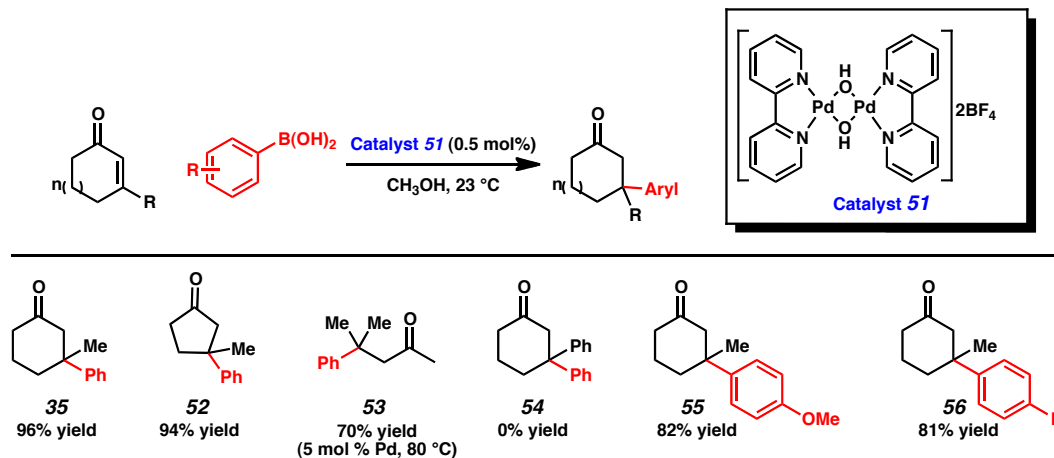
1.4 "Ligand-free" conjugate addition reactions

While "ligand-free" reactions are not amenable to asymmetric catalysis, they do provide a direct route to 1,4-addition products that may be difficult to synthesize by other means. These "ligand-free" reactions, perhaps due to their sterically unencumbered ligand sphere, tolerate highly substituted enone reactants. Lee and coworkers detailed a system using a catalyst derived from palladium(II) acetate and triflic acid to catalyze arylation of hindered enones (e.g., **57**) using arylboroxine reagents (Scheme 1.10).[26] The procedure details treatment of a solution of

palladium(II) acetate with triflic acid, which forms dicationic palladium(II) triflate species *in situ*. Another important advance promoted by Lee was the addition of sodium nitrate to the reaction mixture, which they found to suppress the undesired homocoupling side reaction. This additive is particularly necessary when utilizing sterically hindered enones, however, they observed it was not useful for facile, sterically unencumbered substrates.

Scheme 1.10 "Ligand-free" conjugate addition of arylboroxines to hindered enones
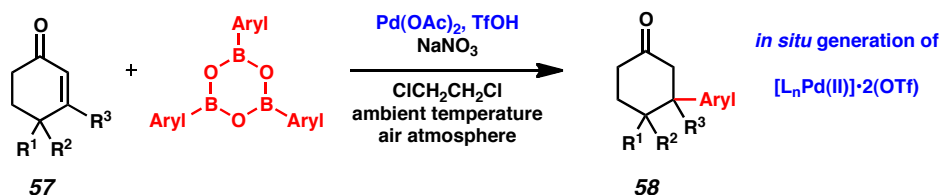
Lee and coworkers next disclosed a link between oxidation chemistry and 1,4-addition reactions, whereby choice of solvent determines the outcome of a β-arylation reaction.[27] Using coordinating solvents, such as dimethylsulfoxide, simple enone substrates could undergo facile oxidative Heck reaction to form arylated enone (**26**). This reactivity was best suited to arylboronic acid reagents. Conversely, employing non-coordinating solvents, such as dichloroethane, and arylboroxine reagents could tune the reactivity toward 1,4-addition products (**25**). Presumably, the more coordinating solvent must stabilize the cationic palladium(II) intermediates and disfavor protonolysis of the enolate. Furthermore, because carbopalladation proceeds in a *syn*-facial stereochemical relationship, the carbon-bound palladium enolate must isomerizes to have a *syn* β-hydrogen to promote the elimination reaction. Coordinating solvent must either slow protonolysis of these equilibrating enolates sufficiently such that the β-hydride elimination reaction can out-compete the other turnover pathways, or the coordinating solvent itself may somehow promote isomerization and β-hydride elimination to furnish the oxidative Heck product.

Figure 1.4 Solvent effects on products of "ligand-free" palladium-catalyzed arylations
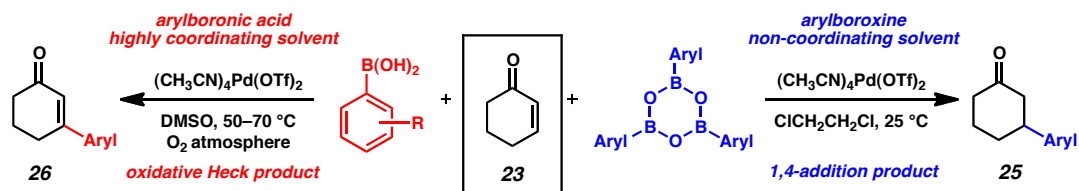
1.5 Direct β-arylation of cyclic ketones

Until recently, β-functionalization of carbonyl compounds required a chemical handle, such as the traditionally-employed α,β-unsaturated carbonyl conjugate acceptor. In 2013, direct β–arylation reactions of ketones was demonstrated. Building on the ketone to enone oxidation work of Stahl and others, which reports the use of molecular oxygen as the stoichiometric oxidant in palladium-catalyzed oxidation reactions,[28] Dong and coworkers reported the first, direct β-arylation of ketones in 2013.[29] Reacting aryl iodides with ketones of a variety of ring sizes, Dong and coworkers postulate the *in situ* formation of the cyclic enone, which in turn reacts *via* palladium-catalyzed 1,4-addition to furnish the β-arylation products (Table 1.3). Successful reactions are reported with 5- (**60**), 6- (**59**) and 7-membered (**61**) ring ketones, as well as an isolated example of a heteoaromatic iodide reactant (**62**) and some linear ketones (**63**).

Table 1.3 Direct β-arylation of ketones
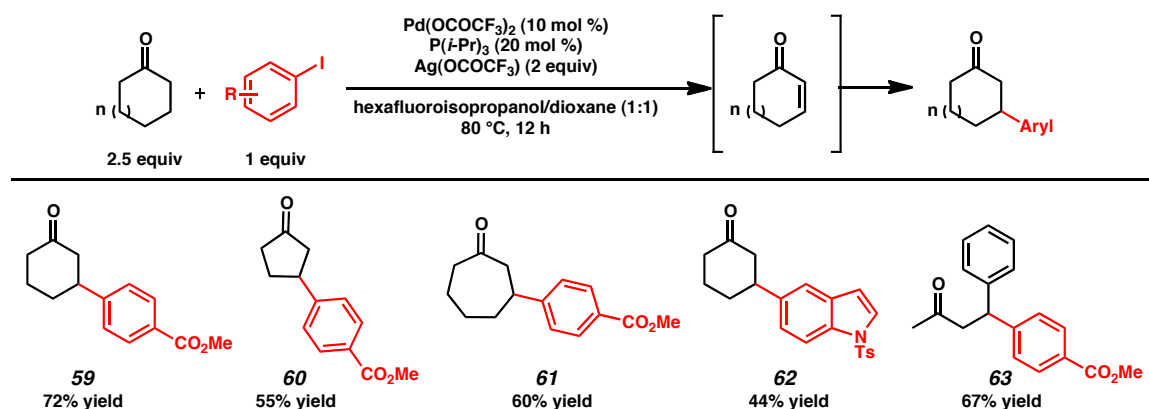
The mechanism Dong proposes is a hybrid of the Stahl oxidation chemistry and the catalytic cycle studied by Miyaura for palladium-catalyzed 1,4-addition. A palladium(II) catalyst (**65**) reacts with an equivalent of ketone/enol substrate (**66**) to afford the equilibrium mixture of carbon– (**67**) and oxygen–bound (**68**) palladium enolates (Figure 1.5). The carbon–bound isomer undergoes β-hydride elimination to afford the corresponding enone and palladium(II) hydride. Reduction of palladium *via* loss of HX generates palladium(0) (**70**), which undergoes oxidative addition with the aryl iodide to furnish arylpalladium(II) **71**. The author of this review speculates that at this point, the reaction pathway becomes cationic by silver-mediated halogen abstraction to precipitate silver iodide and yield arylpalladium(II) **72**, the purported reactive species for enone arylation. Migratory insertion of the enone olefin into the aryl–palladium bond furnishes equilibrating palladium mixture **73** and **74**. Turnover is mediated by protonolysis by an equivalent of HX, formed by reduction of hydride **69** or from initial formation of the palladium enolate to begin the catalytic cycle. HX serves to liberate arylation product **75** and regenerate the catalyst (**65**). The author of this review proposes that the 1,4-addition portion of the cycle is likely facilitated by cationic arylpalladium(II),

and that the reaction may best be thought of as two half-cycles that must link together to form a closed catalytic cycle: 1) a palladium(II)-catalyzed ketone oxidation, which generates palladium(0); and 2) a palladium(0)-catalyzed 1,4-arylation, involving *cationic* palladium(II) during enone arylation and palladium enolate protonolysis. Notably, switching between neutral and cationic palladium(II) is likely required, however the precise mechanistic details are yet unknown.

Figure 1.5 Proposed mechanism of direct β-arylation of ketones
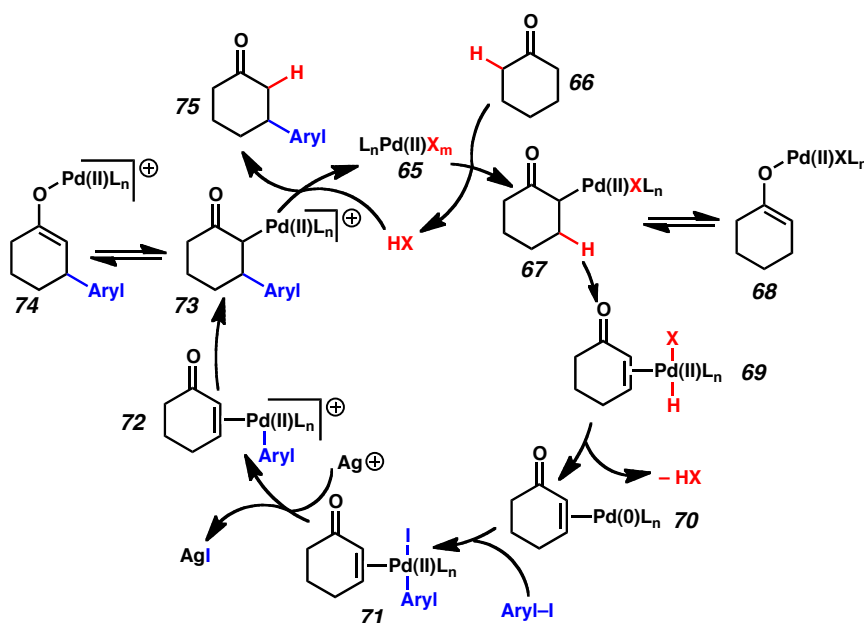
1.6 Asymmetric reactions forging tertiary stereocenters

The application of bidentate ligands to palladium-catalyzed 1,4-addition reactions quickly facilitated the development of asymmetric variants. A comprehensive review of this area was published in 2007.[6] This section will briefly describe a number of approaches that were developed before the advance of quaternary-stereocenter forging palladium-catalyzed conjugate additions.

1.6.1   Dicationic palladium(II)-catalyzed systems

Miyaura and coworkers first reported the asymmetric conjugate addition of triarylbismuth reagents to enones.[30] A variety of cyclic enone ring sizes and acyclic enones were reacted using a catalyst derived from chiral bidentate phosphine ligands, such as dipamp and chiraphos. However, the requisite use of uncommon arylbismuth reagents failed to challenge the popularity of rhodium- and copper-catalyzed systems that employed more common organometallic reagents. Later, Miyaura's group significantly expanded the scope of nucleophiles to include more common reagents such as aryltrifluoroborate salts,[31] and arylboronic acids (Scheme 1.1).[32] In the most general scheme, arylboronic acids are reacted with a dipamp-palladium catalyst (**76**) to deliver phenylated ketone **25** in 95% yield and 93% ee. The catalyst is highly active, and requires sub-zero temperatures to deliver high stereoselectivity. Switching to acetone as the cosolvent and (*S,S*)-chiraphos as the ligand allowed high stereoselectivity to be obtain at ambient temperature, and while aryltrifluoroborate reagents were found to react more rapidly at ambient temperature than arylboronic acids the addition of catalytic $AgBF_4$ induced significantly greater turnover numbers for the arylboronic acids.[33] This advance facilitated the delivery of **25** in 99% yield and 89% ee with catalyst loadings as low as 0.01 mol % on 5 mmol scale. Miyaura's group continued to be extremely productive in this field and has reported a number of further advances in substrate scope, include aldehyde-based conjugate acceptors,[34] nitrogen-containing acceptors,[35] and asymmetric tandem conjugate addition/aldol processes.[36] The authors have since published a retrospective account of their pursuits in the area of palladium-catalyzed conjugate addition.[37]

Scheme 1.11 Chiral dicationic palladium(II) precatalysts based on bidentate bisphosphine ligands
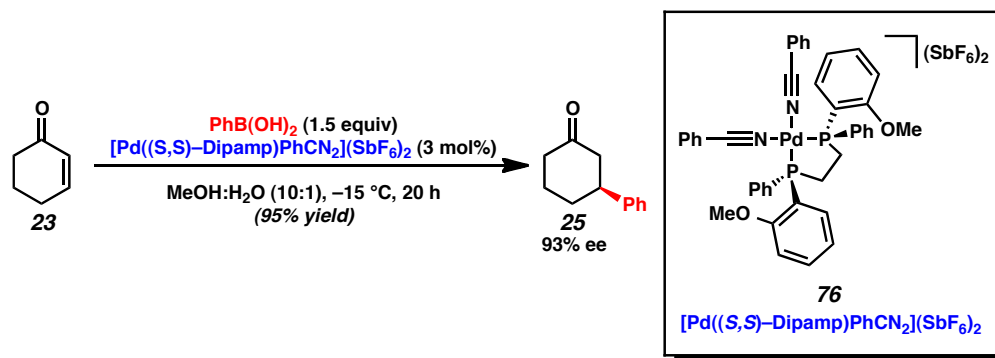
1.6.2   *Palladium(II) trifluoroacetate-catalyzed systems and systems derived in situ*

Minnaard and coworkers reported a system for asymmetric conjugate addition to cyclic enones employing a catalyst derived *in situ* from palladium(II) trifluoroacetate and (*R,R*)-Me-DuPhos as the chiral ligand.[38] This system features a streamlined reaction procedure, as there is no need to pre-form the precatalyst complex. However, because the precatalyst is not cationic or dicationic, elevated temperatures are required to promote the reaction. Presumably, this is because bidentate ligands require that arylpalladium(II) species must necessarily undergo ligand dissociation to form cationic species in order to have an open coordination site for the substrate. Minnaard and coworkers later extended the scope of the nucleophiles to include arylsiloxanes by employing ZnF_2 in conjunction with their Pd/DuPhos catalyst system.[39] Notably, heteroatom-containing substrates were successfully employed in these reactions, such as δ–lactones and 4-piperidinone substrates.

Scheme 1.12 (R,R)-Me-DuPhos as ligand for asymmetric conjugate addition
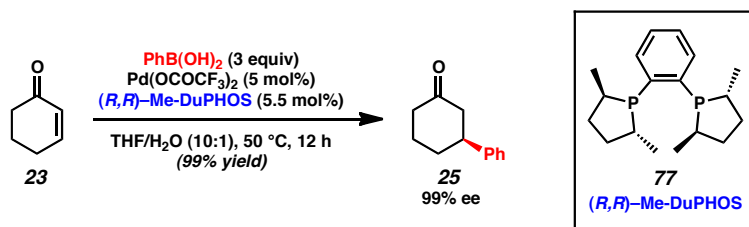
Shi and coworkers reported a bidentate ligand scaffold derived from BINAP and *N*-heterocyclic carbene ligands (Scheme 1.13a, **78**).[40] Related development of bis-NHC ligands derived from anthrocene has been reported recently by Viege.[41] The advance of this work is that the catalyst (**80**) can be derived *in situ* from palladium(II) acetate and the triflate salt of the NHC precursor (Scheme 1.13b, **79**).

Scheme 1.13 N-heterocyclic carbene ligand scaffolds for asymmetric 1,4-addition to cyclic enones

a. Pre-formed NHC-Pd catalysts

ArylB(OH)$_2$ (1.5 equiv)
Catalyst *78* (3 mol%)

THF:H$_2$O (10:1), 20 °C, 36h
(78–99% yield)

23

25
88–99% ee

Catalyst *78*

a. NHC-Pd catalysts generated *in situ*

Pd(OAc)$_2$

− 2 HOAc

79

80
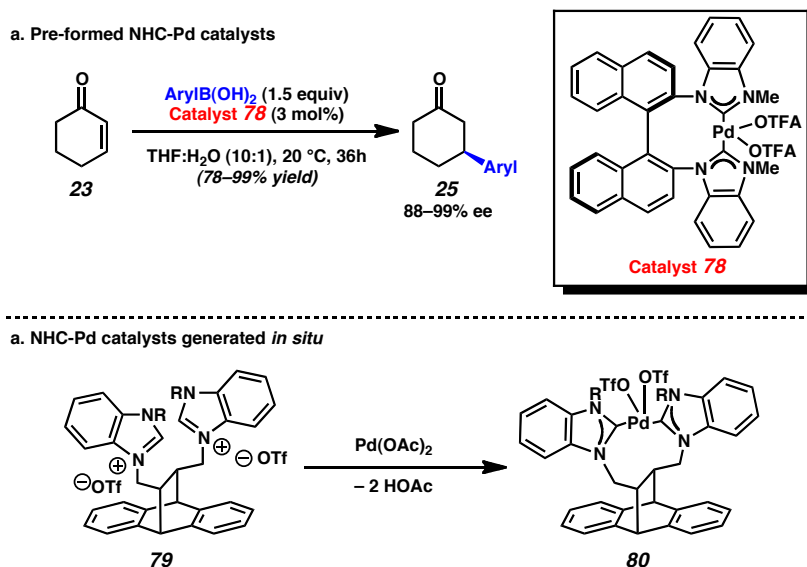
Bedford and Hu independently pioneered the application of palladacycle catalysts to 1,4-addition reactions.[42] These catalysts were suitable for use at loadings of 1 mol % or lower, and functioned with both arylboronic acids and arylsiloxanes. Notably, reactions employing these palladacycles do not facilitate homocoupling of the arylmetal reagent. Otha and coworkers developed an asymmetric variant of these palladacycle-catalyzed reactions.[43] They hypothesize a palladium(II) hydroxide catalyst, presumably by a bromide/hydroxide ligand exchange similar to that detailed in Scheme 1.5. Follow up work saw modest success applying the transformation to

acyclic enones, reporting 42–52% ee with moderate chemical yields, and 1,2-addition to

aldehydes, albeit in poor ee.[44]

Scheme 1.14 Chiral ferrocene-based ligand designs for palladium-catalyzed conjugate addition
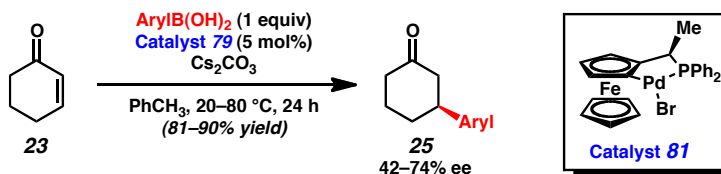
1.7 Asymmetric reactions forging quaternary stereocenters

1.7.1 C_1 symmetric ligands

In 2011, Stoltz reported the first palladium-catalyzed asymmetric conjugate addition of

arylboronic acids to cyclic enones to form quaternary stereocenters utilizing a catalyzed formed

in situ from palladium(II) trifluoroacetate and the *(S)-tert*-butylpyridinooxazoline ligand (Table

1.4).[45] This reaction delivered arylated ketones of five- (**52**), six- (**35**), and seven-membered rings

(**83**) all in greater than 90% ee. Bulky β-substituents (**86**) and heteroatom-containing tethers (**87**)

were all tolerated. The reaction exhibited high functional group compatibility, and reactions of

esters (**88**), fluorinated groups (**89**) and even aryl bromides (**90**) proceeded in high yields.

Additionally, the ligand was easy to synthesize,[46] and the process was found amenable to

heterocyclic conjugate acceptors (**84**, **85**).[47]

Table 1.4 Pd/PyOx-catalyzed asymmetric conjugate addition product scope
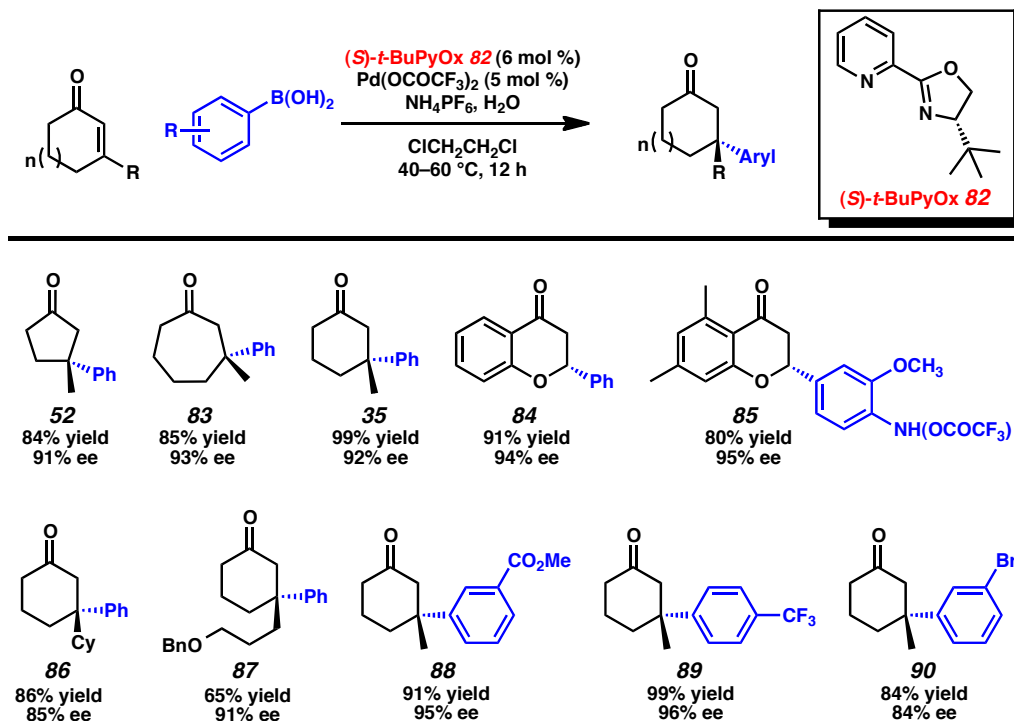
Stoltz and Houk jointly reported a computational and experimental study of the stereochemical model for induction of enantioselectivity and the mechanistic details of the conjugate addition.[48] Steric repulsion between the α-methylene protons of the enone substituent and the *tert*-butyl group of the ligand was implicated as the interaction that determined the preferred transition state geometry (Figure 1.6). Computational studies indicate a cationic palladium(II) hydroxide catalyst, and experiments detailed the addition of water and non-coordinating counterions increased the reaction rate, facilitating a lower reaction temperature and a broader, more functional-group tolerant substrate scope.

Figure 1.6 Stereochemical model for induction of asymmetry in Pd/PyOx conjugate addition

Enantioselectivity-Determining Step
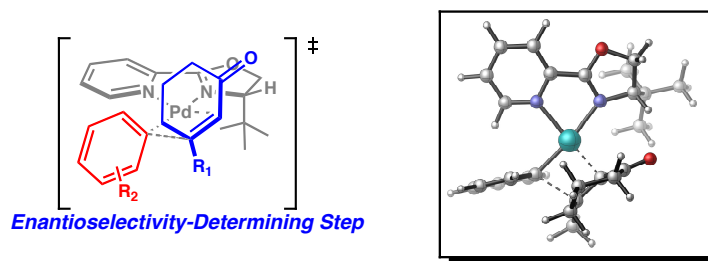
1.7.2   *C₂ symmetric ligands*

Minnaard and de Vries reported the asymmetric conjugate addition of boronic acids to enones utilizing a dicationic palladium catalyzed derived *in situ* from (PhBOX)PdCl$_2$ (**91**).[49] Treatment of dichloride **91** with silver hexafluoroantimonate furnishes the active, dicationic palladium(II) catalyst. The C_2 symmetry of the ligand tolerates enones of five- (**52**), six- (**35**), and seven-membered ring size (**83**), providing the corresponding β-aryl ketones all in greater than 93% ee. Lactone **92** serves as a selective substrate, with an 88% ee. This substrate provided only 50% ee in the Stoltz Pd/PyOx manifold, as the substrate lacks the α-methylene protons that are implicated in the enantiodetermining steric interactions with the ligand. Linear ketones (e.g., **93**) react with modest to good yields, but poor ee. Additionally, the researchers demonstrated that more functionally diverse arylboronic acids could react successfully, furnishing **94** in 93% yield and 93% ee.

Table 1.5 Dicationic palladium(II) asymmetric conjugate addition with bisoxazoline ligands
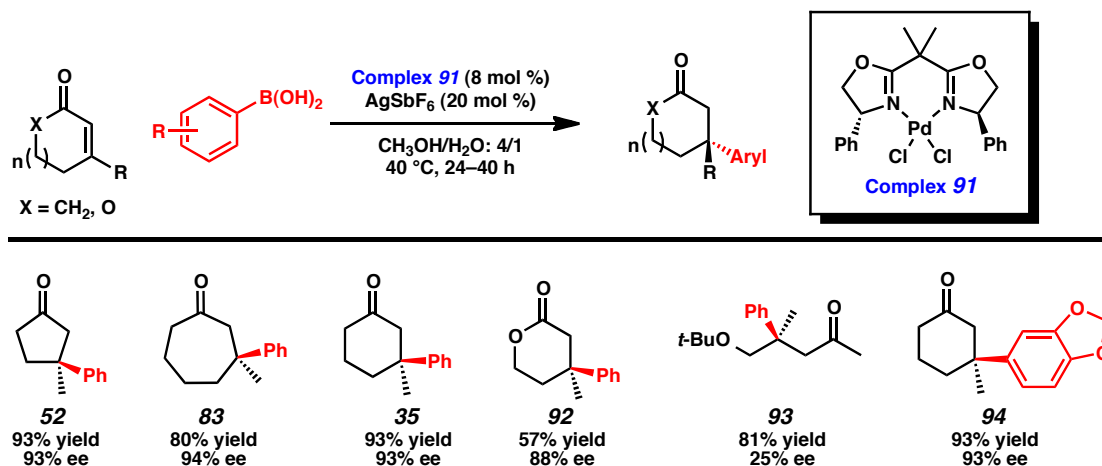
1.8 Conclusion and outlook

The study of palladium-catalyzed conjugate addition is significantly less developed than systems employing rhodium or copper. These palladium catalysts provide an excellent contrast to the other metals in several respects. For example, copper systems generally have lower functional group tolerance due to the necessity of employing highly reactive organometallic reagents for transmetallation with copper, and therefore these reactions also require rigorously anhydrous reaction conditions. The rhodium catalysts can be impractical because they require expensive, sensitive precursors, complicated and difficult to synthesize ligands, and must be run in thoroughly degassed solvents. In contrast, the palladium-catalyzed reactions provide user-friendly advantages in several key areas: 1) the use of bench-stable and easily-handled boron-based aryl reagents, 2) high tolerance for aqueous reaction media and protic solvents, 3) insensitive to oxygen atmosphere, 4) high functional group tolerance, 5) mild reaction conditions and straightforward reaction procedure.

However, palladium-catalyzed conjugate addition significantly lags behind the rhodium and copper manifolds in other areas, most notably the narrow substrate scope. To date, palladium conjugate addition is specific to *aryl* organometallic reagents, and do not tolerate alkenyl or alkyl

nucleophiles. Alkenyl reagents undergo rapid transmetallation, and may dimerize or polymerize under typical reaction conditions. Likewise, alkylpalladium species are often subject to rapid, off-cycle β-hydride elimination. This is particularly true of many of the putative alkylpalladium species formed in the reactions catalyzed by chiral ligands because they frequently employ small ligand-metal bite angles, a geometry that does not retard β-hydride elimination. Indeed, generation of palladium hydrides and subsequent reduction to palladium(0) is one of the factors that prevents lower catalyst loadings in several palladium conjugate addition systems discussed herein. Despite some current drawbacks, the advantages conveyed by palladium-catalyzed conjugate addition should continue to attract researchers to the subject, and perhaps this continued study will enable the technological advance required to significantly expand the substrate scope and synthetic utility of this reaction.

1.9 **Notes and citations**

(1)   (a) Krause, N.; Hoffmann-Röder, A. *Synthesis* **2001**, *2*, 171–196. (b) Sibi, M. P.; Manyem, S. *Tetrahedron* **2000**, *56*, 8033–8061. (c) Rossiter, B. E.; Swingle, N. M. *Chem. Rev.* **1992**, *92*, 771–806.

(2)   (a) Harutyunyan, S. R.; den Hartog, T.; Geurts, K.; Minnaard, A. J.; Feringa, B. L. *Chem. Rev.* **2008**, *108*, 2824–2852. (b) Alexakis, A.; Benhaim, C. *Eur. J. Org. Chem.* **2002**, 3221–3236. (c) Feringa, B. L. *Acc. Chem. Res.* **2000**, *33*, 346–353.

(3)   (a) Hayashi, T.; Yamasaki, K. *Chem. Rev.* **2003**, *103*, 2829–2844.

(4)   Hawner, C.; Alexakis, A. *Chem. Commun.* **2010**, *46*, 7295–7306.

(5)   Larock, R. C.; Yum, E. K.; Yang, H. *Tetrahedron* **1994**, *50*, 305–321.

(6)   Gutnov, A. *Eur. J. Org. Chem.* **2008**, 4547–4554.

(7)   (a) Cacchi, S.; Misiti, D.; Palmieri, G. *Tetrahedron* **1981**, *37*, 2941–2946. (b) Cacchi, S.; La Torre, F.; Misiti, D.; Palmieri, G. *Tetrahedron Lett.* **1979**, *20*, 4591–4595.

(8)   (a) Ohe, T.; Uemura, S. *Tetrahedron Lett.* **2002**, *43*, 1269–1271. (b) Ohe, T.; Wkita, T.; Motofua, S.-I.; Cho, C. S.; Ohe, K.; Uemura, S. *Bull. Chem. Soc. Jpn.* **2000**, *73*, 2149–2155. (c) Cho, C. S.; Motofusa, S.-I.; Ohe, K.; Uemura, S. *Bull. Chem. Soc. Jpn.* **1996**, *69*, 2341–2348. (d) Cho, C. S.; Motofusa, S.-I.; Ohe, K.; Uemura, S.; Shim, S. C. *J. Org. Chem.* **1995**, *60*, 883–888. (e) Cho, C. S.; Motofusa, S.-I.; Uemura, S. *Tetrahedron Letters* **1994**, *35*, 1739–1742.

(9)   Denmark, S. E.; Amishiro, N. *J. Org. Chem.* **2003**, *68*, 6997–7003.

(10)   Wang, H.; Li, Y.; Zhang, R.; Jin, K.; Zhao, D.; Duan, C. *J. Org. Chem.* **2012**, *77*, 4849–4853.

(11)   Nishimura, T.; Katoh, T.; Takatsu, K.; Shintani, R.; Hayashi, T. *J. Am. Chem. Soc.* **2007**, *129*, 14158–14159.

(12)   Yamamoto, T.; Iizuka, M.; Takenaka, H.; Ohta, T.; Ito, Y. *Journal of Organometallic Chemistry* **2009**, *694*, 1325–1332.

(13) Poláčková, V.; Bariak, V.; Sebesta, R.; Toma, S. *Chem. Pap.* **2011**, *65*, 338–344.

(14)   Carrow, B. P.; Hartwig, J. F. *J. Am. Chem. Soc.* **2011**, *133*, 2116–2119.

(15)   Nishikata, T.; Yamamoto, Y.; Miyaura, N. *Angew. Chem., Int Ed.* **2003**, *42*, 2768–2770.

(16)   Mecking, S. *Coord. Chem. Rev.* **2000**, *203*, 325–351.

(17)   Miyaura, N. *Top. Curr. Chem.* **2002**, *219*, 11.

(18)   Albeniz, A. C.; Marta Catalina, N.; Espinet, P.; Redon, R. *Organometallics* **1999**, *18*, 5571–5576.

(19)   Culkin, D. A.; Hartwig, J. F. *J. Am. Chem. Soc.* **2001**, *123*, 5816–5817.

(20)   Nishikata, T.; Yamamoto, Y.; Miyaura, N. *Organometallics* **2004**, *23*, 4317–4324.

(21)   Lu, X.; Lin, S. *J. Org. Chem.* **2005**, *70*, 9651–9653.

(22)   Lin, S.; Lu, X. *Tetrahedron Letters* **2006**, *47*, 7167–7170.

(23)   Mori, S.; Nambo, M.; Chi, L.-C.; Bouffard, J.; Itami, K. *Org. Lett.* **2008**, *10*, 4609–4612.

(24)   Lin, S.; Lu, X. *Org. Lett.* **2010**, *12*, 2536–2539.

(25)   Gottumukkala, A. L.; Suljagic, J.; Matcha, K.; de Vries, J. G.; Minnaard, A. J.

         Chem. Sus. Chem. **2013**, *6*, 1636–1639.

(26)   Jordan-Hore, J. A.; Sanderson, J. N.; Lee, A.-L. *Org. Lett.* **2012**, *14*, 2508–2511.

(27)   Walker, S. E.; Boehnke, J.; Glen, P. E.; Levey, S.; Patrick, L.; Jordan-Hore, J. A.;

         Lee, A.-L. *Org. Lett.* **2013**, *15*, 1886–1889.

(28)   (a) Campbell, A. N.; Stahl, S. S. *Acc. Chem. Res.* **2012**, *45*, 851–863. (b) Stahl, S.

         S. *Science* **2005**, *309*, 1824–1826.

(29)   Huang, Z.; Dong, G. *J. Am. Chem. Soc.* **2013**, *135*, 17747–17750.

(30)   Nishikata, T.; Yamamoto, Y.; Miyaura, N. *Chem. Commun.* **2004**, 1822–1823.

(31)   Nishikata, T.; Yamamoto, Y.; Miyaura, N. *Chem. Lett.* **2005**, *34*, 720–721.

(32)   Nishikata, T.; Yamamoto, Y.; Gridnev, I. D.; Miyaura, N. *Organometallics*, **2005**,

         24, 5025–5032.

(33)   Nishikata, T.; Yamamoto, Y.; Miyaura, N. *Adv. Synth. Catal.* **2007**, *349*,

         1759–1764.

(34)   Nishikata, T.; Yamamoto, Y.; Miyaura, N. *Tetrahedron Lett.* **2007**, *48*,

         4007–4010.

(35)   Nishikata, T.; Yamamoto, Y.; Miyaura, N. *Chem. Lett.* **2007**, *36*,1442–1443.

(36)   Nishikata, T.; Kobayashi, Y.; Kobayashi, K.; Yamamoto, Y.; Miyaura, N. *Synlett*

         2007, *19*, 3055–3057.

(37)   Yamamoto, Y.; Nishikata, T.; Miyaura, N. *Pure Appl. Chem.* **2008**, *80*, 807–817.

(38)   Gini, F.; Hessen, B.; Minnaard, A. J. *Org. Lett.* **2005**, *7*, 5309–5312.

(39)   Gini, F.; Hessen, B.; Feringa, B. L.; Minnaard, A. J. *Chem. Commun.* **2007**, 710.

(40)   Zhang, T.; Shi, M. *Chem. Eur.–J.* **2008**, *14*, 3759–3764.

(41)   Mullick, A. B.; Jeletic, M. S.; Powers, A. R.; Ghiviriga, I.; Abboud, K. A.; Viege, A. S. *Polyhedron* **2013**, *52*, 810–819.

(42)   (a) Bedford, R. B.; Betham, M.; Charmant, J. P. H.; Haddow, M. F.; Guy Orpen, A.; Pilarski, L. T. *Organometallics* **2007**, *26*, 6346–6353. (b) He, P.; Lu, Y.; Dong, C.-G.; Hu, Q.-S. *Org. Lett.* **2007**, *9*, 343–346.

(43)   Suzuma, Y.; Yamamoto, T.; Ohta, T.; Ito, Y. *Chem. Lett.* **2007**, *36*, 470–471.

(44)   Suzuma, Y.; Hayashi, S.; Yamamoto, T.; Oe, Y.; Ohta, T.; Ito, Y. *Tetrahedron: Asymmetry* **2009**, *20*, 2751–2758.

(45)   Kikushima, K.; Holder, J. C.; Gatti, M.; Stoltz, B. M. *J. Am. Chem. Soc.* **2011**, *133*, 6902–6905.

(46)   Shimizu, H.; Holder, J. C.; Stoltz, B. M. *Beilstein J. Org. Chem.* **2013**, *9*, 1637–1642.

(47)   Holder, J. C.; Marziale, A. N.; Gatti, M.; Mao, B.; Stoltz, B. M. *Chem. Eur. J.* **2012**, *19*, 74–77.

(48)   Holder, J. C.; Zou, L.; Marziale, A. N.; Liu, P.; Lan, Y.; Gatti, M.; Kikushima, K.; Houk, K. N.; Stoltz, B. M. *J. Am. Chem. Soc.* **2013**, *135*, 14996–15007.

(49)   Gottumukkala, A. L.; Matcha, K.; Lutz, M.; de Vries, J. G.; Minnaard, A. J. *Chem. Eur. J.* **2012**, *18*, 6907–6914.

CHAPTER 2

The development of a palladium-catalyzed asymmetric conjugate addition of

arylboronic acids to cyclic conjugate acceptors÷
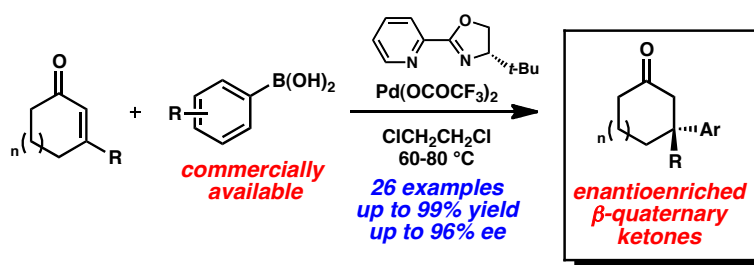
Abstract
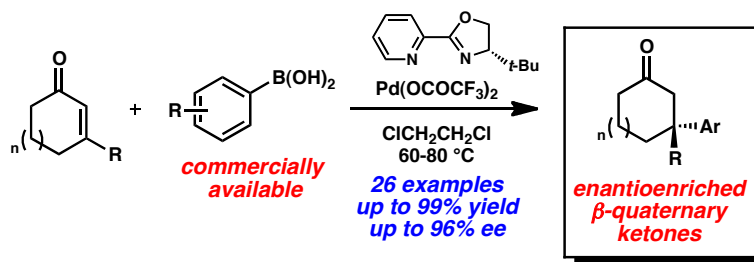
The first enantioselective Pd-catalyzed, asymmetric construction of all-carbon quaternary stereocenters via 1,4-addition of arylboronic acids to cyclic, β-substituted enones is reported. A wide range of arylboronic acids and cyclic enones are reacted utilizing a catalyst prepared from palladium(II) trifluoroacetate and a chiral pyridinooxazoline ligand to yield enantioenriched products bearing benzylic stereocenters. Notably, this transformation is insensitive to air or moisture, providing a practical and operationally simple method of synthesizing enantioenriched all-carbon quaternary stereocenters.

2.1 Introduction

The catalytic enantioselective construction of all-carbon quaternary stereocenters remains a difficult problem in synthetic chemistry.[1] A reliable approach toward this challenge has been the asymmetric conjugate addition of carbon-based nucleophiles to suitable α,β-unsaturated carbonyl acceptors.[2] Pioneered by the groups of Feringa, Alexakis, and Hoveyda, the majority of asymmetric conjugate additions for the synthesis of quaternary centers involve the use of highly reactive organometallic reagents (e.g., diorganozinc,[3] triorganoaluminum,[4] and organomagnesium reagents[5]) to a variety of unsaturated electrophiles with copper catalysts.[6] These reactions uniformly involve air and moisture sensitive organometallic reagents that require rigorously anhydrous reaction conditions. Alternatively, Hayashi has championed the use of chiral rhodium catalysts in combination with air stable, easily handled nucleophilic organoboron reagents to produce a wide array of conjugate addition adducts in exceptional yield and ee.[7,8] In contrast to the copper systems, relatively few examples in the rhodium series lead to the formation of products containing quaternary centers.[9] Notably, Hayashi and Shintani have recently developed a rhodium•diene-catalyzed conjugate addition of sodium tetraaryl borates (Ar_4BNa) and arylboroxines $(ArBO)_3)$ to β,β-disubstituted enones to provide ketone products bearing b-chiral all-carbon quarternary stereocenters.[10,11] Unfortunately, in these examples commercially available arylboronic acids $(ArB(OH)_2)$ are not competent nucleophiles.[10,11,12]

The conjugate addition of arylboronic acids and their derivatives to enones with palladium catalysis has been investigated for some time and has resulted in the development of addition reactions that produce enantioenriched tertiary β-substituted

ketones.[13] In 2010, Lu reported the use of a dicationic bipyridine-derived palladium catalyst for additions to β-substituted enones that deliver racemic products containing the quaternary center in high yield.[14] Notably absent from the Lu report and from the work of others in the area are examples of Pd-catalyzed enantioselective conjugate addition reactions that forge a quaternary center.[13] Herein, we report the first palladium-catalyzed asymmetric conjugate addition of arylboronic acids to β-substituted cyclic enones employing an easily accessible chiral pyridinooxazoline (PyOx) ligand.[15] These reactions generate a wide array of benzylic all-carbon quaternary stereocenters while exhibiting extraordinary tolerance to both air and water.

2.2 Development and optimization of reaction conditions

2.2.1 Identification of chemically competent ligand and solvent conditions

To achieve the desired enantioselective conjugate addition, the reaction of 3-methylcyclohexen-2-one (**1**) with phenylboronic acid (**2**) was investigated in the presence of various palladium catalysts and chiral ligands (Table 2.1). After a preliminary ligand search that included an array of standard chiral ligand frameworks,[16] we noted that bis-nitrogen ligands were generally successful in the literature, and bipyridine (bpy, **96**) provided full conversion of enone **95** when treated with palladium(II) acetate and phenylboronic acid in protic solvents. Unfortunately, a number of standard privileged ligand scaffolds failed to afford any conversion to the desired conjugate addition product under identical reaction conditions. Sparteine (**98**), PyBox (**99**), and a variety of bis-oxazoline (**101** and **102**) and phosphinooxazoline (**100**) did not enable the transformation. "Ligand-less" conditions (**97**) also failed to provide any product. Notably, pyridine (**103**,

12 mol %) failed to deliver any product, insinuating that architechtural features of the bidentate bpy scaffold enabled the desired reaction.

Table 2.1 diamine ligand screen [a]
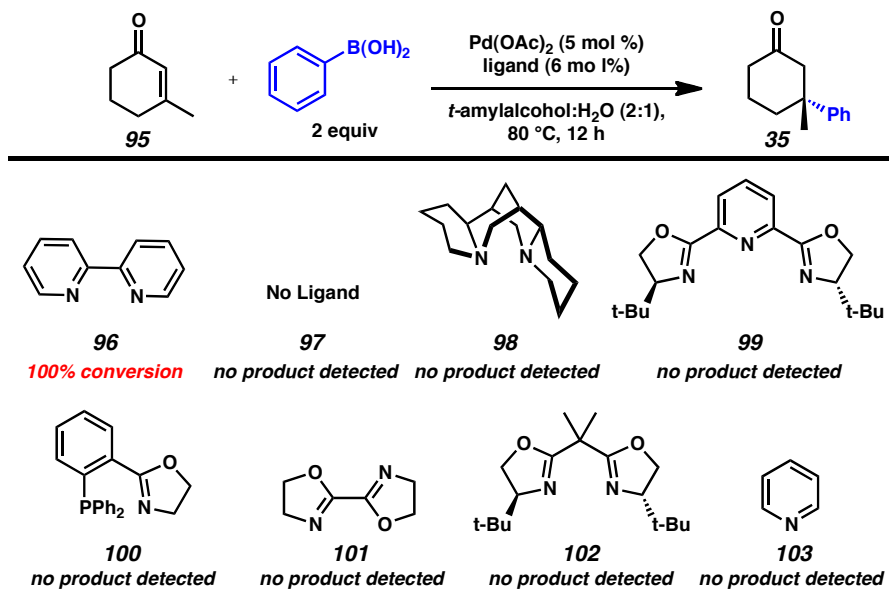
^{a} Conditions: enone (0.25 mmol), phenylboronic acid (0.50 mmol), Pd(OAc)$_2$ (5 mol %), ligand (6 mol %), solvent (1 mL), 24 h. NMR yield. ee determined by chiral HPLC.

Success with bpy and lack of success with chiral bis-oxazoline ligands led us to hypothesize that a C_1 symmetry chiral ligand based on the bpy scaffold would be a suitable catalyst. The presence of a pyridine was required, however the small bite angle and 5-membered metallocycle chelate seemed equally important. We reasoned that modification of one pyridine moiety of bpy would allow the introduction of a chiral group (Figure 2.1, **104**), while still maintaining the 5-membered chelate and narrow bite-angle. We quickly discovered that substituted PyOx ligands (**105**)[15] provided high levels of enantioselection.

Figure 2.1 Motivating the use of pyridinooxazoline ligands

· **5-membered metallocycle chelate**
· **Narrow bite-angle**
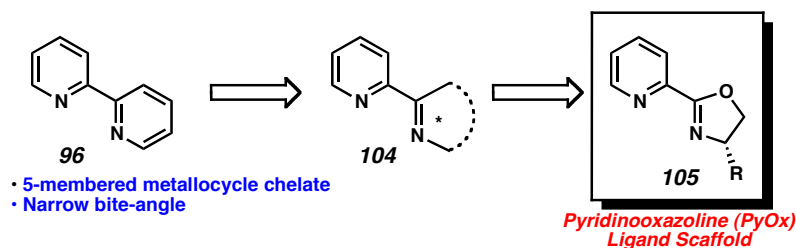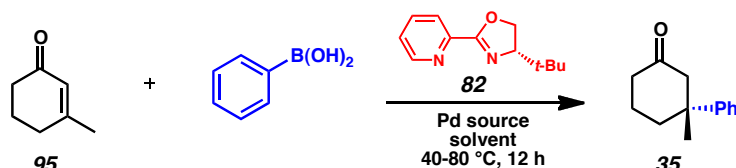
Identification of a functioning chiral ligand (**82**) prompted us to consider the effects of solvent on the yield and enantioselectivity of the reaction. A preliminary solvent screen led us to observe that polar, coordinating solvents hindered the reaction (Table 2.2, entries 1–3). Moving toward non-polar solvents, such as toluene (entry 4), encouraged higher conversions and modest enantioinduction, however, heating these reactions (entries 6–7) failed to drive the reactions to full conversion. Fortuitously, dichloromethane (entry 5) provided 87% isolated yield of the desired conjugate addition adduct in 91% ee.

Table 2.2 Preliminary solvent screen [a]

entry	solvent	temperature (°C)	yield (%)	ee (%)
1	*t*-amyl alcohol	40	14 (NMR)	--
2	dioxane	40	17 (NMR)	--
3	THF	40	31 (NMR)	--
4	toluene	40	65 (NMR)	82
5	CH$_2$Cl$_2$	40	87 (isolated)	91
6	toluene	60	63 (isolated)	77
7	hexane	60	68 (isolated)	62

[a] Conditions: enone (0.25 mmol), phenylboronic acid (0.50 mmol), Pd(OCOCF$_3$)$_2$ (5 mol %), (*S*)-*t*-BuPyOx (6 mol %), solvent (1 mL), 24 h. NMR yield. ee determined by chiral HPLC

To further optimize the reaction, we next looked at palladium sources. The use of palladium(II) halides afforded no reaction (Table 2.3, entry 1–2). The reactivity could be rescued by treatment with AgOTf, presumably abstracting the halides and leading to a dicationic palladium(II) catalyst (entry 3). However, this reaction produced ketone **35** in low enantioselectivity. In the presence of ligand **82**, palladium(II) carboxylate sources were capable of catalyzing the desired reaction (entries 4–5). The acetate counterion (entry 4) led to modest chemical yields of the desired conjugate addition adduct in 93% ee. A catalyst derived from palladium(II) trifluoroacetate and pyridinooxazoline **82** produced the desired ketone product **35**[17] in 87% yield and 91% ee (entry 5).[18] By using 1,2-dichloroethane in place of dichloromethane as solvent, and increasing the reaction temperature from 40 to 60 °C, ketone **35** was isolated in 99% yield and 93% ee (entry 6).[19] The high yield and enantioselectivity were maintained even upon addition of 10 equiv of water (entry 7). Furthermore, the amount of phenylboronic acid was reduced to 1.1 equiv with no detrimental effects (entry 8).

Table 2.3 Optimization of palladium source [a]

entry	Pd source	solvent	temp (°C)	yield (%)[b]	ee (%)[c]
1	PdCl$_2$	CH$_2$Cl$_2$	40	–	–
2	Pd(MeCN)$_2$Cl$_2$	CH$_2$Cl$_2$	40	–	–
3[d]	Pd(MeCN)$_2$Cl$_2$, AgOTf	CH$_2$Cl$_2$	40	69	17
4	Pd(OAc)$_2$	CH$_2$Cl$_2$	40	65	92
5	Pd(OCOCF$_3$)$_2$	CH$_2$Cl$_2$	40	87	91
6	Pd(OCOCF$_3$)$_2$	ClCH$_2$CH$_2$Cl	60	99	93
7[e]	Pd(OCOCF$_3$)$_2$	ClCH$_2$CH$_2$Cl	60	99	91
8[f]	Pd(OCOCF$_3$)$_2$	ClCH$_2$CH$_2$Cl	60	99	93

[a] Conditions: Reactions were performed with phenylboronic acid (0.50 mmol), 3-methylcyclohexen-2-one (0.25 mmol), Pd(OCOCF$_3$)$_2$ (5 mol%), and ligand **4** (6 mol%) in solvent (1 mL) for 12 h, unless otherwise noted. [b] Isolated yield. [c] ee was determined by chiral HPLC. [d] 12 mol% AgOTf. [e] Reaction performed in the presence of added H$_2$O (2.5 mmol, 10 equiv). [f] Phenylboronic acid loading reduced to 1.1 equiv.

A final examination of solvent and palladium sources was undertaken to finalize the reaction conditions before examining a wider range of pyridinooxazoline ligands. Highly polar solvents (Table 2.4, entries 2–3) failed to produce product. Switching to dicationic palladium by employing tetrakis acetonitrile palladium(II) tetrafluoroborate facilitate no conversion in methanol at a variety of temperatures, or as a mixture with dichloroethane as cosolvent (entries 4–6). Finally, we failed to generate a catalyst *in situ* from isolated (PyOx)PdCl$_2$ by treatment with sodium hexafluorophosphate (entry 7).

Table 2.4 Screen of related conjugate addition conditions [a]

entry	solvent	metal source	temp (°C)	yield	ee
1	DCE	Pd(OAc)$_2$	60	Low	--
2	Acetone	Pd(TFA)$_2$	60	---	--
3	DMF	Pd(TFA)$_2$	60	---	--
4	MeOH	Pd(CH$_3$CN)$_4$(BF$_4$)$_2$	60	Trace	--
5	MeOH	Pd(CH$_3$CN)$_4$(BF$_4$)$_2$	25	---	--
6	DCE-MeOH	Pd(CH$_3$CN)$_4$(BF$_4$)$_2$	25	---	--
7	Acetone	tBuPyOXPdCl2 - NaPF6	25	---	--

[a] Conditions: Reactions were performed with phenylboronic acid (0.50 mmol), 3-methylcyclohexen-2-one (0.25 mmol), Pd(OCOCF$_3$)$_2$ (5 mol%), and ligand **4** (6 mol%) in solvent (1 mL) for 12 h, unless otherwise noted. [b] Isolated yield. [c] ee was determined by chiral HPLC.

2.2.2 Investigation of Other Ligands

Having successfully optimized the reaction conditions, we next examined the reaction with other members of the PyOx or related quinolinooxazoline (QuinOx) and isoquinolinooxazoline (IQuinOx) ligand series (Table 2.5, entries 9–16). PyOx ligands bearing isopropyl (**106**) or phenyl (**107**) substitution instead of *tert*-butyl at the 4-position of the oxazoline resulted in low enantioselectivity, although the desired product was obtained in nearly quantitative yield. Similarly, it was found that the PyOx ligands with a 4,5-diphenyl oxazoline (**108**) or simply 5-phenyl substitution (**109**) resulted in poor enantioselectivity. Next, employing QuinOx ligands **110** or **111** resulted in a dramatic decrease in both the reactivity and enantioselectivity, whereas IQuinOx ligands **112**and **113** provided little difference in yield and enantioselectivity to *t*-BuPyOx **82**.

Table 2.5 PyOx, QuinOx, IQuinOx Ligand Screen [a]
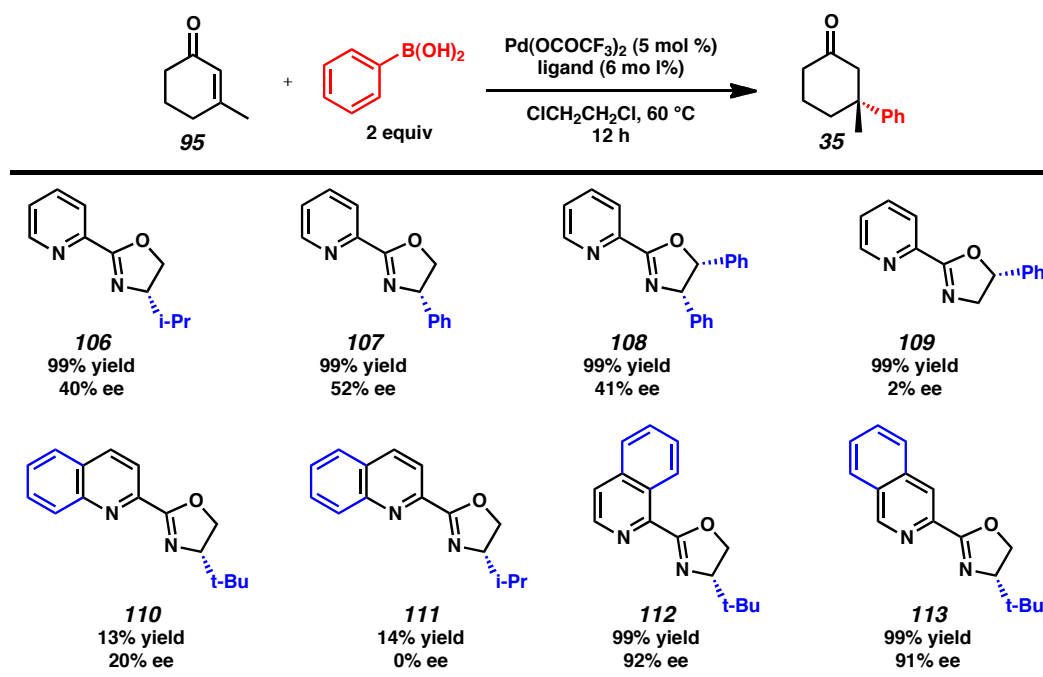
106 99% yield 40% ee	**107** 99% yield 52% ee	**108** 99% yield 41% ee	**109** 99% yield 2% ee
110 13% yield 20% ee	**111** 14% yield 0% ee	**112** 99% yield 92% ee	**113** 99% yield 91% ee

[a] Conditions: Reactions were performed with phenylboronic acid (0.50 mmol), 3-methylcyclohexen-2-one (0.25 mmol), Pd(OCOCF₃)₂ (5 mol%), and ligand (6 mol%) in ClCH₂CH₂Cl (1 mL) for 12 h, unless otherwise noted. Isolated yield. ee was determined by chiral HPLC.

However, later developments of improved reaction conditions encouraged us to reconsider our initial ligand screen. The use of ammonium hexafluorophosphate and water as additives greatly improved reaction rates. We re-screened a large number of chiral and achiral ligands to determine if the new conditions facilitated an expanded class of ligands to successfully catalyze the reaction. Unfortunately, all phosphine ligands we tried failed to product appreciable conversion (Table 2.6, **114, 115** and **116**). The drop in conversion from dppe (**115**) to dppbz (**114**) led us to question whether ligand rigidity was detrimental to conversion. However, the nearly identical results observed with bpy (**96**), phenanthroline (**117**) and bathophenanthroline (**118**) suggest that rigidity of the ligand scaffold has no effect on conversion.

We screened a number of chiral diamine ligands under the optimized conditions as well. The best conversion was observed with a bisoxazoline with a similar bite-angle to bpy (Table 2.6, **125**), followed by proline-derived **123**, which also features a 5-membered metallocycle chelate. Ligands forming 6-membered metallocycles (**119** and **120**) performed poorly, however those containin *gem*-dimethyl (**122**) or cyclopropyl (**126**) substituted bridging methylene groups showed improved conversion. We believe this to be the result of the fully substititued carbon on the ligand backbone enforcing a smaller bite angle. Additionally, sparteine (**98**), PHOX (**124**) and PyBox (**121**) ligands delivered no conversion to the desired product.

Table 2.6 Expanded ligand screen [a]
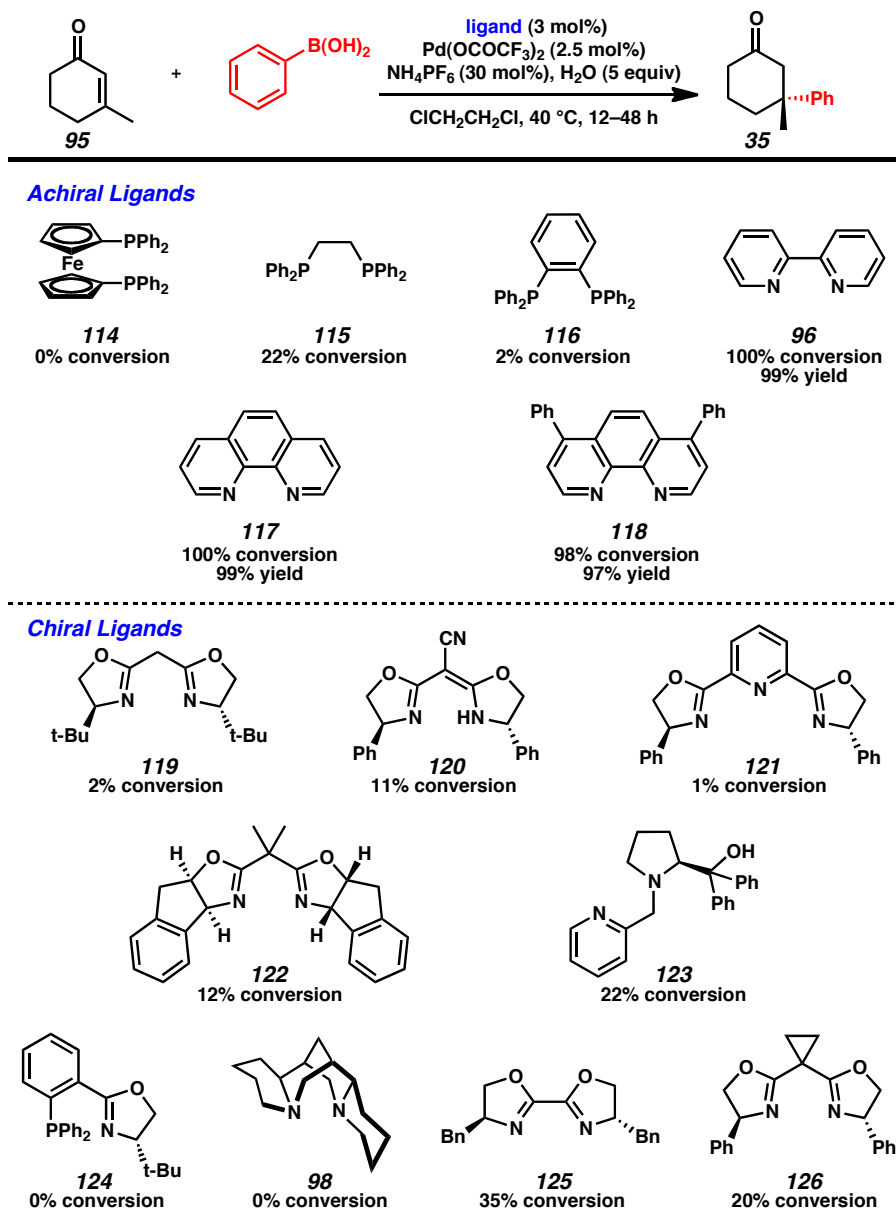
Achiral Ligands

114
0% conversion

115
22% conversion

116
2% conversion

96
100% conversion
99% yield

117
100% conversion
99% yield

118
98% conversion
97% yield

Chiral Ligands

119
2% conversion

120
11% conversion

121
1% conversion

122
12% conversion

123
22% conversion

124
0% conversion

98
0% conversion

125
35% conversion

126
20% conversion

[a] Conditions: Reactions were performed with phenylboronic acid (0.50 mmol), 3-methylcyclohexen-2-one (0.25 mmol), Pd(OCOCF$_3$)$_2$ (2.5 mol%), and ligand (3 mol%) in ClCH$_2$CH$_2$Cl (1 mL) for 12 h, unless otherwise noted. Conversion was determined by ^{1}H NMR.

2.2.3 Investigation of Substrate Scope

To investigate the reaction scope, we explored various arylboronic acids as nucleophiles for this process (Table 2.7). Generally, *para*-substituted arylboronic acids are well tolerated (entries 1–9). Reactions with 4-methyl and 4-ethylboronic acid proceeded well to give high yields of the desired products with good asymmetric induction (entries 1 and 2). While electron-rich nucleophiles tend to be reliable reaction partners, they often furnish products in moderate enantioselectivity (entries 3–5). Electron-deficient nucleophiles fared particularly well, producing ketone products in excellent ee (entries 6–9). Specifically, these electron-poor nucleophiles can possess a wide range of functional groups, such as ketone (entry 6), halide (entries 7 and 8) and a trifluoromethyl group (entry 9). Reactions involving *meta*-substituted arylboronic acids were also broadly successful with alkyl (entry 10), halide (entries 11 and 12), ester (entry 13) and even nitro (entry 14) groups on the nucleophile.[20]

Table 2.7 Scope of Arylboronic Acids [a]

entry	R =	temp (°C)	time (h)	yield (%)[b]	ee (%)[c]
1	4-Me– (127)	60	12	99	87
2	4-Et– (128)	60	12	90	85
3	4-MeO– (129)	40	24	58	69
4	4-BnO– (130)	60	18	96	74
5	4-TBSO– (131)	40	24	52	82
6	4-Ac– (132)	60	18	99	96
7	4-Cl– (133)	60	12	94	95
8	4-F– (134)	80	12	84	92
9	4-F₃C– (89)	60	12	99	96
10	3-Me– (135)	60	24	99	91
11	3-Cl– (136)	60	18	55	96
12	3-Br– (90)	60	24	44	85
13	3-MeO₂C– (88)	60	24	91	95
14	3-O₂N– (137)	60	18	40	92

[a] Conditions: Reactions were performed with phenylboronic acid (0.50 mmol), 3-methylcyclohexen-2-one (0.25 mmol), Pd(OCOCF₃)₂ (5 mol%), and ligand **4** (6 mol%) in (ClCH₂)₂ (1 mL) at 40–80 °C for 12–24 h. [b] Isolated yield. [c] ee was determined by chiral HPLC,

We sought to further examine the scope of the reaction by exploring cyclic enones of different ring sizes and with a range of β-substitution (Table 2.8). Importantly, altering the ring size to the 5- or 7-membered ring series had no deleterious effect on the transformation and fashioned ketones **52** and **83** in high yield and ee. To the best of our knowledge this represents the first time that quaternary centers have been constructed by asymmetric conjugate addition of boronic acids to these differing ring sized enones using a single catalyst.[2] Cyclohexenones bearing other β-alkyl substituents, such as ethyl, *n*-butyl, and benzyl furnished ketone products (i.e., **138**–**140**) in good yield and excellent ee as well. In addition to linear alkyl substitution, ketones with branched β-alkyl substituents

such as *iso*-propyl (**141**) and cyclopropyl (**142**) and cyclohexyl (**86**) are produced in good

yield and enantioselectivity. Finally, products containing functionalized side-chains, such

as benzyl ether **88**, are readily obtained, providing a useful chemical handle for further

transformations.

Table 2.8 Asymmetric synthesis of β,β-disubstituted cyclic ketones [a]
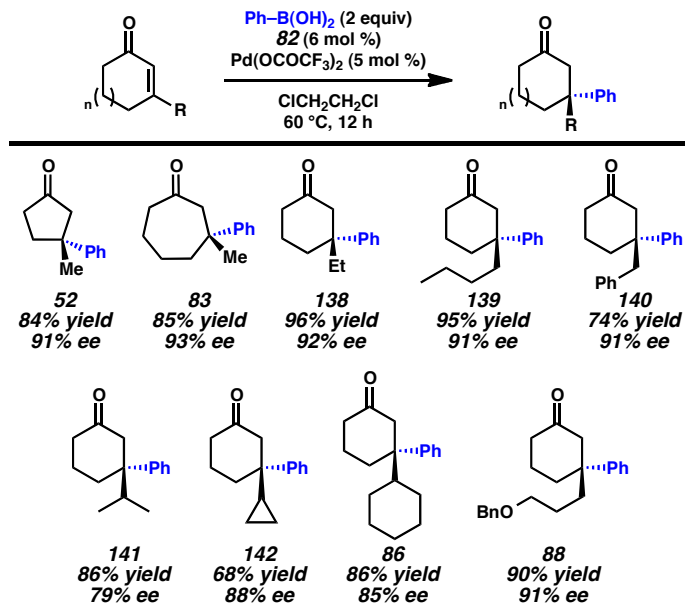
[a] Conditions: Reactions were performed with phenylboronic acid (0.50 mmol), cycloalkenone (0.25 mmol), Pd(OCOCF$_3$)$_2$ (5 mol%), and ligand **82** (6 mol%) in (ClCH$_2$)$_2$ (1 mL) at 60 °C for 12 h.

2.2.4 Substrate Limitations

Despite the many substrates that undergo facile conjugate addition, a number of

substrates proved incompatible with the newly developed methodology (Figure 2.2).

Pyridine **143** presumably coordinates Pd and inhibits the catalyst, yielding no conjugate

addition product. Allyl enone **144** also did not react, nor did enyneone **145**. β-aromoatic

enones also failed, such as thiopene **146** and chloroarene **147**. Each of these substrates

has functionality that can potentially interact with palladium; such interactions are likely

detrimental to the catalytic cycle. Curiously, β–aryl enones are problematic for many

conjugate addition systems, including other palladium-catalyzed systems.

Figure 2.2 Unsuccessful enone substrates

| 143 | 144 | 145 | 146 | 147 |
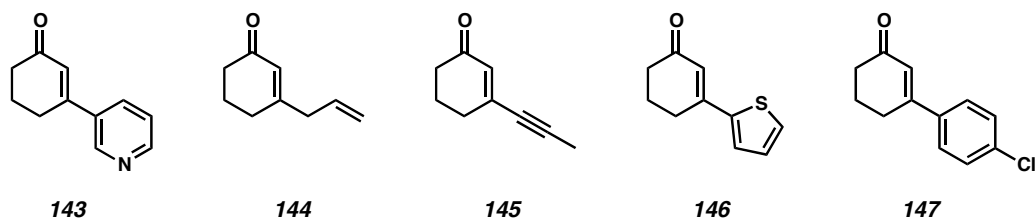
A broader representation of enone substrate scope leads to some observations

about the limitations of the catalyst (Figure 2.3). First, linear substrates are generally less

reactive, and lead to lower ee than their cyclic counterparts (row 1). Second, lactones of

varying ring sizes, and other electron donating substituents that mitigate the

electrophilicity of the carbonyl are less reactive and lead to low ee (row 2). Third, steric

modification of the substrate backbone generally leads to low conversion, if any (row

3–4). Finally, nitrogen-containing substrates are tolerated, though they require electron-

withdrawing carbamate protecting groups (row 4–5). Lactams and imides with less

electron-withdrawing groups are unreactive (row 4–5).

Figure 2.3 Steric considerations of enone substrates
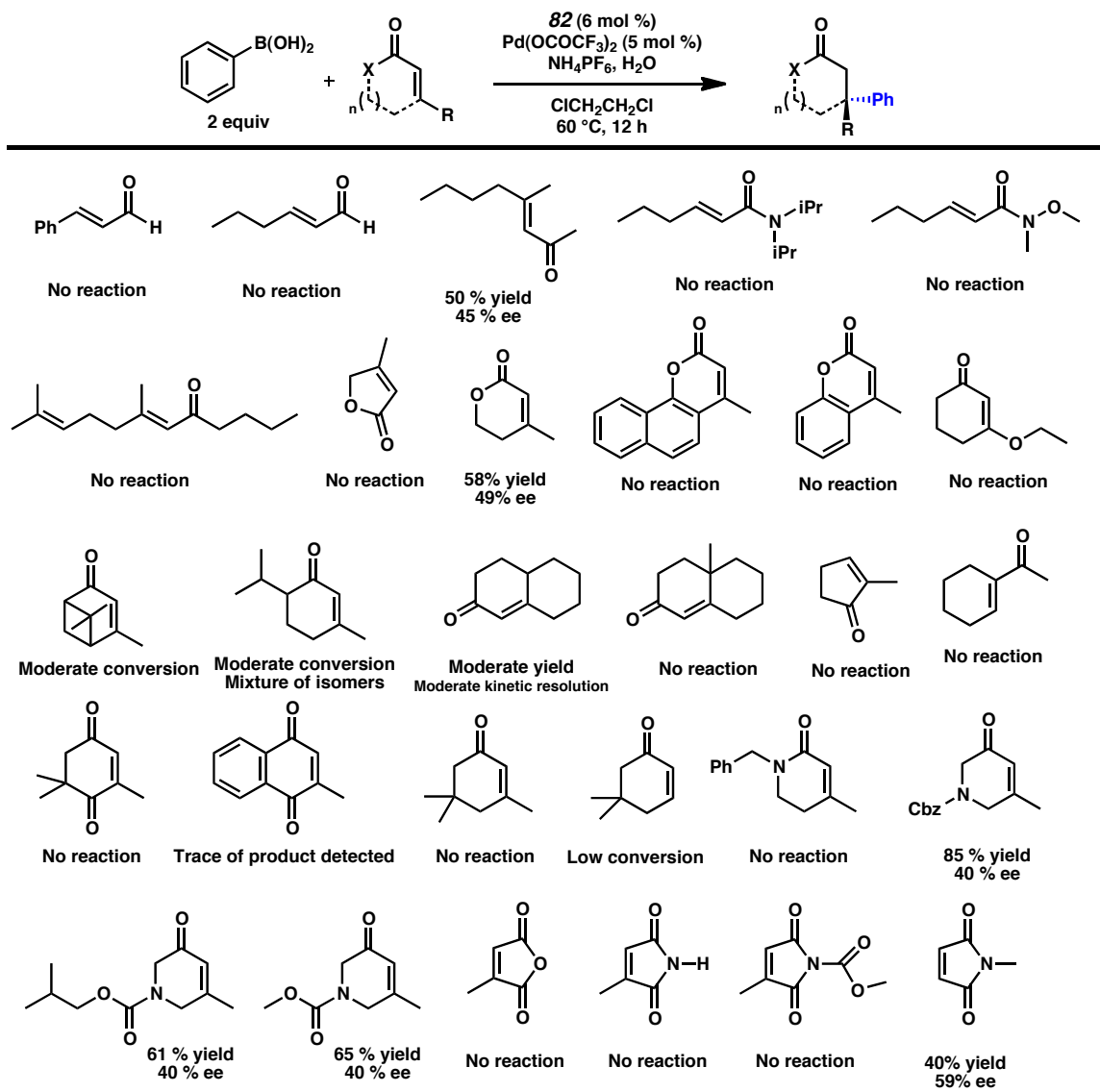
Some arylboronic acids also proved to be poor nucleophiles. *Ortho*-substituted arylboronic acids were generally poor substrates; 2-chlorophenylboronic acid (Figure 2.4, **148**) yielded only 2% of its corresponding product in 37% ee, while 2-methylphenylphenylboronic acid (**149**) yielded 13% product in 25% ee. Arylboronic

acids with reactive groups, such as iodide **151** and furan **152,** were all not reactive. Other

heterocycles such as indole **153** failed, as did the very electron poor fluoroarene **154**,

though steric congestion likely contributes to its poor performance. Interestingly, styrene

moieties **155** and **156** also did not undergo addition. Additionally, it should be noted that

electron-rich arylboronic acids (e.g., dimethoxyphenylboronic acid **150**) undergo rapid

homocoupling and proteodeborylation under the optimized reaction conditions. Thus, it is

difficult to achieve synthetically useful yields of these electron-rich adducts.

Additionally, the enantioselectivity seems to be lower these electron-rich arylboronic

acids. We hypothesize that this may be attributed to the lower energy barrier in

transmetallation for electron-rich arylboronic acids.

Figure 2.4 Unreactive arylboronic acid nucleophiles
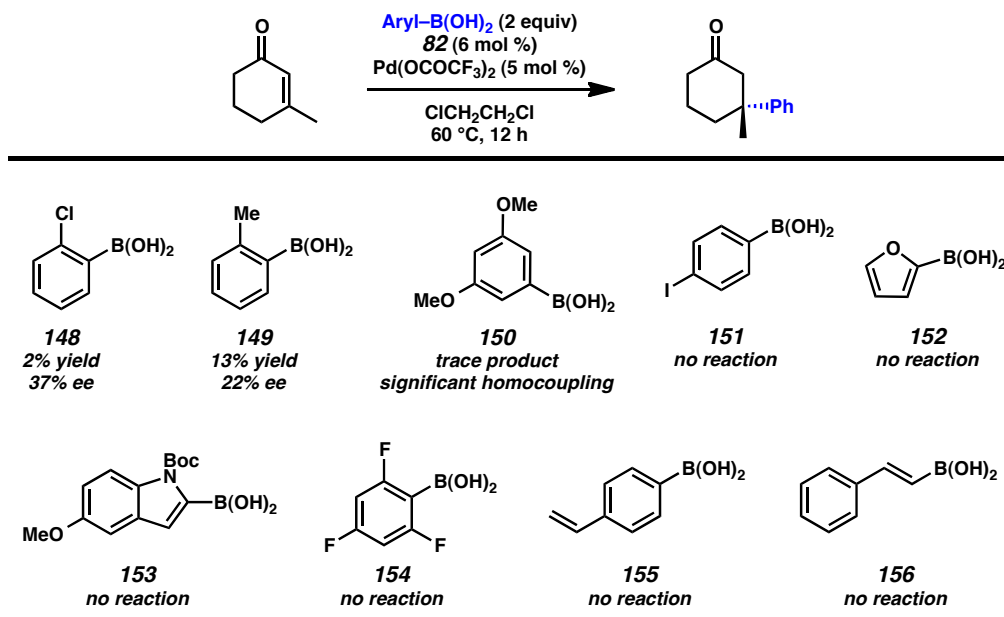
2.2.5 Identification of new substrates

The discovery that reaction rates were dramatically increased by the addition of hexafluorophosphate salts and additional water represented a major opportunity to expand the substrate scope.[21] The additives promoted successful reaction at 40 °C or lower, and thus substantially facilitated the reaction of substrates with temperature-sensitive functionalities (such as silyl ethers), or groups that may react with trace palladium(0) that is formed by off-cycle pathways (such as arylbromides). We next turned our attention to two other broad substrate classes: 1) enones bearing β-substituents that are not merely alkyl chains, and 2) arylboronic acids containing nitrogen and other heteroatoms.

The synthesis of 1,4-dicarbonyl compounds is a nontrivial transformation. This motif is significantly less common that 1,3-dicarbonyl (made from aldol reactions) or 1,5-dicarbonyl (often made through Michael additions) stereochemical relationships. Furthermore, asymmetric synthesis of 1,4-dicarbonyl compounds is exceedingly rare. We considered that our β-arylation reaction constituted a synthetically useful means of synthesizing asymmetric 1,4-dicarbonyl compounds. Beginning with β-acyl cyclic enones (**157**), we were able to react a variety of arylboronic acids to synthesize asymmetric 1,4-dicarbonyl compounds (Table 2. 9, **158a–g**).

Table 2.9 β-arylation of cyclic β-acyl enones
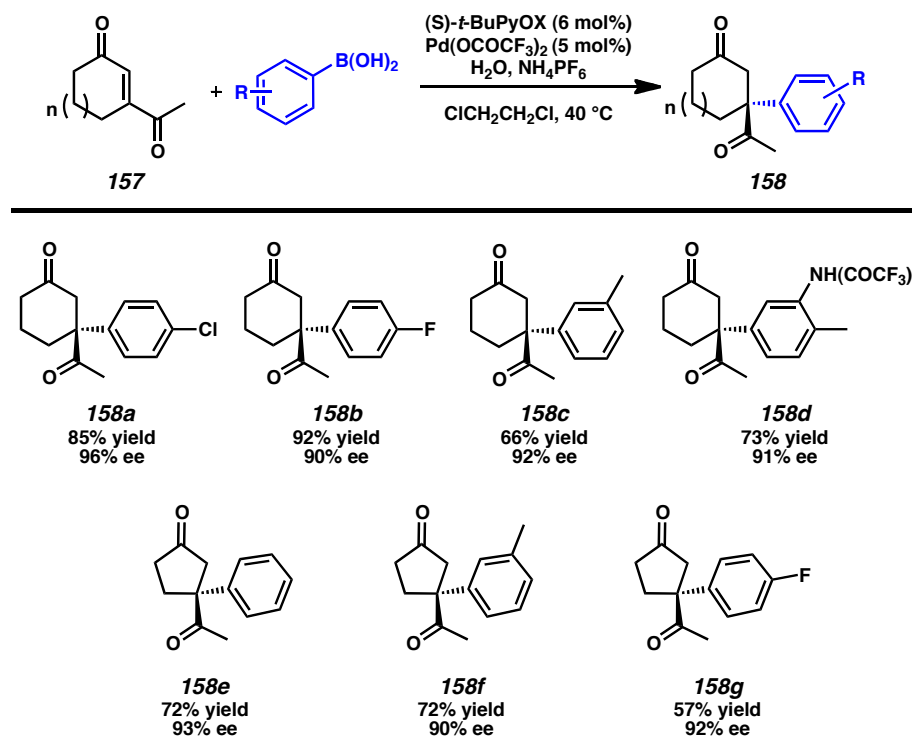
a Conditions: Reactions were performed with phenylboronic acid (0.50 mmol), cycloalkenone (0.25 mmol), Pd(OCOCF₃)₂ (5 mol%), and ligand **4** (6 mol%) in (ClCH₂)₂ (1 mL) at 60 °C for 12 h.

Next, we strived to demonstrate that the reaction was tolerant of heteroatom substitution on the arylboronic acid. Having demonstrated that nitrogen atoms bearing electron-withdrawing groups were competent enone substrates (Figure 2.3, rows 4–5), we proposed that aniline-derived boronic acids could be reacted when protected with electron-withdrawing functional groups. Cbz-protected aniline boronic acid **160** reacted with modest yield (Table 2.10), but a promising 76% ee. Modification to the pivalyl protected boronic acid **161**, facilitated higher yields, but minimal effect on enantioselectivity. Finally, trifluoroacetyl-protected **162** afforded clean conversion to afford 98% of the conjugate addition adduct in 89% ee. The trifluroacetyl group facilitated the reaction on a number of aniline-derived arylboronic acids, including methoxyphenyl aniline **163**, trisubstituted aniline **164**, and *m*-anilines **165** and **166**. Their successful reactions demonstrate the broad utility of these substrates.

Table 2.10 Trifluoroacetamide boronic acid nucleophiles

35 → **159**

(S)-t-BuPyOX (6 mol%)
Pd(OCOCF₃)₂ (5 mol%)
arylboronic acid (1.5 equiv)
H₂O, NH₄PF₆
ClCH₂CH₂Cl 60 °C

160
45% yield
76% ee

161
72% yield
78% ee

162
98% yield
89% ee

163
75% yield
88% ee

164
93% yield
90% ee

165
60% yield
92% ee

166
77% yield
88% ee
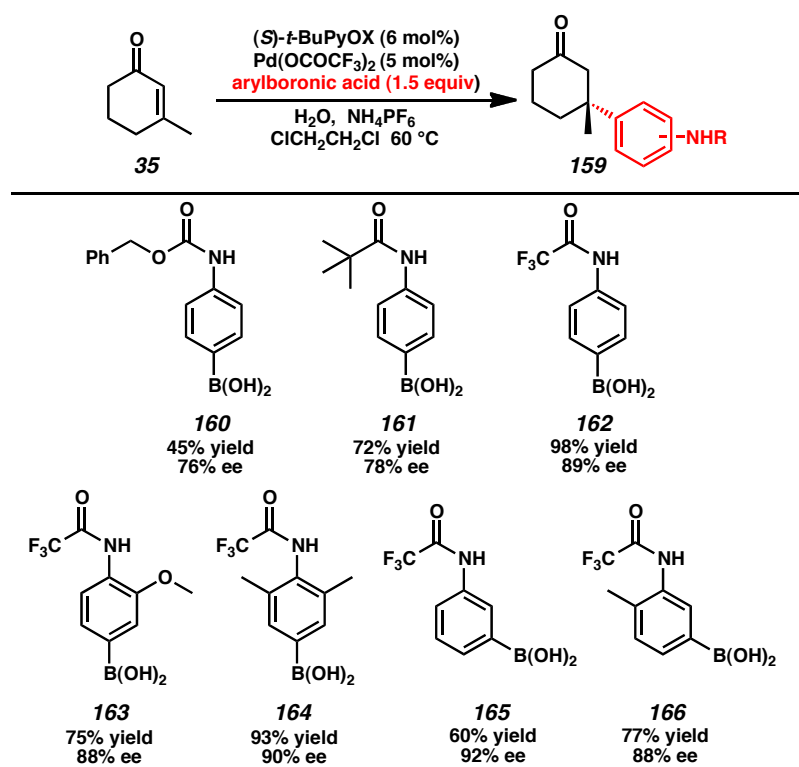
2.2.6 Catalytic Cycle

Computational and experimental work by Stoltz and Houk suggests that the reaction is catalyzed by a palladium(II) cationic species (Figure 2.5, **167**).[22] We propose that the active catalyst is likely a palladium(II) hydroxide cation, which is known to undergo rapid transmetallation with arylboronic acids to afford cationic arylpalladium(II) **168**. Ligand substitution and substrate coordination, likely through the oxygen of the enone to make complex **170**, leads to insertion of the aryl-palladium bond when coordination via the enone olefin occurs (**169**). Insertion affords palladium enolate **171**, formed from its tautomer, carbon–bound palladium enolate **172**. Hydrolysis of this latent

cationic palladium enolate affords the product ketone (**35**) and regenerates the catalyst (**167**).

Figure 2.5 Plausible catalytic cycle
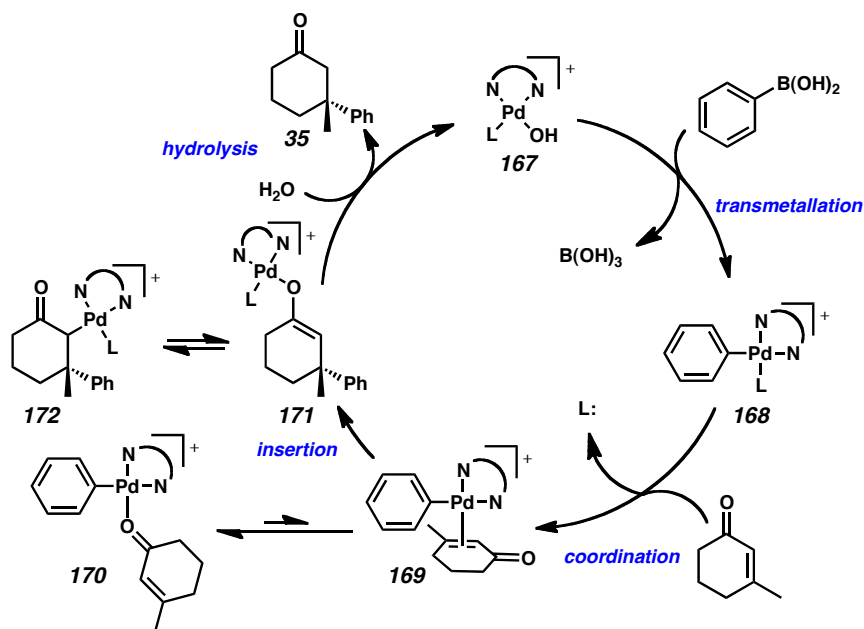
2.3 Conclusion

In summary, we report the first palladium-catalyzed enantioselective conjugate addition of arylboronic acids to β-substituted cyclic enones to deliver products containing an all-carbon quaternary stereocenter. Critically, 5-, 6-, and 7-membered ring enones function well in the process, delivering products of uniformly high ee using a single catalyst. A wide variety of commercially available arylboronic acids and substituted enones can be employed in the asymmetric transformation, while exhibiting broad functional group tolerance. Furthermore, the reaction displays a remarkable tolerance to

water and oxygen, and reactions are typically performed open to air in screw-top vials and without the need for purification or distillation of any commercially obtained materials. Finally, the optimal chiral ligand, (*S*)-*t*-BuPyOx (**82**), is expediently prepared, rendering this process an experimentally simple, practical method for enantioselective construction of all-carbon quaternary stereocenters. Continuing investigations of this method and application of this chemistry in the context of natural product synthesis are currently underway and will be reported in due course.

2.4 Experimental Procedures

2.4.1 Materials and Methods

Unless otherwise stated, reactions were performed with no extra precautions taken to exclude air or moisture. Commercially available reagents were used as received from Sigma Aldrich unless otherwise stated. Enone substrates (Table 3) were prepared according to literature procedure.[23] Reaction temperatures were controlled by an IKAmag temperature modulator. Thin-layer chromatography (TLC) was performed using E. Merck silica gel 60 F254 precoated plates (250 nm) and visualized by UV fluorescence quenching, potassium permanganate, or *p*-anisaldehyde staining. Silicycle Silia*Flash* P60 Academic Silica gel (particle size 40-63 nm) was used for flash chromatography. Analytical chiral HPLC was performed with an Agilent 1100 Series HPLC utilizing a Chiralcel OJ column (4.6 mm x 25 cm) obtained from Daicel Chemical Industries, Ltd with visualization at 254 nm and flow rate of 1 mL/min, unless otherwise stated. ^{1}H and ^{13}C NMR spectra were recorded on a Varian Inova 500 (500 MHz and 125 MHz, respectively) and a Varian Mercury 300 spectrometer (300 MHz and 75 MHz, respectively). Data for ^{1}H NMR spectra are reported as follows: chemical shift (δ ppm)

(multiplicity, coupling constant (Hz), integration). Data for ^{1}H NMR spectra are referenced to the centerline of CDCl$_3$ (δ 7.26) as the internal standard and are reported in terms of chemical shift relative to Me$_4$Si (δ 0.00). Data for ^{13}C NMR spectra are referenced to the centerline of CDCl$_3$ (δ 77.0) and are reported in terms of chemical shift relative to Me$_4$Si (δ 0.00). Infrared spectra were recorded on a Perkin Elmer Paragon 1000 Spectrometer and are reported in frequency of absorption (cm^{-1}). High resolution mass spectra (HRMS) were obtained on an Agilent 6200 Series TOF with an Agilent G1978A Multimode source in electrospray ionization (ESI), atmospheric pressure chemical ionization (APCI) or mixed (MultiMode ESI/APCI) ionization mode. Optical rotations were measured on a Jasco P-2000 polarimeter using a 100 mm path-length cell at 589 nm.

2.4.2 Synthesis of Compounds
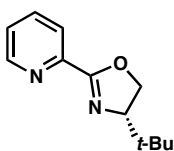
(*S*)-4-(*tert*-butyl)-2-(pyridin-2-yl)-4,5-dihydrooxazole (82).

The ligand was prepared according to literature procedures.[24] All characterization data matches previously reported data. We have recently reported alternative conditions, see Chapter 5 for modified synthetic procedures and references.

Representative General Procedure for the Enantioselective 1,4-Addition of Arylboronic Acids to β-Substituted Cyclic Enones

A screw-top 1 dram vial was charged with a stir bar, Pd(OCOCF$_3$)$_2$ (4.2 mg, 0.0125 mmol, 5 mol%), (*S*)-*t*-BuPyOx (3.1 mg, 0.015 mmol, 6 mol%), and PhB(OH)$_2$ (61 mg, 0.50 mmol, 2.0 equiv). The solids were dissolved in dichloroethane (0.5 mL) and 3-

methyl-2-cyclohexenone (29 μL, 0.25 mmol) was added. The walls of the vial were rinsed with an additional portion of dichloroethane (0.5 mL). The vial was capped with a Teflon/silicone septum and stirred at 60 °C in an oil bath for 12 h. Upon complete consumption of the starting material (monitored by TLC, 4:1 hexanes/EtOAc, *p*-anisaldehyde stain) the reaction was purified directly by column chromatography (CH$_2$Cl$_2$) to afford a clear colorless oil (47 mg, 99% yield).

General Procedure for the Synthesis of Racemic Products

Racemic products were synthesized in a manner analogous to the general procedure using bipyridine (2.1 mg, 0.015 mmol, 6 mol%) as an achiral ligand.

Spectroscopic Data for Enantioenriched β,β-Disubstituted Cyclic Ketones
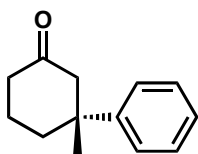
(*R*)-3-phenyl-3-methylcyclohexanone (35)

Synthesized according to the general procedure and purified by flash chromatography (CH$_2$Cl$_2$) to afford a colorless oil (93% yield). $[\alpha]^{25}_D$ –56.1° (*c* 1.36, CHCl$_3$, 92% ee). All characterization data matches previously reported data.[25, 26, 27, 28, 29, 30, 31]
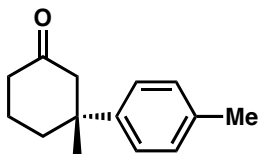
(*R*)-3-(4-methylphenyl)-3-methylcyclohexanone (127)

Synthesized according to the general procedure and purified by flash chromatography (CH$_2$Cl$_2$) to afford a colorless oil (99% yield). $[\alpha]^{25}_D$ –60.9° (*c* 1.11, CH$_2$Cl$_2$, 87% ee). All characterization data matches previously reported data.[25, 27, 29]

(*R*)-3-(4-ethylphenyl)-3-methylcyclohexanone (128)

Synthesized according to the general procedure and purified by flash chromatography (hexanes/EtOAc = 100:0 to 95:5) to afford a colorless oil (90% yield). ^{1}H NMR (500 MHz, CDCl$_3$) δ 7.23 (ddd, *J* = 2.0, 8.5 Hz, 2H), 7.16 (ddd, *J* = 2.0, 8.5 Hz, 2H), 2.87 (d, *J* = 14.0 Hz, 1H), 2.62 (q, *J* = 7.5, 2H), 2.42 (d, *J* = 14.0 Hz, 1H), 2.35–2.26 (m, 2H), 2.20–2.15 (m, 1H), 1.93–1.83 (m, 2H), 1.73–1.64 (m, 1H), 1.31 (s, 3H), 1.23 (t, *J* = 7.5 Hz, 3H); ^{13}C NMR (125 MHz, CDCl$_3$) δ 211.6, 144.7, 142.0, 127.9, 125.5, 53.2, 42.5, 40.8, 38.0, 29.8, 28.2, 22.0, 15.4; IR (Neat Film, NaCl): 2957, 2933, 2863, 1710, 1513, 1453, 1416, 1315, 1288, 1226, 1078 cm^{-1}; HRMS (MultiMode ESI/APCI) *m/z* calc'd for C$_{15}$H$_{21}$O [M+H]$^+$: 217.1587, found 217.1592; [α]$^{25}_D$ –56.8° (*c* 1.61, CHCl$_3$, 85% ee).

(*R*)-3-(4-methoxyphenyl)-3-methylcyclohexanone (129)

Synthesized according to the general procedure and purified by flash chromatography (hexanes/EtOAc = 100:0 to 90:10) as colorless oil (58% yield). [α]$^{25}_D$ –47.9° (*c* 1.05, CHCl$_3$, 69% ee). All characterization data matches previously reported data.[26, 27, 28, 29, 30]

(*R*)-3-(4-benzyloxylphenyl)-3-methylcyclohexanone (130)

Synthesized according to the general procedure and purified by flash chromatography (hexanes/EtOAc = 100:0 to 95:5) to afford a colorless oil (96% yield). ^{1}H NMR (500 MHz, CDCl$_3$) δ 7.43 (ddd, *J* = 1.5, 2.0, 7.5 Hz, 2H), 7.39 (ddd, *J* = 1.0, 7.0, 7.5 Hz, 2H), 7.33 (tt, *J* = 1.5, 7.0 Hz, 1H), 7.22 (ddd, *J* = 2.0, 3.5, 10.0 Hz, 2H), 6.93 (ddd, *J* = 2.0,

3.5, 10.0 Hz, 2H), 5.04 (s, 2H), 2.85 (d, $J = 14.0$ Hz, 1H), 2.42 (d, $J = 14.0$ Hz, 1H), 2.30 (t, $J = 7.0$ Hz, 2H), 2.18–2.13 (m, 1H), 1.92–1.83 (m, 2H), 1.71–1.62 (m, 1H), 1.30 (s, 3H), 0.97 (s, 9H), 0.19 (s, 6H); ^{13}C NMR (125 MHz, CDCl$_3$) δ 211.6, 157.0, 139.7, 137.0, 128.6, 127.9, 127.5, 126.7, 114.7, 70.0, 53.3, 42.3, 40.8, 38.0, 30.0, 22.0; IR (Neat Film, NaCl) 3066, 3027, 2947, 2873, 1710, 1609, 1579, 1510, 1453, 1426, 1379, 1312, 1290, 1246, 1181, 1021 cm^{-1}; HRMS (MultiMode ESI/APCI) *m/z* calc'd for C$_{20}$H$_{23}$O$_2$ [M+H]$^+$: 295.1693, found 295.1673; [α]$^{25}_D$ −26.8° (*c* 4.90, CHCl$_3$, 74% ee).

(*R*)-3-(4-*tert*-butyldimethylsiloxylphenyl)-3-methylcyclohexanone (131)

Synthesized according to the general procedure and purified by flash chromatography (hexanes/EtOAc = 100:0 to 95:5) to afford a colorless oil (52% yield). ^{1}H NMR (500 MHz, CDCl$_3$) δ 7.15 (ddd, $J = 2.0, 3.0, 9.0$ Hz, 2H), 6.71 (ddd, $J = 2.0, 3.0, 9.0$ Hz, 2H), 2.83 (d, $J = 14.0$ Hz, 1H), 2.40 (d, $J = 14.0$ Hz, 1H), 2.30 (t, $J = 7.0$ Hz, 2H), 2.16–2.10 (m, 1H), 1.90–1.81 (m, 2H), 1.70–1.61 (m, 1H), 1.29 (s, 3H), 0.97 (s, 9H), 0.19 (s, 6H); ^{13}C NMR (125 MHz, CDCl$_3$) δ 211.7, 153.8, 140.1, 126.5, 119.8, 53.3, 42.3, 40.8, 38.1, 29.9, 25.6, 22.0, 18.1, −4.4; IR (Neat Film, NaCl) 2952, 2933, 2858, 1713, 1607, 1510, 1473, 1458, 1263, 1181 cm^{-1}; HRMS (MultiMode ESI/APCI) *m/z* calc'd for C$_{19}$H$_{31}$O$_2$Si [M+H]$^+$: 319.2088, found 319.2090; [α]$^{25}_D$ −36.4° (*c* 1.11, CHCl$_3$, 82% ee).

(*R*)-3-(4-acetylphenyl)-3-methylcyclohexanone (132)

Synthesized according to the general procedure and purified by flash chromatography (CH$_2$Cl$_2$/EtOAc = 100:0 to 98:2) to afford colorless oil (99% yield). ^{1}H NMR (500 MHz, CDCl$_3$) δ 7.92 (ddd, $J = 2.0, 9.0$ Hz, 2H), 7.42 (ddd, $J = 2.0, 9.0$ Hz, 2H), 2.90 (d, $J = 14.0$ Hz, 1H), 2.58 (s, 1H), 2.47 (d, $J = 14.0$ Hz, 1H), 2.38–2.26 (m, 2H), 2.25–2.20 (m,

1H), 1.98–1.88 (m, 2H), 1.68–1.59 (m, 1H), 1.34 (s, 3H); ^{13}C NMR (125 MHz, CDCl$_3$) δ 210.8, 197.6, 152.9, 135.2, 128.6, 125.9, 52.8, 43.2, 40.7, 37.8, 29.7, 26.5, 22.0; IR (Neat Film, NaCl) 2957, 2868, 1708, 1683, 1607, 1569, 1456, 1421, 1404, 1359, 1312, 1268, 1228, 1194 cm^{-1}; HRMS (MultiMode ESI/APCI) *m/z* calc'd for C$_{15}$H$_{19}$O [M+H]$^+$: 231.1379, found 231.1380; [α]$^{25}_D$ –58.9° (*c* 1.39, CHCl$_3$, 96% ee).

(*R*)-3-(4-chlorophenyl)-3-methylcyclohexanone (133)

Synthesized according to the general procedure and purified by flash chromatography (hexanes/EtOAc = 100:0 to 95:5) to afford a white solid (94% yield). [α]$^{25}_D$ –69.4° (*c* 0.56, CHCl$_3$, 95% ee). All characterization data matches previously reported data.[26]

(*R*)-3-(4-fluorophenyl)-3-methylcyclohexanone (134)

Synthesized according to the general procedure and purified by flash chromatography (hexanes/EtOAc = 100:0 to 95:5) to afford a colorless oil (84% yield). [α]$^{25}_D$ –59.5° (*c* 1.00, CHCl$_3$, 92% ee). All characterization data matches previously reported data.[25, 26]
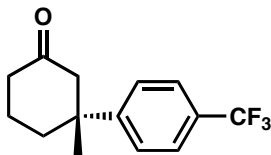
(*R*)-3-(4-trifluoromethylphenyl)-3-methylcyclohexanone (89) Synthesized according to the general procedure and purified by flash chromatography (hexanes/EtOAc = 100:0 to 95:5) to afford a colorless oil (99% yield). [α]$^{25}_D$ –58.5° (*c* 0.92, CHCl$_3$, 96% ee). All characterization data matches previously reported data.[27, 28, 29]
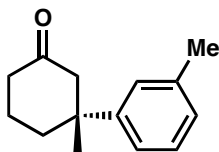
(*R*)-3-methyl-3-(*m*-tolyl)cyclohexanone (135)

Synthesized according to the general procedure and purified by flash chromatography (CH$_2$Cl$_2$) to afford a colorless oil (99% yield). [α]$^{25}_D$ –59.8° (*c* 2.95, CH$_2$Cl$_2$, 91% ee). All characterization data matches previously reported data.[25, 27, 29]
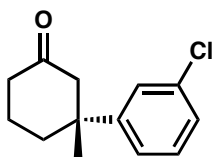
(*R*)-3-(3-chlorophenyl)-3-methylcyclohexanone (136)

Synthesized according to the general procedure and purified by flash chromatography (hexanes/EtOAc = 100:0 to 95:5) to afford a colorless oil (55% yield). [α]$^{25}_D$ –56.7° (*c* 1.48, CHCl$_3$, 96% ee). All characterization data matches previously reported data.[25, 26]
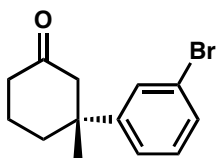
(*R*)-3-(3-bromophenyl)-3-methylcyclohexanone (90)

Synthesized according to the general procedure and purified by flash chromatography (CH$_2$Cl$_2$) to afford a colorless oil (44% yield). [α]$^{25}_D$ –56.7° (*c* 0.68, CHCl$_3$, 85% ee). All characterization data matches previously reported data.[29]
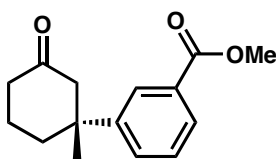
(*R*)-3-(3-methoxycarbonylphenyl)-3-methylcyclohexanone (88)

Synthesized according to the general procedure and purified by flash chromatography (CH$_2$Cl$_2$/EtOAc 100:0 to 98:2) to afford a white solid (91% yield). ^{1}H NMR (500 MHz,

CDCl$_3$) δ 8.03 (dd, *J* = 1.5, 2.0 Hz, 1H), 7.88 (dd, *J* = 1.5, 9.0 Hz, 1H), 7.51 (dd, *J* = 2.0, 9.0 Hz, 1H), 7.39 (dd, *J* = 9.0 Hz, 1H), 3.91 (s, 3H), 2.88 (d, *J* = 14.0 Hz, 1H), 2.47 (d, *J* = 14.0 Hz, 1H), 2.37–2.28 (m, 2H), 2.24-2.19 (m, 1H), 1.98–1.86 (m, 2H), 1.73–1.65 (m, 1H), 1.33 (s, 3H); ^{13}C NMR (125 MHz, CDCl$_3$) δ 210.9, 167.1, 147.9, 130.4, 130.2, 128.6, 127.5, 126.7, 53.0, 52.1, 42.8, 40.7, 37.7, 29.3, 22.0; IR (Neat Film, NaCl) 2952, 2878, 1720, 1604, 1582, 1438, 1350, 1310, 1273, 1243, 1209, 1194, 1120, 1085 cm^{-1}; HRMS (MultiMode ESI/APCI) *m/z* calc'd for C$_{15}$H$_{19}$O$_3$ [M+H]$^+$: 247.1329, found 247.1334; [α]$^{25}_D$ –58.9° (*c* 1.39, CHCl$_3$, 95% ee).
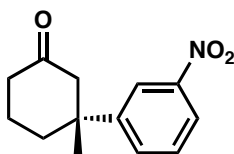
(*R*)-3-(3-nitrophenyl)-3-methylcyclohexanone (137)

Synthesized according to the general procedure and purified by flash chromatography (CH$_2$Cl$_2$) to afford a colorless oil (40% yield). ^{1}H NMR (500 MHz, CDCl$_3$) δ 8.22 (t, *J* = 2.0 Hz, 1H), 8.08 (ddd, *J* = 1.0, 2.0, 8.0 Hz, 1H), 7.66 (ddd, *J* = 1.0, 2.0, 8.0 Hz, 1H), 7.50 (t, *J* = 8.0 Hz, 1H), 2.88 (d, *J* = 14.0 Hz, 1H), 2.53 (ddd, *J* = 1.0, 1.5, 14.0 Hz, 1H), 2.41–2.31 (m, 2H), 2.26–2.20 (m, 1H), 2.03–1.90 (m, 2H), 1.74–1.66 (m, 1H), 1.37 (s, 3H); ^{13}C NMR (125 MHz, CDCl$_3$) δ 210.1, 149.7, 148.6, 131.9, 129.5, 121.4, 120.7, 52.8, 43.1, 40.6, 37.6, 29.4, 22.0; IR (Neat Film, NaCl) 2957, 2873, 1713, 1525, 1480, 1453, 1426, 1347, 1298, 1226, 1107, 1075 cm^{-1}; HRMS (MultiMode ESI/APCI) *m/z* calc'd for C$_{13}$H$_{15}$O$_3$N [M]: 233.1052, found 233.1055; [α]$^{25}_D$ –61.5° (*c* 0.96, CHCl$_3$, 92% ee)
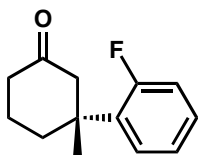
(*R*)-3-(2-fluorophenyl)-3-methylcyclohexanone (134a)

Synthesized according to the general procedure and purified by flash chromatography (hexanes/EtOAc = 100:0 to 95:5) to afford a colorless oil (32% yield). ^{1}H NMR (500 MHz, CDCl$_3$) d 7.25–7.19 (m, 2H), 7.07 (ddd, *J* = 1.5, 2.0, 7.5 Hz, 2H), 7.39 (ddd, *J* =

1.0, 7.0, 7.5, 2H), 7.33 (tt, *J* = 1.5, 7.0 Hz, 1H), 7.22 (ddd, *J* = 1.5, 7.5 Hz, 1H), 7.02 (ddd, *J* = 1.5, 8.0, 13.0 Hz, 1H), 2.94 (d, *J* = 14.5 Hz, 1H), 2.44 (d, *J* = 14.5 Hz, 1H), 2.48–2.44 (m, 1H), 2.37–2.28 (m, 2H), 1.96–1.87 (m, 2H), 1.67-1.60 (m, 1H), 1.41 (s, 3H), ^{13}C NMR (125 MHz, CDCl$_3$) d 211.3, 128.3, 128.0, 127.9, 124.1, 116.7, 53.2, 42.4, 40.9, 35.7, 27.1; IR (Neat Film, NaCl) 2957, 2933, 2873, 1710, 1611, 1577, 1488, 1443, 1315, 1290, 1214, 1117, 1083 cm^{-1}; HRMS (MultiMode ESI/APCI) *m/z* calc'd for C$_{13}$H$_{16}$OF [M+H]$^+$: 207.1180, found 207.1188; [a]$^{25}_D$ –41.0° (*c* 0.64, CHCl$_3$, 77% ee).
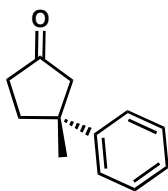
(*R*)-3-phenyl-3-methylcyclopentanone (52)

Synthesized according to the general procedure and purified by flash chromatography (hexanes/EtOAc = 100:0 to 95:5) to afford a colorless oil (84% yield). [α]$^{25}_D$ +21.3° (*c* 1.51, CHCl$_3$, 91% ee). All characterization data matches previously reported data.[27, 28, 29]
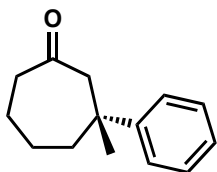
(*R*)-3-phenyl-3-methylcycloheptanone (83)

This product was synthesized according to the general procedure and purified by flash chromatography (hexanes/EtOAc = 100:0 to 95:5) to afford a colorless oil (85% yield). [α]$^{25}_D$ –75.1° (*c* 1.34, CHCl$_3$, 93% ee). All characterization data matches previously reported data.[25, 27, 29]
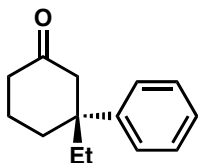
(*R*)-3-phenyl-3-ethylcyclohexanone (138)

Synthesized according to the general procedure and purified by flash chromatography (hexanes/EtOAc = 100:0 to 95:5) to afford a colorless oil (96% yield). $[\alpha]^{25}_D$ –74.5° (*c* 3.39, CHCl$_3$, 92% ee). All characterization data matches previously reported data.[25, 27, 29, 30]
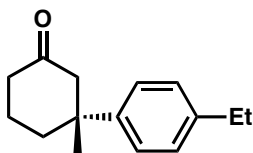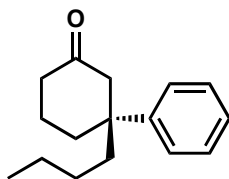

(*R*)-3-phenyl-3-*n*-butylcyclohexanone (139)

Synthesized according to the general procedure and purified by flash chromatography (hexanes/EtOAc = 100:0 to 95:5) to afford colorless oil (95% yield). $[\alpha]^{25}_D$ –56.7° (*c* 1.48, CHCl$_3$. 91% ee). All characterization data matches previously reported data.[30]
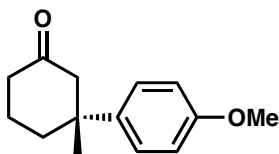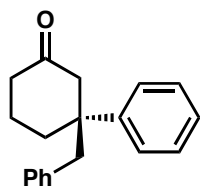

(*R*)-3-benzyl-3-phenylcyclohexanone (140)

Synthesized according to the general procedure and purified by flash chromatography (hexanes/EtOAc = 100:0 to 95:5) to afford a colorless oil (74% yield). $[\alpha]^{25}_D$ +01.0°(*c* 3.83, CHCl$_3$, 91% ee). All characterization data matches previously reported data.[31]
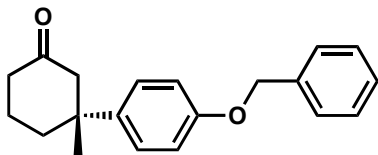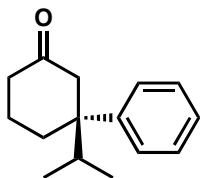
(*R*)-3-phenyl-3-*iso*-propylcyclohexanone (141)

Synthesized according to the general procedure and purified by flash chromatography (hexanes/EtOAc = 100:0 to 95:5) to afford a colorless oil (86% yield). $[\alpha]^{25}_{D}$ –79.4° (*c* 3.24, CHCl$_3$, 79% ee). All characterization data matches previously reported data.[31]
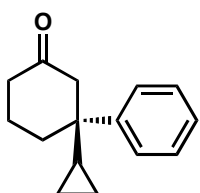
(*R*)-3-phenyl-3-methylcyclohexanone (142)

Synthesized according to the general procedure and purified by flash chromatography (CH$_2$Cl$_2$) to afford a colorless oil (68% yield). ^{1}H NMR (500 MHz, CDCl$_3$) δ 7.30–7.28 (m, 4H), 7.21–7.17 (m, 1H), 2.90 (dt, *J* = 2.0, 14.5 Hz, 1H), 2.48 (d, *J* = 14.5 Hz, 1H), 2.31–2.19 (m, 3H), 1.94–1.86 (m, 2H), 1.60–1.51 (m, 1H), 0.99 (tt, *J* = 5.5, 8.5, 1H), 0.45–0.39 (m, 1H), 0.35–0.29 (m, 1H), 0.24–0.19 (m, 1H), 0.17–0.12 (m, 1H); ^{13}C NMR (125 MHz, CDCl$_3$) δ 210.8, 143.2, 127.6, 126.5, 125.7, 50.0, 44.9, 40.3, 34.1, 23.1, 20.8, 1.1, 0.0; IR (Neat Film, NaCl) 3081, 3057, 3007, 2947, 2873, 1708, 1498, 1443, 1421, 1315, 1285, 1226, 1046, 1023 cm^{-1}; HRMS (MultiMode ESI/APCI) *m/z* calc'd for C$_{15}$H$_{19}$O [M+H]$^+$: 215.1430, found 215.1425; $[\alpha]^{25}_{D}$ –83.1° (*c* 1.39, CHCl$_3$, 88% ee).
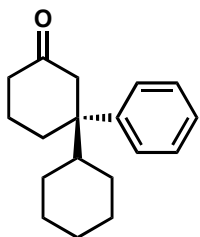
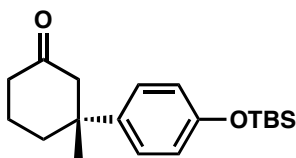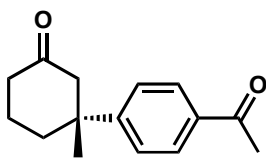**(*R*)-3-phenyl-3-cyclohexylcyclohexanone (86)**

Synthesized according to the general procedure and purified by flash chromatography (hexanes/EtOAc = 100:0 to 95:5) to afford a colorless oil (86% yield). ^{1}H NMR (500

MHz, CDCl$_3$) δ 7.29 (ddd, *J* = 2.0, 7.0, 8.0 Hz, 2H), 7.23 (ddd, *J* = 1.0, 2.0, 8.0 Hz, 2H),

7.18 (tt, *J* = 1.0, 7.0 Hz, 1H), 2.97 (dd, *J* = 2.0, 15.0 Hz, 1H), 2.46 (d, *J* = 15.0 Hz, 1H),

2.26–2.17 (m, 3H), 2.07 (ddd, *J* = 3.5, 12.5, 13.5 Hz, 1H), 1.94–1.88 (m, 1H), 1.84–1.75

(m, 2H), 1.68–1.56 (m, 2H), 1.52–1.45 (m, 1H), 1.44–1.38 (m, 1H), 1.37–1.31 (m, 1H),

1.26–1.17 (m, 1H), 1.11–0.95 (m, 2H), 0.88–0.75 (m, 2H); ^{13}C NMR (125 MHz, CDCl$_3$)

δ 212.0, 143.8, 128.1, 127.4, 125.9, 49.5, 49.0, 47.2, 41.0, 33.6, 27.5, 27.4, 26.9, 26.5,

21.4; IR (Neat Film, NaCl) 2928, 2853, 1713, 1495, 1443, 1315, 1285, 1228 cm^{-1}; HRMS

(MultiMode ESI/APCI) *m/z* calc'd for C$_{18}$H$_{24}$O [M+H]$^+$: 257.1900, found 257.1888;

[α]$^{25}_D$ −52.4° (*c* 3.87, CHCl$_3$, 85% ee).

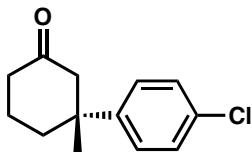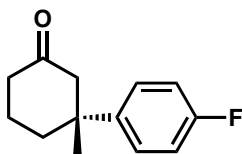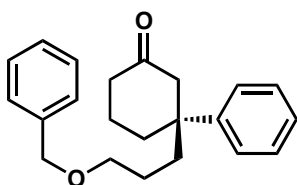**(*S*)-3-(3-(benzyloxy)propyl)-3-phenylcyclohexanone (88)**

Synthesized according to the general procedure and purified by flash chromatography
(hexanes/EtOAc = 100:0 to 95:5) to afford a colorless oil (65% yield). ^{1}H NMR (500

MHz, CDCl$_3$) δ 7.33–7.28 (m, 4H), 7.27–7.24 (m, 5H), 7.18 (tt, *J* = 1.5, 7.0 Hz, 1H), 4.37

(s, 2H), 3.30 (dt, *J* = 1.5, 6.5 Hz, 2H), 2.93 (d, *J* = 14.5 Hz, 1H), 2.43 (d, *J* = 14.5 Hz,

1H), 2.33–2.26 (m, 2H), 2.22–2.16 (m, 1H), 1.98 (ddd, *J* = 3.0, 10.0, 13.5 Hz, 1H),

1.86–1.77 (m, 2H), 1.68 (ddd, *J* = 4.5, 12.0 Hz, 1H), 1.61–1.53 (m, 1H), 1.43–1.32 (m,

1H), 1.23–1.14 (m, 1H); ^{13}C NMR (125 MHz, CDCl$_3$) δ 211.2, 144.8, 138.4, 128.5,

128.3, 127.6, 127.5, 126.4, 126.2, 72.7, 70.4, 51.0, 45.9, 41.0, 39.7, 36.6, 23.9, 21.4; IR

(Neat Film, NaCl) 3057, 3027, 2947, 2858, 1710, 1602, 1495, 1451, 1359, 1312, 1280,

1228, 1100, 1075, 1026 cm^{-1}; HRMS (MultiMode ESI/APCI) *m/z* calc'd for C$_{22}$H$_{26}$O$_2$

[M+H]$^+$: 323.2006, found 323.1993; [α]$^{25}_D$ −42.9° (*c* 4.25, CHCl$_3$, 91% ee).

Representative procedure for the synthesis of *N*-trifluoroacetamide boronic acids
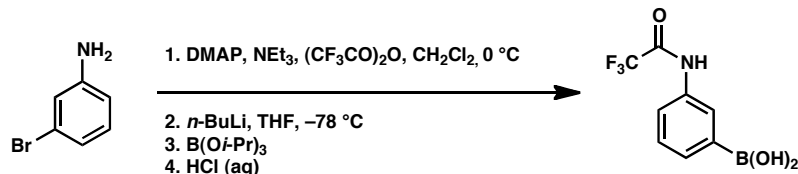
N-(3-bromophenyl)-2,2,2-trifluoroacetamide.

In a 100 ml round bottom flask were added consecutively 3-bromoaniline (1.7 g, 10.0 mmol, 1 eq), DMAP (0.12 g, 1.0 mmol, 0.1 eq), 20 mL of CH_2Cl_2 and Et_3N (1.7 ml, 12.0 mmol, 1.2 eq). The solution was cooled to 0 °C and trifluoroacetic anhydride (2.1 ml, 15.0 mmol, 1.5 eq) was added dropwise. The obtained mixture was stirred at room temperature until all the starting material was consumed (TLC Hexane-EtOAc 4:1) and then it was extracted with CH_2Cl_2 (3 x 20 mL) and washed with brine (2 x 20 mL). The combined organic phases were dried with $MgSO_4$ and the solvent was evaporated to give an off-white solid that was purified via silica gel column chromatography (2.35 g, 88 % yield). ^{1}H NMR (300 MHz, $CDCl_3$) δ 7.84 (t, J = 2.0 Hz, 1H), 7.80 (bs, 1H), 7.51 (dd, J = 8.1, 1.2 Hz, 1H), 7.39 (d, J = 8.2 Hz, 1H), 7.30-7.24 (m, 1H); ^{13}C NMR (125 MHz, $CDCl_3$) δ 155.1 (q, J_{C-F} = 37.7 Hz), 136.3, 130.7, 129.7, 123.8, 123.0, 119.3, 115.6 (q, J_{C-F} = 288.5 Hz); ^{19}F NMR (282 MHz, $CDCl_3$) δ −75.72, −75.73; FTIR (Neat Film, NaCl) 3288, 1709, 1593, 1538, 1470, 1429, 1338, 1263, 1251, 1171, 1153, 1069, 997, 975, 925, 873, 865, 785, 739 cm^{-1}; HRMS (MultiMode ESI/APCI) m/z calc'd for $C_8H_5BrF_3NO$ [M-H]$^-$: 265.9434, found: 295.9426.

3-(2,2,2-trifluroacetamide)-phenylboronic acid.

A flame dried one neck round bottom flask was charged with the required trifluoroacetanilide (1.0 g, 3.7 mmol, 1 eq). The flask was sealed, evacuated and

backfilled with argon. THF (20 ml) was added via syringe and the obtained mixture was cooled to -78 °C. nBuLi (2.3 M solution in hexane, 3.6 ml, 8.2 mmol, 2.2 eq) was added dropwise and the obtained mixture was stirred for 2 h at this temperature. Triisopropylborate (2.7 ml, 11.7 mmol, 3 eq) was then added via syringe and the mixture was stirred for 10 minutes at -78 °C and for one hour at room temperature. A solution of HCl (2 M in water, 10 ml) was added and the biphasic mixture was vigorously stirred for another hour and then extracted with EtOAc (3 x 30 mL). The combined organic phases where washed with brine (2 x 20 ml) and dried over $MgSO_4$. Upon evaporation of the solvent under reduced pressure an off-white solid was obtained. It was suspended in hexane and stirred until a fine powder was formed. It was filtered and dried in high vacuum for 30 minutes (0.58 g, 67 % yield). If the obtained product is not perfectly clean from NMR analysis a 10:1 mixture of hexane-Et_2O or hexane-CH_2Cl_2 can be used instead of hexanes to suspend the compound. In some cases the desired aryl boronic acid is obtained as an oil and does not solidify. This is usually due to the presence of a large amount of byproducts. In these cases it is necessary to add ether, water and a 1 M solution of NaOH (4 to 5 equivalents are normally enough) to the crude mixture. After extraction, the isolated water phase can be acidified with a 1 M aqueous HCl solution and extracted with EtOAc. *It is important to wash this organic phase with water to eliminate possible residual salt*. Upon evaporation of the solvent and trituration with pentane or hexane the desired product should be obtained as an off-white solid in 66% yield. ^{1}H NMR (300 MHz, acetone-d6) δ 8.11 (bs, 1H), 7.81 (m, 1H), 7.74 (dt, *J* = 7.4, 1.0 Hz 1H), 7.40 (t, *J* = 7.7 Hz, 1H), 7.28 (s, 1H); (The obtained ^{13}C NMR is complex due to the presence of two rotamers in solution) ^{13}C NMR (125 MHz, $CDCl_3$) δ 154.8 (q, *J* = 36.9

Hz), 154.7 (q, *J* = 36.8 Hz), 135.8, 135.7, 131.5, 128.2, 126.7, 126.6, 123.0, 122.9, 116.2

(q, *J* = 288.1 Hz); ^{19}F NMR (282 MHz, CDCl$_3$) δ – 76.22, −76.25; FTIR (Neat Film,

, NaCl): 3305, 1701, 1585, 1554, 1437, 1334, 1264, 1182, 1031, 780 cm^{-1}; HRMS

(MultiMode ESI/APCI) *m/z* calc'd for C$_8$H$_7$BrF$_3$NO [M-H]$^-$: 231.0435, found: 231.0433.

4-(2,2,2-trifluroacetamide)-phenylboronic acid

Obtained using the representative procedure in 65% yield. ^{1}H NMR (300 MHz, acetone-

d$_6$) δ 10.22 (bs, 1H), 7.91 (d, *J* = 8.4 Hz, 2H), 7.72 (d, *J* = 8.4 Hz, 1H), 7.20 (s, 1H); ^{13}C

NMR (125 MHz, acetone-d$_6$) d 155.6 (q, J_{C-F} = 37.2 Hz), 136.3, 139.2, 135.9, 120.5,

119.2 (q, J_{C-F} = 288.3 Hz); ^{19}F NMR (282 MHz, acetone-d$_6$) δ –76.21, −76.24; FTIR

(Neat Film, NaCl) 3297, 1714, 1595, 1539, 1408, 1275, 1244, 1183, 1113, 1008, 832,

798 cm^{-1}; HRMS (MultiMode ESI/APCI) *m/z* calc'd for C$_8$H$_7$BrF$_3$NO [M-H]$^-$: 231.0435,

found: 231.0443.
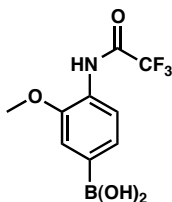
3-(2,2,2-trifluroacetamide)-4-methylphenylboronic acid

Obtained as an off-white solid in 35 % yield following the general procedure and using

the required trifluoroacetanilide (1.4 g, 4.9 mmol, 1 eq), nBuLi (4.4 ml of a 2.4M

solution, 10.7 mmol, 2.2 eq) and triisopropylborate (3.4 mL, 14.6 mmol, 3 eq). ^{1}H NMR

(300 MHz, acetone-d$_6$) δ 9.34 (s, 1H), 8.05 (dd, J = 3.0, 6.9 Hz, 1H), 7.58 (s 1H), 7.54

(dd, J = 7.9, 1.0 Hz, 1H) 7.29 (s, 1H), 3.93 (s, 3H); ^{13}C NMR (125 MHz, acetone-d$_6$) δ

154.3 (q, $J_{C\text{-}F}$ = 150 Hz), 149.3, 126.8, 126.6, 120.5, 116.1, 115.8 (q, $J_{C\text{-}F}$ = 288 Hz),

112.5, 55.4; IR (Neat Film, NaCl): 3298, 1708, 1591, 1537, 1503, 1465, 1404, 1342,

1294, 1273, 1224, 1161, 1123, 1015; HRMS (MultiMode ESI/APCI) *m/z* calc'd for

C$_9$H$_8$BO$_4$NF$_3$ [M-H]$^-$: 261.0590, found: 261.0497.
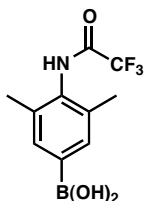
4-(2,2,2-trifluroacetamide)-2,6-dimethyl-phenylboronic acid

Obtained as an off-white solid in 66 % yield following the general procedure and using

the required trifluoroacetanilide (1.0 g, 3.4 mmol, 1 eq), nBuLi (3.2 ml of a 2.3M

solution, 7.44 mmol, 2.2 eq) and triisopropylborate (2.3 mL, 10.1 mmol, 3 eq). ^{1}H NMR

(300 MHz, acetone-d$_6$) δ 7.62 (s, 2H), 7.20 (s, 1H), 2.25 (s, 6H); ^{13}C NMR (125 MHz,

acetone-d$_6$) δ 155.1 (q, J = 36.5 Hz), 134.2, 134.2, 134.1, 133.9, 116.5 (q, J = 286.0 Hz),

17.1; ^{19}F NMR (282 MHz, acetone-d$_6$) δ − 75.97, −75.99; FTIR (Neat Film, NaCl): 3233,

1705, 1602, 1533, 1340, 1219, 1192, 1160 cm^{-1}; HRMS (MultiMode ESI/APCI) *m/z*

calc'd for C$_{10}$H$_{11}$NBrF$_3$O [M-H]$^-$: 259.0748, found 259.0749.
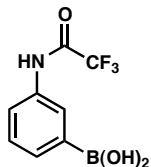
3-(2,2,2-trifluroacetamide)-phenylboronic acid

Obtained as an off-white solid in 66 % yield following the general procedure and using the proper trifluoroacetanilide (1.0 g, 3.7 mmol, 1 eq), nBuLi (3.6 ml of a 2.3M solution, 8.2 mmol, 2.2 eq) and triisopropylborate (2.6 mL, 11.2 mmol, 3 eq). ^{1}H NMR (300 MHz, acetone-d$_6$) δ 8.11 (bs, 1H), 7.81 (m, 1H), 7.74 (dt, J = 7.4, 1.0 Hz 1H), 7.40 (t, J = 7.7 Hz, 1H), 7.28 (s, 1H); (The obtained ^{13}C NMR is complex due to the presence of two rotamers in solution) ^{13}C NMR (125 MHz, acetone-d$_6$) δ 154.8 (q, J = 36.9 Hz), 154.7 (q, J = 36.8 Hz), 135.8, 135.7, 131.5, 128.2, 126.7, 126.6, 123.0, 122.9, 116.2 (q, J = 288.1 Hz); ^{19}F NMR (282 MHz, acetone-d$_6$) δ − 76.22, −76.25; FTIR (Neat Film, NaCl): 3305, 1701, 1585, 1554, 1437, 1334, 1264, 1182, 1031, 780 cm^{-1}; HRMS (MultiMode ESI/APCI) m/z calc'd for C$_8$H$_7$BrF$_3$NO [M-H]$^-$: 231.0435, found: 231.0433.

3-(2,2,2-trifluroacetamide)-4-methylphenylboronic acid

Obtained as an off-white solid in 66 % yield following the general procedure and using the required trifluoroacetanilide (2.0 g, 3.7 mmol, 1 eq), nBuLi (3.6 ml of a 2.3M solution, 8.2 mmol, 2.2 eq) and triisopropylborate (2.6 mL, 11.2 mmol, 3 eq). ^{1}H NMR (300 MHz, acetone-d$_6$) δ 7.82 (s, 1H), 7.75 (dd, J = 6.5, 10 Hz, 1H), 7.32 (d, J = 7.5 Hz, 1H) 7.24 (s, 1H); ^{13}C NMR (125 MHz, acetone-d$_6$) δ 155.4 (q, J = 37.5 Hz), 136.2,

133.5, 132.9, 132.1, 130.1, 116.4 (q, $J = 288.0$ Hz); FTIR (Neat Film, NaCl) 3270, 1708, 1617, 1533, 1406, 1351, 1259, 1180, 1162, 1092, 1036, 898, 825 cm^{-1}; **HRMS** (MultiMode ESI/APCI) *m/z* calc'd for C$_9$H$_8$BF$_3$NO$_3$ [M-H]$^-$: 245.0477, found 245.0591.

Representative General Procedure for the Enantioselective 1,4-Addition of Arylboronic Acids to β-Substituted Cyclic Enones.
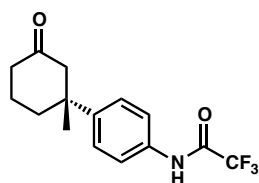
(*R*)-3-(4-(2,2,2-trifluoroacetamide)phenyl)-3-methylcyclohexanone (162a)

A screw-top 5 ml vial was charged with a stir bar, Pd(OCOF$_3$)$_2$ (4.5 mg, 0.014 mmol, 0.05 eq), (*S*)-*t*-BuPyOx (3.3 mg, 0.016 mmol, 0.06 eq), boronic acid (95 mg, 0.41 mmol, 1.5 eq) and NH$_4$PF$_6$ (13 mg, 0.08 mmol, 0.3 eq). Dichloroethane (1 mL) was added and the mixture was stirred until a homogeneous suspension was formed (around 1 minute). 3-methyl-2-cyclohexenone (30 mg, 0.27 mmol, 1 eq) was then added dissolved in 1.7 mL of dichloroethane (yields are improved with the addition of enone as a solution). Water (25 µl, 1.3 mmol, 5 eq) was added, and the vial was sealed and the reaction was stirred at 60 °C for 3h. After this time almost all the solid in the vial was consumed and from TLC (Hexane- EtOAc 4:1) all the starting enone disappeared. The mixture was cooled to ambient temperature and it was charged directly into a silica gel column for purification. The desired product was isolated as white powder (80 mg, 98 % yield, 89 % ee SFC column 6 (IC) 5 ml/min 4 % MeOH). ^{1}H NMR (300 MHz, CDCl$_3$) δ 7.91 (bs, 1H), 7.53

(m, 2H), 7.36 (m, 2H), 2.85 (d, J = 14.2 Hz, 1H), 2.45 (d, J = 14.0 Hz, 1H), 2.32 (m, 2H),

2.25 - 2.12 (m, 1H), 1.98 - 1.82 (m, 2H), 1.71 - 1.57 (m , 1H), 1.32 (s, 3H); ^{13}C NMR

(125 MHz, CDCl$_3$) δ 211.8, 154.9 (q, J = 37.4 Hz), 145.2, 133.5, 126.7, 120.6, 115.7 (q, J

= 289.0 Hz), 52.9, 42.9, 40.7, 37.9, 30.4, 22.0; FTIR (Neat Film, NaCl) 3292, 2958,

1706, 1609, 1545, 1517, 1412, 1285, 1252, 1193, 1155, 901, 835 cm^{-1}; HRMS

(MultiMode ESI/APCI) m/z calc'd for C$_{15}$H$_{16}$F$_3$NO [M-H]$^-$: 298.106, found 289.1049;

$[\alpha]_D^{25}$ – 47.5° (c 2.10, CHCl$_3$, 89% ee).
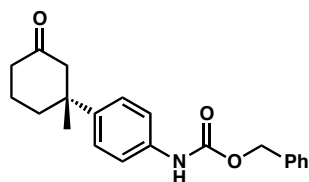
(*R*)-3-(4-(N-carbobenzyloxy)phenyl)-3-methylcyclohexanone (160)

Following the general procedure the desired product was obtained as a clear oil (35 mg,

45 % yield, 76 % ee, SFC column 6 (IC) 5 ml/min 15 % MeOH). ^{1}H NMR (300 MHz,

CDCl$_3$) δ 7.44-7.30 (m, 6H), 7.25-7.22 (m, 3H), 6.63 (bs, 1H), 5.20 (s, 2H), 2.84 (d, J =

14.2 Hz, 1H), 2.42 (d, J = 14.1 Hz, 1H), 2.31 (m, 2H), 2.21–2.10 (m, 1H), 1.95–1.80 (m,

2H), 1.73–1.60 (m, 1H), 1.30 (s, 3H); ^{13}C NMR (125 MHz, CDCl$_3$)

δ 211.6, 153.5, 142.7, 136.1, 135.9, 128.7, 128.5, 128.4, 126.5, 118.9, 67.2, 53.3, 42.6, 40

.9, 38.0, 30.1, 22.1; FTIR (Neat Film, NaCl) 3306, 2953, 1705, 1597, 1534, 1454, 1409,

1323, 1220, 1052 cm^{-1}; HRMS (MultiMode ESI/APCI) m/z calc'd for C$_{21}$H$_{24}$NO$_3$

[M+H]$^+$: 338.1756, found 338.1760; $[\alpha]_D^{25}$ – 26.8° (c 1.40, CHCl$_3$, 76% ee).
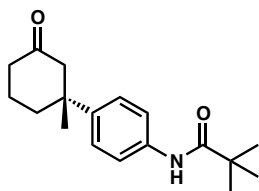
(*R*)-3-(4-(N-pyvaloyl)phenyl)-3-methylcyclohexanone (161)

Following the general procedure the desired product was obtained as a white solid (56 mg, 72% yield, 76% ee SFC column 5 (OB-H) 5 ml/min 10 % MeOH). ^{1}H NMR (300 MHz, CDCl$_3$) δ 7.47 (d, *J* = 8.7 Hz, 2H), 7.33-7.24 (m, 3H), 2.85 (d, *J* = 14.2 Hz, 1H), 2.42 (d, *J* = 14.2 Hz, 1H), 2.31 (m, 2H), 2.21–2.11 (m, 1H), 1.95–1.80 (m, 2H), 1.72–1.58 (m, 1H), 1.30 (s, 9H); ^{13}C NMR (125 MHz, CDCl$_3$) δ 211.6, 176.7, 143.4, 136.2, 126.3, 120.1, 53.2, 42.7, 40.9, 39.7, 38.1, 30.1, 27.8, 22.1; F TIR(Neat Film ,NaCl) 3379, 2961, 1685, 1594, 1518, 1400, 1318, 1301, 1255, 1189 cm^{-1}; HRMS (MultiMode ESI/APCI) *m/z* calc'd for C$_{18}$H$_{26}$NO$_2$ [M+H]$^+$: 2881964, found 288.1969; $[\alpha]_D^{25}$ – 52.5° (c 1.01, CHCl$_3$, 76% ee).
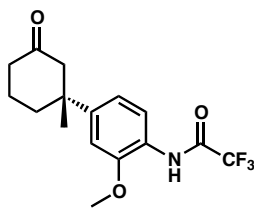
(*R*)-3-(4-(2,2,2-trifluoroacetamide)-3-methoxyphenyl)-3-methylcyclohexanone (163)

Following the general procedure the desired product was obtained as white solid (67 mg, 75 % yield). ^{1}H NMR (300 MHz, CDCl$_3$) δ 8.50 (bs, 1H), 8.24 (d, *J* = 8.5 Hz, 2H), 6.96 (dd, *J* = 8.5, 2.1 Hz, 1H), 6.87 (d, *J* = 2.1 Hz, 1H), 3.93 (s, 3H), 2.87 (d, J = 14.1 Hz, 1H), 2.45 (d, J = 14.2 Hz, 1H), 2.32 (m, 2H), 2.24-2.14 (m, 1H), 2.0-1.8 (m, 2H), 1.68-2.5 (m,

1H), 1.32 (s, 3H); FTIR (neat, NaCl): 3362, 2960, 2871, 1706, 1665, 1594, 1515, 1479, 1402, 1321, 1228, 1193, 1164 cm^{-1}; HRMS (MultiMode ESI/APCI) *m/z* calc'd for C$_{16}$H$_{17}$F$_3$NO$_3$ [M-OH]: 328.1161, found: 328.1167; [α]$_D^{25}$ − 61.3° (c 1.25, CHCl$_3$, 88% ee).
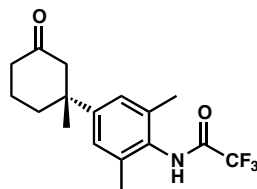
(*R*)-3-(4-(2,2,2-trifluoroacetamide)-2,6-dimethylphenyl)-3-methylcyclohexanone (164)

Following the general procedure the desired product was obtained in 93 % yield as a white solid (90 % ee, SFC column 1 (AD-H) 5ml/min 5 % MeOH). ^{1}H NMR (300 MHz, CDCl$_3$) δ 7.41 (bs, 1H), 7.05 (s, 2H), 2.84 (d, *J* = 14.2 Hz, 1H), 2.42 (d, *J* = 14.1 Hz, 1H), 2.32 (m, 2H), 2.24 (s, 6H), 2.21–2.10 (m, 1H), 1.96–1.80 (m, 2H), 1.76–1.60 (m, 1H), 1.30 (s, 3H); ^{13}C NMR (125 MHz, CDCl$_3$) δ 211.8, 156.2 (q, *J* = 36.4 Hz), 147.6, 135.1, 128.9, 125.7, 118.2 (q, *J* = 279.9 Hz), 52.8, 42.4, 40.6, 37.6, 29.4, 21.9, 18.2; FTIR (Neat Film, NaCl) 2958, 2863, 1715, 1651, 1583, 1568, 1538, 1479, 1441, 1359, 1314, 1228, 1198, 1157, 1101 cm^{-1}; HRMS (MultiMode ESI/APCI) *m/z* calc'd for C$_{17}$H$_{20}$F$_3$NO$_2$ [M-H]$^-$: 326.1373, found 326.1370; [α]$_D^{25}$ − 54.3° (c 2.10, CHCl$_3$, 90% ee).
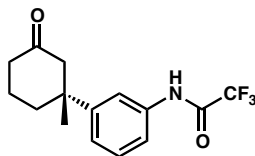
(*R*)-3-(3-(2,2,2-trifluoroacetamide)phenyl)-3-methylcyclohexanone (165)

Following the general procedure the desired product was obtained in 60 % yield as transparent oil (92 % ee, SFC column 1 (AD-H) 5ml/min 5 % MeOH). ^{1}H NMR (300 MHz, CDCl$_3$) δ 7.91 (bs, 1H), 7.55–7.45 (m, 2H), 7.36 (t, *J* = 7.9 Hz,, 1H), 7.20 (m , 1H), 2.87 (d, *J* = 14.2 Hz, 1H), 2.46 (d, *J* = 14.2 Hz, 1H), 2.32 (m, 2H), 2.27–2.17 (m, 1H), 1.98–1.82 (m, 2H), 1.71–1.57 (m , 1H), 1.33 (s, 3H); ^{13}C NMR (125 MHz, CDCl$_3$) δ 211.5, 154.9 (q, *J* = 37.0 Hz), 148.9, 135.5, 129.5, 123.6, 118.5, 118.0, 115.6 (q, *J* = 289.2 Hz), 52.9, 43.0, 40.7, 37.8, 30.0, 22.0; FTIR (Neat Film, NaCl) 3298, 3157, 3111, 2959, 2876, 1713, 1616, 1595, 1563, 1493, 1442, 1421, 1291, 1239, 1201, 1156. cm^{-1}; HRMS (MultiMode ESI/APCI) *m/z* calc'd for C$_{15}$H$_{16}$F$_3$NO$_2$ [M-H]$^-$: 298.1055, found: 298.1050; [α]$_D^{25}$ – 28.9° (c 2.10, CHCl$_3$, 92 % ee).
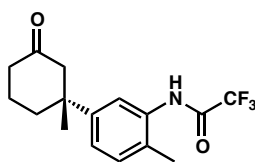
(*R*)-3-(3-(2,2,2-trifluoroacetamide)-4-methylpheny)-3-methylcyclohexanone (166).

Following the general procedure the desired product was obtained in 77 % yield as a white solid (91% ee, OD-H column, 5 mL/min, 5% MeOH). ^{1}H NMR (300 MHz, CDCl$_3$) δ 7.94 (bs, 1H), 7.66 (s, 1H), 7.16 (d, *J* = 8.1 Hz, 1H), 7.11 (dd, *J* = 8.1, 1.9 Hz, 1H), 2.85 (d, *J* = 14.1 Hz, 1H), 2.44 (d, *J* = 14.1 Hz, 1H), 2.32 (m, 2H), 2.26 (s, 3H), 2.24–2.07 (m, 1H), 1.97–1.80 (m, 2H), 1.78–1.60 (m, 1H), 1.31 (s, 3H). ^{13}C NMR (125
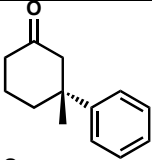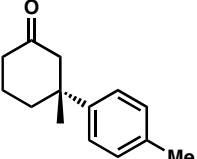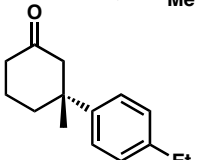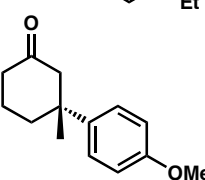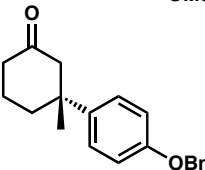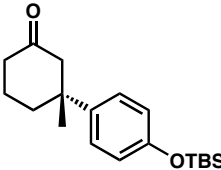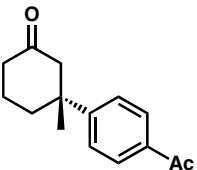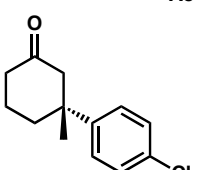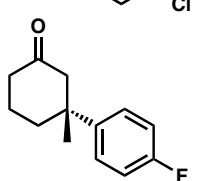
MHz, CDCl$_3$) δ 211.3, 156.2 (q, J = 36.4 Hz), 146.6, 132.9, 131.4, 130.9, 128.3, 124.4,

118.1 (q, J = 279.8 Hz), 53.0, 42.7, 40.7, 37.7, 29.6, 22.0, 16.9; FTIR (Neat Film, NaCl)

3277, 3060, 2959, 2873, 1711, 1617, 1577, 1540, 1507, 1452, 1420, 1316, 1281, 1257,

1200, 1162 cm^{-1}; HRMS (MultiMode ESI/APCI) m/z calc'd for C$_{16}$H$_{18}$F$_3$NO$_2$ [M+H]$^+$:

314.1362, found: 314.1370. [α]$_D^{25}$ – 45.6° (c 5.3, CHCl$_3$, 88% ee).
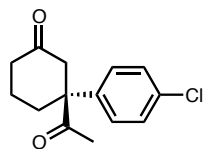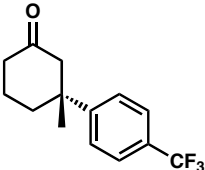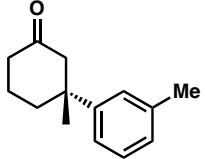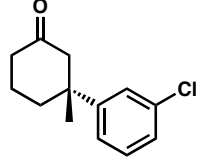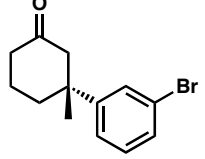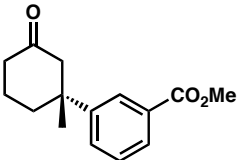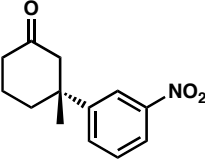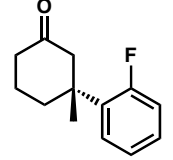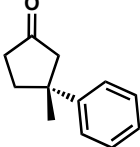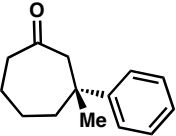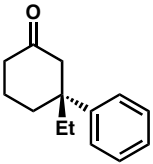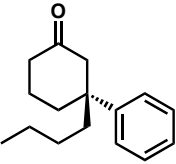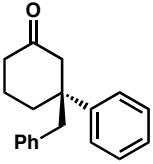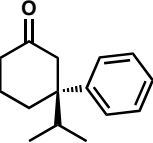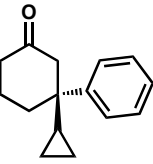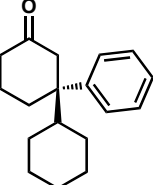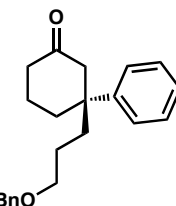
(*R*)-3-(4-chloropheny)-3-acetylcyclohexanone (158)

Following the general procedure and using 3-acetylcyclohexenone (34 mg, 0.25 mmol, 1

eq), 4-chlorophenyl boronic acid (78 mg, 0.5 mmol, 2 eq), water (25 μL, 1.25 mmol, 5

eq), ^{t}BuPyOX (3 mg, 0,015 mmol, 0.06 eq), Pd(OCOF$_3$)$_2$ (4.1 mg, 0.012 mmol, 0.05 eq),

NH$_4$PF$_6$ (12 mg, 0.075 mmol, 0.3 eq) and ClCH$_2$CH$_2$Cl (2 mL) the desired product were

isolated as a white solid (53 mg, 85 % yield, 96 % ee, SFC column 3 (OJ-H) 5 ml/min 15

% MeOH). ^{1}H NMR (300 MHz, CDCl$_3$) δ 7.35 (m, 2H), 7.18 (m, 2H), 2.85 (dt, J = 1.4,

14.8 Hz, 1H), 2.63 (dt, J =1.1, 14.8 Hz, 1H), 2.48–2.20 (m, 4H), 1.87 (s, 3H), 1.80–1.69

(m, 2H); ^{13}C NMR (125 MHz, CDCl$_3$) 208.3, 208.1, 139.3, 133.8, 129.5, 127.8, 59.6,

48.6, 40.3, 31.5, 25.3, 21.1; FTIR (Neat Film , NaCl) 3397, 2951, 2875, 1708, 1490,

1455, 1420, 1402, 1356, 1319, 1235, 1183, 1140, 1097, 1012, 970, 829, 717 cm^{-1}; HRMS

(MultiMode ESI/APCI) m/z calc'd for C$_{14}$H$_{15}$ClO$_2$ [M+H]$^+$: 251.0833, found: 251.0829;

[α]$_D^{25}$ – 6.74° (c 3.2, CHCl$_3$, 96 % ee).

Table 2.11 Chiral assays

entry	product	HPLC conditions	retention time of major isomer (min)	retention time of minor isomer (min)	% ee
1		Chiralcel OJ-H 1% IPA/Hexanes isocratic 1 mL/min	15.3	19.6	92
2		Chiralcel OJ-H 1% IPA/Hexanes isocratic 1 mL/min	15.2	17.1	87
3		Chiralcel OJ-H 0.5% IPA/Hexanes isocratic 1 mL/min	25.9	34.4	85
4		Chiralcel OJ-H 1% IPA/Hexanes isocratic 1 mL/min	29.5	37.1	69
5		Chiralpak AD-H 5% IPA/Hexanes isocratic 1 mL/min	37.9	35.3	74
6		Chiralcel OJ-H 0.5% IPA/Hexanes isocratic 1 mL/min	16.6	24.9	82
7		Chiralpak AD-H 5% IPA/Hexanes isocratic 1 mL/min	30.4	29.5	96
8		Chiralpak AD-H 1% IPA/Hexanes isocratic 1 mL/min	12.8	11.7	95
9		Chiralcel OJ-H 1% IPA/Hexanes isocratic 1 mL/min	13.9	16.9	92

entry	product	HPLC conditions	retention time of major isomer (min)	retention time of minor isomer (min)	% ee
10		Chiralcel OJ-H 0.5% IPA/Hexanes isocratic 1 mL/min	35.0	41.1	96
11		Chiralcel OJ-H 1% IPA/Hexanes isocratic 1 mL/min	11.0	13.0	91
12		Chiralcel OJ-H 1% IPA/Hexanes isocratic 1 mL/min	17.2	20.4	96
13		Chiralcel OJ-H 1% IPA/Hexanes isocratic 1 mL/min	14.7	16.9	85
14		Chiralpak AD-H 5% IPA/Hexanes Isocratic 1mL/min	11.1	10.4	95
15		Chiralpak AD-H 1% IPA/Hexanes Isocratic 1mL/min	29.0	30.6	92
16		Chiralcel OJ-H 1% IPA/Hexanes isocratic 1 mL/min	9.3	10.9	77
17		Chiralpak AD-H 1% IPA/Hexanes Isocratic 1mL/min	12.6	10.2	91

entry	product	HPLC conditions	retention time of major isomer (min)	retention time of minor isomer (min)	% ee
18		Chiralcel OJ-H 1% IPA/Hexanes isocratic 1 mL/min	14.5	19.8	93
19		Chiralcel OJ-H 1% IPA/Hexanes isocratic 1 mL/min	15.5	18.0	92
20		Chiralcel OJ-H 1% IPA/Hexanes isocratic 1 mL/min	8.2	9.2	91
21		Chiralpak AD-H 5% IPA/Hexanes isocratic 1 mL/min	7.3	9.4	91
22		Chiralcel OJ-H 1% IPA/Hexanes isocratic 1 mL/min	13.1	14.7	79
23		Chiralcel OJ-H 1% IPA/Hexanes isocratic 1 mL/min	18.7	20.6	88
24		Chiralpak AD-H 1% IPA/Hexanes isocratic 1 mL/min	8.9	8.2	85
25		Chiralpak AD-H 1% IPA/Hexanes isocratic 1 mL/min	28.3	26.8	91

2.5 Notes and Citations

(1)   For reviews on the synthesis of quaternary stereocenters, see: (a) Denissova, I.;

Barriault, L. *Tetrahedron* **2003**, *59*, 10105. (b) Douglas, C. J.; Overman, L. E.

Proc. Natl. Acad. Sci. U.S.A. **2004**, *101*, 5363. (c) Christoffers, J.; Baro, A. *Adv.

Synth. Catal.* **2005**, *347*, 1473. (d) Trost, B. M.; Jiang, C. *Synthesis* **2006**, 369.

(e) Mohr, J. T.; Stoltz, B. M. *Chem. Asian J.* **2007**, 1476. (f) Cozzi, P. G.;

Hilgraf, R.; Zimmermann, N. *Eur. J. Org. Chem.* **2007**, *36*, 5969.

(2)   For an excellent comprehensive review, see: Hawner, C.; Alexakis, A. *Chem.

Commun.* **2010**, *46*, 7295.

(3)   (a) Wu, J.; Mampreian, D. M.; Hoveyda, A. H. *J. Am. Chem. Soc.* **2005**, *127*,

4584. (b) Hird, A. W.; Hoveyda, A. H. *J. Am. Chem. Soc.* **2005**, *127*, 14988. (c)

Lee, K.-S.; Brown, M. K.; Hird, A. W.; Hoveyda, A. H. *J. Am. Chem. Soc.* **2006**,

128, 7182. (d) Brown, M. K.; May, T. L.; Baxter, C. A.; Hoveyda, A. H. *Angew.

Chem., Int. Ed.* **2007**, *46*, 1097. (e) Wilsily, A.; Fillion, E. *J. Am. Chem. Soc.*

2006, *128*, 2774. (f) Wilsily, A.; Fillion, E. *J. Org. Chem.* **2009**, *74*, 8583. (g)

Dumas, A. M.; Fillion, E. *Acc. Chem. Res.* **2010**, *43*, 440. (h) Feringa, B. L. *Acc.

Chem. Res.* **2000**, *33*, 346. (i) Wilsily, A.; Fillion, E. *Org. Lett.* **2008**, *10*, 2801.

(4)   (a) d'Augustin, M.; Palais, L.; Alexakis, A. *Angew. Chem., Int. Ed.* **2005**, *44*,

1376. (b) Vuagnoux-d'Augustin, M.; Alexakis, A. *Chem. Eur. J.* **2007**, *13*, 9647.

(c) Palais, L.; Alexakis, A. *Chem. Eur. J.* **2009**, *15*, 10473. (d) Fuchs, N.;

d'Augustin, M.; Humam, M.; Alexakis, A.; Taras, R.; Gladiali, S. *Tetrahedron:

Asymm.* **2005**, *16*, 3143. (e) Vuagnoux-d'Augustin, M.; Kehrli, S.; Alexakis, A.

Synlett **2007**, 2057. (f) May, T. L.; Brown, M. K.; Hoveyda, A. H. *Angew.*

Chem., Int. Ed. **2008**, *47*, 7358. (g) Ladjel, C.; Fuchs, N.; Zhao, J.; Bernardinelli, G. Alexakis, A. *Eur. J. Org. Chem.* **2009**, 4949. (h) Palais, L.; Mikhel, I. S.; Bournaud, C.; Micouin, L.; Falciola, C. A.; Vuagnoux-d'Augustin, M.; Rosset, S.; Bernardinelli, G.; Alexakis, A. *Angew. Chem., Int. Ed.* **2007**, *46*, 7462. (i) Hawner, C.; Li, K.; Cirriez, V.; Alexakis, A. *Angew. Chem., Int. Ed.* **2008**, *47*, 8211. (j) Müller, D.; Hawner, C.; Tissot, M.; Palais, L.; Alexakis, A. *Synlett* **2010**, 1694. (k) Hawner, C.; Müller, D.; Gremaud, L.; Felouat, A.; Woodward, S.; Alexakis, A. *Angew. Chem., Int. Ed.* **2010**, *49*, 7769.

(5)   (a) Martin, D.; Kehrli, S.; d'Augustin, M.; Clavier, H.; Mauduit, M.; Alexakis, A. *J. Am. Chem. Soc.* **2006**, *128*, 8416. (b) Kehrli, S.; Martin, D.; Rix, D.; Mauduit, M.; Alexakis, A. *Chem. Eur. J.* **2010**, *16*, 9890. (c) Hénon, H.; Mauduit, M.; Alexakis, A. *Angew. Chem., Int. Ed.* **2008**, *47*, 9122. (d) Matsumoto, Y.; Yamada, K.-I.; Tomioka, K. *J. Org. Chem.* **2008**, *73*, 4578.

(6)   Recently, an asymmetric conjugate addition of cyanide in the presence of a catalyst derived from Sr(O*i*-Pr)3 has been reported, see: Tanaka, Y.; Kanai, M.; Shibasaki, M. *J. Am. Chem. Soc.* **2010**, *132*, 8862.

(7)   (a) For the seminal report in this area, see: Takaya, Y.; Ogasawara, M.; Hayashi, T.; Sakai, M.; Miyaura, N. *J. Am. Chem. Soc.* **1998**, *120*, 5579. (b) For an excellent review, see: Hayashi, T.; Yamasaki, K. *Chem Rev.* **2003**, *103*, 2829.

(8)   For selected recent examples, see: (a) Hayashi, T.; Ueyama, K.; Tokunaga, N.; Yoshida, K. *J. Am. Chem. Soc.* **2003**, *125*, 11508. (b) Fischer, C.; Defieber, C.; Suzuki, T.; Carreira, E. M. *J. Am. Chem. Soc.* **2004**, *126*, 1628. (c) Shintani, R.; Ueyama, K.; Yamada, I.; Hayashi, T. *Org. Lett.* **2004**, *6*, 3425. (d) Otomaru, Y.;

Okamoto, K.; Shintani, R.; Hayashi, T. *J. Org. Chem.* **2005**, *70*, 2503. (e)

Paquin,J.-F.; Defieber, C.; Stephenson, C. R. J.; Carreira, E. M. *J. Am. Chem. Soc.* **2005**, *127*, 10850.

(9)   (a) Mauleón, P.; Carretero, J. C. *Chem. Commun.* **2005**, 4961. (b) Shintani, R.; Duan, W.-L.; Hayashi, T. *J. Am. Chem. Soc.* **2006**, *128*, 5628.

(10)   (a) Shintani, R.; Tsutsumi, Y.; Nagaosa, M.; Nishimura, T.; Hayashi, T. *J. Am. Chem. Soc.* **2009**, *131*, 13588. (b) Shintani, R.; Takeda, M.; Nishimura, T.; Hayashi, T. *Angew. Chem., Int. Ed.* **2010**, *49*, 3969.

(11)   The same group also reported additions to β,β-disubstituted α,β-unsaturated esters, see: Shintani, R.; Hayashi, T. *Org. Lett.* **2011**, *13*, 350.

(12)   A recent paper describing the use of a Rh•OlefOX (olefin-oxazoline) complex provided a single example of a phenylboronic acid addition to 3-methylcyclohexen-2-one (i.e., **1** + **2** → **3**). Unfortunately, ketone **3** was isolated in only 36% yield and 85% ee, see: Hahn, B. T.; Tewes, F.; Fröhlich, R.; Glorius, F. *Angew Chem., Int. Ed.* **2010**, *49*, 1143.

(13)   For excellent review articles, see: (a) Gutnov, A. *Eur. J. Org. Chem.* **2008**, 4547. (b) Christoffers, J.; Koripelly, G.; Rosiak, A.; Rössle, M. *Synthesis* **2007**, 1279. (c) For a recent example, see: Xu, Q.; Zhang, R.; Zhang, T.; Shi, M. *J. Org. Chem.* **2010**, *75*, 3935.

(14)   Lin, S.; Lu, X. *Org. Lett.* **2010**, *12*, 2536.

(15)   Brunner, H.; Obermann, U. *Chem. Ber.* **1989**, *122*, 499.

(16)   Our preliminary ligand search was conducted under a range of conditions that varied solvent, temperature, additives, and palladium source. Ligand frameworks

tested included a variety of chiral bis(oxazolines) (BOX), pyridino(bis)oxazolines (PyBOX), phosphinooxazolines (PHOX), and quinolinooxazolines (QuinOX).

(17)   The absolute stereochemistry for all products shown was assigned by analogy to the product from Table 2, entry 2 as described in ref 3c.

(18)   See experimental section.

(19)   Other solvents proved to be inferior to dichloroethane.18

(20)   Substituents at the 2-position of the arylboronic acid were detrimental to the yields and stereoselectivity of the reaction with enone **1**, although 2-fluorophenylboronic acid underwent the desired reaction to provide a product in 32% yield and 77% ee.18

(21)   See Chapter 4 for full discussion of these results.

(22)   This work is the subject of Chapter 4 of this thesis. See: Holder, J. C.; Zou, L.; Marziale, A. N.; Liu, P.; Lan, Y.; Gatti, M.; Kikushima, K.; Houk, K. N.; Stoltz, B. M. *J. Am. Chem. Soc.* **2013**, *135*, 14996–15007.

(23)   (a) 3-ethylcyclohex-2-enone: Kehrli, S.; Alexakis, A.; Martin, D.; Rix, D.; Mauduit, M. *Chem.–Eur. J.* **2010**, *16*, 9890. (b) 3-isopropylcyclohex-2-enone: Martin, N. J. A.; List, B. *J. Am. Chem. Soc.* **2006**, *128*, 13368. (c) 3-butylcyclohex-2-enone: Moritani, Y.; Appella, D. H.; Jurkauskas, V.; Buchwald, S. L. *J. Am. Chem. Soc.* **2000**, *122*, 6797. (d) 3-cyclopropylcyclohex-2-enone: Piers, E.; Banville, J.; Lau, C. K.; Nagakura, I. *Can. J. Chem.* **1982**, *60*, 2965. (e) 3-benzylcyclohex-2-enone: Wang, X.; Reisinger, C. M.; List, B. *J. Am. Chem. Soc.* **2008**, *130*, 6070. (f) [1,1'-bi(cyclohexan)]-1-en-3-one: Yeh, M. C.; Knochel, P.; Butler, W. M.; Berk, S. C. *Tetrahedron Lett.* **1988**, *29*, 6693. (g) 3-

(3-(benzyloxy)propyl)cyclohex-2-enone: Kim, S.; Koh, J. S. *J. Chem. Soc., Chem. Commun.* **1992**, *18*, 1377. (h) 3-methylcyclohept-2-enone: Martin, N. J. A.; List, B. *J. Am. Chem. Soc.* **2006**, *128*, 13368.

(24) (a) Brunner, H.; Obermann, U. *Chem. Ber.* **1989**, *122*, 499. (b) Malkov, A. V.; Stewart Liddon, A. J.; Ramirez-Lopez, P.; Bendova, L.; Haigh, D.; Kocovsky, P. *Angew. Chem., Int. Ed.* **2006**, *45*, 1432.

(25) Shintani, R.; Tsutsumi, Y.; Nagaosa, M.; Nishimura, T.; Hayashi, T. *J. Am. Chem. Soc.* **2009**, *131*, 13588.

(26) Shintani, R.; Takeda, M.; Nishimura, T.; Hayashi, T. *Angew. Chem., Int. Ed.* **2010**, *49*, 3969.

(27) Hawner, C.; Muller, D.; Gremaud, L.; Fellouat, A.; Woodward, S.; Alexakis, A. *Angew. Chem., Int. Ed.* **2010**, *49*, 7769.

(28) May, T. L.; Brown, M. K.; Hoveyda, A. H. *Angew. Chem., Int. Ed.* **2008**, *47*, 7358.

(29) Hawner, C.; Li, K.; Cirriez, V.; Alexakis, A. *Angew. Chem., Int. Ed.* **2008**, *47*, 8211.

(30) Palais, L.; Alexakis, A. *Chem.–Eur. J.* **2009**, *15*, 10473.

(31) Lin, S.; Lu, X. *Org. Lett.* **2010**, *12*, 2536.

APPENDIX 1

Spectra relevant to Chapter 2:
The development of a palladium-catalyzed asymmetric conjugate
addition of arylboronic acids to cyclic conjugate acceptors
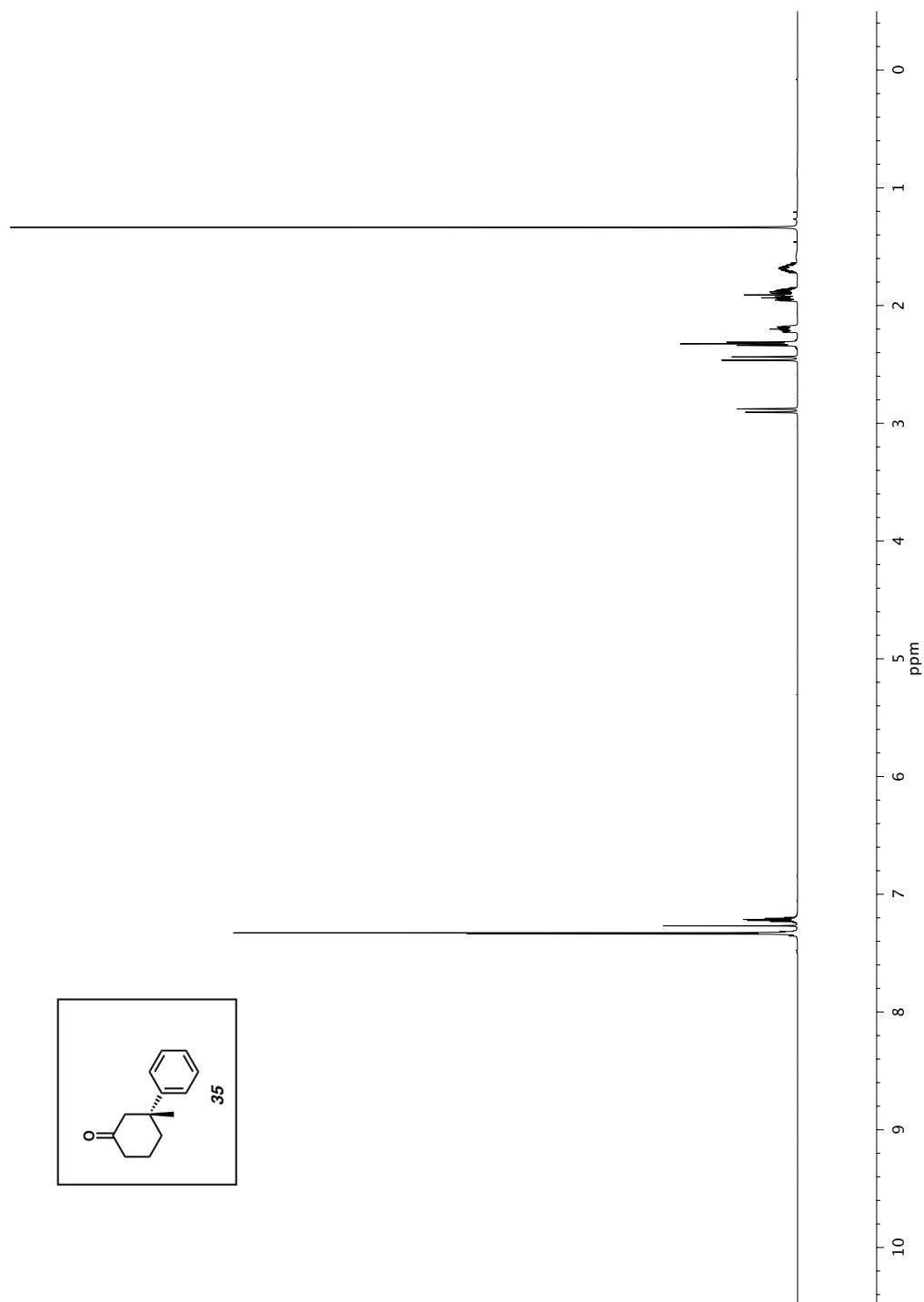
Figure A1.1 ^{1}H NMR (500 MHz, CDCl$_3$) of compound **35**
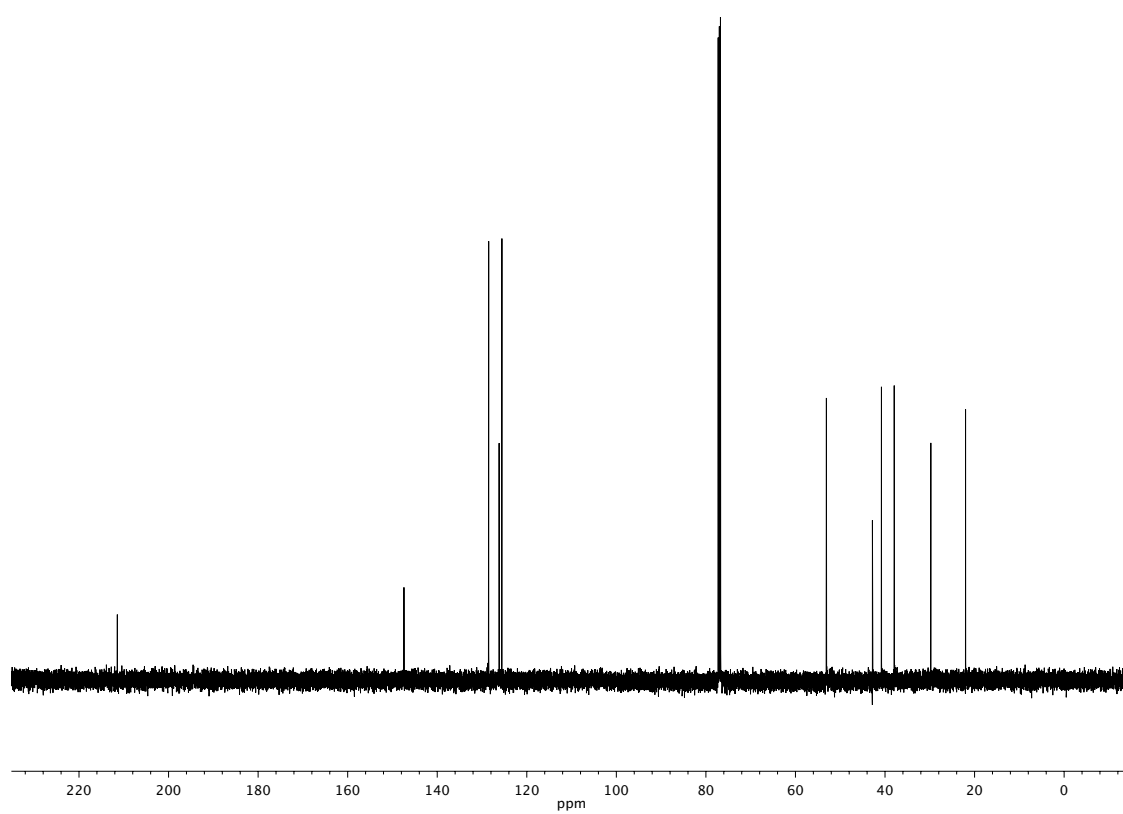
Figure A1.2 ^{13}C NMR (126 MHz, CDCl$_3$) of compound **35**
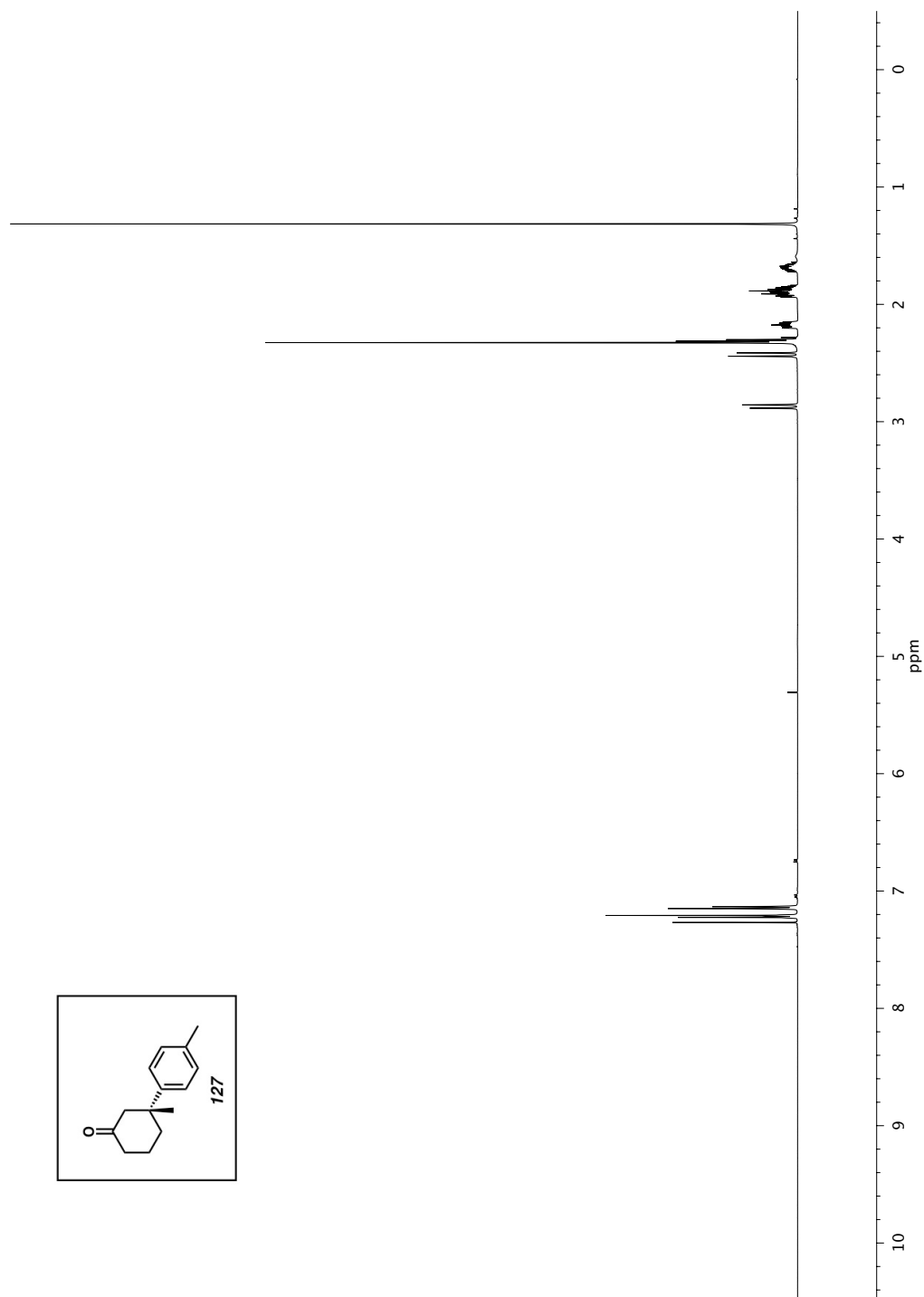
Figure A1.3 ^{1}H NMR (500 MHz, CDCl$_3$) of compound **127**
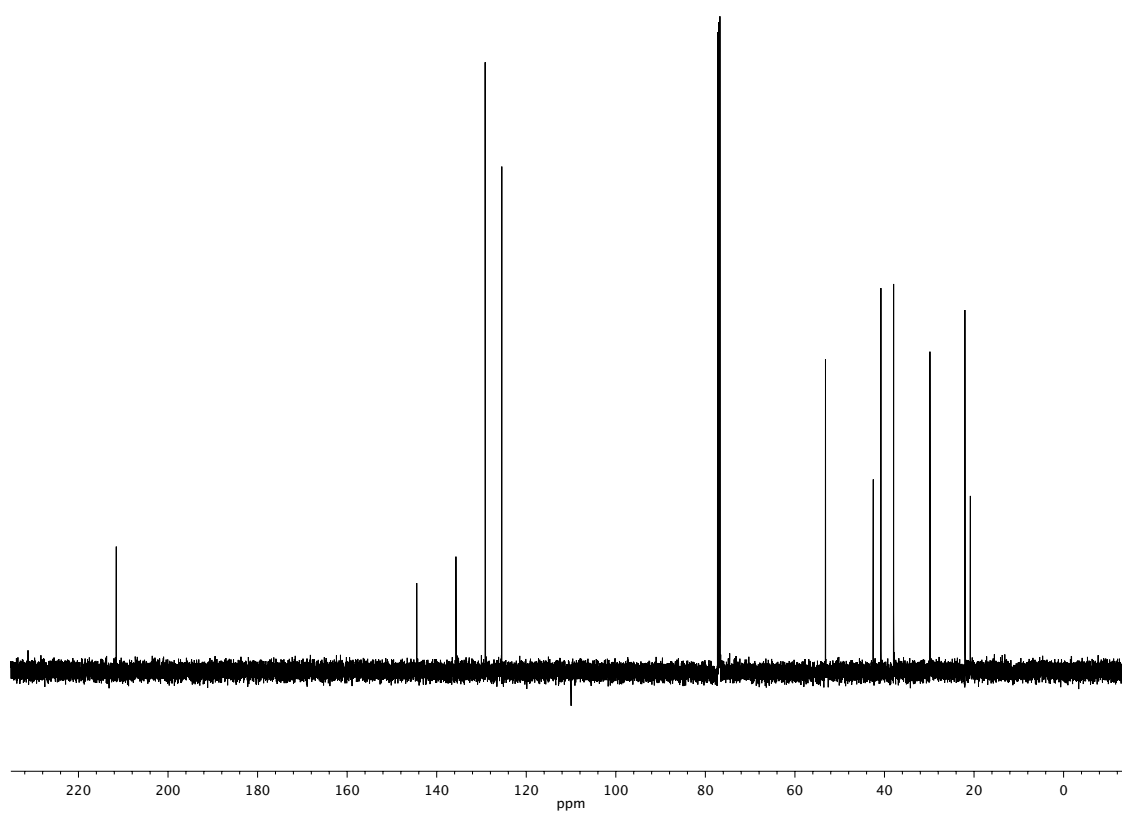
Figure A1.4 ^{13}C NMR (126 MHz, CDCl$_3$) of compound **127**
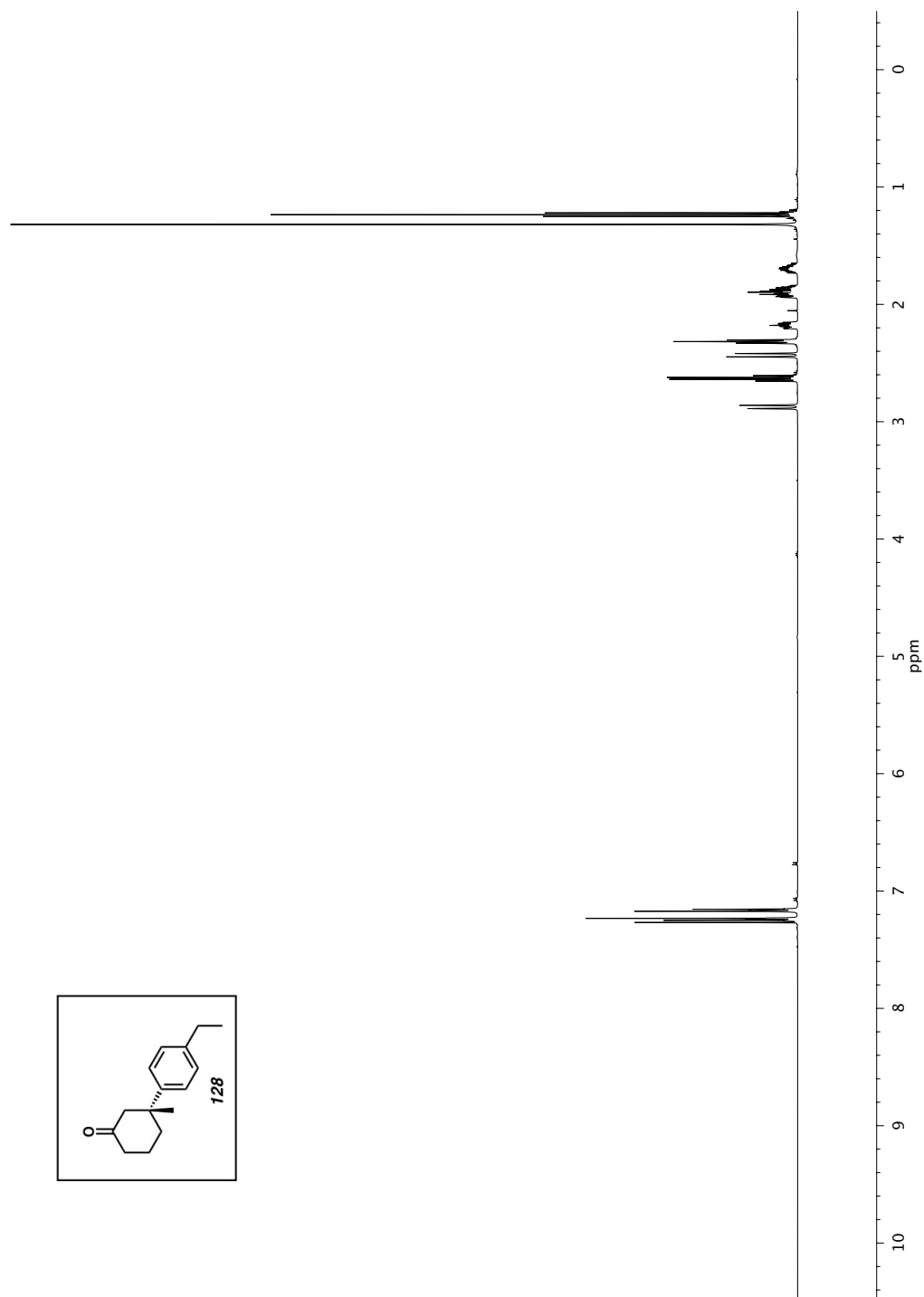
Figure A1.5 ^{1}H NMR (500 MHz, CDCl$_3$) of compound **128**
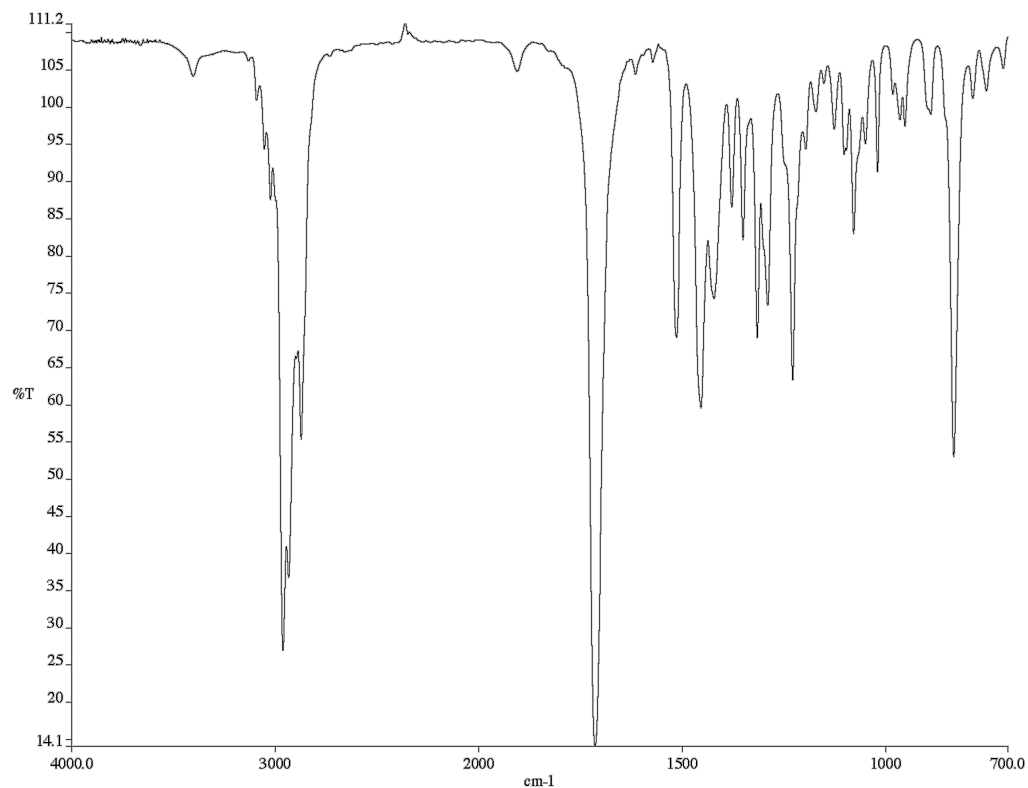
Figure A1.6 Infrared spectrum (Thin Film, NaCl) of compound **128**
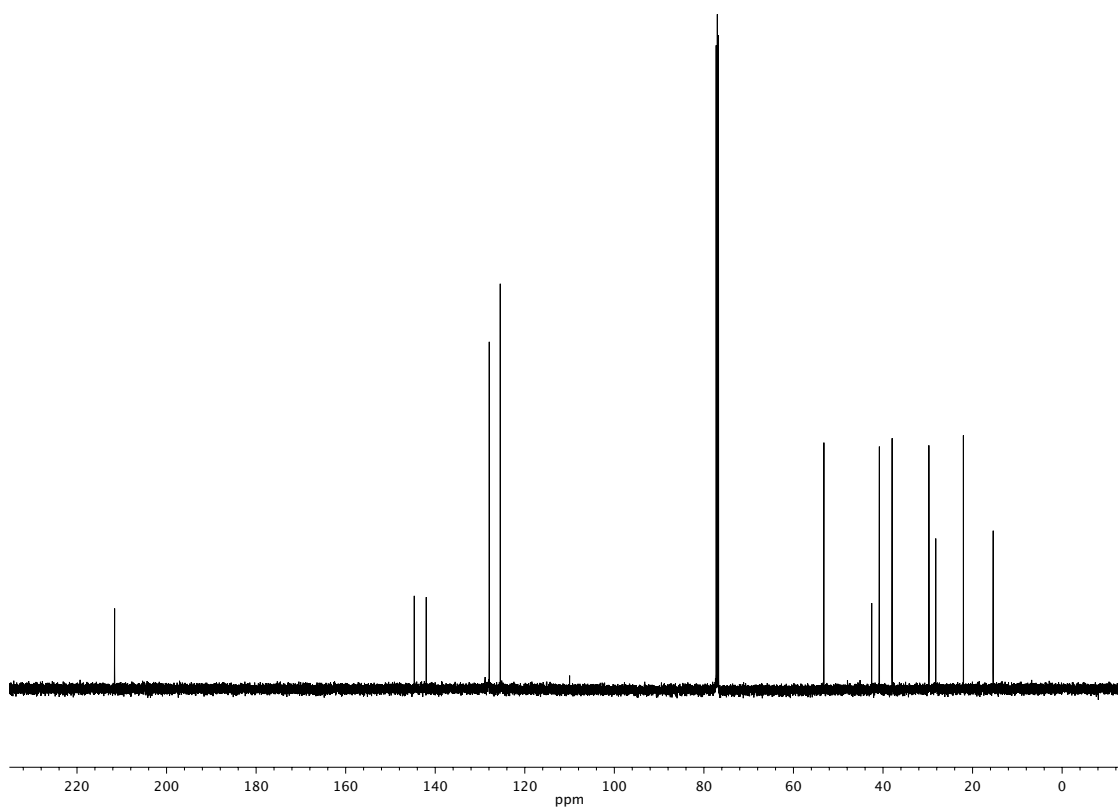
Figure A1.7 ^{13}C NMR (126 MHz, CDCl$_3$) of compound **128**
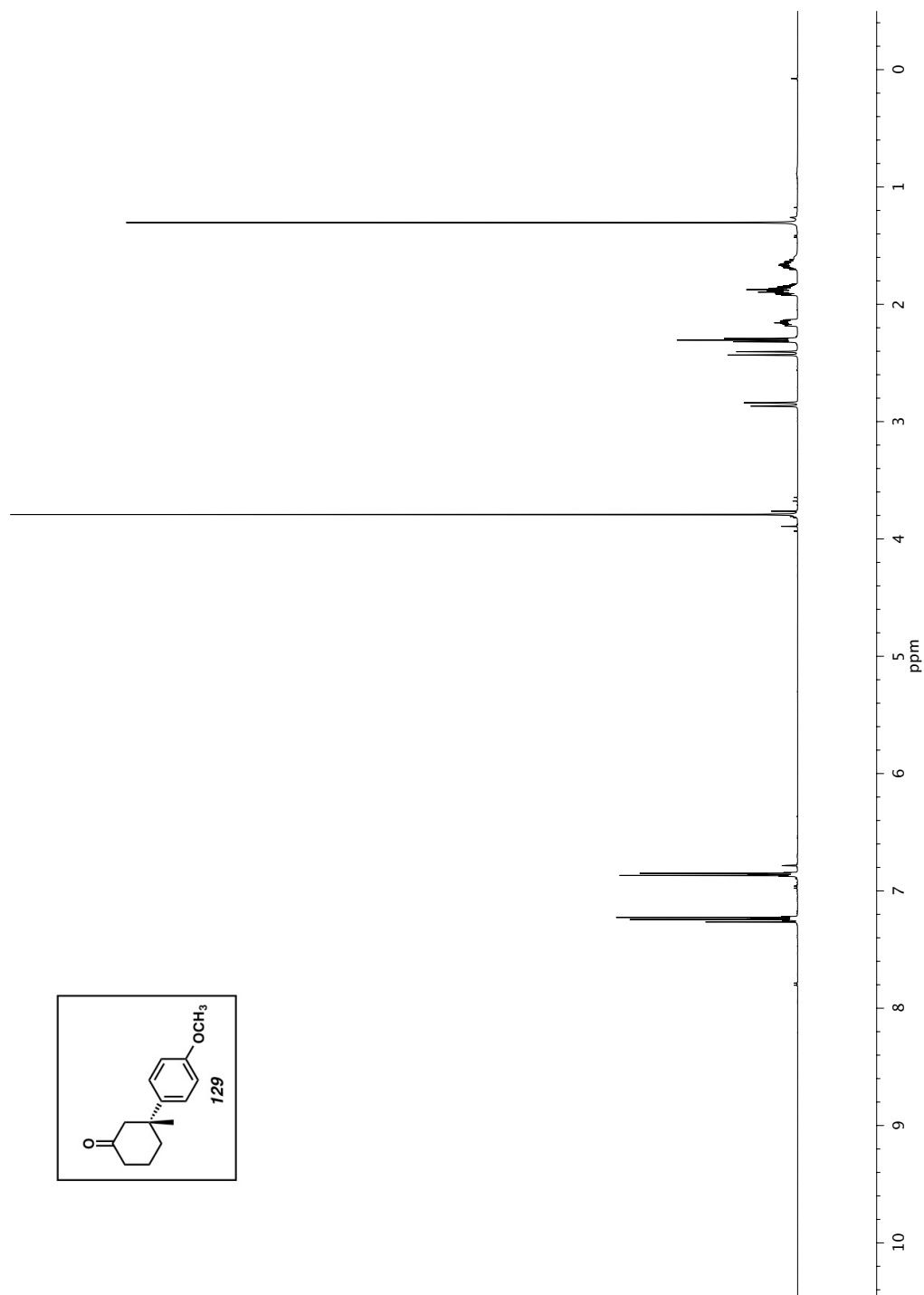
Figure A1.8 ^{1}H NMR (500 MHz, CDCl$_3$) of compound **129**
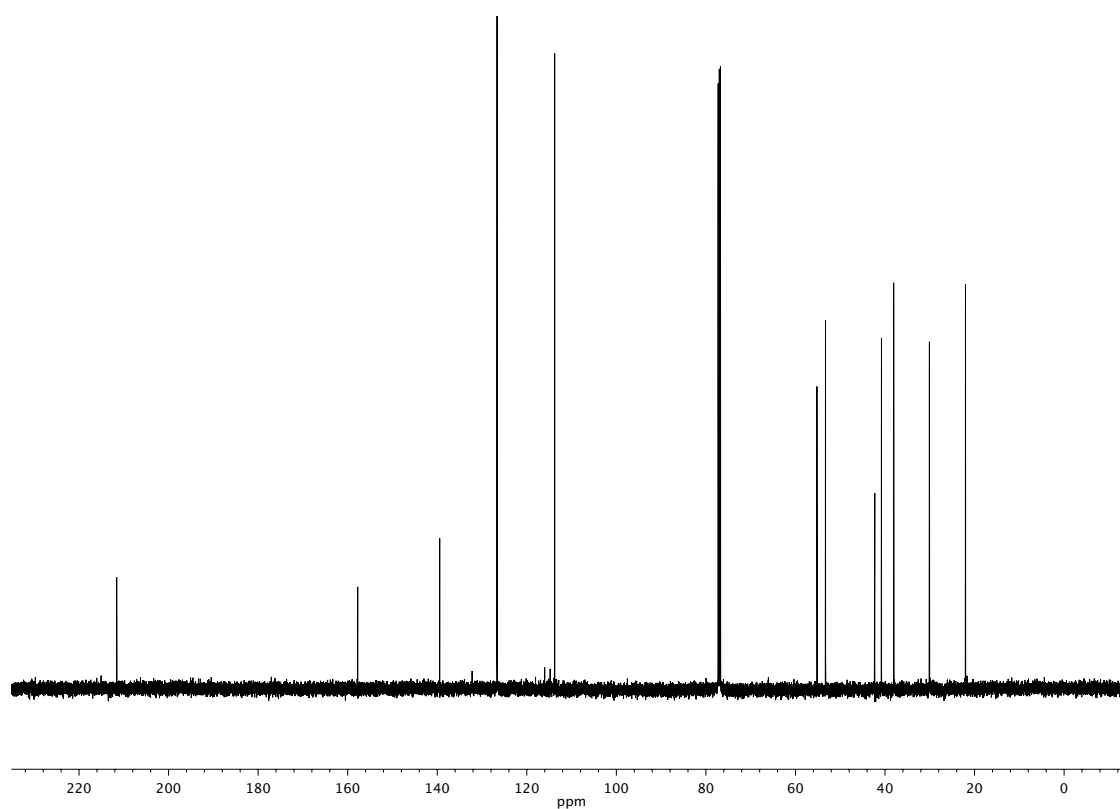
Figure A1.9 ^{13}C NMR (126 MHz, CDCl$_3$) of compound **129**

Figure A1.10 ^{1}H NMR (500 MHz, CDCl$_3$) of compound **130**
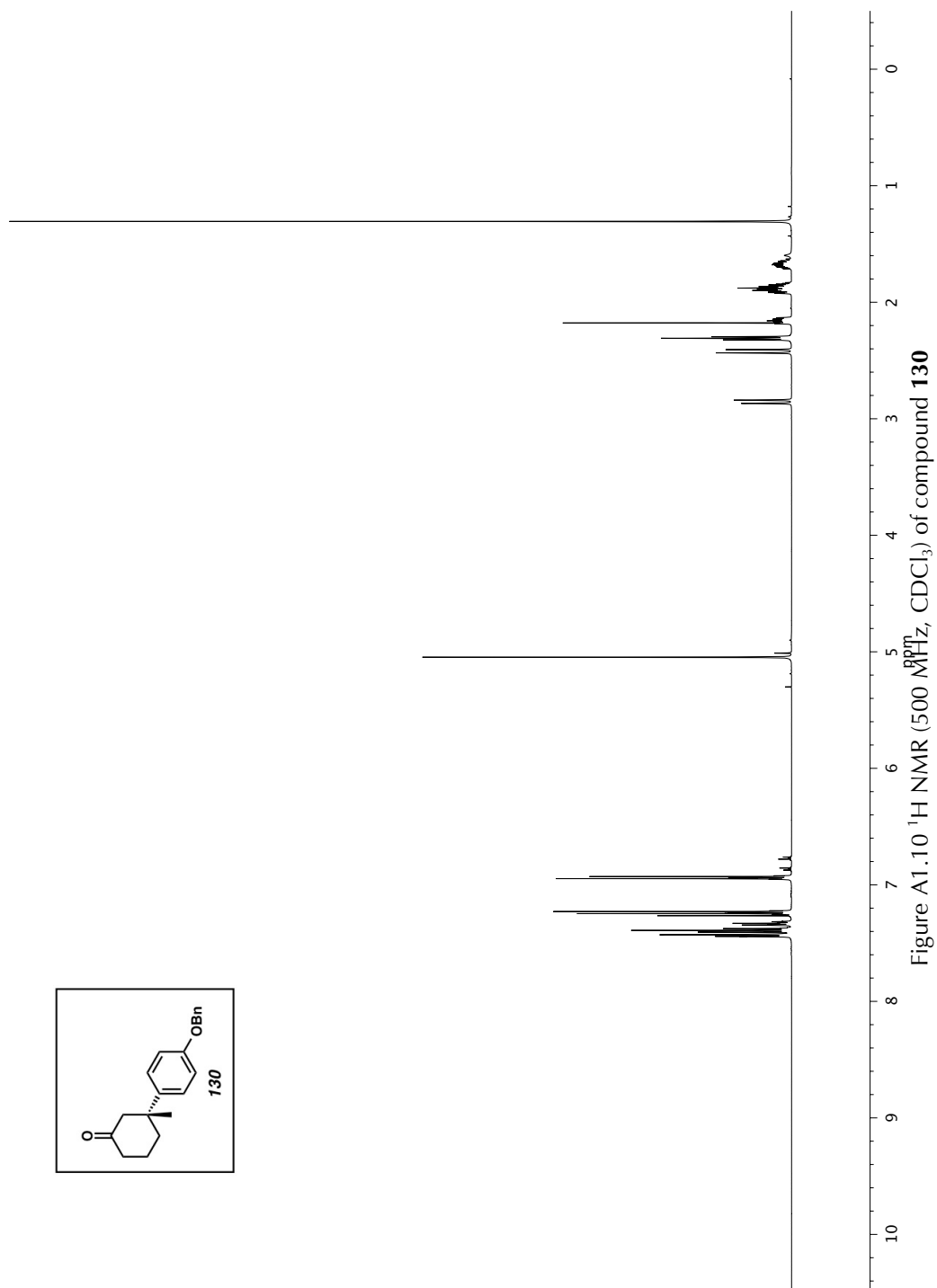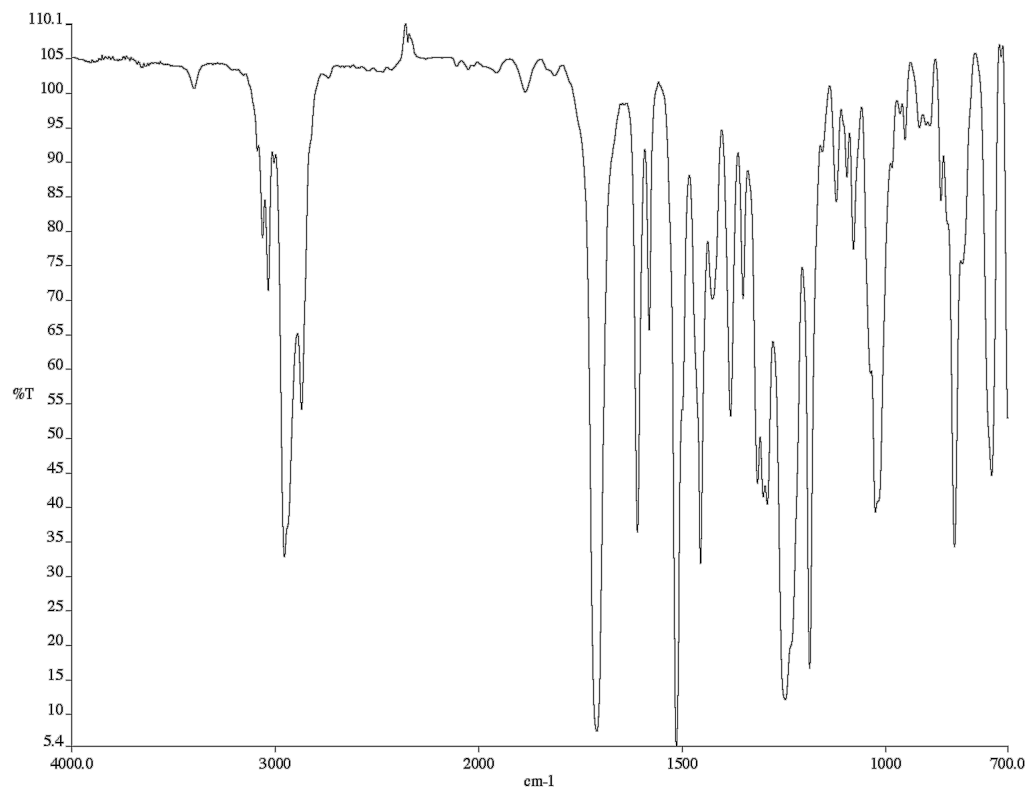
Figure A1.11 Infrared spectrum (Thin Film, NaCl) of compound **130**
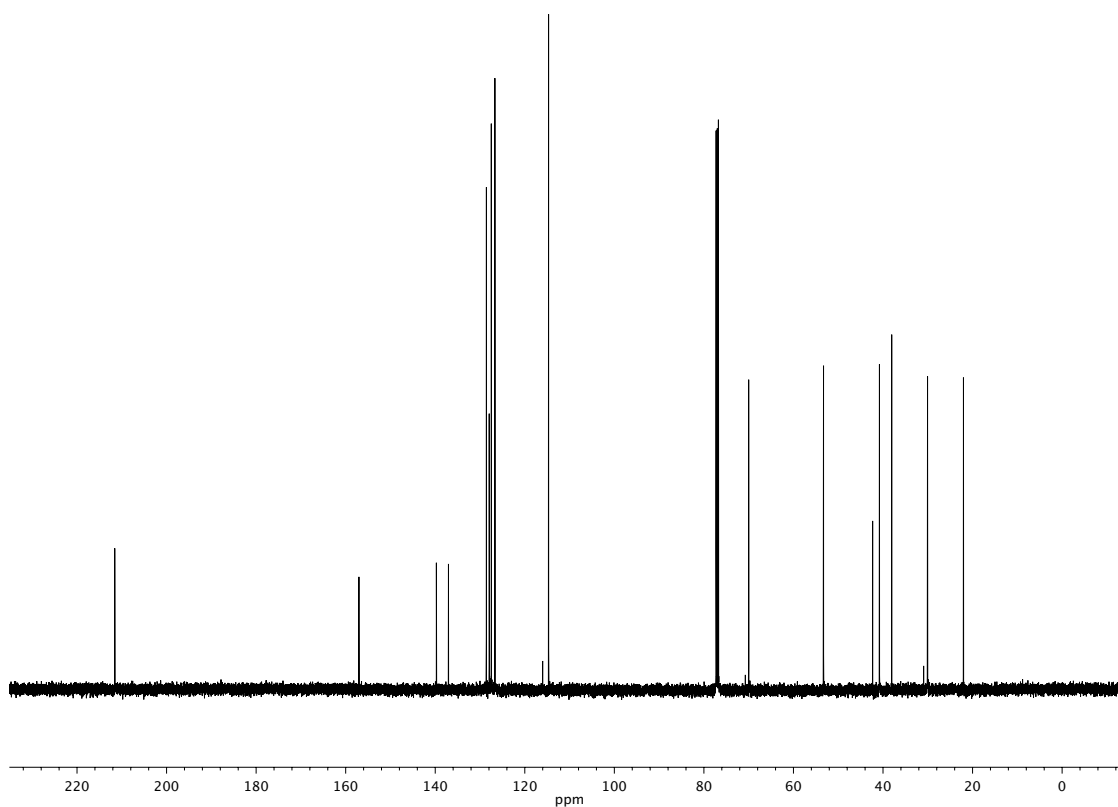
Figure A1.12 ^{13}C NMR (126 MHz, CDCl$_3$) of compound **130**
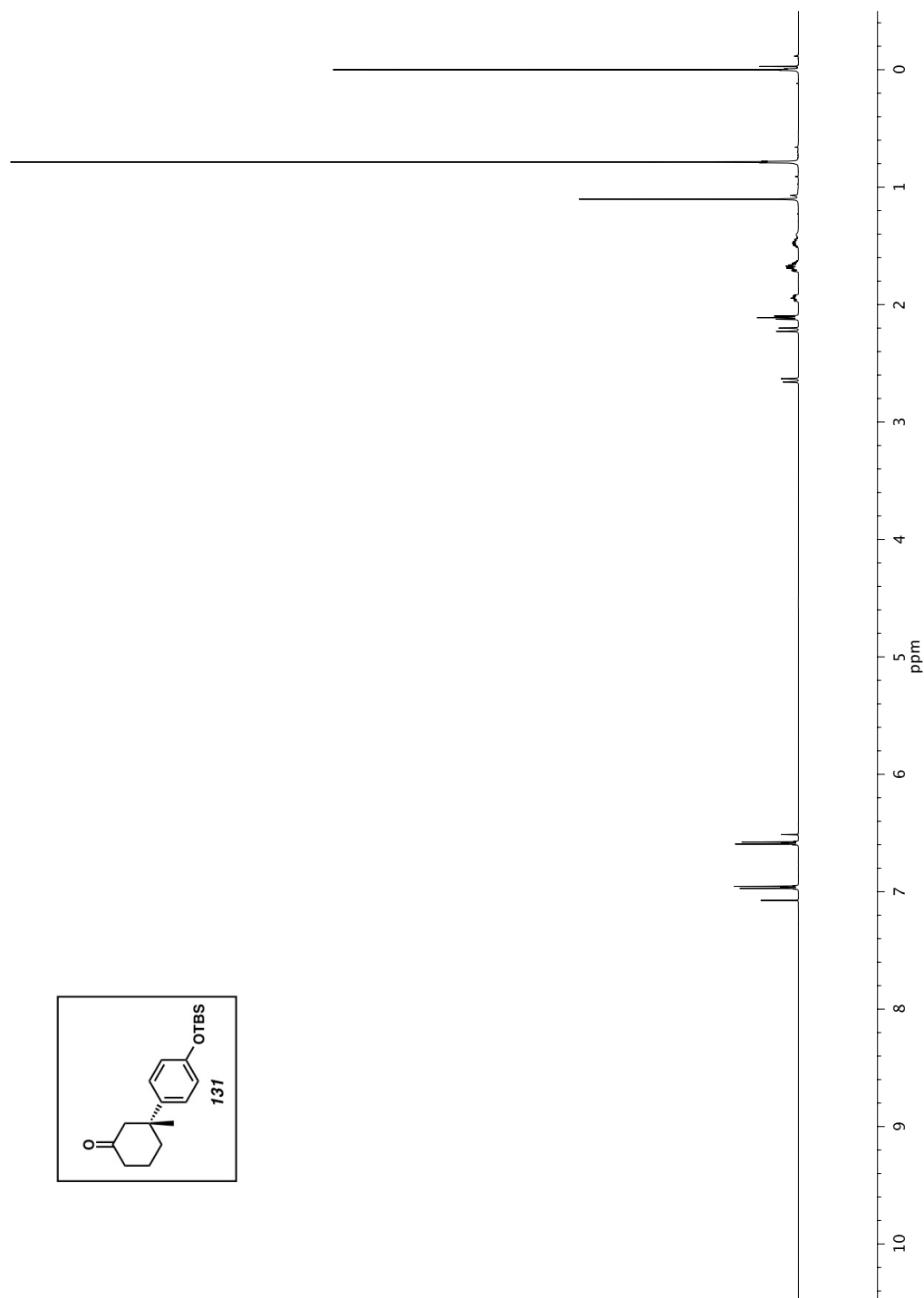
Figure A1.13 ^{1}H NMR (500 MHz, CDCl$_3$) of compound **131**
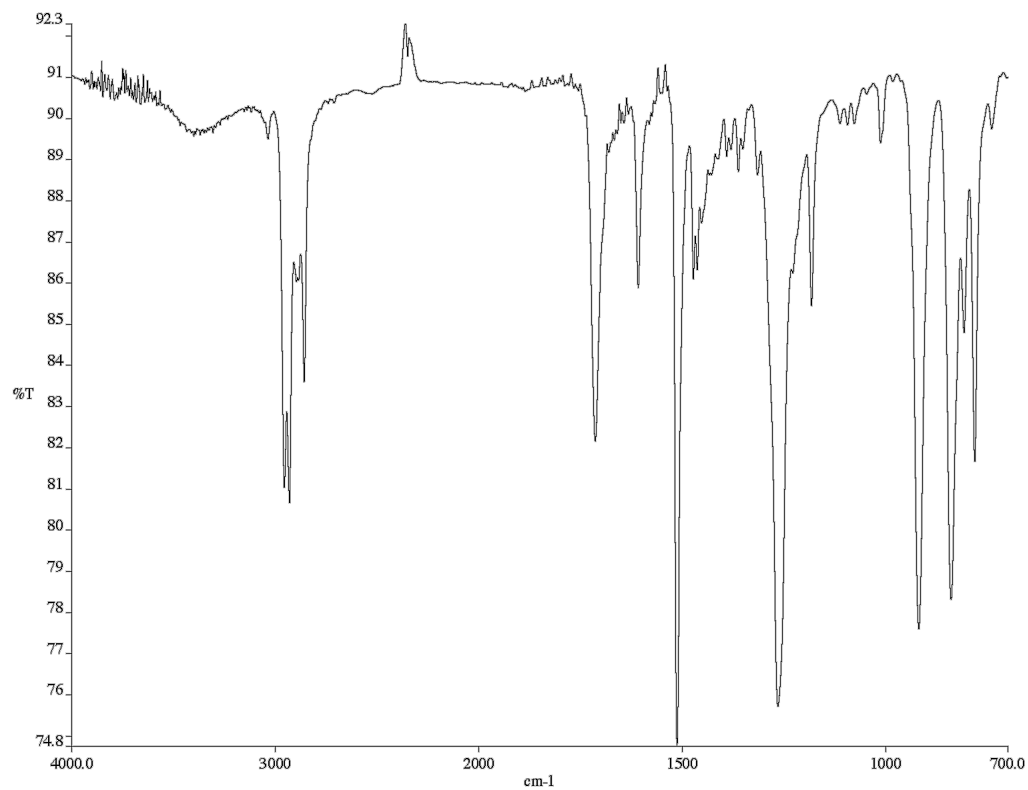
Figure A1.14 Infrared spectrum (Thin Film, NaCl) of compound **131**
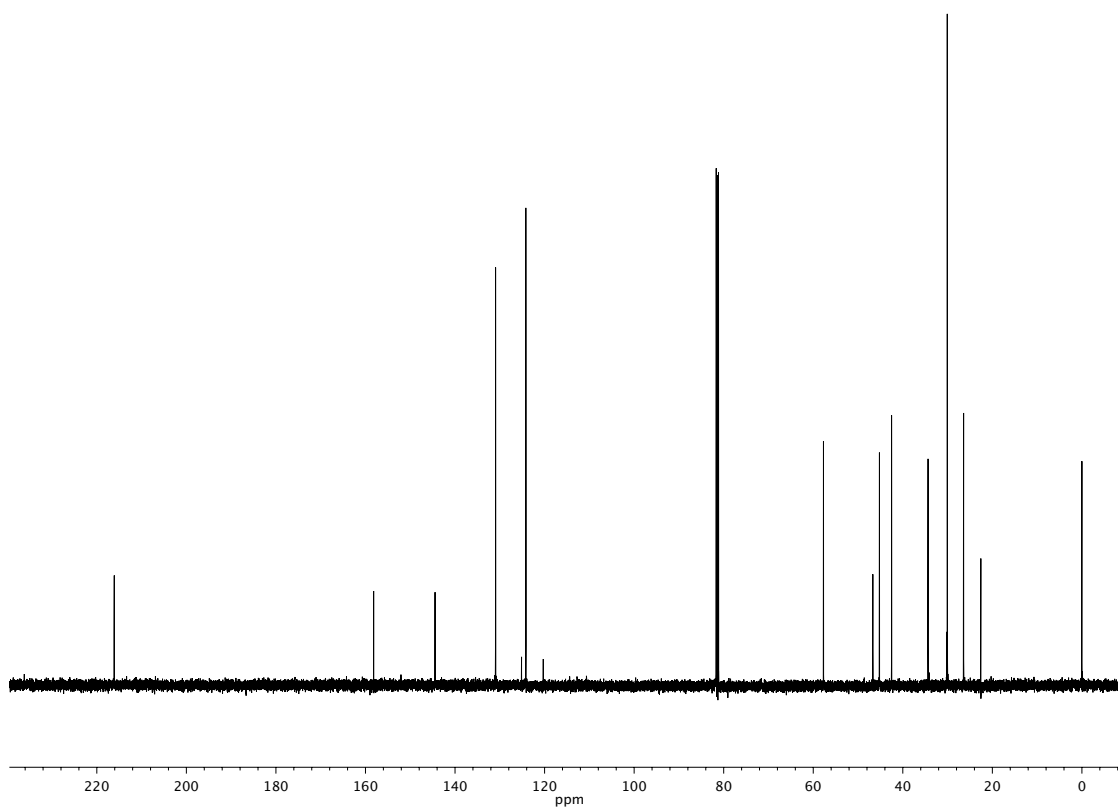
Figure A1.15 ^{13}C NMR (126 MHz, CDCl$_3$) of compound **131**
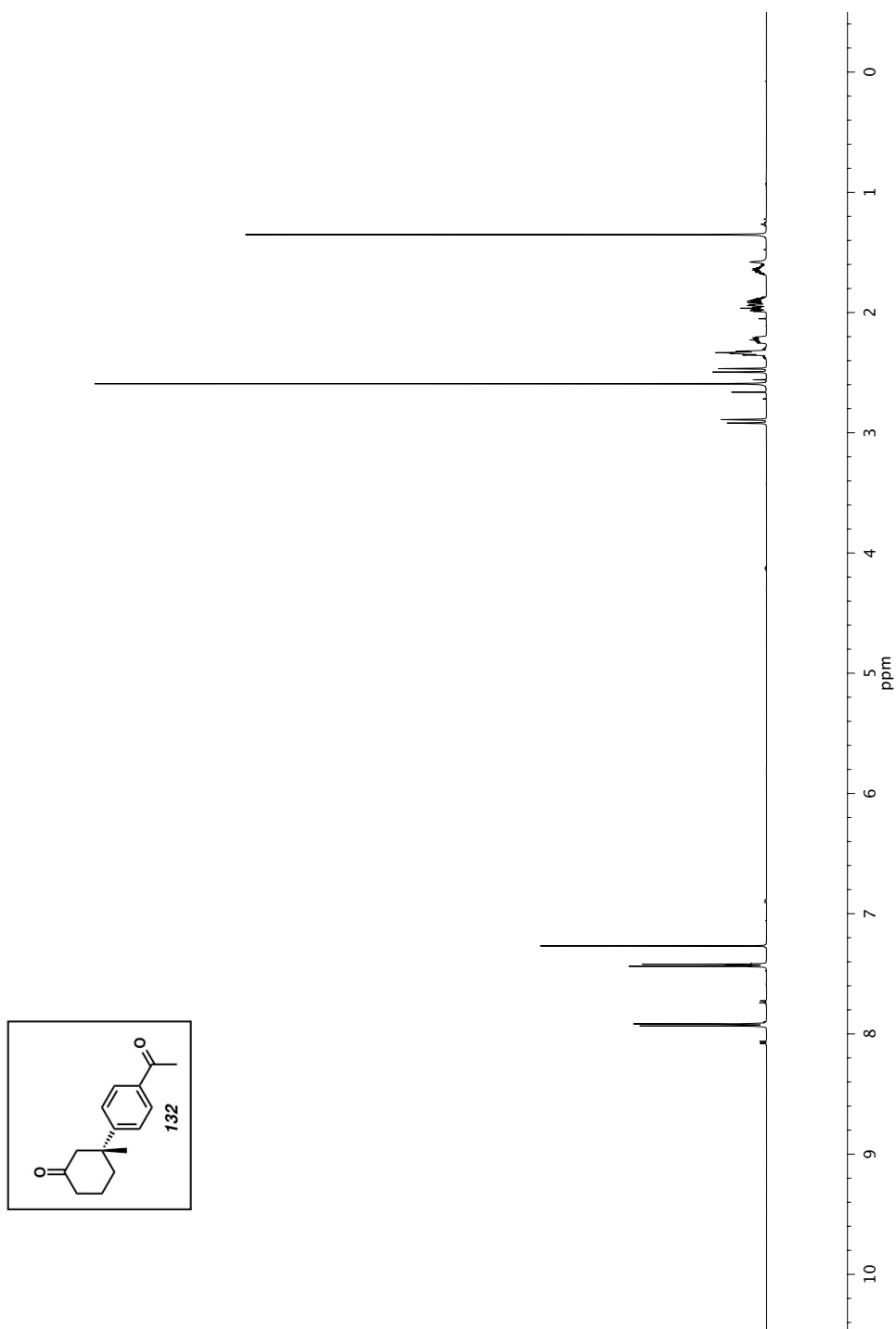
Figure A1.16 ^{1}H NMR (500 MHz, CDCl$_3$) of compound **132**
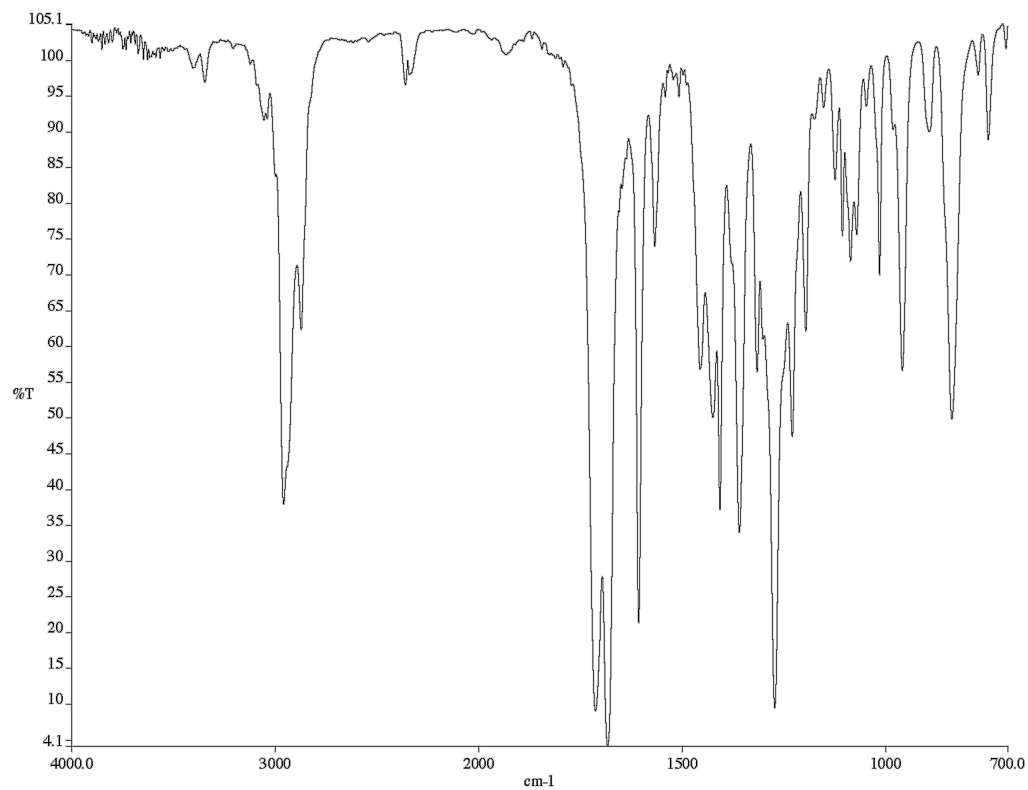
Figure A1.17 Infrared spectrum (Thin Film, NaCl) of compound **132**
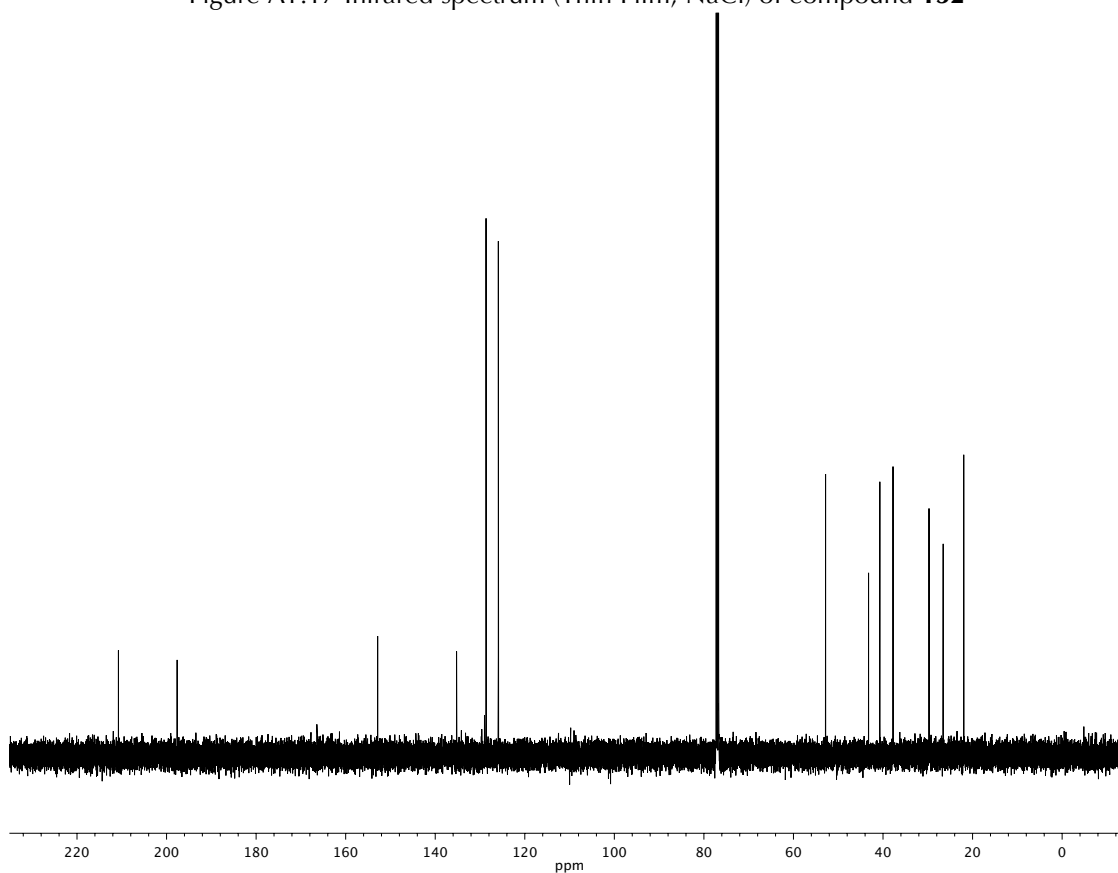
Figure A1.18 ^{13}C NMR (126 MHz, CDCl$_3$) of compound **132**
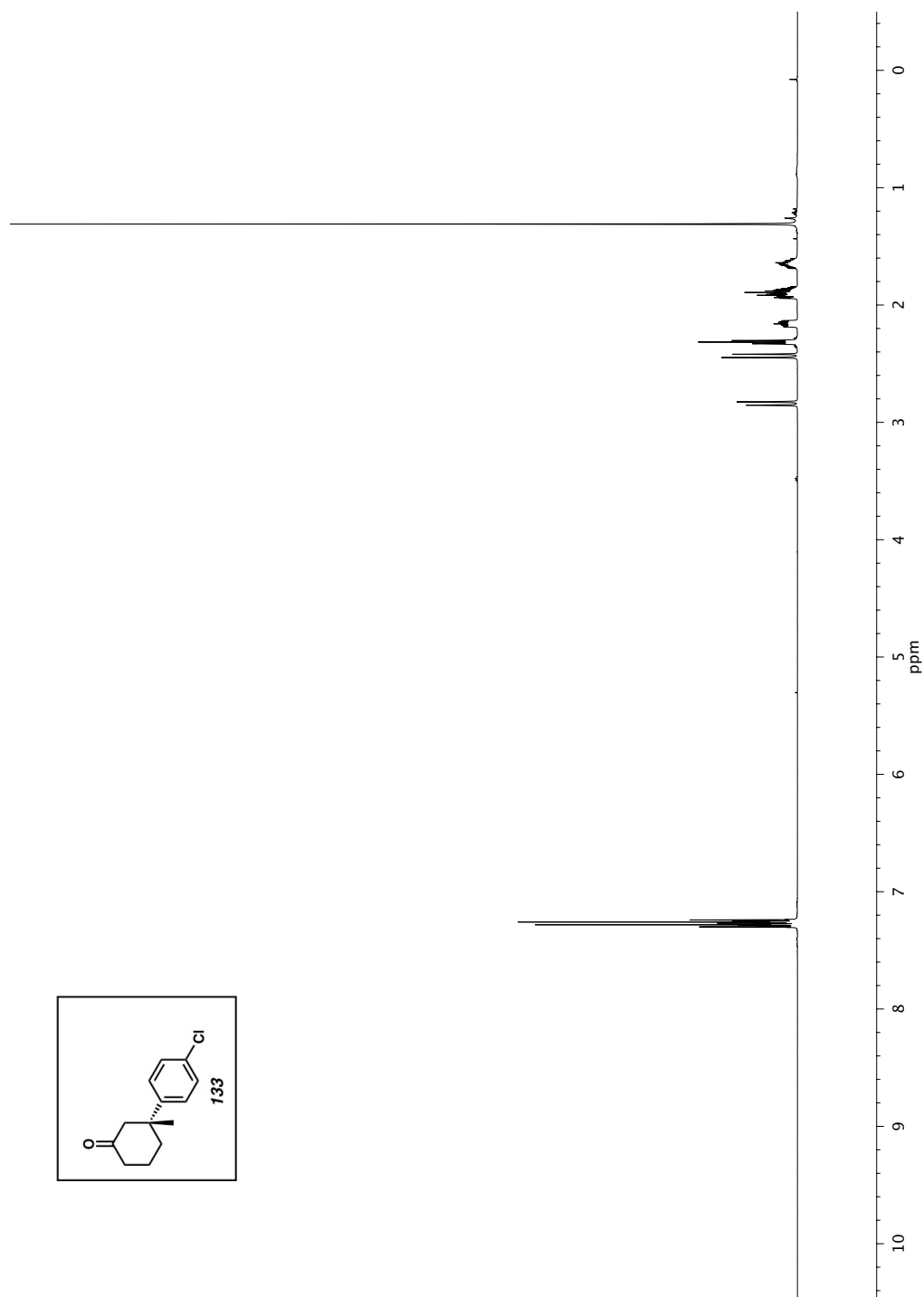
Figure A1.19 ^{1}H NMR (500 MHz, CDCl$_3$) of compound **133**
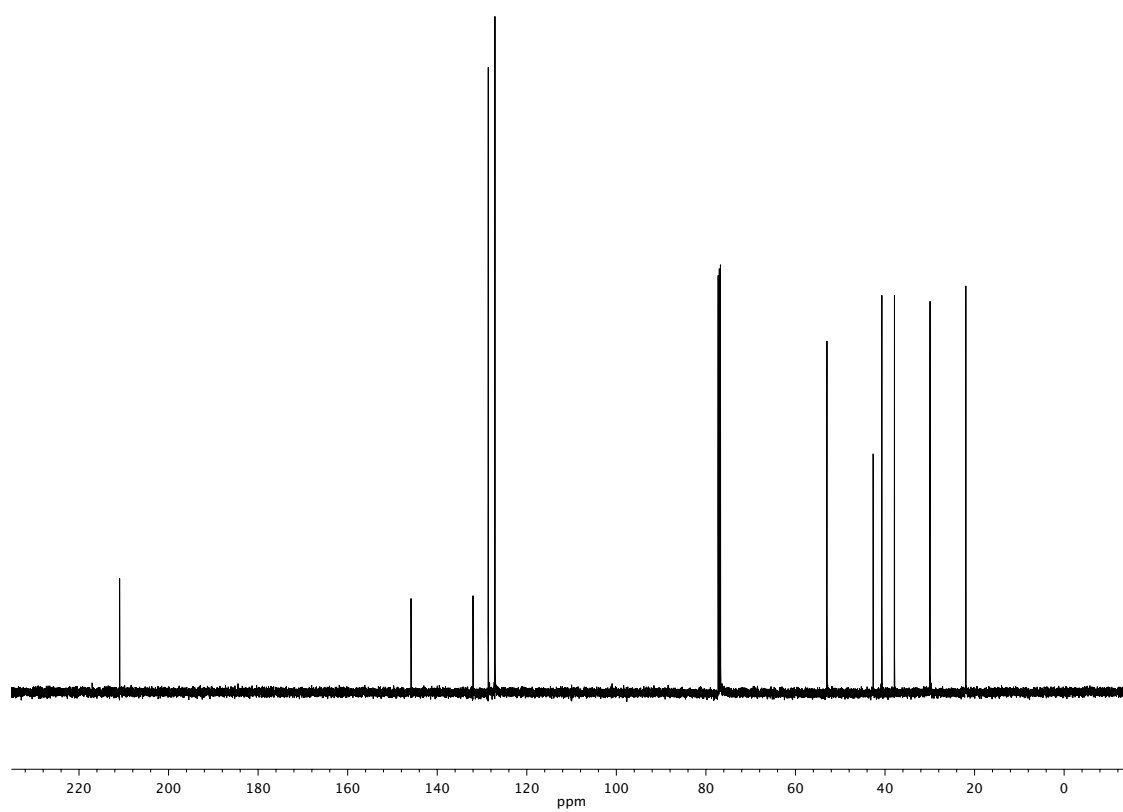
Figure A1.20 ^{13}C NMR (126 MHz, CDCl$_3$) of compound **133**
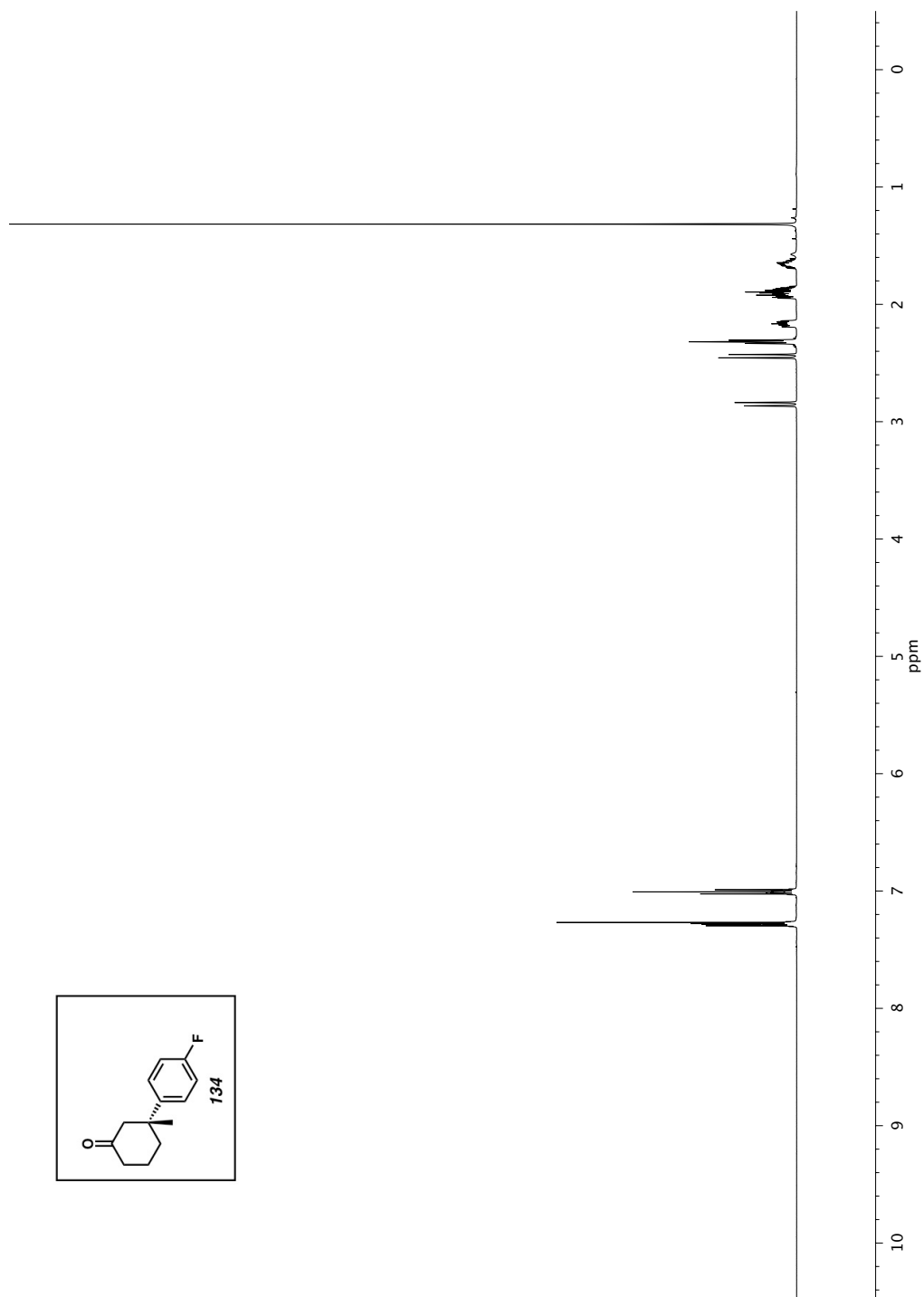
Figure A1.21 ^{1}H NMR (500 MHz, CDCl$_3$) of compound **134**
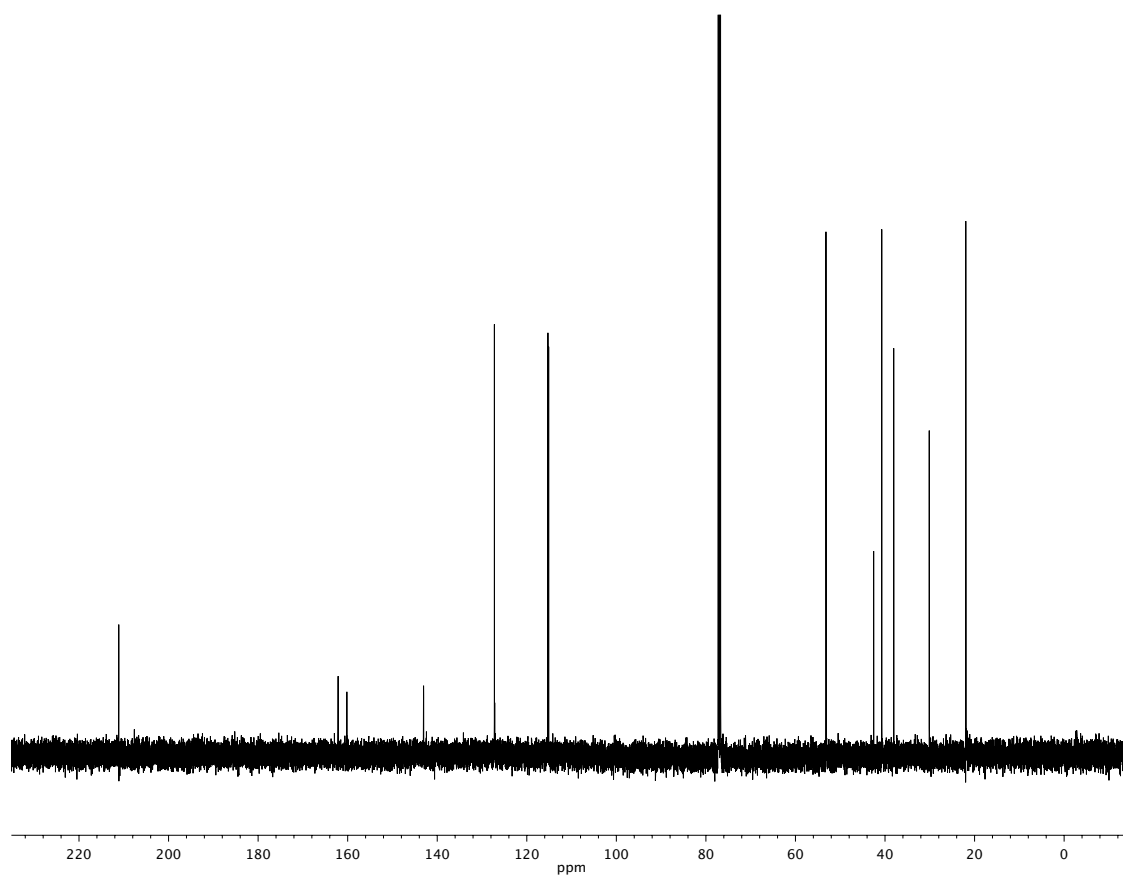
Figure A1.22 ^{13}C NMR (126 MHz, CDCl$_3$) of compound **134**
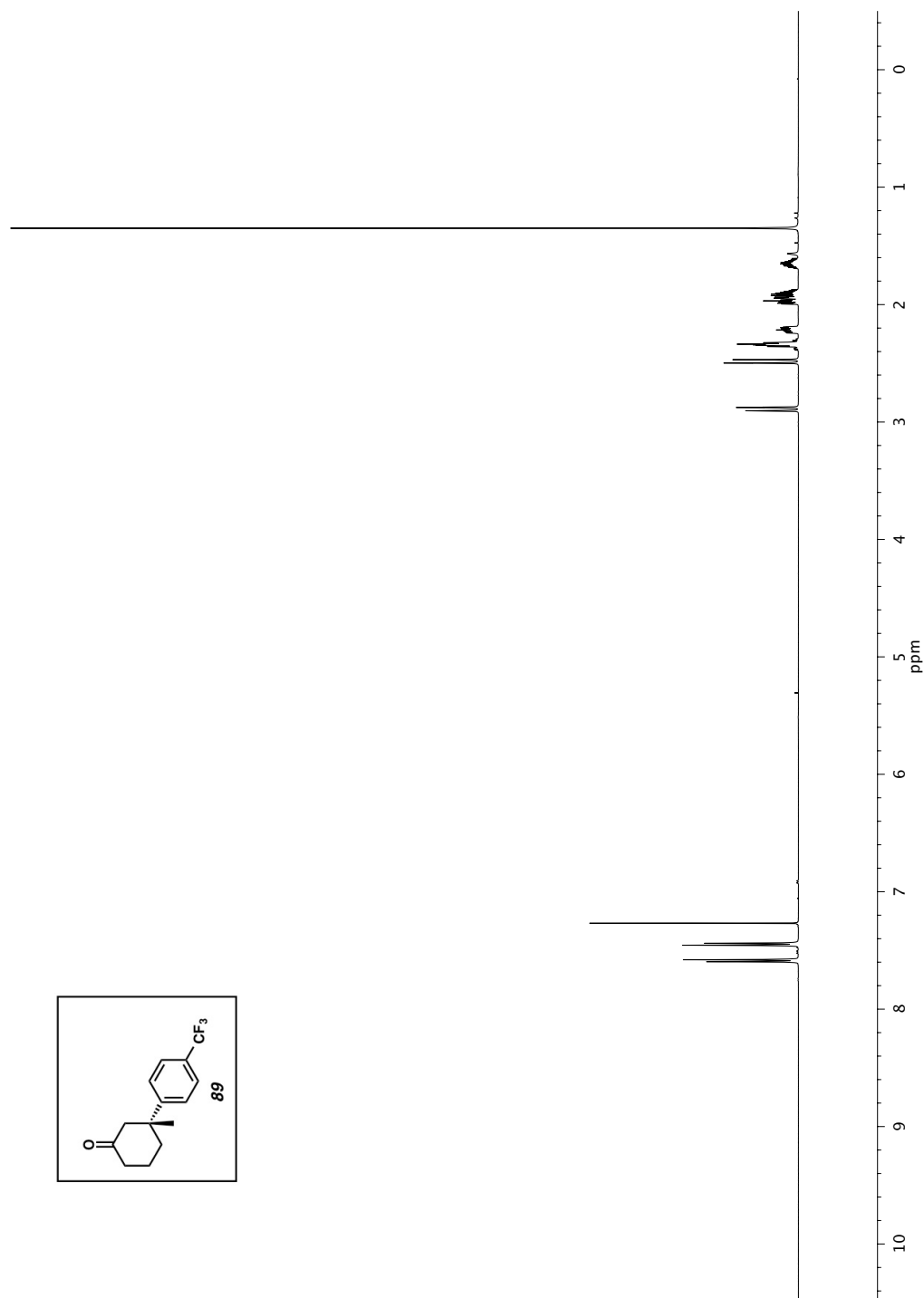
Figure A1.23 ^{1}H NMR (500 MHz, CDCl$_3$) of compound **89**
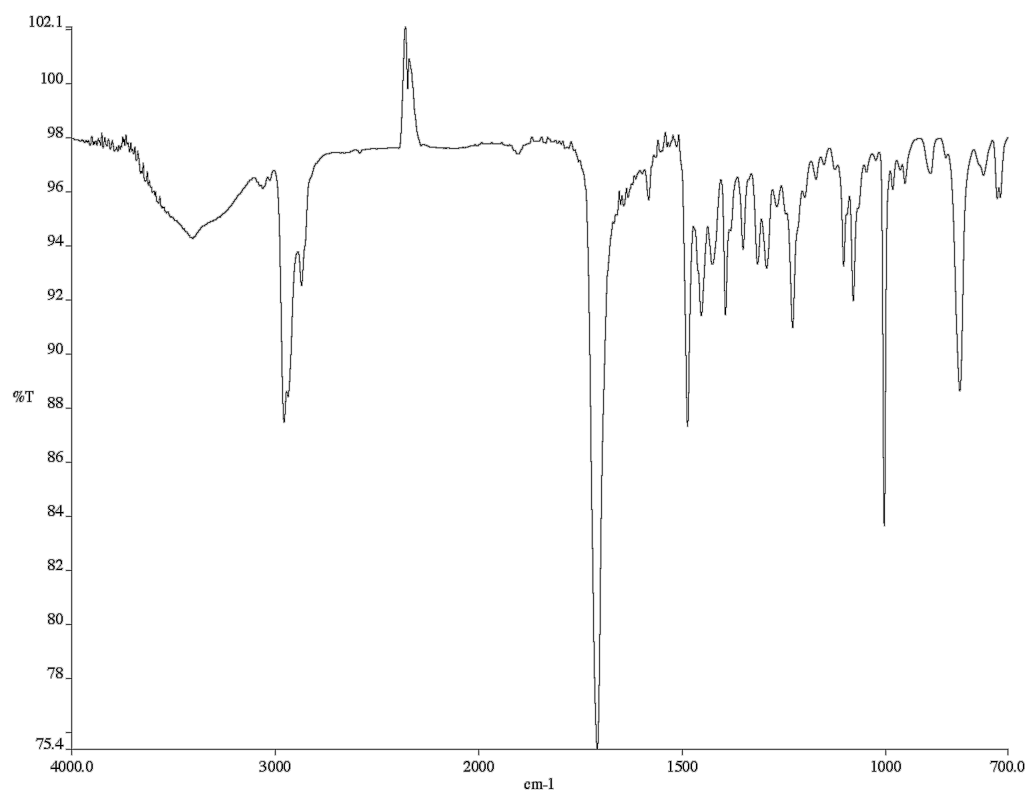
Figure A1.24 Infrared spectrum (Thin Film, NaCl) of compound **89**
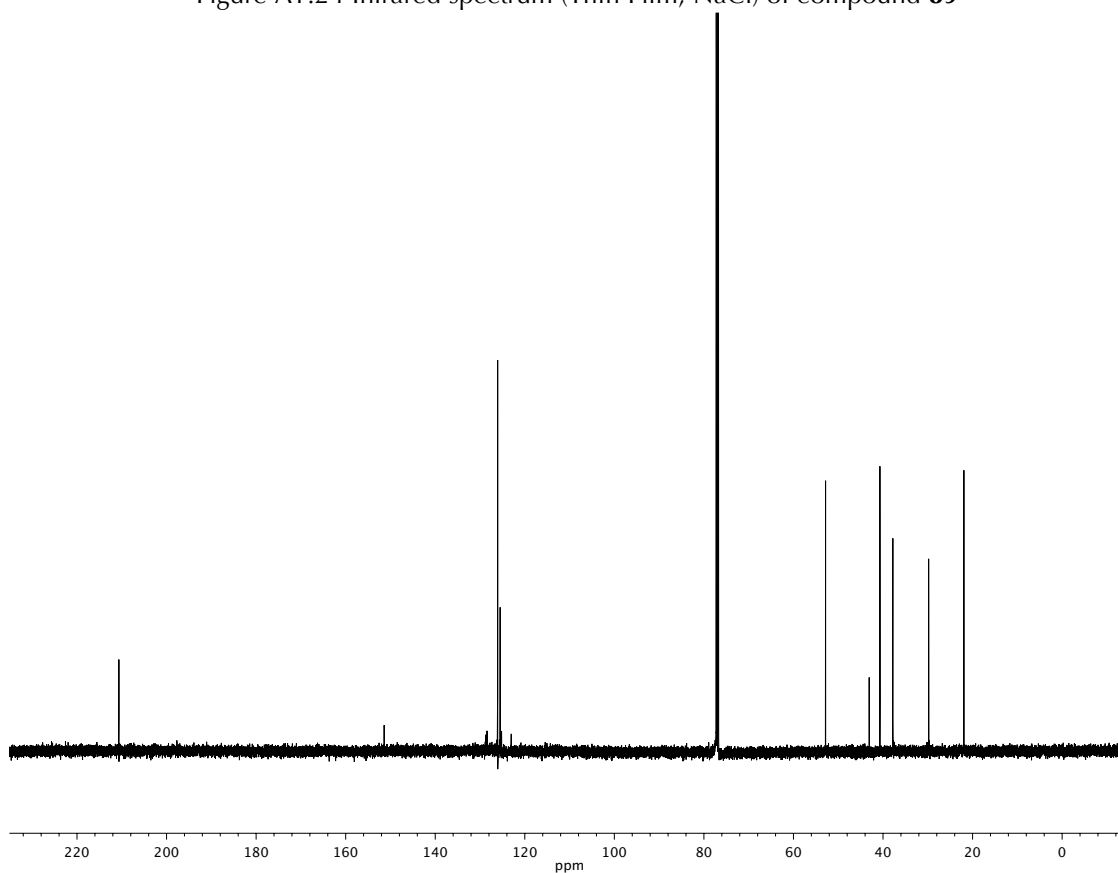
Figure A1.25 ^{13}C NMR (126 MHz, CDCl$_3$) of compound **89**
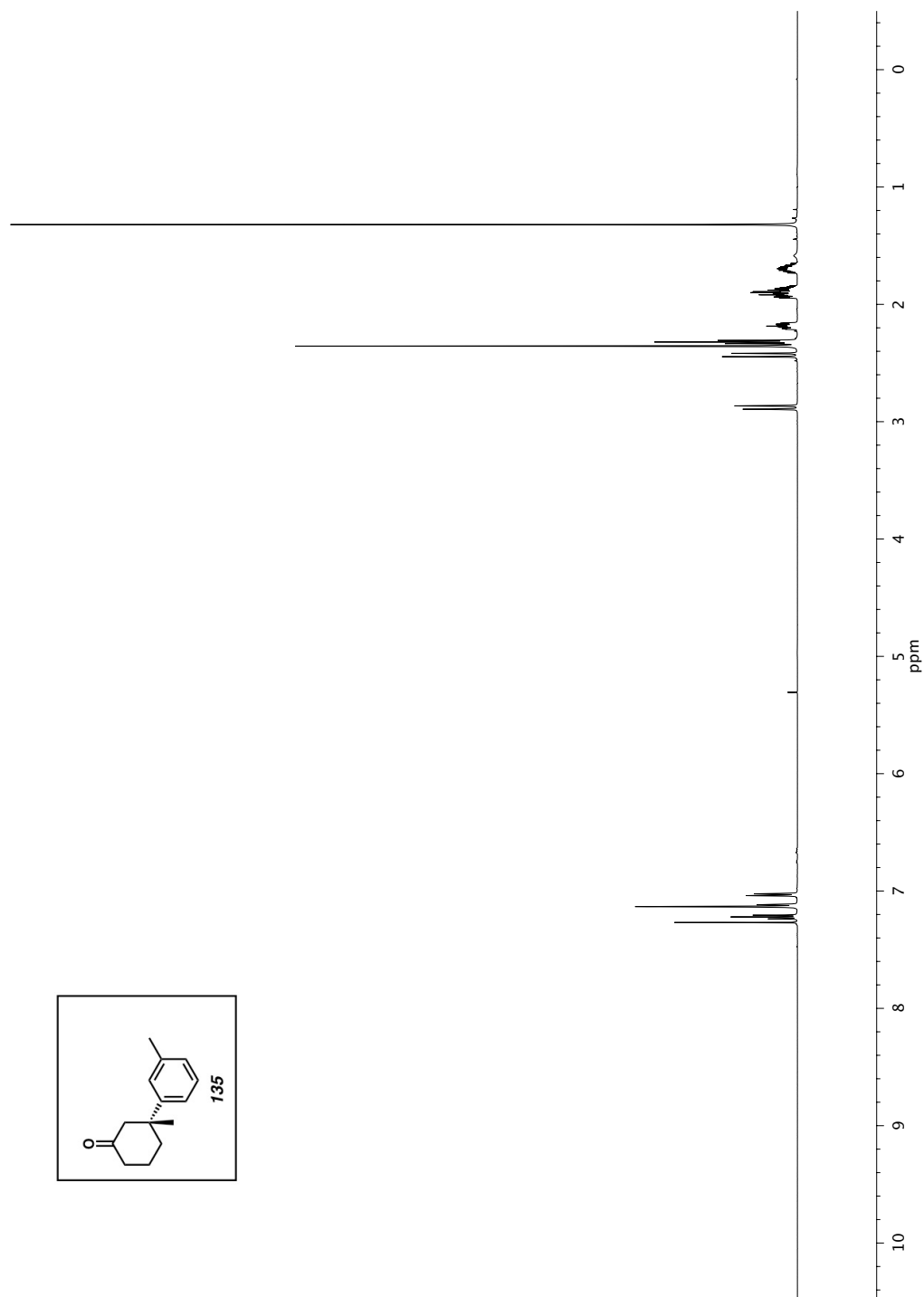
Figure A1.26 ^{1}H NMR (500 MHz, CDCl$_3$) of compound **135**
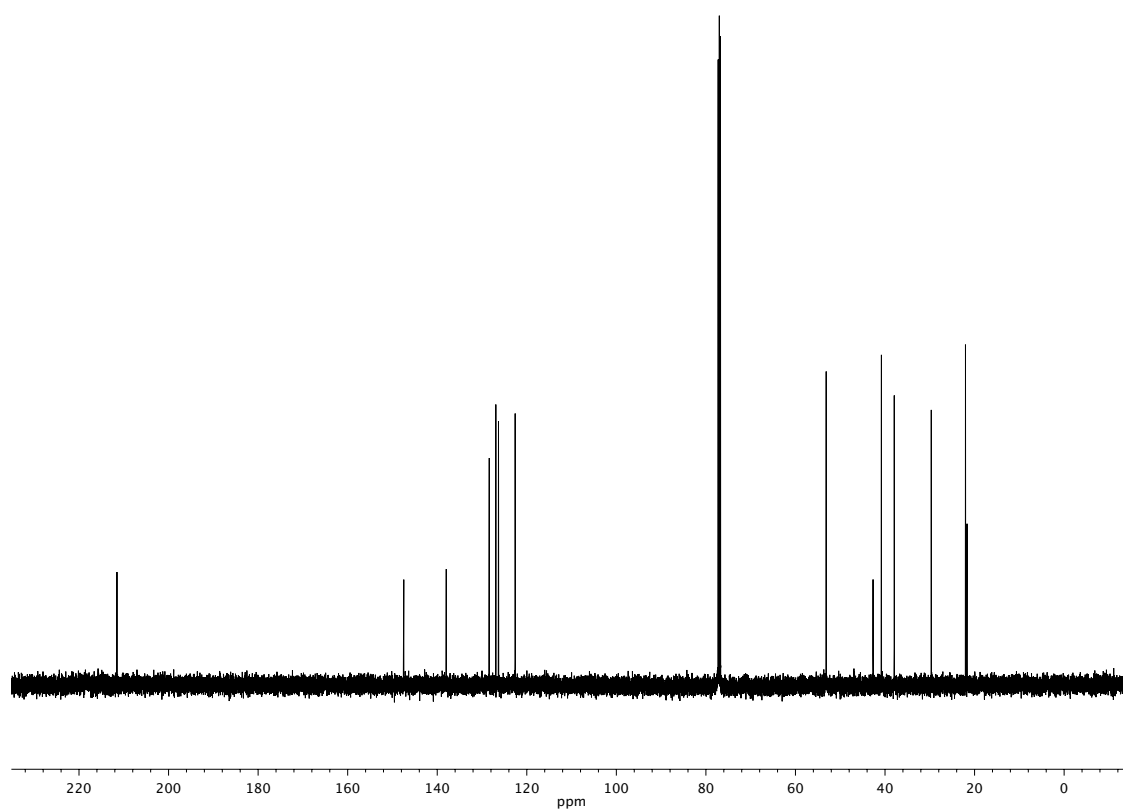
Figure A1.27 ^{13}C NMR (126 MHz, CDCl$_3$) of compound **135**
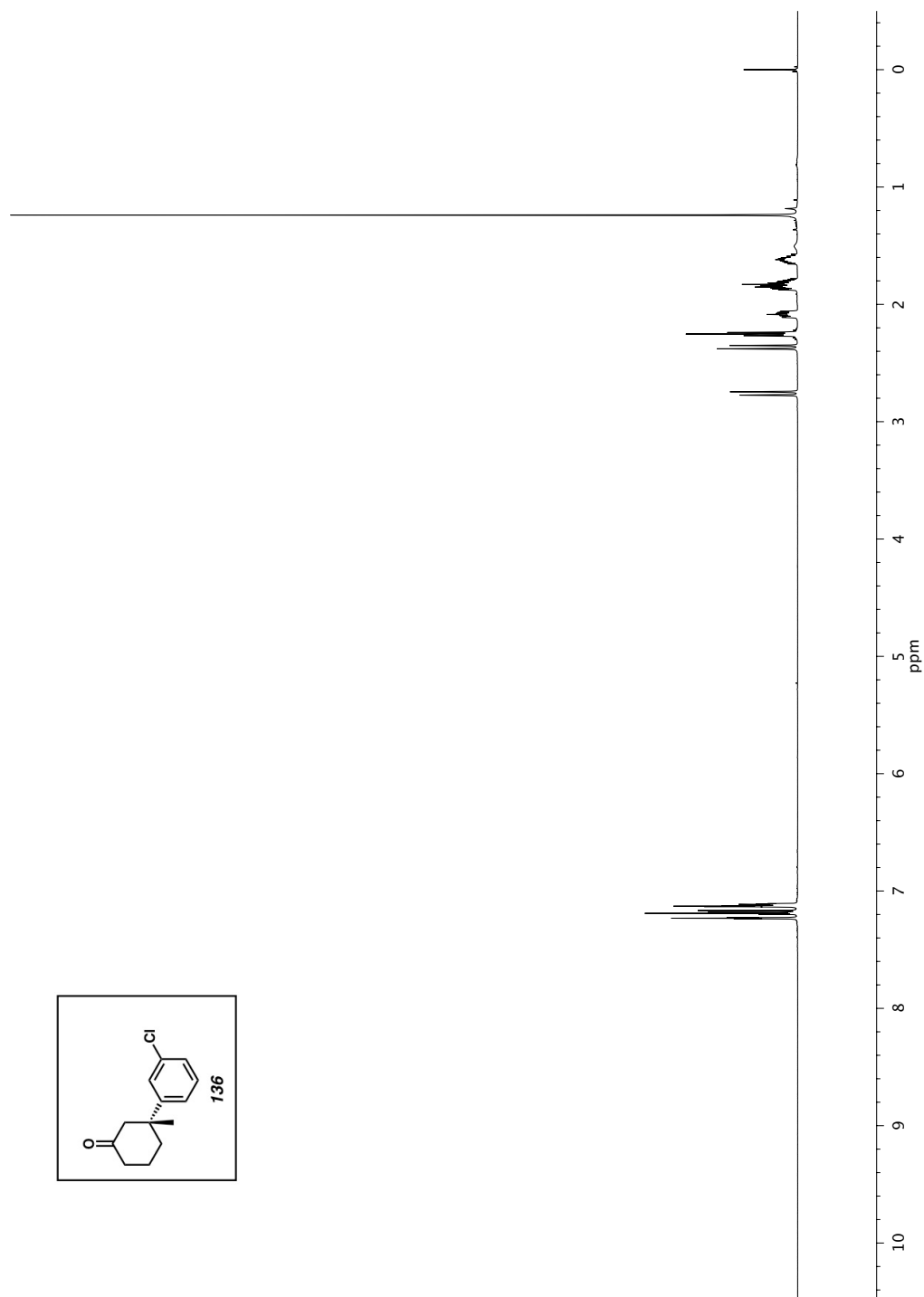
Figure A1.28 ^{1}H NMR (500 MHz, CDCl$_3$) of compound **136**

Figure A1.24 Infrared spectrum (Thin Film, NaCl) of compound **89**
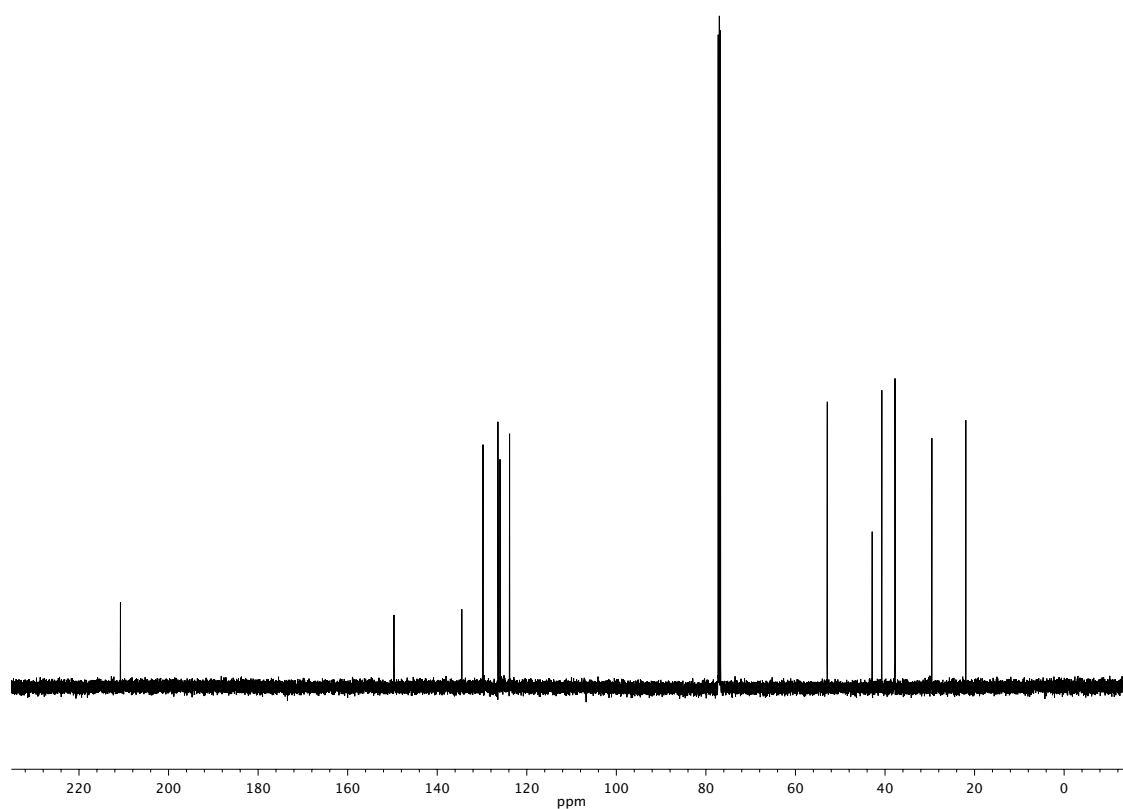
Figure A1.29 ^{13}C NMR (126 MHz, CDCl$_3$) of compound **136**
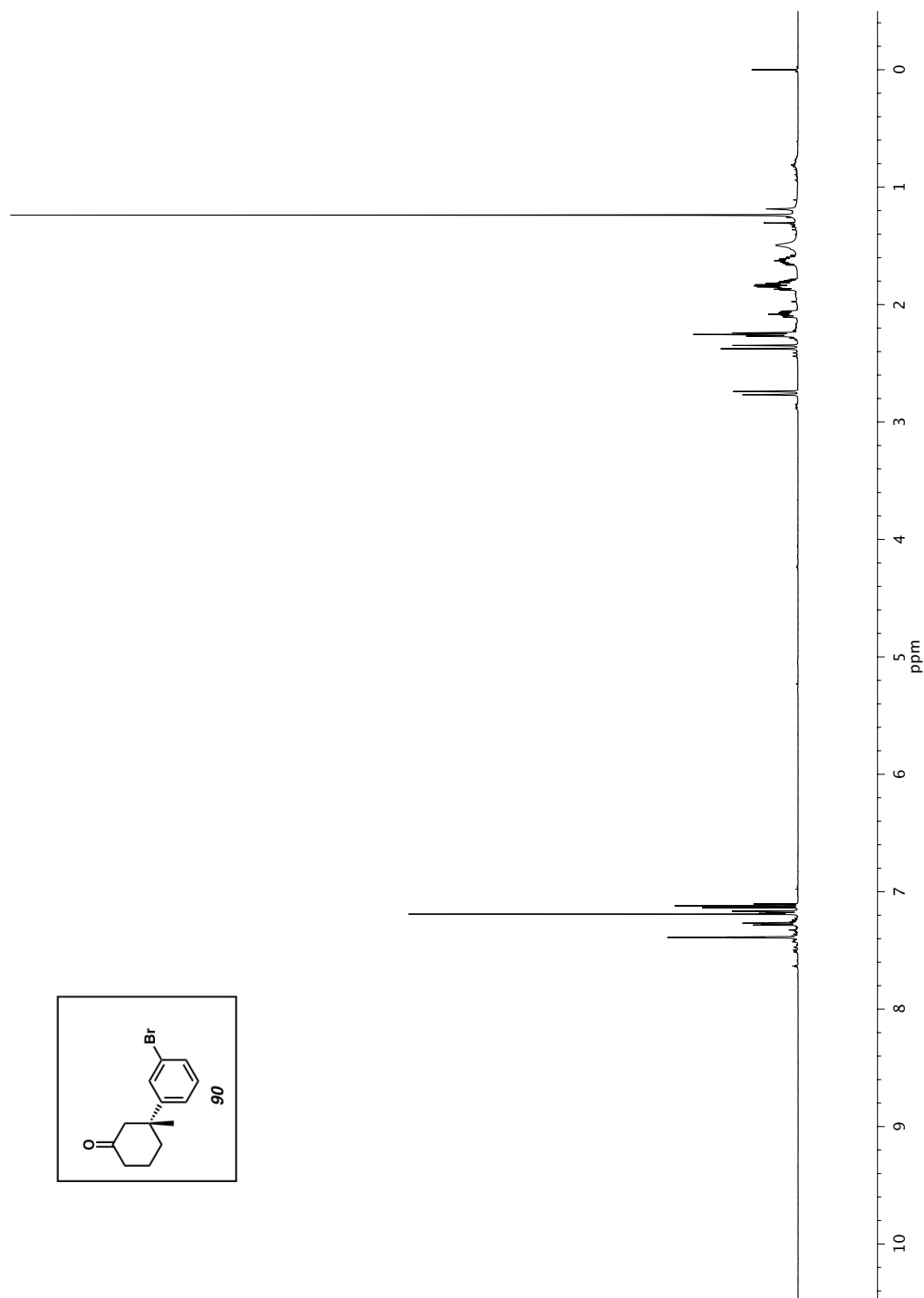
Figure A1.30 ^{1}H NMR (500 MHz, CDCl$_3$) of compound **90**
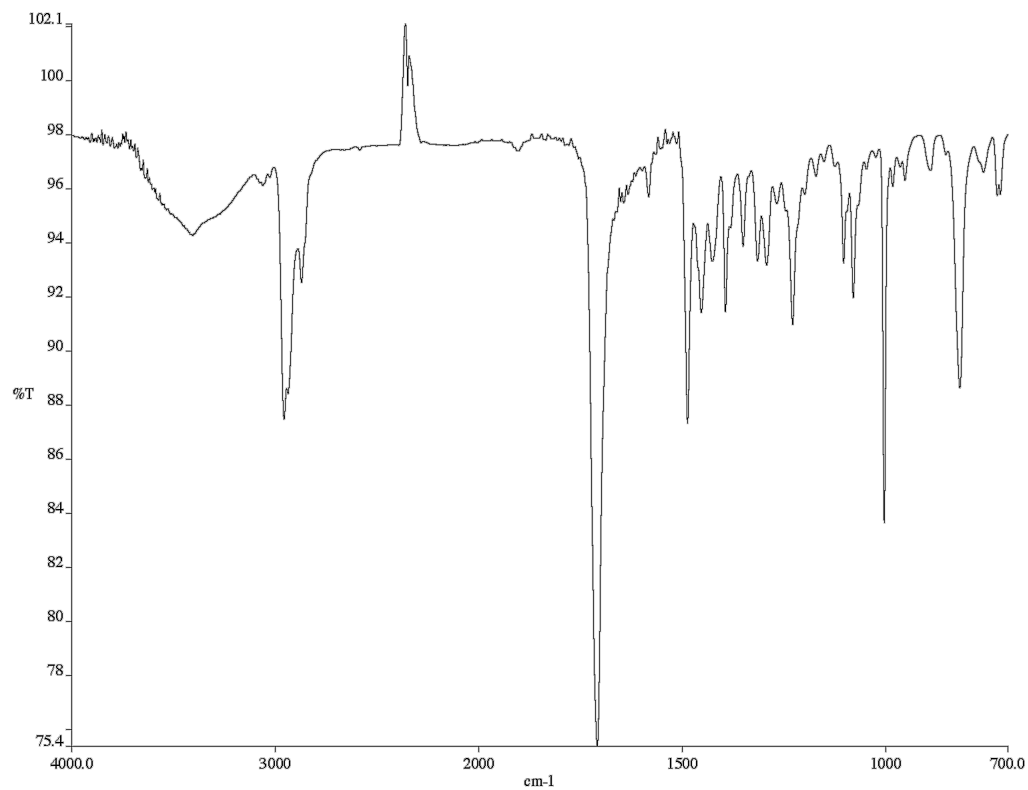
Figure A1.31 Infrared spectrum (Thin Film, NaCl) of compound **90**
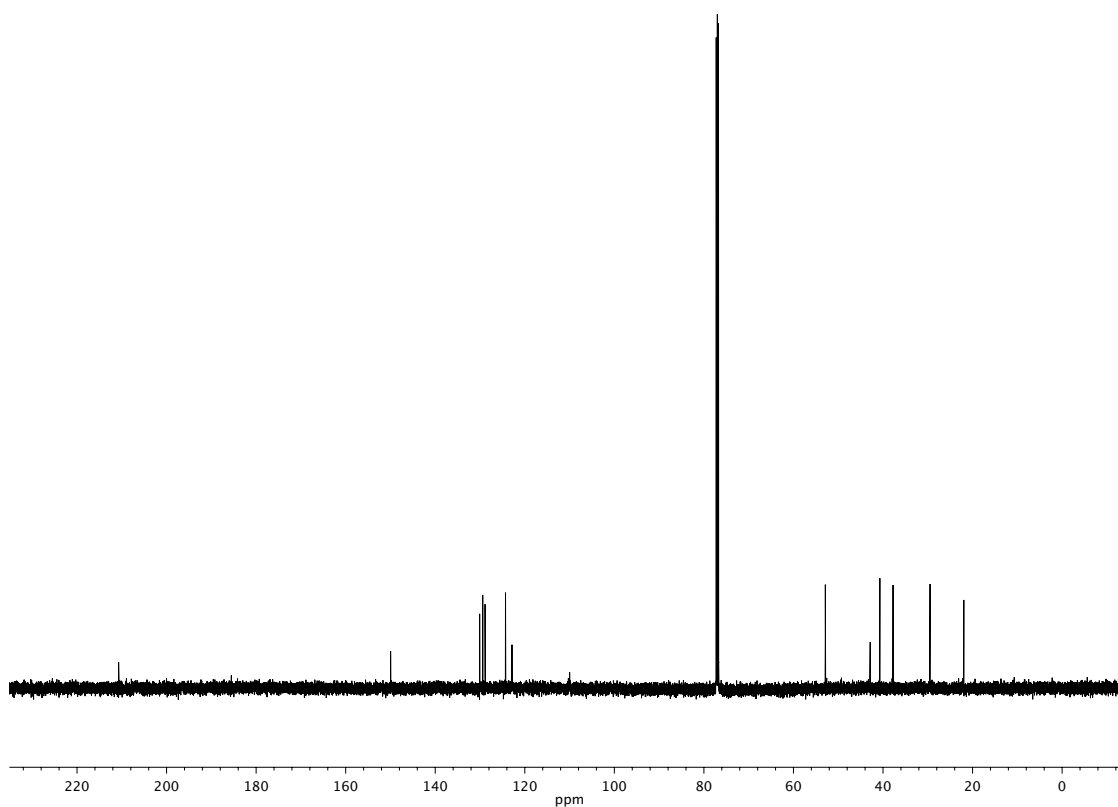
Figure A1.32 ^{13}C NMR (126 MHz, CDCl$_3$) of compound **90**
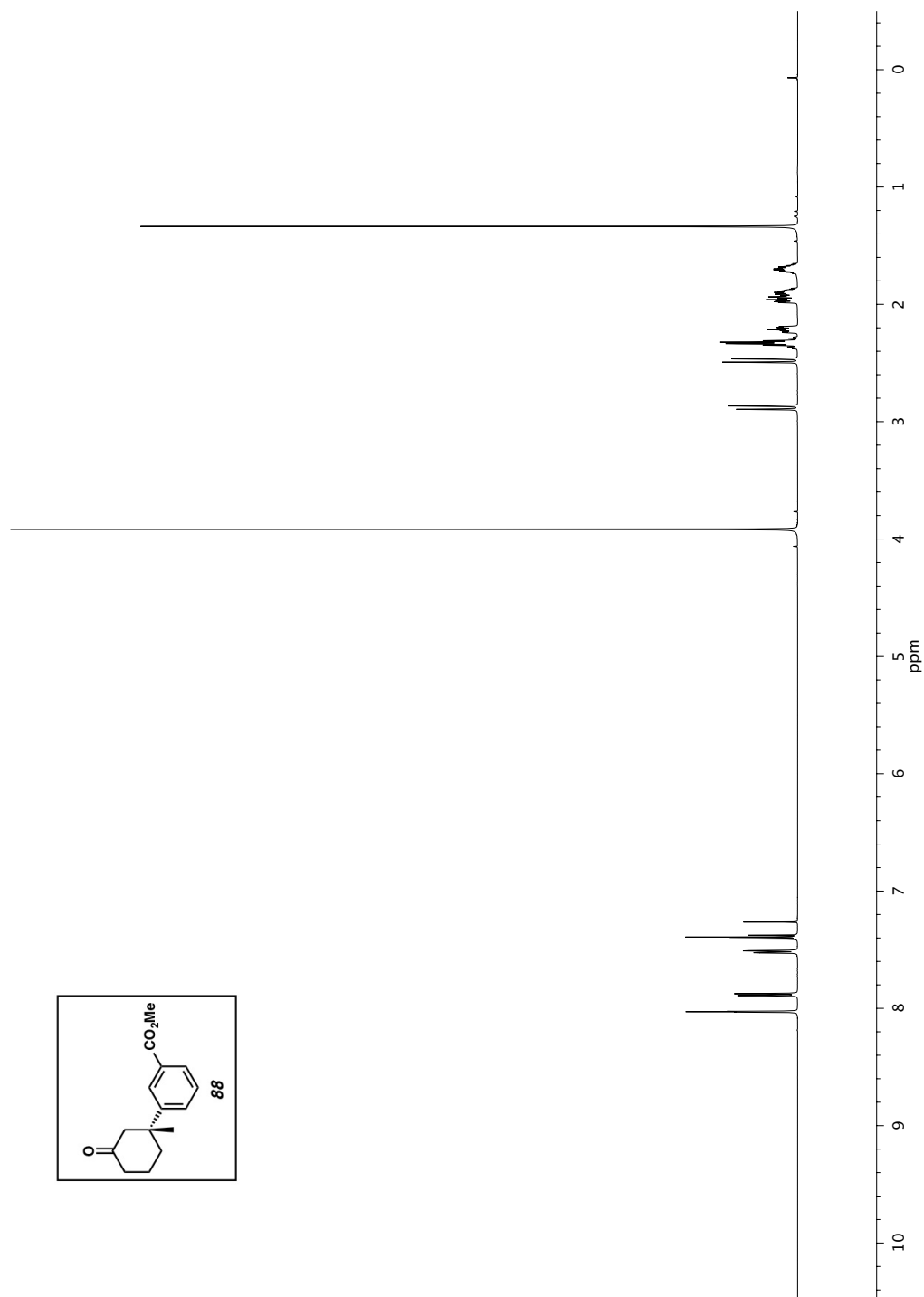
Figure A1.33 ^{1}H NMR (500 MHz, CDCl$_3$) of compound **88**
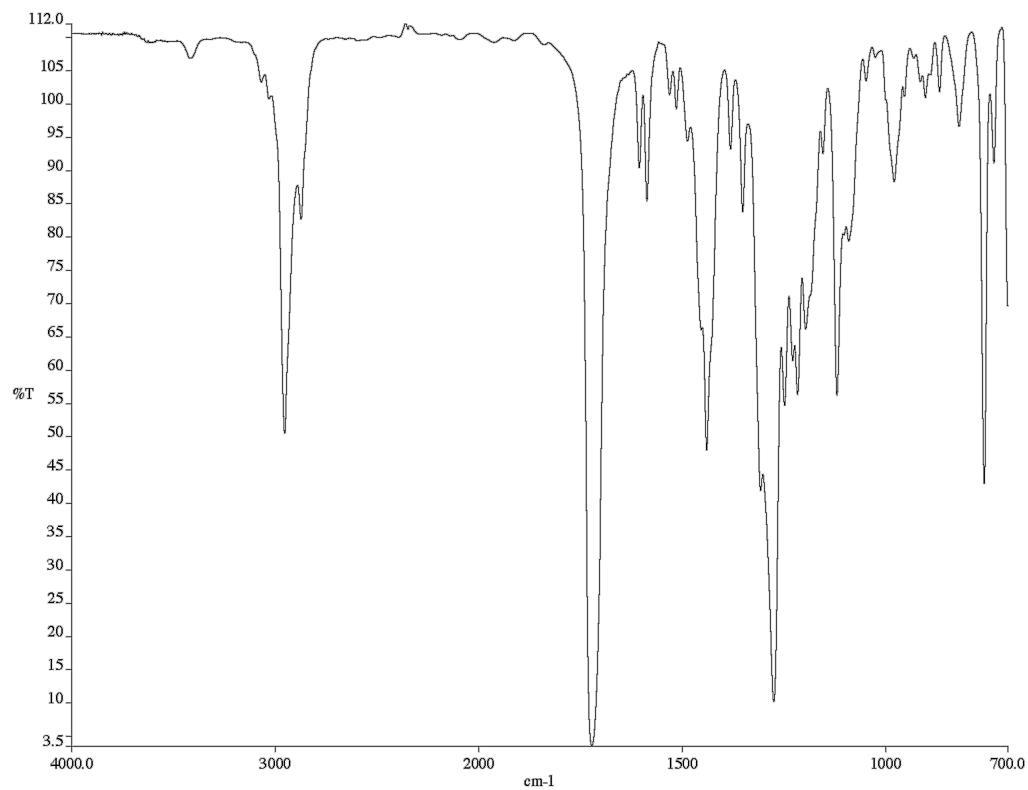
Figure A1.34 Infrared spectrum (Thin Film, NaCl) of compound **88**
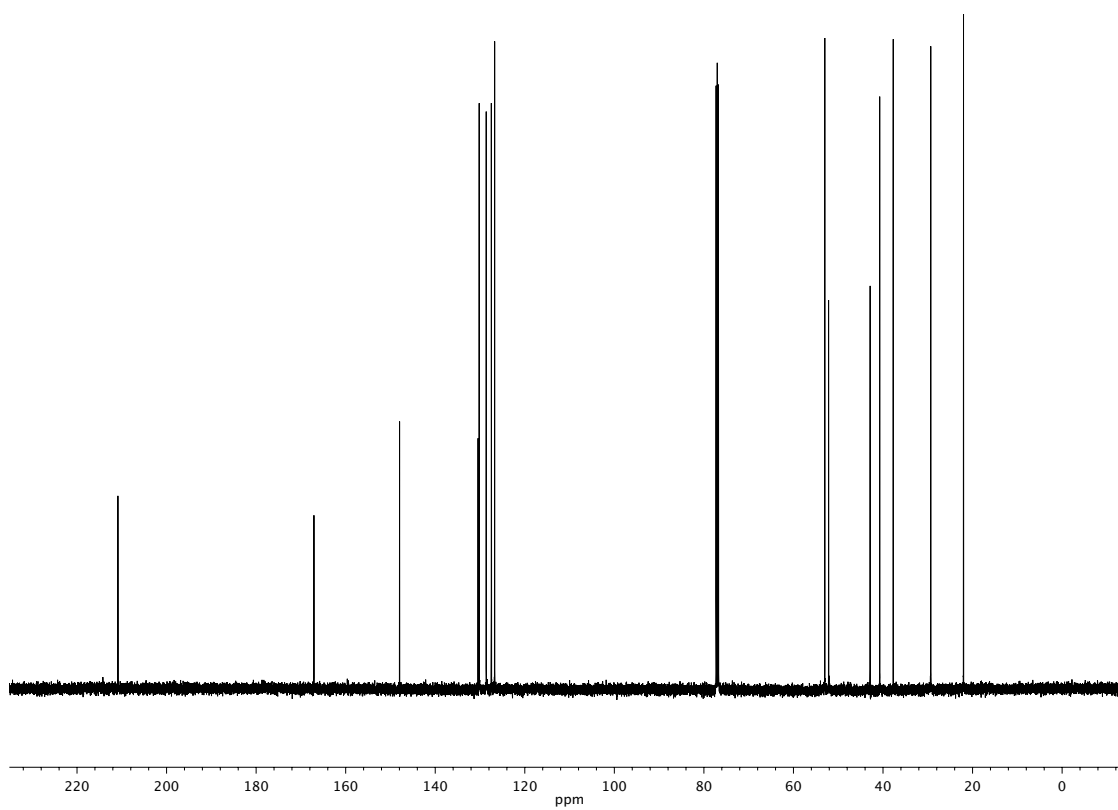
Figure A1.35 ^{13}C NMR (126 MHz, CDCl$_3$) of compound **88**

Figure A1.36 ^{1}H NMR (500 MHz, CDCl$_3$) of compound **137**
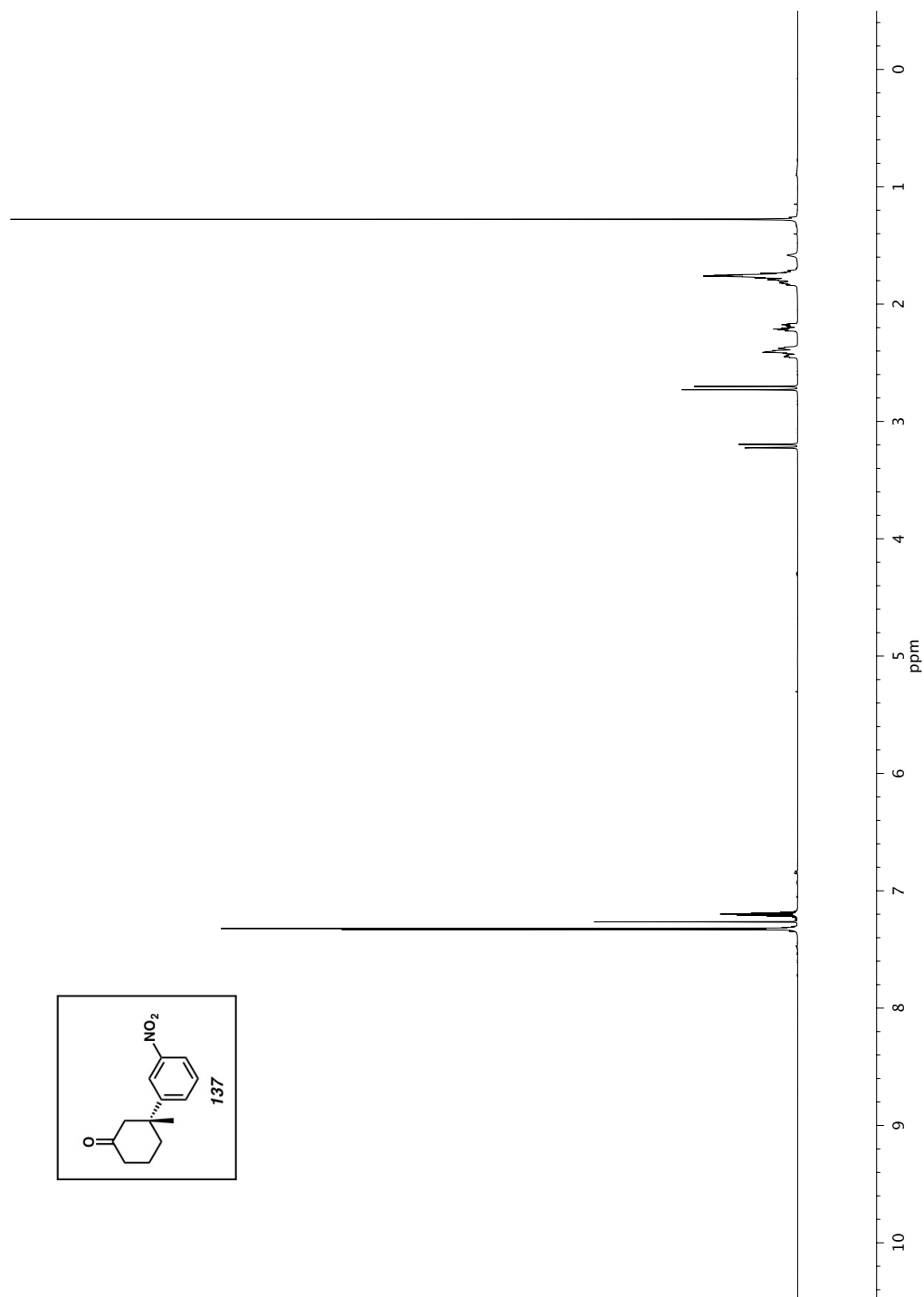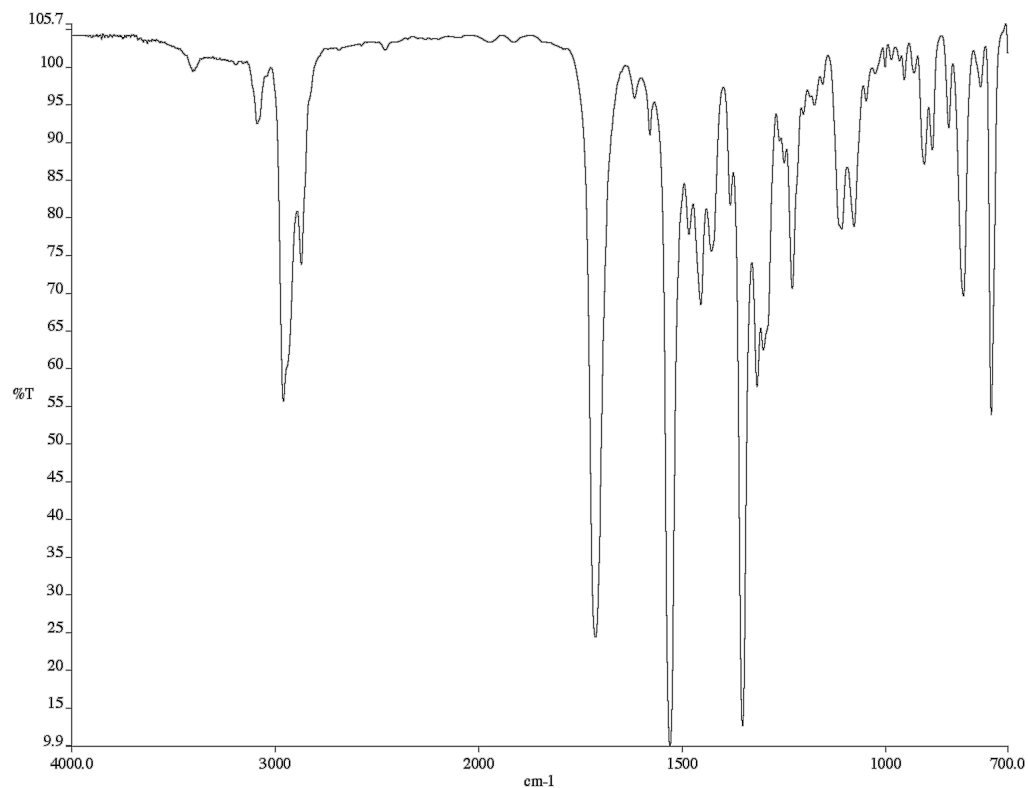
Figure A1.37 Infrared spectrum (Thin Film, NaCl) of compound **137**
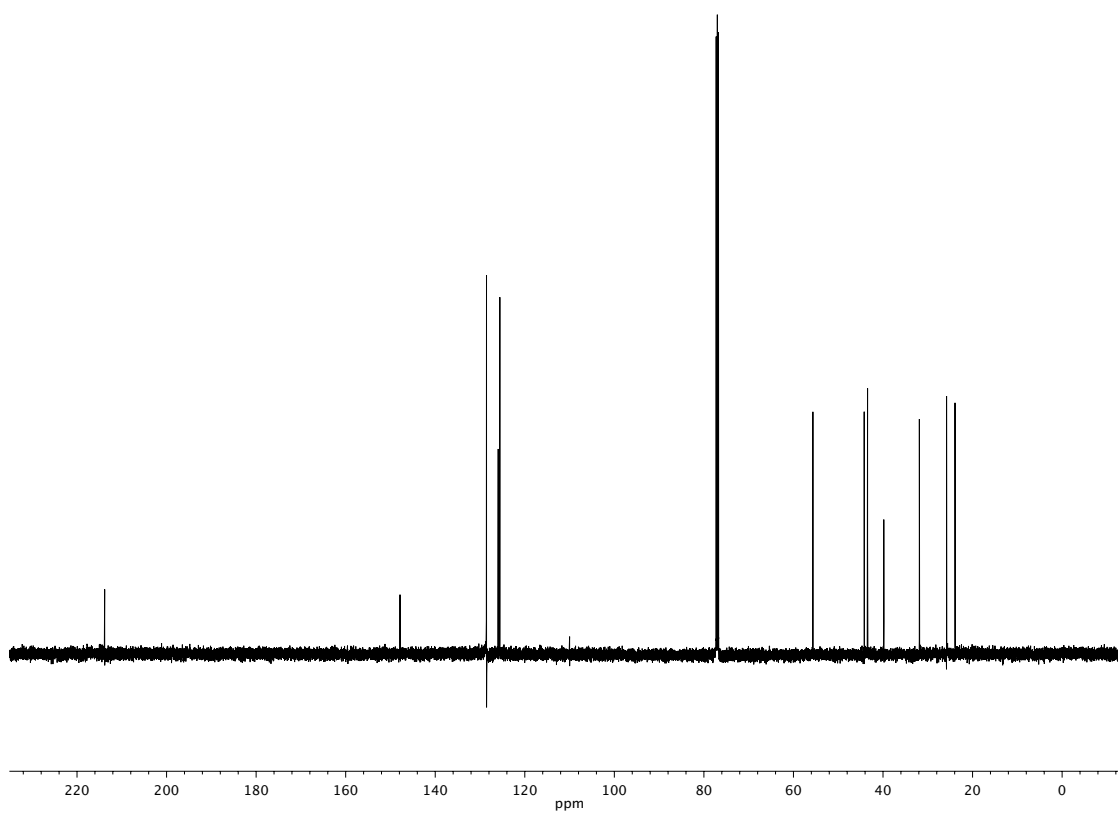
Figure A1.38 ^{13}C NMR (126 MHz, CDCl$_3$) of compound **137**
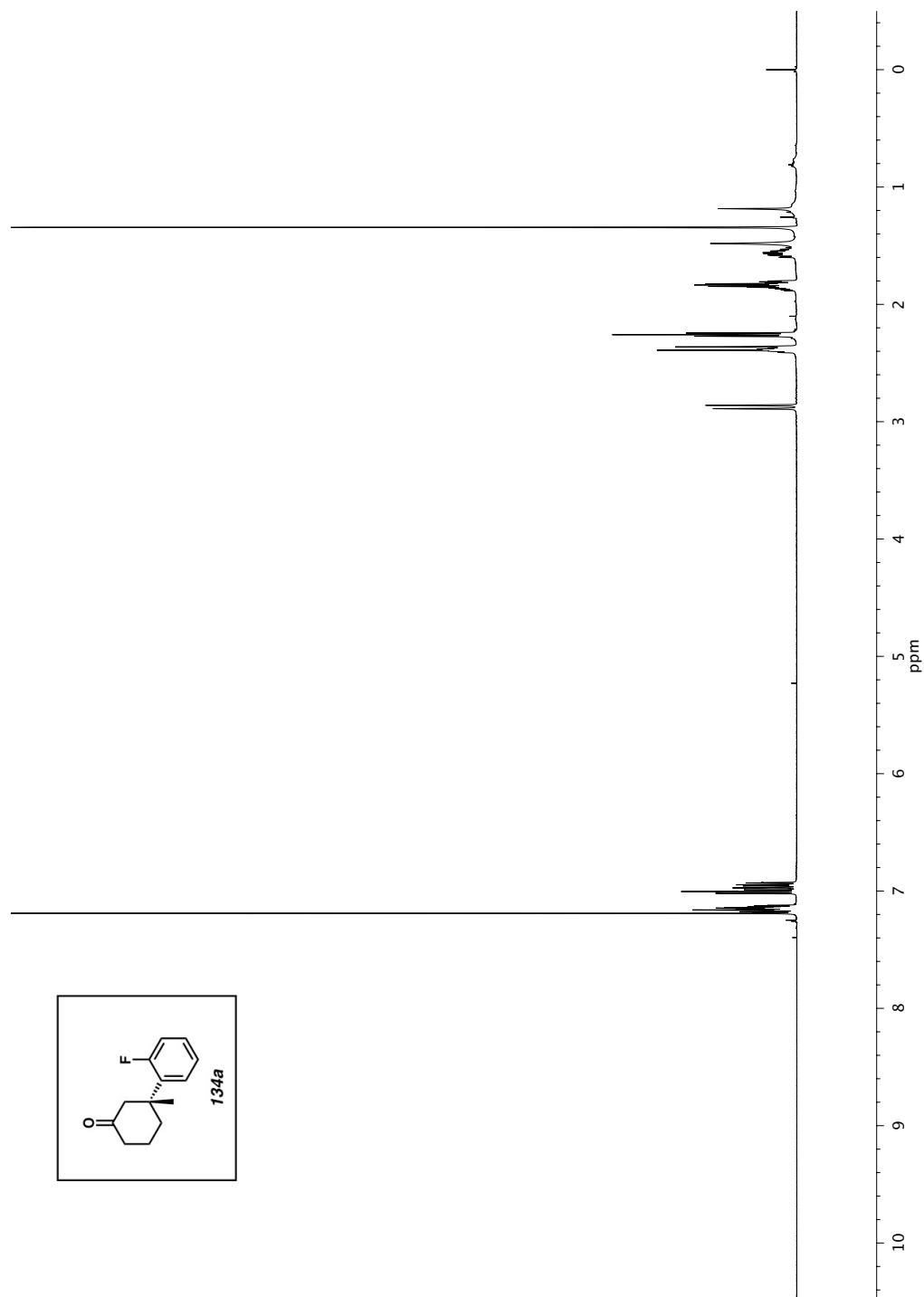
Figure A1.39 ^{1}H NMR (500 MHz, CDCl$_3$) of compound **134a**
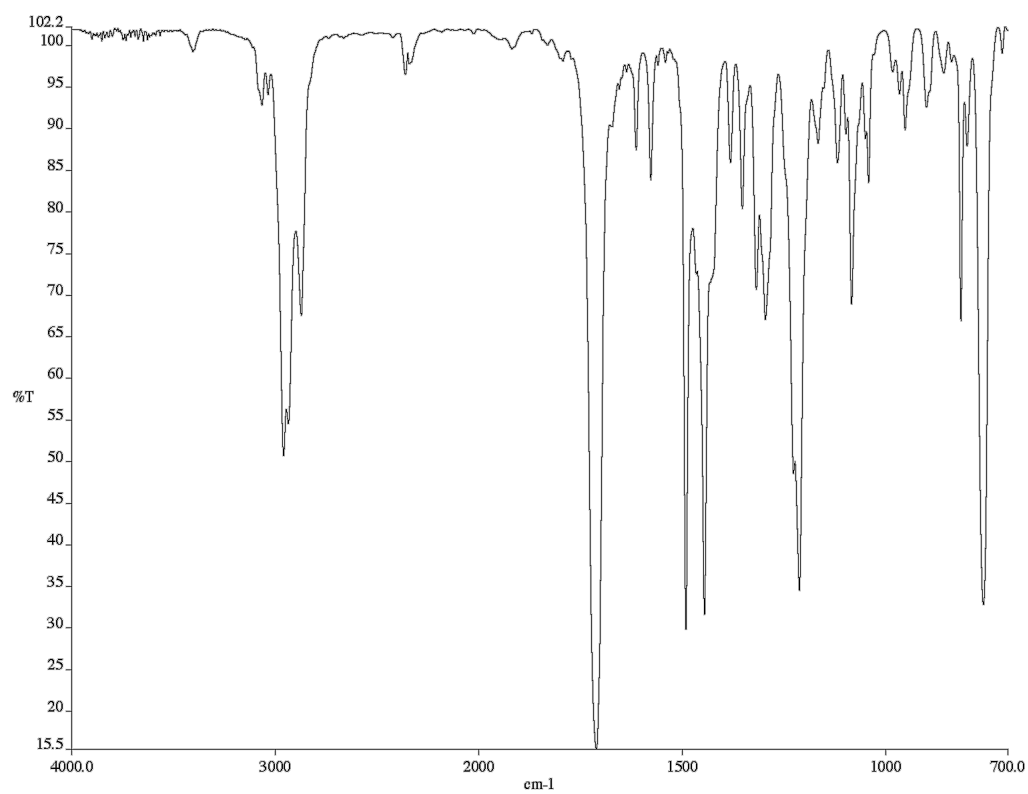
Figure A1.40 Infrared spectrum (Thin Film, NaCl) of compound **134a**
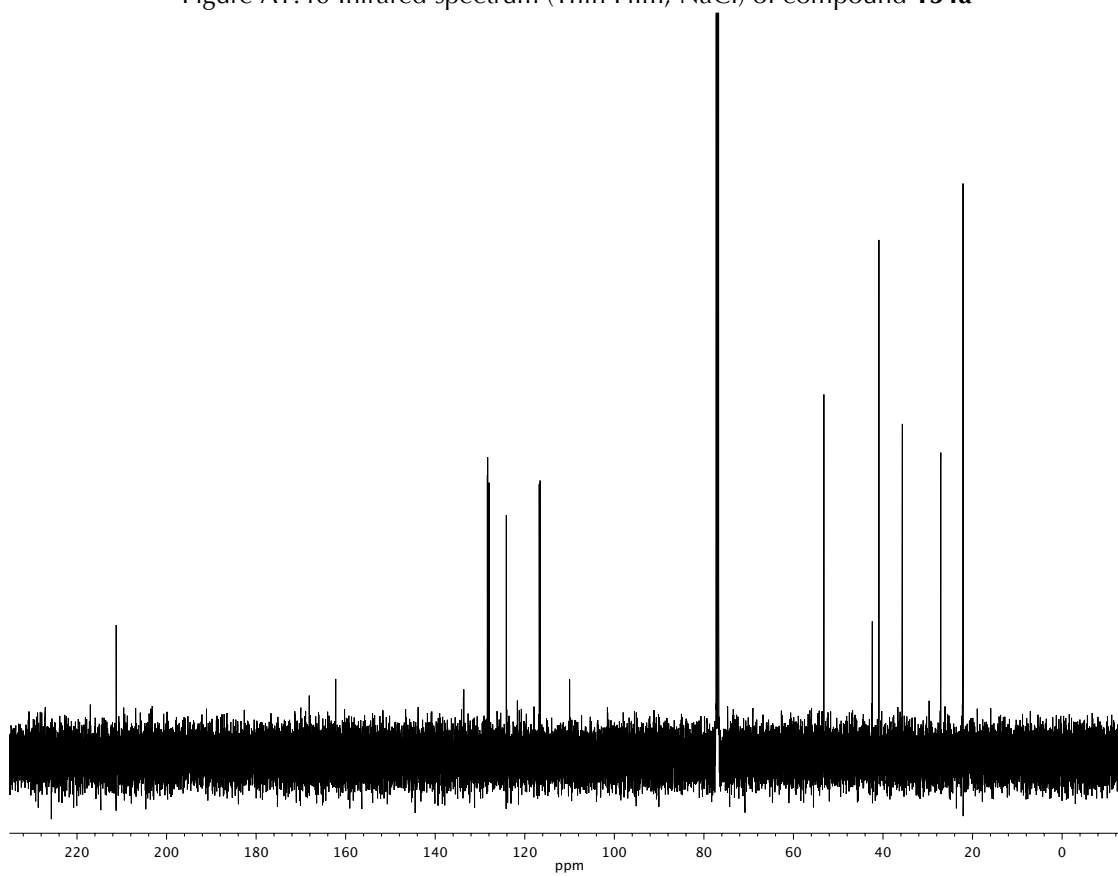
Figure A1.41 ^{13}C NMR (126 MHz, CDCl$_3$) of compound **134a**
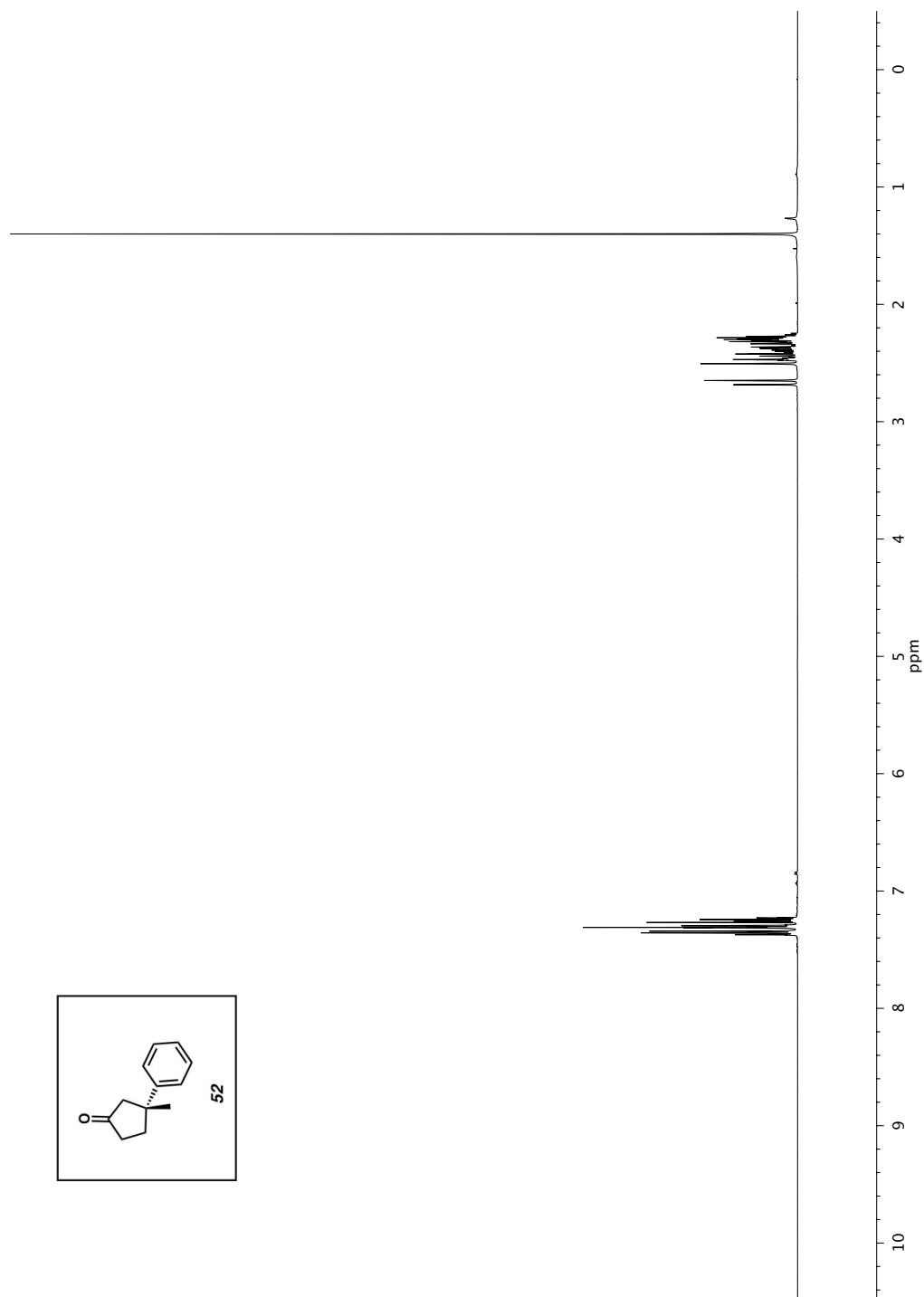
Figure A1.42 ^{1}H NMR (500 MHz, CDCl$_3$) of compound **52**
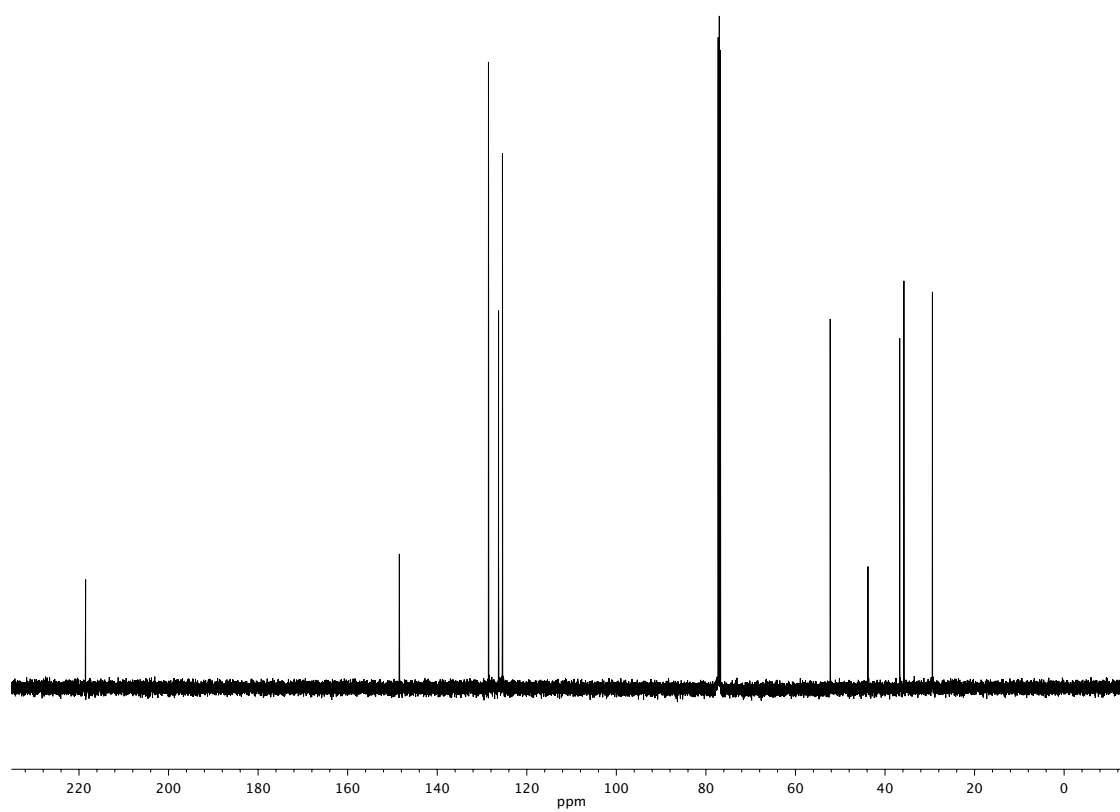
Figure A1.43 ^{13}C NMR (126 MHz, CDCl$_3$) of compound **52**
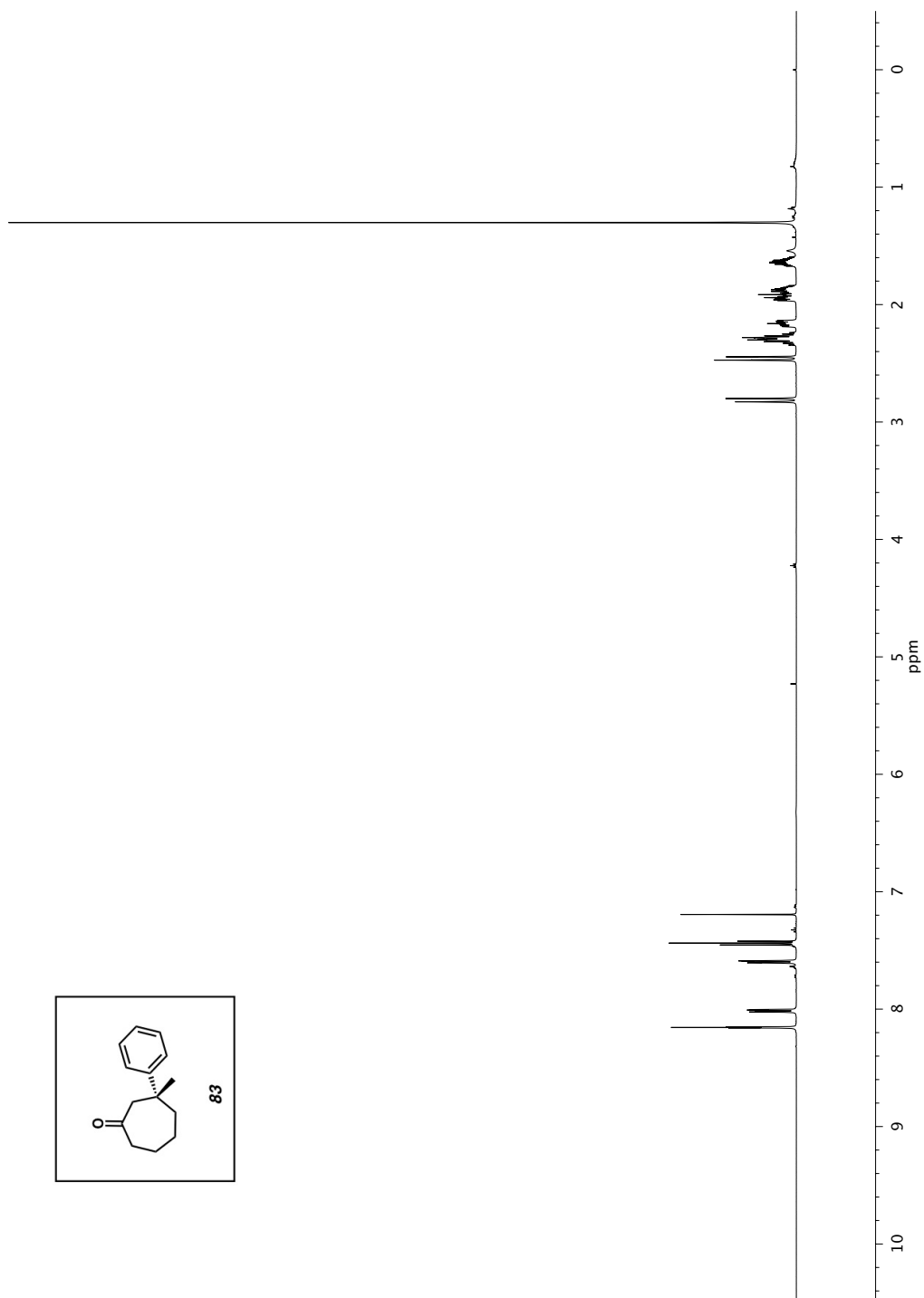
Figure A1.44 ^{1}H NMR (500 MHz, CDCl$_3$) of compound **83**
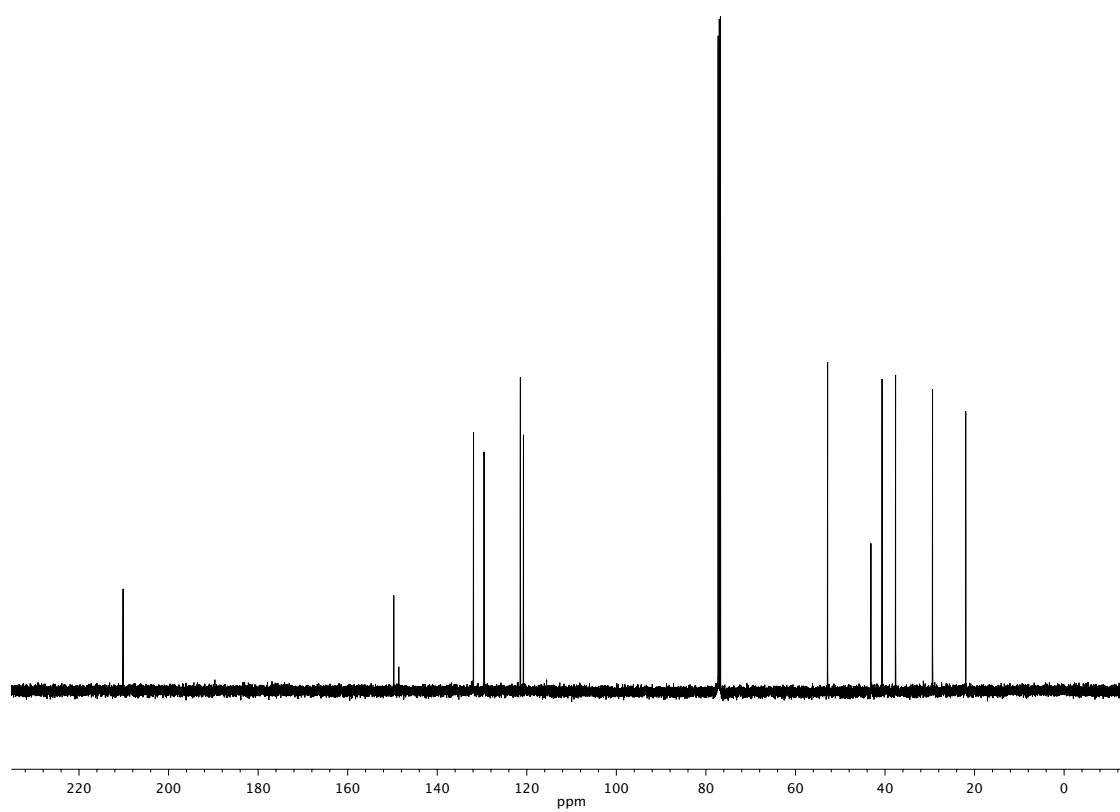
Figure A1.45 ^{13}C NMR (126 MHz, CDCl$_3$) of compound **83**
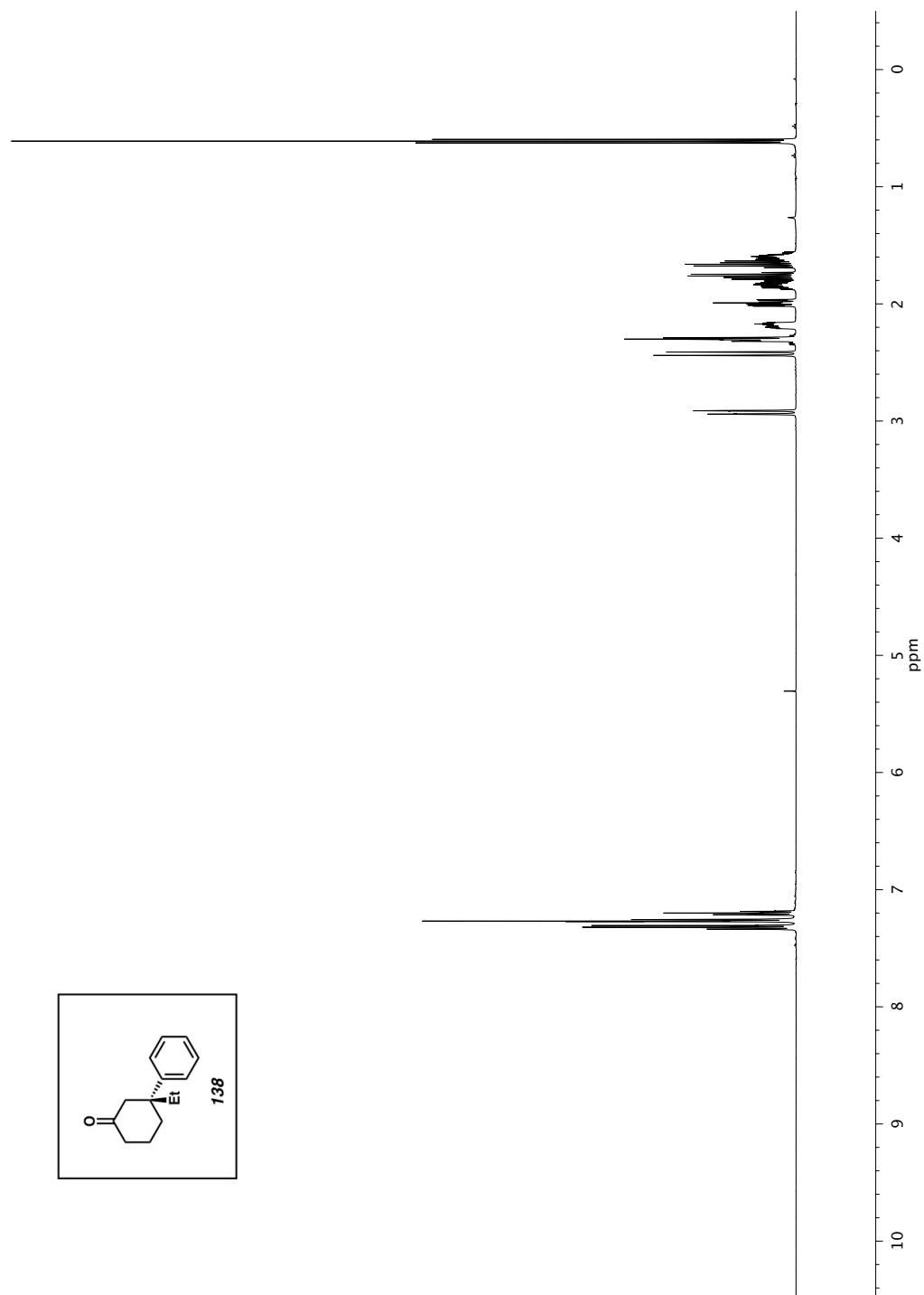
Figure A1.46 ^{1}H NMR (500 MHz, CDCl$_3$) of compound **138**
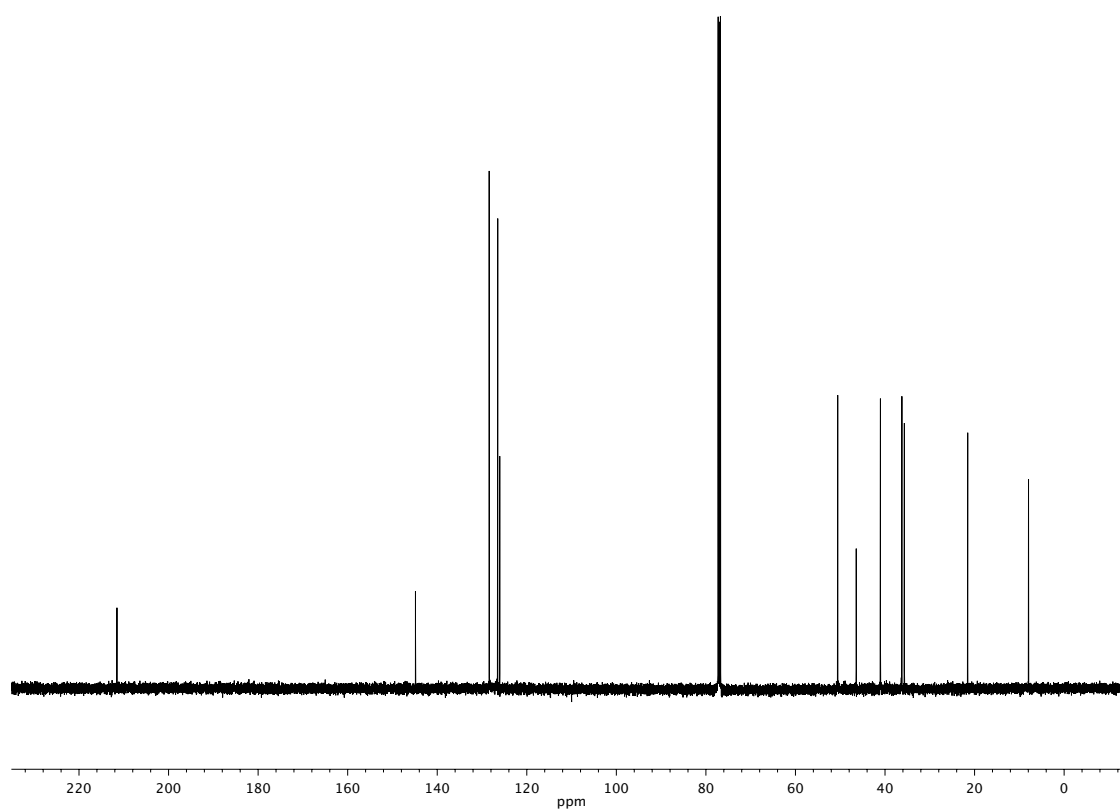
Figure A1.47 ^{13}C NMR (126 MHz, CDCl$_3$) of compound **138**
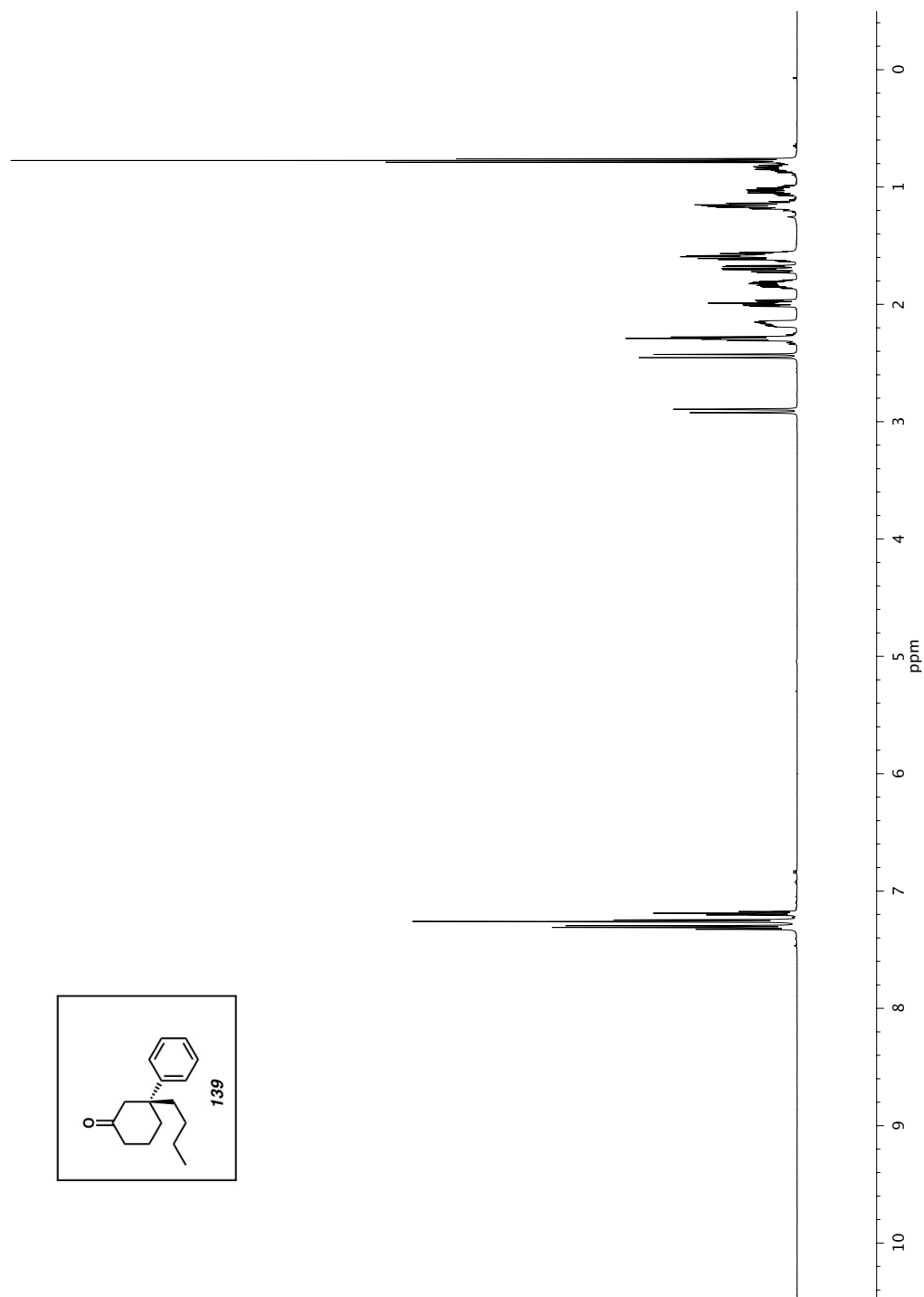
Figure A1.48 ^{1}H NMR (500 MHz, CDCl$_3$) of compound **139**
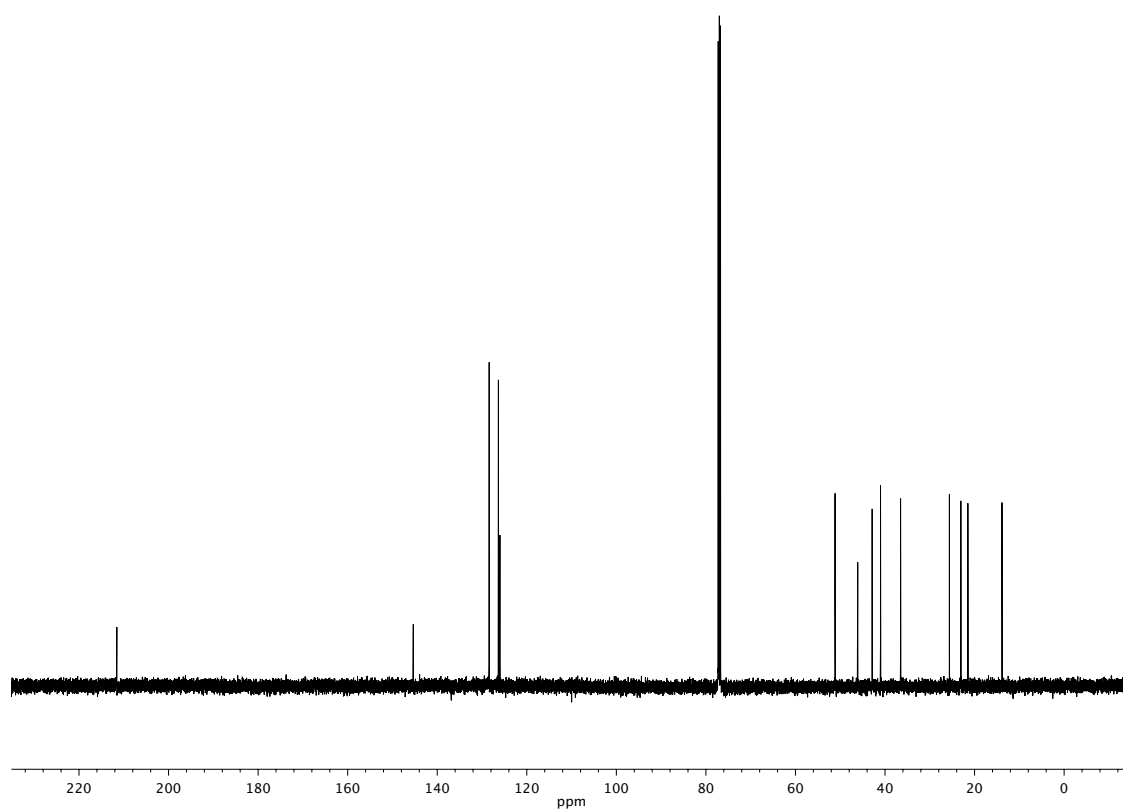
Figure A1.49 ^{13}C NMR (126 MHz, CDCl$_3$) of compound **139**
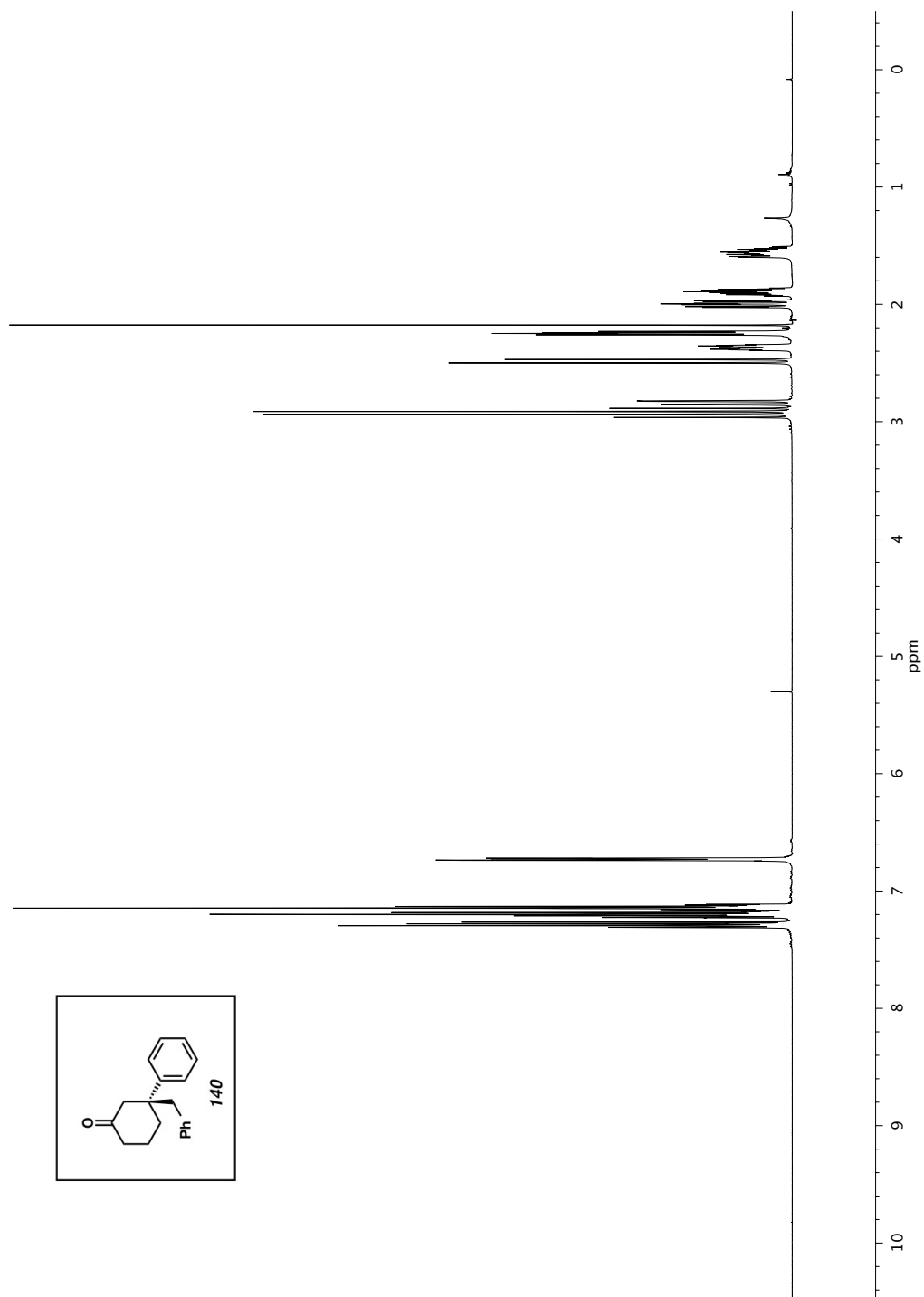
Figure A1.50 ^{1}H NMR (500 MHz, CDCl$_3$) of compound **140**
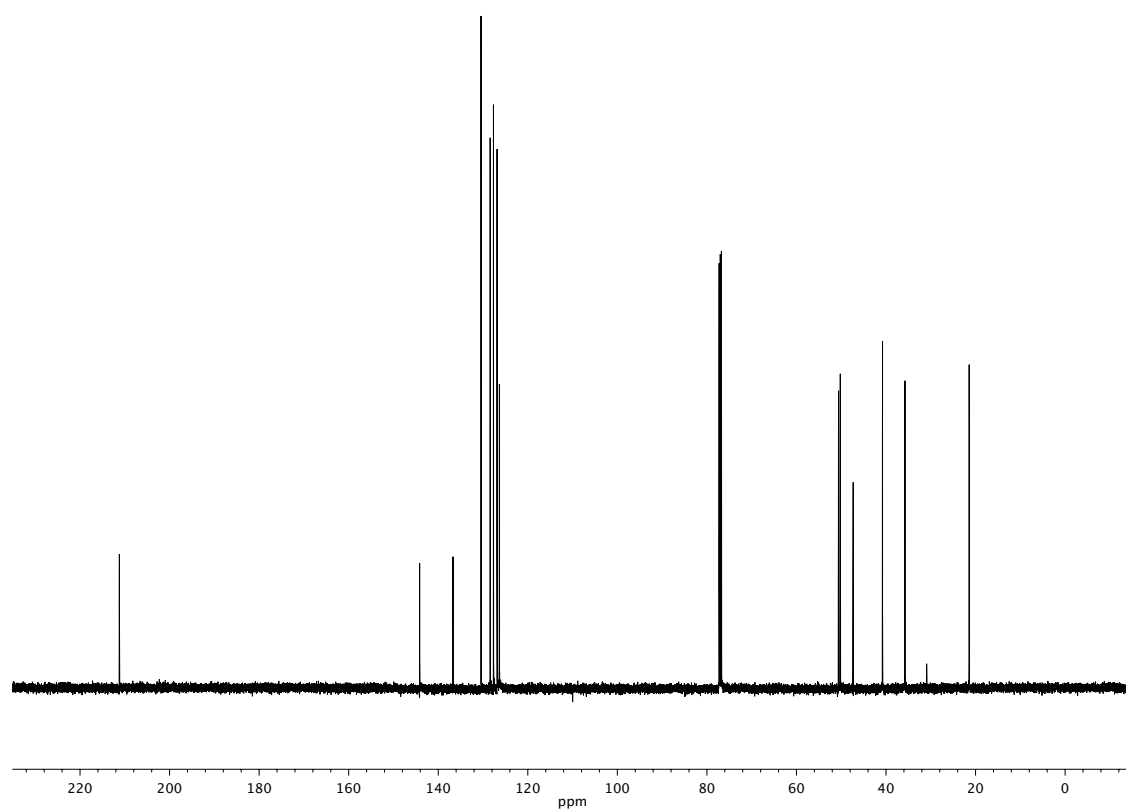
Figure A1.51 ^{13}C NMR (126 MHz, CDCl$_3$) of compound **140**
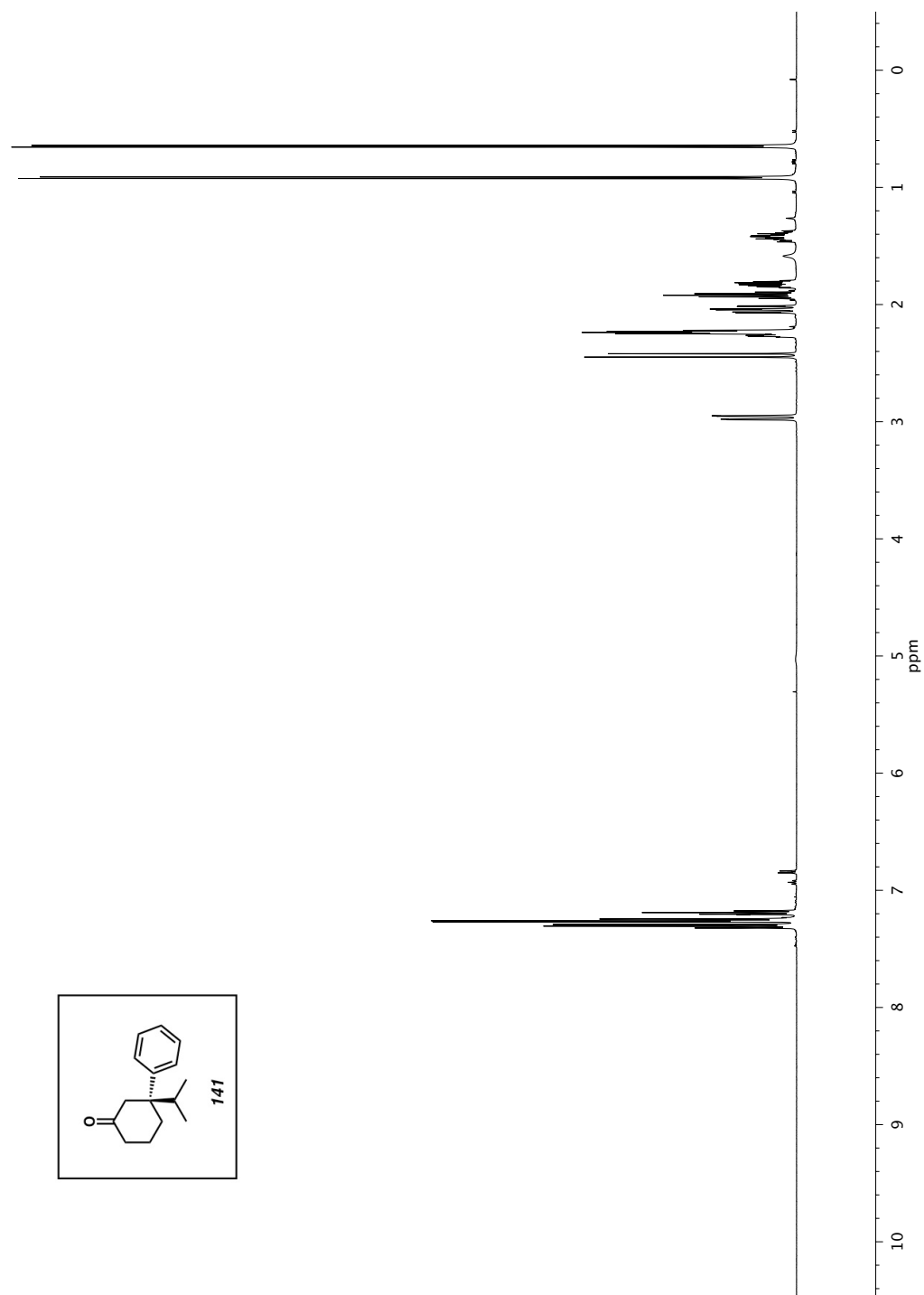
Figure A1.52 ^{1}H NMR (500 MHz, CDCl$_3$) of compound **141**
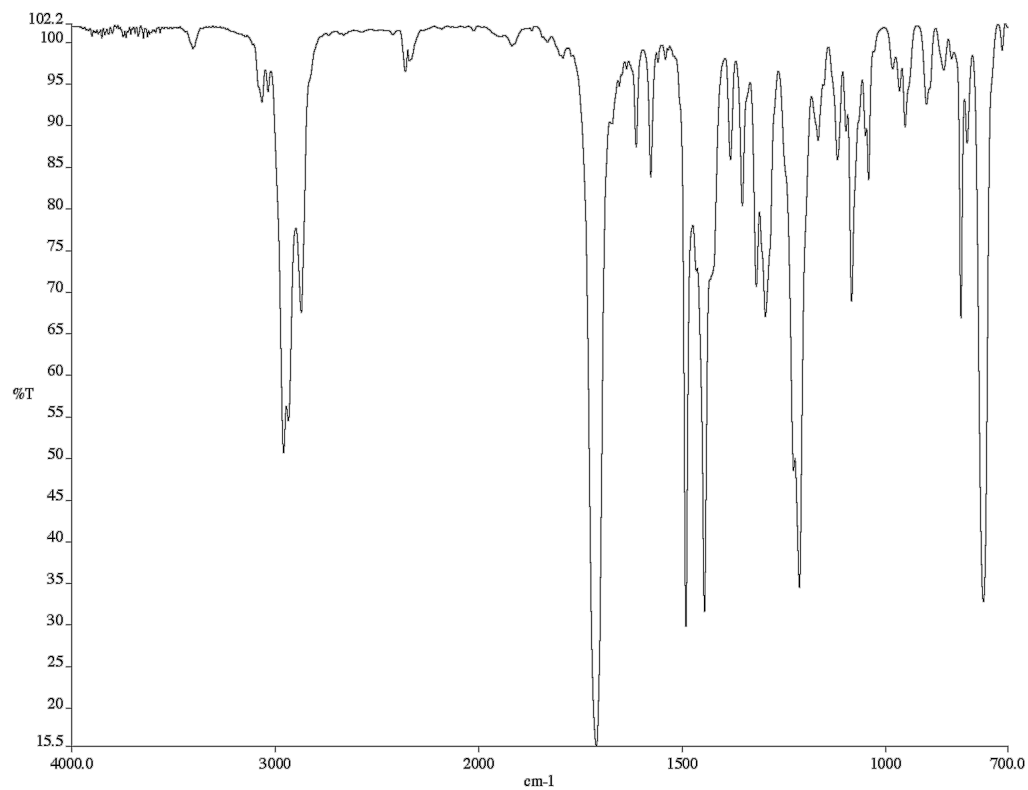
Figure A1.53 Infrared spectrum (Thin Film, NaCl) of compound **141**
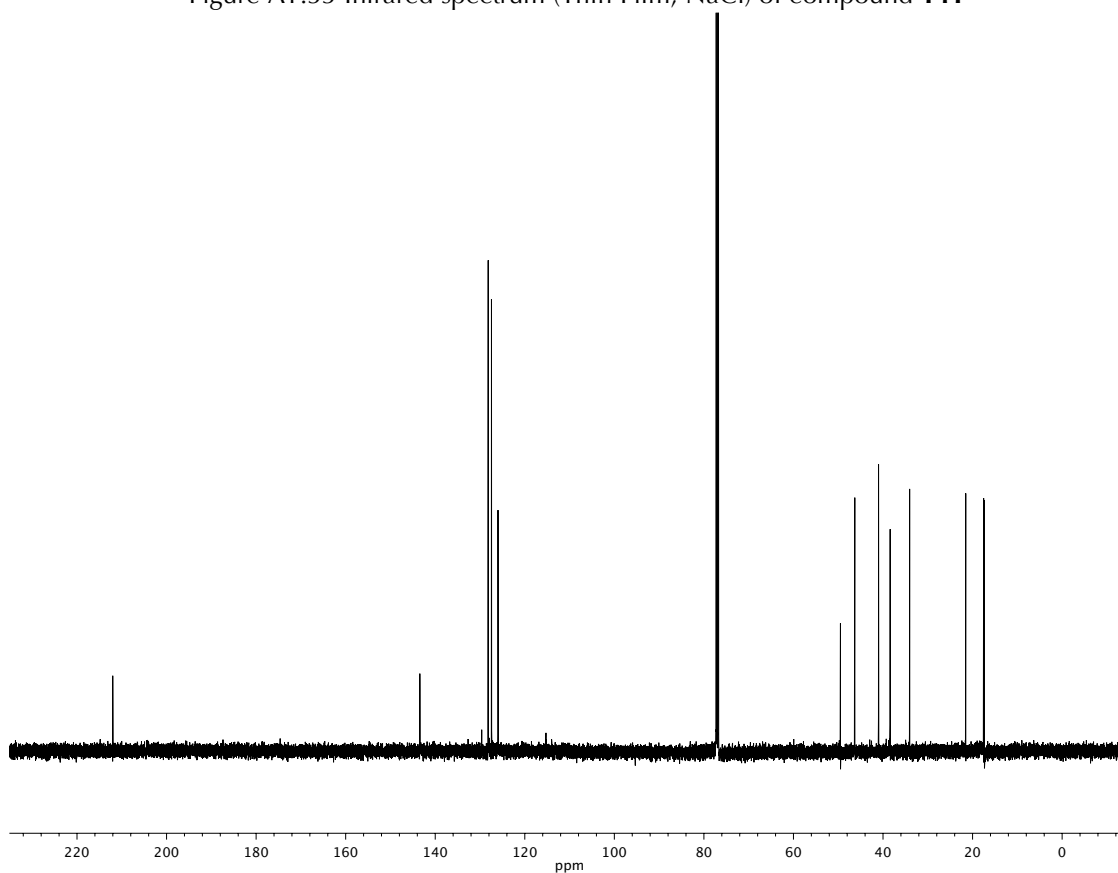
Figure A1.54 ^{13}C NMR (126 MHz, CDCl$_3$) of compound **141**
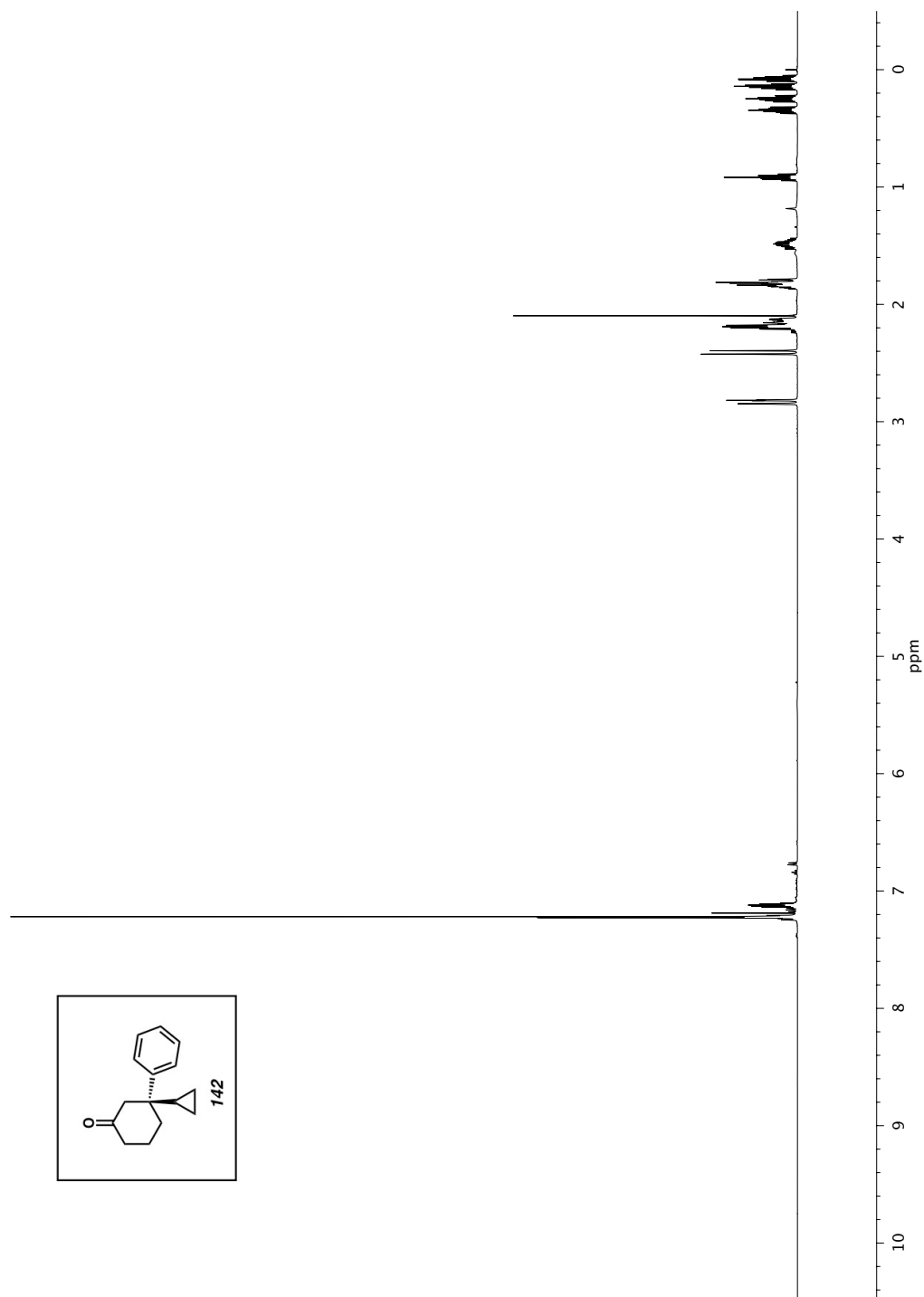
Figure A1.55 ^{1}H NMR (500 MHz, CDCl$_3$) of compound **142**
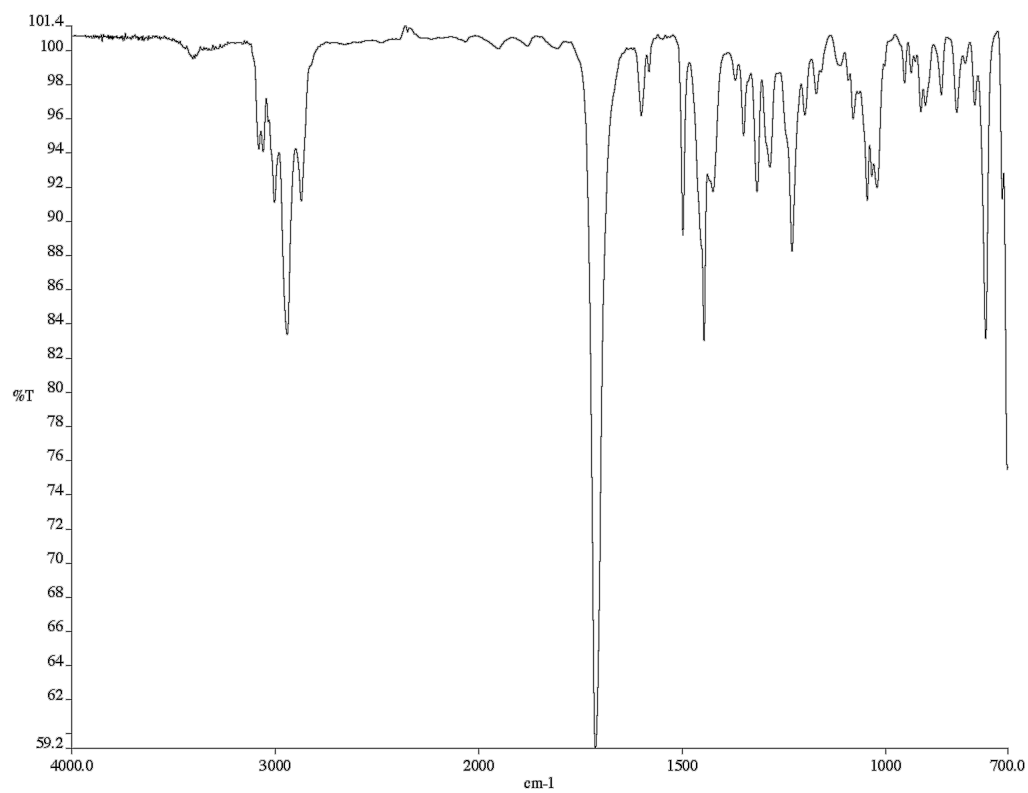
Figure A1.56 Infrared spectrum (Thin Film, NaCl) of compound **142**
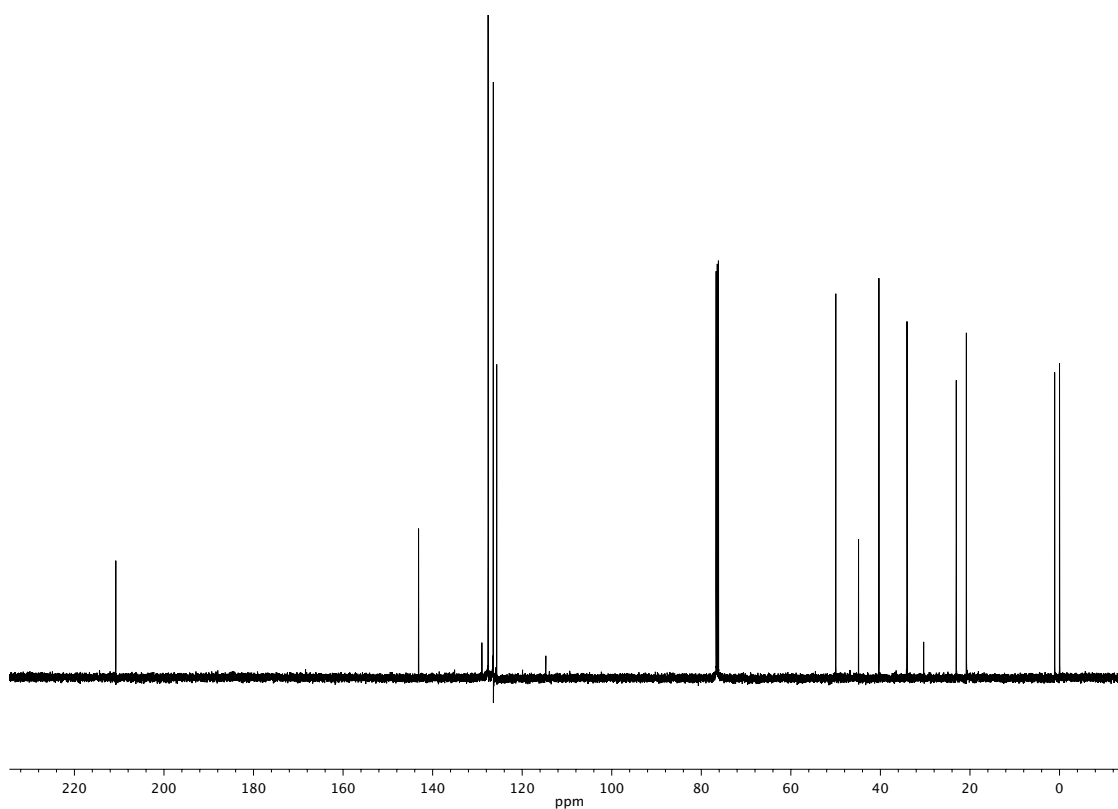
Figure A1.57 ^{13}C NMR (126 MHz, CDCl$_3$) of compound **142**
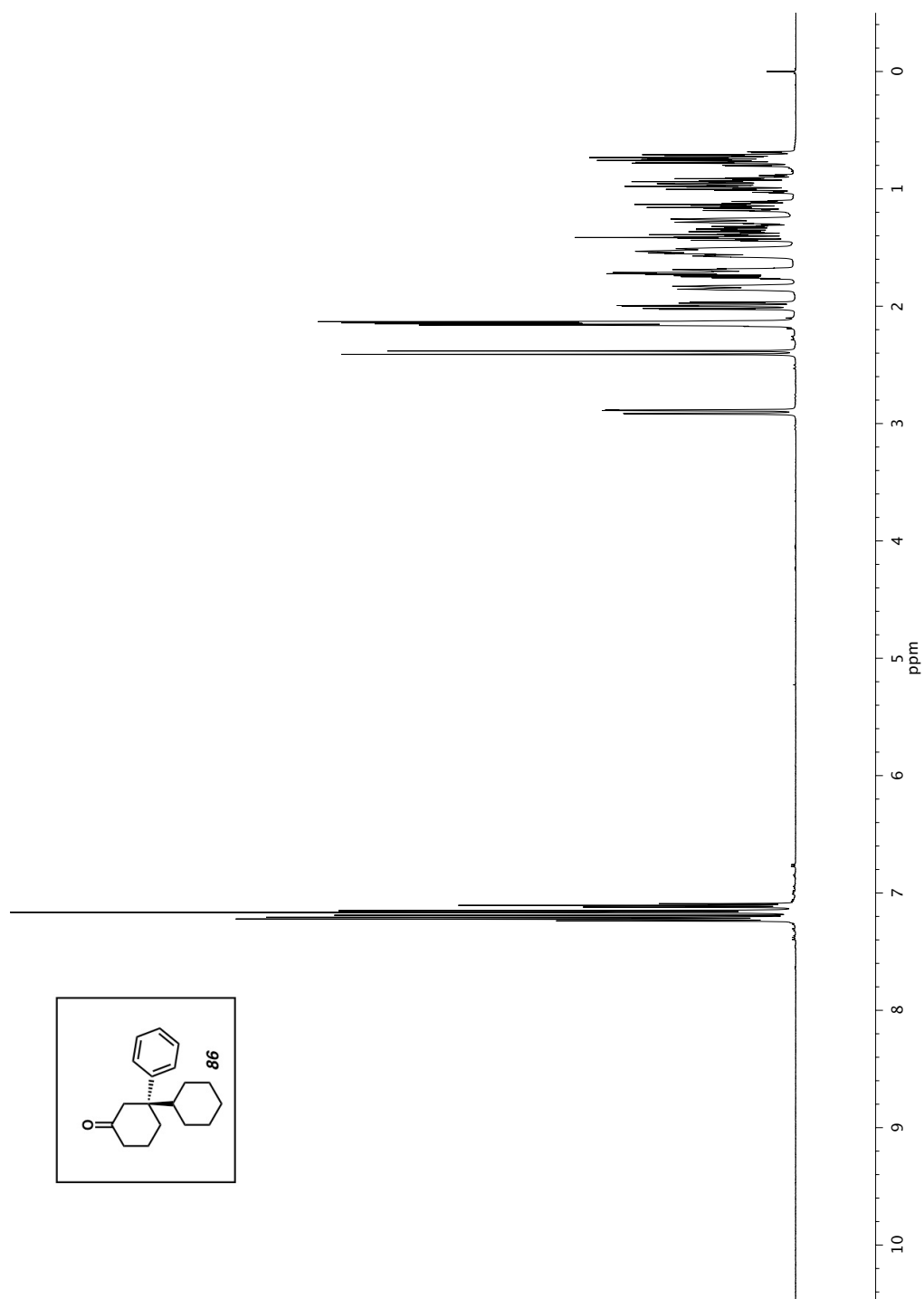
Figure A1.58 ^{1}H NMR (500 MHz, CDCl$_3$) of compound **86**
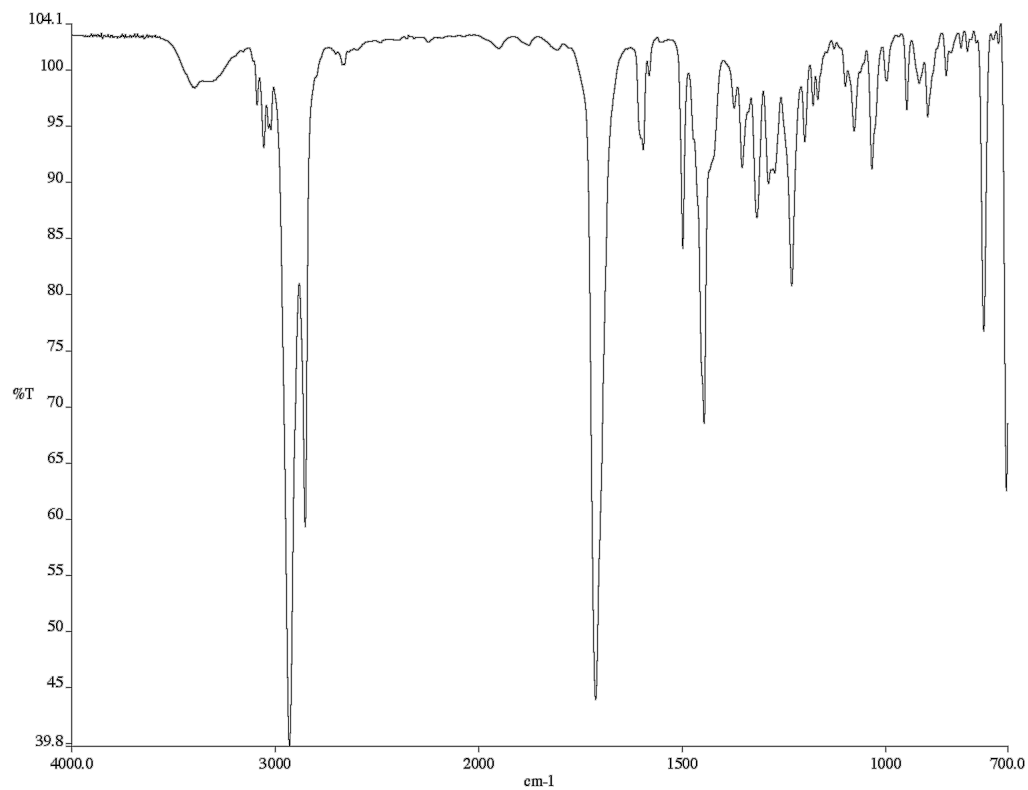
Figure A1.59 Infrared spectrum (Thin Film, NaCl) of compound **86**
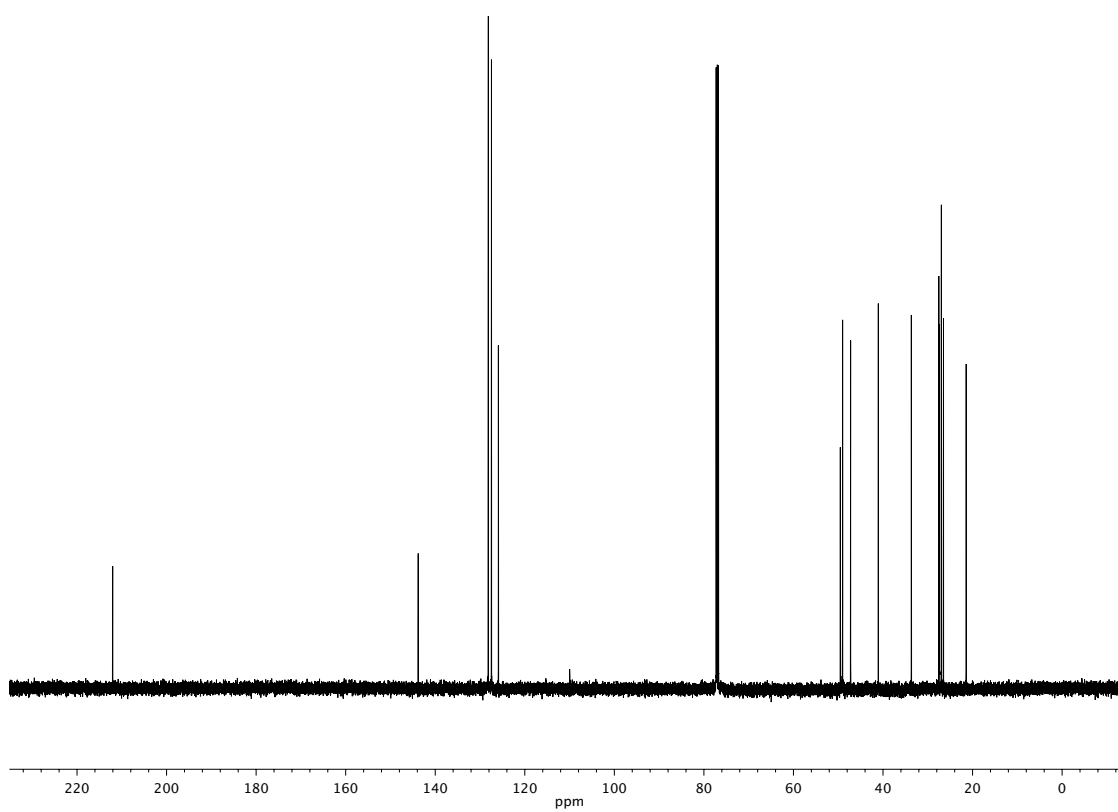
Figure A1.60 ^{13}C NMR (126 MHz, CDCl$_3$) of compound **86**

Figure A1.61 ^{1}H NMR (500 MHz, CDCl$_3$) of compound **88**
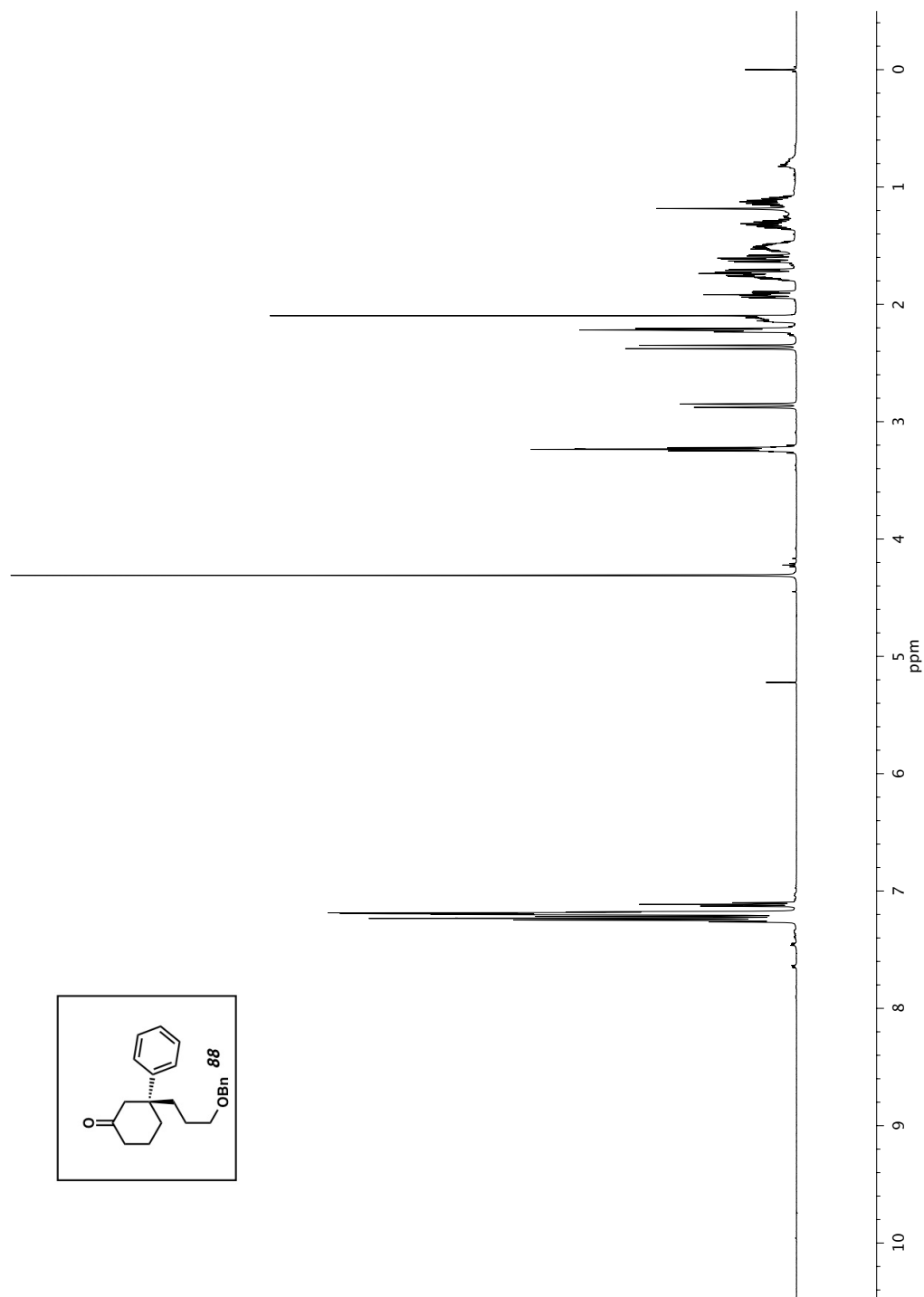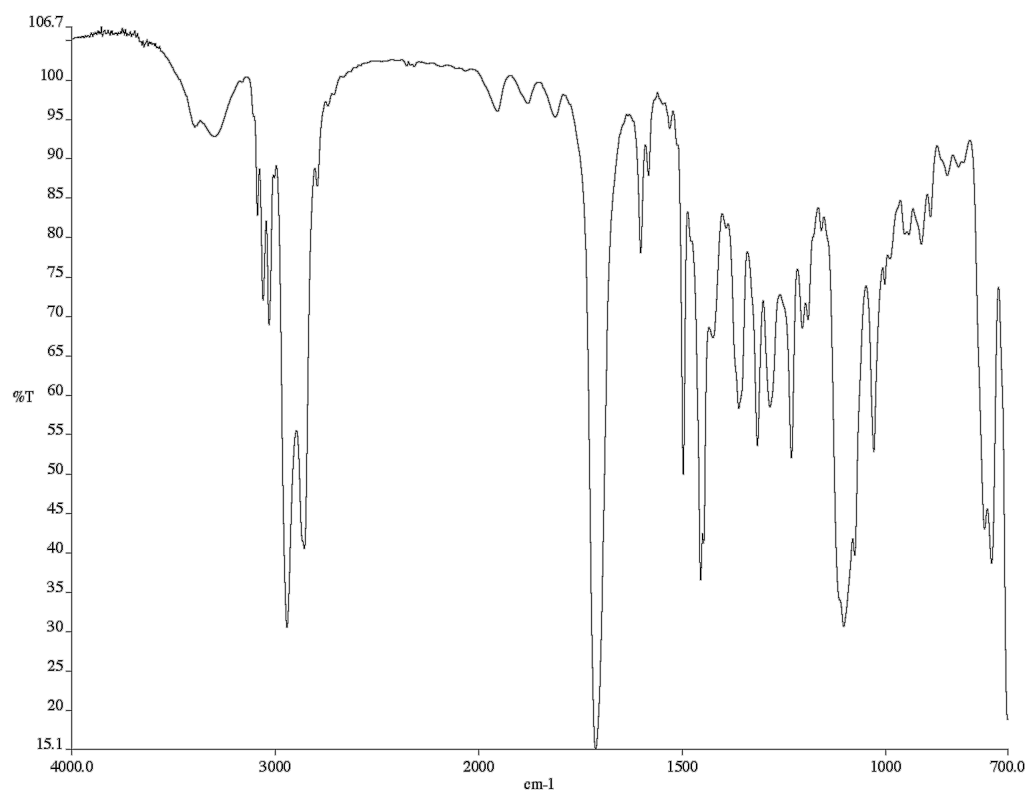
Figure A1.62 Infrared spectrum (Thin Film, NaCl) of compound **88**
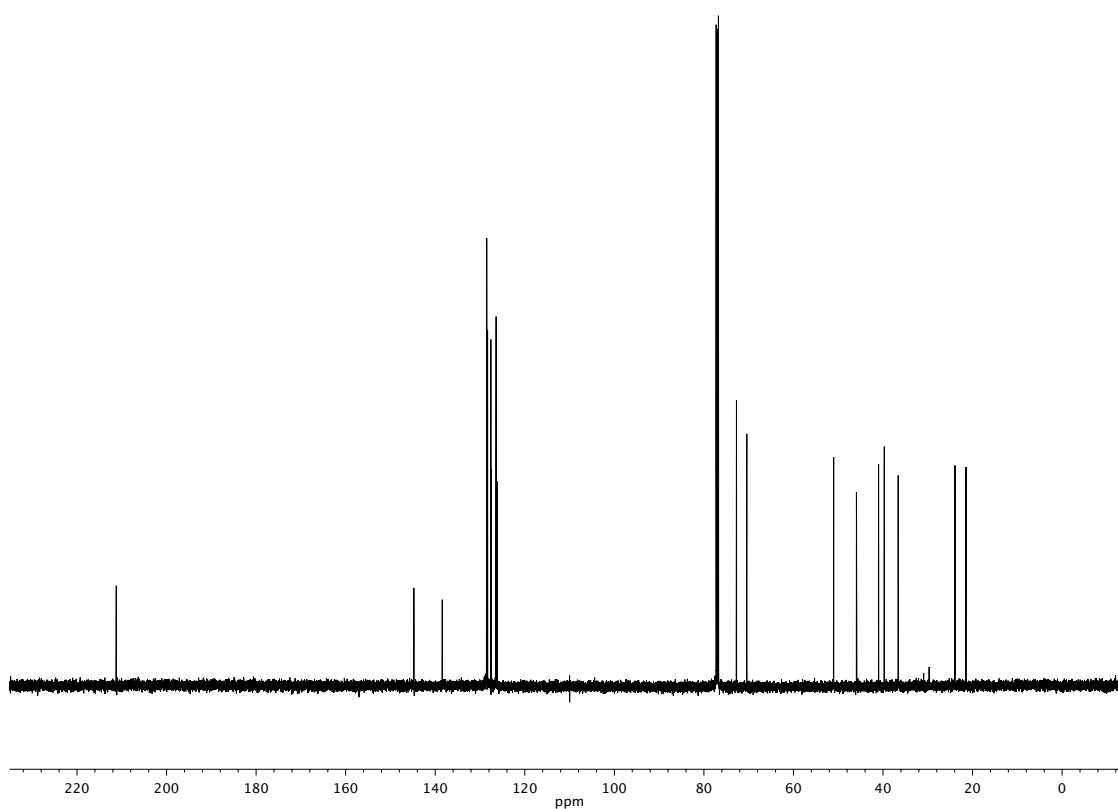
Figure A1.63 ^{13}C NMR (126 MHz, CDCl$_3$) of compound **88**
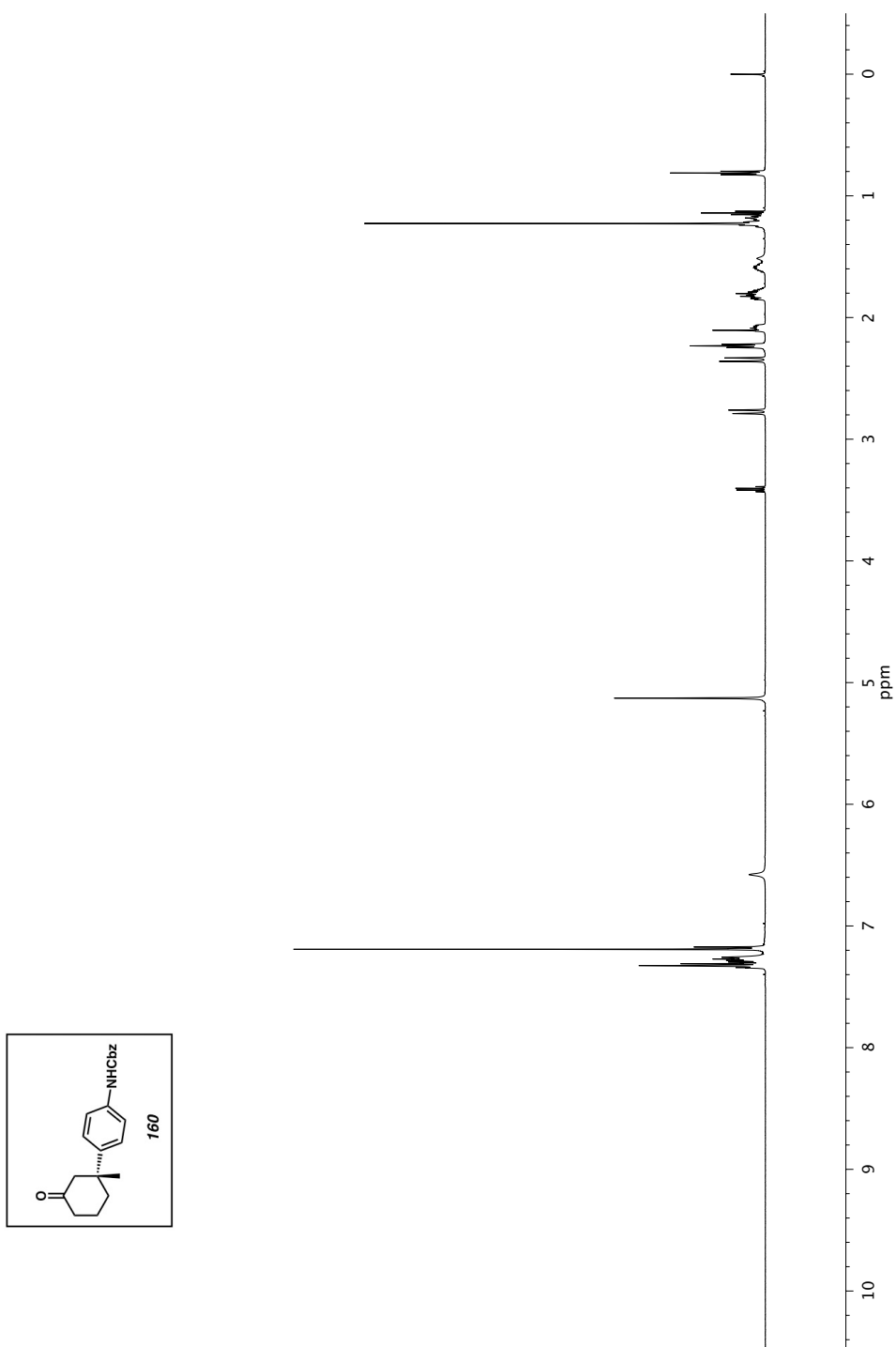
Figure A1.64 ^{1}H NMR (500 MHz, CDCl$_3$) of compound **160**
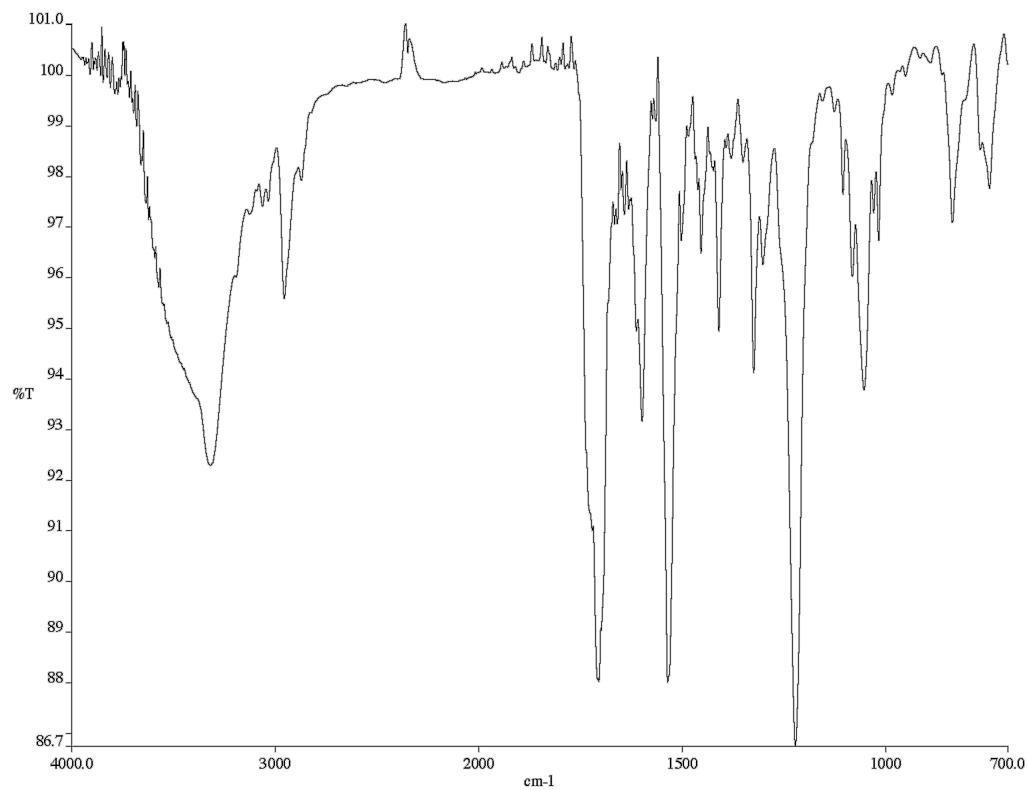
Figure A1.65 Infrared spectrum (Thin Film, NaCl) of compound **160**
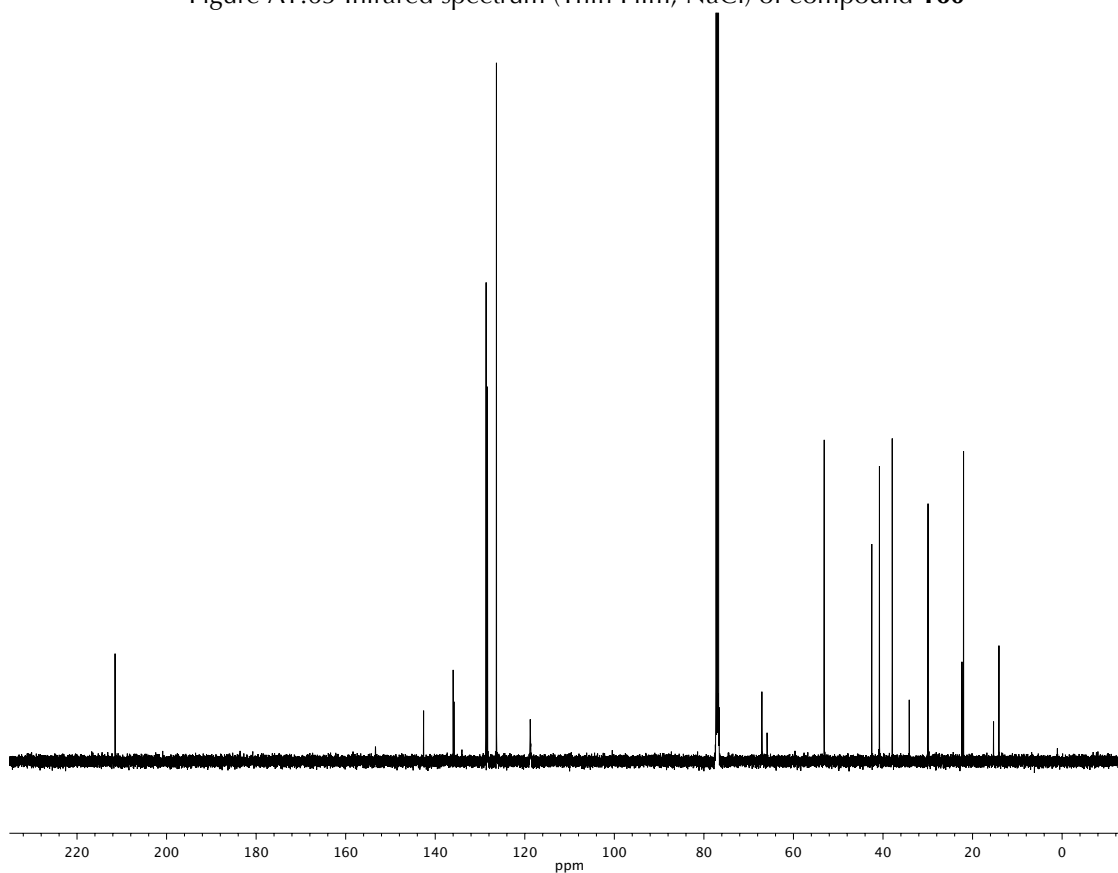
Figure A1.66 ^{13}C NMR (126 MHz, CDCl$_3$) of compound **160**
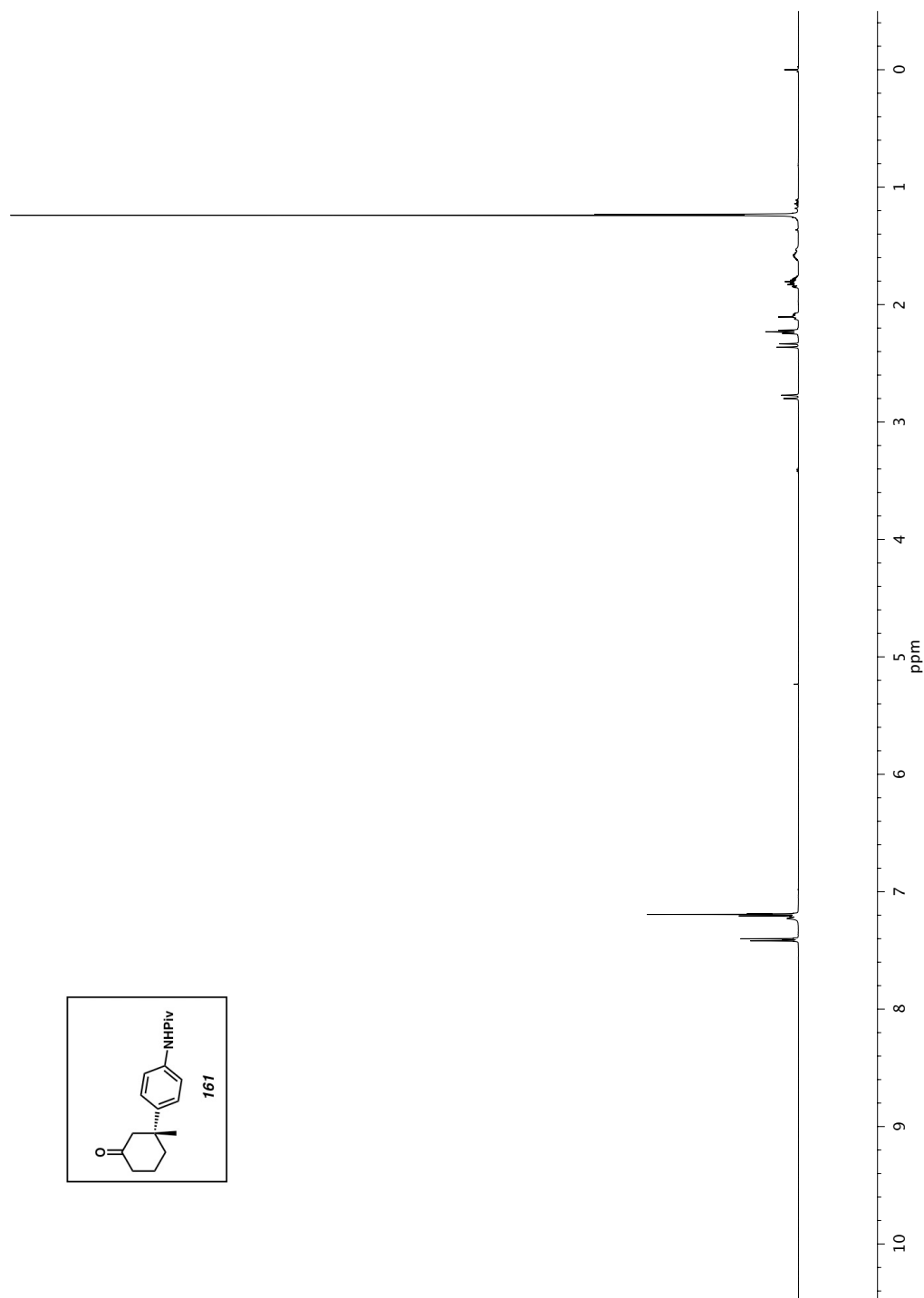
Figure A1.67 ^{1}H NMR (500 MHz, CDCl$_3$) of compound **161**
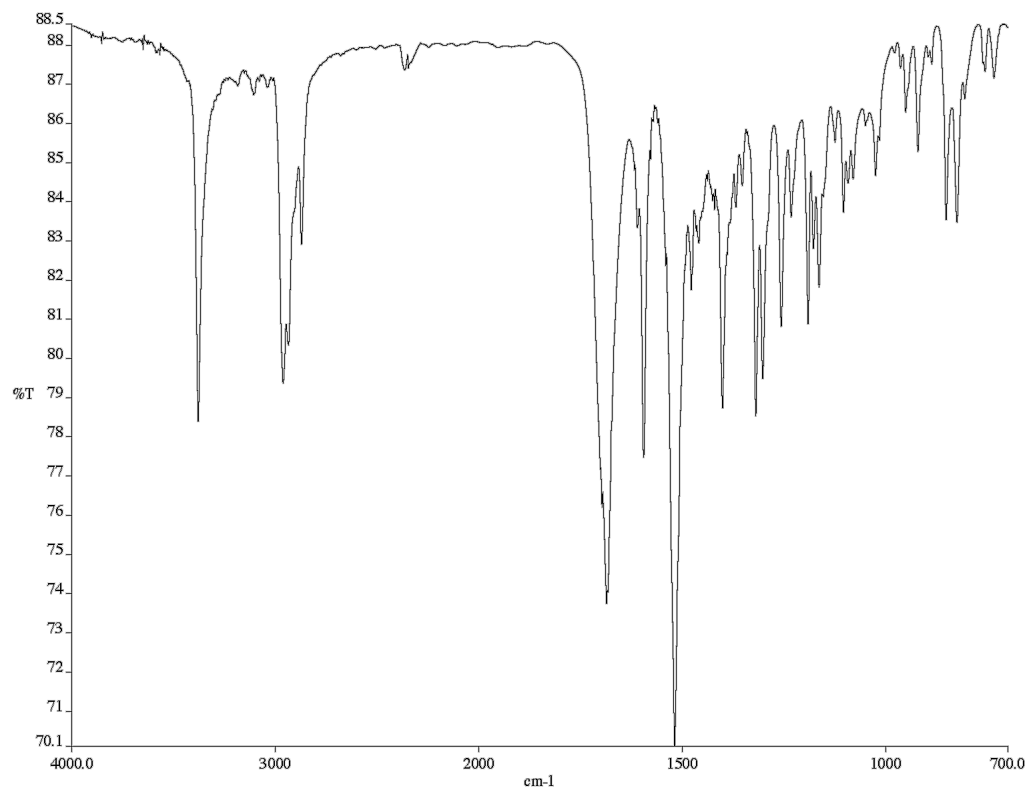
Figure A1.68 Infrared spectrum (Thin Film, NaCl) of compound **161**
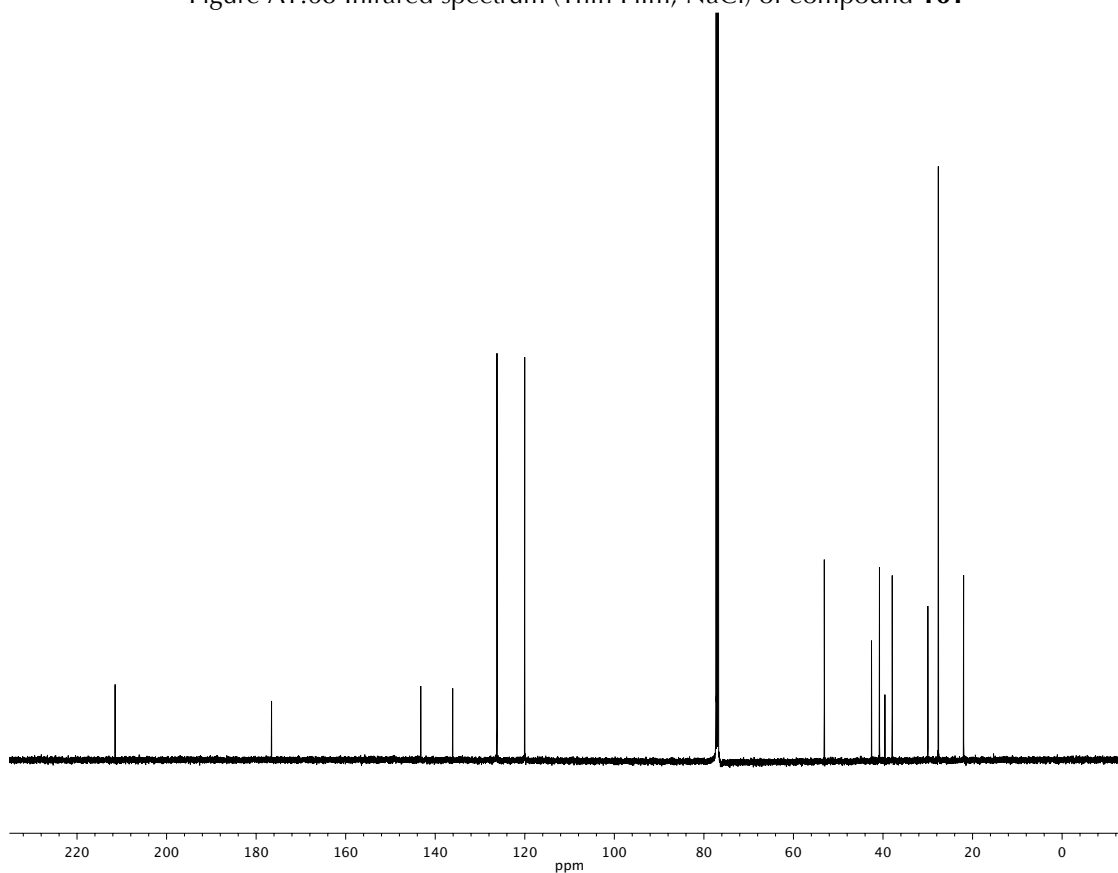
Figure A1.69 ^{13}C NMR (126 MHz, CDCl$_3$) of compound **161**
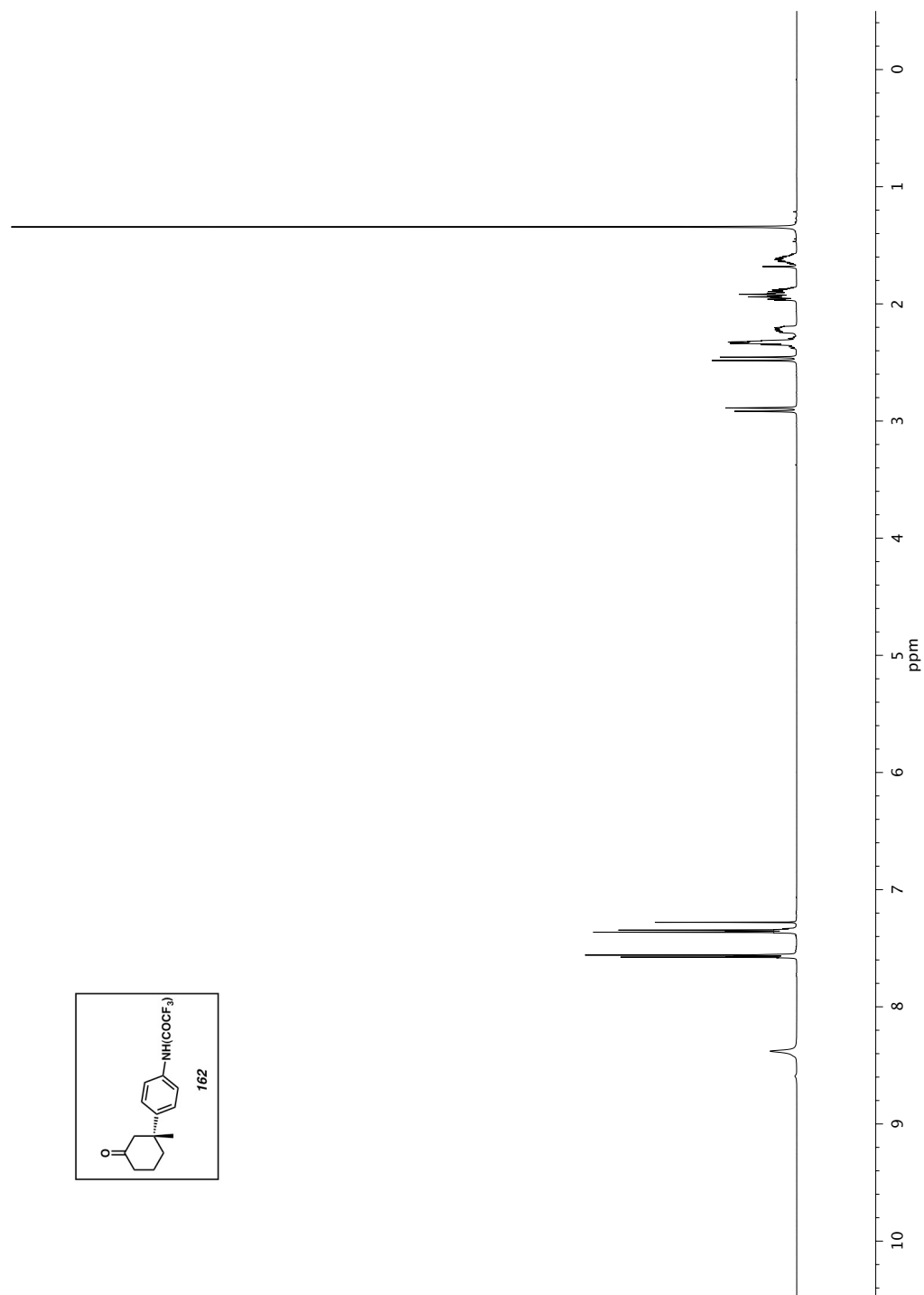
Figure A1.70 ^{1}H NMR (500 MHz, CDCl$_3$) of compound **162**
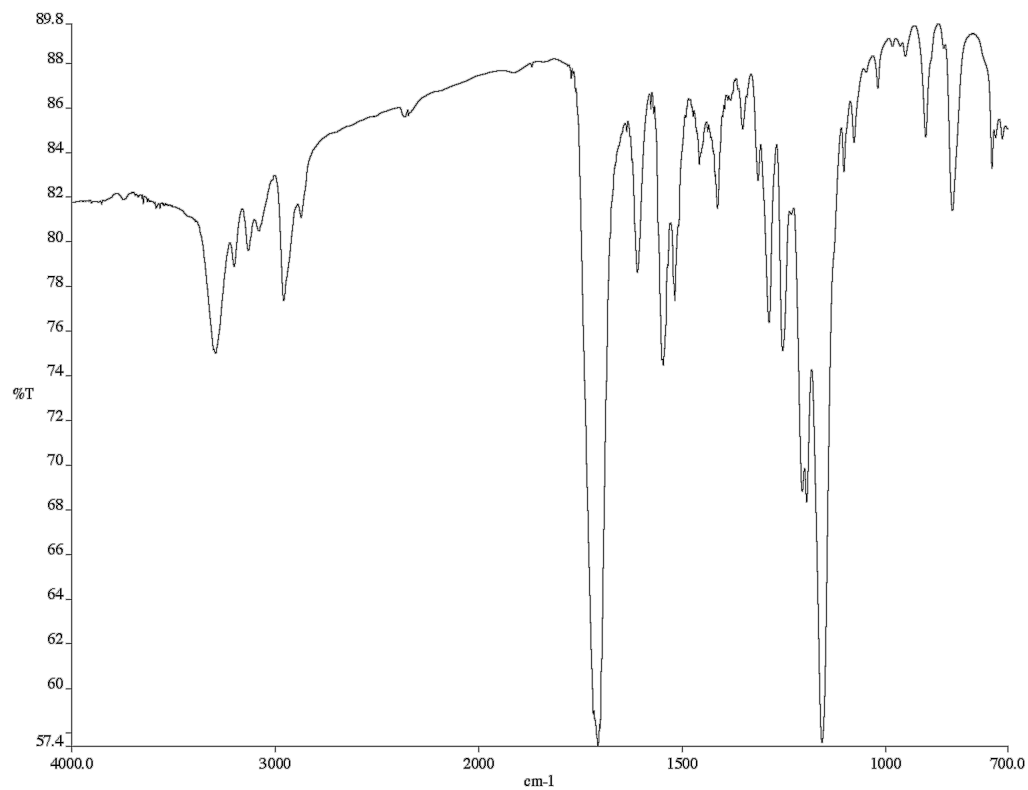
Figure A1.71 Infrared spectrum (Thin Film, NaCl) of compound **162**
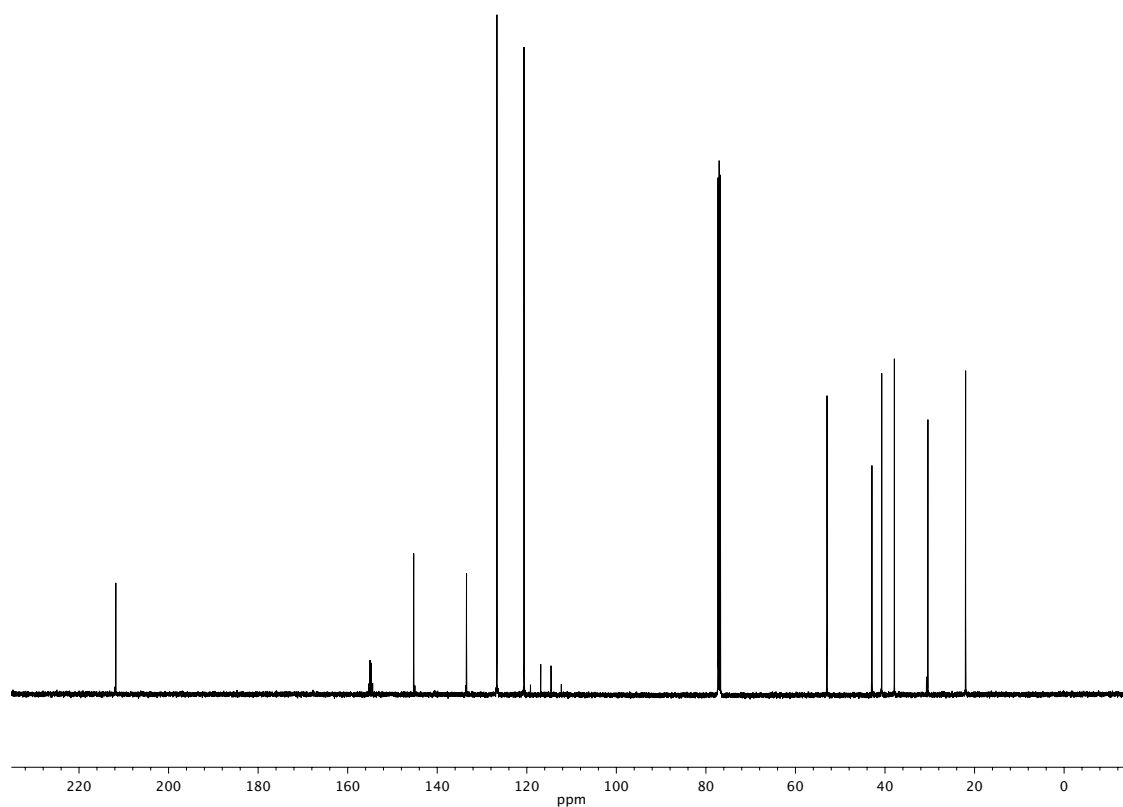
Figure A1.72 ¹³C NMR (126 MHz, CDCl₃) of compound **162**
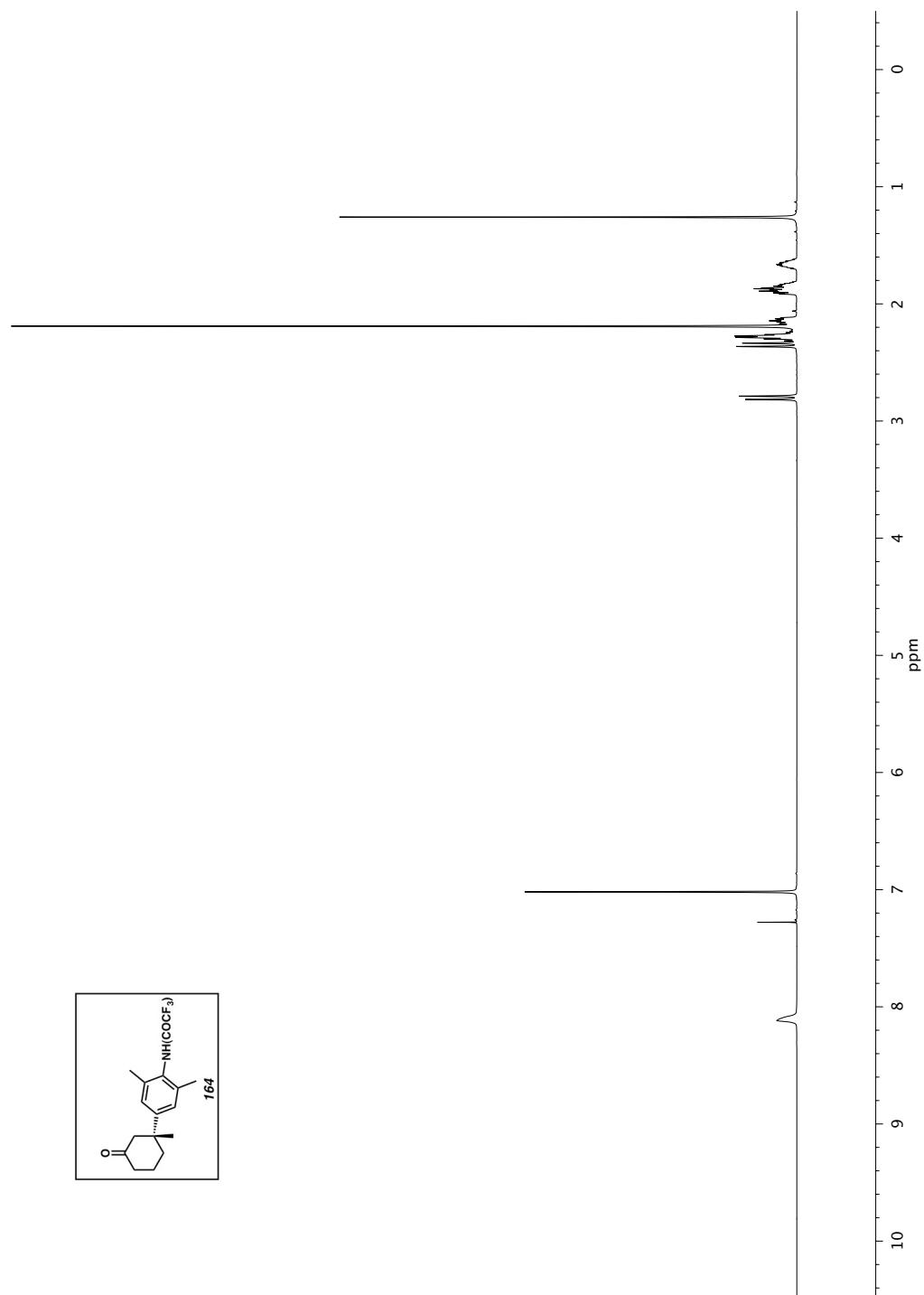
Figure A1.73 ^{1}H NMR (500 MHz, CDCl$_3$) of compound **164**
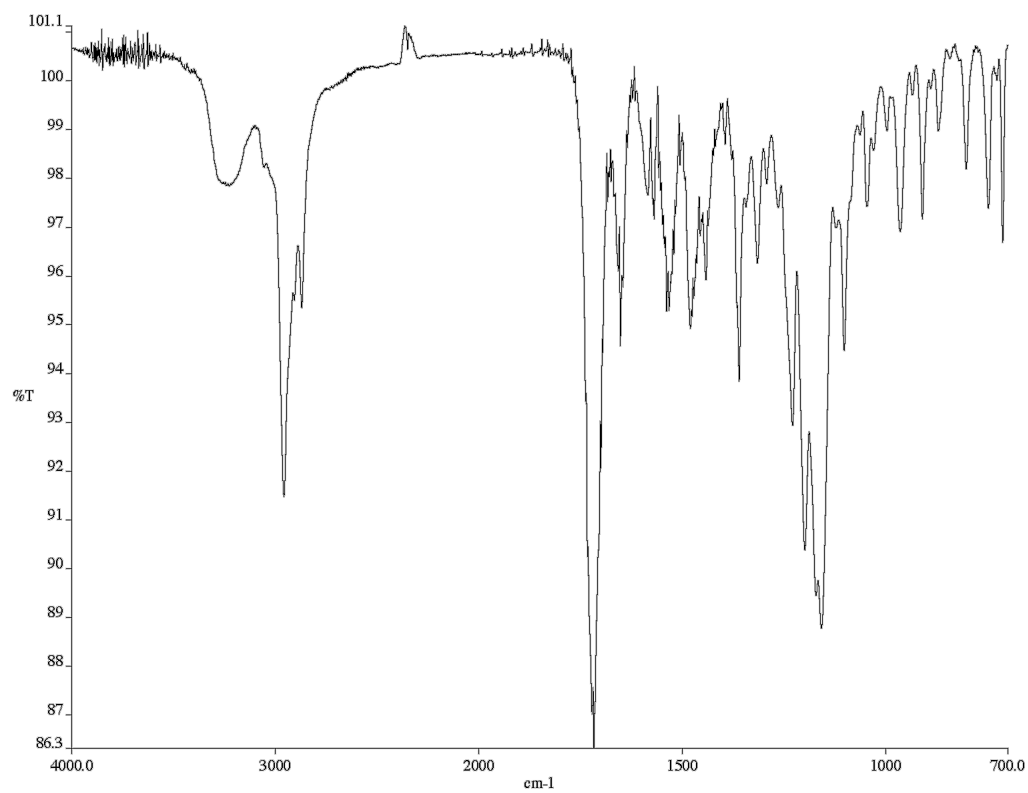
Figure A1.74 Infrared spectrum (Thin Film, NaCl) of compound **164**
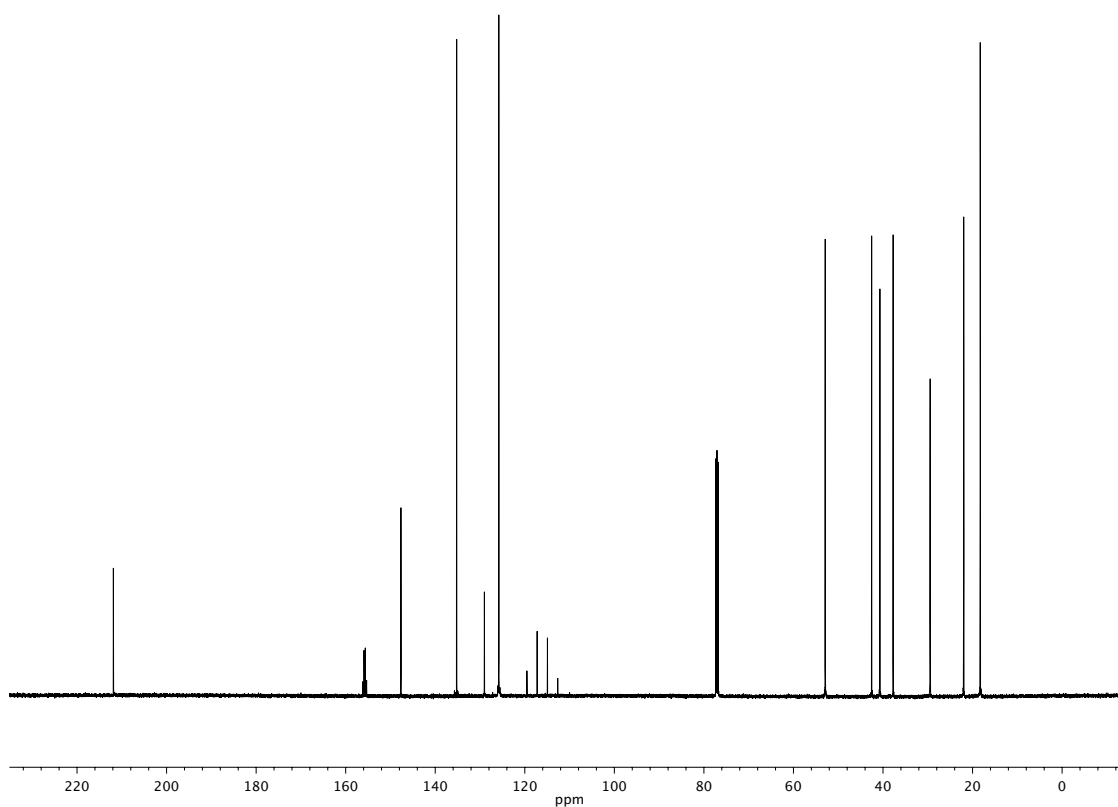
Figure A1.75 ^{13}C NMR (126 MHz, CDCl$_3$) of compound **164**
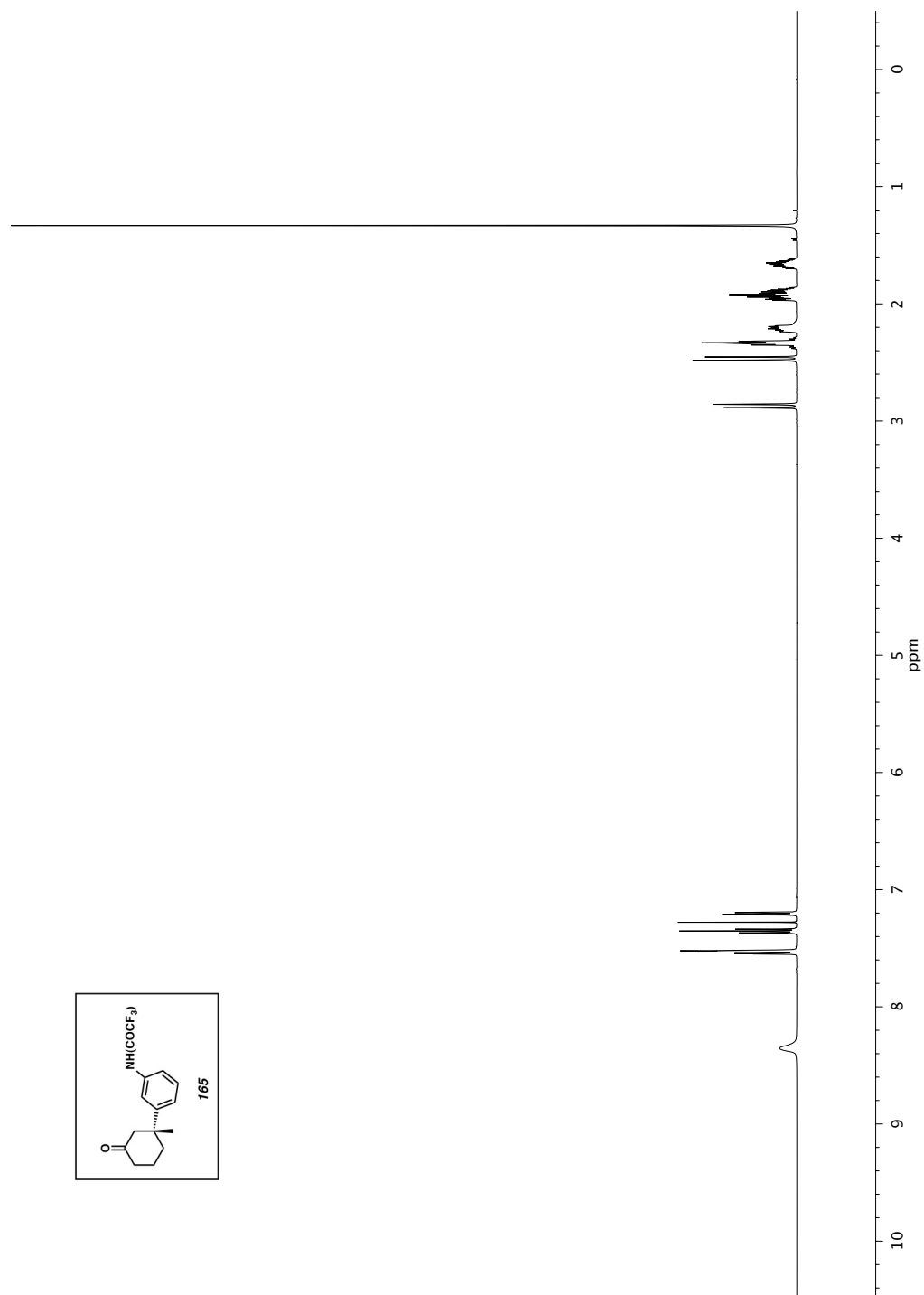
Figure A1.76 ^{1}H NMR (500 MHz, CDCl$_3$) of compound **165**
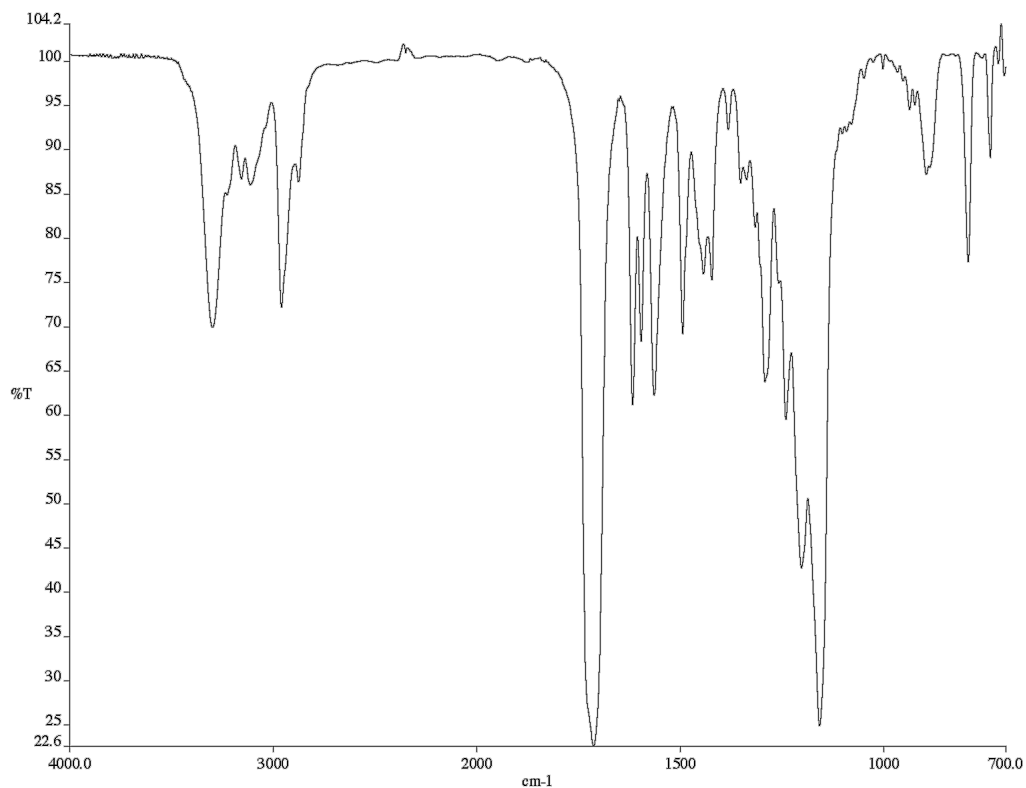
Figure A1.77 Infrared spectrum (Thin Film, NaCl) of compound **165**
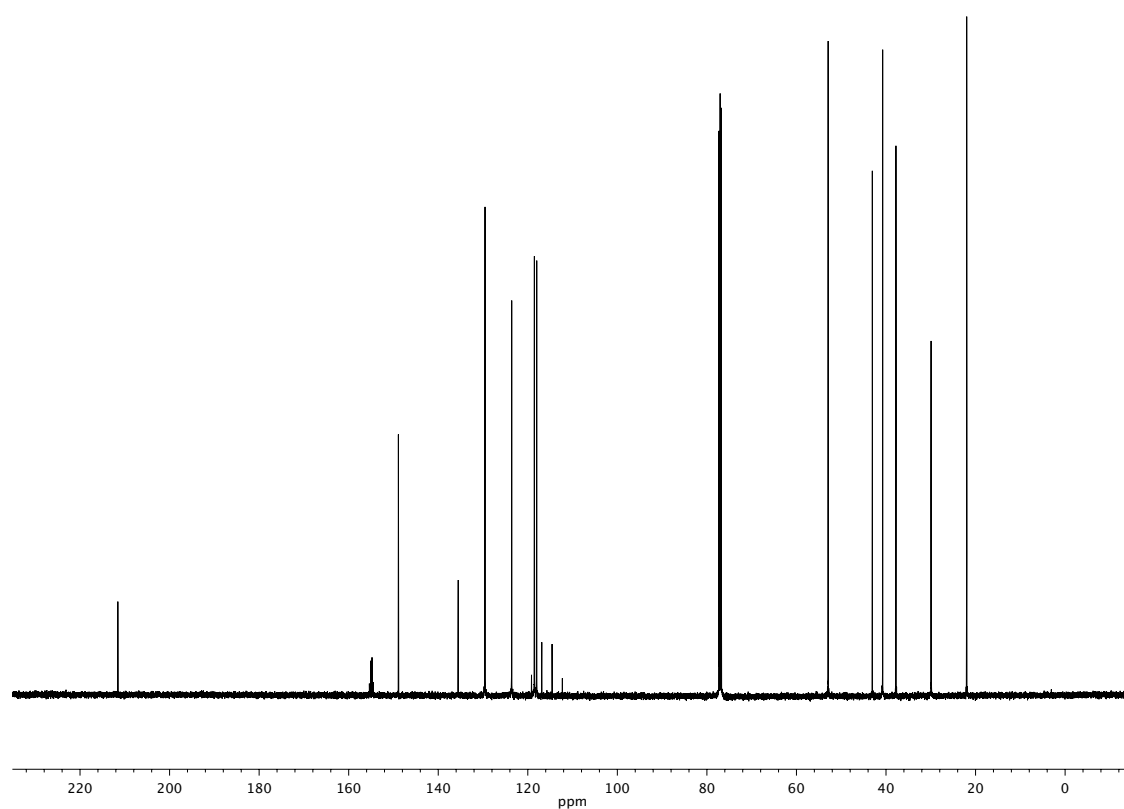
Figure A1.78 ^{13}C NMR (126 MHz, CDCl$_3$) of compound **165**
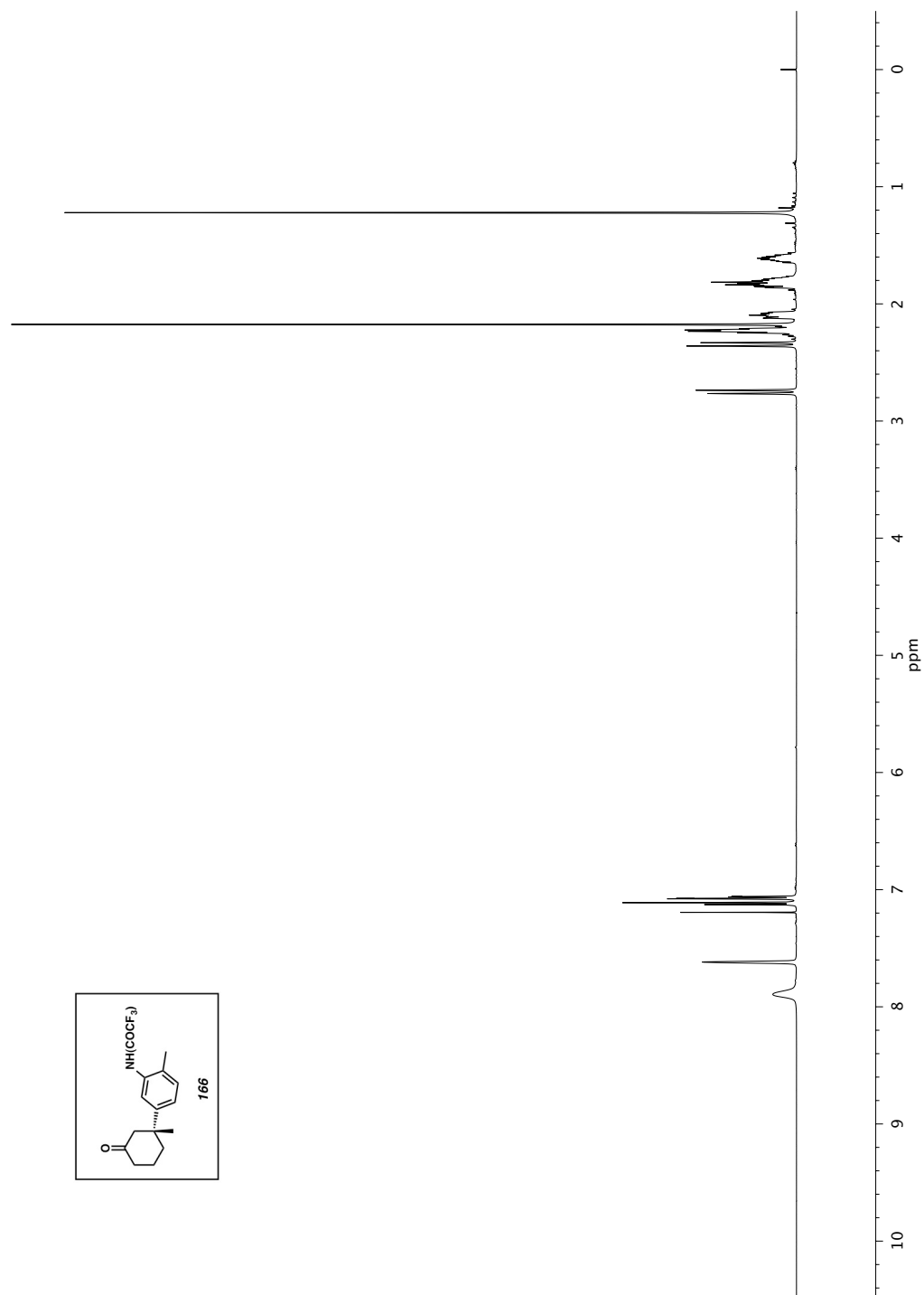
Figure A1.79 ^{1}H NMR (500 MHz, CDCl$_3$) of compound **166**
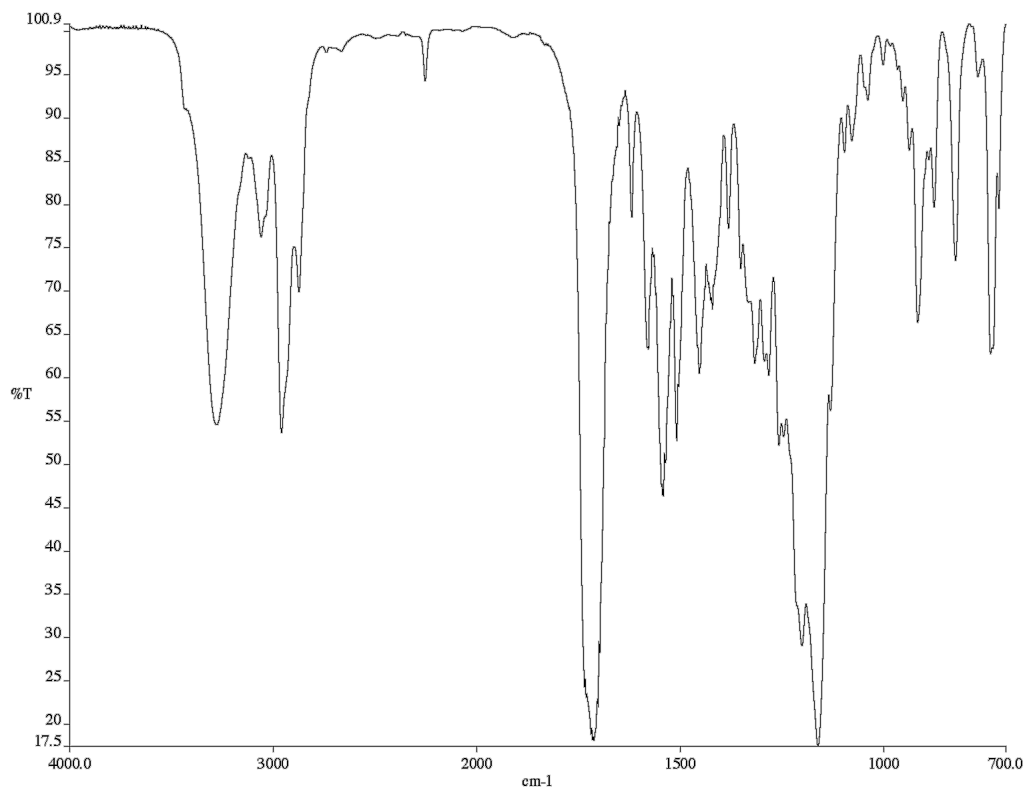
Figure A1.80 Infrared spectrum (Thin Film, NaCl) of compound **166**
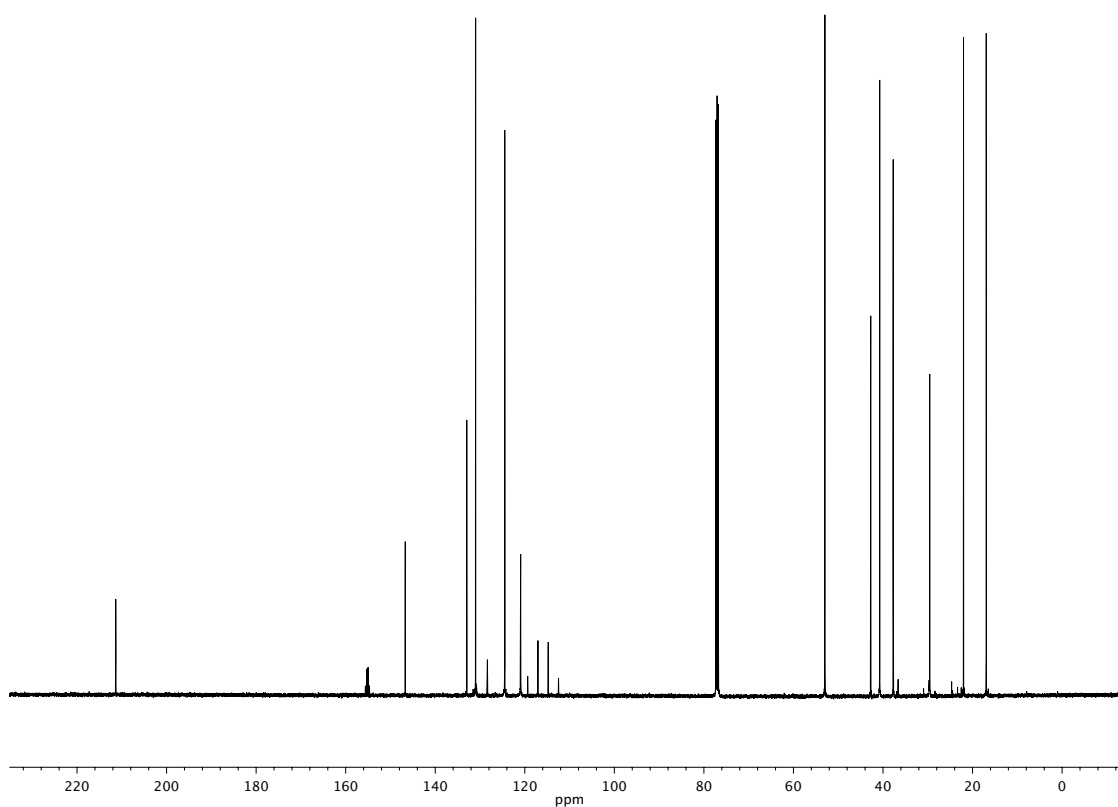
Figure A1.81 ^{13}C NMR (126 MHz, CDCl$_3$) of compound **166**

CHAPTER 3

Palladium-catalyzed asymmetric conjugate addition

of arylboronic acids to heterocyclic acceptors[±]

Single Catalyst System

X = O, NCbz

38 examples
up to 98% yield
up to 98% ee

Range of Heterocyclic Products

Abstract

Single Catalyst System

Range of Heterocyclic Products

X = O, NCbz

38 examples
up to 98% yield
up to 98% ee
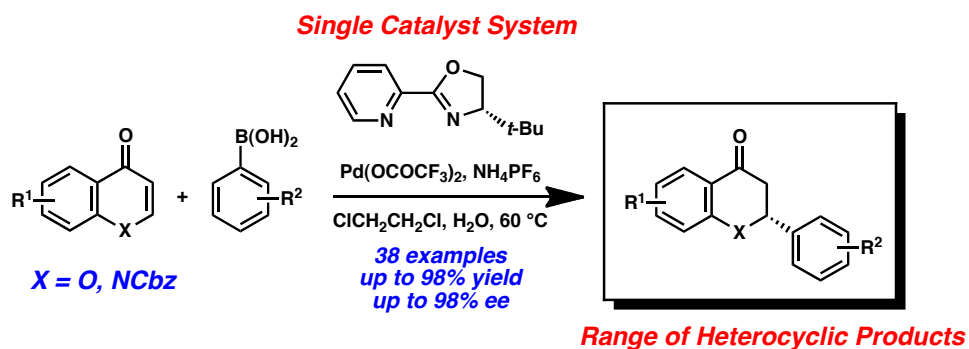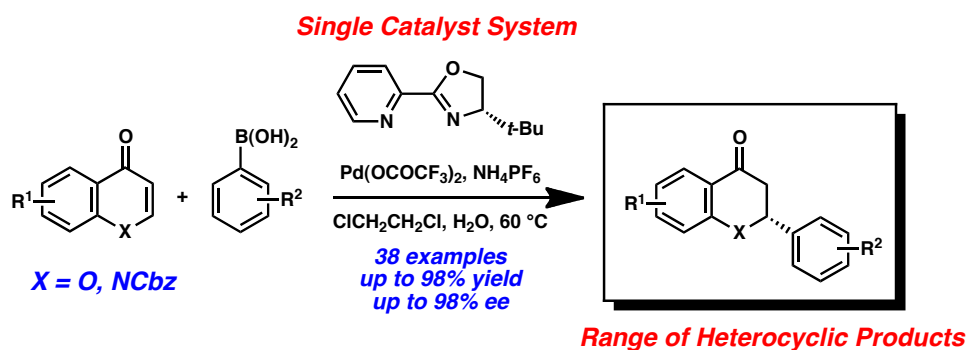
Asymmetric conjugate additions to chromones and 4-quinolones are reported utilizing a single catalyst system formed *in situ* from Pd(OCOCF$_3$)$_2$ and (*S*)-*t*-BuPyOx. Notably, these reactions are performed in wet solvent under ambient atmosphere, and utilize readily available arylboronic acids as the nucleophile, thus providing ready access to these asymmetric heterocycles.

3.1 Introduction

Palladium-catalyzed asymmetric conjugate additions are an increasingly versatile class of enantioselective reactions that allow for stereoselective alkylation and arylation of α,β-unsaturated conjugate acceptors.[1] These processes often utilize easily-handled, air- and water-stable boron nucleophiles that render these reactions highly tolerant of oxygen and moisture.[2] Recently, our group disclosed the asymmetric conjugate addition of arylboronic acids to cyclic enones facilitated by a palladium catalyst derived *in situ* from palladium(II) trifluoroacetate and a chiral pyridinooxazoline (PyOx) ligand (**82**).[3] Notably, our catalyst system was generally applicable for 5-, 6-, and 7-membered carbocyclic enones.

The numerous advantages of this system encouraged us to seek application to heterocyclic molecules, in order to demonstrate the broad utility of this reaction for the synthesis of pharmaceutically relevant molecules. Herein, we report the first general enantioselective conjugate addition of arylboronic acids to heterocyclic conjugate acceptors derived from chromones and 4-quinolones utilizing the Pd/PyOx catalyst system. These reactions are performed under an atmosphere of air and deliver a large variety of asymmetric products with high enantioselectivity in moderate to excellent yields. The stereoselective conversion of chromones through conjugate addition renders access to flavanones, a class of heterocyclic molecules that have demonstrated numerous medicinal properties.[4] Recent literature suggests that intramolecular oxa-Michael additions are among the best-studied synthetic methods for asymmetric flavanone synthesis.[5] However, examples for the retrosynthetic disconnection of flavanones via conjugate addition of an aryl moiety to a chromone derivative remain scarce.[6,7]

3.2 Results and discussion

3.2.1 Identification of chromones as substrates for Pd/PyOx asymmetric 1,4-addition

While chromones have been successfully employed in rhodium-catalyzed conjugate addition,[7] to the best of our knowledge, no palladium-catalyzed asymmetric conjugate addition syntheses of flavanones have been reported.[8] We identified chromone as a functioning conjugate acceptor with our Pd/PyOx system during a screen developed to analyze the effect of a β-substituent on reactivity and enantioselectivity (Table 3.1). As reported in our initial communication,[3] 3-methylcyclohexenone reacts with phenylboronic acid to give nearly quantitative yield of the conjugate addition adduct in 93% ee (entry 2). With only hydrogen in the β-position, enantioselectivity drops precipitously to 18% ee (entry 1). Interestingly, 2-methyl-4-chromone reacts poorly, with only trace conjugate addition adduct detected by 1H NMR spectroscopy (entry 4), yet chromone reacts with high yield and excellent enantioselectivity (94% ee, entry 3).

Table 3.1 Comparison of asymmetric conjugate additions to various enone substrates [a]

entry	product	product	yield (%)[b]	ee (%)[c]
1		*25 (R = H)*	87[d]	18
2		*35 (R = Me)*	99	93
3		*84 (R = H)*	91	94
4		*173 (R = Me)*	trace	--

[a] Conditions: chromone (0.25 mmol), arylboronic acid (0.50 mmol), Pd(OCOCF$_3$)$_2$ (5 mol %), Ligand (6 mol %), NH$_4$PF$_6$ (30 mol %), H$_2$O (5 equiv), ClCH$_2$CH$_2$Cl (1 mL), 60 °C, 12 h; [b] isolated yield; [c] ee determined by chiral SFC or HPLC; [d] no NH$_4$PF$_6$ was used.

3.2.1 Application of Pd/PyOx conjugate addition to asymmetric flavanone syntheses

We sought to explore the scope of the asymmetric conjugate addition of arylboronic acids to chromones with respect to the range of substrates and functional groups tolerated. Moderate yields and enantioselectivity were realized with sterically challenging 2-fluorophenylboronic acid (Table 3.2, entry 2). Arylboronic acid substitution at the *meta* position is generally tolerated with high enantioselectivity and moderate to good yields (entries 3–7). Notably, arylboronic acids with halogen substitutents in the *para* position (entry 10) and 3-carbomethoxyphenylboronic acid undergo conjugate addition with high enantioselectivity (entry 4). Furthermore, nitrogen-

containing substitution was well tolerated when protected as a trifluoroacetamide, producing the flavanone in 77% yield and 98% ee (entry 6). Other *para*-substituted arylboronic acids also reacted with high enantioselectivity: alkyl substituents on the phenylboronic acid yielded 94% and 85% ee (entries 8 and 9, respectively). With 3,5-dimethoxyphenylboronic acid, bearing multiple substituents, high enantioselectivity (95% ee) was obtained (entry 11). Remarkably, a heteroarylboronic acid was successfully reacted with chromone as the conjugate acceptor for the first time (entry 12), as 4-dibenzofuranboronic acid was converted with 64% yield and 77% ee in this case.

Table 3.2 Asymmetric conjugate addition of arylboronic acids to chromone [a]

entry	R =	yield (%)[b]	ee (%)[c]
1	H (84)	91	94
2	2-F-C_6H_4 (174)	50	76
3	3-Me-C_6H_4 (175)	66	90
4	3-CO_2Me-C_6H_4 (176)	72	93
5	3-Br-C_6H_4 (177)	40	89
6	3-NH(CO)CF_3-C_6H_4 (178)	77	98
7	3-Cl-C_6H_4 (179)	52	94
8	4-Me-C_6H_4 (180)	64	94
9	4-Et-C_6H_4 (181)	36	85
10	4-F-C_6H_4 (182)	51	90
11	3,5-OMe-C_6H_3 (183)	69	95
12	4-dibenzofuran (184)	64	77

[a] Conditions: chromone (0.25 mmol), arylboronic acid (0.50 mmol), Pd(OCOCF$_3$)$_2$ (5 mol %), Ligand (6 mol %),

NH$_4$PF$_6$ (30 mol %), H$_2$O (5 equiv), ClCH$_2$CH$_2$Cl (1 mL), 60 °C, 12 h; [b] isolated yield; [c] ee determined by

chiral SFC.

Substituted chromones were also found to perform well with the PyOx/Pd catalytic system. 5,7-dimethyl-6-acetylchromone was successfully converted with a variety of arylboronic acids (Table 3.3, i.e., **185–187**). Addition of phenylboronic acid gave nearly quantitative yield and 90% ee (**185**), while 3-methylphenylboronic acid saw diminished yield with comparable ee of 88% (**186**), and 4-ethylphenylboronic acid reacted with modest yield and 86% ee (**187**). Furthermore, a variety of *para-* and *meta-* substituted arylboronic acids were successfully converted with the corresponding 5,7-dimethyl-8-acetylchromone as well (i.e., **188–193**). Nucleophiles bearing functional group handles such as 3-carbomethoxy-phenylboronic acid and 3-bromophenylboronic acid reacted to yield flavanone products **192** and **190**, respectively, with good to moderate yield (60% and 65%) and high ee (i.e., 86% and 95%). Notably, with the present catalytic protocol 7-hydroxychromone could be successfully applied, yielding flavanones **196**, **197**, and **198** without protection of the phenol (Table 3.3). To our knowledge, this is the first example of an unprotected phenol reacted in asymmetric conjugate additions and serves to highlight the high functional group tolerance as compared to other systems.[7] 7-hydroxychromone underwent smooth conjugate addition with a range of boronic acids in good yield and enantioselectivity: phenylboronic acid (**196**, 77% yield, 93% ee), 3-methylphenylboronic acid (**197**, 66% yield, 90% ee), and 4-fluorophenylboronic acid (**198**, 50% yield, 93% ee). Finally, we found reaction of phenylboronic acids with substituted chromones to be general for a number of other substituted chromones including 5,7-dimethylchromone (flavanones **194** and **85**, 92% ee and 95% ee), 7-acetoxychromone (flavanone **195**, 93% ee) and 7-methoxychromone (flavanones **199** and **200**, 94% ee and 96% ee).

Table 3.3 Asymmetric conjugate addition of arylboronic acids to substituted chromones [a]
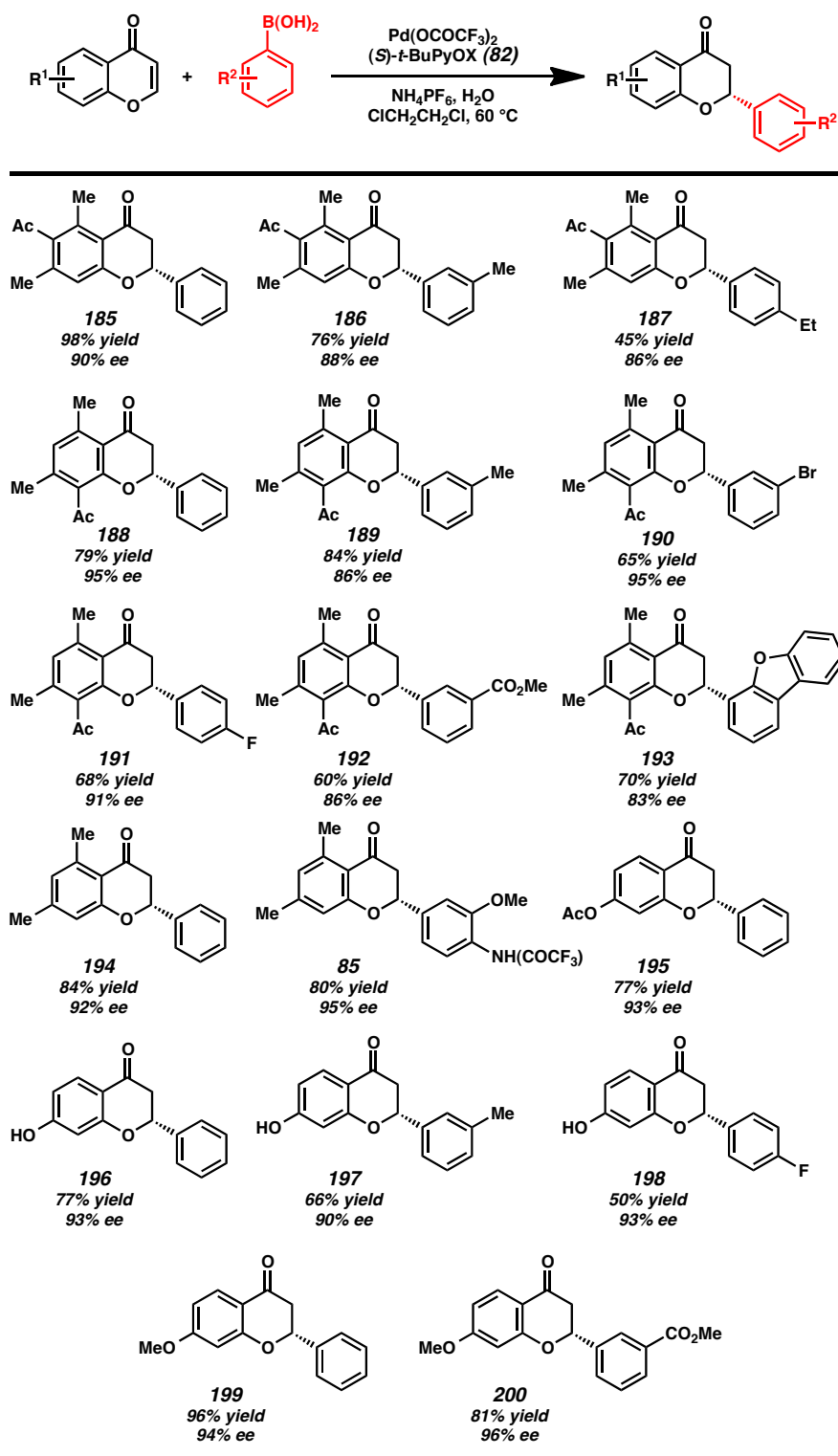
185
98% yield
90% ee

186
76% yield
88% ee

187
45% yield
86% ee

188
79% yield
95% ee

189
84% yield
86% ee

190
65% yield
95% ee

191
68% yield
91% ee

192
60% yield
86% ee

193
70% yield
83% ee

194
84% yield
92% ee

85
80% yield
95% ee

195
77% yield
93% ee

196
77% yield
93% ee

197
66% yield
90% ee

198
50% yield
93% ee

199
96% yield
94% ee

200
81% yield
96% ee

[a] Conditions: chromone (0.25 mmol), arylboronic acid (0.50 mmol), Pd(OCOCF$_3$)$_2$ (5 mol %), Ligand (6 mol %), NH$_4$PF$_6$ (30 mol %), H$_2$O (5 equiv), ClCH$_2$CH$_2$Cl (1 mL), 60 °C, 12 h, yields given are isolated yields, ee determined by chiral SFC.

3.2.2 Application of Pd/PyOx conjugate addition to 4-quinolone acceptors

We next turned our attention to 4-quinolones as a class of potential substrates. Like flavanones, 4-quinolones have been reported as potential pharmaceutical agents.[9] Yet, despite their promising antimitotic and antitumor activity, the enantioselective synthesis of 2-aryl-2,3-dihydro-4-quinolones remains a challenge in asymmetric conjugate addition. Hayashi and coworkers reported a rhodium-catalyzed asymmetric conjugate addition, which utilized 3 equivalents of arylzinc chloride nucleophiles and superstoichiometric chlorotrimethylsilane to react with Cbz-protected 4-quinolones.[10] While Hayashi notes that phenylboronic acid is a particularly poor nucleophile in reactions with protected 4-quinolones, giving the desired conjugate addition adduct in only 10% yield, Liao and coworkers reported rhodium-catalyzed asymmetric 1,4-addition of sodium tetraarylborate reagents to *N*-substituted 4-quinolones.[11] To the best of our knowledge, there are no literature reports of palladium-catalyzed conjugate additions to 4-quinolones, nor are there any robust examples of additions to the latter utilizing simple boronic acid nucleophiles

To our delight, Carboxybenzyl-protected (Cbz) 4-quinolone reacted with phenylboronic acid to yield conjugate addition adduct **201** in modest yield and 80% ee (Table 3.4). Investigation of further *N*-protecting groups demonstrated that the Carboxybenzyl-protected substrates gave the best results in terms of reactivity and stereoselectivity. Gratifyingly, a range of addition products could be prepared in yields up to 65% yield and 89% ee (Table 3.4). Nitrogen-containing, heteroaromatic and simpler boronic acid derivatives were successfully employed as nucleophiles in the 1,4-addition to 4-quinolones. For the corresponding alkyl- and halogen-substituted boronic acids,

reasonable yields (45–65%) and enantioselectivities (67–89% ee) were observed in the conjugate addition of 4-quinolones. Disubstituted boronic acids were well tolerated and gave similar results (**202** and **204**). Both compounds were obtained in 85% ee. For addition products **205**, **208**, and **209** yields and enantioselectivities ranging from 31% to 36% and 40% to 60% ee were achieved (Table 4). While the decreased yield of quinolone **209** can be rationalized by the sterically demanding nature of the boronic acid, the lower ee could not be readily explained.

Table 3.4 Asymmetric conjugate addition of arylboronic acids to 4-quinolones [a]
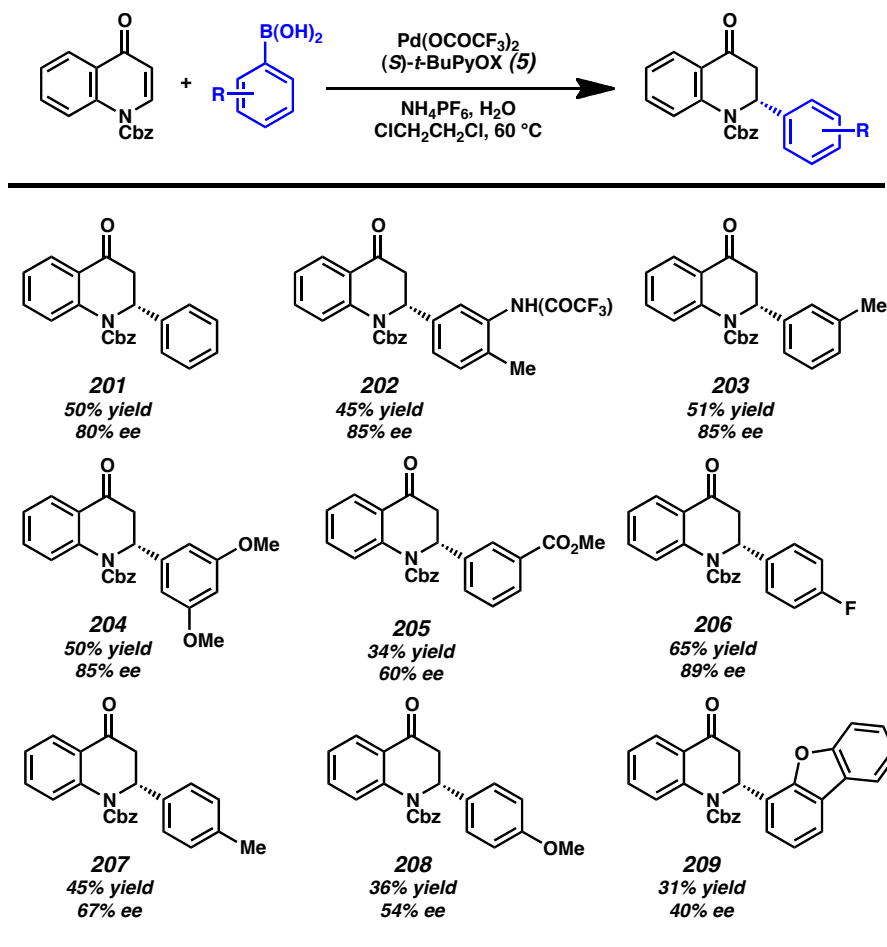
[a] Conditions: 4-quinolone (0.25 mmol), arylboronic acid (0.50 mmol), Pd(OCOCF$_3$)$_2$ (5 mol %), Ligand (6 mol %), NH$_4$PF$_6$

(30 mol %), H$_2$O (5 equiv), ClCH$_2$CH$_2$Cl (1 mL), 60 °C, 12 h, yields given are isolated yields, ee determined by chiral SFC.

3.2.3 Experiments excluding Pd(0) nanoparticles as heterogeneous catalysts

To confirm the homogenous nature of our catalyst system and exclude the possibility of erosion of enantiomeric excess due to the presence of catalytically active, achiral Pd nanoparticles, a mercury drop test was performed. The addition of mercury to a catalytic reaction is widely used to exclude catalysis by Pd- nanoparticles as the amalgamation should only deactivate heterogeneous metal particles.[12] For the conversion of chromone with phenylboronic acid in presence of 200 equiv of mercury, with respect to the catalyst, only a slight drop of the yield from 91% to 80% was observed, while the ee of 94% remained unaltered. Addition of mercury to the reaction of 3-Me-cyclohexenone and phenylboronic acid resulted in quantitative yield and a slightly reduced ee of 90% for addition product **2**, which is within error margins. Hence, the formation of zerovalent Pd-nanoparticles could be excluded.

3.3 Summary and Concluding Remarks

In conclusion, we report the palladium-catalyzed conjugate addition of arylboronic acids to chromones and 4-quinolones using a single, easily prepared catalyst system. To our knowledge this is the first report of a palladium-catalyzed asymmetric conjugate addition to chromones and 4-quinolones using either palladium catalysis or arylboronic acid nucleophiles. Overall, a total of 38 addition products could be synthesized in moderate to excellent yield and generally high enantioselectivity. The present catalytic protocol exhibits particularly mild reaction conditions and renders the use of silver salts for catalyst activation obsolete. Furthermore, moisture and air are well tolerated; this results in an unprecedented functional group tolerance. Hence, the direct

synthesis of flavanones bearing free hydroxyl-groups via conjugate addition and the application of *N*-substituted, as well as heterocyclic boronic acids, is realized. Kinetic and computational studies to elucidate the present catalytic reaction mechanism are presented in Chapter 4. Furthermore, continued study of the substrate scope of the Pd/PyOx system and its reactivity, as well as the application of these operationally simple asymmetric conjugate addition reactions to total synthesis are underway in our laboratory

3.4 Experimental procedures

3.4.1 Materials and methods

Unless otherwise stated, reactions were performed with no extra precautions taken to exclude air or moisture. Commercially available reagents were used as received from Sigma Aldrich unless otherwise stated. Enone substrates were purchased from Sigma Aldrich (3-methylcyclohexenone, 2-cyclohexene-1-one, chromone) or prepared according to literature procedure.[10] Reaction temperatures were controlled by an IKAmag temperature modulator. Thin-layer chromatography (TLC) was performed using E. Merck silica gel 60 F254 precoated plates (250 nm) and visualized by UV fluorescence quenching, potassium permanganate, or *p*-anisaldehyde staining. Silicycle Silia*Flash* P60 Academic silica gel (particle size 40-63 nm) was used for flash chromatography. Analytical chiral HPLC was performed with an Agilent 1100 Series HPLC utilizing a Chiralcel OJ column (4.6 mm x 25 cm) obtained from Daicel Chemical Industries, Ltd with visualization at 254 nm and flow rate of 1 mL/min, unless otherwise stated. Analytical chiral SFC was performed with a JASCO 2000 series instrument utilizing Chiralpak (AD-H or AS-H) or Chiralcel (OD-H, OJ-H, or OB-H) columns (4.6

mm x 25 cm), or a Chiralpak IC column (4.6 mm x 10 cm) obtained from Daicel Chemical Industries, Ltd with visualization at 210 or 254 nm. ^{1}H and ^{13}C NMR spectra were recorded on a Varian Inova 500 (500 MHz and 125 MHz, respectively) and a Varian Mercury 300 spectrometer (300 MHz and 75 MHz, respectively). Data for ^{1}H NMR spectra are reported as follows: chemical shift (δ ppm) (multiplicity, coupling constant (Hz), integration). Data for ^{1}H NMR spectra are referenced to the centerline of CHCl$_3$ (δ 7.26) or (CH$_3$)$_2$CO (δ 2.05) as the internal standard and are reported in terms of chemical shift relative to Me$_4$Si (δ 0.00). Data for ^{13}C NMR spectra are referenced to the centerline of CDCl$_3$ (δ 77.0) or (CD$_3$)$_2$CO (δ 29.8, 206.3) and are reported in terms of chemical shift relative to Me$_4$Si (δ 0.00). Infrared spectra were recorded on a Perkin Elmer Paragon 1000 Spectrometer and are reported in frequency of absorption (cm^{-1}). High resolution mass spectra (HRMS) were obtained on an Agilent 6200 Series TOF with an Agilent G1978A Multimode source in electrospray ionization (ESI), atmospheric pressure chemical ionization (APCI) or mixed (MultiMode ESI/APCI) ionization mode. Optical rotations were measured on a Jasco P-2000 polarimeter using a 100 mm path-length cell at 589 nm.

3.4.2 Experimental procedures
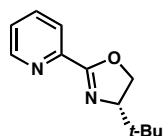
(*S*)-4-(*tert*-butyl)-2-(pyridin-2-yl)-4,5-dihydrooxazole (82)

Adapted from: Brunner, H.; Obermann., U. *Chem. Ber.* **1989**, *122*, 499–507.

A flame-dried round bottom flask was charged with a stir bar and MeOH (110 mL). Sodium metal ingot (295 mg, 12.8 mmol, 0.1 equiv) was cut with a razor into small portions, washed in a beaker of hexanes, and added in five portions over 5 min to the stirring flask of MeOH. The reaction mixture was stirred vigorously at ambient temperature until no sodium metal remained, at which time it was cooled to 0 °C in an ice/water bath. At this time, 2-cyanopyridine (13.0 g, 125 mmol, 1.0 equiv) was added dropwise, and the clear, colorless reaction mixture was allowed to warm to ambient temperature with stirring. When all the starting material was consumed as indicated by TLC analysis (50% EtOAc/Hexanes, *p*-anisaldehyde stain), the reaction was cooled to 0 °C in an ice/water bath and quenched by dropwise addition of glacial AcOH (1 mL). The crude reaction mixture was evaporated *in vacuo*, redissolved in CH_2Cl_2 (100 mL) and washed with brine (2 x 50 mL). The organic phase was dried ($MgSO_4$), concentrated *in vacuo*, and dried under high vacuum for 1 h. The resulting crude methoxyimidate (light yellow oil) was suitable for use in the next step without further purification.

To a flame-dried round bottom flask charged with a stir bar was added crude methoxyimidate (2.55 g, 18.7 mmol, 1.0 equiv), (*S*)–*tert*-leucinol (2.10 g, 17.9 mmol, 0.96 equiv), and toluene (100 mL), and *p*-TsOH•H_2O (167 mg, 0.88 mmol, 5 mol%). The mixture was stirred at 80 °C in an oil bath for 3 h, at which time the starting material was consumed as indicated by TLC analysis (20% acetone/hexanes, *p*-anisaldehyde stain). The reaction was cooled to ambient temperature and quenched with sat. $NaHCO_3$ (60 mL). The reaction was partitioned with EtOAc and water, and the aqueous phase was extracted with EtOAc (3 x 50 mL). The combined organic extracts were washed with water (2 x 50 mL), brine (1 x 25 mL), dried ($MgSO_4$) and concentrated in vacuo. The

crude mixture was purified by flash column chromatography (eluent: 20% acetone/hexanes) to afford 1.85 g (9.06 mmol, 51%) (*S*)-*t*-BuPyOX as an off-white solid. R_f = 0.44 with 3:2 hexanes/acetone; mp 70.2 - 71.0 °C; ^{1}H NMR (500 MHz, CDCl$_3$) δ 8.71 (ddd, *J* = 4.8, 1.8, 0.9 Hz, 1H), 8.08 (dt, *J* = 7.9, 1.1 Hz, 1H), 7.77 (dt, *J* = 7.7, 1.7 Hz, 1H), 7.37 (ddd, *J* = 7.0, 4.5, 1.0 Hz, 1H), 4.45 (dd, *J* = 10.2, 8.7 Hz, 1H), 4.31 (t, *J* = 8.5 Hz, 1H), 4.12 (dd, *J* = 10.2, 8.5 Hz, 1H), 0.98 (s, 9H); ^{13}C NMR (125 MHz, CDCl$_3$) δ 162.4, 149.6, 147.0, 136.5, 125.4, 124.0, 76.5, 69.3, 34.0, 26.0; IR (Neat film, NaCl): 2981, 2960, 2863, 1641, 1587, 1466, 1442, 1358, 1273, 1097, 1038, 968 cm^{-1}; HRMS (MultiMode ESI/APCI) *m/z* calc'd for C$_{12}$H$_{17}$ON$_2$ [M+H]$^+$: 205.1335, found 205.1327; $[\alpha]^{25}_D$ –90.5° (c 1.15, CHCl$_3$).

Representative General Procedure for the Enantioselective 1,4-Addition of Arylboronic Acids to Heteroaromatic Conjugate Acceptors

A screw-top 1 dram vial was charged with a stir bar, Pd(OCOCF$_3$)$_2$ (4.2 mg, 0.0125 mmol, 5 mol%), (*S*)-*t*-BuPyOX (3.1 mg, 0.015 mmol, 6 mol%), NH$_4$PF$_6$ (12.5 mg, 0.075 mmol, 30 mol%) and PhB(OH)$_2$ (61 mg, 0.50 mmol, 2.0 equiv). The solids were suspended in dichloroethane (0.5 mL) and stirred for 2 min at ambient temperature, at which time a yellow color was observed. Not all solids were dissolved at this time. Conjugate acceptor substrate (0.25 mmol) and water (0.025 mL, 1.25 mmol, 5.0 equiv) were added. The walls of the vial were rinsed with an additional portion of dichloroethane (0.5 mL), and the vial was capped with a Teflon/silicone septum and stirred at 60 °C in an oil bath for 12 h. Upon complete consumption of the starting material (monitored by TLC, 4:1 hexanes/EtOAc, *p*-anisaldehyde or iodine/silica gel

stain) the reaction mixture was filtered through a pipet plug of silica gel using CH_2Cl_2 as the eluent and concentrated *in vacuo*. The crude residue was purified by column chromatography (gradient: 9:1 hexanes/EtOAc to 7:3 hexanes/EtOAc) to afford the title compound.

General Procedure for the Synthesis of Racemic Products

Racemic products were synthesized in a manner analogous to the general procedure using PyOX synthesized from racemic *tert*-leucinol (3.1 mg, 0.015 mmol, 6 mol%) as an achiral ligand.

General Procedure for the synthesis of *N*-trifluoroacetamide Boronic Acids from Bromo-trifluoroacetanilides

A flame round bottom flask was charged with bromo-trifluoroacetanilide (3.7 mmol, 1 equiv). The flask was sealed, evacuated and backfilled with argon. THF (20 ml) was added via syringe and the obtained mixture was cooled to -78 °C. *n*-BuLi (2.3 M solution in hexane, 3.6 mL, 8.2 mmol, 2.2 equiv) was added dropwise and the reaction was stirred for 2 h. Triisopropylborate (2.7 mL, 11.7 mmol, 3 equiv) was then added via syringe and the mixture was stirred for 10 minutes, at which time the cooling bath was removed and the reaction was allowed to stir and warm to room temperature for 1 h. A solution of HCl (2 M in water, 10 mL) was added and the biphasic mixture was vigorously stirred for 1 and then extracted with EtOAc (3 x 30 mL). The combined organic extracts where washed with brine (2 x 20 ml) and dried over $MgSO_4$. Upon concentration *in vacuo* an off-white solid was obtained. The solid was suspended in

hexane and stirred until a fine powder was formed, filtered, and dried in high vacuum for 30 minutes to obtain the title boronic acid.

3-(2,2,2-trifluroacetamide)-4-methylphenylboronic acid

Obtained as an off-white solid in 35% yield following the general procedure. ^{1}H NMR (300 MHz, acetone) δ 9.34 (s, 1H), 8.05 (dd, J = 3.0, 6.9 Hz, 1H), 7.58 (s 1H), 7.54 (dd, J = 7.9, 1.0 Hz, 1H) 7.29 (s, 1H), 3.93 (s, 3H); 13C NMR (125 MHz, acetone) δ 154.3 (q, J_{C-F} = 150 Hz), 149.3, 126.8, 126.6, 120.5, 116.1, 115.8 (q, J_{C-F} = 288 Hz), 112.5, 55.4; IR (Neat Film, NaCl): 3298, 1708, 1591, 1537, 1503, 1465, 1404, 1342, 1294, 1273, 1224, 1161, 1123, 1015; HRMS (MultiMode ESI/APCI) m/z calc'd for $C_9H_8BO_4NF_3$ [M-H]$^-$: 261.0590, found: 261.0497.

3-(2,2,2-trifluroacetamide)-phenylboronic acid

Obtained as an off-white solid in 66 % yield following the general procedure. ^{1}H NMR (300 MHz, acetone-d6) δ 8.11 (bs, 1H), 7.81 (m, 1H), 7.74 (dt, J = 7.4, 1.0 Hz 1H), 7.40 (t, J = 7.7 Hz, 1H), 7.28 (s, 1H); (The obtained ^{13}C NMR is complex due to the presence of two rotamers in solution) ^{13}C NMR (125 MHz, CDCl$_3$) δ 154.8 (q, J = 36.9 Hz), 135.8, 135.7, 131.5, 128.2, 126.7, 126.6, 123.0, 122.9, 116.2 (q, J = 288.1 Hz); IR (Neat

Film, NaCl): 3305, 1701, 1585, 1554, 1437, 1334, 1264, 1182, 1031, 780 cm^{-1}; HRMS

(MultiMode ESI/APCI) *m/z* calc'd for $C_8H_7BrF_3NO$ [M-H]$^-$: 231.0435, found: 231.0433.
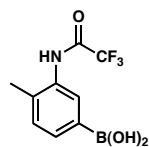
3-(2,2,2-trifluroacetamide)-4-methylphenylboronic acid.

Obtained as an off-white solid in 66% yield following the general procedure. ^{1}H NMR

(300 MHz, acetone) δ 9.91 (bs, 1H), 7.82 (s, 1H), 7.75 (dd, *J* = 6.5, 10 Hz, 1H), 7.32 (d, *J*

= 7.5 Hz, 1H) 7.24 (s, 1H), 2.29 (s, 3H); ^{13}C NMR (125 MHz, acetone-d$_6$) δ 155.4 (q, *J* =

37.5 Hz), 136.2, 133.5, 132.9, 132.1, 130.1, 116.4 (q, *J* = 288.0 Hz), 16.8; FTIR (Neat

Film, NaCl) 3270, 1708, 1617, 1533, 1406, 1351, 1259, 1180, 1162, 1092, 1036, 898,

825 cm^{-1}; HRMS (MultiMode ESI/APCI) *m/z* calc'd for $C_9H_8BF_3NO_3$ [M-H]$^-$: 245.0477,

found 245.0591.

General Procedure for the Synthesis of Substituted Chromones

A known literature procedure was used.[13] An Erlenmeyer flask charged with the

corresponding hydroxy acetophenone (26.2 mmol, 1 equiv) was suspended in

triethylorthoformate (12 mL). A 70 % aqueous solution of $HClO_4$ was added rapidly via

syringe (1.3 mL) and the obtained mixture was stirred for 30 minutes at room

temperature. A moderate increase in temperature is observed. Et_2O was added to

precipitate a red-brown solid that was filtered and transferred into a flask. Water (10 mL)

was added and the flask was warmed to 100 °C for 10 minutes. The solid rapidly

dissolve and re-precipitate. The mixture is cooled to room temperature and filtered. The

obtained solid can be purified via crystallization from ethanol (17 mL EtOH/ 4 mL H_2O, 80 °C) and the obtained powder is pure by NMR analysis, but often contains colored impurities. This compound is typically further purified by flash chromatography to obtain off-white powders. All characterization data for the following chromones matches previously reported data: 7-hydroxychromone,[2] 7-methoxychromone,[14] 7-acetoxy-chromone,[15] 5,7-dimethylchromone,[16]
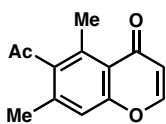
7-acetoxy-chromen-4-one

Synthesized from 1,1'-(4-hydroxy-2,6-dimethyl-1,3-phenylene)diethanone in 82% yield by the general procedure, obtained as an off-white powder solid. ^{1}H NMR (500 MHz, CDCl$_3$) δ 7.68–7.62 (m, 1H), 7.06 (d, J = 3.5 Hz, 1H), 6.18–6.13 (m, 1H), 2.71–2.65 (m, 3H), 2.44 (q, J = 1.4 Hz, 3H), 2.28–2.23 (m, 3H); ^{13}C NMR (125 MHz, CDCl$_3$) δ 207.3, 179.3, 157.4, 153.4, 140.8, 138.5, 135.4, 121.1, 117.5, 114.4, 32.5, 19.5, 18.8; IR (Neat Film, NaCl): 3086, 2987, 2918, 1701, 1649, 1604, 1443, 1354, 1339, 1245, 1221, 1182, 1060 cm^{-1}; HRMS (MultiMode ESI/APCI) m/z calc'd for $C_{13}H_{13}O_3$ [M+H]$^+$: 217.0859, found: 217.0858.

3.4.3 Spectroscopic Data for Enantioenriched Products
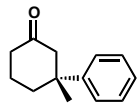
(*R*)-3-phenyl-3-methylcyclohexanone (35)

Synthesized according to the general procedure and purified by flash chromatography (9:1 hexanes/EtOAc) to afford a pale yellow oil (99% yield). $[\alpha]^{25}_D$ –56.1° (*c* 1.36, CHCl$_3$, 93% ee). All characterization data matches previously reported data.[17, 18, 19, 20, 21, 22, 23]
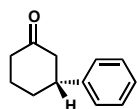
(*R*)-3-phenylcyclohexanone (25)

Synthesized according to the general procedure and purified by flash chromatography (9:1 hexanes/EtOAc) to afford a pale yellow oil (89% yield). $[\alpha]^{25}_D$ –2.93° (*c* 1.01, CHCl$_3$, 18% ee). All characterization data matches previously reported data.[24]

(*R*)-2-phenylchroman-4-one (84)

Synthesized according to the general procedure and purified by flash chromatography (9:1 hexanes/EtOAc) to afford an off-white solid (91% yield). $[\alpha]^{25}_D$ 67.3° (*c* 0.95, CHCl$_3$, 92% ee). All characterization data matches previously reported data.[7]

(*R*)-2-(2-fluorophenyl)chroman-4-one (174)

Synthesized according to the general procedure and purified by flash chromatography

(9:1 hexanes/EtOAc) to afford an off-white solid (50% yield). ^{1}H NMR (500 MHz,

CDCl$_3$) δ 7.97 (dd, *J* = 1.5, 7.5 Hz, 1H), 7.67 (dt, *J* = 1.7, 7.6 Hz, 1H), 7.54 (ddd, *J* = 1.8,

7.1, 8.2 Hz, 1H), 7.39 (ddt. *J* = 1.7, 5.4, 7.8 Hz, 1H), 7.25–7.28 (m, 1H), 7.07–7.16 (m,

3H), 5.81 (dd, *J* = 2.9, 13.4 Hz, 1H), 3.08 (dd, *J* = 13.4, 16.9 Hz, 1H), 2.93 (dd, *J* = 2.9,

16.9 Hz, 1H); ^{13}C NMR (125 MHz, CDCl$_3$) δ 191.5, 161.5, 160.6, 158.6, 136.2, 130.6,

130.2, 127.5, 127.4, 126.2, 126.1, 124.5, 124.5, 121.8, 120.9, 118.9, 118.0, 115.8, 115.6,

73.8, 73.8, 43.7; IR (Neat Film, NaCl): 1698, 1609, 1577, 1493, 1463, 1370, 1305, 1224,

1149, 1116, 1068 cm^{-1}; HRMS (MultiMode ESI/APCI) *m/z* calc'd for C$_{15}$H$_{12}$FO$_2$

[M+H][+]: 243.0816, found 243.0814; [α]$^{25}_D$ 63.6° (*c* 3.0, CHCl$_3$, 76% ee).

(*R*)-2-(m-tolyl)chroman-4-one (175)

Synthesized according to the general procedure and purified by flash chromatography

(9:1 hexanes/EtOAc) to afford an off-white solid (66% yield). [α]$^{25}_D$ 45.5° (*c* 6.9, CHCl$_3$,

90% ee). All characterization data matches previously reported data.[25]

(*R*)-methyl 3-(4-oxochroman-2-yl)benzoate (176)

Synthesized according to the general procedure and purified by flash chromatography

(9:1 hexanes/EtOAc) to afford an off-white solid (72% yield). ^{1}H NMR (500 MHz,

CDCl$_3$) δ 8.18 (t, *J* = 1.8 Hz, 1H), 8.06 (dt, *J* = 1.4, 7.8 Hz, 1H), 7.93 (dd, *J* = 1.7, 8.1

Hz, 1H), 7.68 (dq, *J* = 1.2, 7.8 Hz, 1H), 7.57–7.44 (m, 2H), 7.10–6.93 (m, 2H), 5.53 (dd,

J = 2.8, 13.4 Hz, 1H), 3.93 (s, 3H), 3.07 (dd, *J* = 13.4, 16.8, Hz, 1H), 2.91 (dd, *J* = 2.9,

16.8 Hz, 1H); ^{13}C NMR (125 MHz, CDCl$_3$) δ 191.6, 166.7, 161.4, 139.4, 136.4, 130.9,

130.6, 130.0, 129.1, 127.4, 127.2, 121.9, 121.0, 118.2, 79.00, 52.4, 44.8; IR (Neat Film,

NaCl): 2951, 1720, 1691, 1606, 1577, 1463, 1431, 1359, 1304, 1225, 1214, 1149, 1114,

1068 cm^{-1}; HRMS (MultiMode ESI/APCI) *m/z* calc'd for C$_{17}$H$_{15}$O$_4$ [M+H]$^+$: 283.0965,

found 285.0967; [α]$^{25}_D$ 66.5° (*c* 1.00, CHCl$_3$, 93% ee).

(*R*)-2-(3-bromophenyl)chroman-4-one (177)

Synthesized according to the general procedure and purified by flash chromatography

(9:1 hexanes/EtOAc) to afford an off-white solid (40% yield). ^{1}H NMR (500 MHz,

CDCl$_3$) δ 7.94 (dd, *J* = 2.0, 8.5 Hz, 1H), 7.68 (bs, 1H), 7.53 (dt, *J* = 1.7, 7.8 Hz, 2H), 7.39

(d, *J* = 7.6 Hz, 1H), 7.31 (t, *J* = 7.8 Hz, 1H), 7.08 (t, *J* = 7.6 Hz, 2H), 5.46 (dd, *J* = 2.9,

13.2 Hz, 1H), 3.04 (dd, *J* = 13.2, 16.9 Hz, 1H), 2.89 (dd, *J* = 2.9, 16.9 Hz, 1H); ^{13}C NMR

(125 MHz, CDCl$_3$) δ 191.3, 161.2, 140.9, 136.3, 131.7, 130.3, 129.2, 127.0, 124.6, 122.9,

121.8, 121.6, 118.1, 78.6, 44.6; IR (Neat Film, NaCl): 1691, 1605, 1575, 1463, 1362,

1304, 1226, 1152, 1115, 1067 cm^{-1}; HRMS (MultiMode ESI/APCI) *m/z* calc'd for

$C_{15}H_{12}BrO_2$ [M+H]$^+$: 300.9871, found 300.9870; [α]$^{25}_D$ 53.5° (*c* 3.0, CHCl$_3$, 89% ee).

(*R*)-2,2,2-trifluoro-N-(3-(4-oxochroman-2-yl)phenyl)acetamide (178)

Synthesized according to the general procedure and purified by flash chromatography

(gradient: 8:2 hexanes/EtOAc to 7:3 hexanes/EtOAc) to afford an off-white solid (40%

yield). ^{1}H NMR (500 MHz, CDCl$_3$) δ 8.07 (bs, 1H), 7.94 (d, *J* = 7.7 Hz, 1H), 7.79 (s,

1H), 7.67–7.58 (m, 1H), 7.54 (t, *J* = 7.8 Hz, 1H), 7.48 (t, *J* = 7.9 Hz, 1H), 7.35 (d, *J* = 7.7

Hz, 1H), 7.08 (t, *J* = 8.9 Hz, 2H), 5.51 (dd, *J* = 3.1, 13.3 Hz, 1H), 3.06 (dd, *J* = 13.1, 16.9

Hz, 1H), 2.92 (dd, *J* = 3.1, 16.9 Hz, 1H); ^{13}C NMR (125 MHz, CDCl$_3$) δ 191.5, 161.2,

154.6–154.9 (m), 140.4, 136.4, 135.7, 129.9, 127.1, 123.9, 121.9, 120.9, 120.6, 118.1,

118.1, 114.4–116.7 (m), 78.9, 44.7; IR (Neat Film, NaCl): 3304, 1718, 1684, 1607, 1565,

1465, 1307, 1208, 1148, 1116 cm^{-1}; HRMS (MultiMode ESI/APCI) *m/z* calc'd for

$C_{17}H_{13}O_3F_3N$ [M+H]$^+$: 336.0847, found 336.0854; [α]$^{25}_D$ 74.4° (*c* 1.02, CHCl$_3$, 98% ee).

(*R*)-2-(*p*-tolyl)chroman-4-one (179)

Synthesized according to the general procedure and purified by flash chromatography

(9:1 hexanes/EtOAc) to afford an off-white solid (64% yield). $[\alpha]^{25}_{D}$ 30.0° (*c* 1.85, CHCl$_3$, 94% ee). All characterization data matches previously reported data.^{Error! Bookmark not defined.}

(*R*)-2-(4-ethylphenyl)chroman-4-one (180)

Synthesized according to the general procedure and purified by flash chromatography (9:1 hexanes/EtOAc) to afford an off-white solid (36% yield). ^{1}H NMR (500 MHz, CDCl$_3$) δ 7.94 (dd, *J* = 1.8, 8.2 Hz, 1H), 7.51 (ddd, *J* = 1.7, 7.1, 8.3 Hz, 1H), 7.45–7.34 (m, 2H), 7.32–7.21 (m, 2H), 7.12 –6.92 (m, 2H), 5.46 (dd, *J* = 2.8, 13.4 Hz, 1H), 3.11 (dd, *J* = 13.5, 16.9 Hz, 1H), 2.88 (dd, *J* = 2.8, 16.9 Hz, 1H), 2.69 (q, *J* = 7.7 Hz, 2H), 1.26 (t, *J* = 7.6 Hz, 3H); ^{13}C NMR (125 MHz, CDCl$_3$) δ 192.1, 161.6, 145.0, 136.1, 135.8, 128.3, 126.9, 126.2, 121.5, 120.8, 118.1, 79.5, 44.5, 28.6, 15.5; IR (Neat Film, NaCl): 2964, 2930, 2896, 2872, 1691, 1605, 1576, 1516, 1472, 1463, 1420, 1367, 1319, 1304, 1225, 1148, 1114, 1068 cm^{-1}; HRMS (MultiMode ESI/APCI) *m/z* calc'd for C$_{17}$H$_{17}$O$_2$ [M+H]$^+$: 253.1223, found 253.1225; $[\alpha]^{25}_{D}$ 20.7° (*c* 0.4, CHCl$_3$, 95% ee).
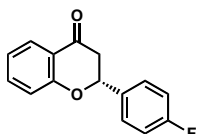
(*R*)-2-(4-fluorophenyl)chroman-4-one (182)

Synthesized according to the general procedure and purified by flash chromatography

(9:1 hexanes/EtOAc) to afford an off-white solid (51% yield). $[\alpha]^{25}_{D}$ 29.6° (*c* 3.4, CHCl$_3$, 90% ee). All characterization data matches previously reported data.[25]
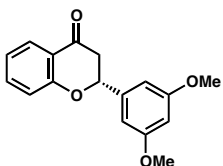
(*R*)-2-(3,5-dimethoxyphenyl)chroman-4-one (183)

Synthesized according to the general procedure and purified by flash chromatography (gradient: 8:2 hexanes/EtOAc to 7:3 hexanes/EtOAc) to afford an off-white solid (69% yield). ^{1}H NMR (500 MHz, CDCl$_3$) δ 7.93 (ddd, *J* = 0.7, 1.8, 7.5 Hz, 1H), 7.52 (ddd, *J* = 1.8, 7.3, 8.3Hz, 1H), 7.15–6.93 (m, 2H), 6.63 (dd, *J* = 0.6, 2.2 Hz, 2H), 6.47 (t, *J* = 2.3 Hz, 1H), 5.51–5.30 (m, 1H), 3.82 (s, 6H), 3.07 (dd, *J* = 13.3, 16.9 Hz, 1H), 2.89 (dd, *J* = 2.9, 16.9 Hz, 1H); ^{13}C NMR (125 MHz, CDCl$_3$) δ 191.9, 161.4, 161.1, 141.0, 136.2, 127.0, 121.6, 120.9, 118.1, 104.1, 100.4, 79.6, 55.4, 44.8; IR (Neat Film, NaCl): 3852, 3744, 3674, 3648, 2933, 1695, 1606, 1464, 1362, 1303, 1205, 1157, 1115, 1063 cm^{-1}; HRMS (MultiMode ESI/APCI) *m/z* calc'd for C$_{17}$H$_{17}$O$_4$ [M+H]$^+$: 285.1127, found 285.1127; $[\alpha]^{25}_{D}$ 46.7° (*c* 0.98, CHCl$_3$, 95% ee).

(*R*)-2-(dibenzo[*b,d*]furan-4-yl)chroman-4-one (184)

Synthesized according to the general procedure and purified by flash chromatography (8:2 hexanes/EtOAc) to afford an off-white solid (64% yield). ^{1}H NMR (500 MHz,

CDCl$_3$) δ 8.08–7.92 (m, 3H), 7.70 (dd, J = 1.2, 7.7 Hz, 1H), 7.62–7.52 (m, 2H), 7.49

(ddt, J = 1.1, 7.2, 8.4 Hz, 1H), 7.44 (td, J = 0.9, 7.6 Hz, 1H), 7.40–7.34 (m, 1H),

7.16–7.07 (m, 2H), 6.11 (dd, J = 2.9, 13.5 Hz, 1H), 3.35 (ddd, J = 1.0, 13.4, 17.0 Hz,

1H), 3.17 (ddd, J = 1.0, 3.0, 17.0 Hz, 1H); ^{13}C NMR (125 MHz, CDCl$_3$) δ 192.0, 161.7,

156.1, 152.8, 136.2, 127.5, 127.6, 124.8, 124.4, 123.9, 123.1, 123.1, 122.9, 121.7, 121.1,

120.9, 120.8, 118.2, 111.9, 75.3, 43.4; IR (Neat Film, NaCl): 3060, 1690, 1604, 1576,

1471, 1463, 1450, 1428, 1303, 1223, 1187, 1118 1066 c m^{-1}; HRMS (MultiMode

ESI/APCI) m/z calc'd for C$_{21}$H$_{15}$O$_3$ [M+H]$^+$: 315.1016, found 315.1017; [α]$^{25}_D$ 74.1° (c

0.77, CHCl$_3$, 77% ee).

(*R*)-6-acetyl-5,7-dimethyl-2-phenylchroman-4-one (185)

Synthesized according to the general procedure and purified by flash chromatography

(8:2 hexanes/EtOAc) to afford a colorless solid (98% yield). ^{1}H NMR (500 MHz, CDCl$_3$)

δ 7.47–7.37 (m, 5H), 6.79 (s, 1H), 5.43 (dd, J = 2.9, 13.1 Hz, 1H), 3.07 (dd, J = 13.2,

16.5 Hz, 1H), 2.87 (dd, J = 3.0, 16.5 Hz, 1H), 2.56 (s, 3H), 2.47 (s, 3H), 2.23 (s, 3H); ^{13}C

NMR (125 MHz, CDCl$_3$) δ 207.7, 192.9, 162.3, 140.8, 138.6, 138.0, 136.5, 128.8, 128.7,

126.0, 117.7, 117.3, 78.8, 46.2, 32.8, 19.8, 18.9; IR (Neat Film, NaCl): 3034, 2974, 2916,

1700, 1696, 1684, 1559, 1425, 1354, 1314, 1278, 1258, 1211, 1182, 1074, 1029, 895,

856, 766 c m^{-1}; HRMS (MultiMode ESI/APCI) m/z calc'd for C$_{19}$H$_{19}$O$_3$ [M+H]$^+$:

295.1329, found 295.1320; [α]$^{25}_D$ 22.2° (c 1.14, CHCl$_3$, 90% ee).

(*R*)-6-acetyl-5,7-dimethyl-2-(*m*-tolyl)chroman-4-one (186)

Synthesized according to the general procedure and purified by flash chromatography (9:1 hexanes/EtOAc to 8:2 hexanes/EtOAc) to afford a colorless solid (76% yield). ^{1}H NMR (500 MHz, CDCl$_3$) δ 7.38–7.18 (m, 4H), 6.79 (m, 1H), 5.38 (dd, *J* = 2.8, 13.3 Hz, 1H), 3.07 (dd, *J* = 13.3, 16.5 Hz, 1H), 2.85 (dd, *J* = 2.9, 16.5 Hz, 1H), 2.56 (s, 3H), 2.48 (s, 3H), 2.40 (s, 3H), 2.22 (d, *J* = 0.6 Hz, 3H); ^{13}C NMR (125 MHz, CDCl$_3$) δ 207.8, 193.0, 162.3, 140.8, 138.6, 138.5, 138.0, 136.5, 129.5, 128.7, 126.7, 123.1, 117.7, 117.3, 78.9, 46.2, 32.8, 21.5, 19.8, 18.9; IR (Neat Film, NaCl): 2918, 1701, 1683, 1600, 1558, 1464, 1427, 1354, 1313, 1278, 1258, 1216, 1182, 1072, 969, 876, 786, 705 cm^{-1}; HRMS (MultiMode ESI/APCI) *m/z* calc'd for C$_{20}$H$_{21}$O$_3$ [M+H]$^+$: 309.1485, found 309.1483; [α]$^{25}_D$ 22.2° (*c* 1.14, CHCl$_3$, 88% ee).
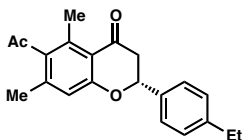
(*R*)-6-acetyl-2-(3-ethylphenyl)-5,7-dimethylchroman-4-one (187)

Synthesized according to the general procedure and purified by flash chromatography (8:2 hexanes/EtOAc to 6:1 hexanes/EtOAc) to afford a colorless solid (45% yield). ^{1}H NMR (500 MHz, CDCl$_3$) δ 7.38–7.36 (m, 2H), 7.27–7.25 (m, 2H), 6.77 (s, 1H), 5.40 (dd, *J* = 2.8, 13.2 Hz, 1H), 3.09 (dd, *J* = 13.2, 16.5 Hz, 1H), 2.86 (dd, *J* = 2.9, 16.5 Hz, 1H), 2.68 (q, *J* = 7.6 Hz, 2H), 2.56 (s, 3H), 2.47 (s, 3H), 2.22 (s, 3H), 1.25 (t, *J* = 7.6 Hz, 3H);

^{13}C NMR (125 MHz, CDCl$_3$) δ 207.7, 193.1, 162.4, 145.0, 140.7, 138.0, 136.5, 135.8, 128.3, 126.2, 117.7, 117.3, 78.8, 46.1, 32.8, 28.6, 19.8, 19.0, 15.6; IR (Neat Film, NaCl): 3379, 2965, 2930, 2873, 1910, 1685, 1601, 1559, 1517, 1465, 1427, 1379, 1354, 1313, 1278, 1258, 1212, 1182, 1117, 1073, 1021, 988, 969, 895, 858, 831, 777, 736 cm^{-1}; HRMS (MultiMode ESI/APCI) *m/z* calc'd for C$_{21}$H$_{23}$O$_3$ [M+H]$^+$: 323.1642, found 323.1627; [α]$^{25}_D$ 8.8° (*c* 1.00, CHCl$_3$, 86% ee).
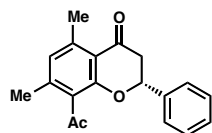
(*R*)-8-acetyl-5,7-dimethyl-2-phenylchroman-4-one (188)

Synthesized according to the general procedure and purified by flash chromatography (8:2 hexanes/EtOAc) to afford a colorless solid (79% yield). ^{1}H NMR (500 MHz, CDCl$_3$) δ 7.44–7.36 (m, 5H), 6.72 (s, 1H), 5.48 (dd, *J* = 2.9, 13.2 Hz, 1H), 3.06 (dd, *J* = 13.2, 16.6 Hz, 1H), 2.89 (dd, *J* = 2.9, 16.6 Hz, 1H), 2.64 (s, 3H), 2.48 (s, 3H), 2.26 (s, 3H); ^{13}C NMR (125 MHz, CDCl$_3$) δ 203.7, 192.4, 159.4, 143.1, 142.2, 138.5, 128.9, 128.7, 127.5, 125.8, 117.6, 110.0, 79.4, 46.1, 32.3, 22.7, 19.7; IR (Neat Film, NaCl): 2946, 2924, 1684, 1599, 1559, 1473, 1444, 1352, 1317, 1281, 1163, 1079, 763 cm^{-1}; HRMS (MultiMode ESI/APCI) *m/z* calc'd for C$_{19}$H$_{17}$O$_3$ [M-H]$^-$: 293.1183, found 293.1178; [α]$^{25}_D$ 65.5° (*c* 1.02, CHCl$_3$, 95% ee).

(*R*)-8-acetyl-5,7-dimethyl-2-(*m*-tolyl)chroman-4-one (189)

Synthesized according to the general procedure and purified by flash chromatography

(5:1 hexanes/EtOAc) to afford a colorless solid (84% yield). ^{1}H NMR (500 MHz, CDCl$_3$)

δ 7.33–7.17 (m, 4H), 6.71 (s, 1H), 5.44 (dd, *J* = 2.9, 13.1 Hz, 1H), 3.05 (dd, *J* = 13.2,

16.6 Hz, 1H), 2.86 (dd, *J* = 3.0, 16.6 Hz, 1H), 2.64 (s, 3H), 2.48 (s, 3H), 2.39 (s, 3H),

2.26 (s, 3H); ^{13}C NMR (125 MHz, CDCl$_3$) δ 203.7, 192.5, 159.4, 143.1, 142.2, 138.6,

138.4, 129.4, 129.3, 128.7, 127.4, 126.5, 122.9, 117.6, 79.5, 46.2, 32.3, 22.7, 21.5, 19.7;

IR (Neat Film, NaCl): 2945, 2923, 1684, 1599, 1558, 1472, 1447, 1353, 1316, 1281,

1173, 1085, 960, 892, 811, 789, 757 cm^{-1}; HRMS (MultiMode ESI/APCI) *m/z* calc'd for

C$_{20}$H$_{21}$O$_3$ [M+H]$^+$: 309.1485, found 309.1494; [α]$^{25}_D$ 60.6° (*c* 1.03, CHCl$_3$, 86% ee).
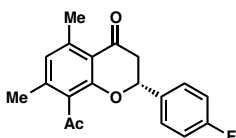
(*R*)-8-acetyl-2-(4-fluorophenyl)-5,7-dimethylchroman-4-one (191)

Synthesized according to the general procedure and purified by flash chromatography

(1:1 hexanes/EtOAc) to afford a colorless solid (68% yield). ^{1}H NMR (500 MHz, CDCl$_3$)

δ 7.40–7.38 (m, 2H), 7.26 (s, 1H), 7.12–7.09 (m, 2H), 5.45 (dd, *J* = 2.9, 13.1 Hz, 1H),

3.03 (dd, *J* = 13.1, 16.6 Hz, 1H), 2.87 (dd, *J* = 2.9, 16.6 Hz, 1H), 2.63 (s, 3H), 2.46 (s,

3H), 2.26 (s, 3H); ^{13}C NMR (125 MHz, CDCl$_3$) δ 203.6, 192.1, 162.8 (d, $^1J_{(C,F)}$ = 247.8

Hz), 159.1, 143.1, 142.2, 134.3 (d, $^4J_{(C,F)}$ = 3.3 Hz), 129.3, 127.7 (d, $^3J_{(C,F)}$ = 8.4 Hz) ,

127.5, 117.5, 115.8 (d, $^2J_{(C,F)}$ = 21.7 Hz), 78.7, 46.0, 32.3, 22.7, 19.7; IR (Neat Film,

NaCl): 3354, 3073, 2967, 2925, 1895, 1685, 1603, 1560, 1513, 1474, 1445, 1353, 1316,

1283, 1265, 1254, 1227, 1187, 1161, 1087, 1041, 1014, 992, 961, 897, 880, 837, 811,

731, 727 cm^{-1}; HRMS (MultiMode ESI/APCI) *m/z* calc'd for $C_{19}H_{18}FO_3$ [M+H]$^+$:

313.1234, found 313.1240; $[\alpha]^{25}_D$ 53.4° (*c* 1.05, CHCl$_3$, 91% ee).

(*R*)-methyl 3-(8-acetyl-5,7-dimethyl-4-oxochroman-2-yl) benzoate (192)

Synthesized according to the general procedure and purified by flash chromatography

(5:1 hexanes/EtOAc) to afford a colorless solid (60% yield). ^{1}H NMR (500 MHz, CDCl$_3$)

δ 8.10 (t, *J* = 1.7 Hz, 1H), 8.06–8.04 (m, 1H), 7.64–7.62 (m, 1H), d 7.51 (t, *J* = 7.7 Hz,

1H), 6.73 (s, 1H), 5.52 (dd, *J* = 2.9, 13.1 Hz, 1H), 3.94 (s, 3H), 3.07 (dd, *J* = 13.3, 16.6

Hz, 1H), 2.90 (dd, *J* = 2.9, 16.6 Hz, 1H), 2.64 (s, 3H), 2.48 (s, 3H), 2.26 (s, 3H); ^{13}C

NMR (125 MHz, CDCl$_3$) δ 203.5, 191.9, 166.5, 159.1, 143.1, 142.3, 138.9, 130.8, 130.2,

129.9, 129.3, 129.1, 127.7, 127.0, 117.5, 78.9, 52.3, 46.0, 32.3, 22.7, 19.7; IR (Neat Film,

NaCl): 2953, 2924, 2360, 1722, 1684, 1600, 1559, 1473, 1436, 1354, 1316, 1283, 1210.

1163, 1084, 961, 892, 860, 822, 755 cm^{-1}; HRMS (MultiMode ESI/APCI) *m/z* calc'd for

$C_{21}H_{21}O_5$ [M+H]$^+$: 353.1384, found 353.1385; $[\alpha]^{25}_D$ 83.5° (*c* 1.53, CHCl$_3$, 86% ee).

(*R*)-8-acetyl-2-(3-bromophenyl)-5,7-dimethylchroman-4-one (190)

Synthesized according to the general procedure and purified by flash chromatography (8:2 hexanes/EtOAc) to afford a colorless solid (65% yield). ^{1}H NMR (500 MHz, CDCl$_3$) δ 7.56 (t, *J* = 1.6 Hz, 1H), 7.53–7.48 (m, 1H), 7.35–7.28 (m, 2H), 6.73 (s, 1H), 5.44 (dd, *J* = 2.9, 13.2 Hz, 1H), 3.02 (dd, *J* = 13.2, 16.6 Hz, 1H), 2.87 (dd, *J* = 3.0, 16.6 Hz, 1H), 2.64 (s, 3H), 2.48 (s, 3H), 2.26 (s, 3H); ^{13}C NMR (125 MHz, CDCl$_3$) δ 203.5, 191.7, 158.9, 143.1, 142.3, 140.7, 131.8, 130.5, 129.3, 128.9, 127.7, 124.4, 122.9, 117.5, 78.6, 46.0, 32.3, 22.7, 19.7; IR (Neat Film, NaCl): 3583, 2919, 1685, 1597, 1559, 1473, 1444, 1355, 1316, 1282, 1263, 1163, 1084, 959, 891, 789 cm^{-1}; HRMS (MultiMode ESI/APCI) *m/z* calc'd for C$_{19}$H$_{18}$BrO$_3$ [M+H]$^+$: 373.0434, found 373.0435; [α]$^{25}_D$ 97.6° (*c* 0.81, CHCl$_3$, 95% ee).
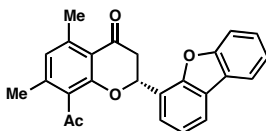
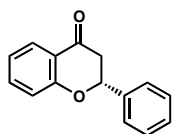**(*R*)-8-acetyl-2-(dibenzo[b,d]furan-4-yl)-5,7-dimethylchroman-4-one (194)**
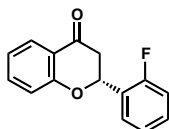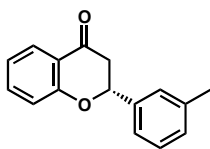
Synthesized according to the general procedure and purified by flash chromatography (8:2 hexanes/EtOAc) to afford a colorless solid (70% yield). ^{1}H NMR (500 MHz, CDCl$_3$) δ 7.97 (d, *J* = 7.7 Hz, 2H), 7.60–7.55 (m, 2H), 7.48 (dt, *J* = 0.9, 7.8 Hz, 1H), 7.46–7.35 (m, 2H), 6.75 (s, 1H), 6.09 (dd, *J* = 3.1, 12.9 Hz, 1H), 3.30 (dd, *J* = 13.0, 16.6 Hz, 1H), 3.16 (dd, *J* = 3.3, 16.7 Hz, 1H), 2.69 (s, 3H), 2.48 (s, 3H), 2.28 (s, 3H); ^{13}C NMR (125 MHz, CDCl$_3$) δ 203.7, 192.4, 159.4, 156.1, 152.8, 143.2, 142.2, 129.3, 127.6, 127.5,

124.8, 124.0, 123.8, 123.1, 123.0, 122.6, 121.0, 120.8, 117.7, 111.8, 75.2, 45.0, 32.3,

22.8, 19.7; IR (Neat Film, NaCl): 3583, 3017, 2963, 2923, 1683, 1600, 1557, 1474, 1450,

1428, 1378, 1352, 1317, 1282, 1188, 1171, 1078, 961, 893, 843, 800, 754 cm^{-1}; HRMS

(MultiMode ESI/APCI) *m/z* calc'd for $C_{25}H_{21}O_4$ [M+H]$^+$: 385.1438, found 385.1440,

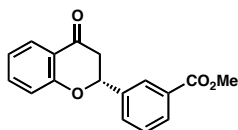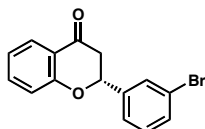found; $[\alpha]^{25}_D$ 52.4° (*c* 0.75, CHCl$_3$, 83% ee).
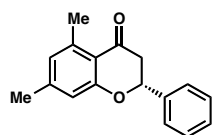
(*R*)-5,7-dimethyl-2-phenylchroman-4-one (195)

Synthesized according to the general procedure and purified by flash chromatography

(6:1 hexanes/EtOAc) to afford a colorless solid (84% yield). ^{1}H NMR (500 MHz, CDCl$_3$)

δ 7.48–7.38 (m, 5H), 6.75 (s, 1H), 6.66 (s, 1H), 5.42 (dd, *J* = 2.8, 13.3 Hz, 1H), 3.05 (dd,

J = 13.3, 16.5 Hz, 1H), 2.84 (dd, *J* = 2.9, 16.5 Hz, 1H), 2.64 (s, 3H), 2.31 (s, 3H); ^{13}C

NMR (125 MHz, CDCl$_3$) δ 193.0, 162.7, 146.1, 141.9, 139.1, 128.8, 128.6, 126.1, 126.0,

117.2, 116.2, 78.8, 46.1, 22.8, 21.7; IR (Neat Film, NaCl): 3650, 3586, 2916, 2360, 1675,

1616, 1559, 1320, 1279, 1159, 1072, 843, 763 cm^{-1}; HRMS (MultiMode ESI/APCI) *m/z*

calc'd for $C_{17}H_{17}O_2$ [M+H]$^+$: 253.1223, found 253.1217; $[\alpha]^{25}_D$ 46.8° (*c* 1.00, CHCl$_3$,

92% ee).
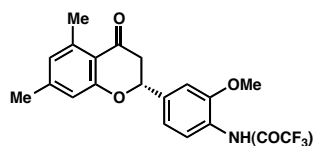
(*R*)-*N*-(4-(5,7-dimethyl-4-oxochroman-2-yl)-2-methoxyphenyl)-2,2,2-

trifluoroacetamide (85)

Synthesized according to the general procedure and purified by flash chromatography (8:2 hexanes/EtOAc) to afford a colorless solid (80% yield). ^{1}H NMR (500 MHz, CDCl$_3$) d 8.57 (s, 1H), 8.35 (dJ = 8.7 Hz, 1H), 7.11-7.07 (m, 2H), 6.75 (s, 1H), 6.67 (s, 1H), 5.40 (dd, J = 2.8, 13.1 Hz, 1H), 3.97 (s, 3H), 3.02 (dd, J = 13.2, 16.5 Hz, 1H), 2.83 (dd, J = 2.9, 16.5 Hz, 1H), 2.63 (s, 3H), 2.32 (s, 3H); ^{13}C NMR (125 MHz, CDCl$_3$) δ 192.6, 162.4, 152.42 (q, $^2J_{(C,F)}$ = 37.3 Hz), 148.5, 146.2, 142.0, 137.1, 126.3, 125.1, 120.3, 118.8, 117.2, 116.1, 112.6 (m, $^1J_{(C,F)}$ = 211.0 Hz), 107.9, 78.4, 56.1, 46.1, 22.7, 21.7; IR (Neat Film, NaCl): 3401, 2917, 2848, 1721, 1682, 1613, 1545, 1499, 1464, 1425, 1362, 1322, 1302, 1291, 1266, 1226, 1156, 1119, 1078, 1033, 901, 864, 846, 826, 790, 733 cm^{-1}; HRMS (MultiMode ESI/APCI) *m/z* calc'd for C$_{20}$H$_{19}$F$_3$NO$_4$ [M]$^+$: 393.1261, found 393.1269; [α]$^{25}_D$ 46.8° (*c* 0.93, CHCl$_3$, 95% ee).
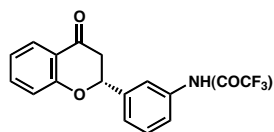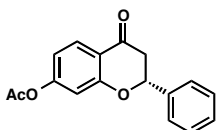

(*R*)-4-oxo-2-phenylchroman-7-yl acetate (196)

Synthesized according to the general procedure and purified by flash chromatography (9:1 hexanes/EtOAc to 8:2 hexanes/EtOAc) to afford a colorless solid (77% yield). ^{1}H NMR (500 MHz, CDCl$_3$) δ 7.96 (d, J = 8.6 Hz, 1H), 7.49–7.38 (m, 5H), 6.85 (d, J = 2.1 Hz, 1H), 6.81 (dd, J = 2.2, 8.6 Hz, 1H), 5.51 (dd, J = 2.9, 13.4 Hz, 1H), 3.08 (dd, J = 13.4, 16.9 Hz, 1H), 2.89 (dd, J = 2.9, 16.9 Hz, 1H), 2.32 (s, 3H); ^{13}C NMR (125 MHz, CDCl$_3$) δ 190.8, 168.5, 162.3, 156.5, 138.3, 128.8, 128.7, 128.4, 126.0, 118.7, 115.6, 111.1, 79.9, 44.3, 21.1; IR (Neat Film, NaCl): 3034, 1768, 1691, 1611, 1580, 1481, 1437,

1369, 1340, 1286, 1243, 1192, 1140, 1117, 1062, 1012, 965, 905, 884, 843, 819, 758 cm^{-1}; HRMS (MultiMode ESI/APCI) m/z calc'd for C$_{17}$H$_{15}$O$_4$ [M+H]$^+$: 283.0965, found 283.0969; $[\alpha]^{25}_D$ 41.7° (c 1.00, CHCl$_3$, 93% ee).
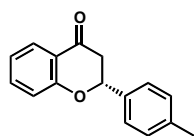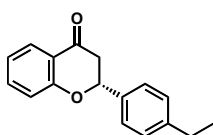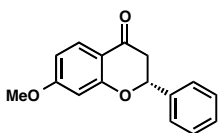

(*R*)-7-methoxy-2-phenylchroman-4-one (199)

Synthesized according to the general procedure and purified by flash chromatography (9:1 hexanes/EtOAc) to afford a colorless solid (96% yield). ^{1}H NMR (500 MHz, CDCl$_3$) δ 7.87 (d, J = 8.8 Hz, 1H), 7.49–7.39 (m, 5H), 6.62 (dd, J = 2.4, 8.8 Hz, 1H), 6.50 (d, J = 2.4 Hz, 1H), 5.47 (dd, J = 2.9, 13.3 Hz, 1H), 3.83 (s, 3H), 3.04 (dd, J = 13.3, 16.9 Hz, 1H), 2.83 (dd, J = 2.9, 16.9 Hz, 1H); ^{13}C NMR (125 MHz, CDCl$_3$) δ 190.6, 166.2, 163.5, 138.8, 128.9, 128.8, 128.7, 126.2, 114.8, 110.3, 100.9, 80.0, 55.7, 44.3; IR (Neat Film, NaCl): 3583, 2915, 1677, 1602, 1496, 1437, 1355, 1255, 1198, 1156, 1113, 1058, 1022, 996, 953, 835, 764 c m^{-1}; HRMS (MultiMode ESI/APCI) m/z calc'd for C$_{16}$H$_{15}$O$_3$ [M+H]$^+$: 255.1016, found 255.1017; $[\alpha]^{25}_D$ 63.5° (c 0.97, CHCl$_3$, 94% ee).
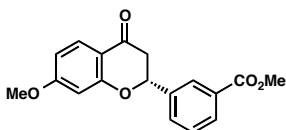
(*R*)-methyl 3-(7-methoxy-4-oxochroman-2-yl)benzoate (200)

Synthesized according to the general procedure and purified by flash chromatography (2:1 hexanes/EtOAc) to afford a colorless solid (81% yield). ^{1}H NMR (500 MHz, CDCl$_3$)

δ 8.18 (s, 1H), 8.06 (dt, *J* = 1.3, 7.7 Hz, 1H), 7.88 (d, *J* = 8.8 Hz, 1H), 7.67 (d, *J* = 7.7 Hz,

1H), 7.52 (t, *J* = 7.7 Hz, 1H), 6.64 (dd, *J* = 2.4, 8.8 Hz, 1H), 6.52 (d, *J* = 2.4 Hz, 1H),

5.52 (dd, *J* = 3.0, 13.2 Hz, 1H), 3.95 (s, 3H), 3.85 (s, 3H), 3.03 (dd, *J* = 13.2, 16.8 Hz,

1H), 2.85 (dd, *J* = 3.1, 16.9 Hz, 1H); ^{13}C NMR (125 MHz, CDCl$_3$) δ 190.1, 166.6, 166.3,

163.3, 139.3, 130.8, 130.5, 129.9, 129.0, 128.8, 127.3, 114.8, 110.5, 100.9, 79.4, 55.7,

52.3, 44.3; IR (Neat Film, NaCl): 3431, 2951, 2841, 1721, 1683, 1608, 1575, 1496, 1443,

1353, 1335, 1289, 1258, 1210, 1159, 1132, 1114, 1060, 1023, 1000, 953, 838, 824, 752

cm^{-1}; HRMS (MultiMode ESI/APCI) *m/z* calc'd for C$_{18}$H$_{17}$O$_5$ [M+H]$^+$: 313.1071, found

313.1067; [α]$^{25}_D$ 86.8° (*c* 0.89, CHCl$_3$, 96% ee).
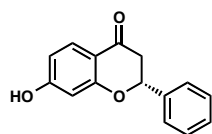
(*R*)-7-hydroxy-2-phenylchroman-4-one (196)

Synthesized according to the general procedure and purified by flash chromatography

(6:4 hexanes/EtOAc) to afford a colorless solid (77% yield). ^{1}H NMR (500 MHz,

(CD$_3$)$_2$CO) δ 9.46 (s, 1H), 7.74 (d, *J* = 8.7 Hz, 1H), 7.62–7.54 (m, 2H), 7.48–7.42 (m,

2H), 7.41–7.36 (m, 1H), 6.60 (dd, *J* = 2.3, 8.7 Hz, 1H), 6.46 (d, *J* = 2.3 Hz, 1H), 5.57 (dd,

J = 2.9, 12.9 Hz, 1H), 3.04 (dd, *J* = 12.9, 16.7 Hz, 1H), 2.75 (dd, *J* = 3.0, 16.7 Hz, 1H);

^{13}C NMR (125 MHz, (CD$_3$)$_2$CO) δ 190.1, 165.2, 164.3, 140.5, 129.5, 129.4, 129.3, 127.3,

115.2, 111.3, 103.7, 80.6, 44.8; IR (Neat Film, NaCl): 3376, 1657, 1601, 1464, 1332,

1279, 1255, 1219, 1156, 1121, 1062, 1002, 963, 850, 752 cm^{-1}; HRMS (MultiMode

ESI/APCI) *m/z* calc'd for C$_{15}$H$_{13}$O$_3$ [M+H]$^+$: 241.0859, found 241.0858; [α]$^{25}_D$ 76.9° (*c*

0.98, CHCl$_3$, 93% ee).
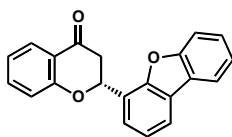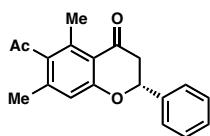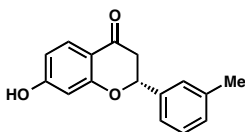
(*R*)-7-hydroxy-2-(m-tolyl)chroman-4-one (197)

Synthesized according to the general procedure and purified by flash chromatography (6:4 hexanes/EtOAc) to afford a colorless solid (66% yield). ^{1}H NMR (500 MHz, (CD$_3$)$_2$CO) δ 9.47 (s, 1H), 7.74 (d, *J* = 8.6 Hz, 1H), 7.43–7.28 (m, 3H), 7.20 (d, *J* = 7.2 Hz, 1H), 6.59 (dd, *J* = 0.9, 8.7 Hz, 1H), 6.46 (d, *J* = 1.4 Hz, 1H), 5.51 (dd, *J* = 2.4, 13.0 Hz, 1H), 3.03 (dd, *J* = 13.0, 16.7 Hz, 1H), 2.72 (dd, *J* = 2.6, 16.7 Hz, 1H), 2.37 (s, 3H); ^{13}C NMR (125 MHz, (CD$_3$)$_2$CO) δ 189.4, 164.4, 163.5, 139.6, 138.1, 129.1, 128.6, 128.5, 127.0, 123.5, 114.4, 110.4, 102.8, 79.8, 44.0, 20.6; IR (Neat Film, NaCl): 3207, 2918, 2360, 1657, 1601, 1575, 1464, 1332, 1279, 1244, 1221, 1189, 1155, 1121, 1065, 1000, 964, 851, 819, 785, 731 cm^{-1}; HRMS (MultiMode ESI/APCI) *m/z* calc'd for C$_{16}$H$_{15}$O$_3$ [M+H]$^+$: 255.1016, found 255.1012; [α]$^{25}_D$ 58.5° (*c* 1.15, CHCl$_3$, 90% ee).
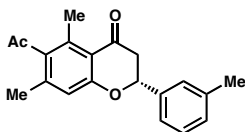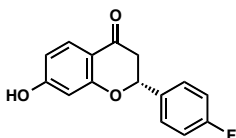

(*R*)-2-(4-fluorophenyl)-7-hydroxychroman-4-one (198)

Synthesized according to the general procedure and purified by flash chromatography (1:1 hexanes/EtOAc) to afford a colorless solid (50% yield). ^{1}H NMR (500 MHz, (CD$_3$)$_2$CO) δ 9.47 (s, 1H), 7.74 (d, *J* = 8.7 Hz, 1H), 7.69–7.55 (m, 2H), 7.28-7.09 (m, 2H), 6.60 (dd, *J* = 2.9, 8.7 Hz, 1H), 6.46 (d, *J* = 2.3 Hz, 1H), 5.59 (dd, *J* = 2.9, 13.0 Hz, 1H), 3.04 (dd, *J* = 13.0, 16.7 Hz, 1H), 2.75 (dd, *J* = 2.9, 16.7 Hz, 1H); ^{13}C NMR (125

MHz, (CD$_3$)$_2$CO) δ 189.1, 164.3, 163.3, 162.6 (d, $^1J_{(C,F)}$ = 245.0 Hz), 135.8 (d, $^4J_{(C,F)}$ = 3.0

Hz), 128.7, 128.6 (d, $^3J_{(C,F)}$ = 8.3 Hz), 115.3 (d, $^2J_{(C,F)}$ = 21.7 Hz), 114.3, 110.5, 102.8,

79.0, 43.8; IR (Neat Film, NaCl): 3256, 2922, 2852, 1661, 1602, 1511, 1464, 1331, 1280,

1225, 1156, 1125, 1003, 853 cm^{-1}; HRMS (MultiMode ESI/APCI) *m/z* calc'd for

C$_{15}$H$_{10}$FO$_3$ [M-H]$^-$: 257.0619, found 257.0623; [α]$^{25}_D$ 54.1° (*c* 1.54, CHCl$_3$, 93% ee).
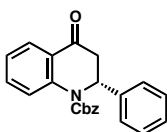
(*R*)-benzyl 4-oxo-2-phenyl-3,4-dihydroquinoline-1(2H)-carboxylate (201)

Synthesized according to the general procedure and purified by flash chromatography

(8:2 hexanes/EtOAc) to afford an off-white solid (50% yield). [α]$^{25}_D$ 110.9° (*c* 0.98,

CHCl$_3$, 80% ee). All characterization data matches previously reported data.[10,11]
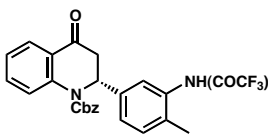
**(*R*)–benzyl 2-(4-methyl-3-(2,2,2-trifluoroacetamido)phenyl)-4-oxo-3,4-**

dihydroquinoline-1(2H)-carboxylate (202)

Synthesized according to the general procedure and purified by flash chromatography

(7:3 hexanes/EtOAc) to afford an off-white solid (45% yield). ^{1}H NMR (500 MHz,

CDCl$_3$) δ 7.86 (dd, *J* = 1.5, 7.8 Hz, 1H), 7.82 (d, *J* = 8.3 Hz, 1H), 7.75 (bs, 1H), 7.64 (s,

1H), 7.45–7.47 (m, 1H), 7.35–7.42 (m, 5H), 7.07 (dd, *J* = 5.6, 7.6 Hz, 2H), 6.98 (dd, *J* =

1.1, 7.9 Hz, 1H), 6.20 (t, *J* = 3.5 Hz, 1H), 5.39 (d, *J* = 12.0 Hz, 1H), 5.33 (d, *J* = 12.0 Hz,

1H), 3.27 (d, *J* = 3.9 Hz, 2H), 2.15 (s, 3H); ^{13}C NMR (125 MHz, CDCl$_3$) δ 192.4, 155.0,

154.9 (q, *J* = 37.2 Hz), 154.2, 141.3, 137.4, 135.4, 134.6, 133.2, 131.1, 129.6, 128.7, 128.5, 128.4, 128.1, 126.8, 124.9, 124.8, 124.5, 124.3, 121.7, 115.8 (m), 68.6, 55.7, 42.1, 16.9; IR (Neat Film, NaCl): 3281, 1719, 1711, 1683, 1600, 1480, 1460, 1390, 1320, 1303, 1268, 1222, 1162, 1041 cm^{-1}; HRMS (FAB+) *m/z* calc'd for $C_{26}H_{22}O_4N_2F_3$ [M+H]$^+$: 483.1532, found 481.1545; [α]$^{25}_D$ 65.3° (*c* 1.0, CHCl$_3$, 79% ee).
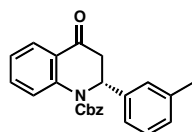
(*R*)-benzyl 4-oxo-2-(*m*-tolyl)-3,4-dihydroquinoline-1(2H)-carboxylate (203)
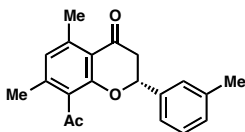
Synthesized according to the general procedure and purified by flash chromatography (2:1 hexanes/EtOAc) to afford an off-white solid (51% yield). [α]$^{25}_D$ 116.5° (*c* 1.05, CHCl$_3$, 87% ee). All characterization data matches previously reported data.**Error! Bookmark not defined.**
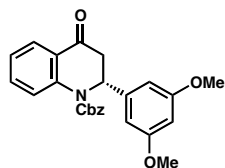
(*R*)-benzyl 2-(3,5-dimethoxyphenyl)-4-oxo-3,4-dihydroquinoline-1(2H)-carboxylate (204)

Synthesized according to the general procedure and purified by flash chromatography (gradient: 9:1 hexanes/EtOAc to 7:3 hexanes/EtOAc) to afford a pale yellow solid (50% yield). ^{1}H NMR (500 MHz, CDCl$_3$) δ 7.90 (dd, *J* = 1.7, 7.8 Hz, 1H), 7.82 (d, *J* = 8.3 Hz, 1H), 7.47 (ddd, *J* = 1.7, 7.2, 8.4 Hz, 1H) 7.35–7.42 (m, 5H), 7.1–7.2 (m, 1H), 6.31 (dd, *J*

= 0.7, 2.2 Hz, 2H), 6.24 (t, *J* = 2.1 Hz, 1H), 6.16 (t, *J* = 3.8 Hz, 1H), 5.38 (d, *J* = 12.2, 1H), 5.33 (d, *J* = 12.2, 1H), 3.64 (s, 6H), 3.26–3.27 (m, 2H); ^{13}C NMR (125 MHz, CDCl$_3$) δ 192.4, 160.9, 154.2, 141.5, 140.5, 135.6, 134.5, 128.7, 128.6, 128.5, 128.4, 128.1, 126.9, 125.3, 125.0, 124.2, 105.0, 99.1, 68.4, 56.2, 55.2, 42.4; IR (Neat Film, NaCl): 2958, 1708, 1686, 1598, 1479, 1460, 1427, 1389, 1315, 1286, 1221, 1159, 1041 cm^{-1}; HRMS (MultiMode ESI/APCI) *m/z* calc'd for C$_{25}$H$_{23}$NO$_5$ [M-H]$^-$: 416.1500, found 416.1520; $[\alpha]^{25}_D$ 116.8° (*c* 1.4, CHCl$_3$, 85% ee).
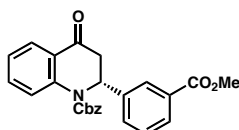
(*R*)-benzyl 2-(3-(methoxycarbonyl)phenyl)-4-oxo-3,4-dihydroquinoline-1(2H)-carboxylate (205)

Synthesized according to the general procedure and purified by flash chromatography (gradient 9:1 hexanes/EtOAc to 7:3 hexanes/EtOAc) to afford a pale yellow solid (34% yield). ^{1}H NMR (500 MHz, CDCl$_3$) δ 7.91 (q, *J* = 1.2 Hz, 1H), 7.89 (ddd, *J* = 0.5, 1.7, 7.8 Hz, 1H), 7.81–7.86 (m, 2H), 7.47 (ddd, *J* = 1.8, 7.3, 8.4 Hz, 1H), 7.35–7.40 (m, 6H), 7.29 (d, *J* = 7.8 Hz, 1H), 7.09 (ddd, *J* = 1.1, 7.6, 7.6 Hz, 1H), 6.27 (t, *J* = 3.8 Hz, 1H), 5.41 (d, *J* = 12.2 Hz, 1H), 5.34 (d, *J* = 12.2 Hz, 1H), 3.87 (s, 3H), 3.34–3.35 (m, 2H); ^{13}C NMR (125 MHz, CDCl$_3$) δ 192.1, 166.5, 154.2, 141.2, 138.5, 134.6, 130.7, 130.6, 128.7, 128.6, 128.5, 128.4, 128.3, 128.1, 127.8, 126.9, 124.9, 124.4, 124.3, 68.6, 55.9, 52.4, 42.2; IR (Neat Film, NaCl): 2950, 1720, 1688, 1600, 1479, 1460, 1389, 1298, 1281, 1221, 1130, 1041 cm^{-1}; HRMS (MultiMode ESI/APCI) *m/z* calc'd for C$_{25}$H$_{21}$NO$_5$ [M-H]$^-$: 415.1420, found 415.1419; $[\alpha]^{25}_D$ 109.7° (*c* 0.9, CHCl$_3$, 69% ee).
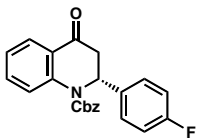
(*R*)-benzyl 2-(4-fluorophenyl)-4-oxo-3,4-dihydroquinoline-1(2H)-carboxylate (206)
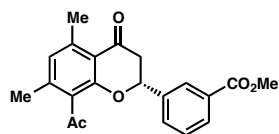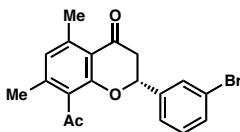
Synthesized according to the general procedure and purified by flash chromatography (gradient: 2:1 hexanes/EtOAc) to afford a colorless solid (65% yield). $[\alpha]^{25}_D$ 96.4° (*c* 1.19, CHCl$_3$, 89% ee). All characterization data matches previously reported data.
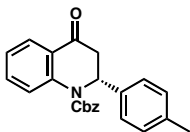
(*R*)-benzyl 4-oxo-2-(*p*-tolyl)-3,4-dihydroquinoline-1(2H)-carboxylate (207)

Synthesized according to the general procedure and purified by flash chromatography (gradient 9:1 hexanes/EtOAc to 8:2 hexanes/EtOAc) to afford a colorless solid (65% yield). $[\alpha]^{25}_D$ 71.2° (*c* 0.5, CHCl$_3$, 67% ee). All characterization data matches previously reported data.
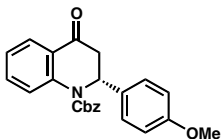
(*R*)-benzyl 2-(4-methoxyphenyl)-4-oxo-3,4-dihydroquinoline-1(2H)-carboxylate

(208)

Synthesized according to the general procedure and purified by flash chromatography

(gradient: 9:1 hexanes/EtOAc to 8:2 hexanes/EtOAc) to afford a colorless solid (36%

yield). ^{1}H NMR (500 MHz, CDCl$_3$) δ 7.91 (dd, J = 1.5, 7.8 Hz, 1H), 7.78 (d, J = 8.5 Hz,

1H), 7.37–7.46 (m, 6H), 7.07–7.12 (m, 3H), 6.72–6.74 (m, 2H), 6.20 (t, J = 3.9 Hz, 1H),

5.41 (d, J = 12.2 Hz, 1H), 5.34 (d, J = 12.2 Hz, 1H), 3.71 (s, 3H), 3.28 (d, J = 3.9 Hz,

2H); ^{13}C NMR (125 MHz, CDCl$_3$) δ192.9, 158.8, 154.2, 141.3, 135.6, 134.5, 130.0,

128.7, 128.4, 128.1, 127.8, 126.8, 125.0, 124.4, 124.1, 113.9, 68.4, 55.7, 55.1, 42.4; IR

(Neat Film, NaCl): 2957, 1705, 1683, 1601, 1513, 1479, 1460, 1380, 1320, 1302, 1252,

1224, 1181, 1128, 1035 cm^{-1}; HRMS (FAB+) m/z calc'd for C$_{24}$H$_{22}$O$_4$N [M+H]$^+$:

388.1549, found 388.1548; $[\alpha]^{25}_D$ 54.8° (c 2.5, CHCl$_3$, 53% ee).
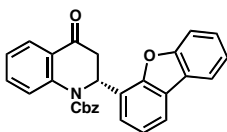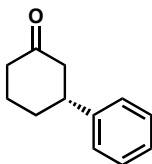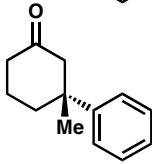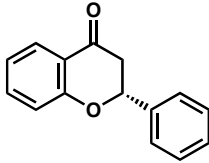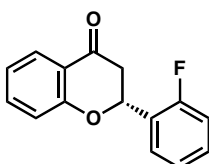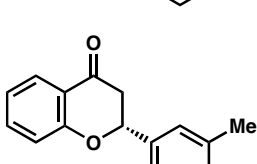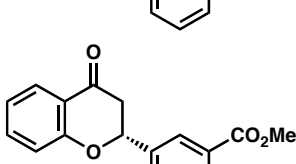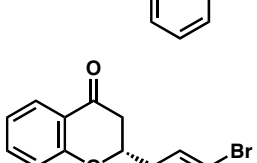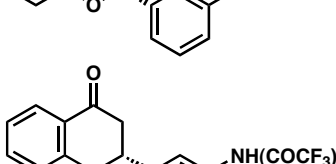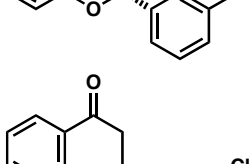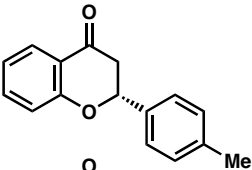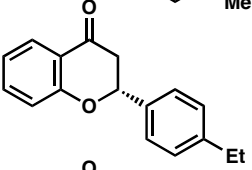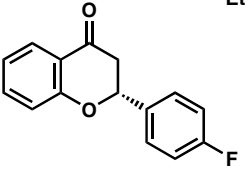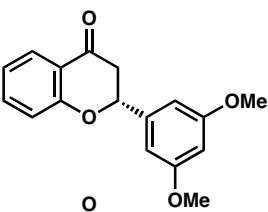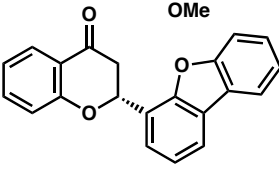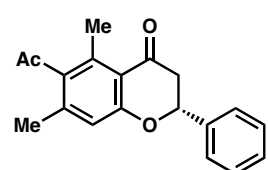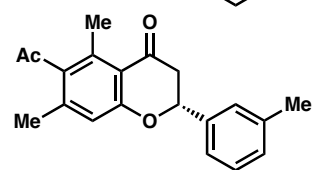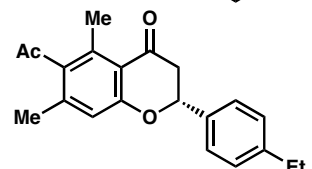
(*R*)-benzyl 2-(dibenzo[b,d]furan-4-yl)-4-oxo-3,4-dihydroquinoline-1(2H)-carboxylate

(209)

Synthesized according to the general procedure and purified by flash chromatography

(gradient: 9:1 hexanes/EtOAc to 8:2 hexanes/EtOAc) to afford a colorless solid (31%

yield). ^{1}H NMR (500 MHz, CDCl$_3$) δ 7.98 (d, J = 8.5 Hz, 1H), 7.92 (dd, J = 1.7, 7.8 Hz,
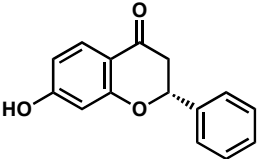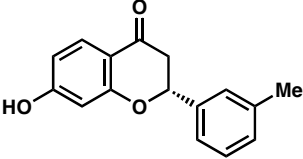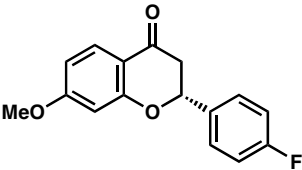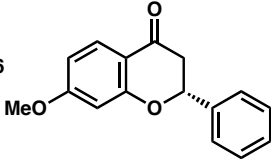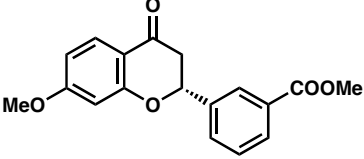
1H), 7.89–7.90 (m, 1H), 7.77–7.79 (m, 1H), 7.44–7.50 (m, 3H), 7.32–7.41 (m, 6H), 7.09–7.13 (m, 2H), 7.05 (td, J = 1.1, 7.8 Hz, 1H), 6.76 (dd, J = 0.9, 5.3 Hz, 1H), 5.44 (d, J = 12.5 Hz, 1H), 5.34 (d, J = 12.2 Hz, 1H), 3.63 (dd, J = 2.0, 17.9 Hz, 1H), 3.44 (dd, J = 6.4, 17.6 Hz, 1H); ^{13}C NMR (125 MHz, CDCl$_3$) δ 192.9, 155.9, 153.9, 153.3, 142.1, 135.7, 134.6, 128.6, 128.3, 128.1, 127.3, 126.9, 124.9, 124.8, 124.7, 124.1, 123.9, 123.7, 122.9, 122.7, 122.6, 120.6, 120.3, 111.7, 68.4, 53.4, 42.3; IR (Neat Film, NaCl): 3032, 1710, 1683, 1600, 1459, 1479, 1420, 1388, 1344, 1319, 1298, 1269, 1223, 1186, 1133, 1041, 1027 cm^{-1}; HRMS (MultiMode ESI/APCI) *m/z* calc'd for C$_{29}$H$_{20}$NO$_4$ [M-H]$^-$: , found 446.1393; $[\alpha]^{25}_{D}$ 27.4° (*c* 2.2, CHCl$_3$, 40% ee).

Table 3.5 Chiral assays
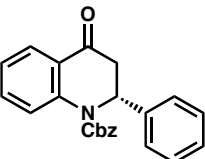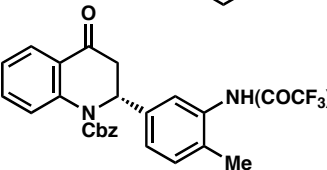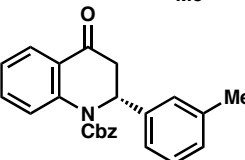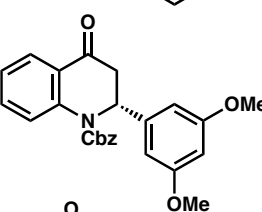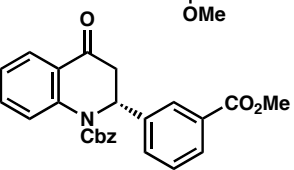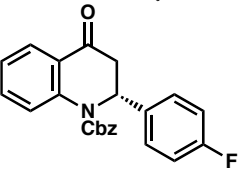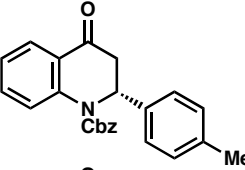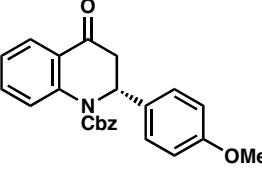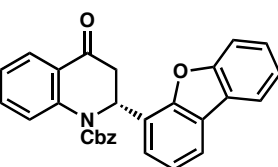
Compound	product	SFC or HPLC conditions	retention time of major isomer (min)	retention time of minor isomer (min)	% ee
Table 1 Entry 1		Chiralcel HPLC OJ-H 1% IPA/Hexanes isocratic 1 mL/min	17.0	19.1	18
Table 1 Entry 2		Chiralcel HPLC OJ-H 1% IPA/Hexanes isocratic 1 mL/min	15.3	19.6	93
Table 1 Entry 3		Chiralcel SFC OB-H 4% MeOH/CO_2 isocratic 5 mL/min	2.71	2.51	94
Table 2 Entry 2		Chiralcel SFC OJ-H 1% MeOH/CO_2 isocratic 5 mL/min	4.57	4.21	76
Table 2 Entry 3		Chiralcel SFC OJ-H 3% MeOH/CO_2 isocratic 5 mL/min	2.53	2.29	90
Table 2 Entry 4		Chiralcel SFC OD-H 20% MeOH/CO_2 isocratic 5 mL/min	2.09	1.85	93
Table 2 Entry 5		Chiralcel SFC OD-H 10% MeOH/CO_2 isocratic 5 mL/min	4.59	3.55	89
Table 2 Entry 6		Chiralcel SFC OD-H 10% MeOH/CO_2 isocratic 5 mL/min	3.21	2.68	98
Table 2 Entry 7		Chiralcel SFC OD-H 10% MeOH/CO_2 isocratic 4 mL/min	4.02	4.96	94

Compound	product	SFC or HPLC conditions	retention time of major isomer (min)	retention time of minor isomer (min)	% ee
Table 2 Entry 8		Chiralcel SFC OB-H 3% MeOH/CO$_2$ isocratic 5 mL/min	3.70	3.44	94
Table 2 Entry 9		Chiralcel HPLC OJ-H 1% IPA/Hexanes isocratic 1 mL/min	15.3	19.6	85
Table 2 Entry 10		Chiralpak HPLC AD-H 10% IPA/Hexanes isocratic 1 mL/min	22.7	27.2	90
Table 2 Entry 11		Chiralcel SFC OD-H 20% MeOH/CO$_2$ isocratic 5 mL/min	2.33	1.98	95
Table 2 Entry 12		Chiralcel SFC OD-H 25% MeOH/CO$_2$ isocratic 4 mL/min	9.92	5.69	77
Table 3 Entry 1		Chiralcel SFC OD-H 15% MeOH/CO$_2$ isocratic 4 mL/min	4.93	3.87	90
Table 3 Entry 2		Chiralcel SFC OD-H 10% MeOH/CO$_2$ isocratic 5 mL/min	4.64	3.37	88
Table 3 Entry 3		Chiralcel SFC OD-H 10% MeOH/CO$_2$ isocratic 5 mL/min	3.67	3.17	86

Compound	product	SFC or HPLC conditions	retention time of major isomer (min)	retention time of minor isomer (min)	% ee
Table 3 Entry 4		Chiralcel SFC AS-H 4% IPA/CO_2 isocratic 5 mL/min	3.49	4.19	95
Table 3 Entry 5		Chiralcel SFC OD-H 10% MeOH/CO_2 isocratic 4 mL/min	4.07	3.76	86
Table 3 Entry 6		Chiralcel SFC OD-H 10% MeOH/CO_2 isocratic 4 mL/min	6.87	5.83	95
Table 3 Entry 7		Chiralcel SFC OD-H 10% MeOH/CO_2 isocratic 4 mL/min	5.89	5.42	91
Table 3 Entry 8		Chiralcel SFC OD-H 15% MeOH/CO_2 isocratic 4 mL/min	3.68	4.13	86
Table 3 Entry 9		Chiralcel SFC OD-H 25% MeOH/CO_2 isocratic 4 mL/min	9.19	6.31	83
Table 3 Entry 10		Chiralcel SFC OJ-H 5% MeOH/CO_2 isocratic 5 mL/min	4.13	3.67	92
Table 3 Entry 11		Chiralcel SFC OD-H 10% MeOH/CO_2 isocratic 4 mL/min	4.30	5.38	95
Table 3 Entry 12		Chiralcel SFC OJ-H 5% MeOH/CO_2 isocratic 5 mL/min	5.45	5.00	93

Compound	product	SFC or HPLC conditions	retention time of major isomer (min)	retention time of minor isomer (min)	% ee
Table 3 Entry 13		Chiralcel HPLC OD-H 10% IPA/Hexanes isocratic 1 mL/min	18.30	16.63	93
Table 3 Entry 14		Chiralcel SFC OD-H 10% MeOH/CO_2 isocratic 4 mL/min	9.01	8.44	90
Table 3 Entry 15*		Chiralcel SFC OD-H 5% MeOH/CO_2 isocratic 4 mL/min	6.71	6.23	93
Table 3 Entry 16		Chiralcel SFC OJ-H 5% MeOH/CO_2 isocratic 5 mL/min	5.88	5.07	94
Table 3 Entry 17		Chiralcel SFC OD-H 15% MeOH/CO_2 isocratic 4 mL/min	5.81	4.70	96

* The free-OH compound from Table 3 Entry 15 was unsuccessfully separated by analytical SFC or HPLC. The compound was methylated under standard conditions, and the methyl ether was used to determine the ee.

Compound	product	SFC or HPLC conditions	retention time of major isomer (min)	retention time of minor isomer (min)	% ee
Table 4 Entry 1		Chiralpak AS-H 5% MeOH/CO$_2$ isocratic 5 mL/min	4.65	4.19	80
Table 4 Entry 2		Chiralcel SFC OB-H 10% MeOH/CO$_2$ isocratic 5 mL/min	3.28	3.67	85
Table 4 Entry 3		Chiralcel SFC AS-H 5% MeOH/CO$_2$ isocratic 5 mL/min	4.93	4.43	85
Table 4 Entry 4		Chiralpak SFC IC 10% MeOH/CO$_2$ isocratic 5 mL/min	4.87	3.71	85
Table 4 Entry 5		Chiralpak SFC AD-H 10% MeOH/CO$_2$ isocratic 5 mL/min	5.47	6.07	60
Table 4 Entry 6		Chiralcel SFC AS-H 5% MeOH/CO$_2$ isocratic 5 mL/min	4.44	3.91	89
Table 4 Entry 7		Chiralpak SFC IC 10% MeOH/CO$_2$ isocratic 5 mL/min	2.91	2.53	67
Table 4 Entry 8		Chiralpak SFC IC 10% MeOH/CO$_2$ isocratic 5 mL/min	3.87	3.36	54
Table 4 Entry 9		Chiralpak AS-H 10% MeOH/CO$_2$ isocratic 5 mL/min	6.24	5.24	40

3.5 Notes and citations

(1)   (a) Perlmutter, P. in *Conjugate Addition Reactions in Organic Synthesis*, Tetrahedron Organic Chemistry Series 9; Pergamon, Oxford, **1992**. (b) Tomioka, K.; Nagaoka, Y. in *Comprehensive Asymmetric Catalysis*, Vol. 3 (Eds: Jacobsen, E. J.; Pfaltz, A.; Yamamoto, H. Springer-Verlag, New York, **1999**; Chapter 31. (c) Gini, F.; Hessen, B.; Feringa, B. L.; Minnaard, A. J. *Chem. Commun.* **2007**, 710–712.

(2)   (a) Xu, Q.; Zhang, R.; Zhang, T.; Shi, M. *J. Org. Chem.* **2010**, *75*, 3935–3937. (b) Zhang, T.; Shi, M. *Chem. Eur. J.* **2008**, *14*, 3759–3764. (c) Gottumukkala, A. L.; Matcha, K.; Lutz, M.; de Vries, J. G.; Minnaard, A. J. *Chem.–Eur. J.* **2012**, *18*, 6907–6914. (d) Gini, F.; Hessen, B.; Minnaard, A. J. *Org. Lett.* **2005**, *7*, 5309–5312.

(3)   Kikushima, K.; Holder, J. C.; Gatti, M.; Stoltz, B. M. *J. Am. Chem. Soc.* **2011**, *133*, 6902–6905.

(4)   (a) Harborne, J. B. in *The Flavonoids: Advances in Research Since 1980*, Chapman and Hall, New York, **1988**. (b) Harborne, J. B.; Williams, C. A. *Nat. Prod. Rep.* **1995**, *12*, 639–642. (c) Chang, L. C.; Kinghorn, A. D. in *Bioactive Compounds from Natural Sources: Isolation, Characterisation and Biological Properties* (Ed: Tringali, C.), Taylor & Francis, London, **2001**, ch. 5. (d) Andersen, O. M.; Markham, K. R. in *Flavonoids: Chemistry, Biochemistry and Applications*, Taylor & Francis, London, **2006**.

(5)   (a) Biddle, M. M.; Lin, M.; Scheidt, K. A. *J. Am. Chem. Soc.* **2007**, *129*, 3830–3831. (b) Dittmer, C.; Taabe, G.; Hintermann, L. *Eur. J. Org. Chem.* **2007**, 5886–5898. (c) Wang, L. J.; Liu, H.; Dong, Fu, X.; Feng, X. M. *Angew. Chem. Int. Ed.* **2008**, *47*, 8670–8673.

(6)   (a) Brown, M. K.; Degrado, S. J.; Hoveyda, A. H. *Angew. Chem. Int. Ed.* **2005**, *44*, 5306–5310. (b) Klier, L.; Bresser, T.; Nigst, T. A.; Karaghiosoff, K.; Knochel, P. *J. Am. Chem. Soc.* **2012**, *134*, 13584–13587. (c) Hodgetts, K. J.; Maragkou, K. I.; Wallace, T. W.; Wooton, R. C. R. *Tetrahedron* **2001**, *57*, 6793–6804.

(7)   (a) Chen, J.; Chen, J.; Lang, F.; Zhang, X.; Cun, L.; Zhu, J.; Deng, J.; Liao, J. *J. Am. Chem. Soc.* **2010**, *132*, 4552–4553. (b) Han, F.; Chen, G.; Zhang, X.; Liao, J. *Eur. J. Org. Chem.* **2011**, 2928–2931. (c) Korenaga, T.; Hayashi, K.; Akaki, Y.; Maenishi, R.; Sakai, T. *Org. Lett.* **2011**, *13*, 2022–2025.

(8)   For an isolated example of a Pd-catalyzed non-enantioselective conjugate addition to a chromone, see: Huang, S.-H.; Wu, T.-M.; Tasi, F.-Y. *Appl. Organometal. Chem.* **2010**, *24*, 619–624.

(9)   (a) Xia, Y.; Yang, Z.-Y.; Xia, P.; Bastow, K. F.; Tachibana, Y.; Kuo, S.-C.; Hamel, E.; Hackl, T.; Lee, K.-H. *J. Med. Chem.* **1998**, *41*, 1155–1162. (b) Zhang, S.-X.; Feng, J.; Kuo, S.-C.; Brossi, A.; Hamel, E.; Tropsha, A.; Lee, K.-H. *J. Med. Chem.* **2000**, *43*, 167–176.

(10)   Shintani, R.; Yamagami, T.; Kimura, T.; Hayashi, T. *Org. Lett.* **2005**, *7*, 5317–5319.

(11)   Zhang, X.; Chen, J.; Han, F.; Cun, L.; Liao, J. *Eur. J. Org. Chem.* **2011**, 1443–1446.

(12)   (a) Inés, B.; San Martin, R.; Moure, M. J.; Domínguez, E. *Adv. Synth. Catal.* **2009**, *351*, 2124-2132. (b) Ogo, S.; Takebe, Y.; Uehara, K.; Yamazaki, T.; Nakai, H.; Watanabe, Y.; Fukuzumi, S. *Organometallics*, **2006**, *25*, 331-338.

(13)   Jaen, J. C.; Wise, L. D.; Heffner, T. G.; Pugsley, T. A.; Meltzer L. T. *J. Med. Chem.* **1991**, *34*, 248–256.

(14)   Morimoto, M.; Tanimoto, K.; Nakano, S.; Ozaki, T.; Nakano, A.; Komai, K. *J. Agric. Food Chem.* **2003,** *51,* 389.

(15)   Pfeiffer, P.; Oberlin, H.; Konermann, E. *Chemische Berichte*, **1925**, *58*, 1947–1958.

(16)   Ullah, E.; Appel, B.; Fischer, C.; Langer, P. *Tetrahedron*, **2006**, *62*, 9694.

(17)   Shintani, R.; Tsutsumi, Y.; Nagaosa, M.; Nishimura, T.; Hayashi, T. *J. Am. Chem. Soc.* **2009**, *131*, 13588–13589.

(18)   Shintani, R.; Takeda, M.; Nishimura, T.; Hayashi, T. *Angew. Chem. Int. Ed.* **2010**, *49*, 3969–3971.

(19)   Hawner, C.; Muller, D.; Gremaud, L.; Fellouat, A.; Woodward, S.; Alexakis, A. *Angew. Chem. Int. Ed.* **2010**, *49*, 7769–7772.

(20) May, T. L.; Brown, M. K.; Hoveyda, A. H. *Angew. Chem. Int. Ed.* **2008**, *47*, 7358–7362.

(21) Hawner, C.; Li, K.; Cirriez, V.; Alexakis, A. *Angew. Chem. Int. Ed.* **2008**, *47*, 8211–8214.

(22) Palais, L.; Alexakis, A. *Chem.–Eur. J.* **2009**, *15*, 10473–*10485*.

(23) Lin, S.; Lu, X. *Org. Lett.* **2010**, *12*, 2536–2539.

(24) Kuriyama, M.; Nagai, K.; Yamada, K.-I.; Miwa, Y.; Taga, T.; Tomioka, K. *J. Am. Chem. Soc.* **2002**, *124*, 8932–8939.

(25) Dauzonne, D.; Monneret, C. *Synthesis* **1997**, 1305–*1308*.

APPENDIX 2

Spectra relevant to Chapter 3: Palladium-catalyzed addition of arylboronic acids to heterocyclic conjugate acceptors

Figure A2.1 ^{1}H NMR (500 MHz, CDCl$_3$) of compound **84**
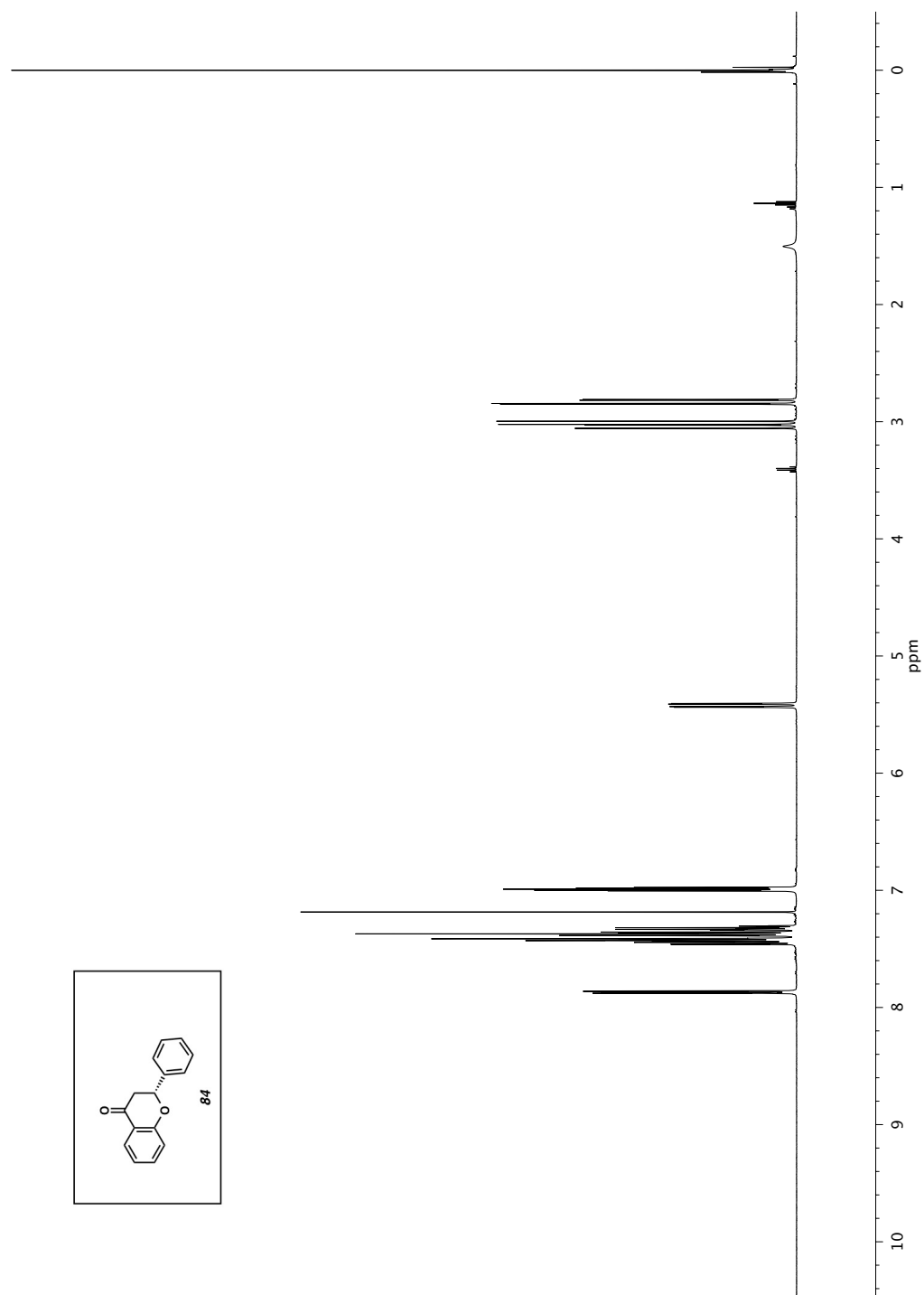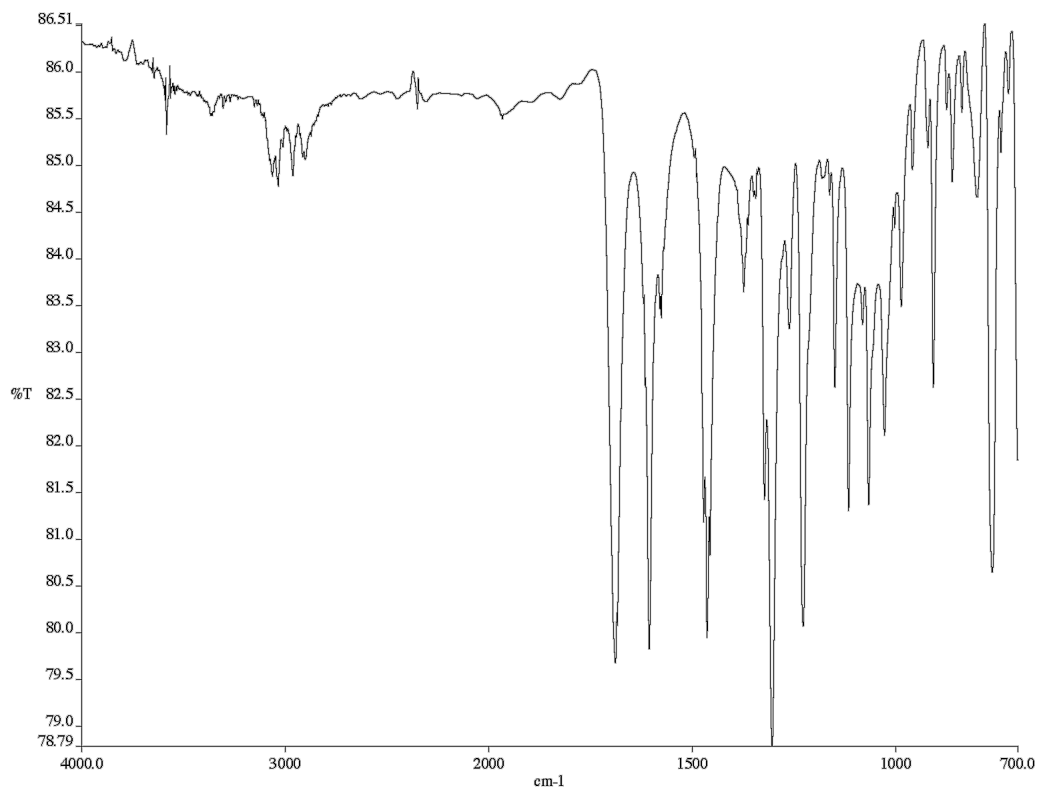
Figure A2.2 Infrared spectrum (Thin Film, NaCl) of compound **84**
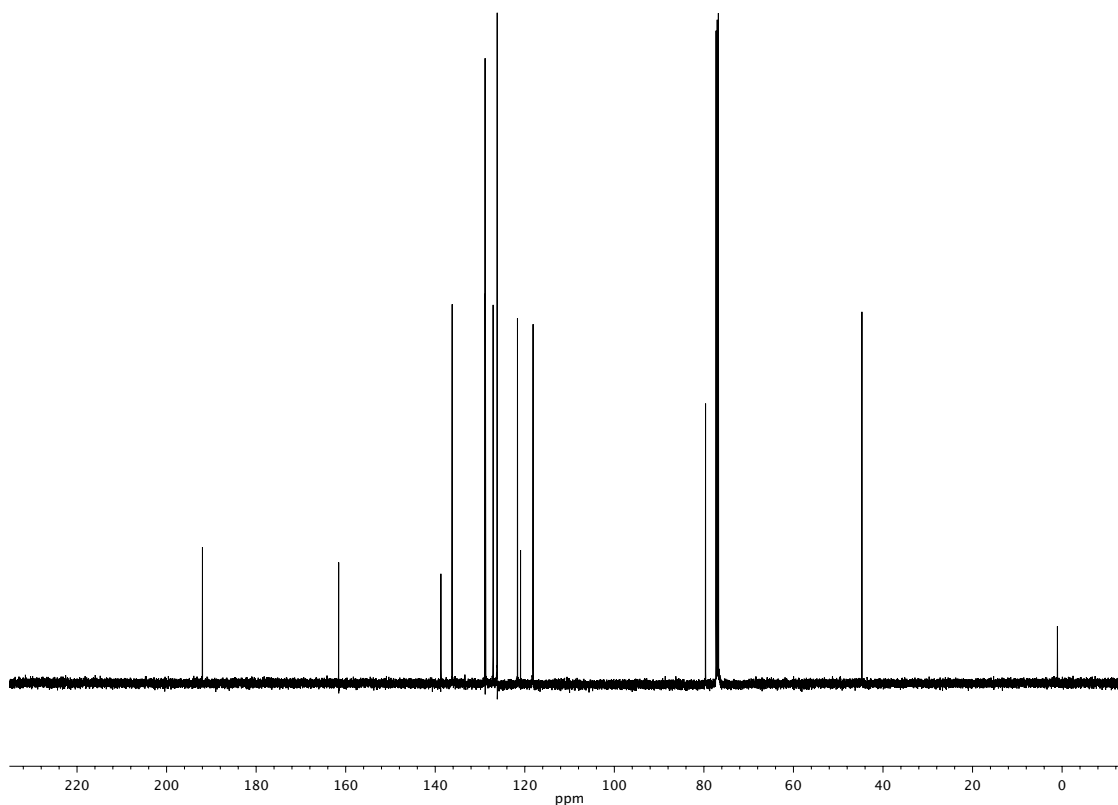
Figure A2.3 ^{13}C NMR (126 MHz, CDCl$_3$) of compound **84**
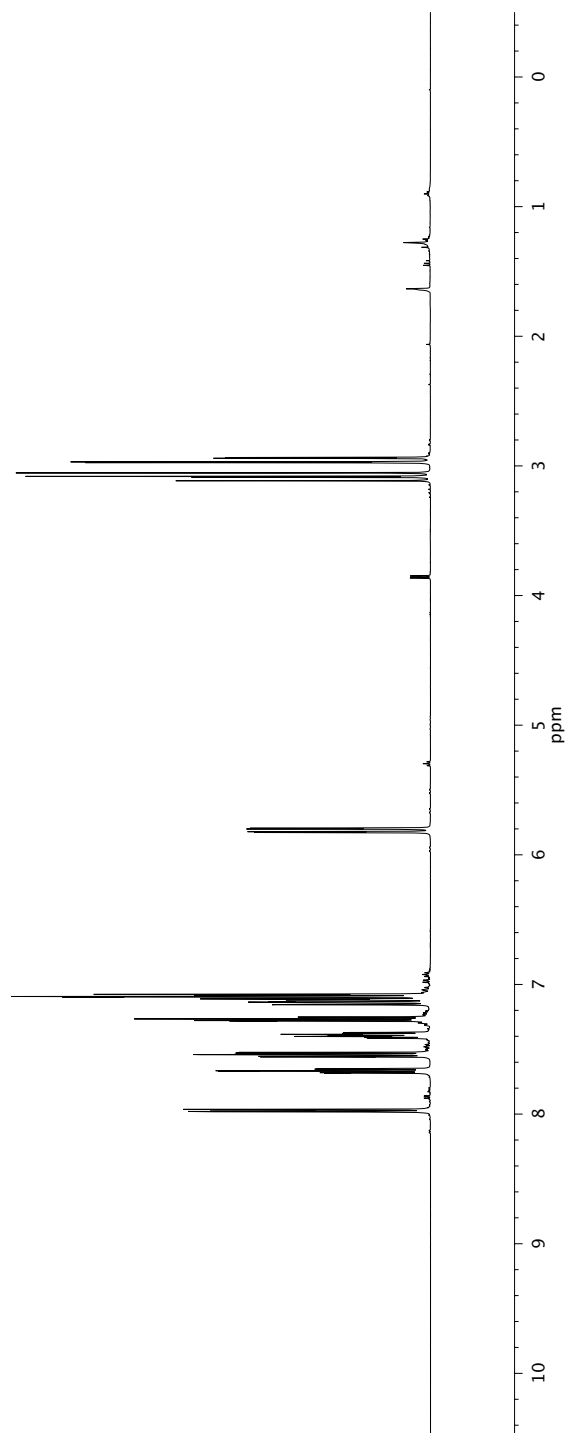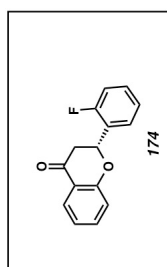
Figure A2.4 ^{1}H NMR (500 MHz, CDCl$_3$) of compound **174**
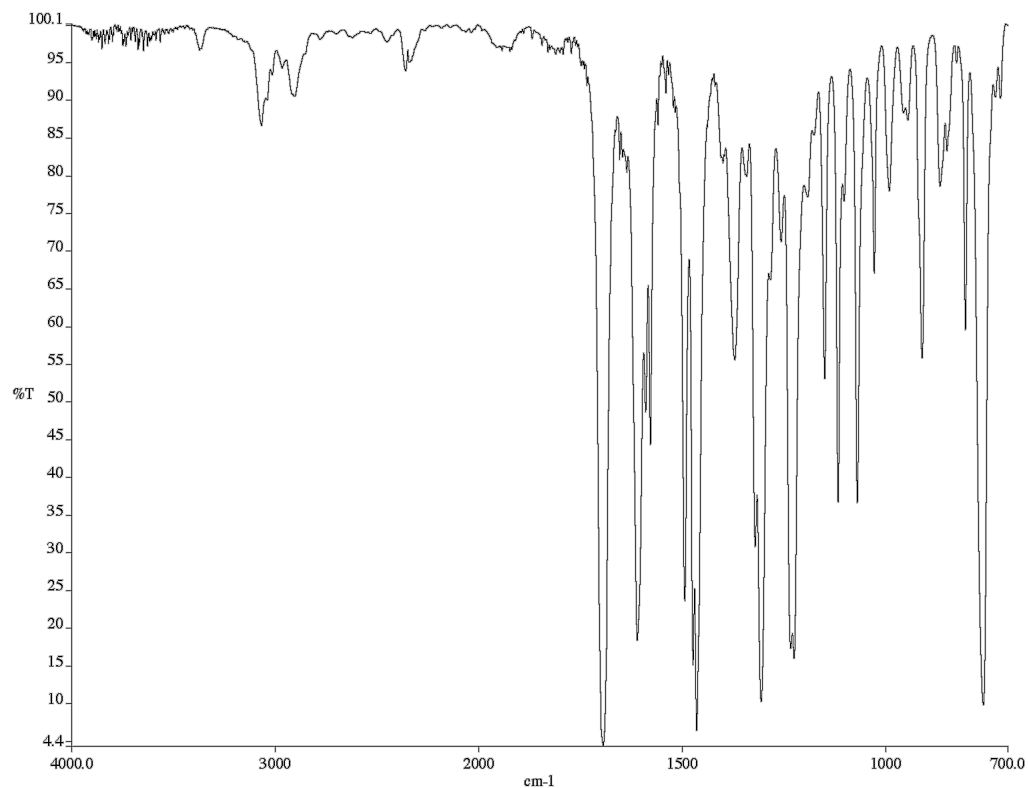
Figure A2.5 Infrared spectrum (Thin Film, NaCl) of compound **174**
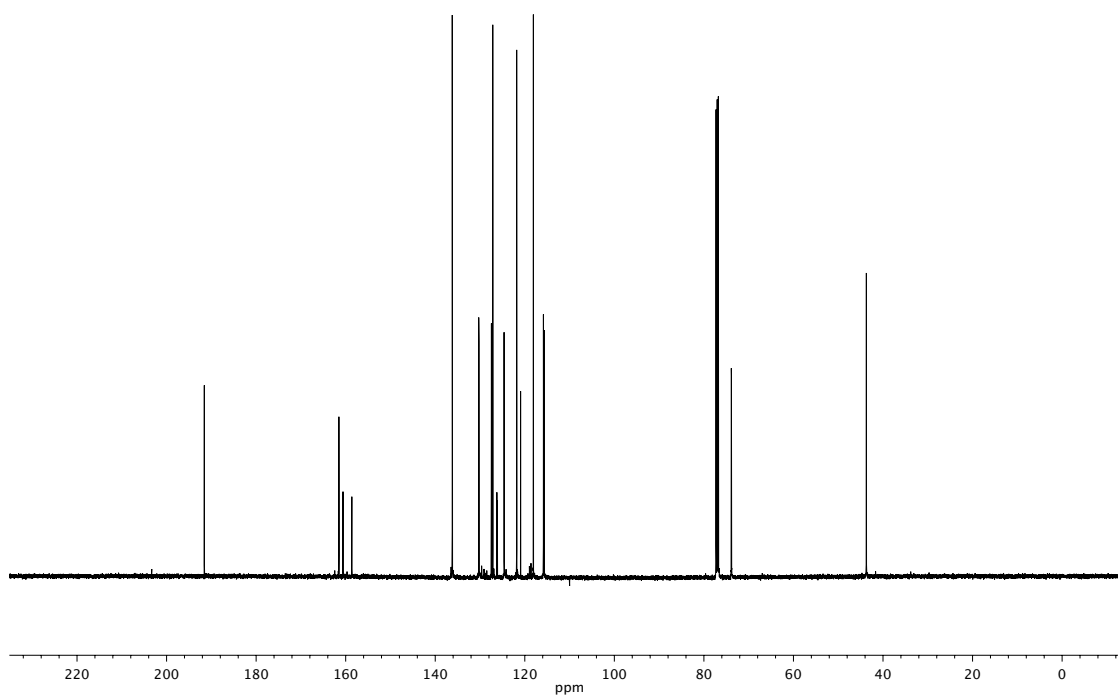
Figure A2.6 ^{13}C NMR (126 MHz, CDCl$_3$) of compound **174**

Figure A2.7 ^{1}H NMR (500 MHz, CDCl$_3$) of compound **175**
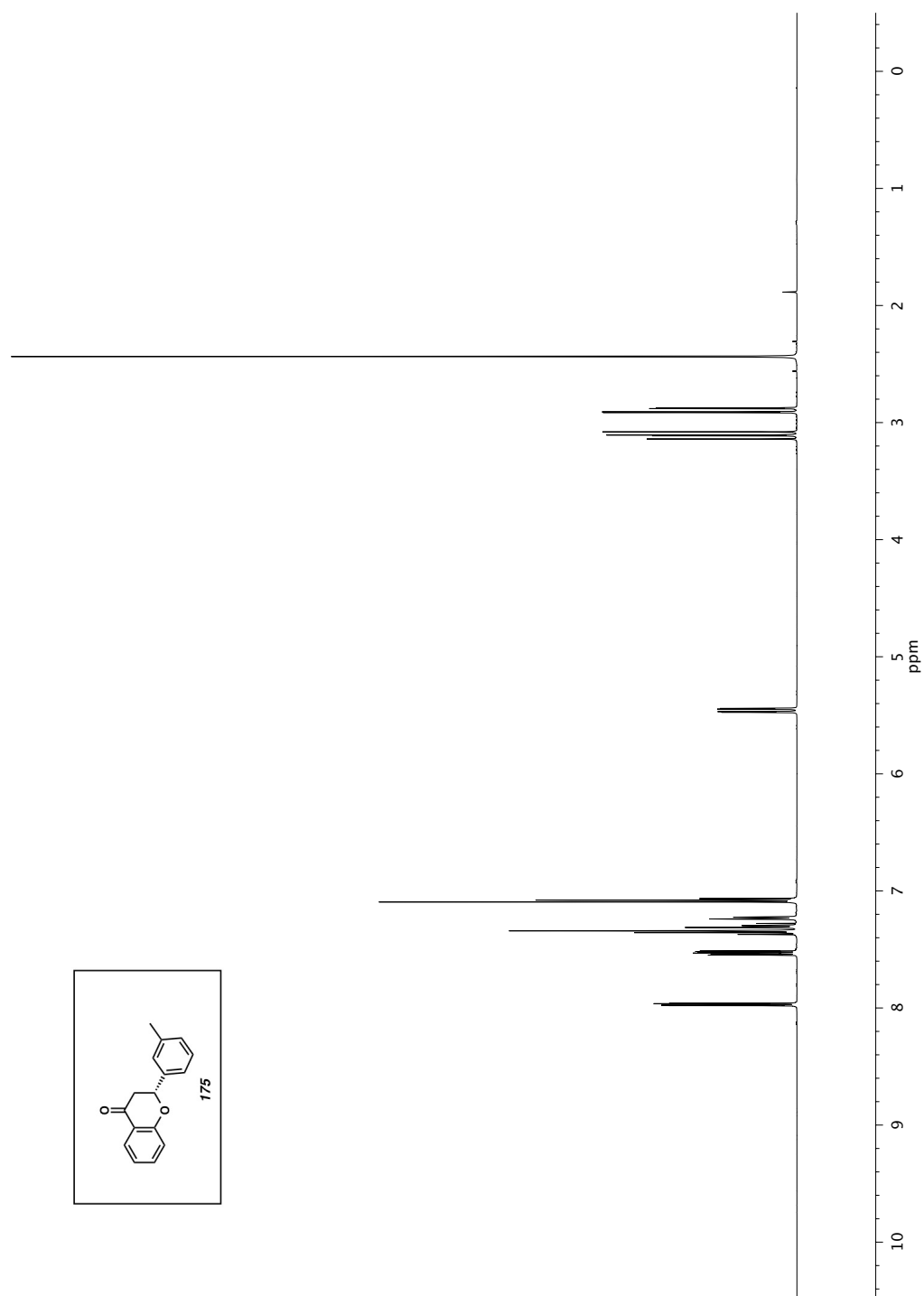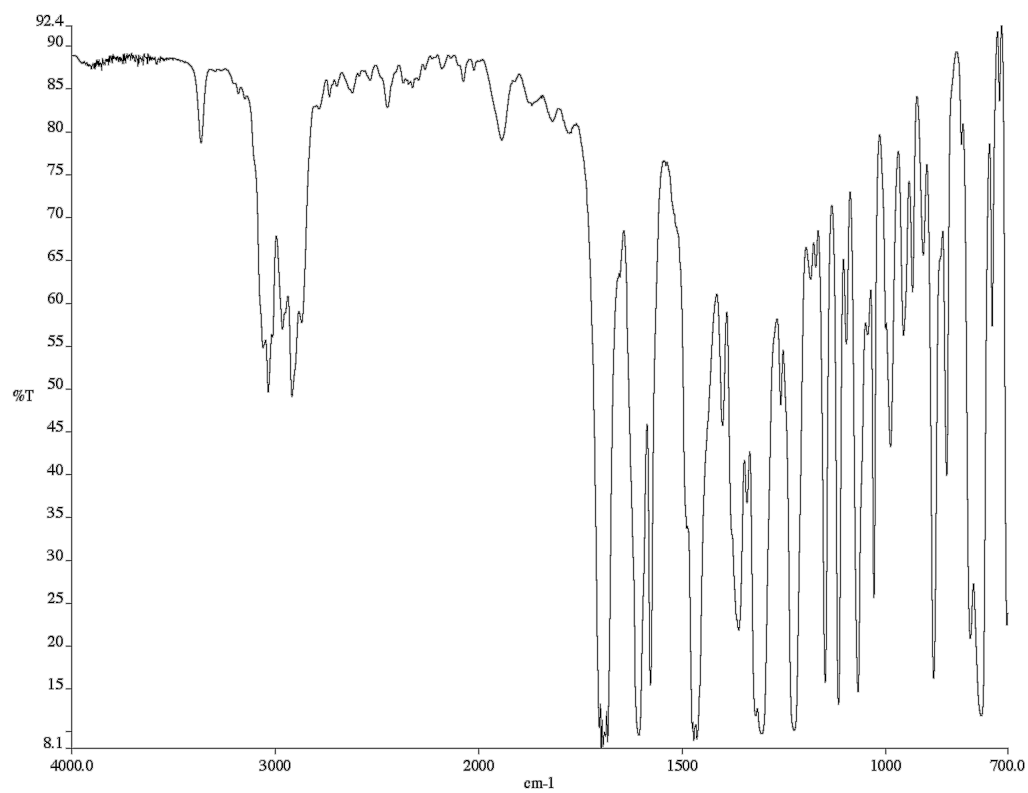
Figure A2.8 Infrared spectrum (Thin Film, NaCl) of compound **175**
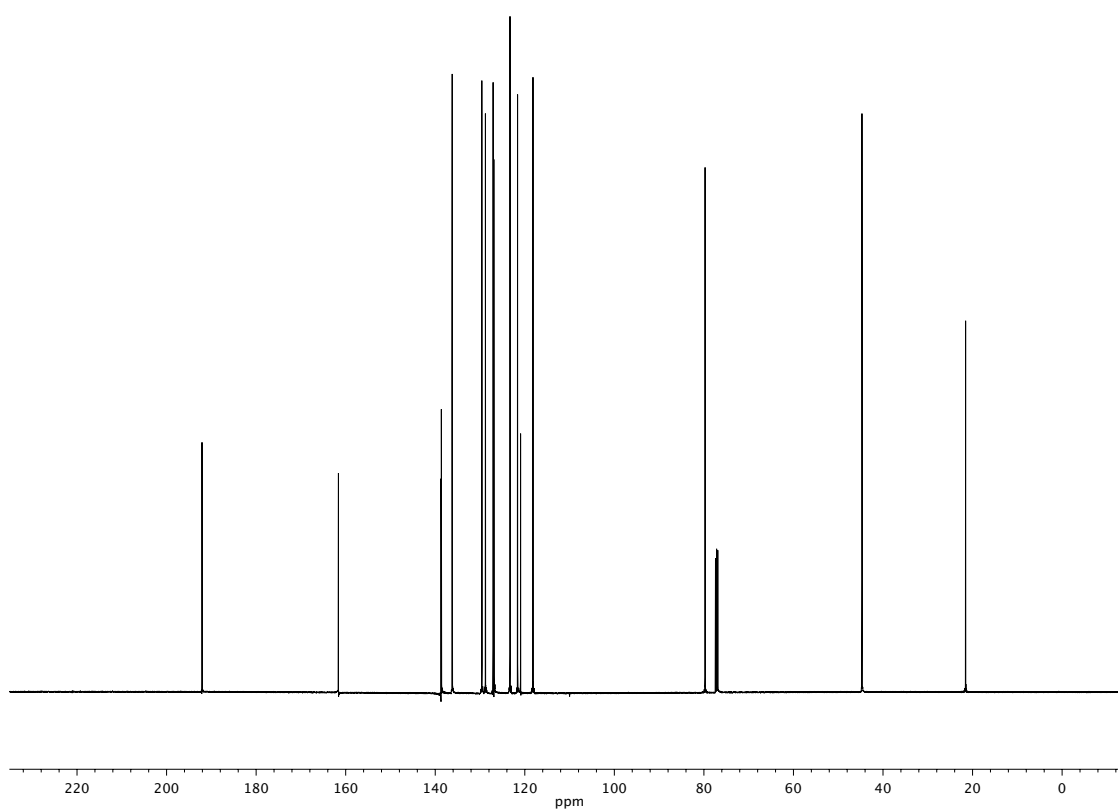
Figure A2.9 ^{13}C NMR (126 MHz, CDCl$_3$) of compound **175**
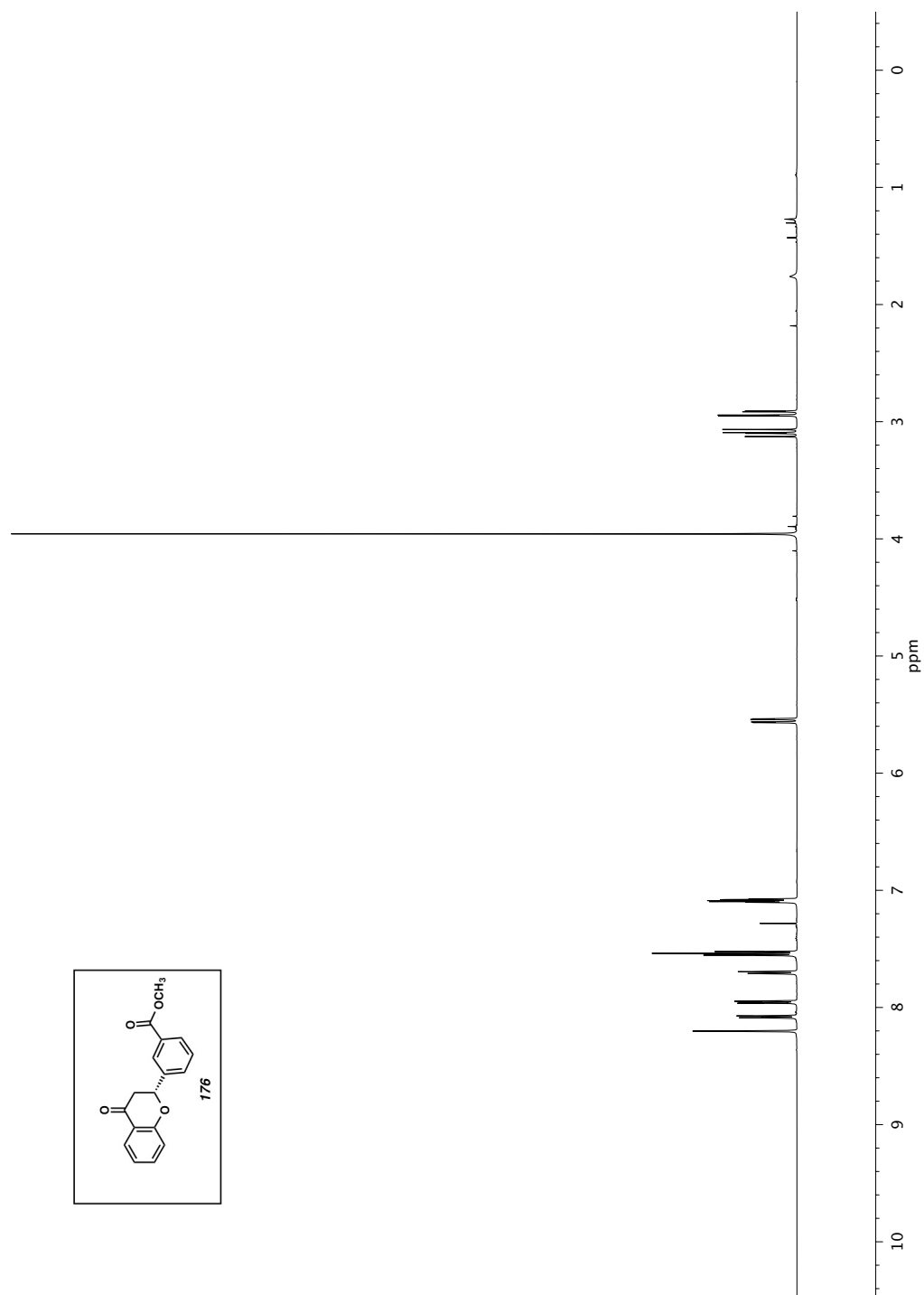
Figure A2.10 ^{1}H NMR (500 MHz, CDCl$_3$) of compound **176**
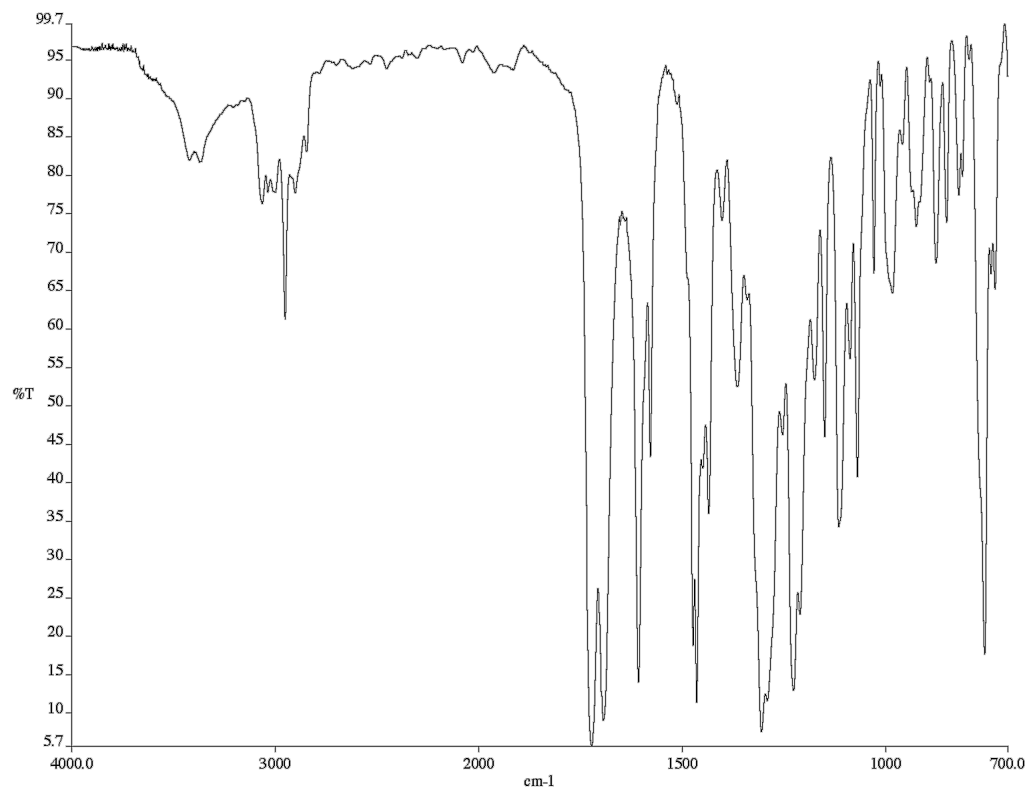
Figure A2.11 Infrared spectrum (Thin Film, NaCl) of compound **176**
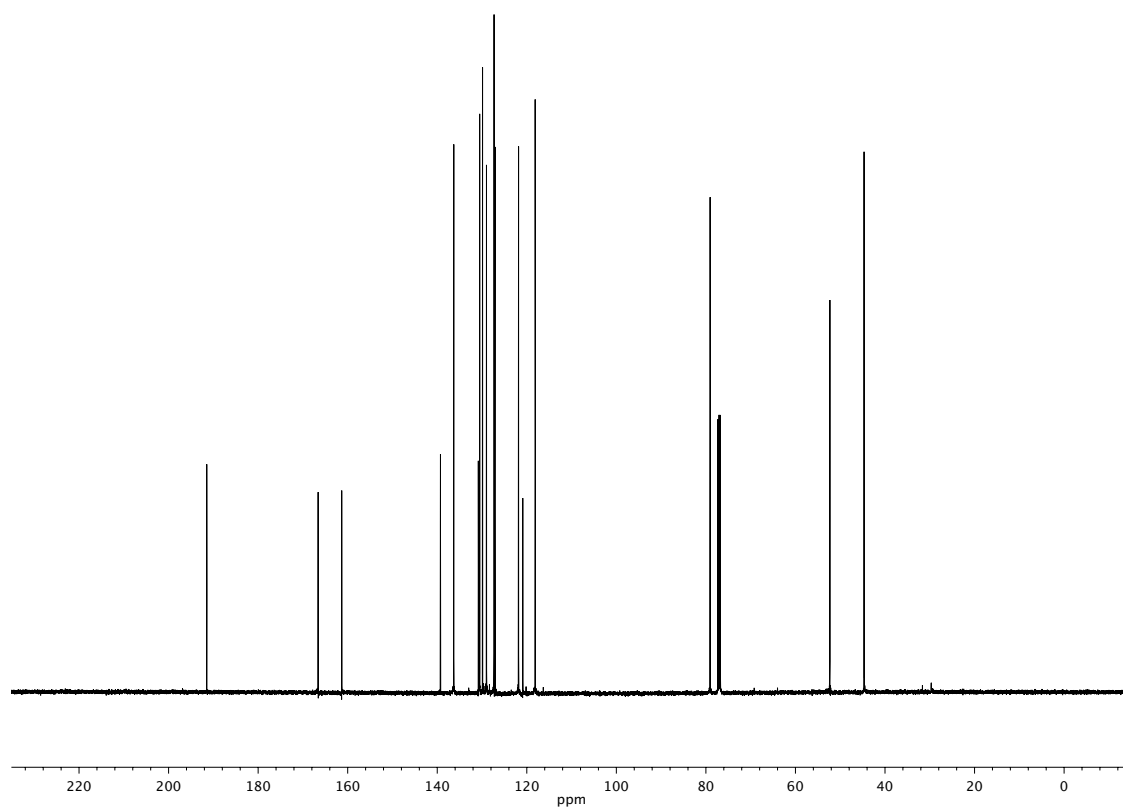
Figure A2.12 ^{13}C NMR (126 MHz, CDCl$_3$) of compound **176**
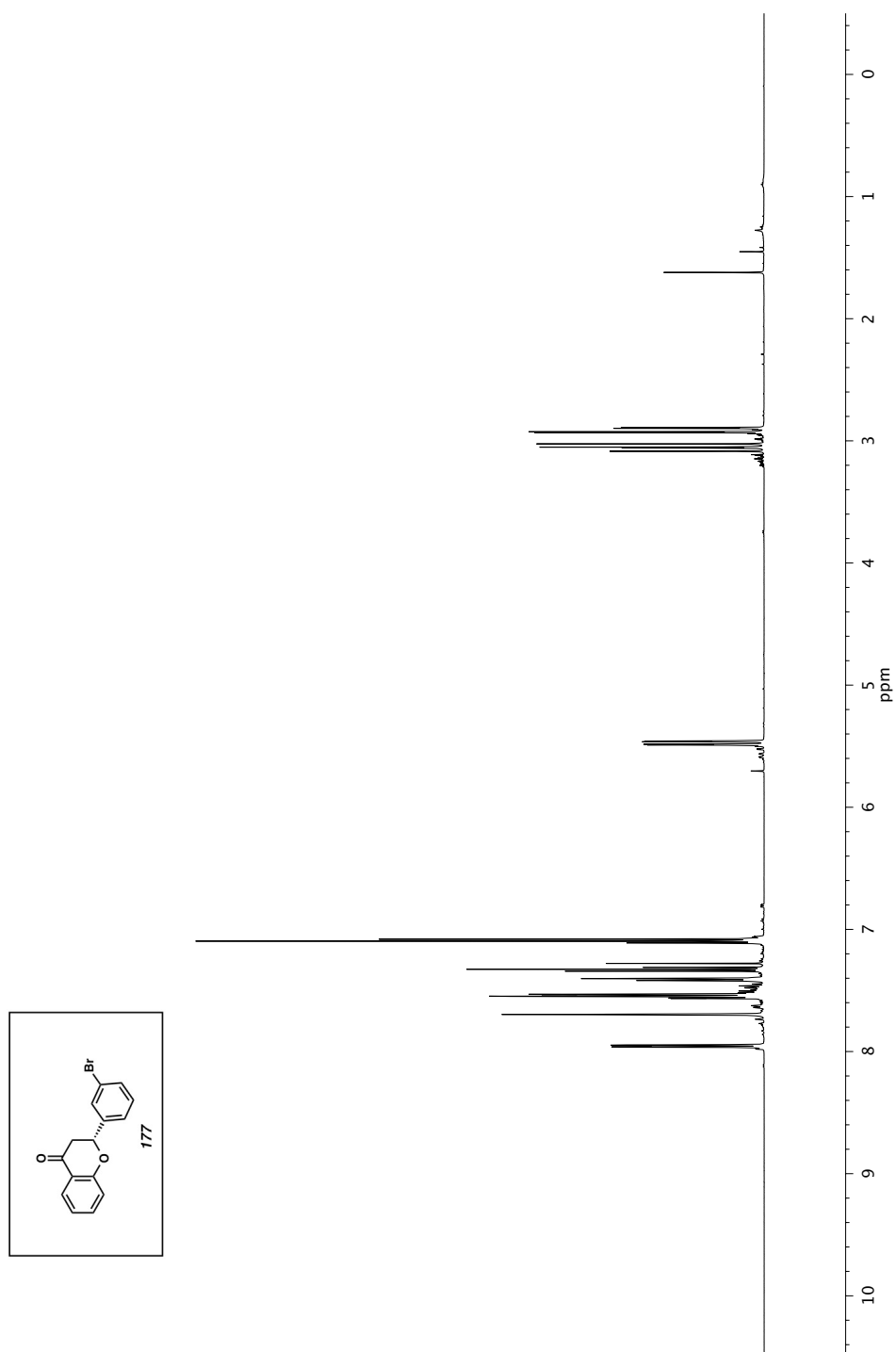
Figure A2.13 ^{1}H NMR (500 MHz, CDCl$_3$) of compound **177**
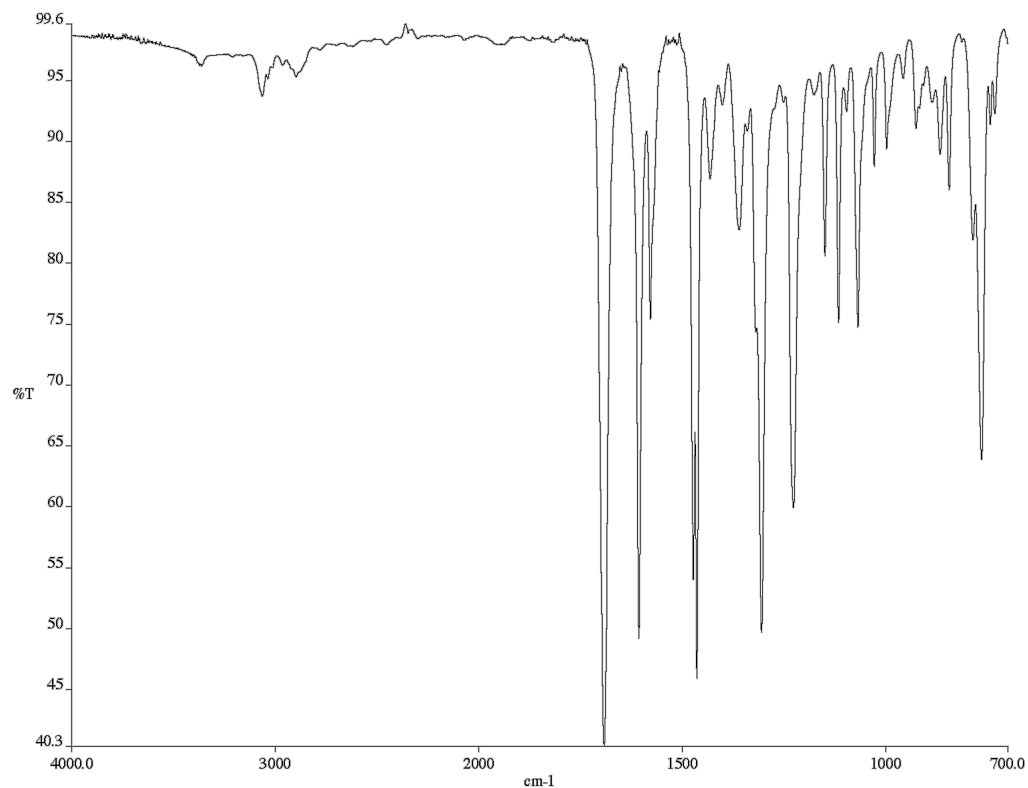
Figure A2.14 Infrared spectrum (Thin Film, NaCl) of compound **177**
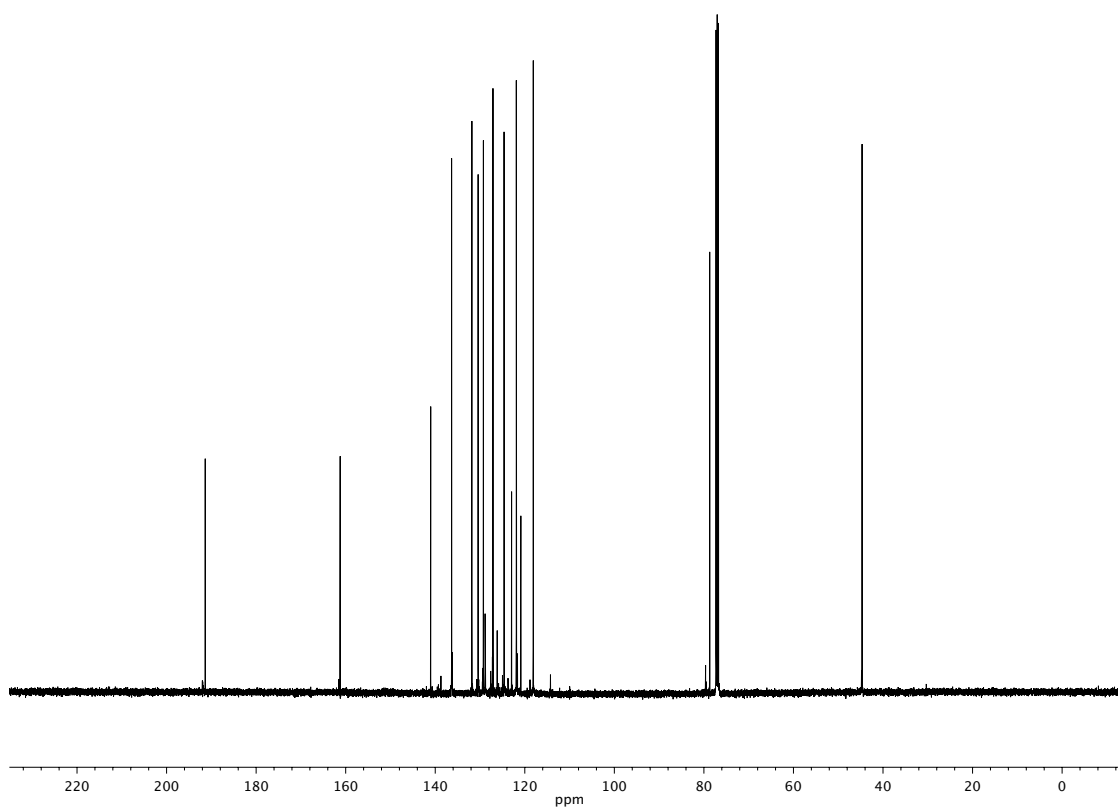
Figure A2.15 ^{13}C NMR (126 MHz, CDCl$_3$) of compound **177**
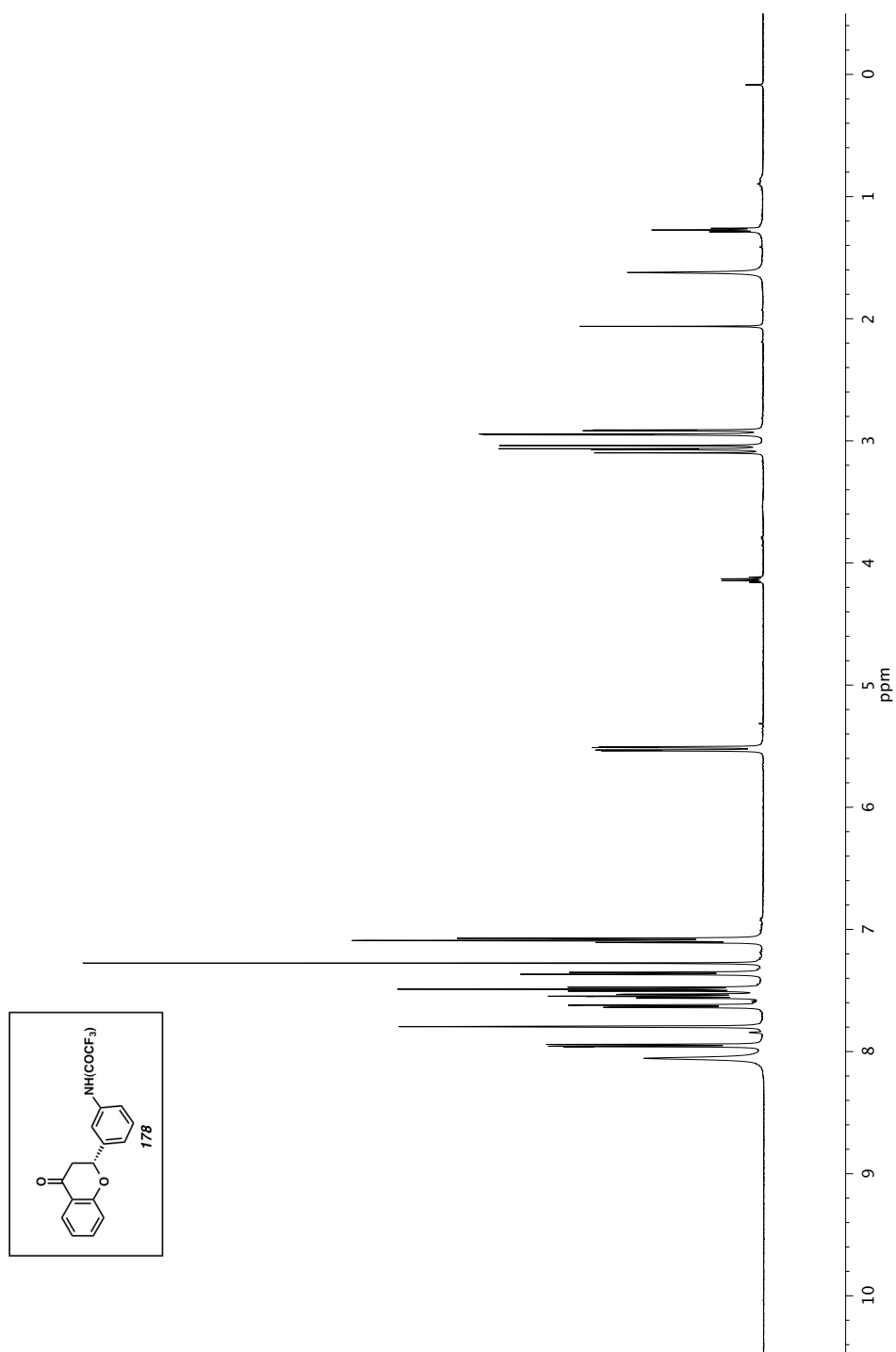
Figure A2.16 ^{1}H NMR (500 MHz, CDCl$_3$) of compound **178**
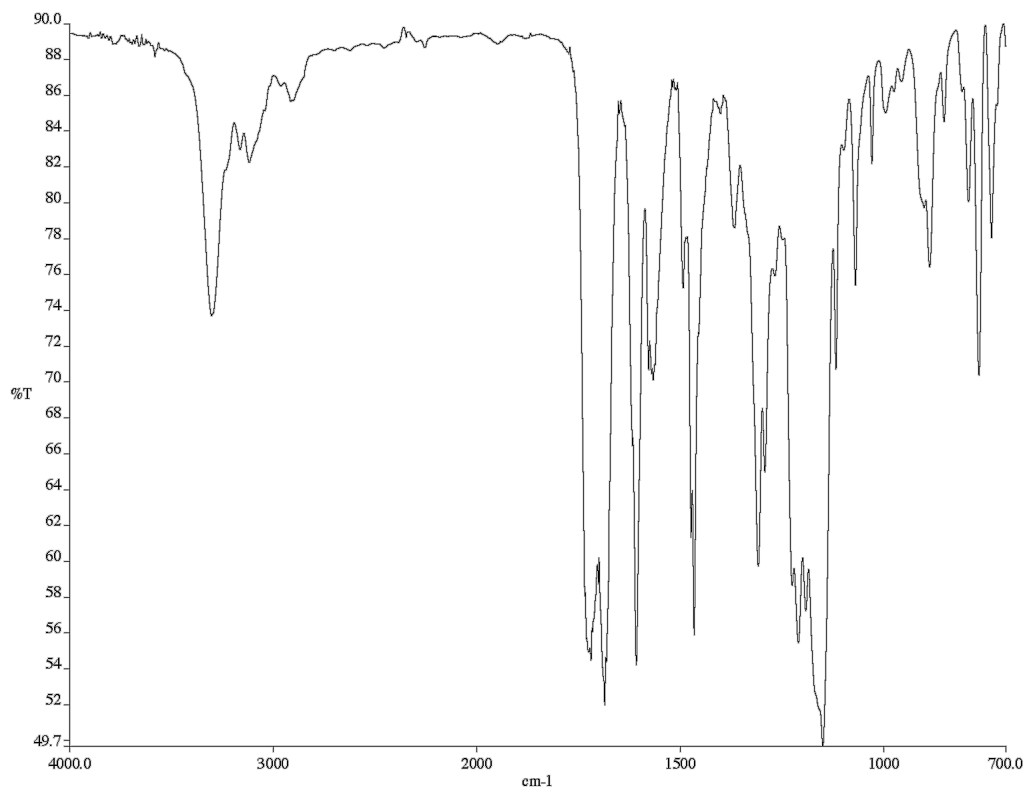
Figure A2.17 Infrared spectrum (Thin Film, NaCl) of compound **178**
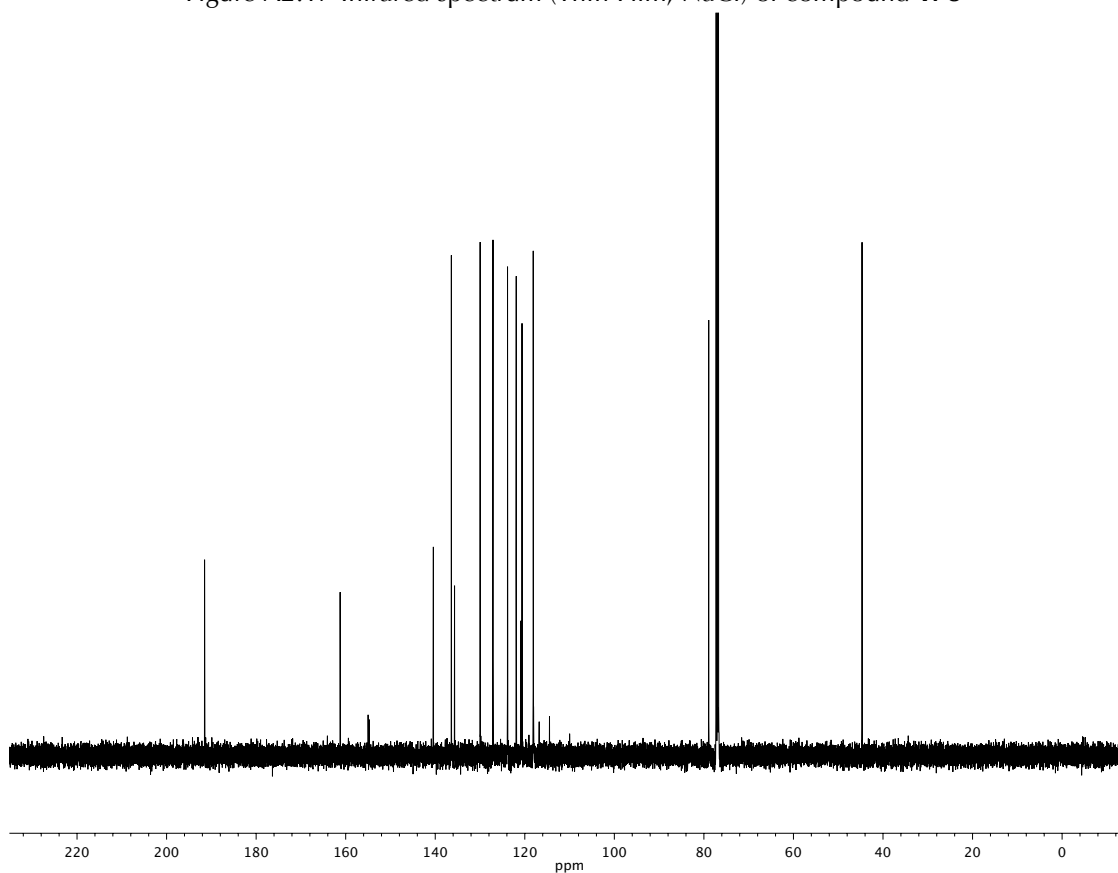
Figure A2.18 ^{13}C NMR (126 MHz, CDCl$_3$) of compound **178**
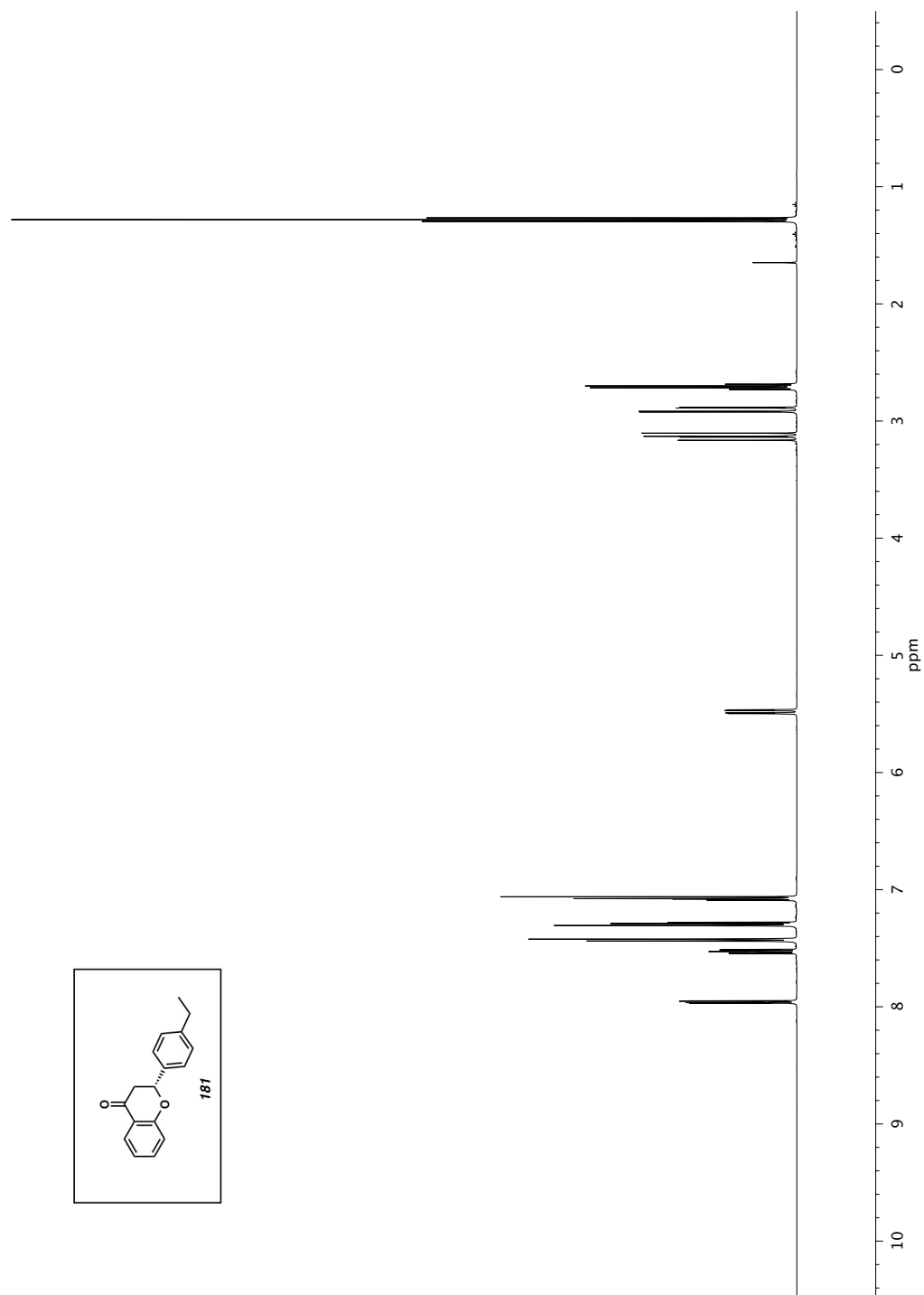
Figure A2.19 ^{1}H NMR (500 MHz, CDCl$_3$) of compound **181**
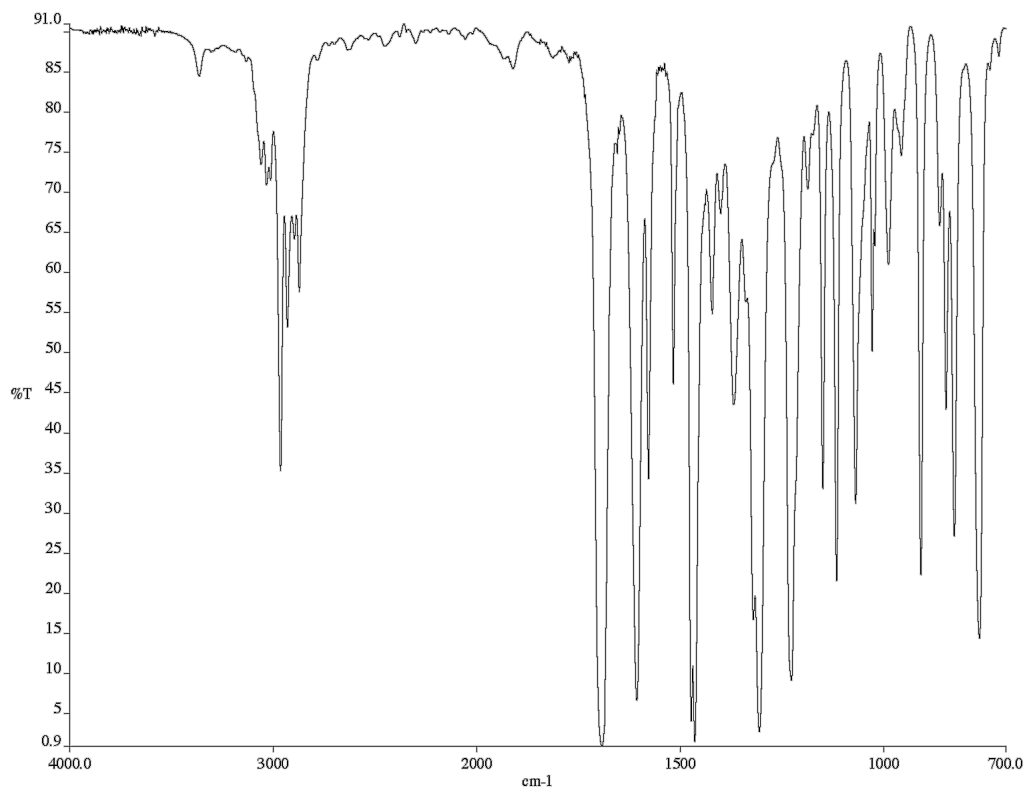
Figure A2.20 Infrared spectrum (Thin Film, NaCl) of compound **181**
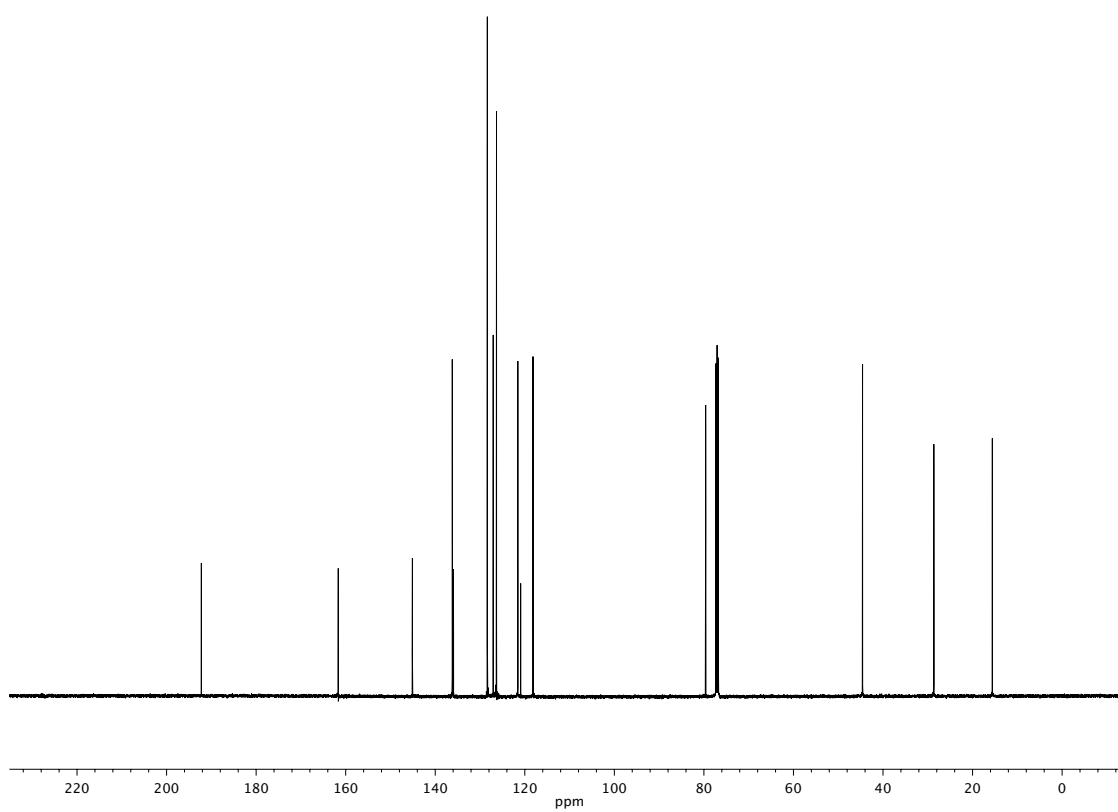
Figure A2.21 ^{13}C NMR (126 MHz, CDCl$_3$) of compound **181**
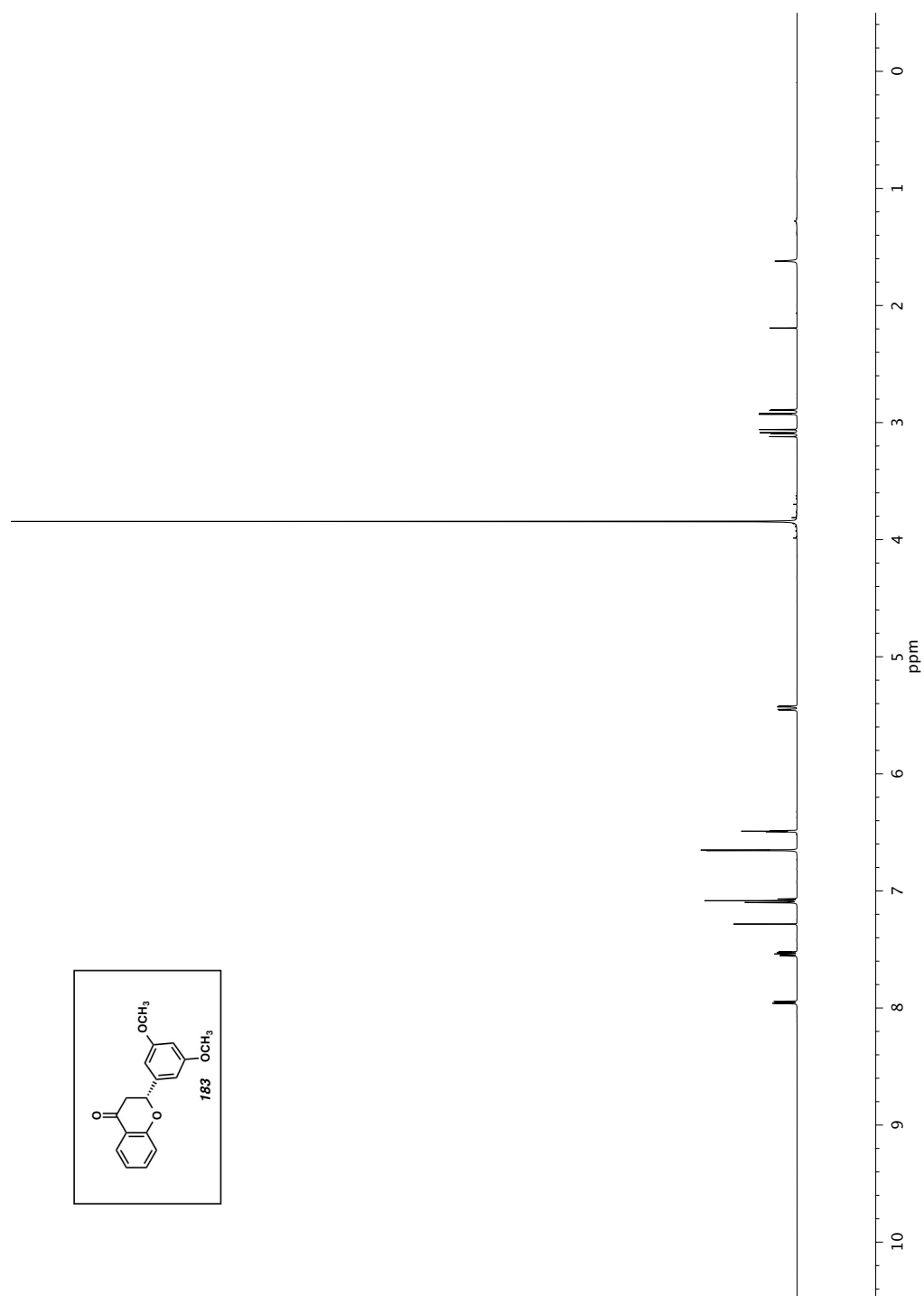
Figure A2.22 ^{1}H NMR (500 MHz, CDCl$_3$) of compound **183**
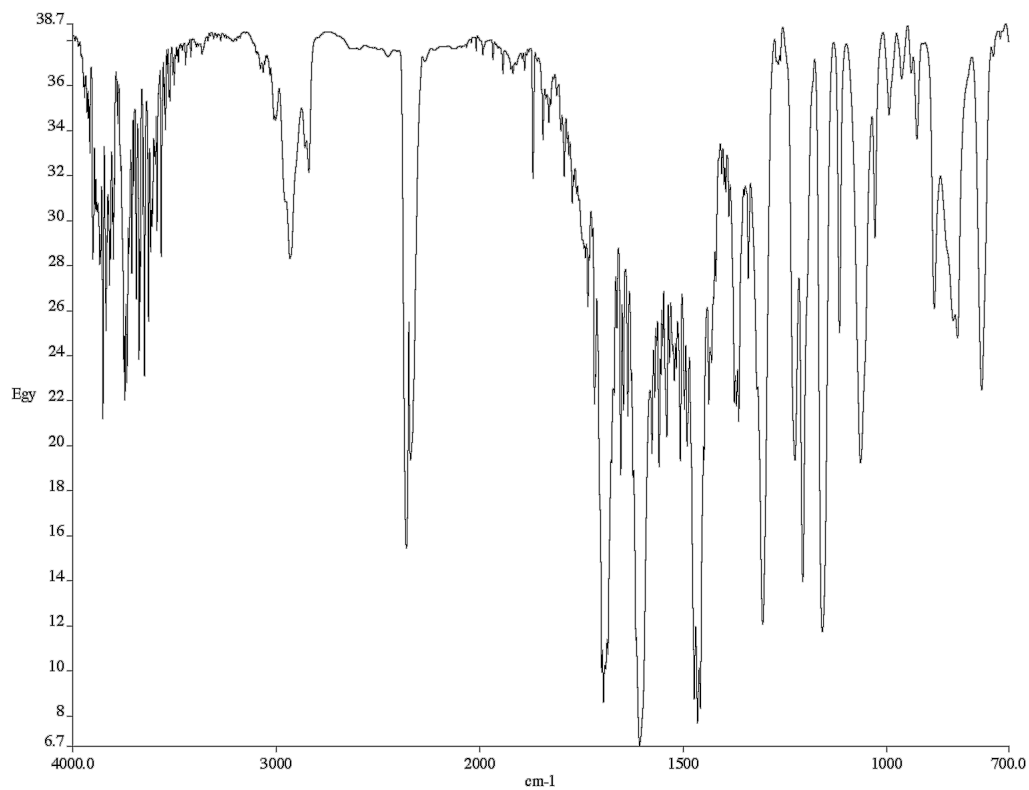
Figure A2.23 Infrared spectrum (Thin Film, NaCl) of compound **183**
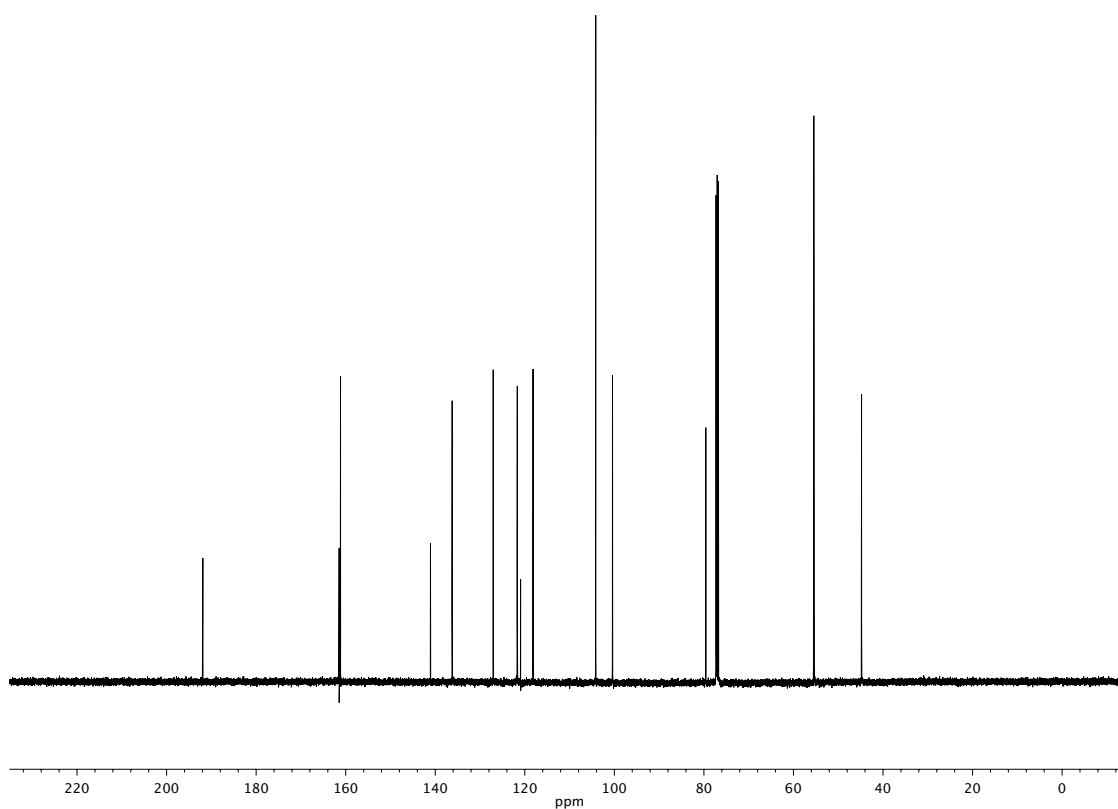
Figure A2.24 ^{13}C NMR (126 MHz, CDCl$_3$) of compound **183**
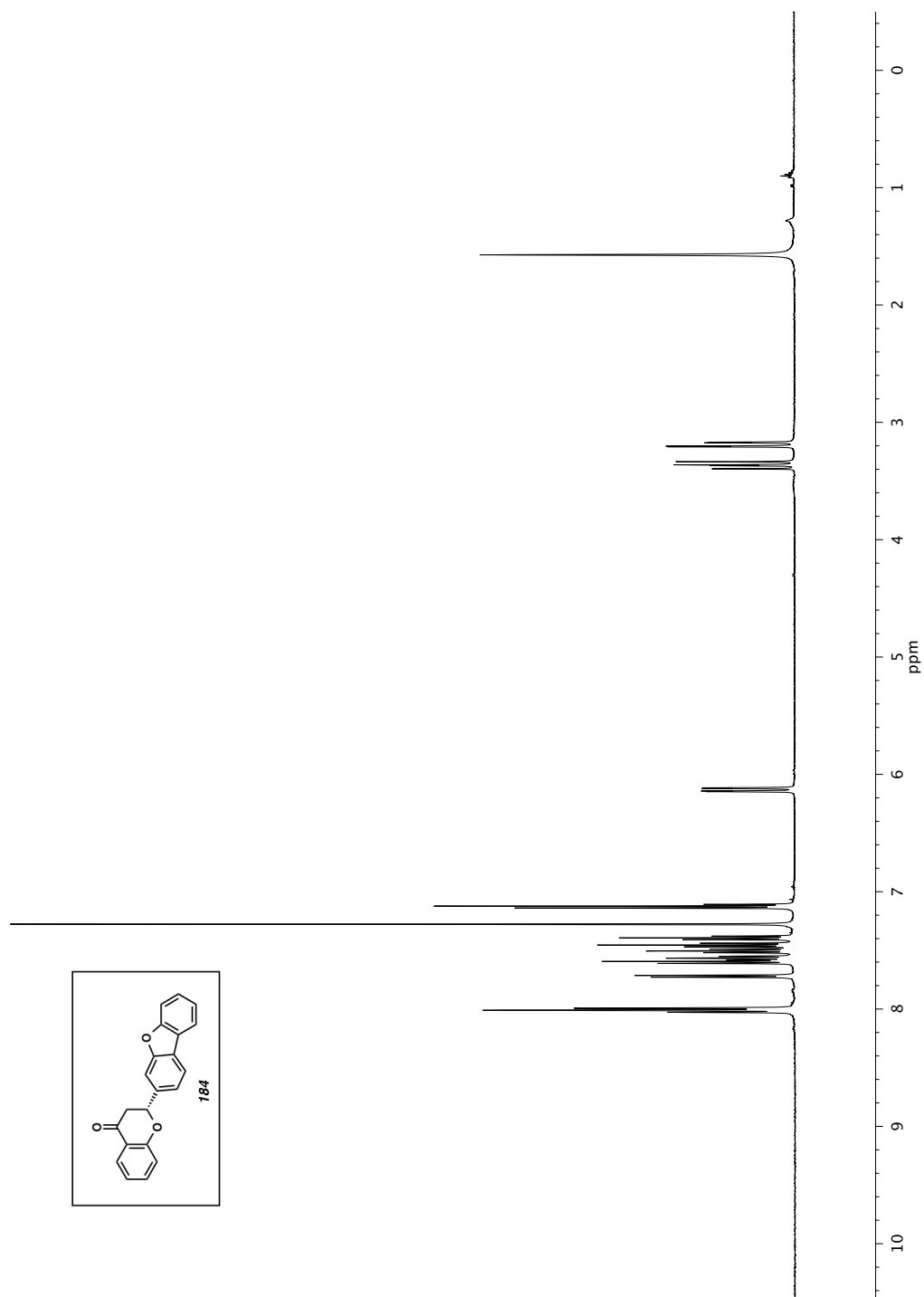
Figure A2.25 ^{1}H NMR (500 MHz, CDCl$_3$) of compound **184**
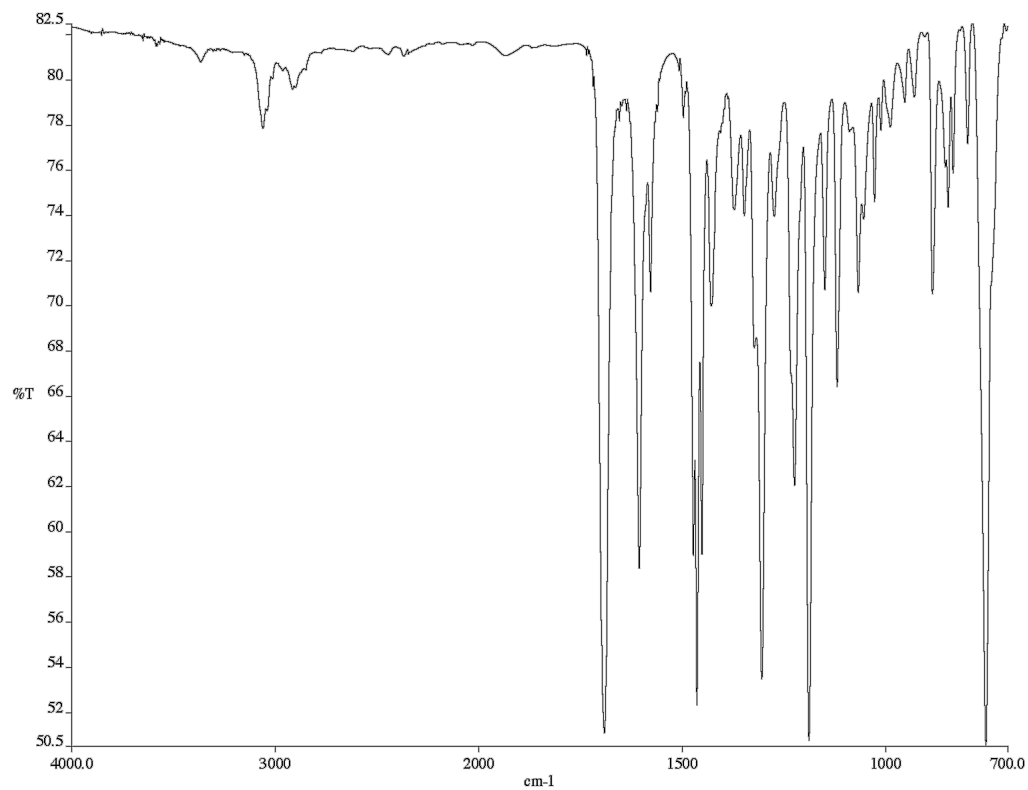
Figure A2.26 Infrared spectrum (Thin Film, NaCl) of compound **184**
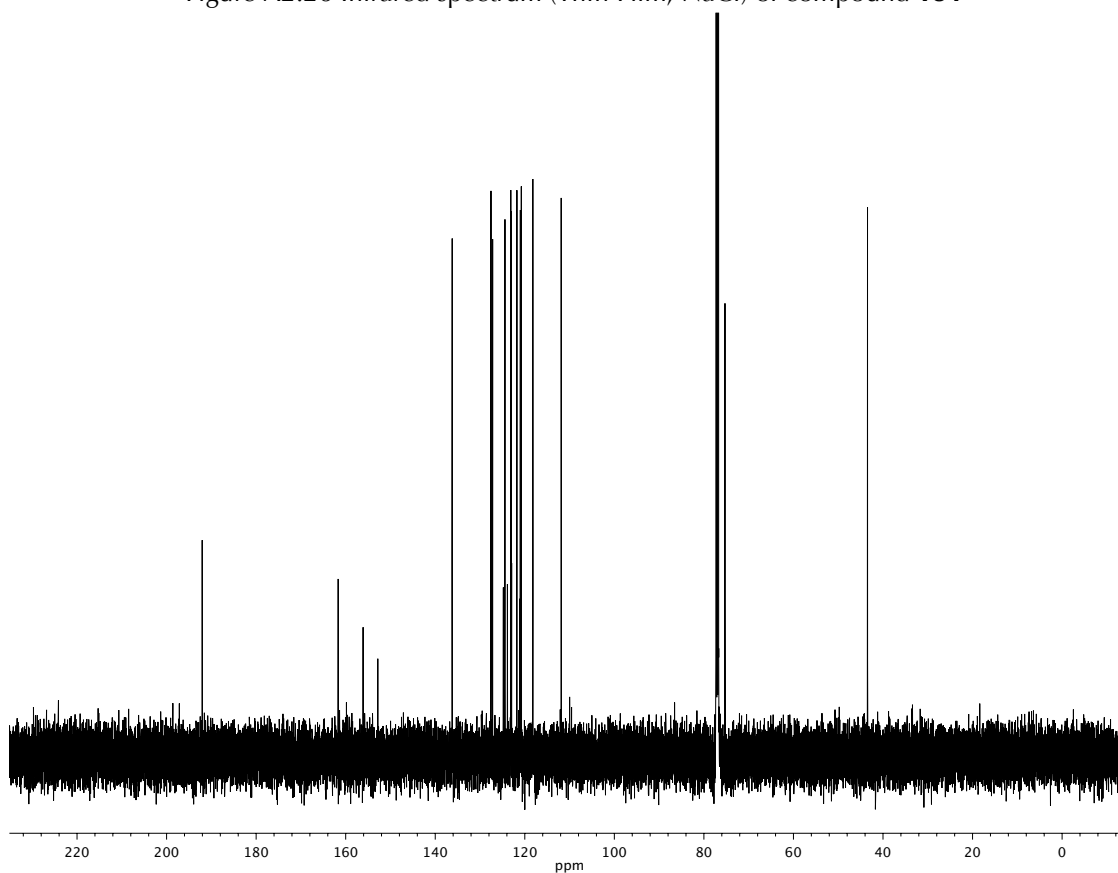
Figure A2.27 ^{13}C NMR (126 MHz, CDCl$_3$) of compound **184**
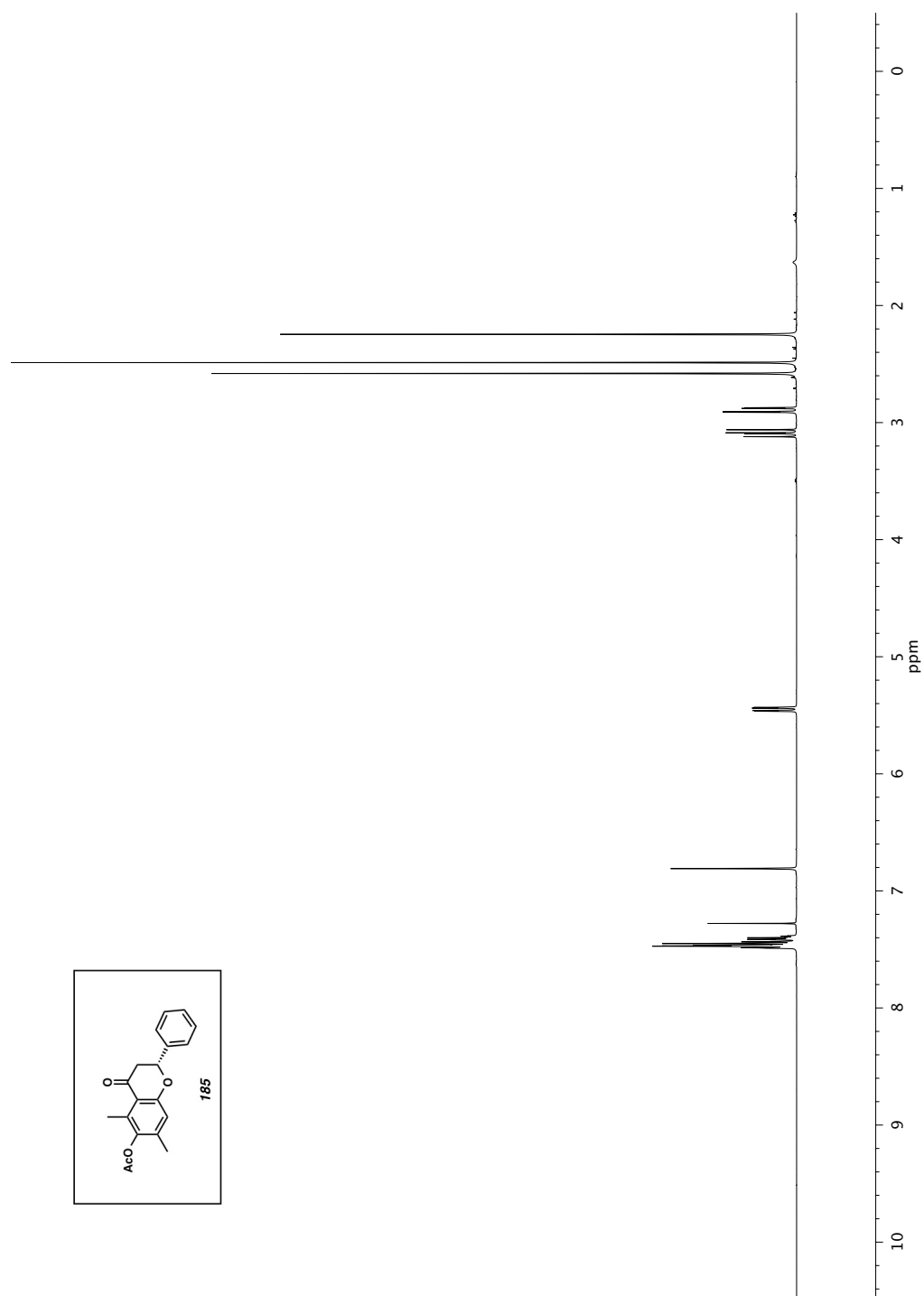
Figure A2.28 ^{1}H NMR (500 MHz, CDCl$_3$) of compound **185**
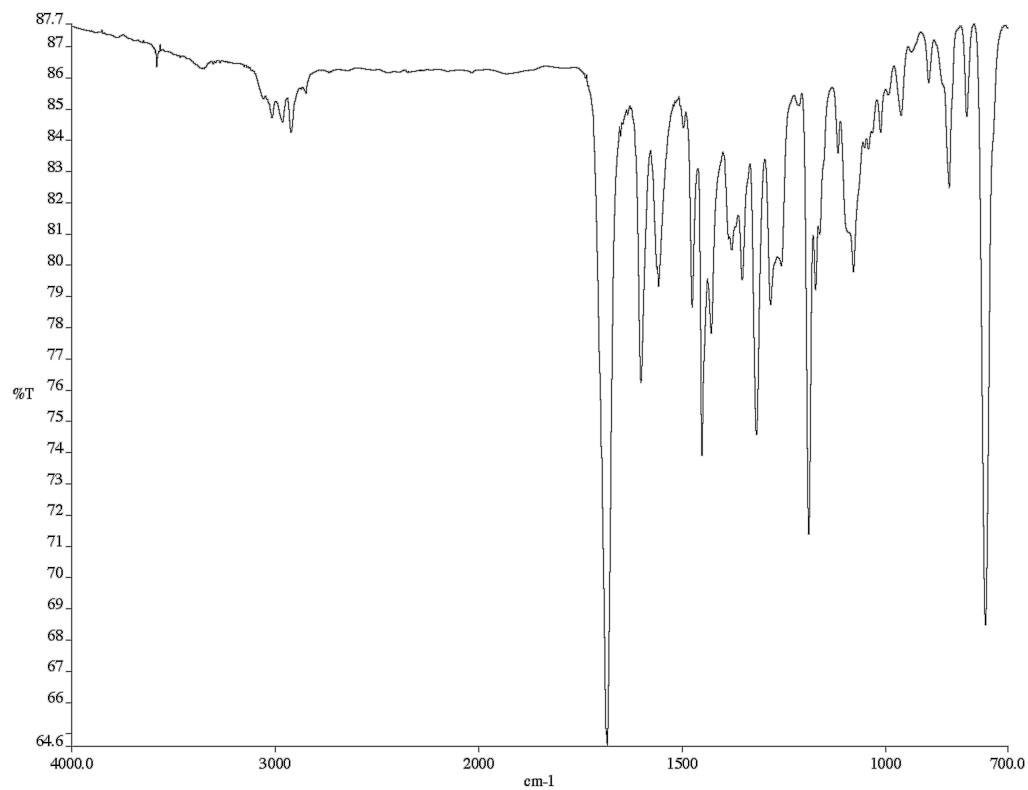
Figure A2.29 Infrared spectrum (Thin Film, NaCl) of compound **185**
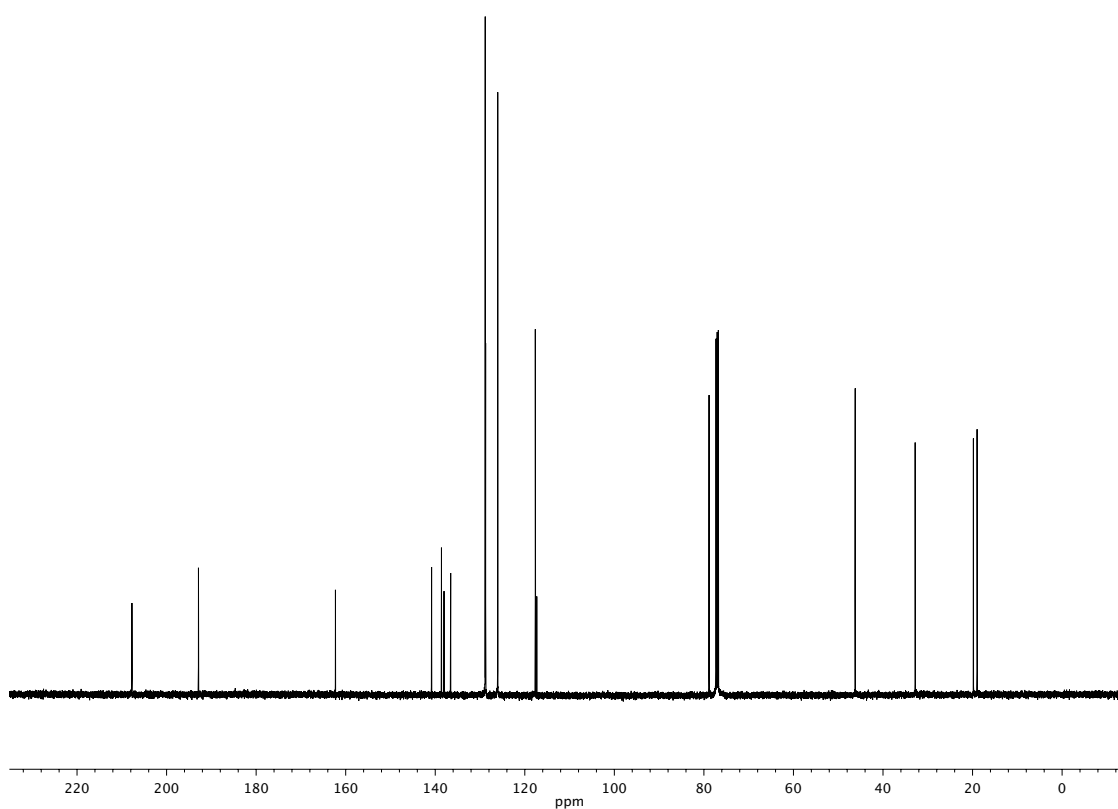
Figure A2.30 ^{13}C NMR (126 MHz, CDCl$_3$) of compound **185**
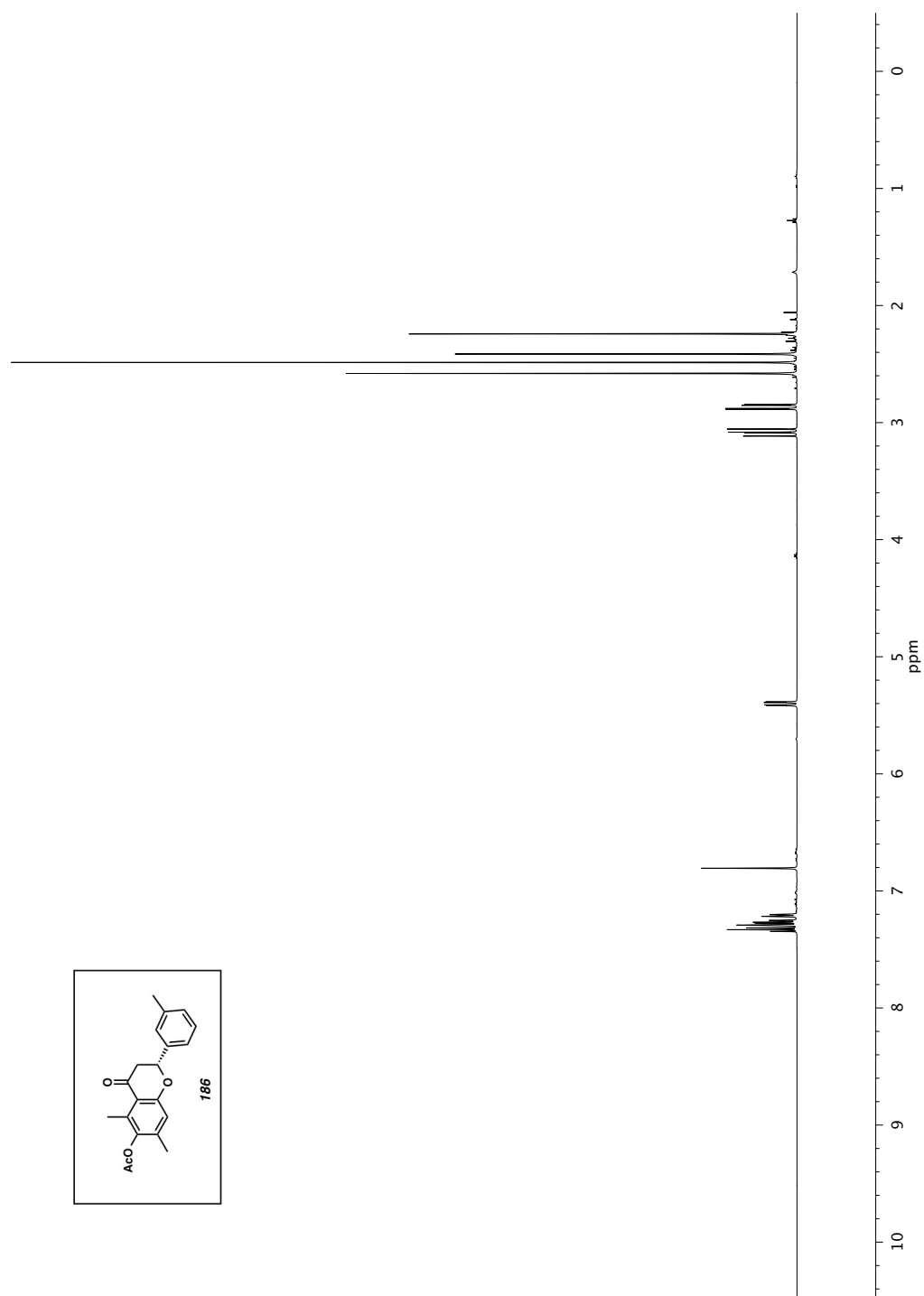
Figure A2.31 ^{1}H NMR (500 MHz, CDCl$_3$) of compound **186**
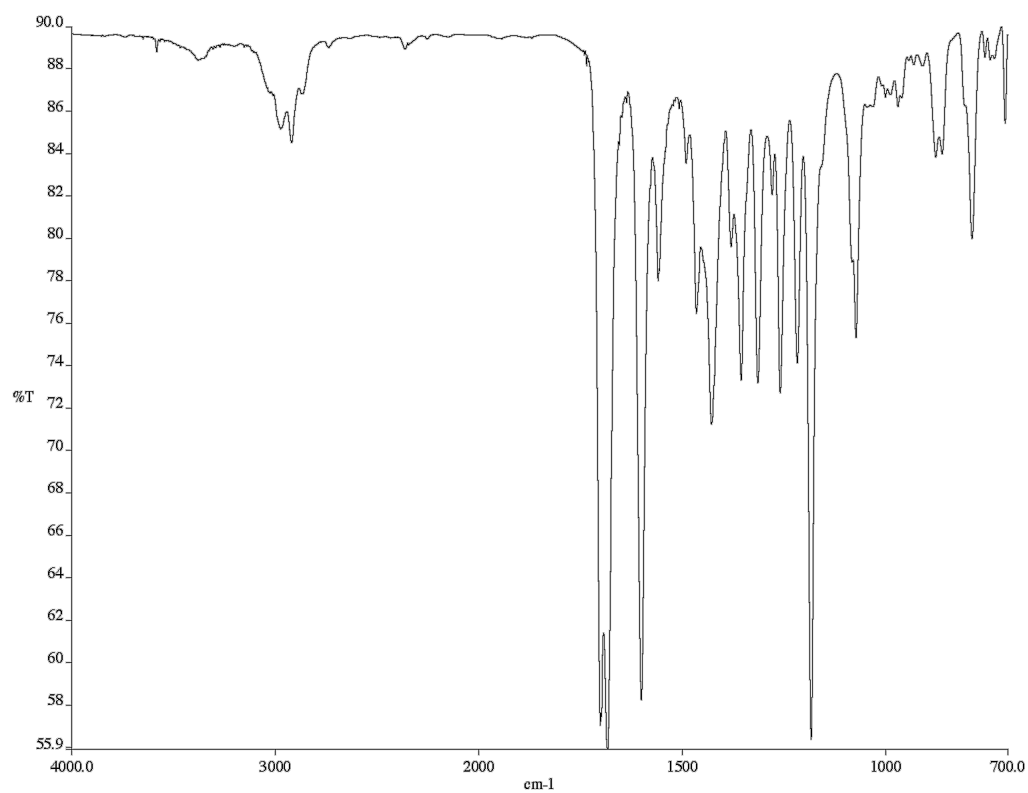
Figure A2.32 Infrared spectrum (Thin Film, NaCl) of compound **186**
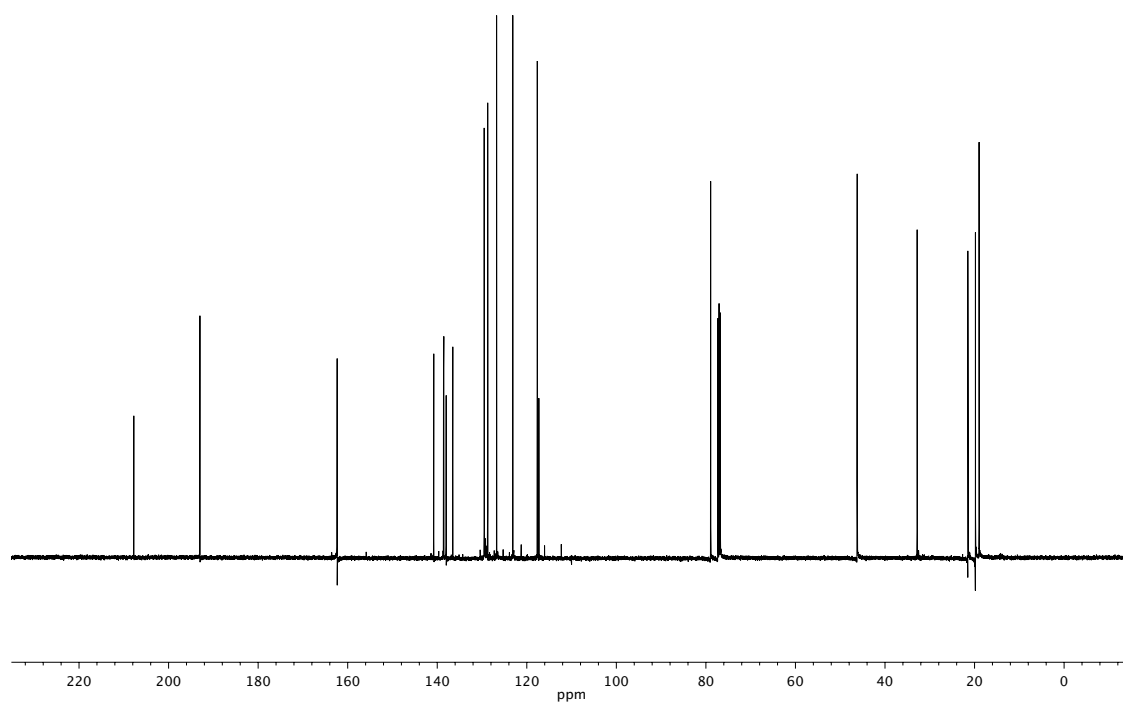
Figure A2.33 ^{13}C NMR (126 MHz, CDCl$_3$) of compound **186**
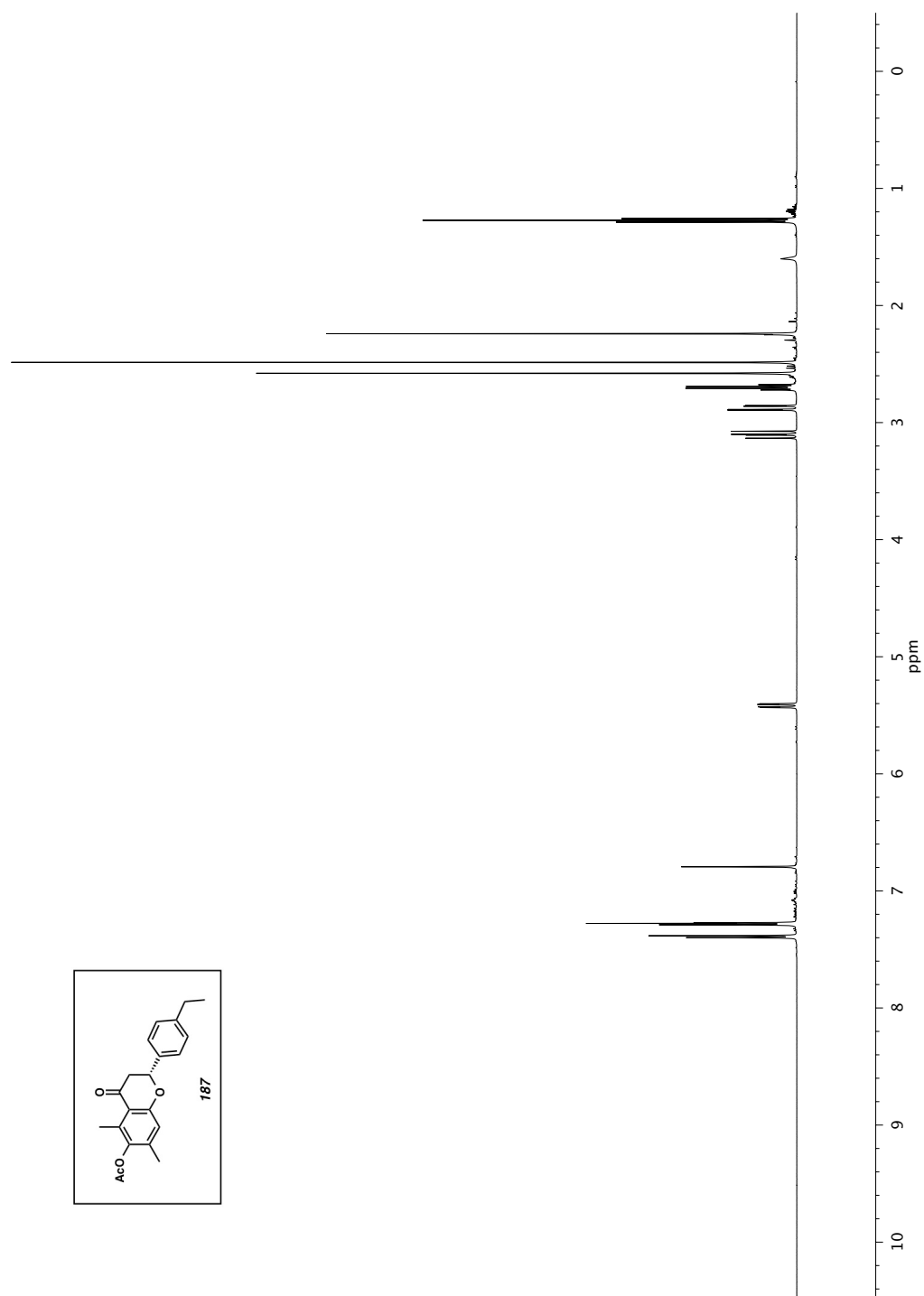
Figure A2.34 ^{1}H NMR (500 MHz, CDCl$_3$) of compound **187**
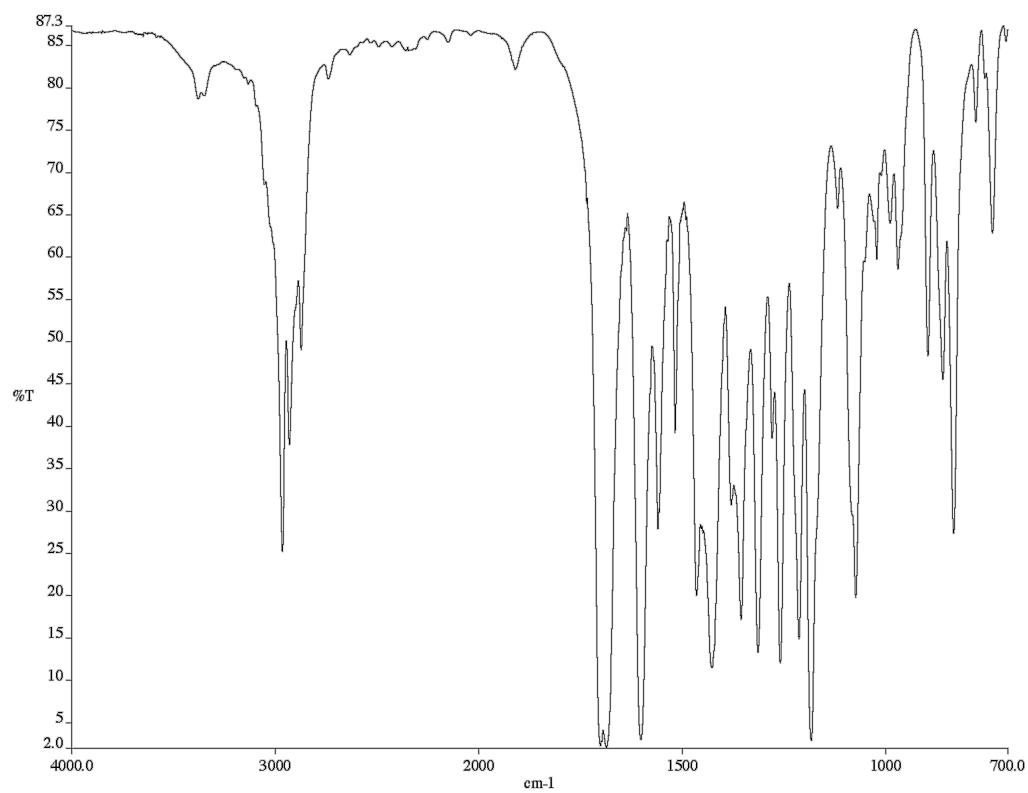
Figure A2.35 Infrared spectrum (Thin Film, NaCl) of compound **187**
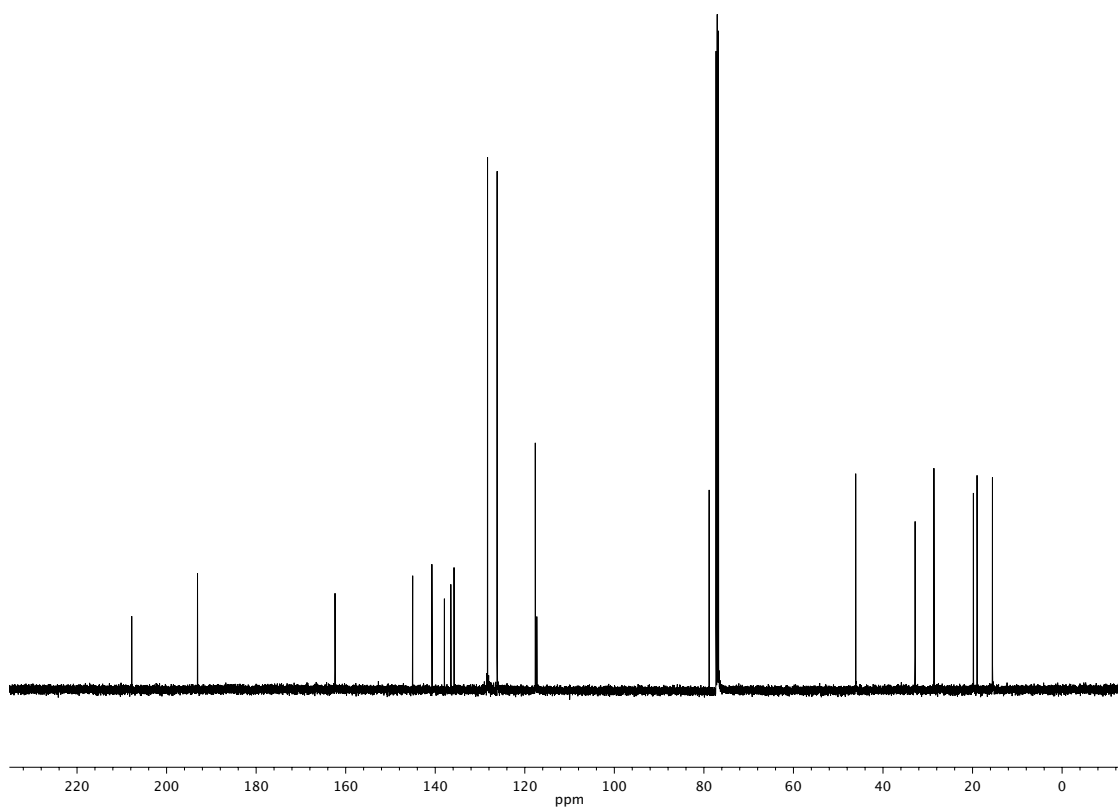
Figure A2.36 ^{13}C NMR (126 MHz, CDCl$_3$) of compound **187**
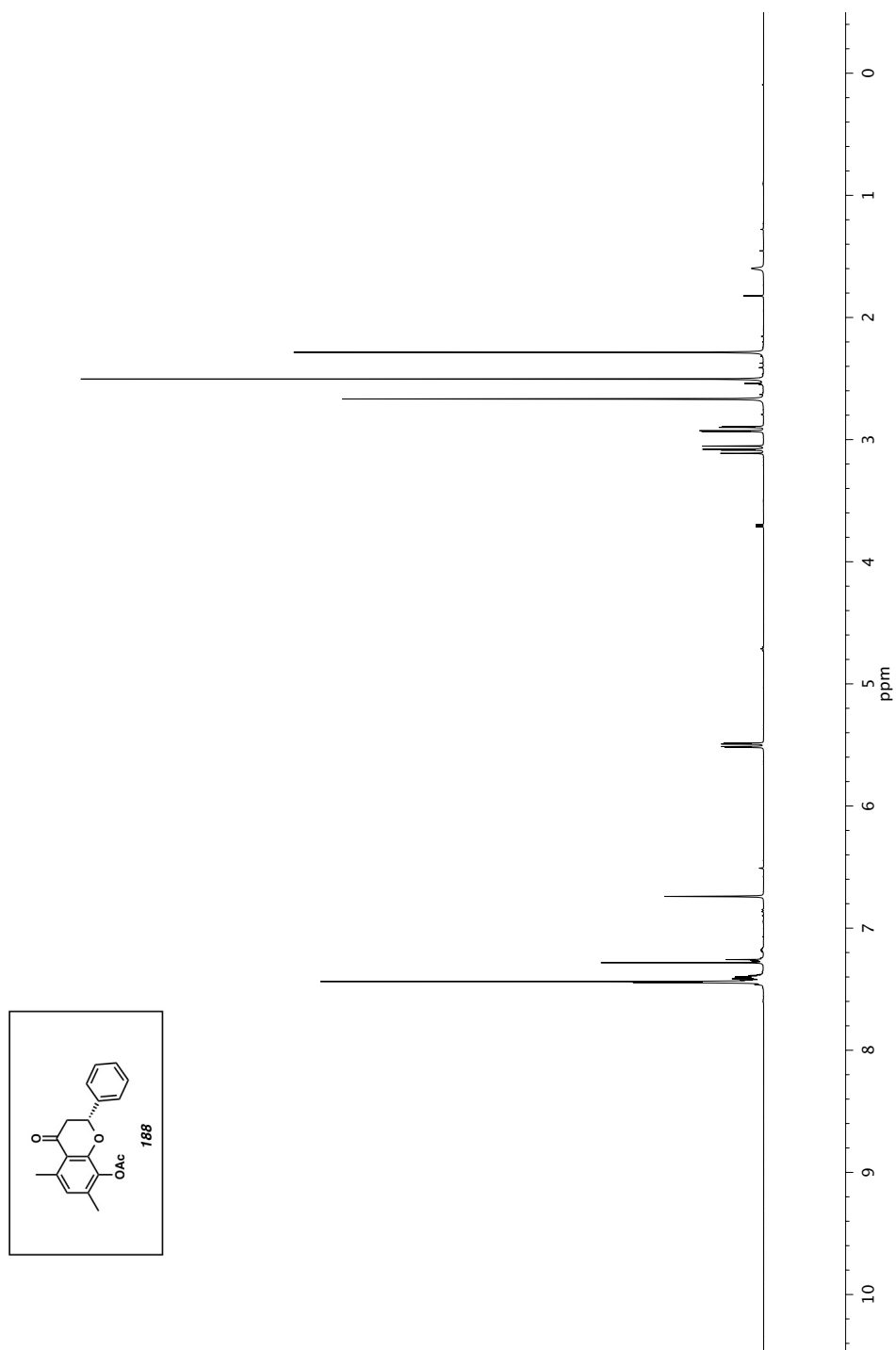
Figure A2.37 ^{1}H NMR (500 MHz, CDCl$_3$) of compound **188**
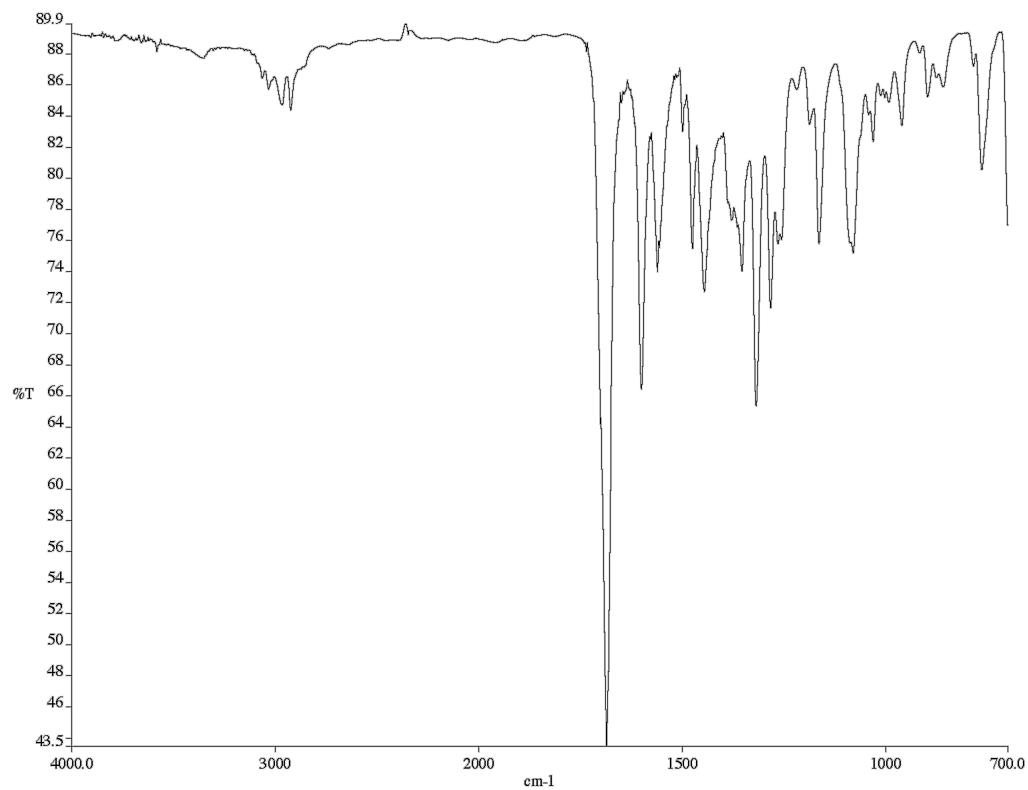
Figure A2.38 Infrared spectrum (Thin Film, NaCl) of compound **188**
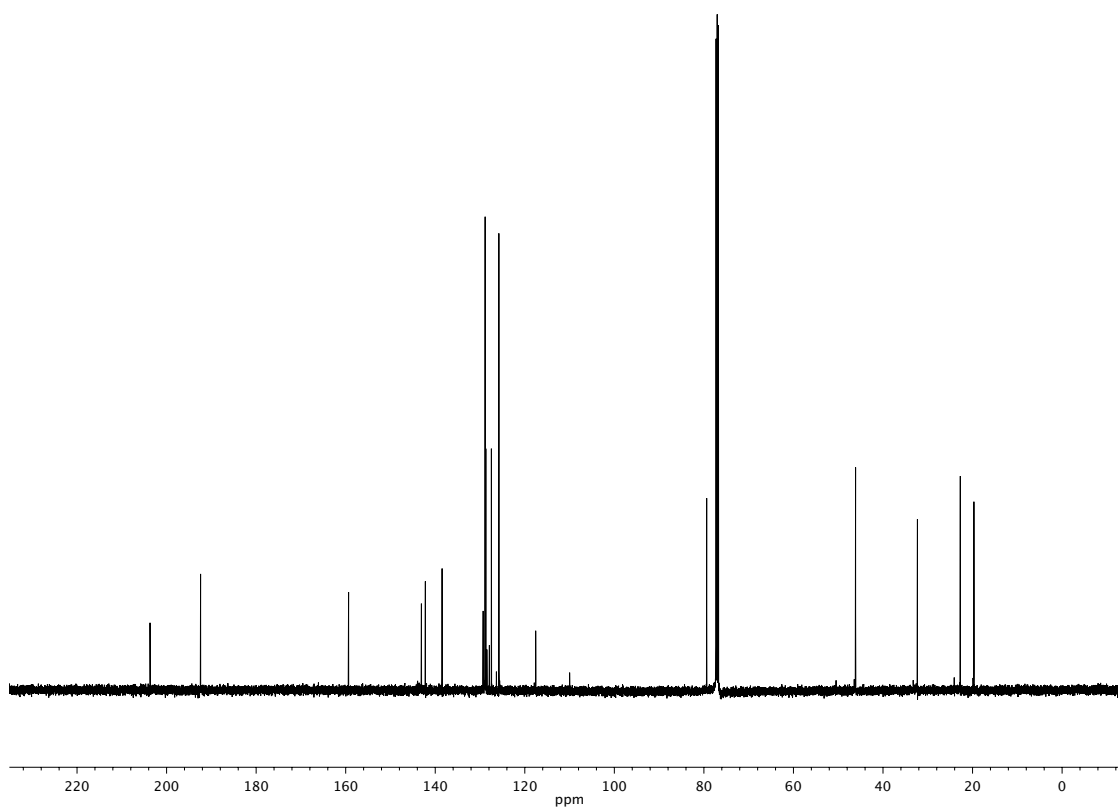
Figure A2.39 ^{13}C NMR (126 MHz, CDCl$_3$) of compound **188**
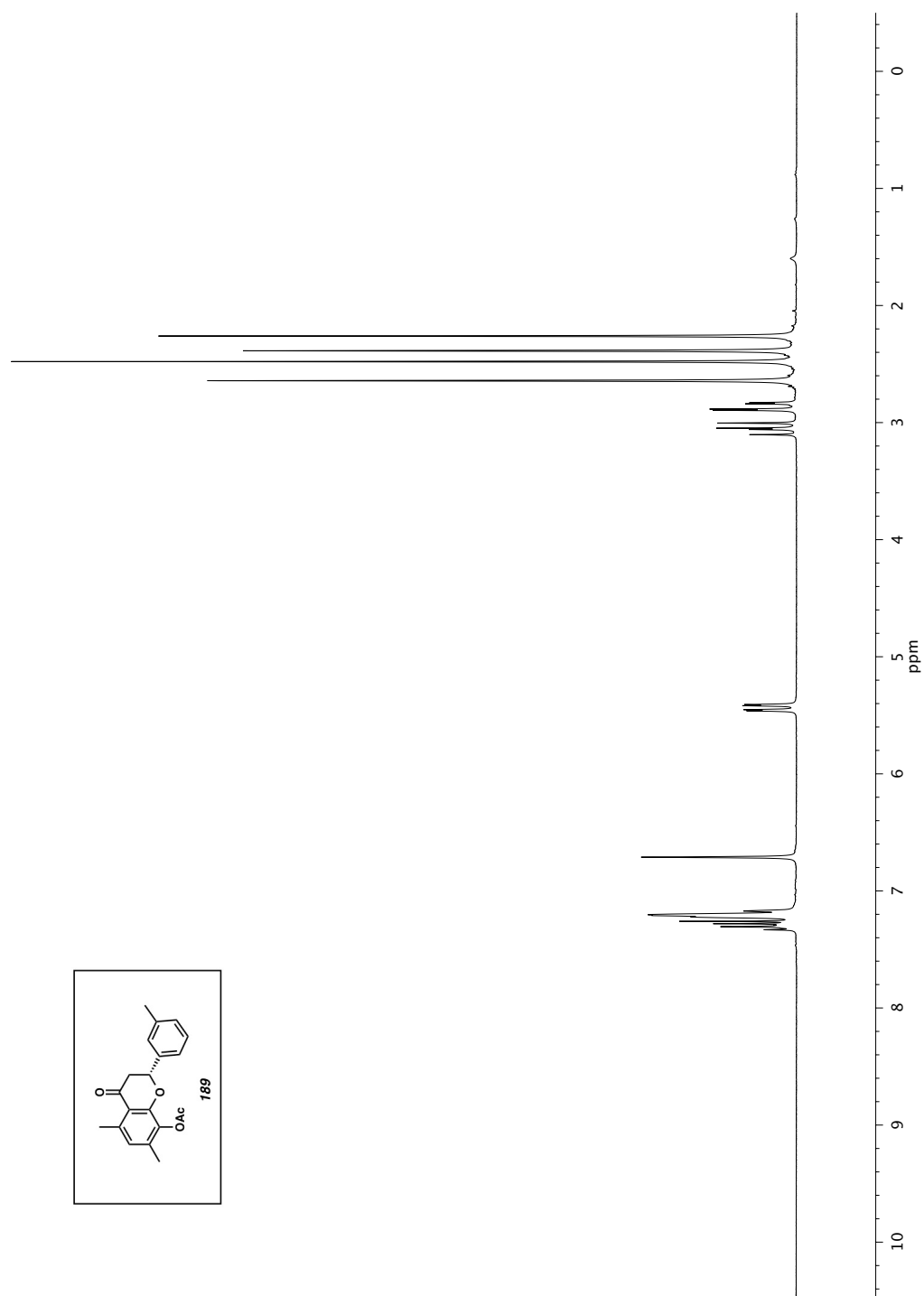
Figure A2.40 ^{1}H NMR (500 MHz, CDCl$_3$) of compound **189**
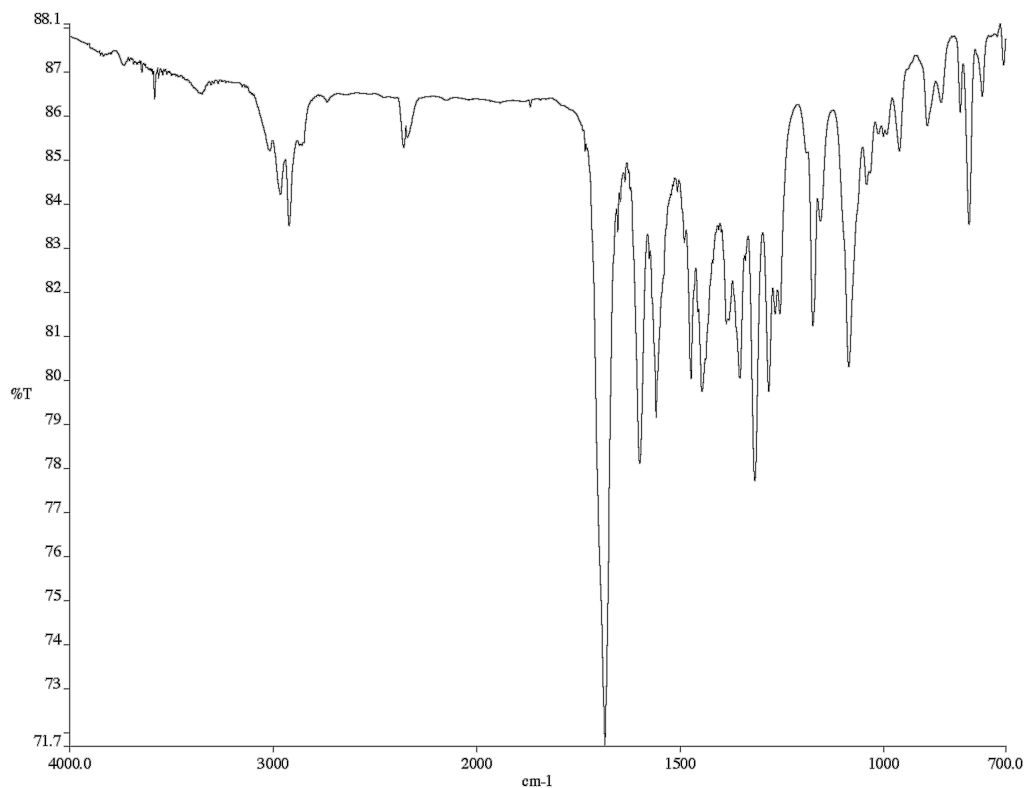
Figure A2.41 Infrared spectrum (Thin Film, NaCl) of compound **189**
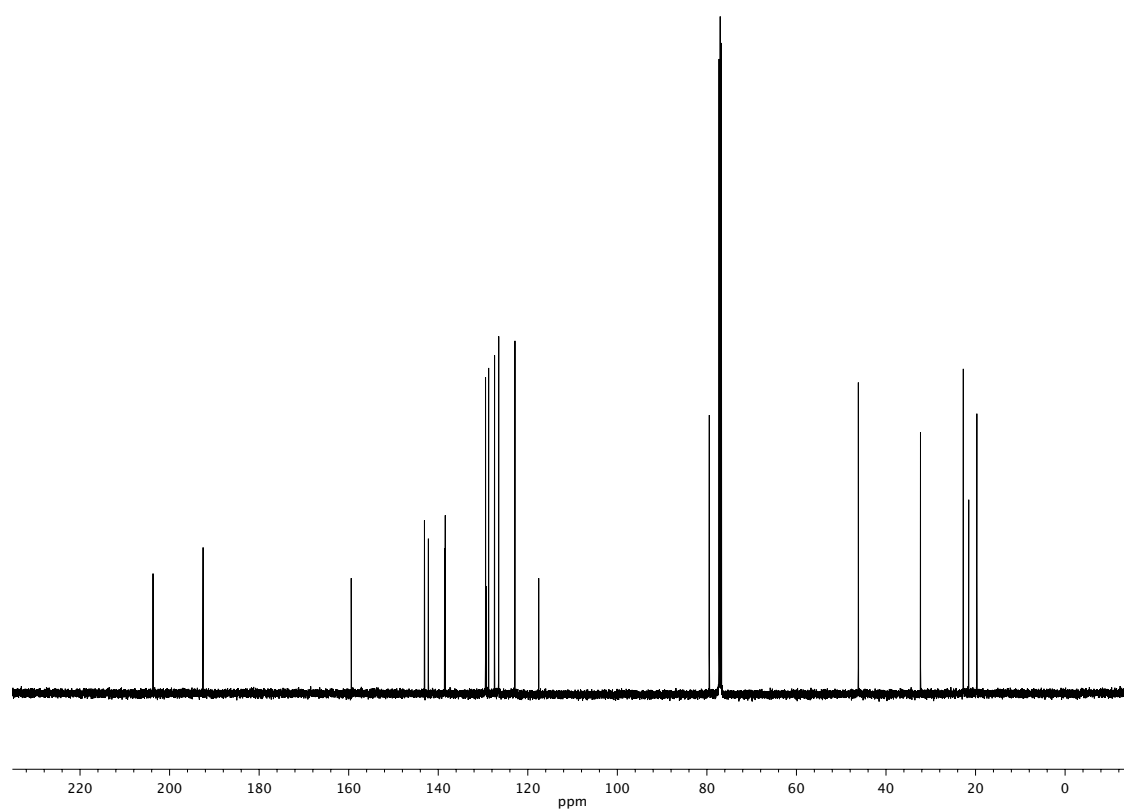
Figure A2.42 ^{13}C NMR (126 MHz, CDCl$_3$) of compound **189**
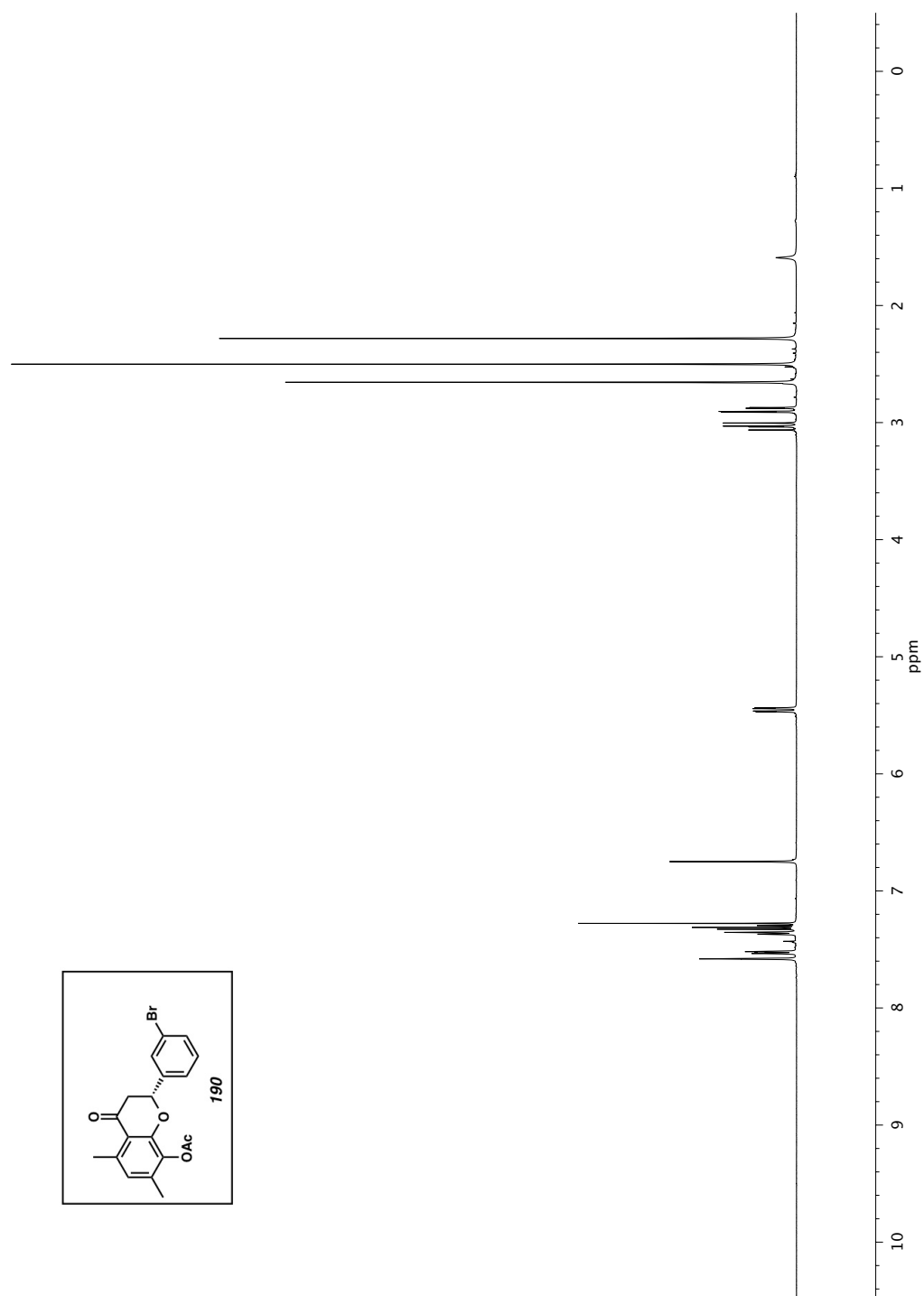
Figure A2.43 ^{1}H NMR (500 MHz, CDCl$_3$) of compound **190**
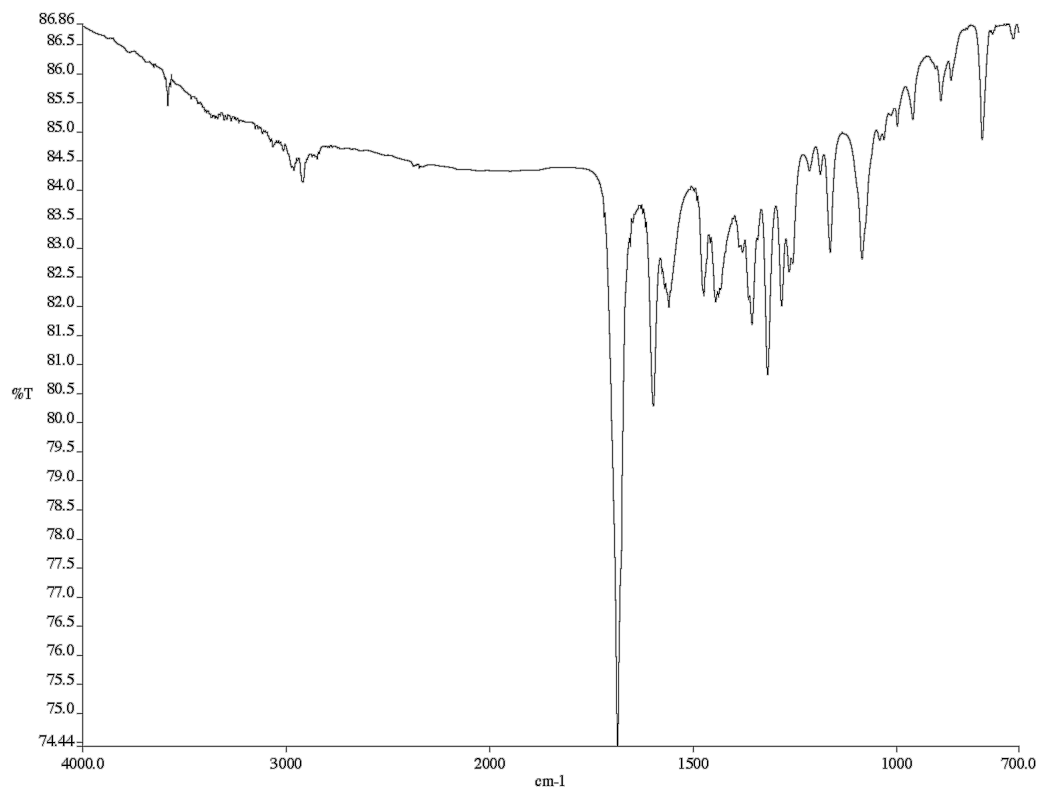
Figure A2.44 Infrared spectrum (Thin Film, NaCl) of compound **190**
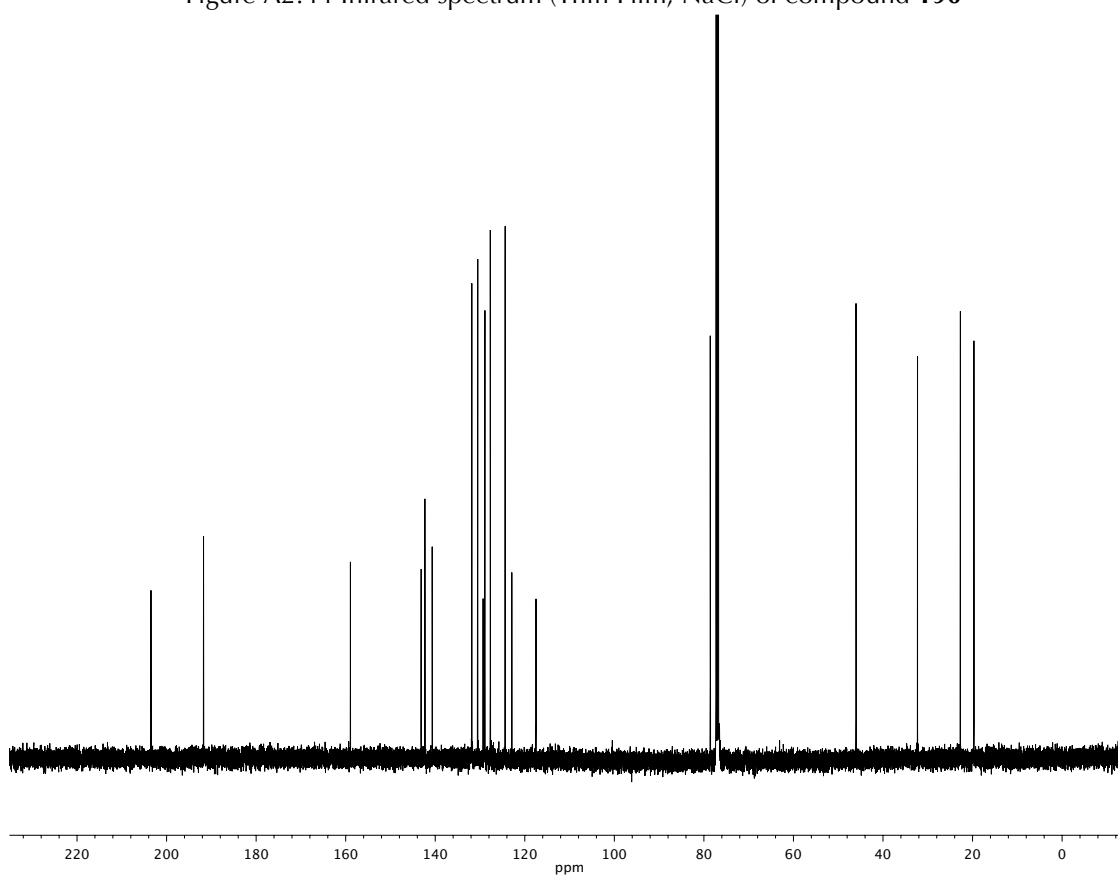
Figure A2.45 ^{13}C NMR (126 MHz, CDCl$_3$) of compound **190**
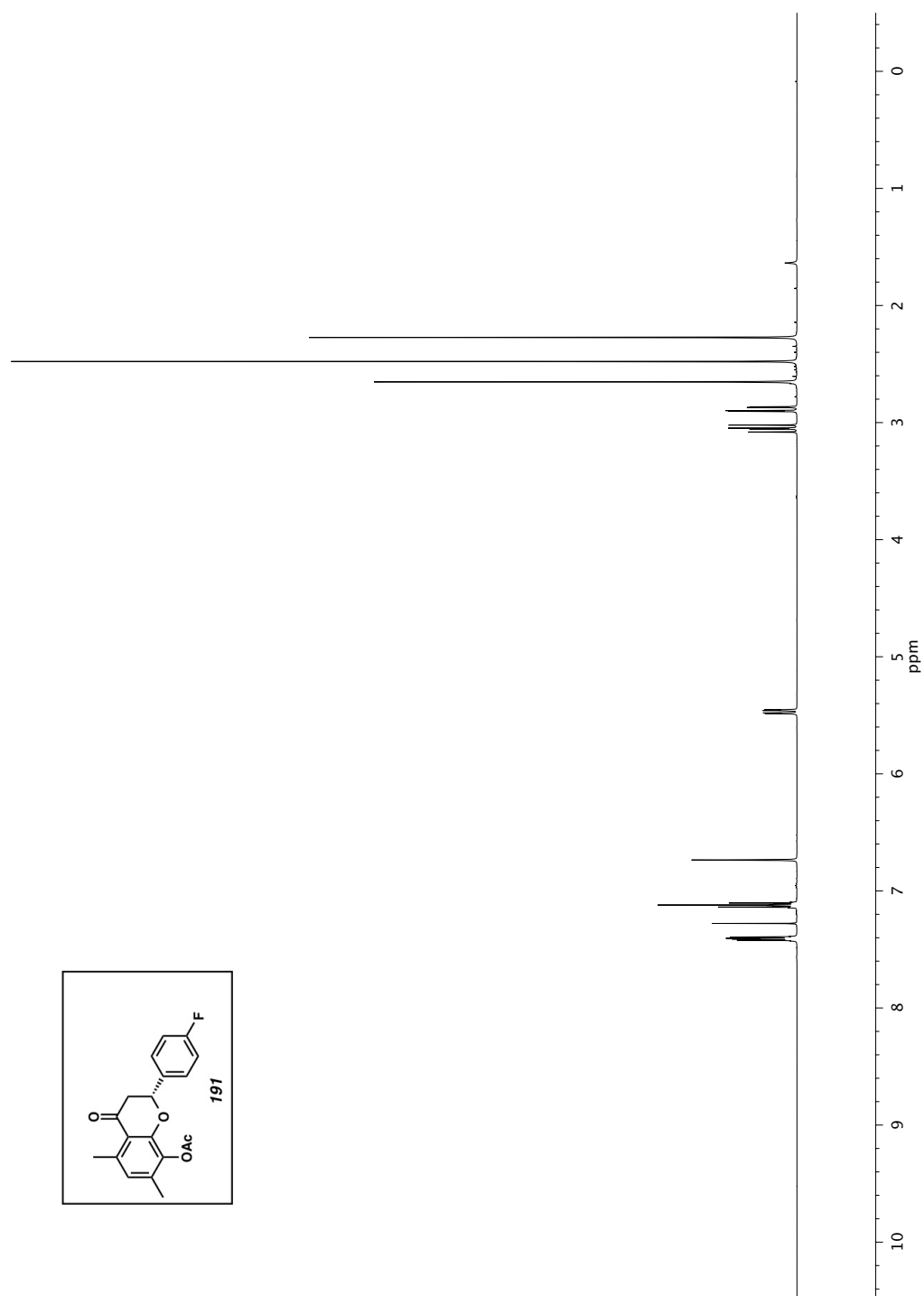
Figure A2.46 ^{1}H NMR (500 MHz, CDCl$_3$) of compound **191**
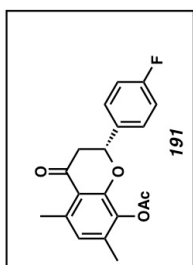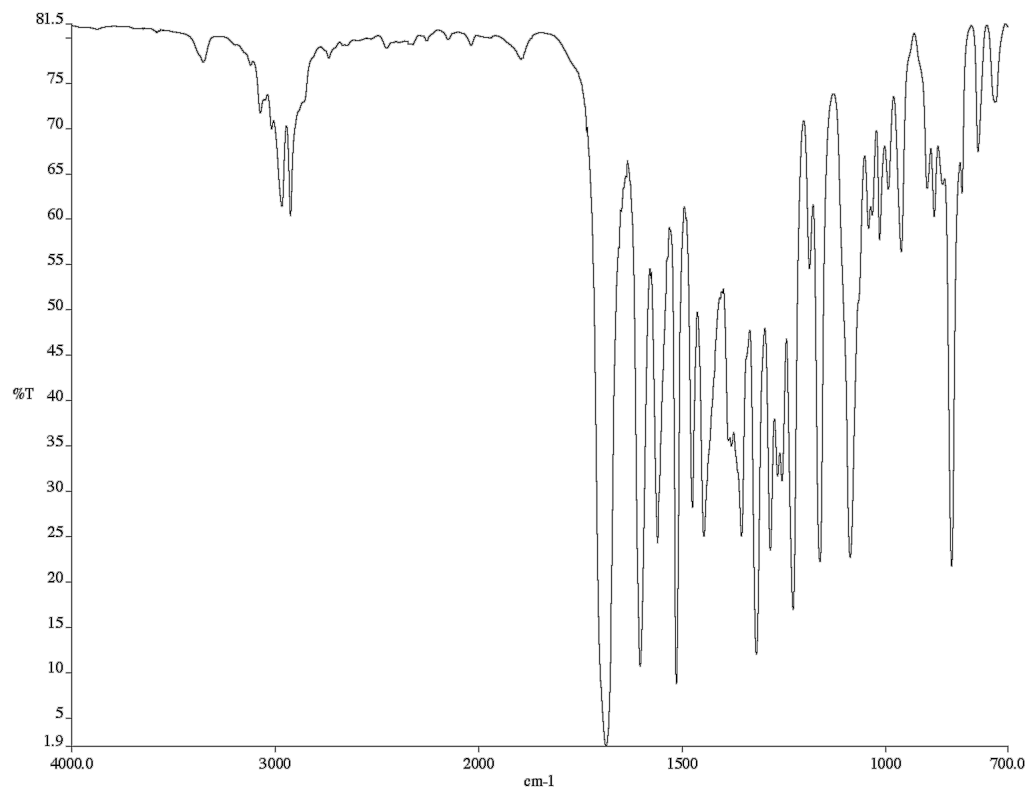
Figure A2.47 Infrared spectrum (Thin Film, NaCl) of compound **191**
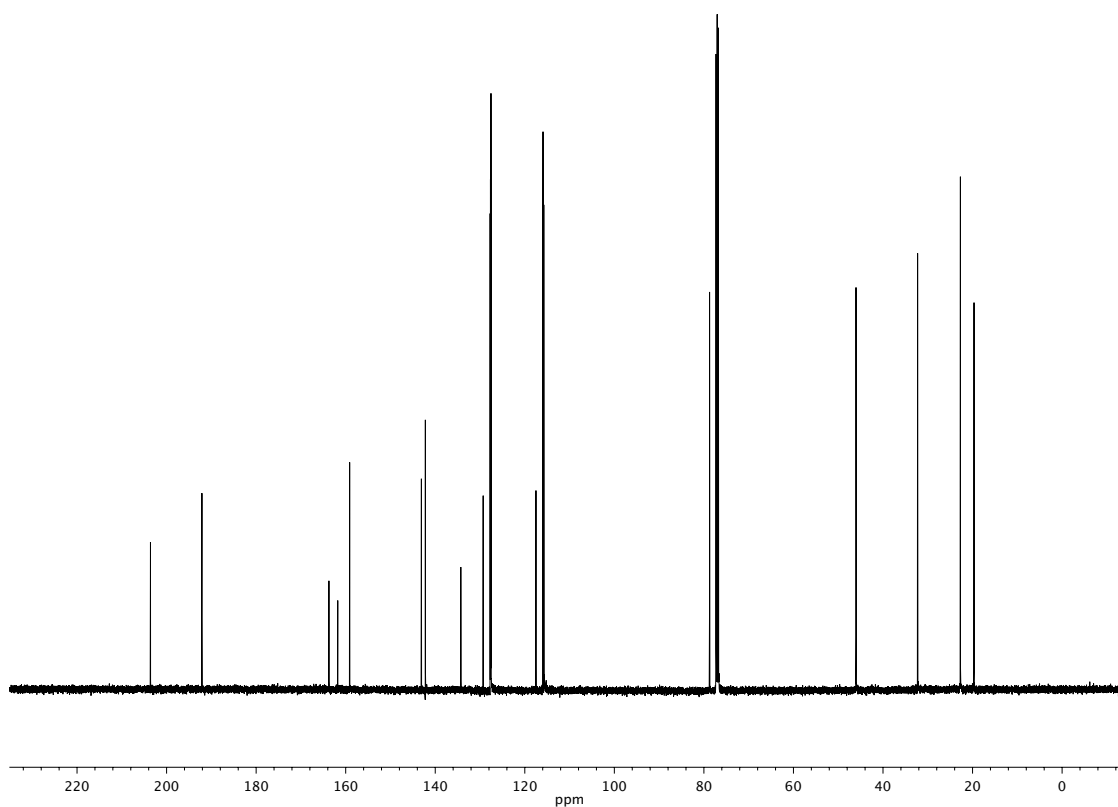
Figure A2.48 ^{13}C NMR (126 MHz, CDCl$_3$) of compound **191**

Figure A2.49 ^{1}H NMR (500 MHz, CDCl$_3$) of compound **192**
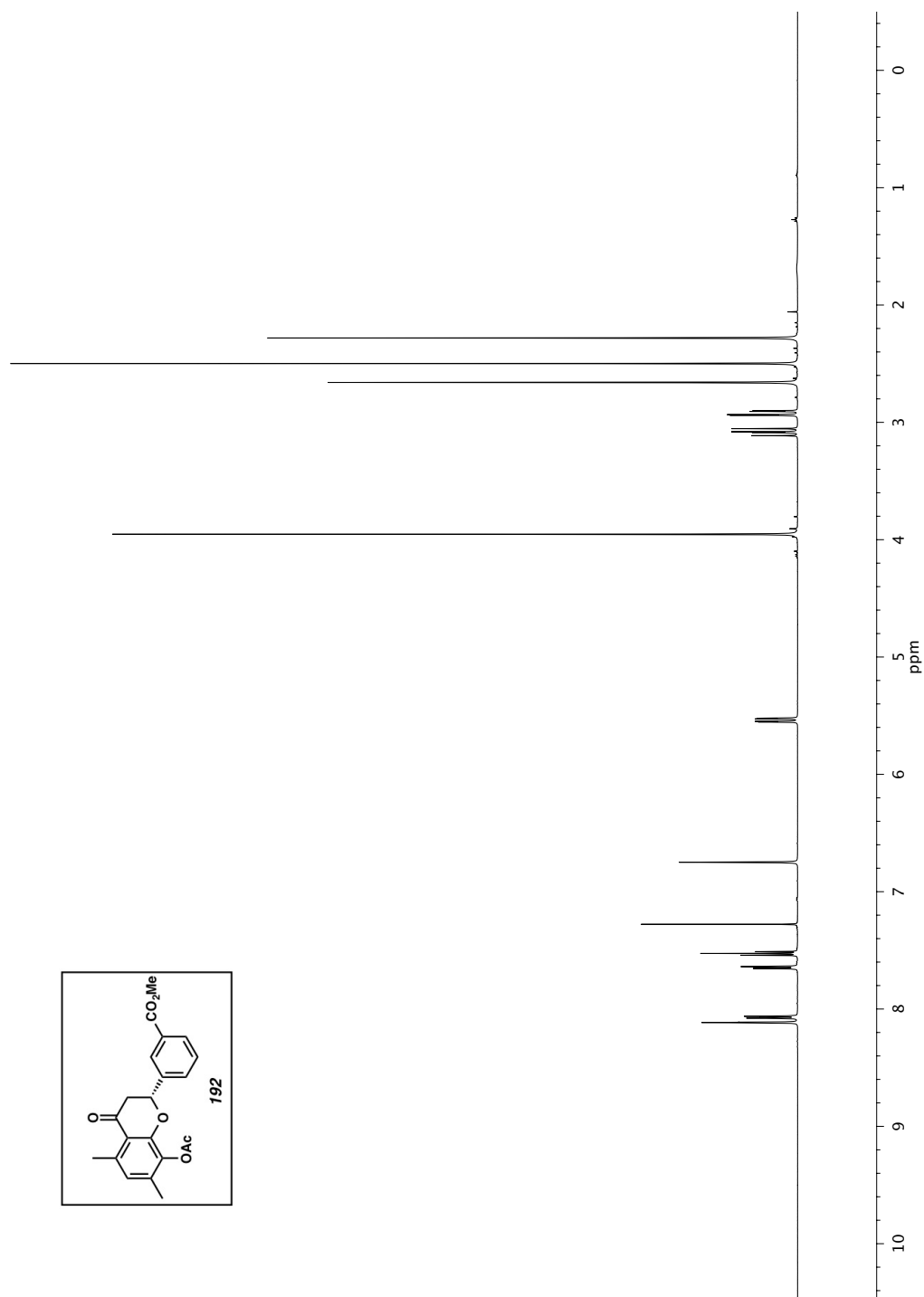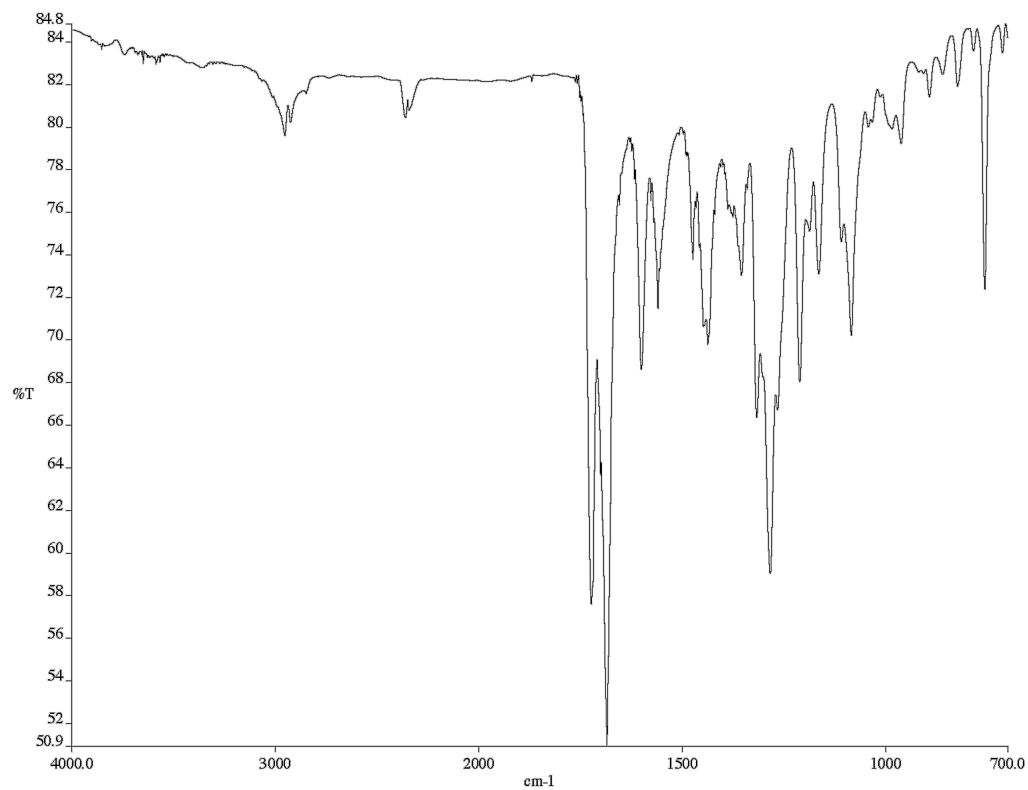
Figure A2.50 Infrared spectrum (Thin Film, NaCl) of compound **192**
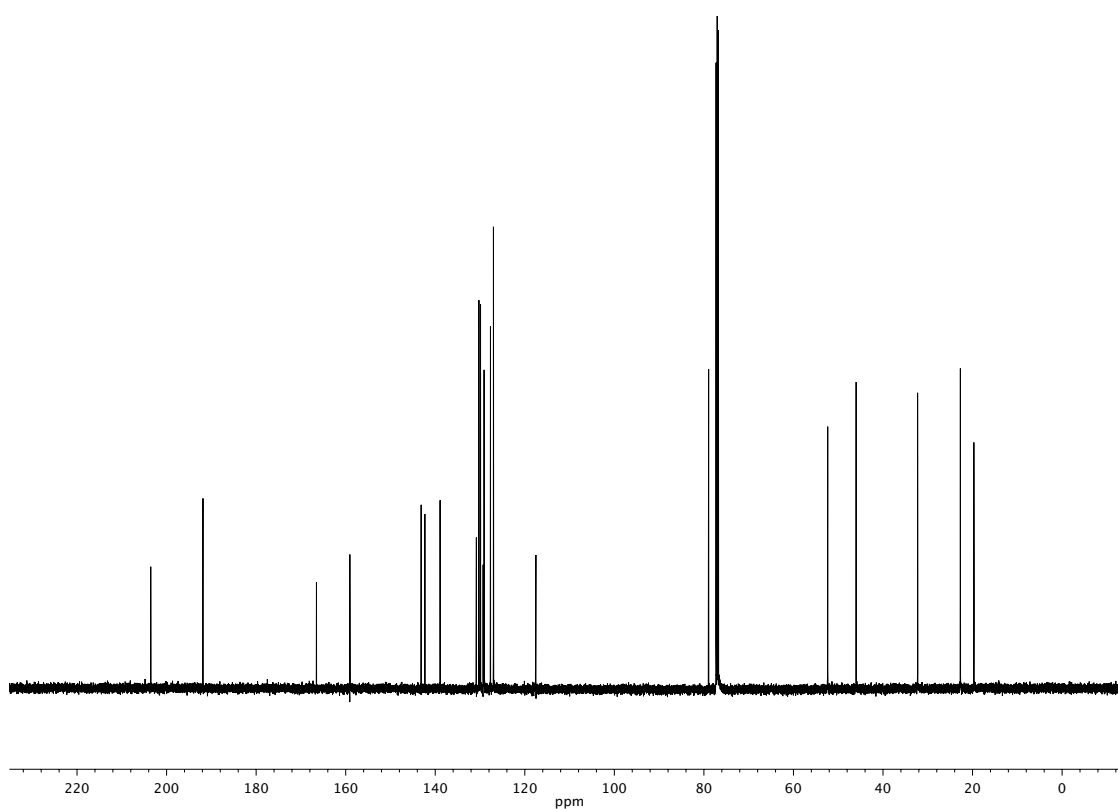
Figure A2.51 ¹³C NMR (126 MHz, CDCl₃) of compound **192**
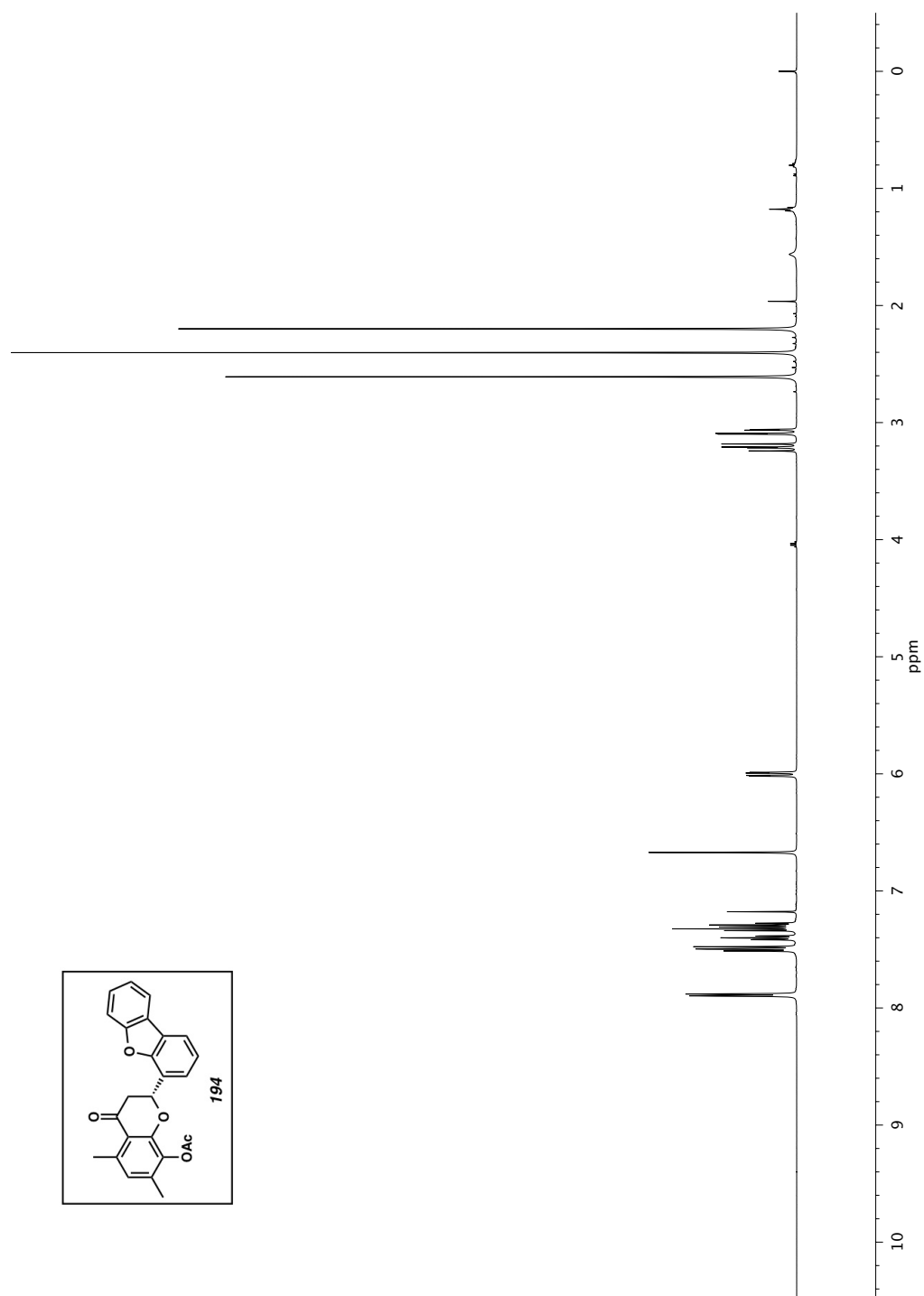
Figure A2.52 ^{1}H NMR (500 MHz, CDCl$_3$) of compound **194**
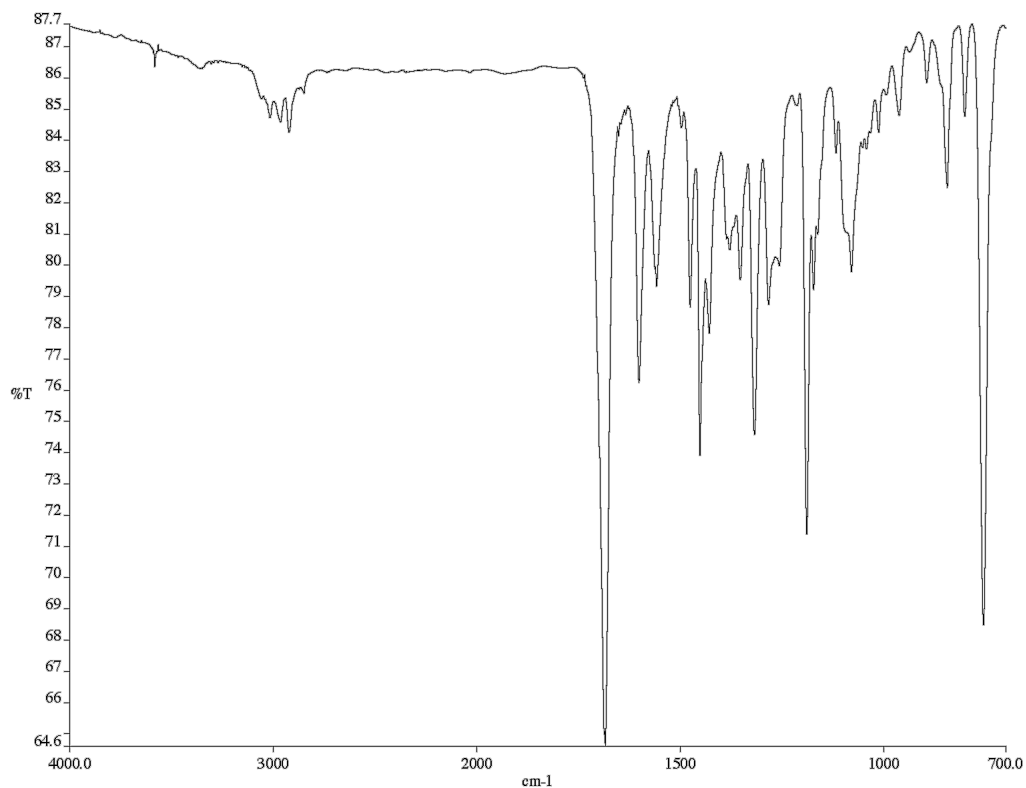
Figure A2.53 Infrared spectrum (Thin Film, NaCl) of compound **194**
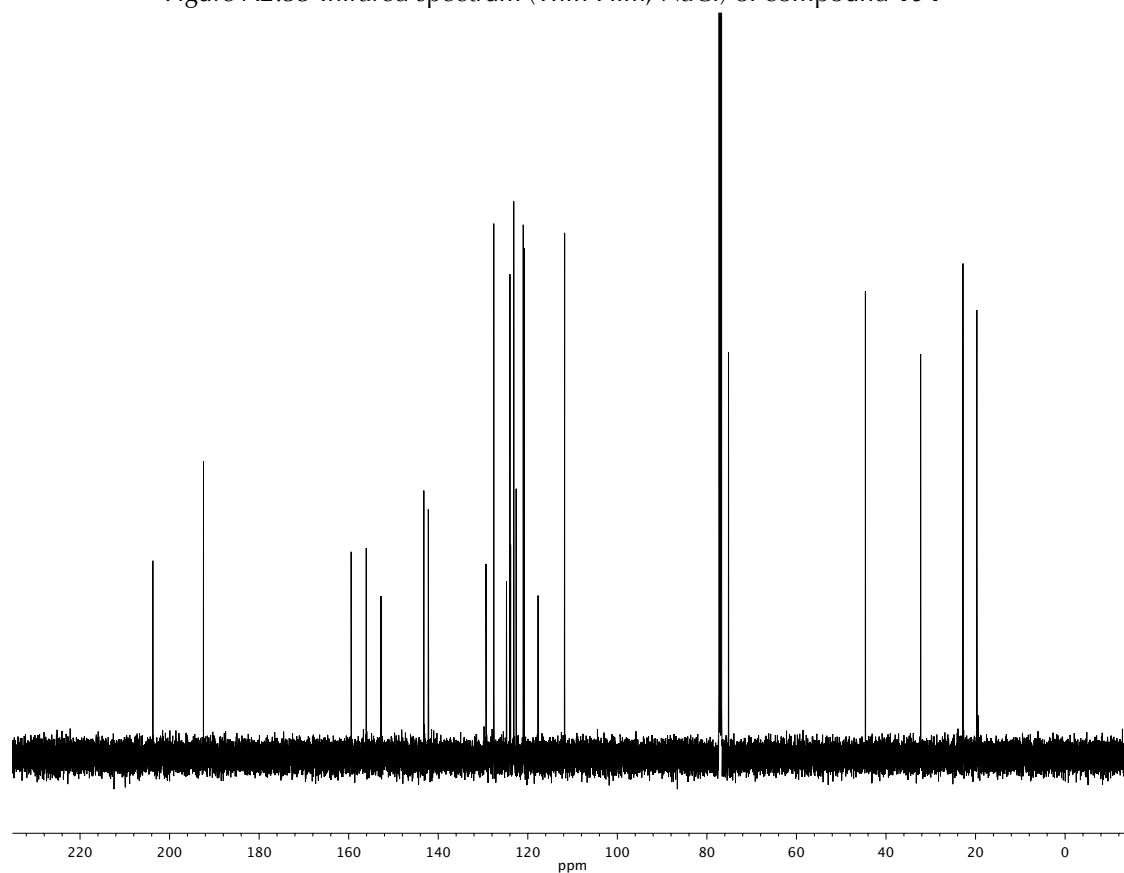
Figure A2.54 ^{13}C NMR (126 MHz, CDCl$_3$) of compound **194**
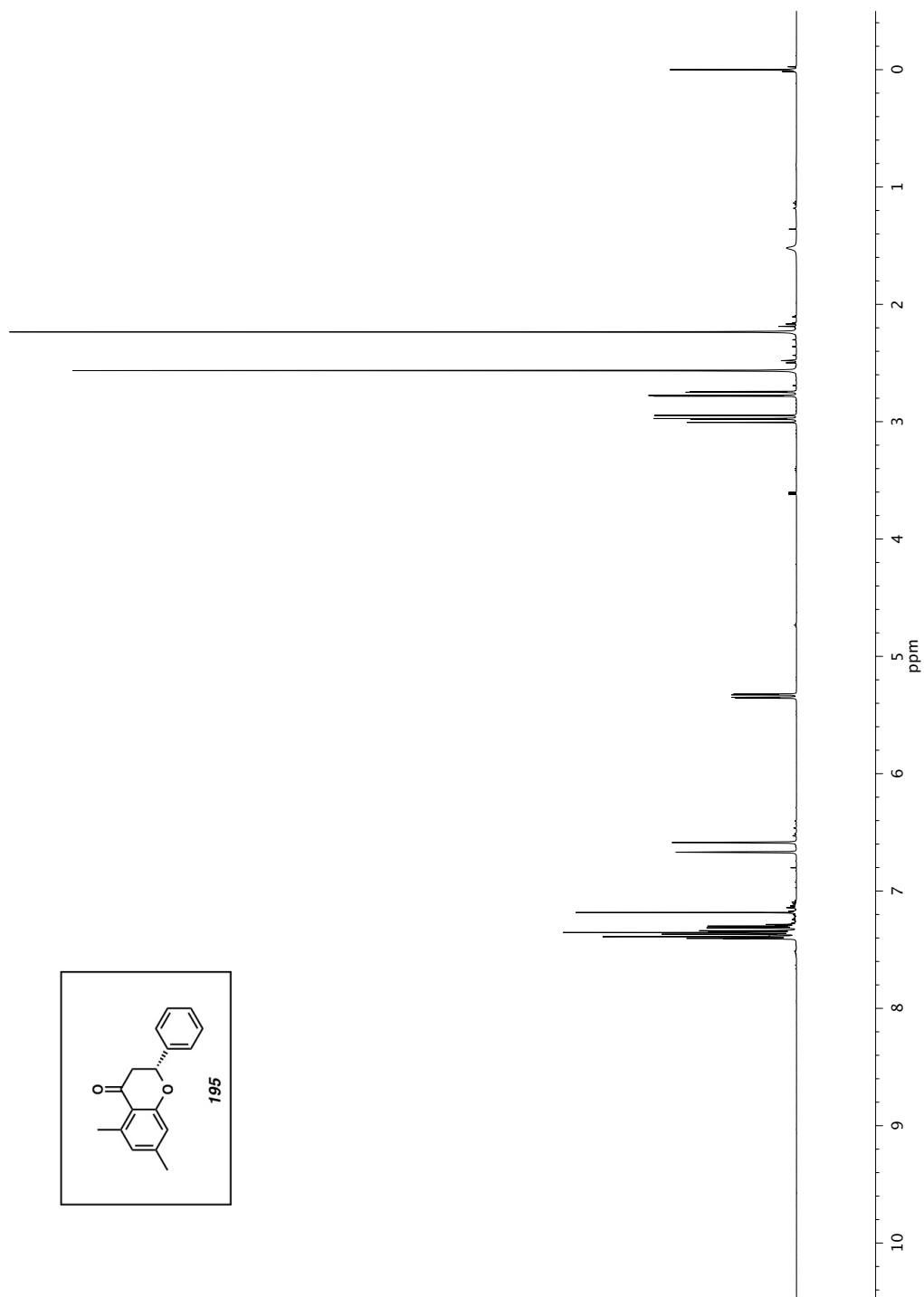
Figure A2.55 ^{1}H NMR (500 MHz, CDCl$_3$) of compound **195**
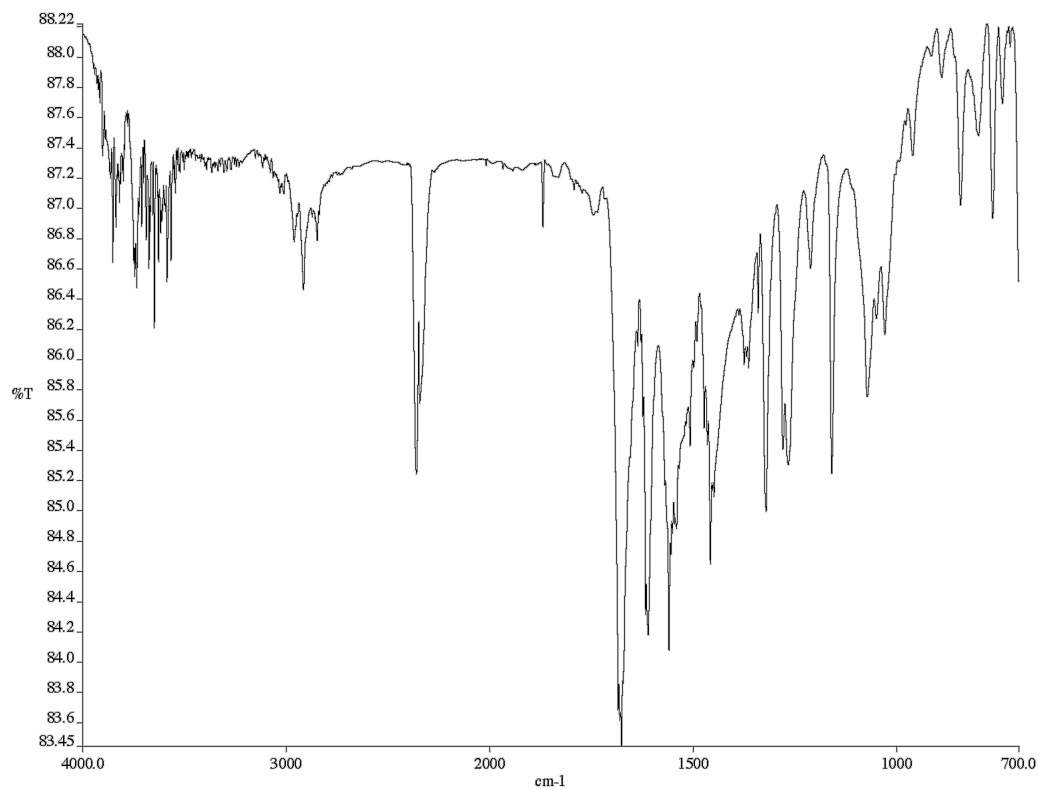
Figure A2.56 Infrared spectrum (Thin Film, NaCl) of compound **195**
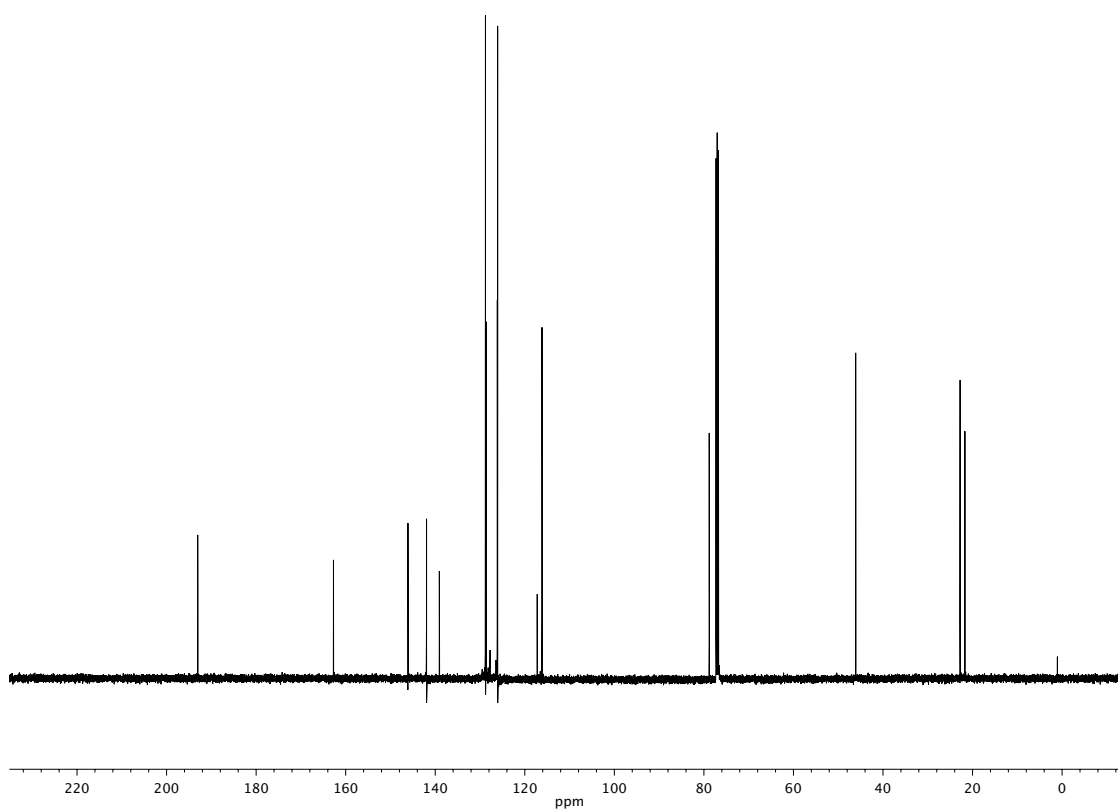
Figure A2.57 ^{13}C NMR (126 MHz, CDCl$_3$) of compound **195**
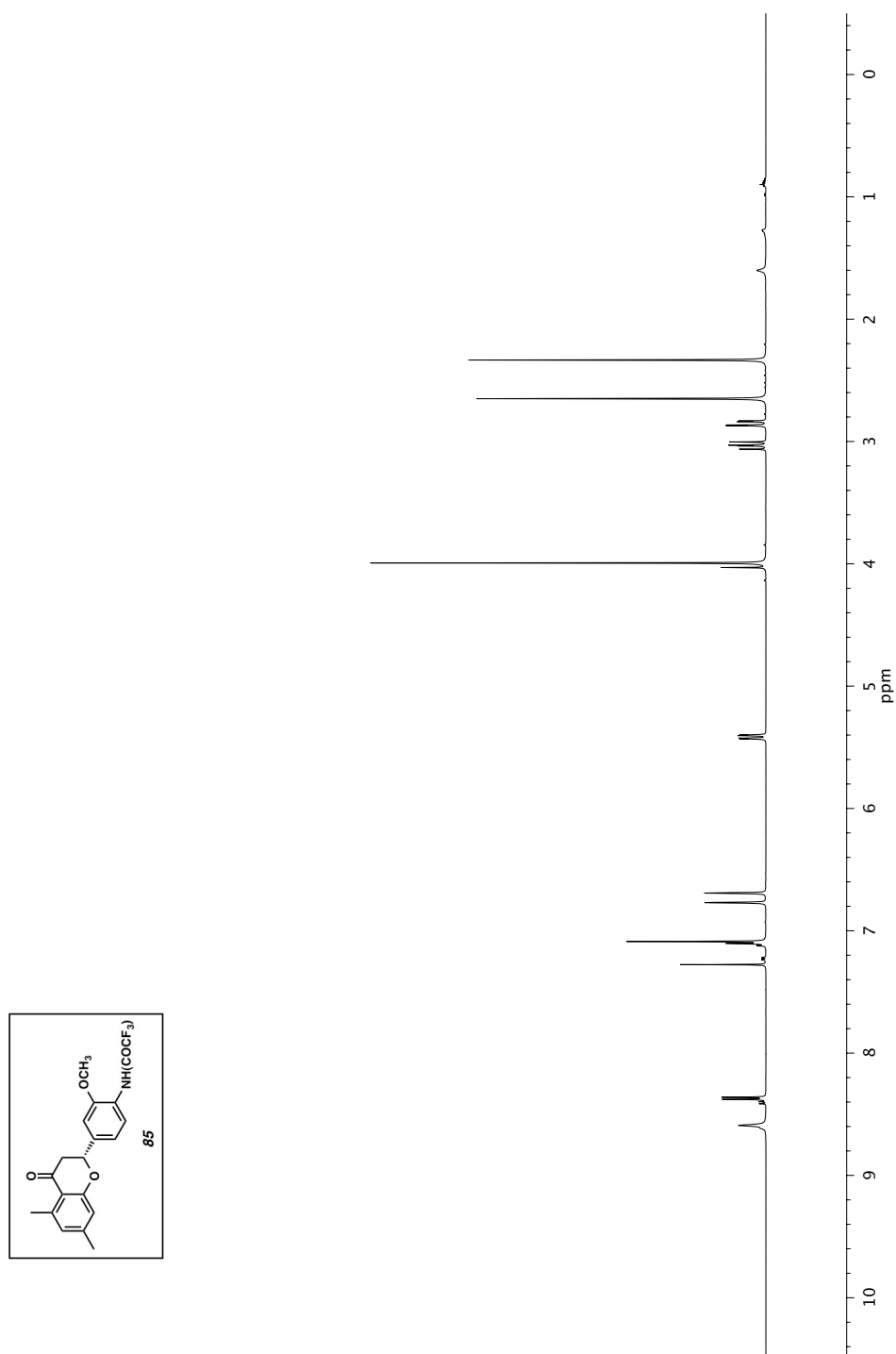
Figure A2.58 ^{1}H NMR (500 MHz, CDCl$_3$) of compound **85**
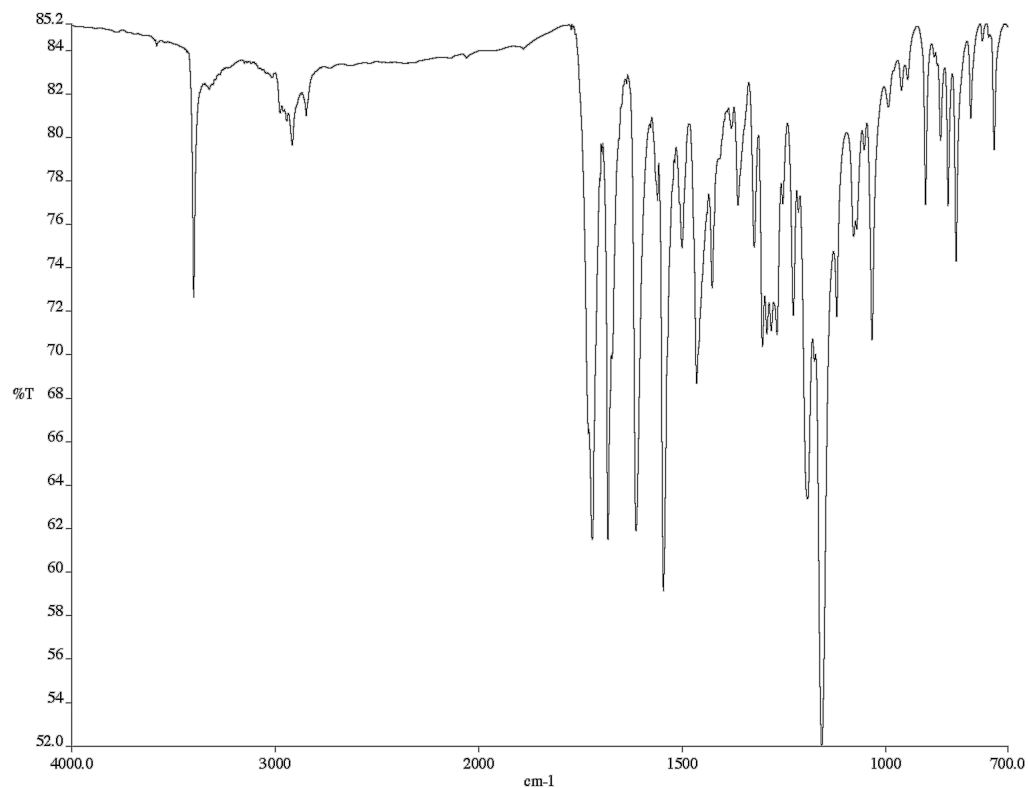
Figure A2.59 Infrared spectrum (Thin Film, NaCl) of compound **85**
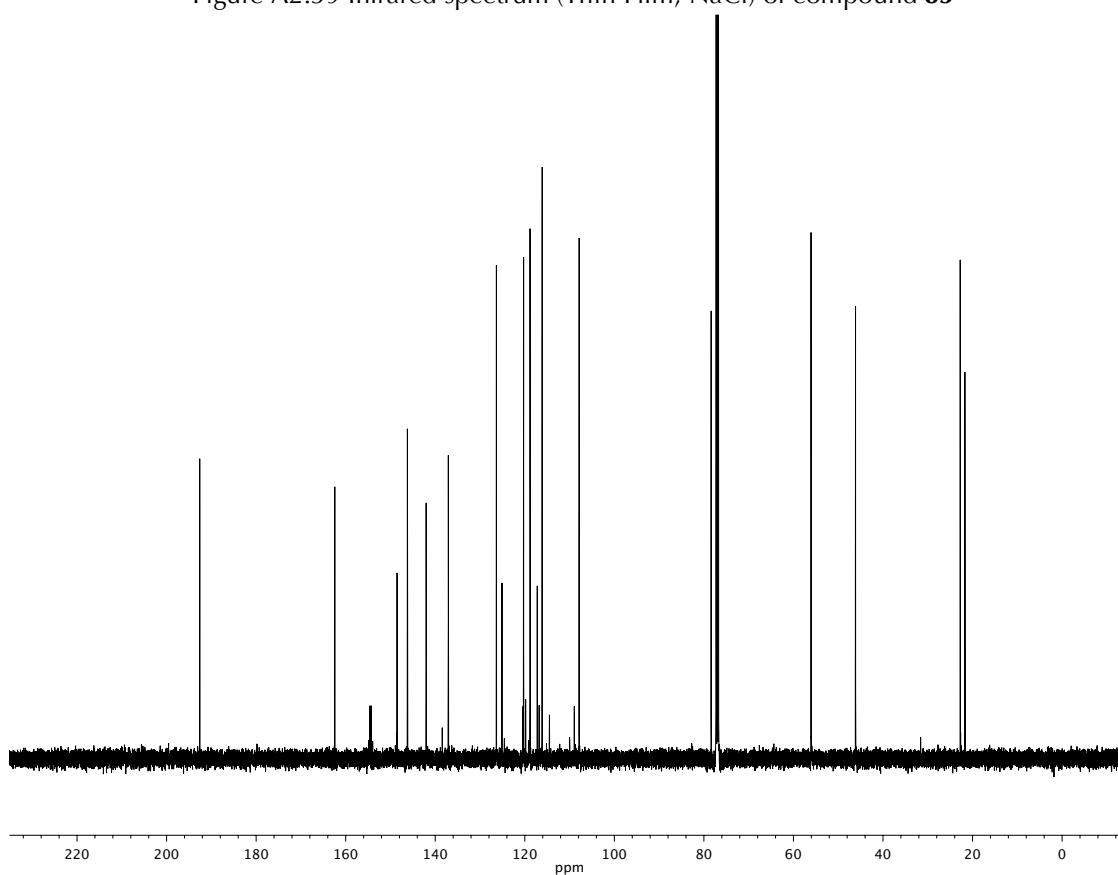
Figure A2.60 ^{13}C NMR (126 MHz, CDCl$_3$) of compound **85**
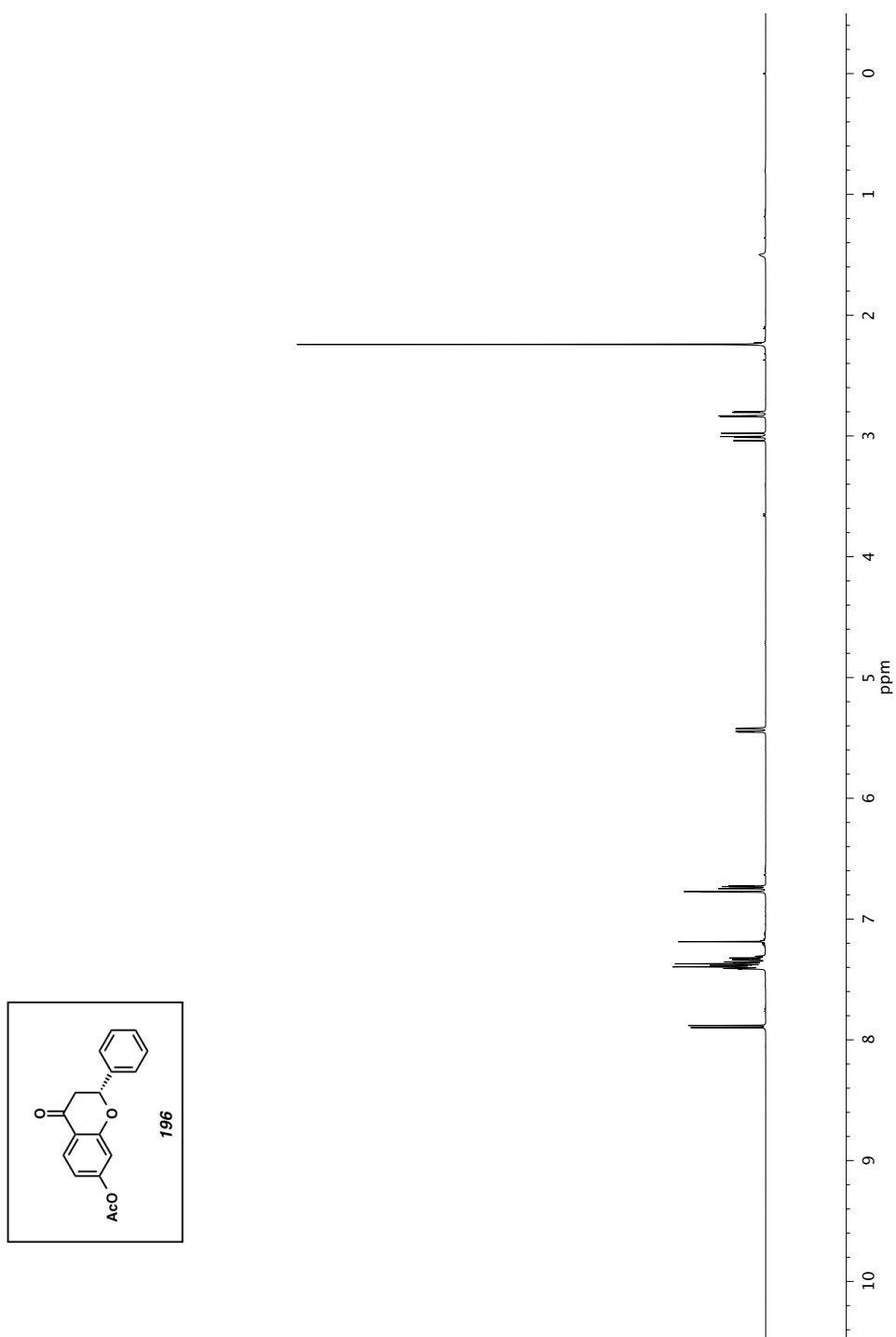
Figure A2.61 ^{1}H NMR (500 MHz, CDCl$_3$) of compound **196**
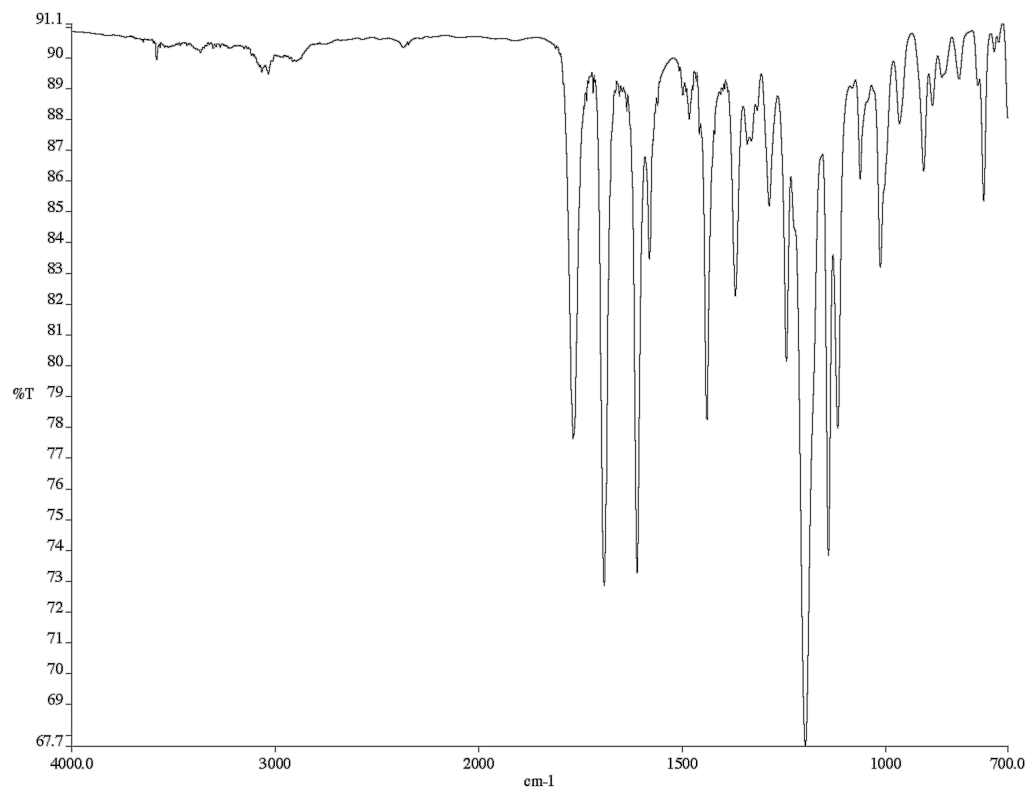
Figure A2.62 Infrared spectrum (Thin Film, NaCl) of compound **196**
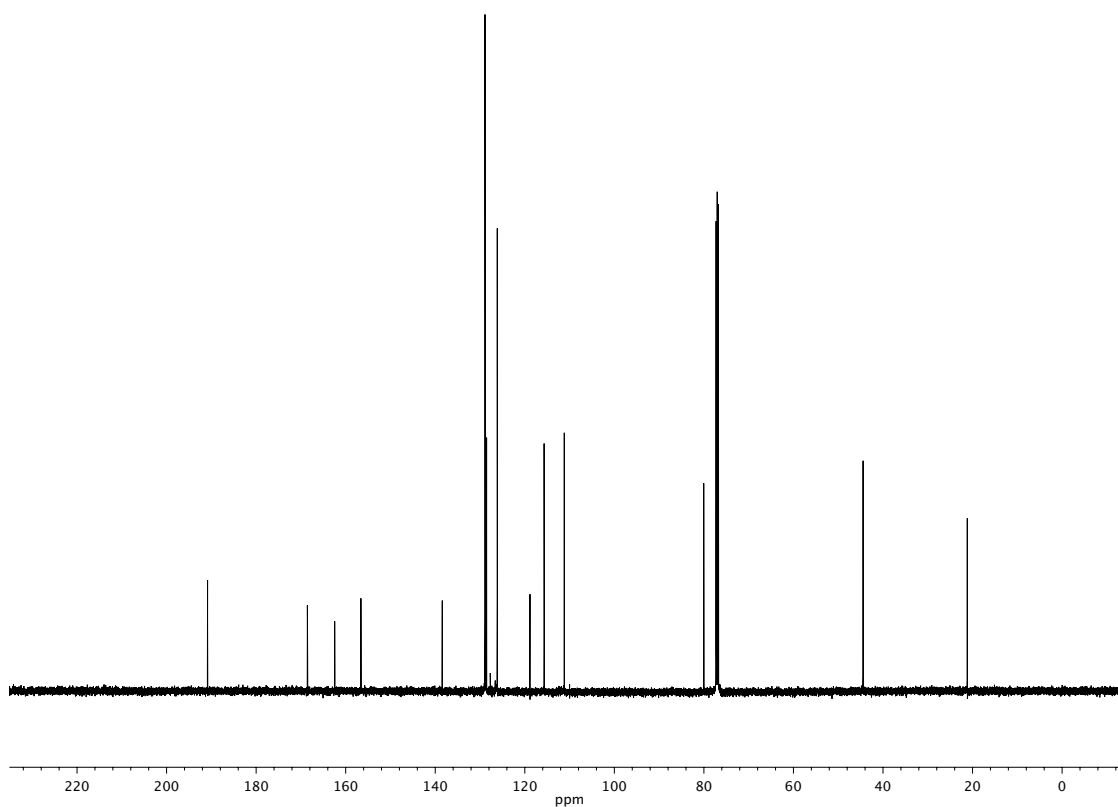
Figure A2.63 ^{13}C NMR (126 MHz, CDCl$_3$) of compound **196**
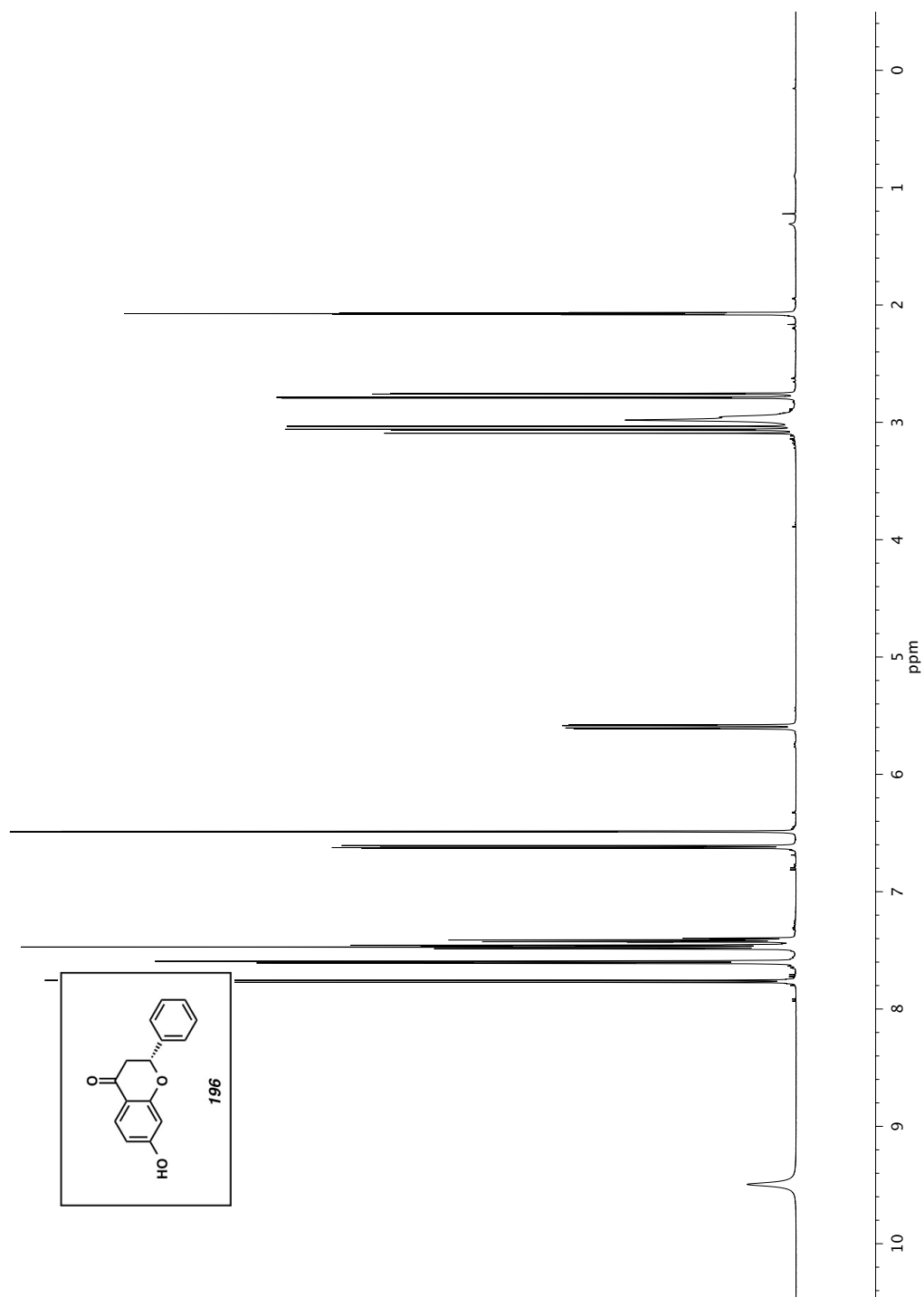
Figure A2.64 ^{1}H NMR (500 MHz, CDCl$_3$) of compound **196**
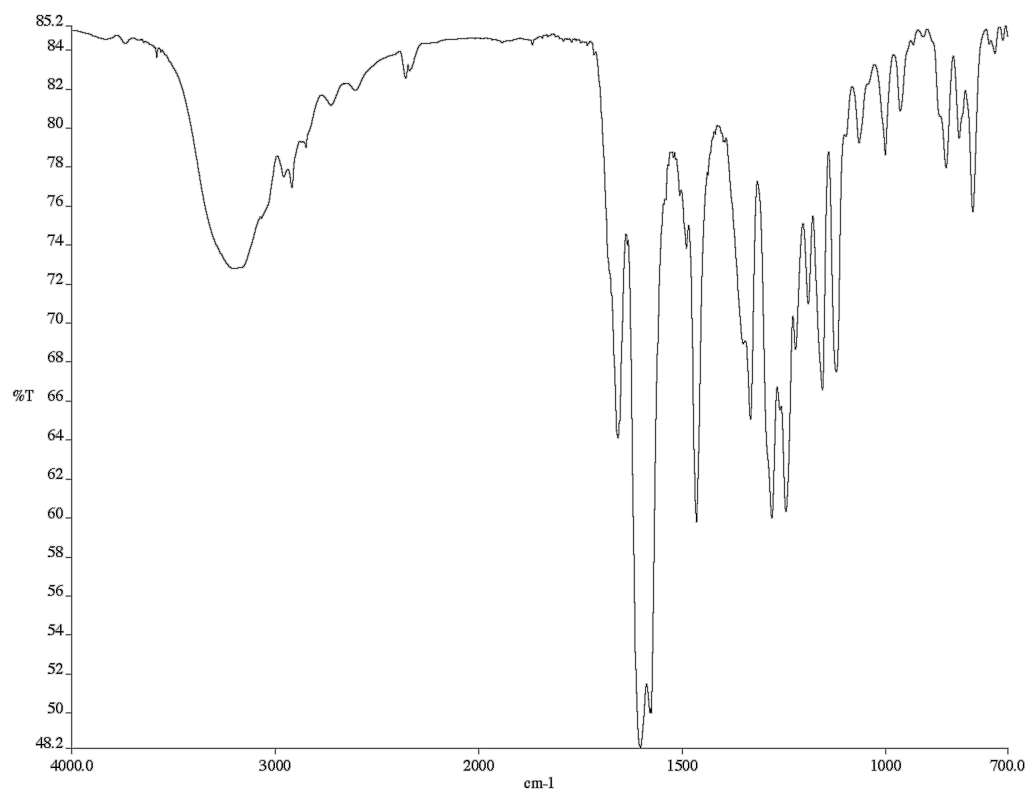
Figure A2.65 Infrared spectrum (Thin Film, NaCl) of compound **196**
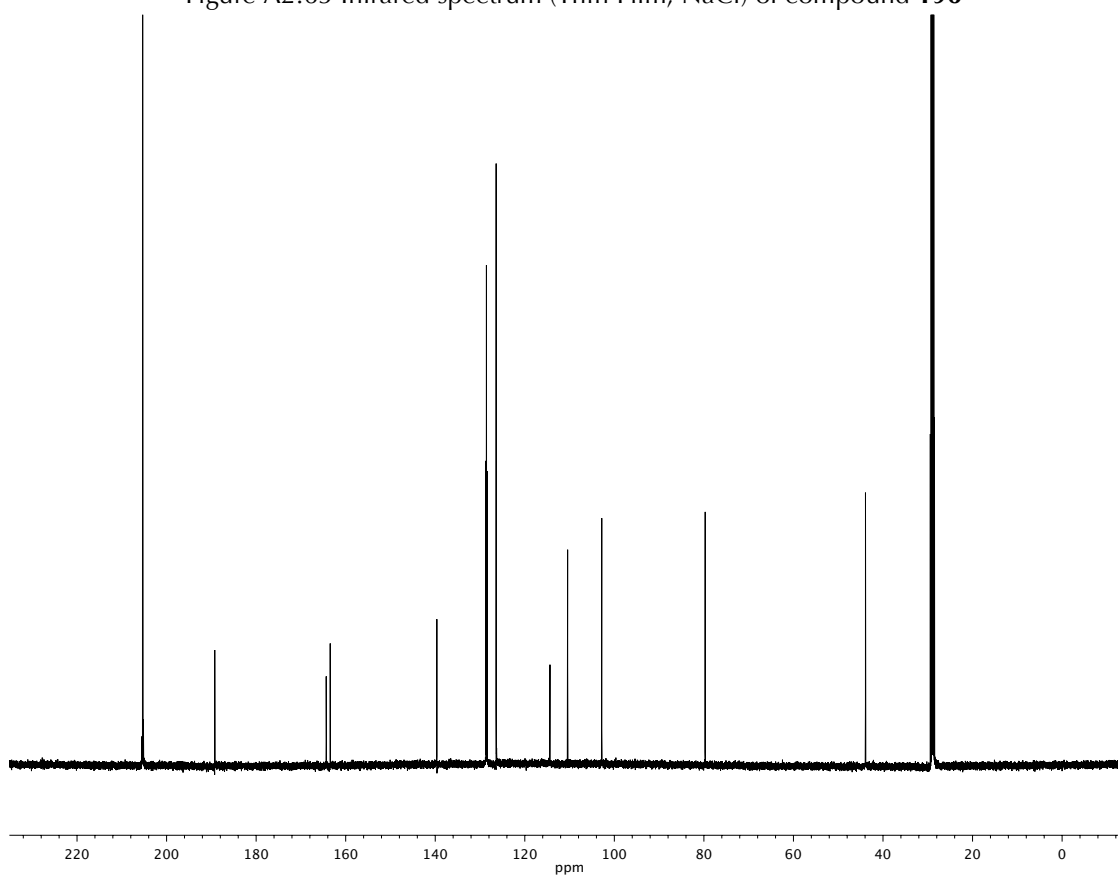
Figure A2.66 ^{13}C NMR (126 MHz, CDCl$_3$) of compound **196**
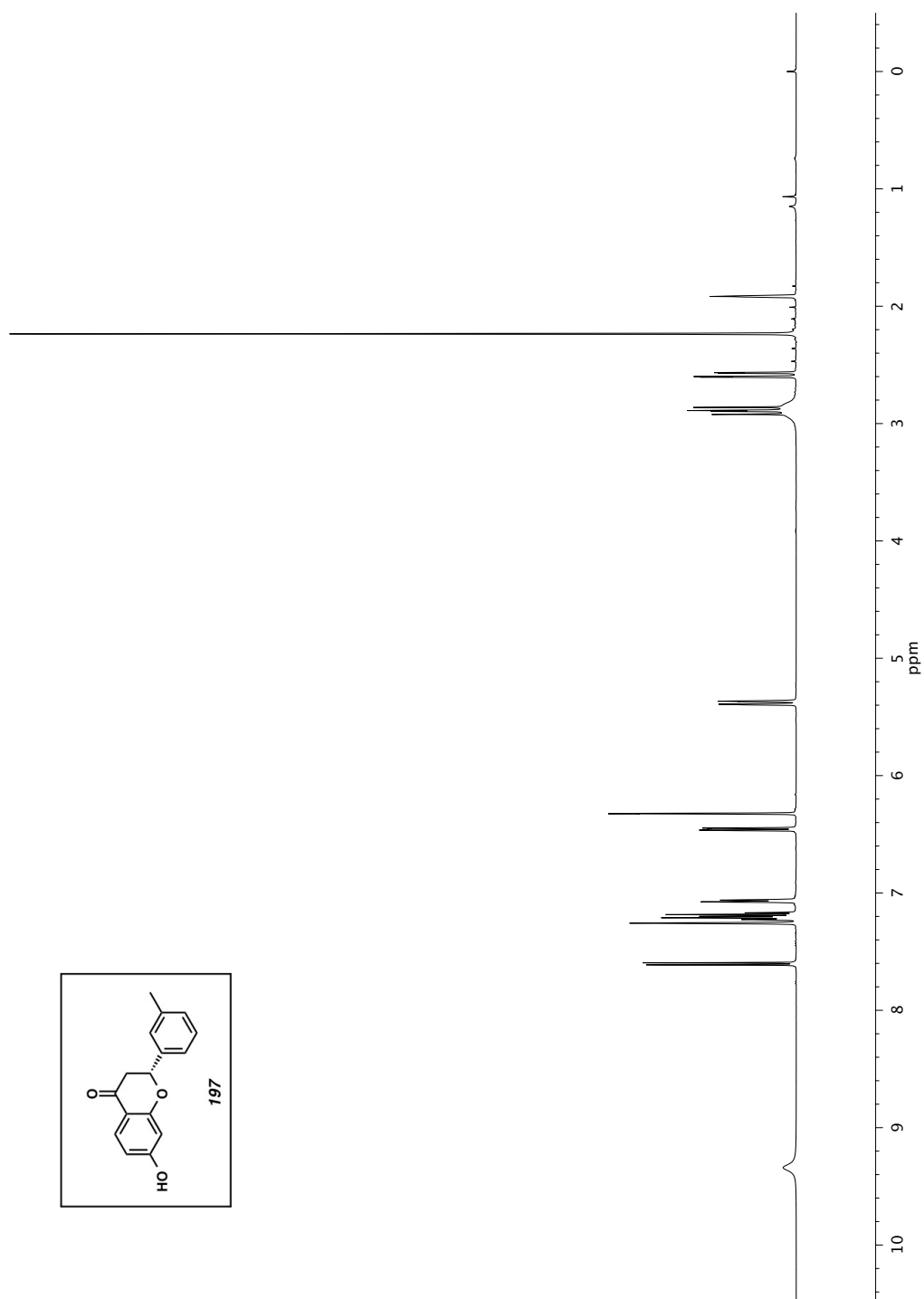
Figure A2.67 ^{1}H NMR (500 MHz, CDCl$_3$) of compound **197**
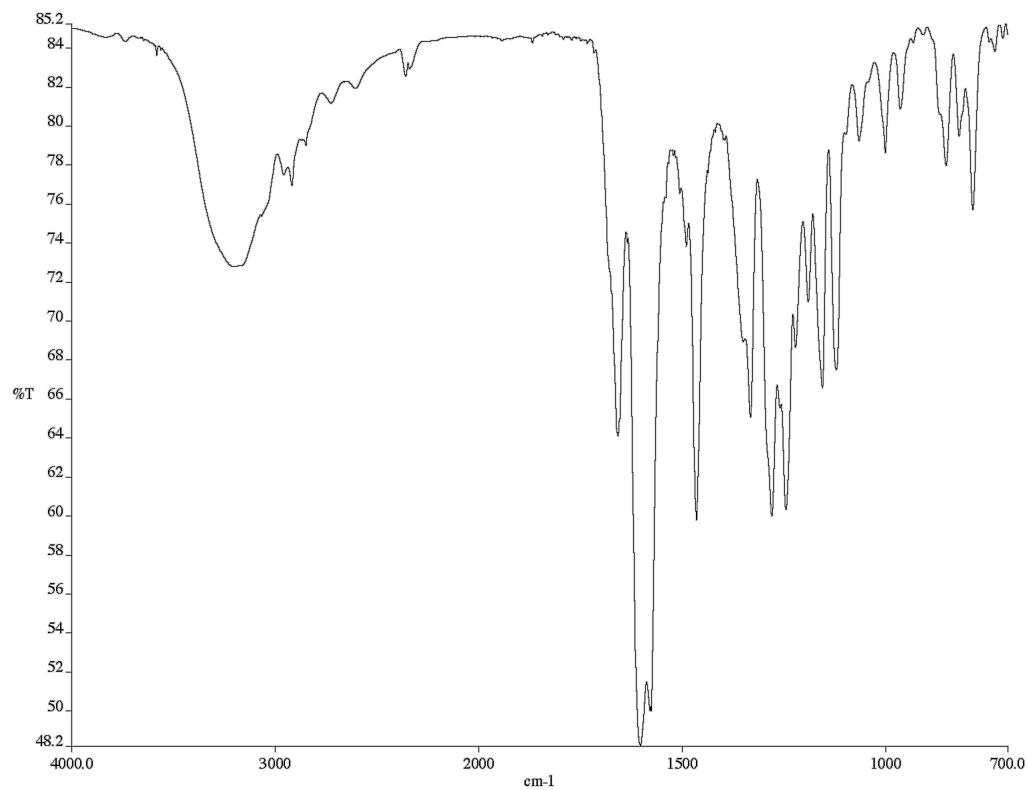
Figure A2.68 Infrared spectrum (Thin Film, NaCl) of compound **197**
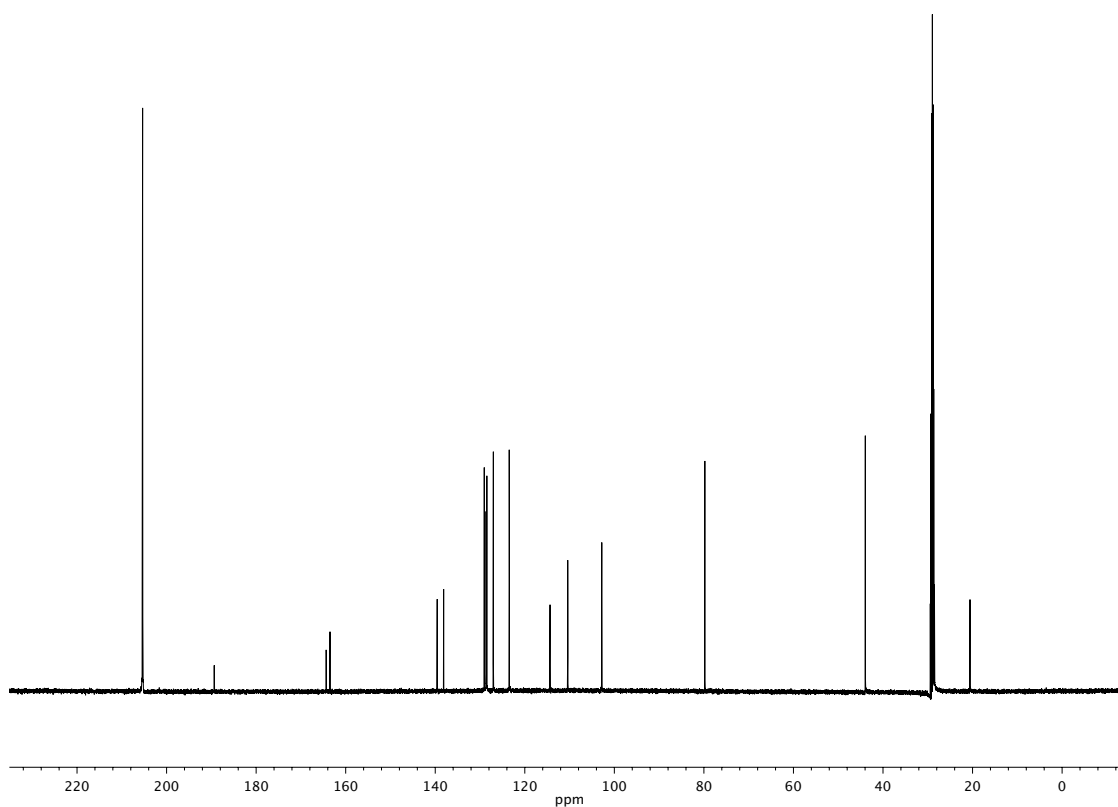
Figure A2.67 ^{13}C NMR (126 MHz, CDCl$_3$) of compound **197**
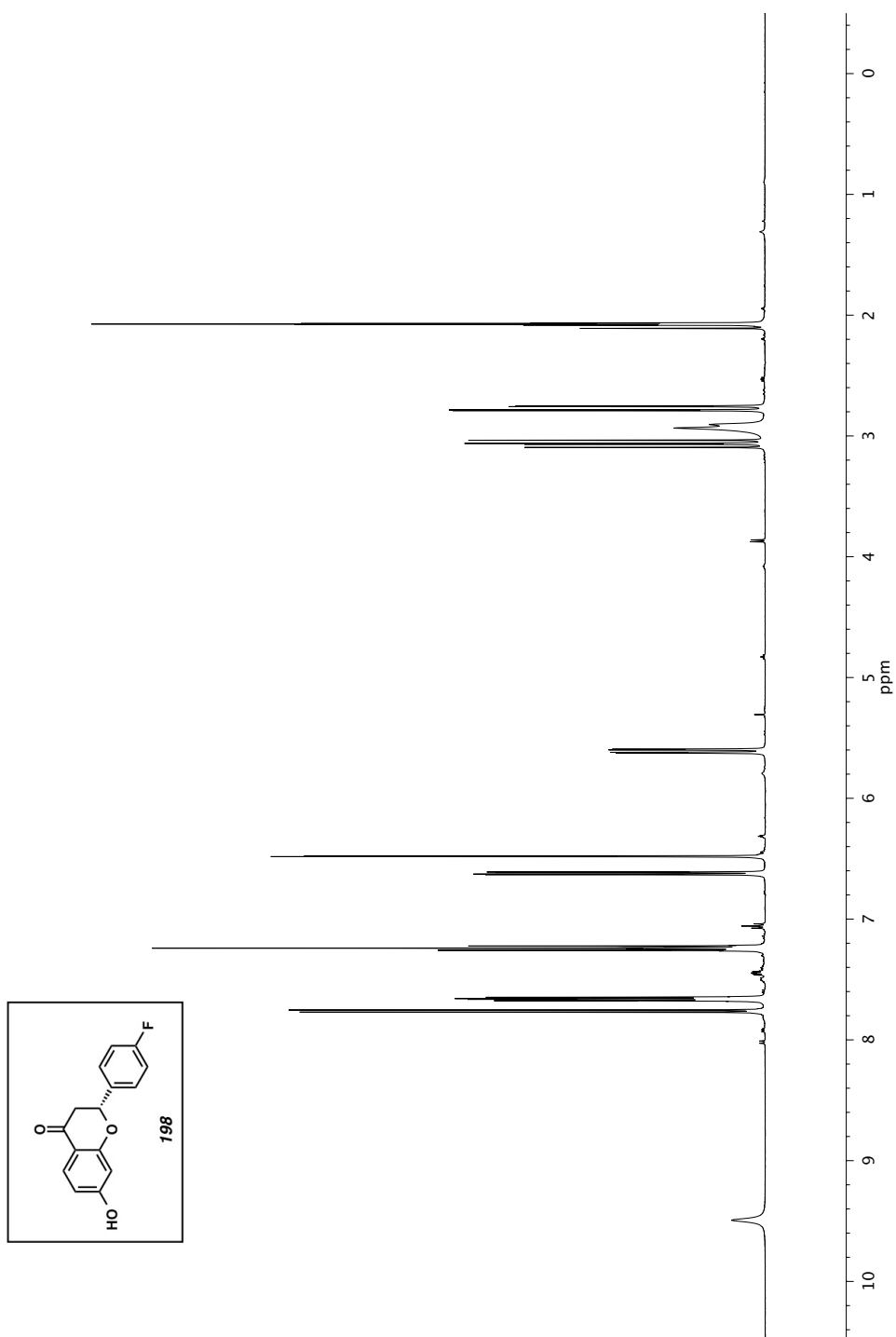
Figure A2.70 ^{1}H NMR (500 MHz, CDCl$_3$) of compound **198**
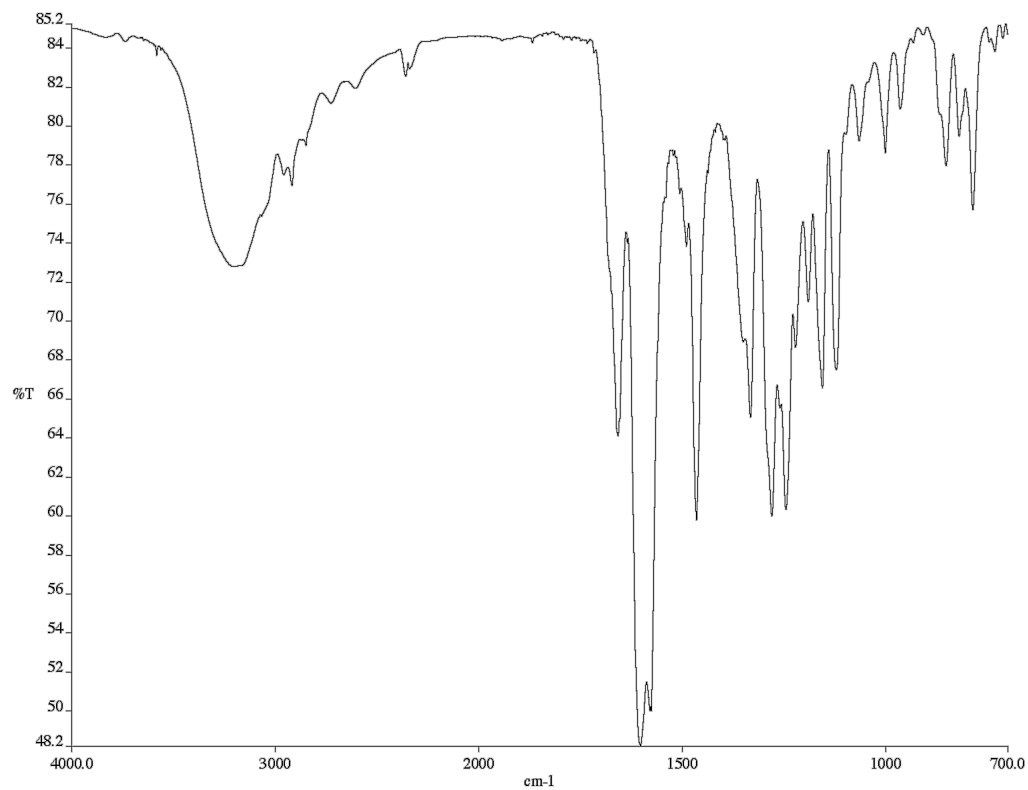
Figure A2.71 Infrared spectrum (Thin Film, NaCl) of compound **198**
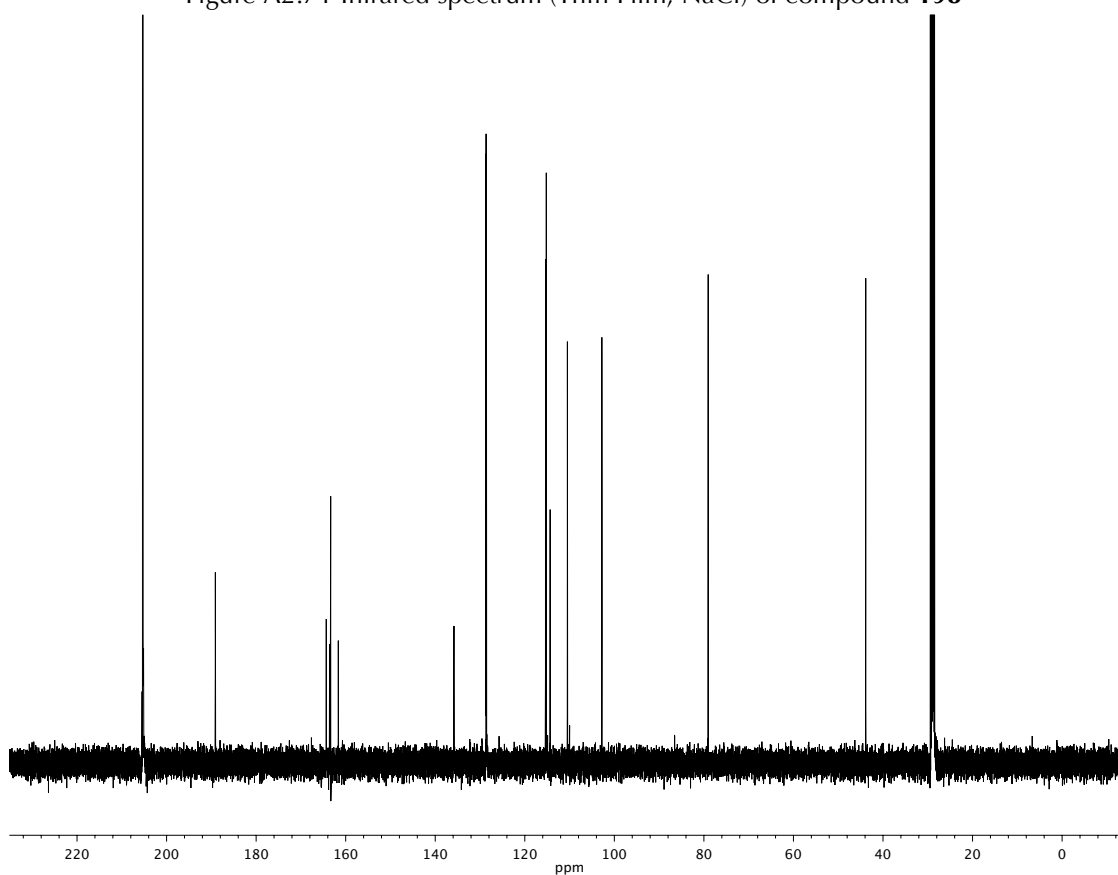
Figure A2.72 ^{13}C NMR (126 MHz, CDCl$_3$) of compound **198**
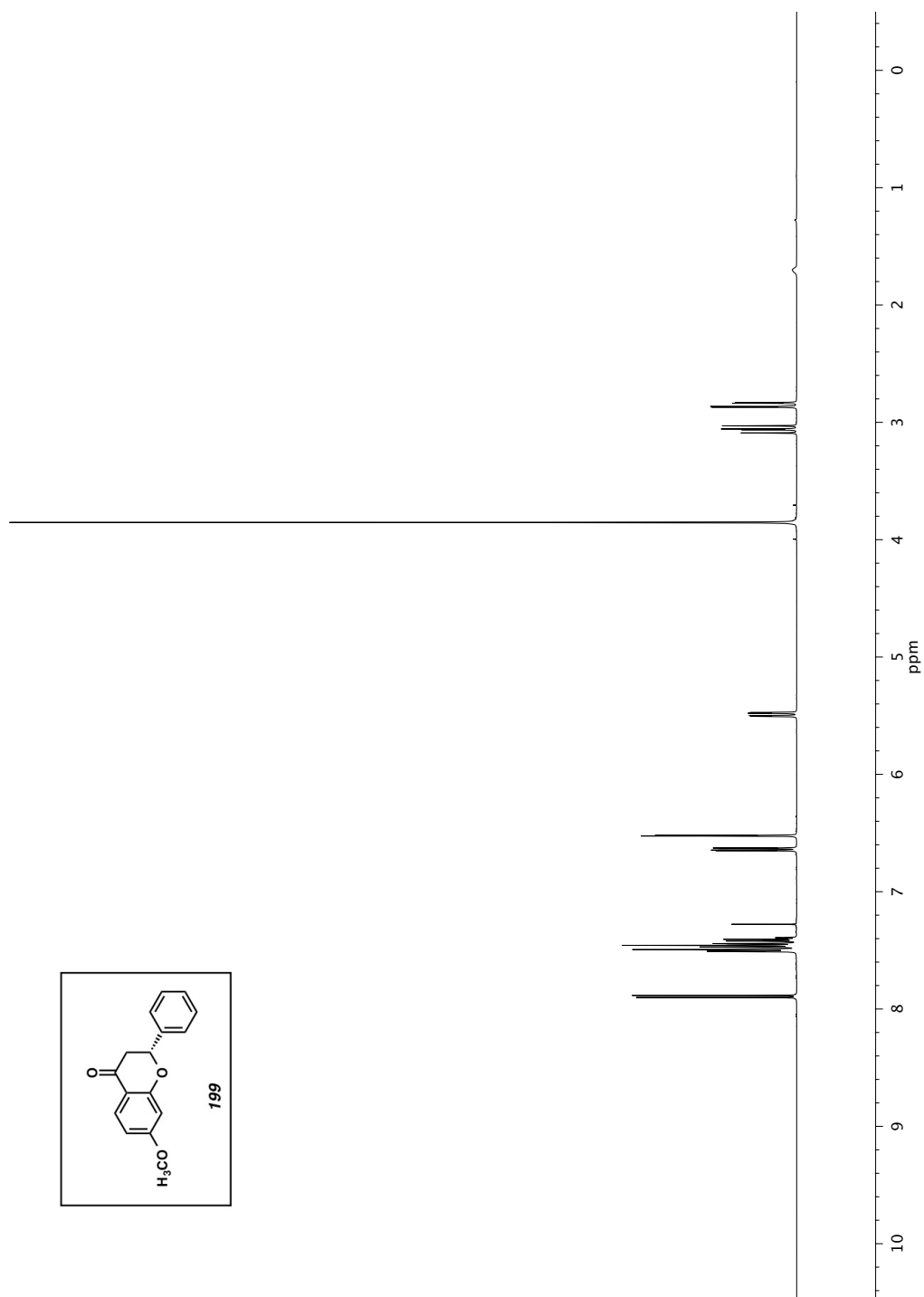
Figure A2.73 ^{1}H NMR (500 MHz, CDCl$_3$) of compound **199**
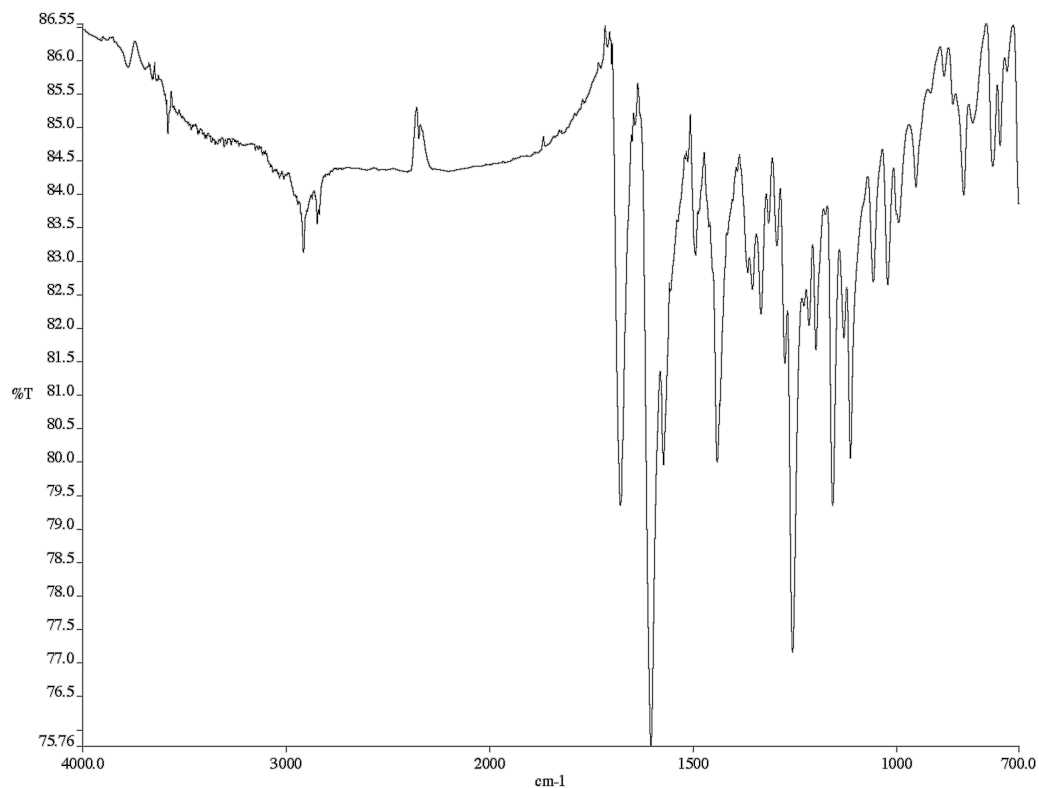
Figure A2.74 Infrared spectrum (Thin Film, NaCl) of compound **199**
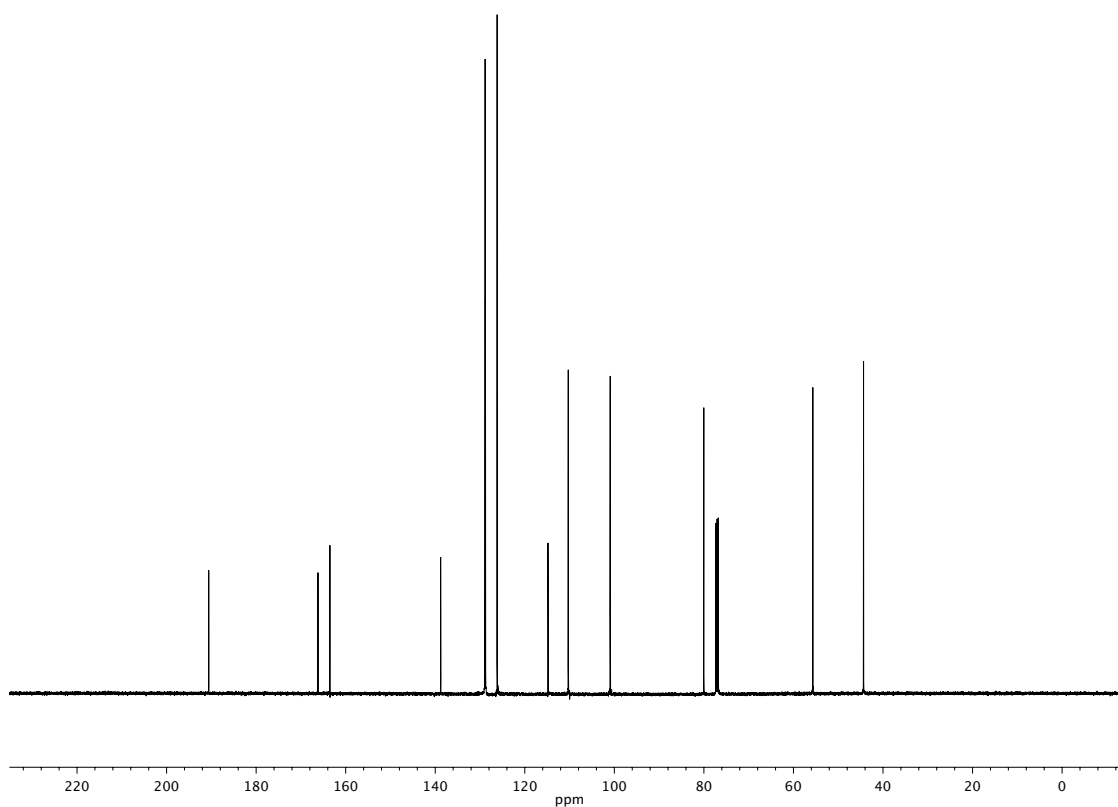
Figure A2.75 ^{13}C NMR (126 MHz, CDCl$_3$) of compound **199**
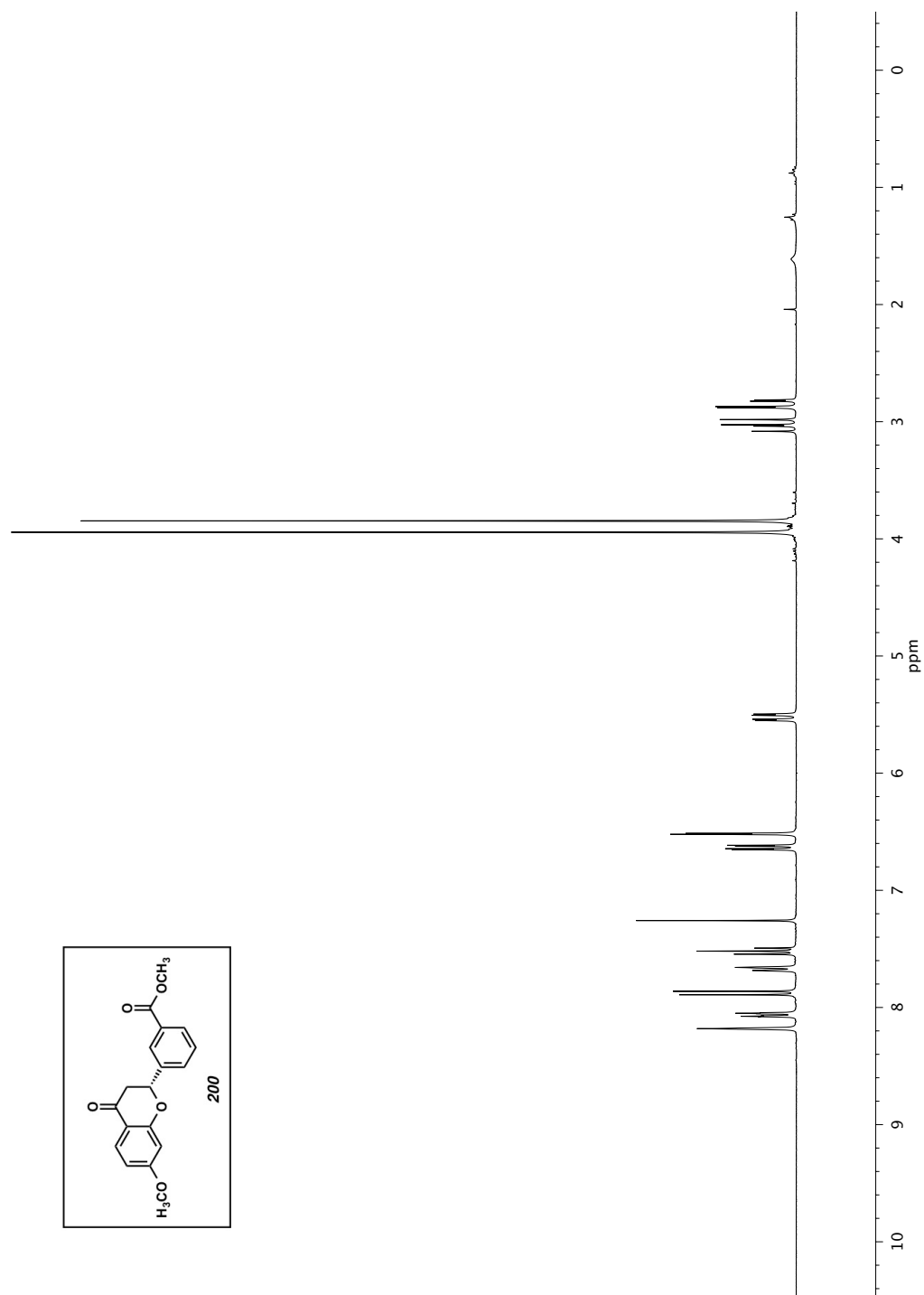
Figure A2.76 ^{1}H NMR (500 MHz, CDCl$_3$) of compound **200**
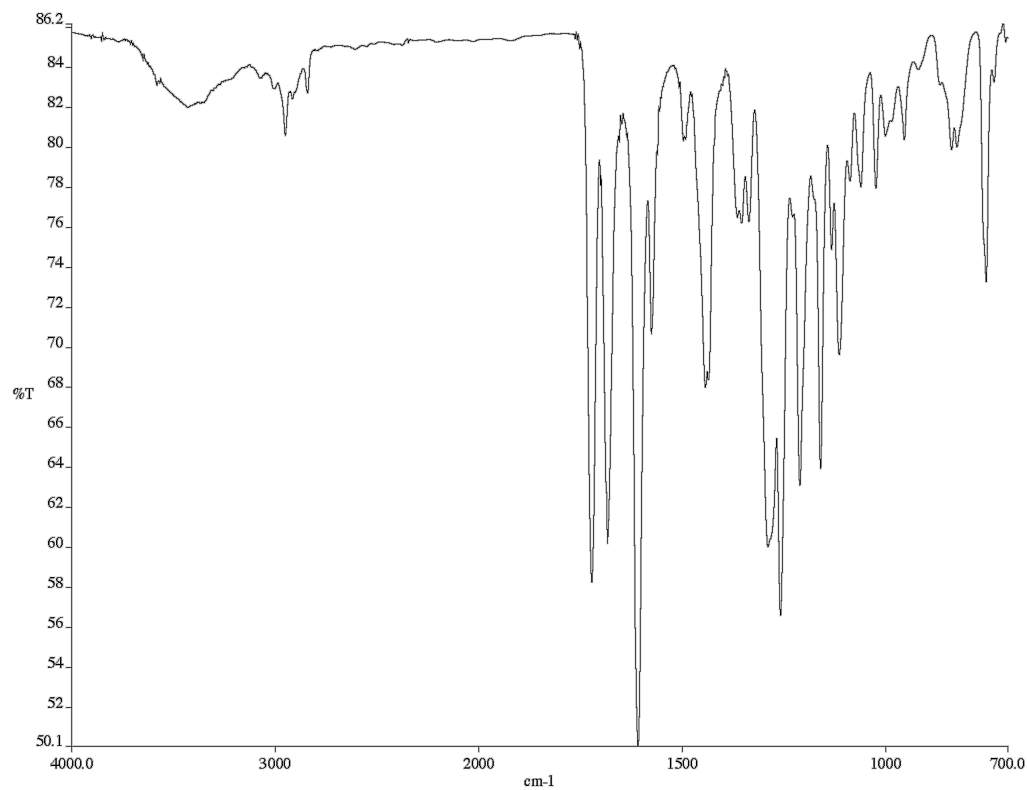
Figure A2.77 Infrared spectrum (Thin Film, NaCl) of compound **200**
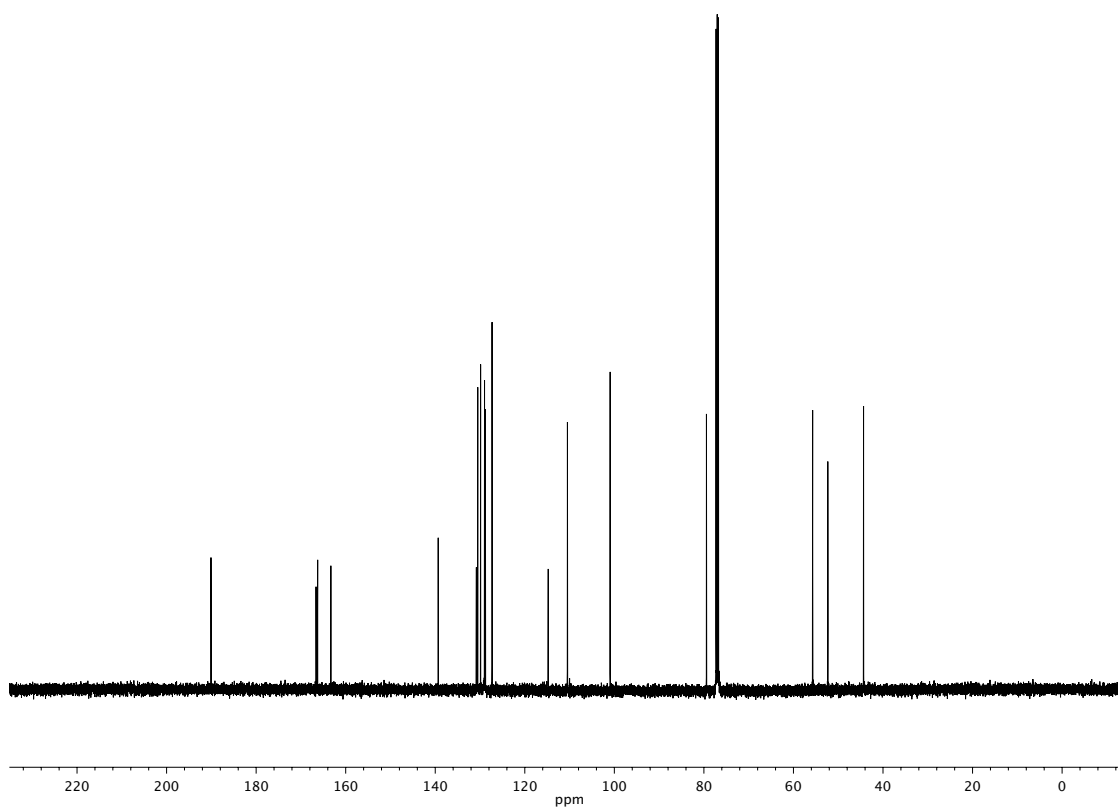
Figure A2.78 ^{13}C NMR (126 MHz, CDCl$_3$) of compound **200**
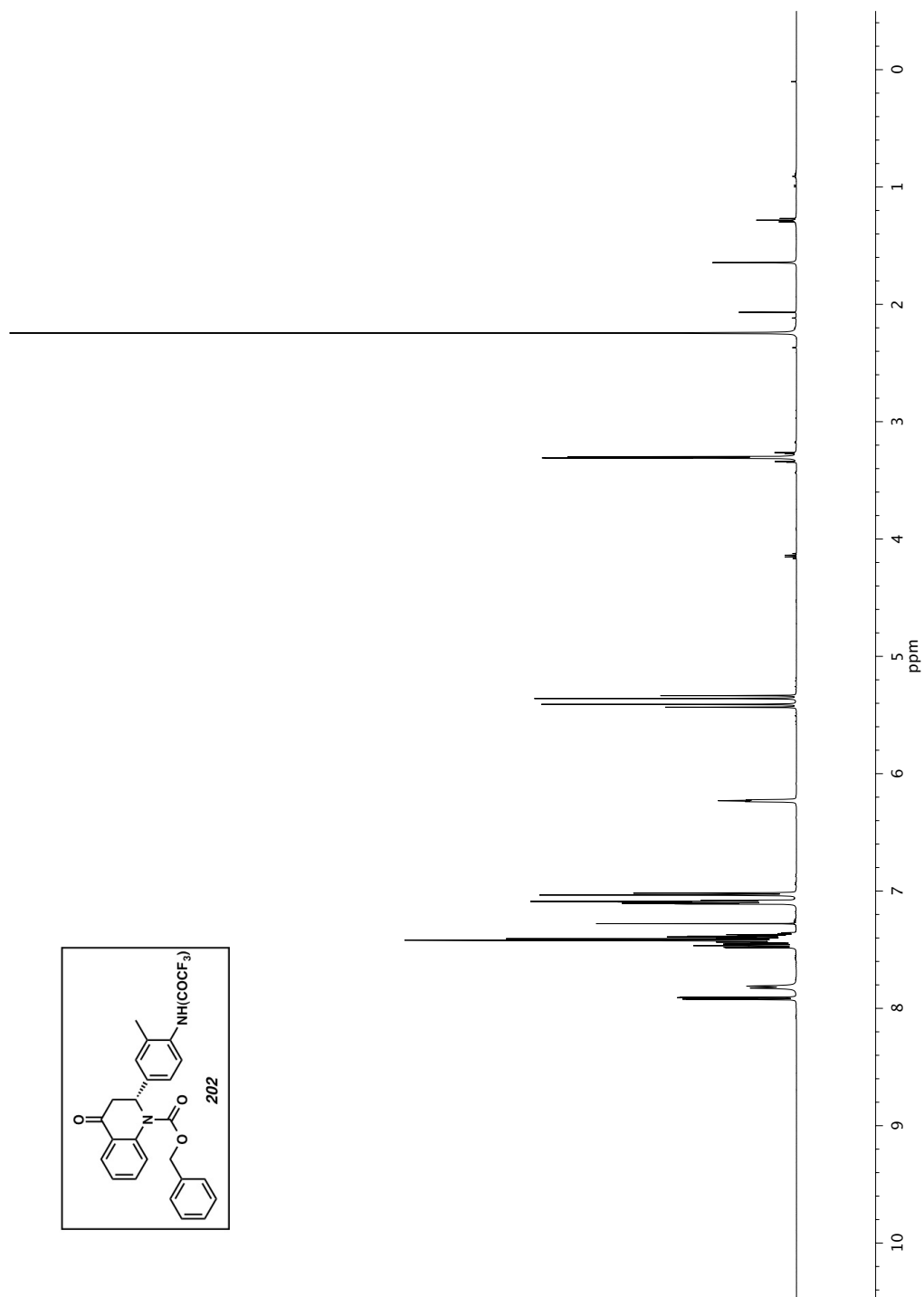
Figure A2.79 ^{1}H NMR (500 MHz, CDCl$_3$) of compound **202**
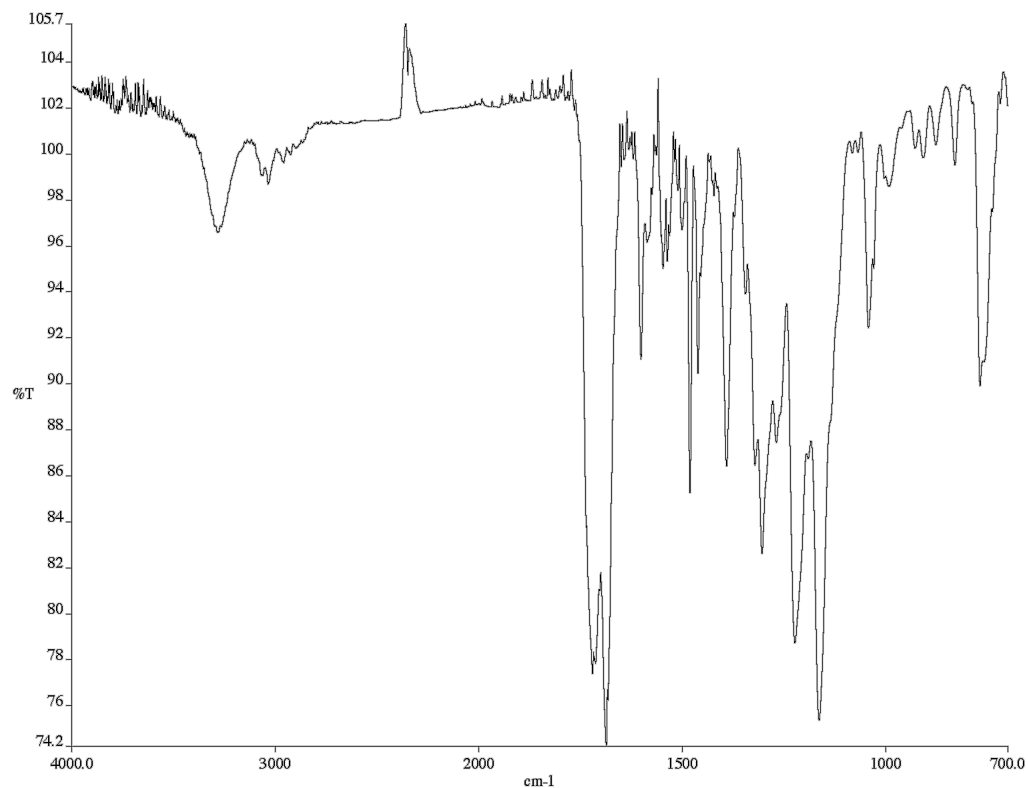
Figure A2.80 Infrared spectrum (Thin Film, NaCl) of compound **202**
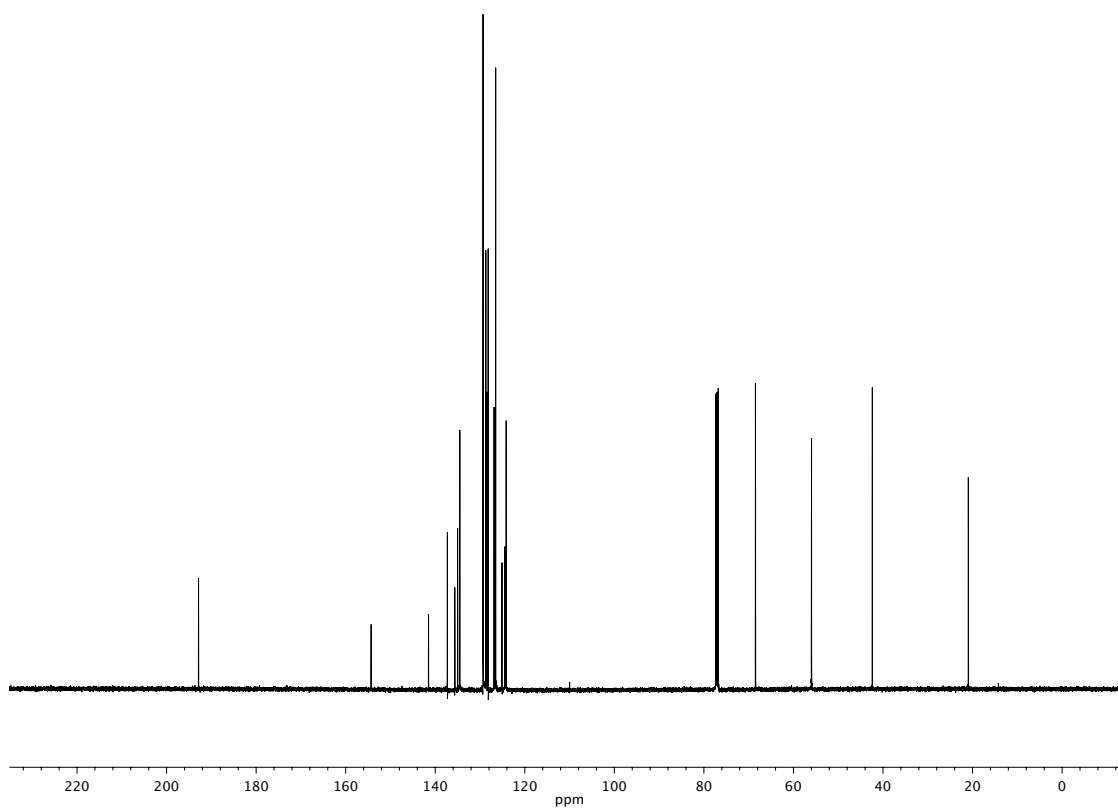
Figure A2.81 ^{13}C NMR (126 MHz, CDCl$_3$) of compound **202**
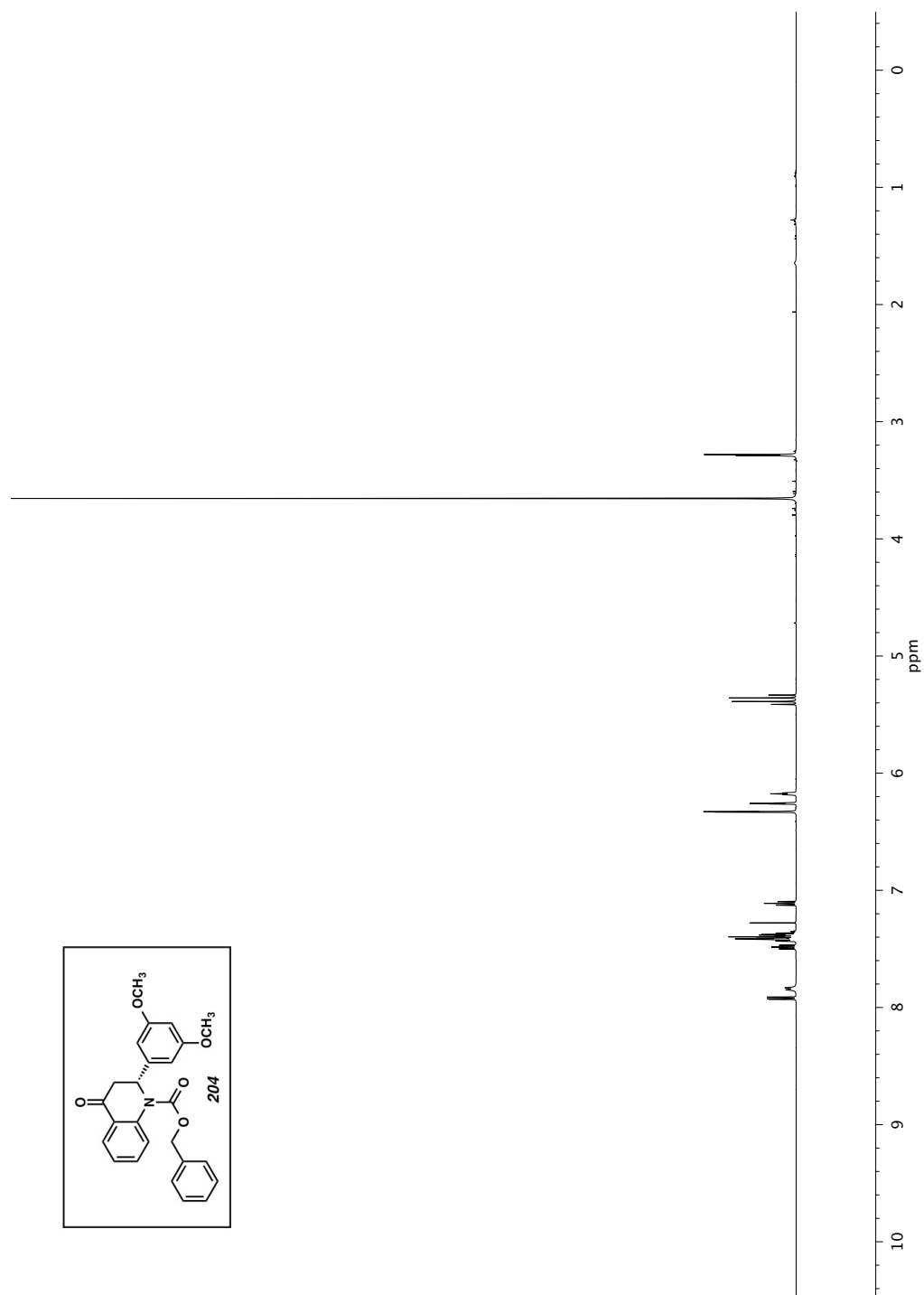
Figure A2.82 ^{1}H NMR (500 MHz, CDCl$_3$) of compound **204**
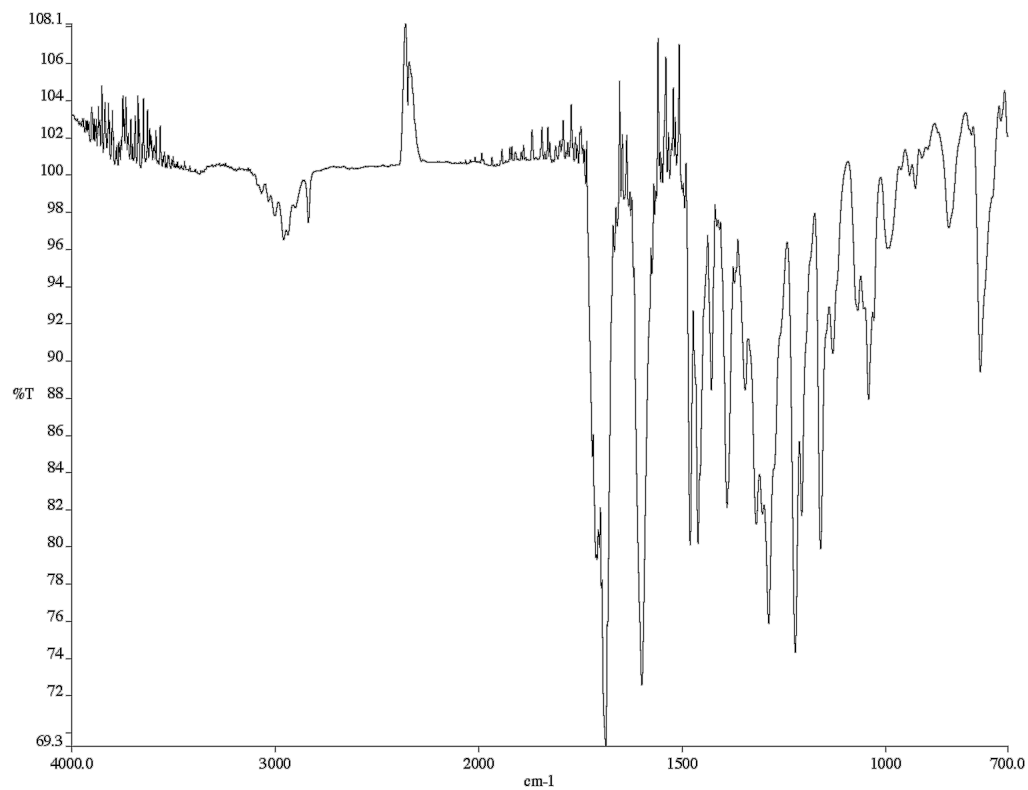
Figure A2.83 Infrared spectrum (Thin Film, NaCl) of compound **204**
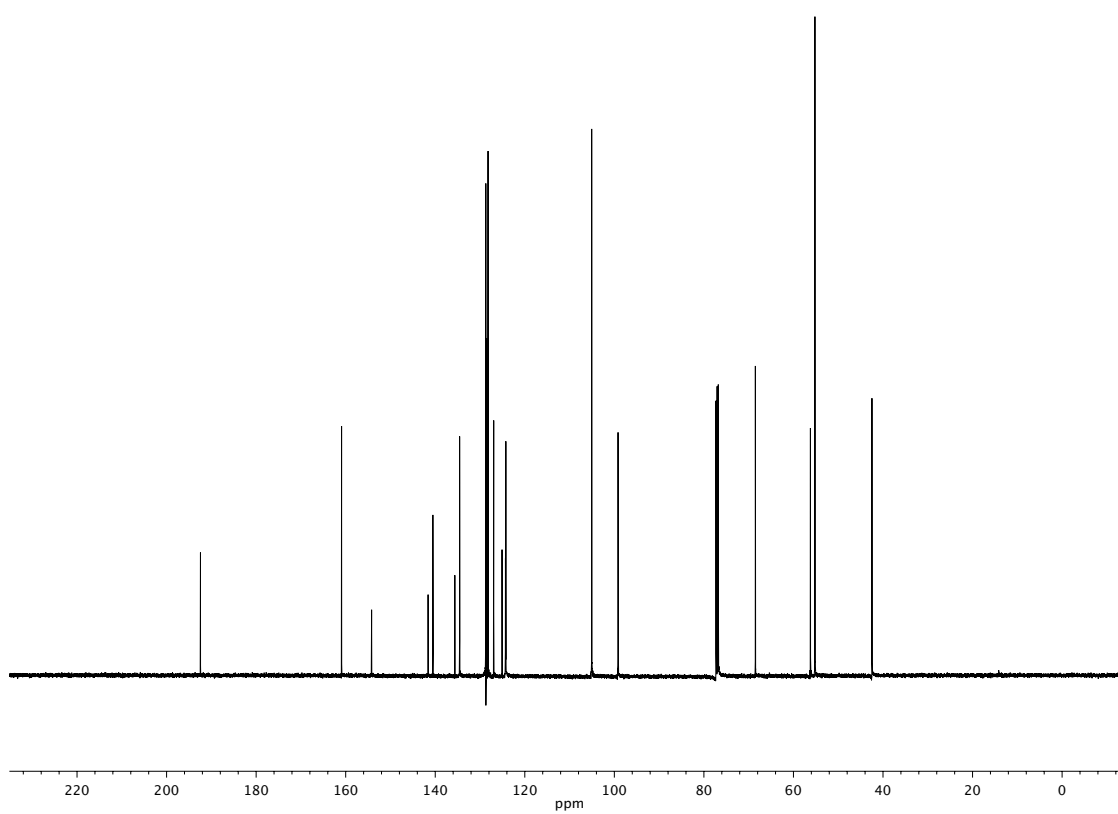
Figure A2.84 ^{13}C NMR (126 MHz, CDCl$_3$) of compound **204**
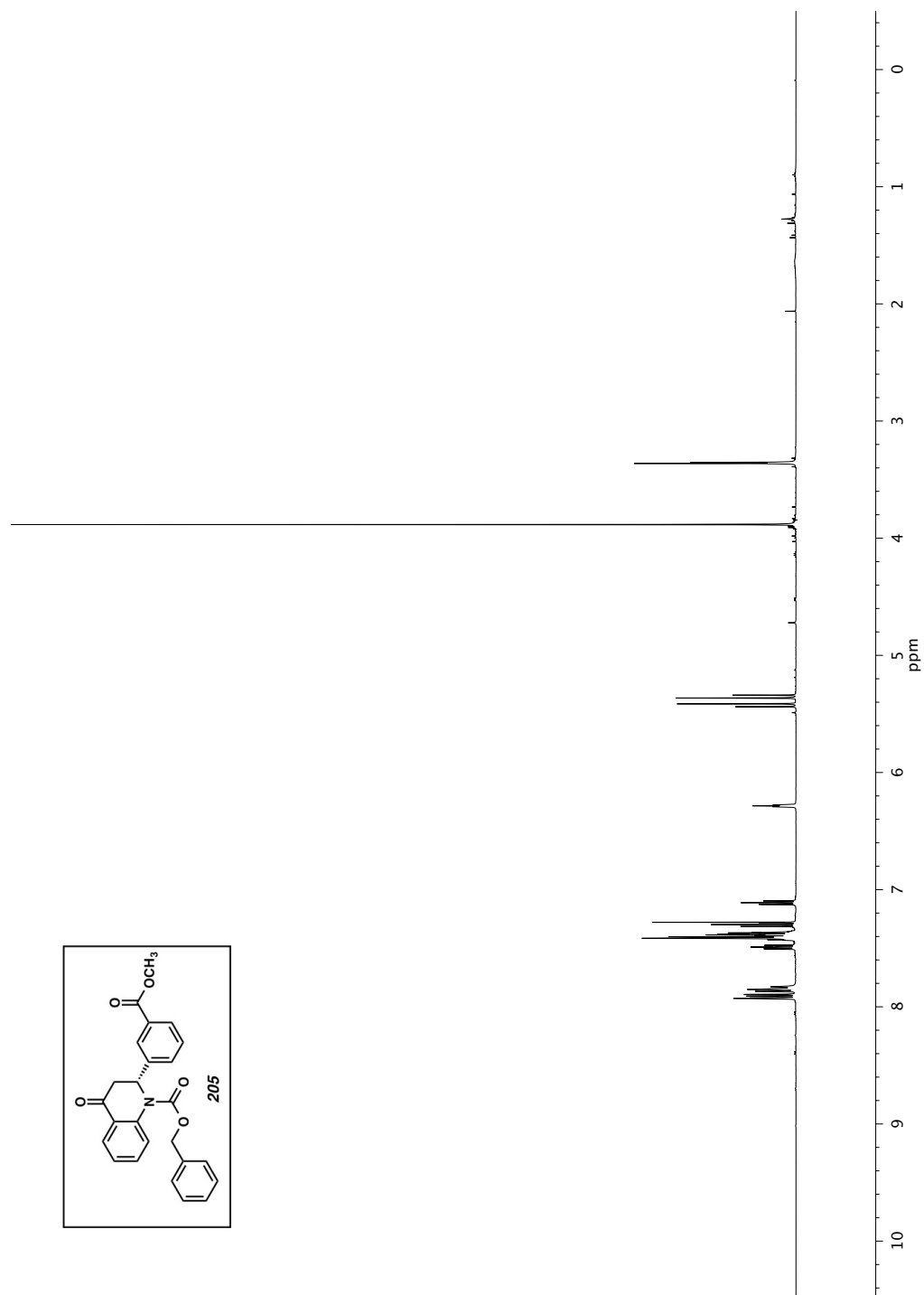
Figure A2.85 ^{1}H NMR (500 MHz, CDCl$_3$) of compound **205**
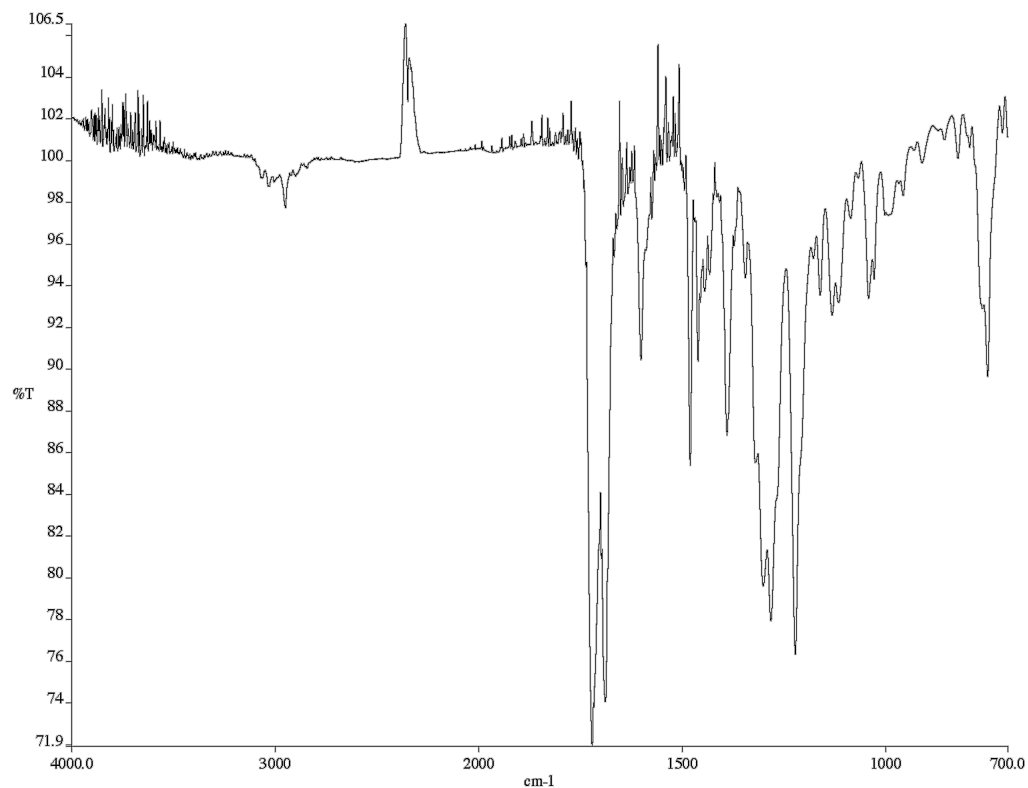
Figure A2.86 Infrared spectrum (Thin Film, NaCl) of compound **205**
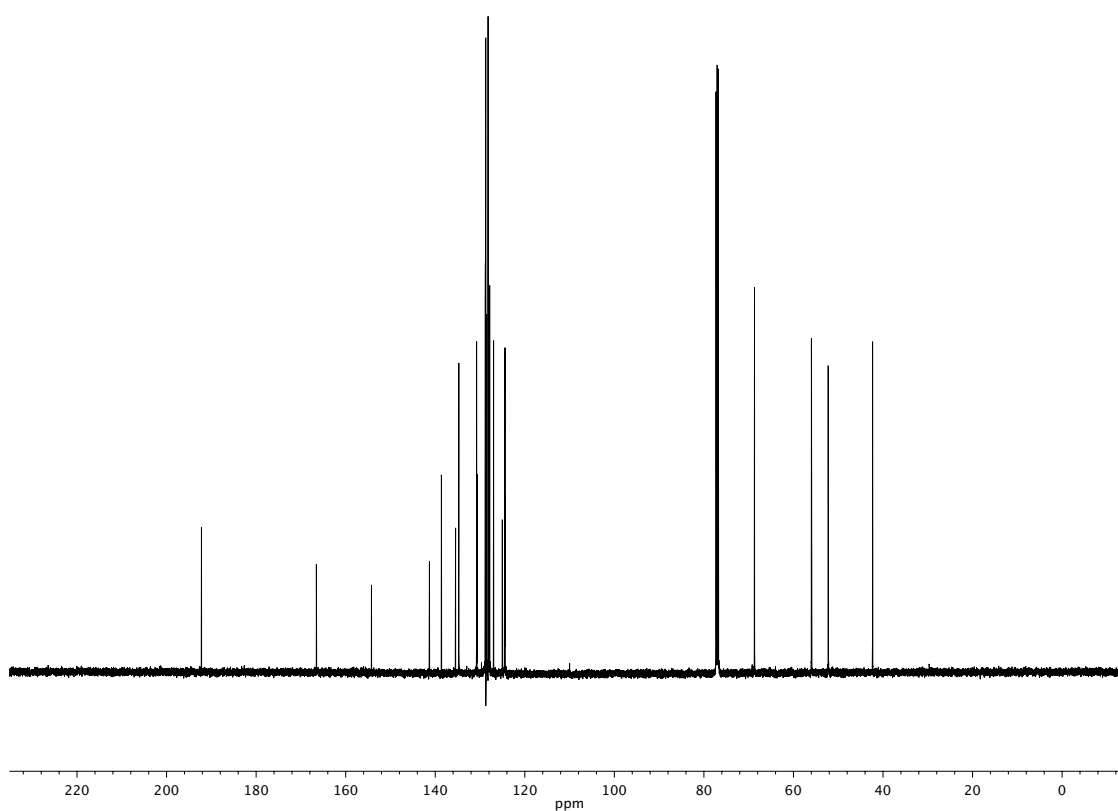
Figure A2.87 ^{13}C NMR (126 MHz, CDCl$_3$) of compound **205**
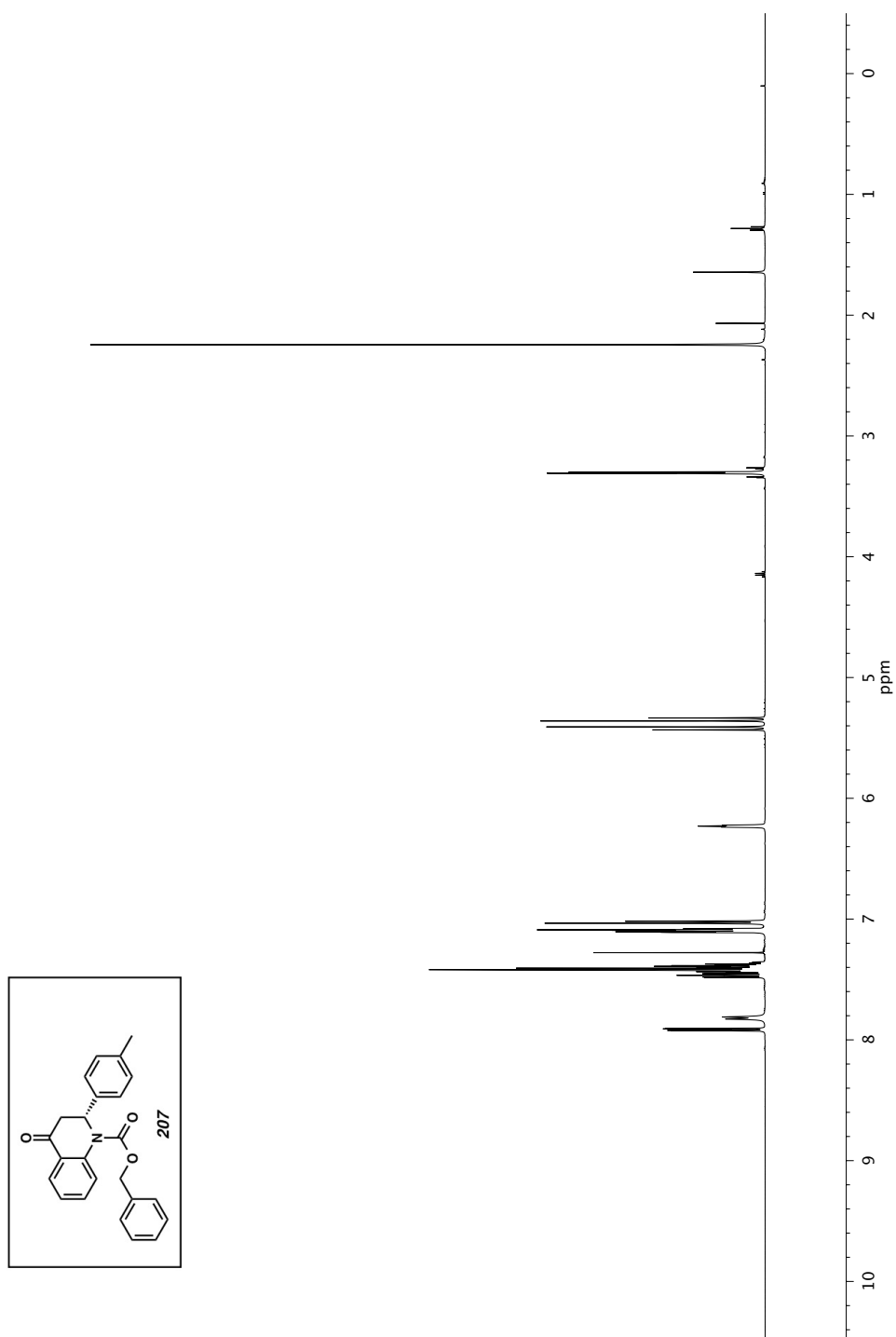
Figure A2.88 ^{1}H NMR (500 MHz, CDCl$_3$) of compound **207**
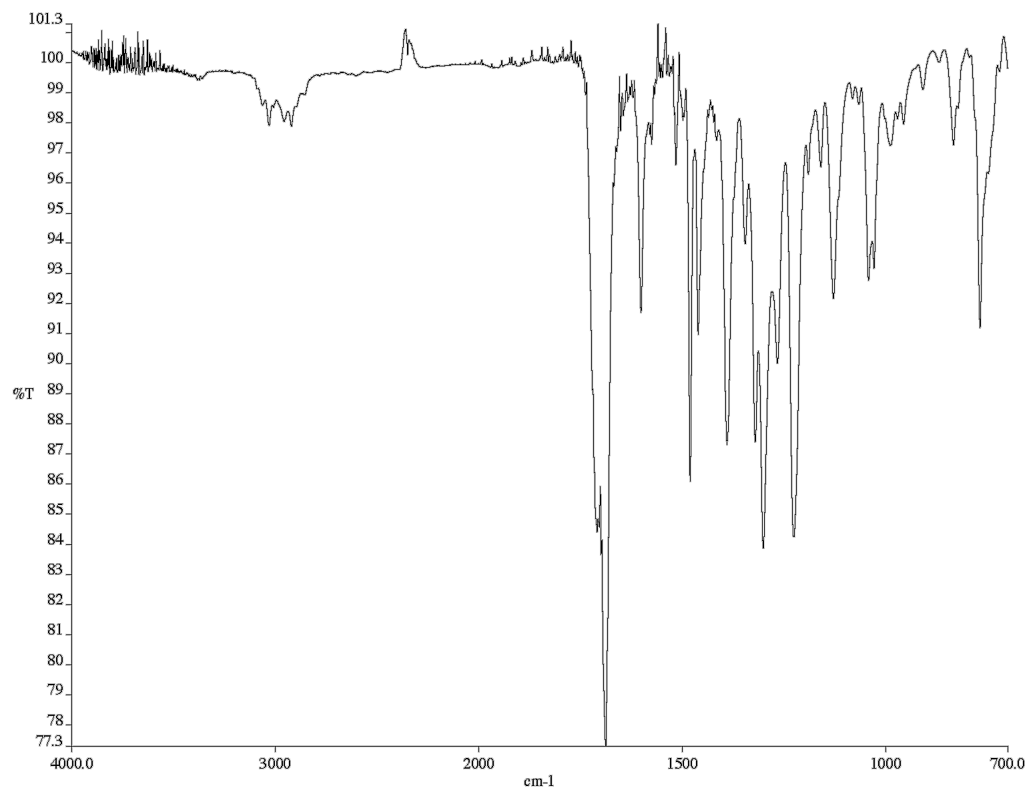
Figure A2.89 Infrared spectrum (Thin Film, NaCl) of compound **207**
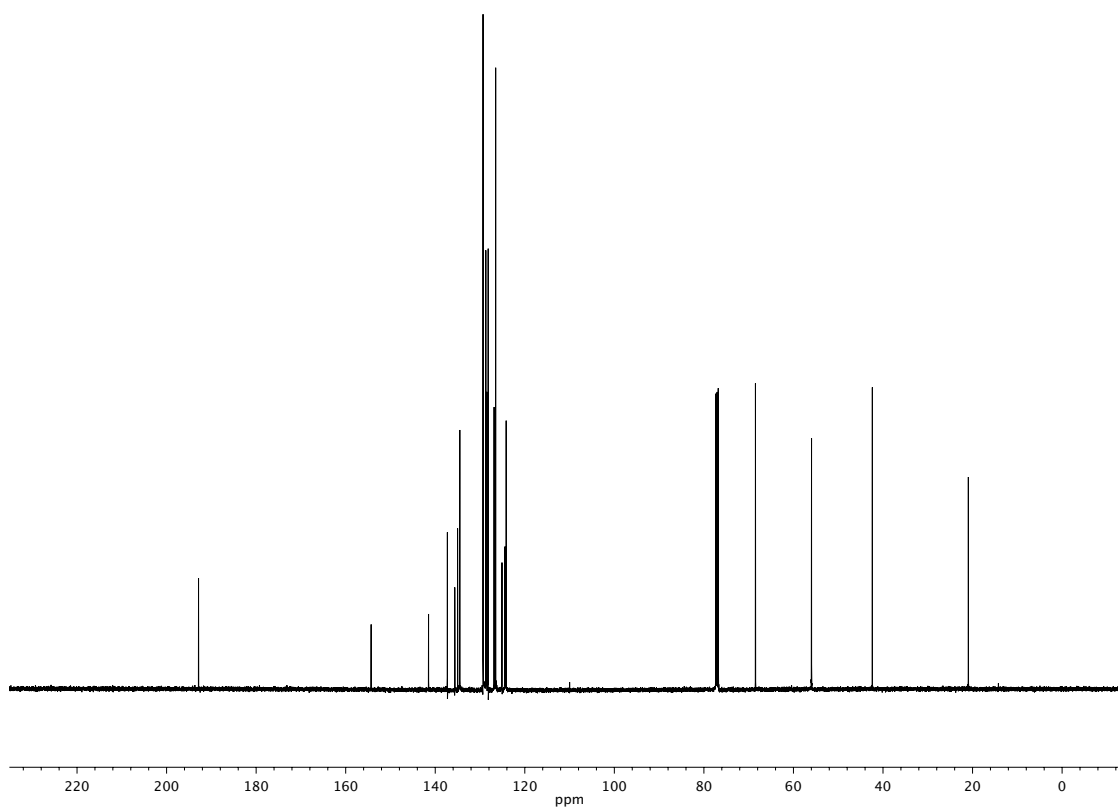
Figure A2.90 ^{13}C NMR (126 MHz, CDCl$_3$) of compound **207**
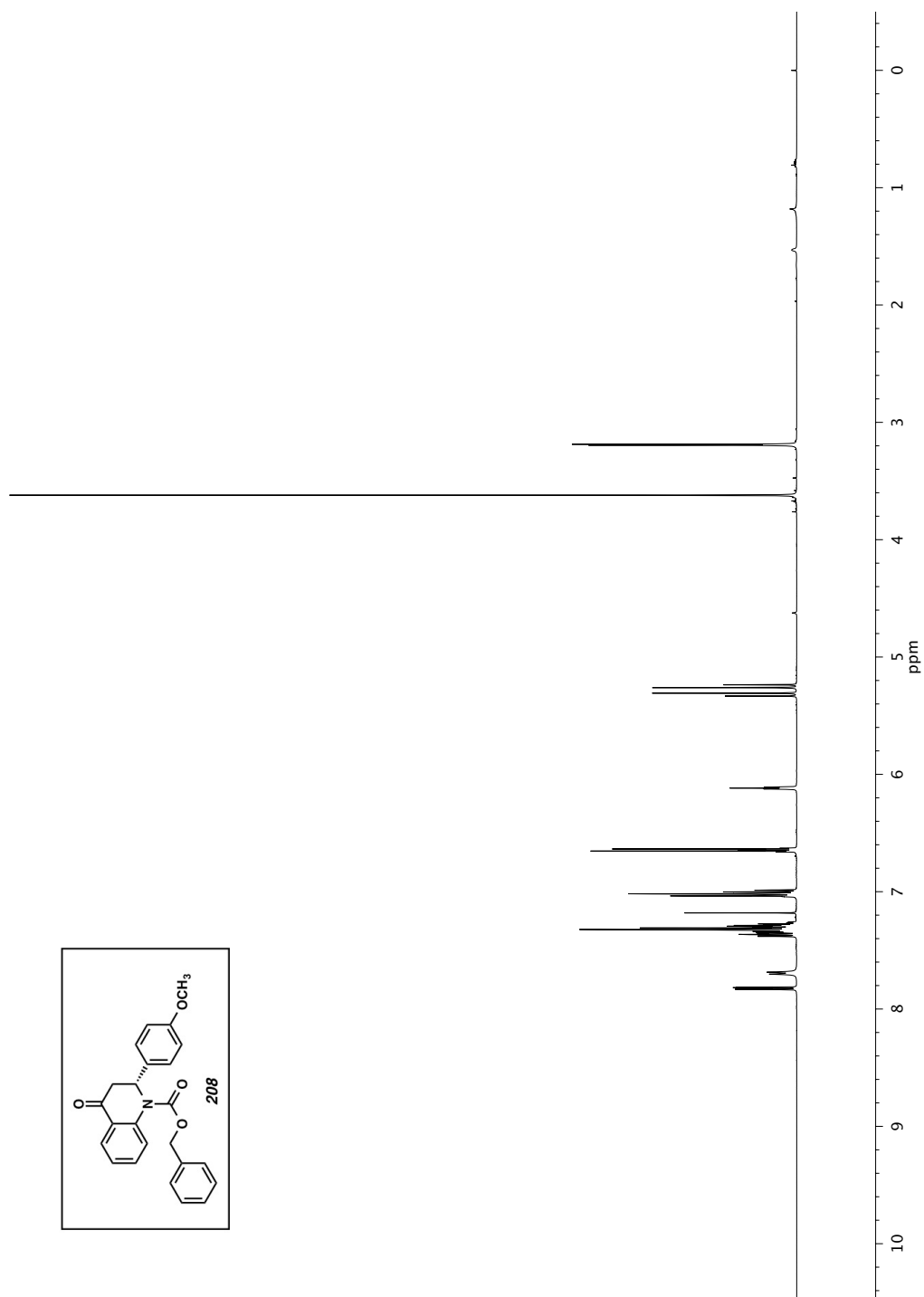
Figure A2.91 ^{1}H NMR (500 MHz, CDCl$_3$) of compound **208**
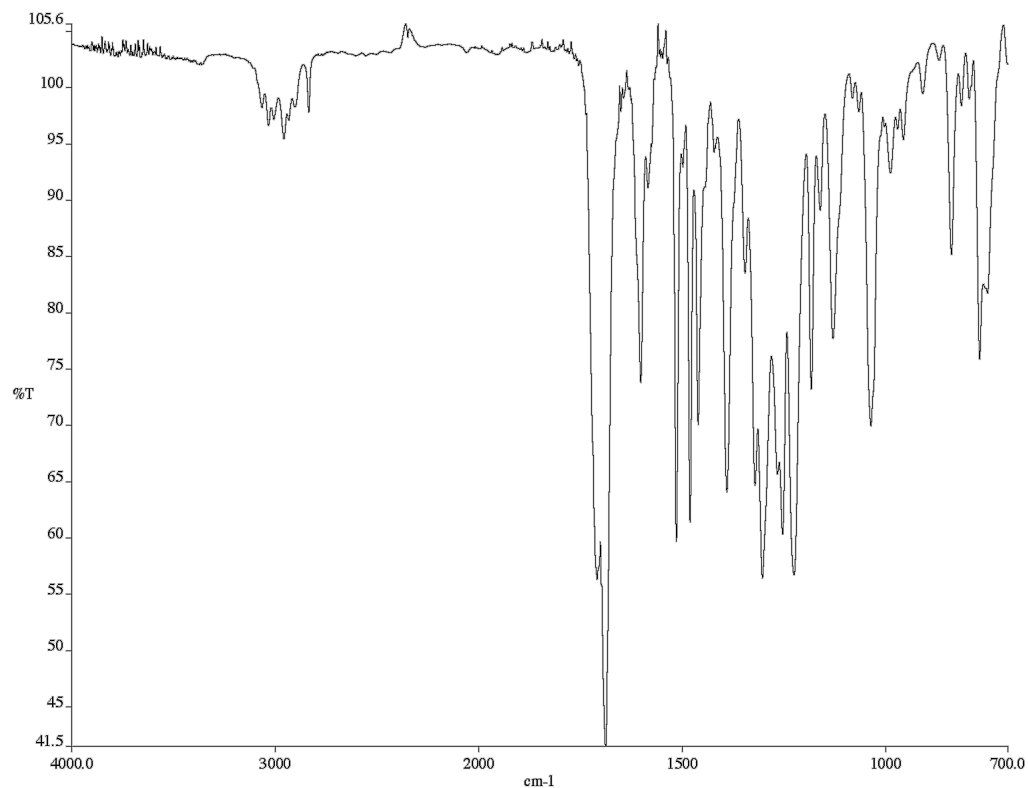
Figure A2.92 Infrared spectrum (Thin Film, NaCl) of compound **208**
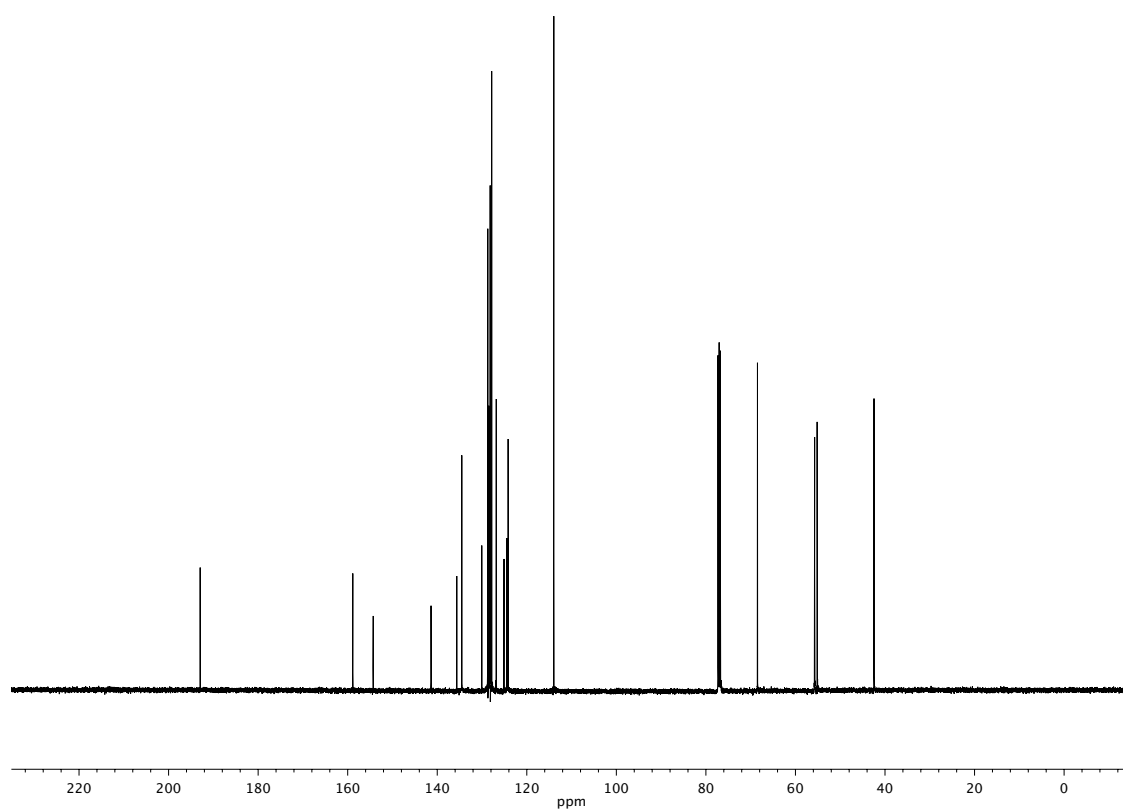
Figure A2.93 ^{13}C NMR (126 MHz, CDCl$_3$) of compound **208**
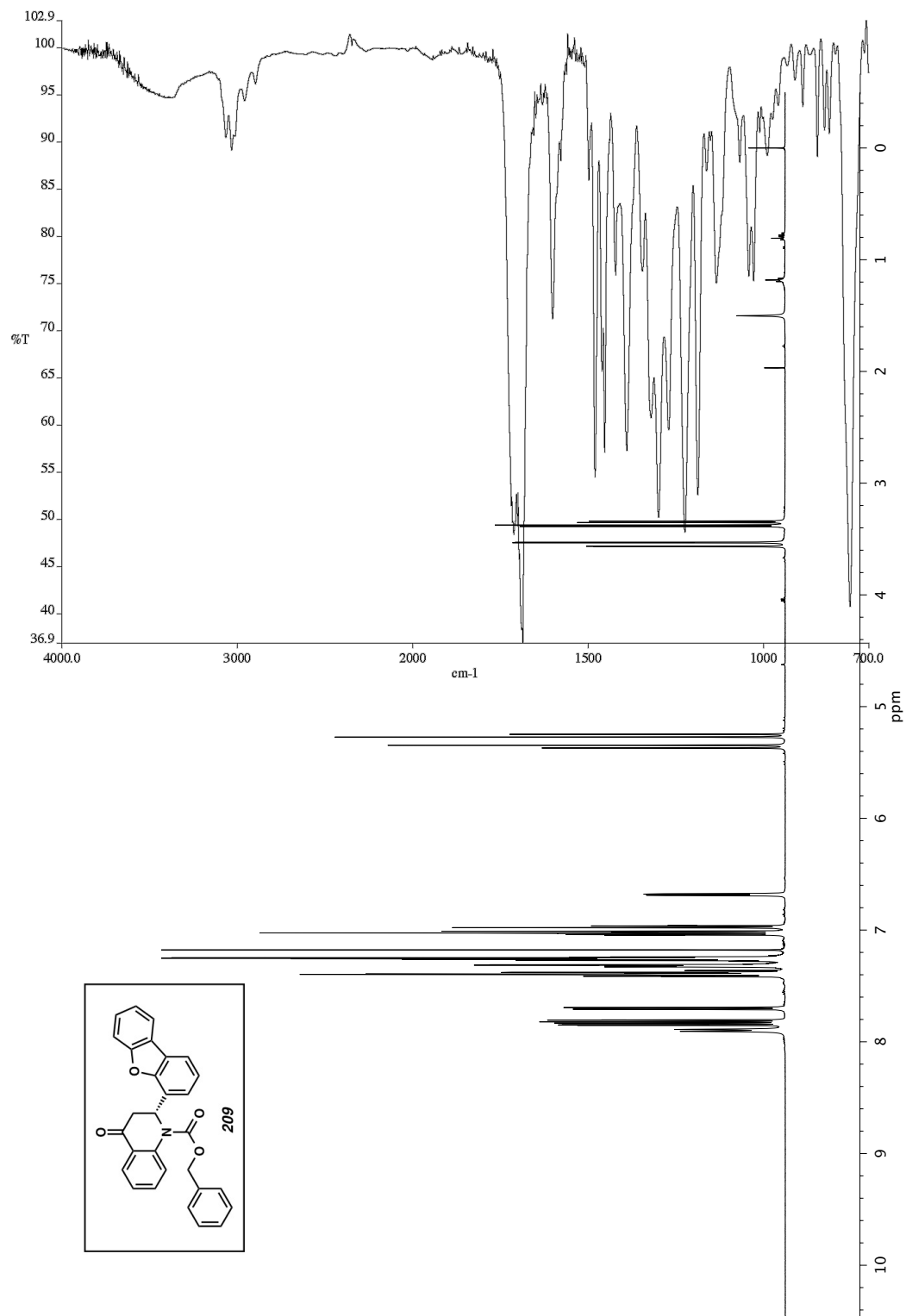
Figure A2.94 ^{1}H NMR (500 MHz, CDCl$_3$) of compound **209**
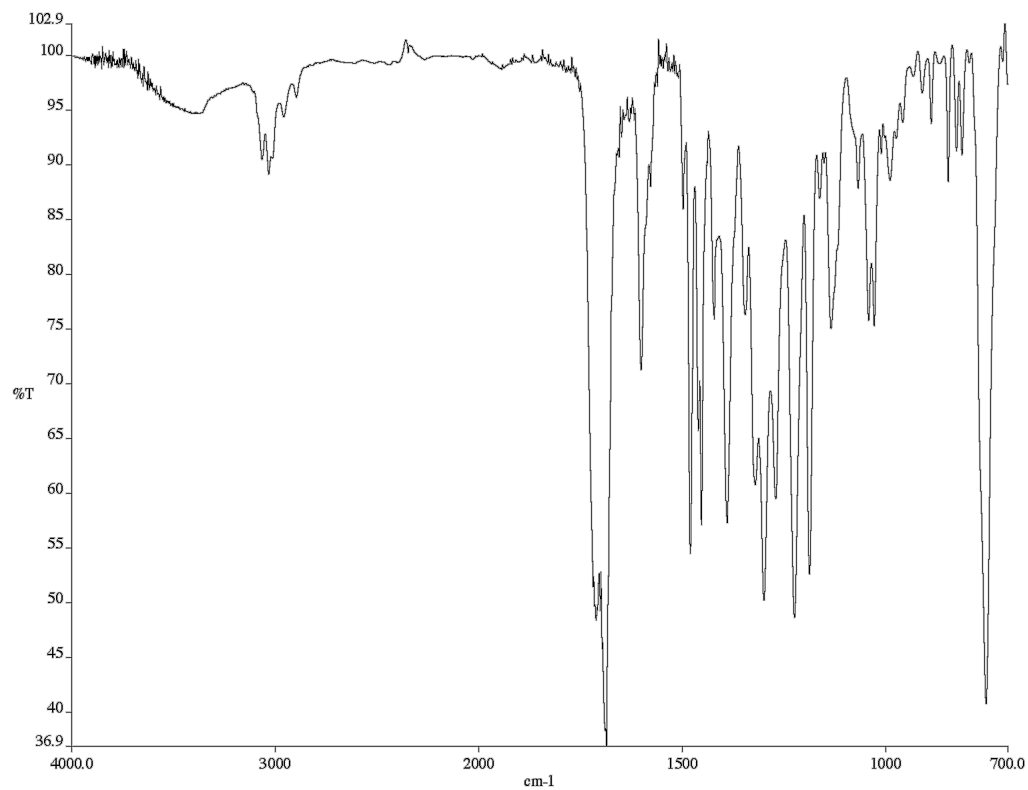
Figure A2.95 Infrared spectrum (Thin Film, NaCl) of compound **209**
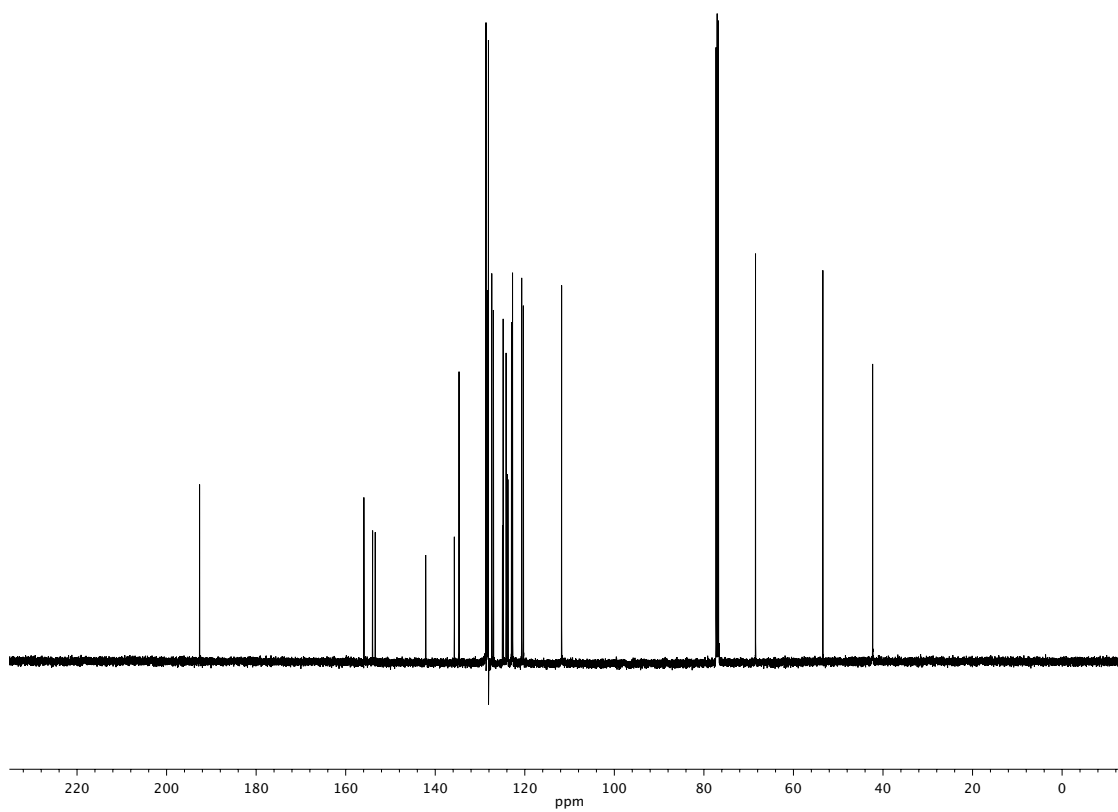
Figure A2.96 ^{13}C NMR (126 MHz, CDCl$_3$) of compound **209**

CHAPTER 4

Mechanism and Enantioselectivity in Palladium-Catalyzed Conjugate

Addition of Arylboronic Acids to β-Substituted Cyclic Enones: Insights

from Computation and Experiment[‡]

Abstract

Enantioselectivity-Determining Step

Enantioselective conjugate additions of arylboronic acids to β-substituted cyclic enones have been reported previously from our laboratories. Air and moisture tolerant conditions were achieved with a catalyst derived *in situ* from palladium(II) trifluoroacetate and the chiral ligand (*S*)-*t*-BuPyOx. We now report a combined experimental and computational investigation on the mechanism, the nature of the active catalyst, the origins of the enantioselectivity, and the stereoelectronic effects of the ligand and the substrates of this transformation. Enantioselectivity is controlled primarily by steric repulsions between the *t*-Bu group of the chiral ligand and the α-methylene hydrogens of the enone substrate in the enantiodetermining carbopalladation step. Computations indicate that the reaction occurs via formation of a cationic arylpalladium(II) species, and subsequent carbopalladation of the enone olefin forms the key carbon-carbon bond. Studies of non-linear effects and stoichiometric and catalytic reactions of isolated (PyOx)Pd(Ph)I complexes show that a monomeric arylpalladium-ligand complex is the active species in the selectivity-determining step. The addition of water and ammonium hexafluorophosphate synergistically increases the rate of the reaction. These additives also allow the reaction to be performed at 40 °C and facilitate an expanded substrate scope.

4.1 Introduction

Asymmetric conjugate addition has become a familiar reaction manifold in the synthetic chemists' repertoire.[1] Though seminal reports involved highly reactive organometallic nucleophiles,[2] systems were rapidly developed that involved functional-group-tolerant organoboron nucleophiles. Namely, Hayashi pioneered the use of rhodium/BINAP catalysts for the asymmetric conjugate addition of a number of boron-derived nucleophiles.[3] As an economical alternative to the rhodium systems, Miyaura pioneered the use of chiral palladium-phosphine catalysts to address similar transformations[4] and Minnaard reported a palladium-catalyzed asymmetric conjugate addition using a catalyst formed *in situ* from palladium trifluoroacetate and commercially available (*S*,*S*)-Me-DuPhos.[5]

More recently, asymmetric conjugate addition has become a useful strategy for the challenge of constructing asymmetric quaternary stereocenters.[6] Again, many earlier developed methods involved highly reactive diorganozinc,[7] triorganoaluminum,[8] and organomagnesium[9] nucleophiles, however, more recently chiral rhodium/diene systems have been shown to construct asymmetric quaternary stereocenters with functional group-tolerant organoboron nucleophiles.[10] While rhodium systems are highly developed and exhibit a wide substrate scope, the high cost of the catalyst precursors and oxygen sensitivity of the reactions are undesirable. Despite progress in palladium-catalyzed conjugate additions for the formation of tertiary stereocenters,[11] no conditions were amenable to the synthesis of even *racemic* quaternary centers until Lu and coworkers disclosed a dicationic, dimeric palladium/bipyridine catalyst in 2010.[12] However, it was not until our recent report that a palladium-derived catalyst was employed to generate an

asymmetric quaternary stereocenter *via* conjugate addition chemistry.[13] We employed a catalyst derived *in situ* from Pd(OCOCF$_3$)$_2$ and a chiral pyridinooxazoline (PyOx) ligand,[14] (*S*)-*t*-BuPyOx (ligand **82**, Scheme 4.1). This catalyst facilitates the asymmetric conjugate addition of arylboronic acids to β-substituted enones in high yield and good enantioselectivity.

Scheme 4.1 Asymmetric conjugate addition with (S)-t-BuPyOx ligand
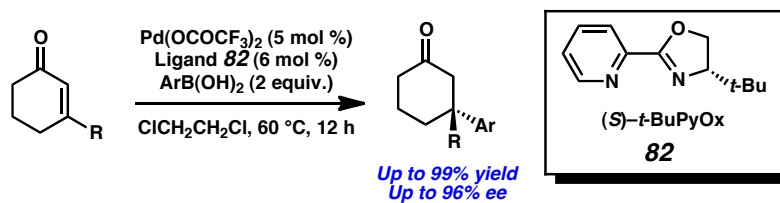
Importantly, this reaction is highly tolerant of air and moisture, and the chiral ligand, while not yet commercially available, is easily prepared.[15] Initial results with the Pd/PyOx system were reported rapidly due to concerns over competition in the field. Indeed, recent publications prove palladium-catalyzed conjugate addition to be a burgeoning field of research.[16] After the initial disclosure, we observed that in addition to catalyzing conjugate additions to 5-, 6-, and 7-membered enones, the Pd/PyOx catalyst successfully reacted with chromones and 4-quinolones.[17] Intrigued by the broad substrate scope and operational simplicity of this highly asymmetric process, we conducted a thorough study to optimize the reaction conditions, including measures to reduce the catalyst loading, lower the reaction temperature, and further generalize the substrate scope. We also performed mechanistic and computational investigations toward

elucidating the catalytic cycle, active catalyst species, and the stereoelectronic effects on enantioselectivity of this reaction.

4.2 Results

4.2.1 Effects of Water on Catalyst Turnover

In our initial report,[13] we were able to demonstrate that the addition of up to 10 equivalents of water had no deleterious effect. Despite this, water was not considered as an important additive in the initially reported conditions because the stoichiometric arylboronic acid was believed to be a sufficient proton source to turn over the catalyst. In considering the overall reaction scheme, a more precise analysis of the mass balance of the reaction led us to reconsider the importance of water as an participant in the overall transformation (Scheme 4.2a). These considerations proved to be essential during the scale up of the reaction. Attempts to use the original conditions (with no water added) failed to convert enone **95** efficiently, generating the desired ketone (**35**) only in moderate yield (Scheme 4.2b). We reasoned that when the reaction is performed on a small scale under ambient atmosphere the moisture present in the air and on the glassware could be sufficient to drive the reaction to completion. On a larger scale, however, where a more significant quantity of water was necessary, this was no longer true. Gratifyingly, upon the addition of as little as 1.5 equivalents of water to the reaction mixture, both reactivity and the enantioselectivity were restored (Scheme 4.2c), affording ketone **35** in high yield and ee.

Scheme 4.2 (a) Examination of reaction mass balance (b) Absence of water prohibits scale-up (c)

Addition of water facilitates larger scale reactions
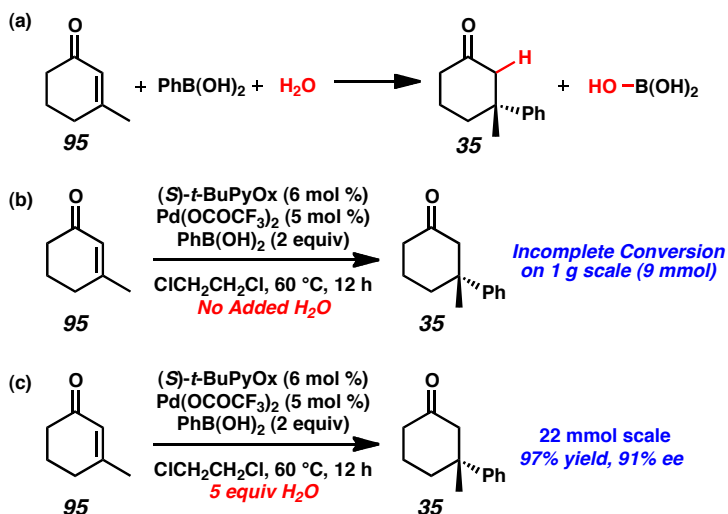
We next sought to measure deuterium incorporation at the carbonyl α-position as a method to determine the source of the proton utilized in reaction turnover. Reactions were performed substituting deuterium oxide for water and observed by ^{1}H and ^{2}H NMR analysis (Figure 4.1). Using phenylboronic acid, the reaction afforded ketone **35** in similar yield and enantioselectivity (Figure 4.1a). Likewise, substitution of phenylboroxine ((PhBO)$_3$) for phenylboronic acid and deuterium oxide for water (Figure 4.1b) resulted in identical yield, albeit with slightly depressed ee observed in ketone **35**. Analysis of ketone **35** by ^{1}H NMR (Figure 4.1c) showed significant deuterium incorporation at the α-position of the carbonyl, even in the presence of phenylboronic acid.[18] As expected, a higher degree of deuterium incorporation was observed in the reaction where phenyl boroxine was substituted for the boronic acid, however, the similar level of incorporation in both experiments suggested that the deuterium oxide was the agent assisting reaction turnover regardless of the use of protic or aprotic boron reagent.

*Figure 4.1 (a) deuterium incorporation using PhB(OH)$_2$ (b) deuterium incorporation using (PhBO)$_3$ (c) ^{1}H NMR data measuring deuterium incorporation by integral comparison of α-protons relative to H$_5$, control: treatment of ketone **35** to deuterium incorporation conditions*
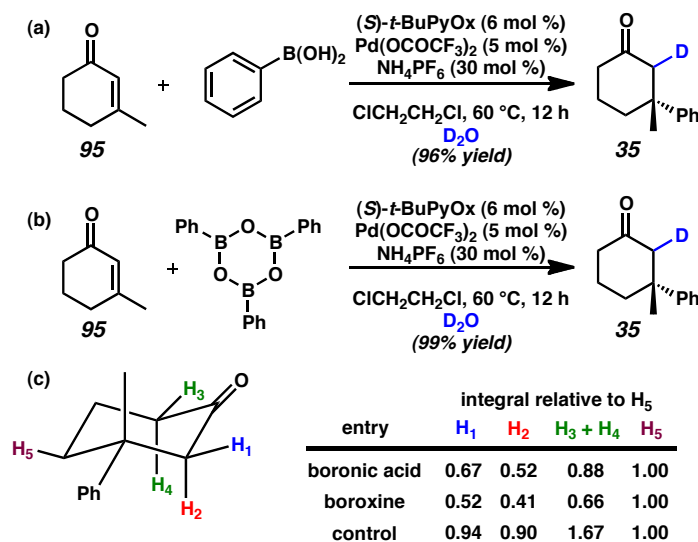
4.2.2. Effects of Salt Additives on Reaction Rate

Satisfied with our ability to perform the reaction on scale, we turned our attention toward improving the catalyst activity. We observed that nearly all previous literature reports regarding palladium-catalyzed conjugate addition utilized cationic precatalysts featuring weakly-coordinative anions (PF$_6^-$, SbF$_6^-$, BF$_4^-$ etc.). We reasoned that the substitution of the trifluoroacetate counterion with a less coordinative species could lead to an increase in reaction rate. With this goal in mind, we examined a series of salt additives containing weakly coordinative counterions. We viewed the strategy for the *in situ* generation of the catalyst as the more practical and operationally simple alternative to the design, synthesis, and isolation of a new dicationic palladium precatalyst.

We investigated a number of salt additives to test this mechanistic hypothesis (Table 4.1). Coordinating counterions like chloride (entry 1) shut down reactivity. Pleasingly, as per our hypothesis, weakly coordinating counterions with sodium cations (entries 2–4) facilitated swift reaction, albeit with depressed ee. Tetrabutylammonium salts (entries 5–6) encountered slow reaction times, but good enantioselectivity. Sodium tetraphenylborate (entry 7), however, failed to deliver appreciable quantities of the quaternary ketone **35**, as rapid formation of biphenyl was observed. Ammonium salts (entries 8–9) provided the desired blend of reaction rate and enantioselectivity. We concluded that the hexafluorophosphate anion (entry 9) gave the optimal combination of short reaction time with minimized loss of enantioselectivity. Perhaps the influence/effect of the salt on the polarity of the medium also effects the enantioselectivity.

Table 4.1 Effect of salt additives on reaction rate [a]

entry[a]	additive	time (h)	yield (%)[b]	ee (%)[c]
1	NaCl	24	trace	---
2	NaBF$_4$	8	81[d]	88
3	NaPF$_6$	6	97	87
4	NaSbF$_6$	5	99	81
5	*n*-(Bu)$_4$PF$_6$	24	98	90
6	*n*-(Bu)$_4$BF$_4$	24	95	88
7	NaBPh$_4$	24	trace	---
8	NH$_4$BF$_4$	15	93	89
9	NH$_4$PF$_6$	12	96	91

[a]Conditions: phenylboronic acid (0.5 mmol), 3-methylcyclohexen-2-one (0.25 mmol), water (5 equiv), additive (30 mol %), Pd(OCOCF$_3$)$_2$ (5 mol %) and (*S*)-*t*-BuPyOx (6 mol %) in ClCH$_2$CH$_2$Cl (1 mL) at 40 °C . [b]GC yield utilizng tridecane standard. [c]ee was determined by chiral HPLC. [d]Reaction checked at 83% conversion as determined by GC analysis.

Based on our previous observations regarding the beneficial nature of water as an additive, we next explored the combined effect of water and hexafluorophosphate counterions. We found addition of both water and ammonium hexafluorophosphate were the most successful for increasing reactivity (Table 4.2). Water alone is insufficient to alter reactivity (entry 1), though the use of water with 30 mol % ammonium hexafluorophosphate greatly reduced the reaction time (entry 2) to only 1.5 hours with minimal effect on yield or ee. Furthermore, this combination of additives allowed the reaction to proceed at temperatures as low as 25 °C with 5 mol % palladium and 6 mol % ligand, and lowering of catalyst loadings to only 2.5 mol % of palladium and 3 mol % ligand at 40 °C (entry 3). We determined that optimal conditions for the reaction with lower catalyst loading to be 5 equivalents of water, 30 mol % ammonium hexafluorophosphate at 40 °C (entry 4), conditions that reproduce the original result at milder temperature and lower catalyst loadings. The reaction was extraordinarily tolerant of the amount of water, with both 10 (entry 5) and 20 (entry 6) equivalents of water having minimal effect on the yield or ee. Loadings of ammonium hexafluorophosphate can be as low as 5 mol % (entry 7) or 10 mol % (entry 8) with reactions completed in 24 hours. Stoichiometric additive (entry 9) gave no additional benefit (entry 4). Thus, we optimized the additive amounts to be 30 mol % ammonium hexafluorophosphate and 5 equivalents of water

Table 4.2 Effect of water and NH$_4$PF$_6$ on reaction rate[a]

entry[a]	H$_2$O (equiv.)	NH$_4$PF$_6$ (mol %)	Pd (mol %)	ligand (mol %)	temp (°C)	time (h)	yield (%)[b]	ee (%)[c]
1	10	---	5	6	60	12	99	91
2	5	30	5	6	60	1.5	93	88
3	5	30	5	6	25	36	98	91
4	5	30	2.5	3	40	12	95	91
5	10	30	2.5	3	40	12	96	89
6	20	30	2.5	3	40	12	95	90
7	5	5	2.5	3	40	24	93	90
8	5	10	2.5	3	40	24	93	92
9	5	100	2.5	3	40	12	97	88

[a]Conditions: phenylboronic acid (1.0 mmol), 3-methylcyclohexen-2-one (0.5 mmol), water, NH$_4$PF$_6$, Pd(OCOCF$_3$)$_2$ and (*S*)-t-BuPyOx in ClCH$_2$CH$_2$Cl (2 mL). [b]Isolated yield. [c]ee was determined by chiral HPLC.

Though increased rates were observed at 60 °C, the newly-found ability to perform reactions at 40 °C promoted superior reactivity of many substrates (Table 4.3). In fact, many substrates that exhibited high enantioselectivities under the original 60 °C reaction conditions suffered from poor yields. Reacting these substrates at 40 °C with the addition of ammonium hexafluorophosphate and water promoted significantly higher isolated yields. Arylboronic acids containing halides, such as *m*-chloro- (**210a**) and *m*-bromophenylboronic acid (**210b**) reacted with good enantioselectivity, but each substrate was originally marred by low yield using our original conditions. However, when reacted under the newly optimized reaction conditions, the isolated yield for the addition of chlorophenylboronic acid increased from 55% to 96% and for bromophenylboronic acid from 44% to 86%. Even *m*-nitroboronic acid (**210c**) reacted with higher isolated yield. Notably, some *ortho*-substituted boronic acids, such as *o*-fluorophenylboronic acid

(**210d**), reacted more successfully under the milder reaction conditions, leading to increased isolated yield of 70%.

Table 4.3 Increased reaction yields with different arylboronic acid substrates under new reaction conditions [a]

<table>
<tr><td>

210a
55 % Yield 97 % ee
96 % Yield 96 % ee

</td><td>

210b
44 % Yield 86 % ee
84 % Yield 84 % ee

</td><td>

210c
40 % Yield 92 % ee
81 % Yield 91 % ee

</td><td>

210d
32 % Yield 77 % ee
70 % Yield 77 % ee

</td></tr>
</table>
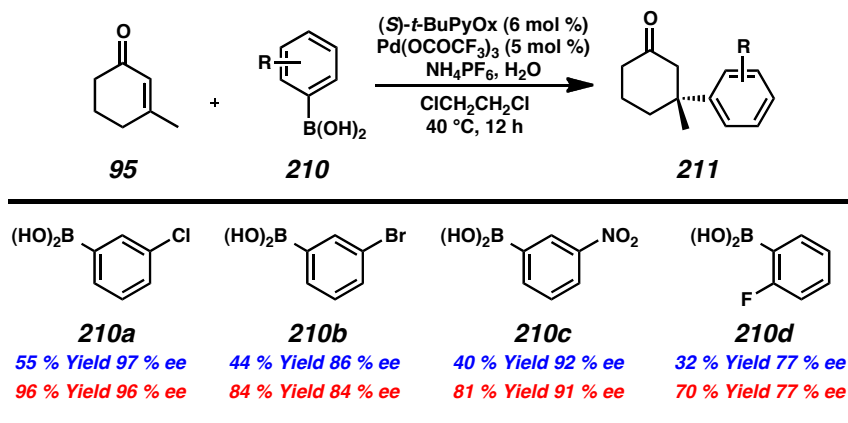
[a]Blue font: reported yield and ee of **211** in the absence of NH_4PF_6 and water with reactions performed at 60 °C; red font: yield and ee of **211** with additives. Conditions: boronic acid (1.0 mmol), 3-methylcyclohexen-2-one (0.5 mmol), NH_4PF_6 (30 mol %), water (5 equiv.), $Pd(OCOCF_3)_2$ (5 mol %) and (*S*)-*t*-BuPyOx (6 mol %) in $ClCH_2CH_2Cl$ (2 mL) at 40 °C . Isolated yield reported, ee was determined by chiral HPLC.

4.2.3 Determination of active catalyst as monomeric (ML)-system

Despite optimization of catalytic conditions for this highly enantioselective process, we were unsure of the nature of the active catalyst. For example, some rhodium conjugate addition systems have been shown to involve trimeric ligand/metal complexes.[19] Furthermore, Lu and coworkers reported the use of the palladium dimer $[(bpy)Pd(OH)]_2 \cdot 2BF_4$ as a precatalyst for conjugate addition.[12] We aimed to rule out the *in situ* formation and kinetic relevance of such dimers in our system. In seeking to support our hypothesized monomeric ligand-metal complex, we performed a non-linear effect study to determine the relationship between the ee of the ligand and the ee of the generated product.[20] The endeavor was to exclude dimeric $(ML)_2$ complexes from kinetic

relevance, clarifying the monomeric nature of the active catalyst.[21] Five reactions were performed using a catalyst with different level of enantiopurity (racemic, 20%, 40%, 60% and 80% ee), and the obtained enantioselectivities were plotted against ee of the catalyst mixture (Figure 4.2). The obtained data clearly demonstrates that a non-linear effect is not present, and this observation strongly supports the action of a single, monomeric (ML)-type Pd/PyOx catalyst as the kinetically relevant species.[21] While the precise nature of the active catalyst species is unknown, isolated $(PyOx)Pd(OCOCF_3)_2$ serves as an identically useful precatalyst, delivering ketone **35** in 99% yield and 92% ee.[22]

Figure 4.2 Determination of linearity between catalyst ee and product ee
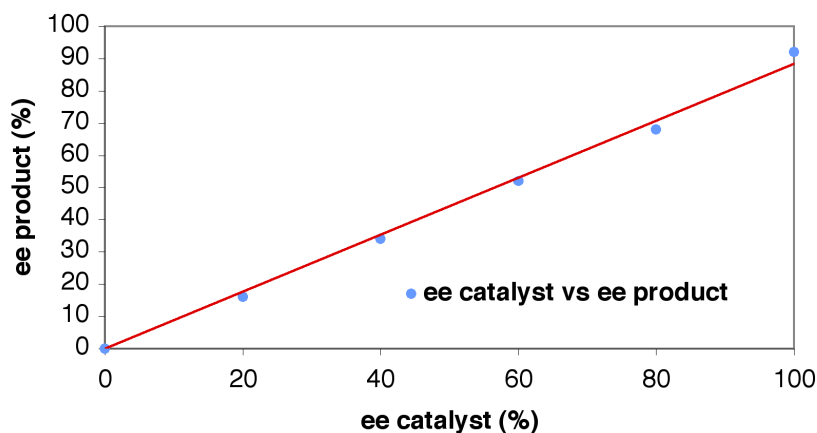
We aimed to augment the result of our non-linear experiment with a qualitative measurement of the molecular weight of the catalyst in solution (Table 4.4). Diffusion oriented spectroscopy (DOSY) NMR studies are a common method of correlating the molecular weight of a solution complex with its diffusion rate, which can be determined by NMR observation.[23] We used the pre-formed complex $(PyOx)Pd(OCOCF_3)_2$ as

standards for molecular weight (entry 1). As a high molecular weight standard for the hypothetical dimer, we measured the diffusion of (dppf)PdCl$_2$ (entry 2). Next, we mixed the PyOx ligand with a Pd(OCOCF$_3$)$_2$, ammonium hexafluorophosphate, and water in CD$_2$Cl$_2$ and observed the diffusion rate of the major species formed *in situ* (entry 3). The major solution species for the complex formed in entry 3 matched the ^{1}H and ^{13}C solution structure of synthesized and isolated (PyOx)Pd(OCOCF$_3$)$_2$ (entry 1), and produced a very reasonable match for diffusion coefficient in the DOSY NMR studies when the value of the solvent's diffusion coefficient (CD$_2$Cl$_2$) is taken into account as a standardization parameter. Furthermore, the high molecular weight standard (entry 2) was observed to diffuse slower than both these complexes, suggesting no change in speciation occurs when (PyOx)Pd(OCOCF$_3$)$_2$ is in solution. Taken together, these data suggest that the major palladium species formed in solution is a monomeric ligand-metal complex. We cannot definitively rule that (PyOx)Pd(OCOCF$_3$)$_2$ is the active catalyst; in fact, this author hypotheses that cationic [(PyOx)Pd(OH)]+ is the likely active catalyst. However, our data does suggest that, initially, the monomeric ligand-metal complex is the major species formed under the reaction conditions. Furthermore, the isolated (PyOx)Pd(OCOCF$_3$)$_2$ complex is chemically competent as a catalyst for the reaction, and delivers ketone **3** according to the general procedure in 99% yield and 92% ee.

Table 4.4 DOSY NMR Values for palladium complexes

entry	Pd species	molecular weight (g/mol)	diffusion coefficent (d)	CD$_2$Cl$_2$ diffusion coefficient (d)
1	(PyOx)Pd(OCOCF$_3$)$_2$	536.72	1.1 x 10^{-4}	3.3 x 10^{-4}
2	(dppf)PdCl$_2$	731.70	0.9 x 10^{-4}	3.2 x 10^{-4}
3	Pd(OCOCF$_3$)$_2$ + PyOx + NH$_4$PF$_6$ + H$_2$O	unknown	1.1 x 10^{-4}	3.2 x 10^{-4}

Conditions: Spectra acquired utilizing complex (0.015 mmol) dissolved in CD$_2$Cl$_2$ (700 mL) at 25 °C. Pulse sequence:Varian 2D DOSY with convection compensation (gradient stimulated echo), with the 90-Grad-90 option and 1.5 ms diffusion gradient length pules (called "DgsteSL_cc" in VnmrJ). Data processed in VnmrJ and corrected for non-uniform gradients. Attached spectra are processed in Mestrenova for clarity, and do not match the numbers shown in the above table.

4.2.4 Computational Investigations of the Reaction Mechanism

Despite the results of the non-linear effect study agreeing with the proposed monomeric Pd/PyOx catalyst, no formal exploration of the mechanism of this transformation has been reported. Our initial hypothesis concerning the mechanism of the Pd/PyOx-catalyzed asymmetric conjugate addition were well informed by the seminal work of Miyaura,[24] however, the heterogeneous nature of the reaction medium, undefined nature of the precise catalyst,[25] and complicating equilibrium of organoboron species make kinetic analysis and thorough mechanistic study extremely challenging.[26]

Previously, Houk performed density functional theory (DFT) calculations to investigate the mechanism of palladium-catalyzed conjugate addition of arylboronic acids to enones, explicitly studying a catalytic palladium(II)/bipyridine system in MeOH solvent similar to that developed by Lu.[12,27,28] Calculations indicated that the mechanism involves three steps: transmetallation, carbopalladation (i.e., alkene insertion), and protonation with MeOH. Monomeric cationic palladium complexes are the active species in the catalytic cycle. The carbopalladation is calculated to be the rate- and stereoselectivity-determining step (Scheme 4.3). Now, Houk and coworkers performed

DFT investigations on the catalytic cycle of reactions with the Pd/PyOx manifold and the effects of substituents and ligand on reactivity and enantioselectivity. The calculations were performed at the theoretical level found satisfactory in their previous study of the Pd/bipyridine system. Geometries were optimized with BP86[29] and a standard 6-31G(d) basis set (SDD basis set for palladium). Solvent effects were calculated with single point calculations on the gas phase geometries with the CPCM solvation model in dichloroethane. All calculations were performed with Gaussian 03.[30]

Scheme 4.3 Enantioselectivity-determining step in asymmetric conjugate addition of arylboronic acids to cyclic enones
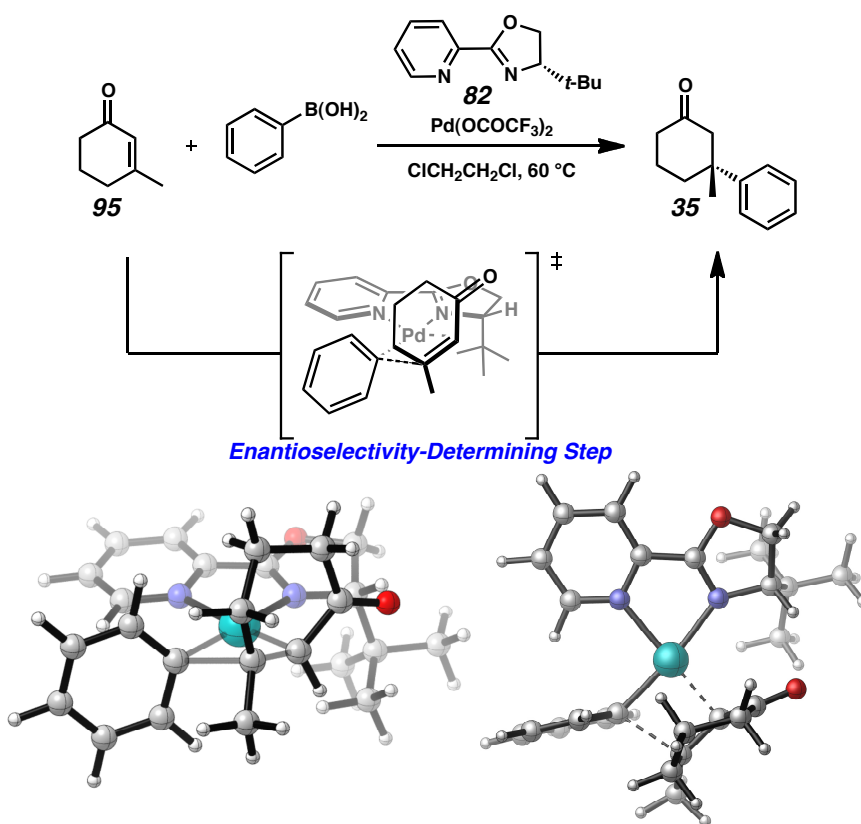
The computed potential energy surface for the catalytic cycle is shown in Figure 4.3. To simplify the computations of the mechanisms, a model ligand, in which the *t*-Bu group on the *t*-BuPyOx ligand was replaced by H, was used in the calculations of the mechanisms and the full ligand was used in the calculations of enantioselectivities which will be discussed below. Calculations on the reaction mechanism with the full ligand scaffold, however, generated a similar reaction diagram, and the rate- and stereo-determining steps were unchanged. The first step involves transmetallation of cationic Pd(II)-phenylborate complex **212** to generate a phenyl palladium complex. Transmetallation requires a relatively low free energy barrier of 15.6 kcal/mol (**213-ts**) with respect to complex **212** and leads to a phenyl palladium complex (**214**). Complex **214** undergoes ligand exchange to form a more stable phenyl palladium-enone complex **218**, in which the palladium binds to the enone oxygen atom. Complex **218** isomerizes to a less stable π complex **219** and then undergoes carbopalladation of the enone (**220-ts**) to form the new carbon–carbon bond. The carbopalladation step requires an activation free energy of 21.3 kcal/mol (**219 → 220-ts**), and is the stereoselectivity-determining step. The regioisomeric carbopalladation transition state **222-ts** requires 5.6 kcal/mol higher activation free energy than **220-ts**, indicating the formation of the α-addition compound **223** is unlikely to occur. Coordination of one water molecule to **221** leads to a water-palladium enolate complex **224**, and finally facile hydrolysis of **224** via **225-ts** affords product complex **226**. Liberation of the product **35** from **226** and coordination with another molecule of phenyl boronic acid regenerates complex **212** to complete the catalytic cycle. The computed catalytic cycle demonstrates some similarities with the Pd/bipyridine system in our previous computational investigation, which also involves

monomeric cationic palladium as the active species and a catalytic cycle of

transmetallation, carbopalladation, and protonation (with MeOH instead of H_2O). Houk

also considered an alternative pathway involving direct nucleophilic attack of the phenyl

boronic acid at the enone while the Pd catalyst is acting as a Lewis acid to activate the

enone and directs the attack of the nucleophile (**215-ts**, Figure 3). This alternative

pathway requires an activation free energy of 58.9 kcal/mol, 43.3 kcal/mol higher than

the transmetallation transition state **213-ts**. Thus, this alternative pathway was excluded

by calculations.

Figure 4.3   Computed potential energy surface of the catalytic cycle (shown in black), the
alternative direct nucleophilic addition pathway (via 9-ts, shown in blue), and the isomeric
carbopalladation pathway (via 16-ts, shown in green)
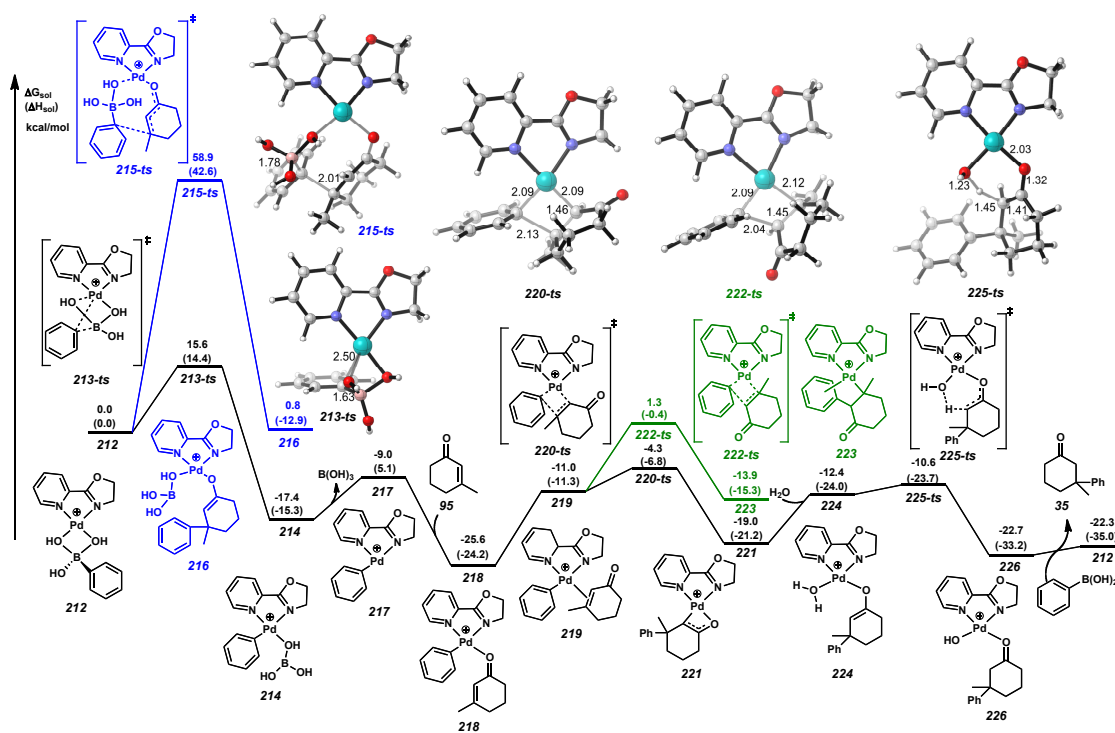
4.2.5 Experimental and Computational Investigations of the Enantioselectivities

With the aforementioned optimized reaction conditions and computational elucidation of the mechanism and stereoselectivity-determining transition states, Houk explored the effects of ligand and substrate on enantioselectivities by both experiment and computations. The enantioselectivity-determining alkene insertion step involves a four-membered cyclic transition state, which adopts a square-planar geometry. When a chiral bidentate ligand, such as (*S*)-*t*-BuPyOx, is employed, there are four possible isomeric alkene insertion transition states. The 3D structures of the alkene insertion transition states in the reaction of 3-methyl-2-cyclohexenone with (*S*)–*t*-BuPyOx ligand are shown in Figure 4.4. In **1-TS-A** and **1-TS-B**, the phenyl group is *trans* to the chiral oxazoline on the ligand, and in **1-TS-C** and **1-TS-D**, the phenyl group is *cis* to the oxazoline. **1-TS-A**, which leads to the predorminant (*R*)-product, is the most stable as the *t*-Bu group is pointing away from other bulky groups. **1-TS-C** leads to the same enantiomer, but with an activation enthalpy 2.6 kcal/mol higher than **1-TS-A**. The difference is likely to result from steric effects between the *t*-Bu on the ligand and the phenyl group, as indicated by the C-H and C-C distances labeled in Figure 4. **1-TS-B** and **1-TS-D** lead to the minor (*S*)-product, which are ~ 3 kcal/mol less stable than **1-TS-A** as a result of the repulsions between the *t*-Bu on the ligand and the phenyl group. In **1-TS-B**, the cyclohexenone ring is *syn* to the *t*-Bu group on the ligand. The shortest H–H distance between the ligand and the enone is 2.30 Å, suggesting some steric repulsions. In contrast, no ligand-substrate steric repulsions are observed in **1-TS-A**, in which the cyclohexenone is *anti* to the *t*-Bu. **1-TS-A** is also stabilized by a weak hydrogen bond between the carbonyl oxygen and the hydrogen geminal to the *t*-Bu group on the

oxazoline. The O–H distance is 2.16Å. Therefore, the enthalpy of **1-TS-B** is 2.3 kcal/mol higher than that of **1-TS-A**. This corresponds to an ee of 94%, which is very similar to the experimental observation (93%). Enantioselectivities were computed from relative enthalpies of the transition states. The selectivities computed from Gibbs free energies are very similar and are given in the experimental procedures section.

Figure 4.4 The optimized geometries of transition states in the enantioselectivity-determining alkene insertion step of the reaction of 3-methyl-2-cyclohexenone and phenyl boronic acid with (S)–t-BuPyOx ligand. Selected H–H, C–H, and O–H distances are labeled in Å
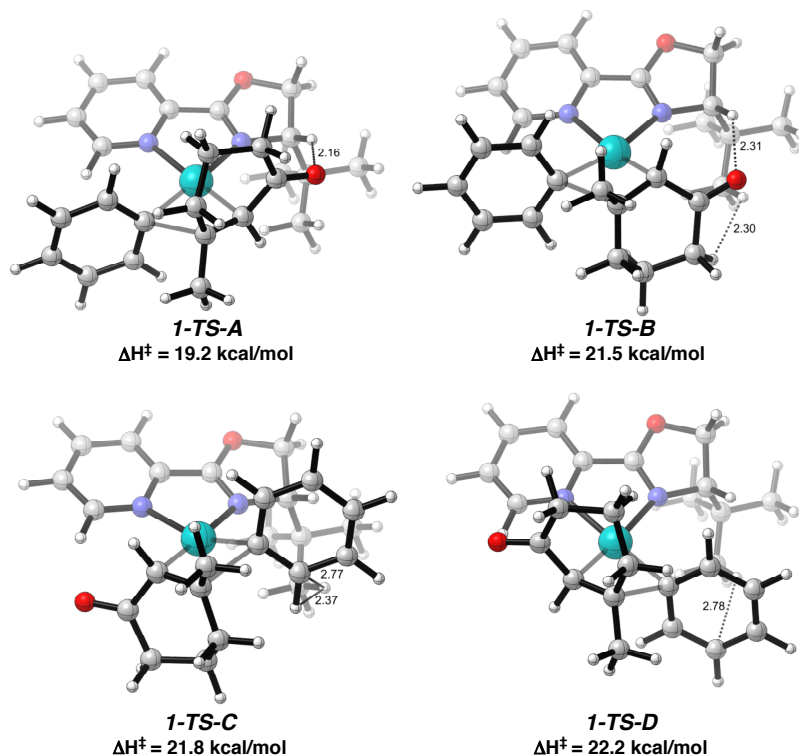
Houk then investigated the effects of substituents on the ligand, in particular, at the 4 position of the oxazoline. The activation enthalpies of four alkene insertion pathways and the computed and experimental ee for the reaction of 3-methyl-2-

cyclohexenone and phenyl boronic acid are summarized in Table 4.5. The *t*-Bu

substituted PyOx ligand is found to be the optimum ligand experimentally (Table 4.5,

entry 1). Replacing *t*-Bu with smaller groups, such as *i*-Pr, *i*-Bu, or Ph, dramatically

reduces the ee.

Table 4.5 Activation energies and enantioselectivities of alkene insertion with (S)-t-BuPyOx, (S)-i-PrPyOx, (S)-i-BuPyOx, and (S)-PhPyOx ligands
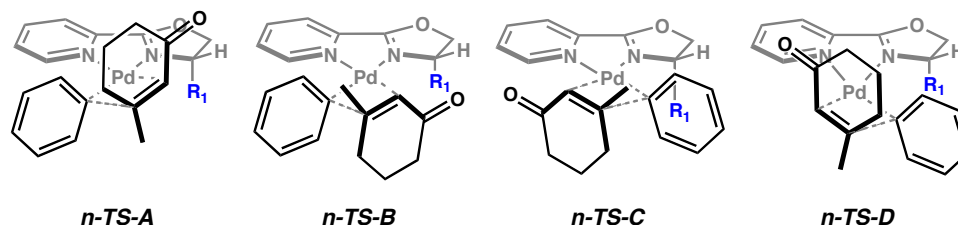
TS	R^1	ΔH$^{‡ a}$				ee ^{b}
		TS-A	**TS-B**	**TS-C**	**TS-D**	
1	*t*-Bu	**19.2**	**21.5**	21.8	22.2	94% [93%]
2	*i*-Pr	**18.6**	**19.7**	20.1	20.0	67% [40%]
3	*i*-Bu	**18.5**	**19.3**	20.4	20.4	52% [24%]
4	Ph	**18.0**	**19.0**	19.6	20.2	65% [52%]

^{a}The values are activation enthalpies in kcal/mol calculated at the BP86/6-31G(d)–SDD level and the CPCM solvation model in dichloroethane. ^{b}Experimental ee were obtained under standard conditions and are given in square brackets.

The bulky *t*-Bu substituent on the ligand is essential not only to discriminate the

diastereomeric transition states **1-TS-A** and **1-TS-B**, but also fix the orientation of the

ligand to point the chiral center *cis* to the cyclohexenone. The energy difference between

1-TS-C and **1-TS-D**, in which the chiral center on the ligand is *trans* to the

cyclohexenone, is diminished. When the (*S*)-*i*-PrPyOx ligand is used, the alkene insertion

transition states with phenyl *trans* to the oxazoline (**2-TS-A** and **2-TS-B**) are also

preferred. Thus, the enantioselectivity is determined by the energy difference between **2-TS-A** and **2-TS-B**. The (*R*)-product (via **2-TS-A**) is favored with a computed ee of 67%, slightly higher than the experimental ee (40%). The optimized geometries of **2-TS-A** and **2-TS-B** are shown in Figure 4.5 and the activation energies of all four transition states are shown in Table 4.5, entry 2. The *i*-Pr substituted ligand manifests via similar steric effects to (*S*)-*t*-BuPyOx, with, as expected, slightly weaker steric control. The lower enantioselectivity is attributed to the weaker steric repulsions between the *i*-Pr and the cyclohexenone in **2-TS-B** than those with the *t*-Bu in **1-TS-B**. The shortest distance between the hydrogen atoms on the ligand and the cyclohexenone is 2.35 Å in **2-TS-B**, slightly longer than the H–H distance in **1-TS-B** (2.30 Å). Less steric repulsions with the (*S*)-*i*-PrPyOx lead to 2.8 kcal/mol lower activation barriers for **2-TS-B** compared to **1-TS-B**. The ligand steric effects on the activation energies of the major pathway **TS-A** are smaller; the *i*-Pr substituted **2-TS-A** is only 0.6 kcal/mol more stable than the *t*-Bu substituted **1-TS-A**.

Figure 4.5 The optimized geometries of transition states in the enantioselectivity-determining alkene insertion step of the reaction of (a) 3-methyl-2-cyclohexenone and phenyl boronic acid with (S)-i-PrPyOx ligand; (b) 3-methyl-δ-2-pentenolide and phenyl boronic acid with (S)-t-BuPyOx ligand. Selected H–H, C–H, and O–H distances are labeled in Å

(a)

2-TS-A
$\Delta H^{\ddagger} = 18.6$ kcal/mol

2-TS-B
$\Delta H^{\ddagger} = 19.7$ kcal/mol

(b)

7-TS-A
$\Delta H^{\ddagger} = 16.7$ kcal/mol

7-TS-B
$\Delta H^{\ddagger} = 18.6$ kcal/mol
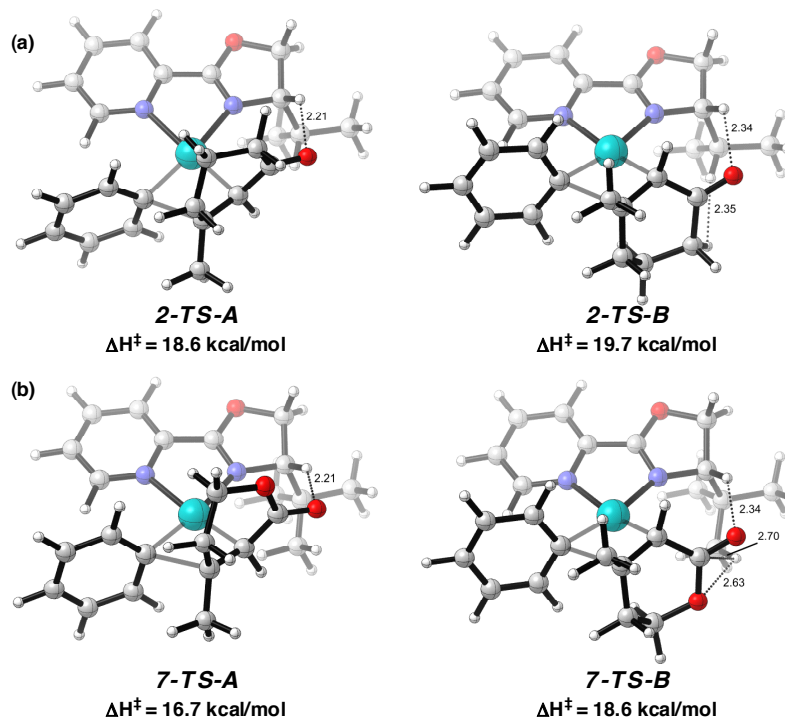
Electronically differentiated PyOx ligands were also studied, and the results are summarized in Table 4.6. Electron-withdrawing or donating groups at the 4-position of the PyOx ligand showed minimal effects on the activation barriers, and were calculated to have minimal effect on product ee. With the electron-withdrawing CF_3 and the electron-donating OCH_3 on the 4-position of the ligand, the activation enthalpies of alkene insertion increase by only 0.3 kcal/mol and 0.1 kcal/mol, respectively. The calculated ee are essentially identical among these three ligands. Experimentally, depressed ee was observed with both the 4-CF_3 and the 4-OCH_3 substituted ligands (entries 5 and 6). This

confirms that the enantioselectivity is mainly attributed to the ligand/substrate steric

repulsions.

Table 4.6 Remote ligand substituent effects on activation energies and enantioselectivities of alkene insertion

n-TS-A *n-TS-B* *n-TS-C* *n-TS-D*
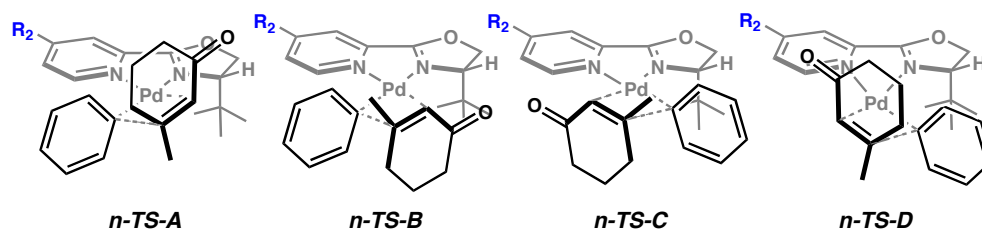
TS	R^2	$\Delta H^{\ddagger\, a}$				ee [b]
		TS-A	**TS-B**	**TS-C**	**TS-D**	
1	H	**19.2**	**21.5**	21.8	22.2	94% [93%]
5	CF$_3$	**19.5**	**21.7**	21.8	22.3	93% [81%]
6	OCH$_3$	**19.3**	**21.5**	21.5	22.2	93% [78%]
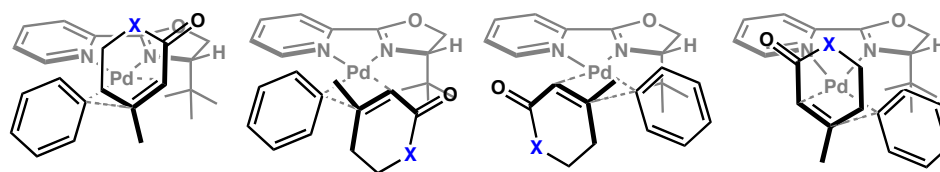
[a]The values are activation enthalpies in kcal/mol calculated at the BP86/6-31G(d)-SDD level and the CPCM solvation model in dichloroethane. [b]Experimental ee are given in square brackets.

The transition state structures shown in Figure 4.5 indicate that the steric control

mainly arises from the repulsion of the C$_{\alpha'}$ hydrogens on the cyclohexenone with the

ligand. Houk then investigated the effects of substitution at the α' position and

replacement of the CH$_2$ group with O. The reactivity and enantioselectivity of the

reactions of lactone (Table 4.7, entry 7) and α',α'-dimethylcyclohexenone (entry 8) with

the (*S*)-*t*-BuPyOx ligand were computed. The enantioselectivity of lactone is predicted to

be lower than cyclohexenone. The enthalpy of **7-TS-B** is 1.8 kcal/mol higher than that of

7-TS-A, corresponding to an ee of 88%. Experimentally, the ee of the lactone product is

59%, also significantly lower than that with cyclohexenone. The optimized geometries of

7-TS-A and **7-TS-B** are shown in Figure 4.5b. Replacing the CH$_2$ group with O decreases the ligand–substrate steric repulsion in **7-TS-B** is smaller than that in **1-TS-B**. This results in decreased enantioselectivity.

Methyl substitution at the α' position of cyclohexenone increases the steric repulsion with the *t*-Bu group on the ligand. Computations predicted increased enantioselectivity with α',α'–dimethylcyclohexenone (99% ee, Table 4.7, entry 8).[31] However, experimentally, the ee is comparable with the reaction of 3-methylcyclohexenone.

Table 4.7 Activation energies and enantioselectivities of alkene insertion with substrates varying at the α'-position

TS	X	ΔH‡ ^{a}				ee ^{b}
		TS-A	**TS-B**	**TS-C**	**TS-D**	
1	CH$_2$	**19.2**	**21.5**	21.8	22.2	94% [93%]
7	O	**16.7**	**18.6**	19.4	19.6	88% [57%]
8	C(CH$_3$)$_2$	**17.9**	22.0	20.0	**20.8**	99% [90%]

^{a}The values are activation enthalpies in kcal/mol calculated at the BP86/6-31G(d)-SDD level and the CPCM solvation model in dichloroethane. ^{b}Experimental ee are given in square brackets. Experimental isolated yields: TS-1: 99%, TS-7: 49%, TS-8: 9%.

Houk also considered the electronic effects of arylboronic acids on enantioselectivity (Table 4.8). Computations predicted that *para*-electron-withdrawing substituents lead to increases in the activation barrier in alkene insertion, probably due to the electrophilicity of the β-carbon of the enone, and thus are predicted to afford slightly decreased enantioselectivities. Both *para*-acetylphenylboronic acid (**9-TS-A**) and *para*-

trifluoromethylphenylboronic acid (**10-TS-A**) are predicted to react with 92% ee. However, both excellent enantioselectivities (96% ee) and excellent yields (99% isolated yield) are observed experimentally. Thus, the electronic effects of phenyl substituents on enantioselectivities are minimal, though slightly increased enantioselectivities are observed experimentally with the use of electron-withdrawing substituents.

Table 4.8 Activation energies and enantioselectivities of alkene insertion with various boronic acids

TS	R³	ΔH‡ ᵃ				ee ᵇ
		TS-A	**TS-B**	**TS-C**	**TS-D**	
1	H	**19.2**	**21.5**	21.8	22.2	94% [93%]
9	CH₃CO	**21.6**	**23.7**	24.5	24.8	92% [96%]
10	CF₃	**21.3**	**23.4**	23.6	24.2	92% [96%]

ᵃThe values are activation enthalpies in kcal/mol calculated at the BP86/6-31G(d)-SDD level and the CPCM solvation model in dichloroethane. ᵇExperimental ee are given in square brackets. Experimental isolated yields: TS-1: 99%, TS-9: 1%, TS-10: 99%, TS-11: 99%.

Permutations of the pyridinooxazoline ligand framework corroborate the calculated data and suggest that a number of factors affect enantioselectivity. First, the steric demand of the chiral group on the oxazoline greatly impacts the observed enantioselectivity in the reaction (Table 4.9). Only *t*-BuPyOx (**82**) yields synthetically tractable levels of enantioselectivity, while the less sterically demanding *i*-PrPyOx (**227**), PhPyOx (**228**), and *i*-BuPyOx (**229**) all exhibit greatly diminished selectivity. Oxazoline substitution patterns also affect enantioselectivity. Substitution at the 4-position appears to be required for high selectivity, as substitution at the 5-position yields practically no

enantioselectivity (ligand **230**). Electronic variation in the PyOx framework was observed

to have a large effect on the *rate* of the reaction but, disappointingly, led to depressed

stereoselectivity. CF$_3$-*t*-BuPyOx (**231**) afforded the conjugate addition product in 99%

yield and 81% ee. Surprisingly, MeO-*t*-BuPyOx (**232**) afforded the product in similar

yield and only 78% ee. Finally, substitution at the 6-position of the pyridine (ligands **233**

and **234**) greatly diminished both reactivity and selectivity, perhaps due to hindered

ligand chelation to palladium.

Table 4.9 Enantioselectivity trends in pyridinooxazoline and related ligand frameworks [a]
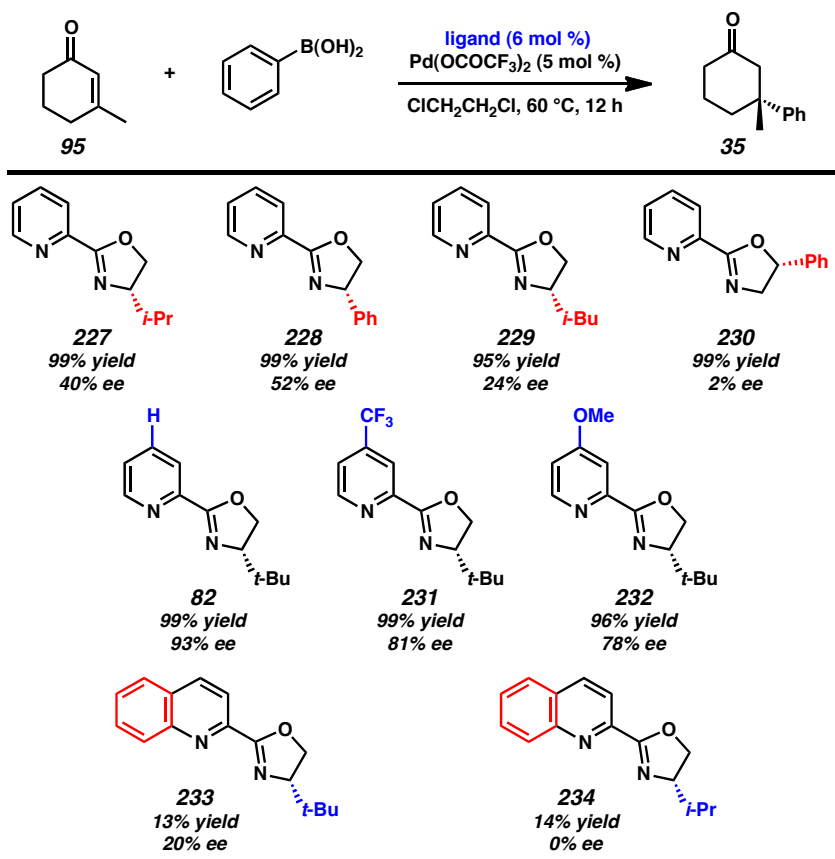
[a]Conditions: 3-methylcyclohexen-2-one (0.25 mmol), phenylboronic acid (0.5 mmol),

ClCH$_2$CH$_2$Cl (1 mL). Yields are isolated yields, ee determined by chiral HPLC.

Thus, we have concluded that enantioselectivity is controlled by the steric repulsion between the substituent on the chiral pyridinooxazoline ligand and the cyclohexyl ring. The bulkier *t*-Bu substituent on the (*S*)-*t*-BuPyOx ligand leads to greater enantioselectivity than the reactions with (*S*)-*i*-PrPyOx or (*S*)-PhPyOx. Similarly, substrates with less steric demand adjacent the carbonyl exhibit lower enantioselectivities; for example the reaction of a lactone substrate (Table 4.7, TS-7) yields lower enantioselectivity due to smaller repulsions between the lactone oxygen and the *t*-Bu group.

4.2.6 Experimental Investigation of Arylpalladium(II) Intermediates and Formation of the Key C–C Bond

Experiments aiming to corroborate the calculated mechanism have been performed. We sought to observe the formation of the key C–C bond between an arylpalladium(II) species and the enone substrate in the absence of exogenous phenylboronic acid. Complexes **235** were synthesized as an intractable mixture of isomers, and were treated with AgPF$_6$ *in situ* to generate the [(PyOx)Pd(Ph)]$^+$ cation. Gratifyingly, complexes **235** serve as a competent precatalyst at 5 mol % loading, and affords ketone **35** in 96% yield and 90% ee (Table 4.10, entry 1). Varying the amount of complex utilized in proportion with phenylboronic acid, however, leads to significant production of biphenyl above 5 mol % (entries 2–5). Utilizing even 25 mol % (entry 2) resulted in significant increase in biphenyl production (16% yield), and reduction in yield of the desired ketone **35** to 79%. Increasing complex loadings to 45 and 65 mol % (entries 3 and 4) leads to negligible production of ketone **35**, and nearly quantitative

formation of biphenyl relative to catalyst loading. Furthermore, attempts to use the complex as a stoichiometric reagent in the place of $PhB(OH)_2$ lead to no observed product (entry 5), and exclusive formation of biphenyl. We hypothesize that quantitative generation of the reactive arylpalladium cation intermediate in high relative concentration leads quickly to disproportionation and formation of biphenyl and palladium(0). Omission of the $AgPF_6$ in favor of 30 mol % NH_4PF_6 leads to isolation of only 22% yield of the conjugate addition product (entry 6). Finally, a control experiment demonstrates that $AgPF_6$ is incapable of catalyzing the reaction itself (entry 7).[32] This control further supports the computational results, which indicate a transmetallation-based mechanism as opposed to a Lewis acid-catalyzed pathway.

Table 4.10 Arylpalladium(II) catalyzed conjugate addition [a]

entry	complex 29 (mol %)	AgPF₆ (mol %)	PhB(OH)₂ (mol %)	yield (%) 3	yield (%) biphenyl
1	5	10	100	96	3
2	25	50	80	79	16
3	45	90	60	11	53
4	65	130	40	5	58
5	105	210	0	0	87
6[b]	5	0	200	22	0
7	0	20	200	0	0

[a] Conditions: 3-methylcyclohexen-2-one (0.25 mmol), phenylboronic acid (equiv as stated), $ClCH_2CH_2Cl$ (1 mL). Yields are isolated yields, ee determined by chiral HPLC. [b] Reaction performed with 30 mol % NH_4PF_6

Concerned by our inability to observe consistent product formation at 40 °C, we sought alternative experimental verification that a putative cationic arylpalladium(II) species is capable of reacting to form conjugate addition products. Thus, we performed the stoichiometric reaction of the isomeric phenyl palladium iodide complexes (**235**) with AgPF$_6$ and 3-methylcyclohexenone at cryogenic temperatures, allowing the mixture to warm slowly to room temperature before quenching with trifluoroethanol.[33] We observed both conjugate addition product and biphenyl, with the desired adduct (**35**) isolated in 30% yield (Scheme 4.4a). Curiously, the conjugate addition adduct was isolated in only 55% ee. We considered that the isomeric mixture of phenyl palladium iodide isomers formed configurationally stable cationic species at cryogenic temperature.[34,] Repeating the experiment, we substituted triphenylphosphine for methylcyclohexenone and observed the reaction at low temperature utilizing ^{1}H and ^{31}P NMR (Scheme 4.4b). Indeed, two ^{31}P signals corresponding to phosphine-bound palladium(II) species (**236**) were observed at 28 and 34 ppm. No isomerization was observed upon warming the isomeric mixture to room temperature.[35] Indeed, we were able to isolate and characterize the mixture of arylpalladiumphosphine cations. With evidence for the configurationally stable arylpalladium cation, we rationalized the observed 55% ee for the direct reaction of mixture **234** with methylcyclohexenone corresponds directly to the isomeric ratio of the complex: a ratio of 1.3:1 represents a 56:44 ratio of isomers. Assuming that the major isomer reacts with 92% ee, and the minor isomer reacts with no stereoselectivity to give racemic products,[36] a net stereoselectivity of 53.7% ee would be predicted for the product. Presuming configurational stability of the arylpalladium(II) cation as suggested by the triphenylphosphine trapping experiment, the diminished enantioselectivity

observed in this result is unsurprising. Thus, we have obtained experimental verification

of the key C–C bond forming event of the Pd/PyOx asymmetric conjugate addition

occurring from a quantitative generated arylpalladium(II) cation in the presence of enone

substrate and absence of an exogenous arylboronic acid.

Scheme 4.4 (a) Direct formation of C–C bond from arylpalladium(II) cation. (b) Triphenylphosphine

trapping experiments demonstrates configurational stability of arylpalladium cation
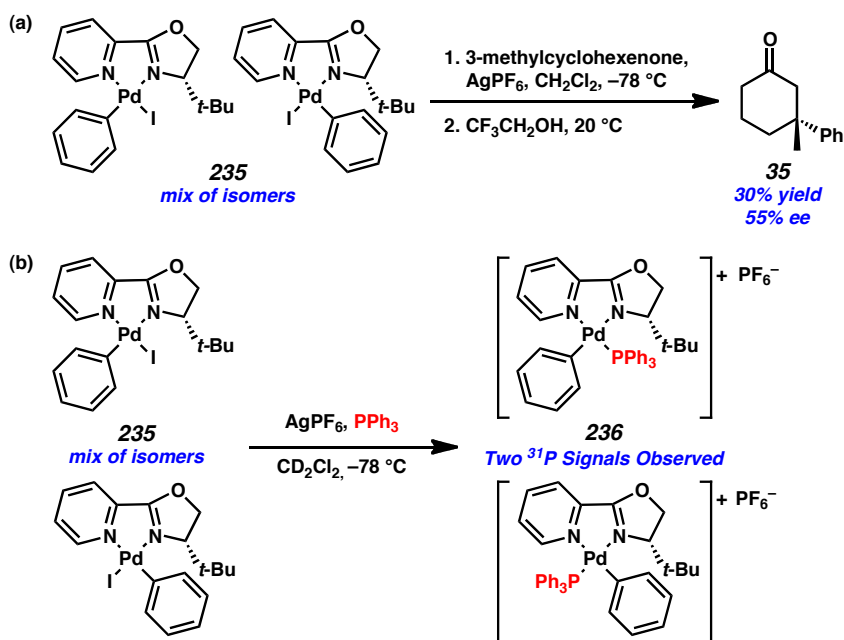
Attempts to optimize the transition state of the isomerization of the tricoordinated

cationic phenylpalladium(II) complexes **217** and **217'** failed. Houk then performed a scan

of the reaction coordinates by calculating structures with fixed N-Pd-C angle. The results

are summarized in Figure 4.6. Based on the scan of the reaction coordinate (i.e., N-Pd-C

angle), they estimated the activation barrier for the isomerization of **217** to **217'** is higher

than 10 kcal/mol with respect to **217**. Thus, the isomerization has higher activation

energy than subsequent alkene insertion (**220-ts** is only 1.7 kcal/mol less stable than **217**).

*Figure 4.6 Scan of the reaction coordinate of the interconversion between **217** and **217′**. The*

energies in kcal/mol are calculated at the BP86/6-31G(d)-SDD level without solvent corrections
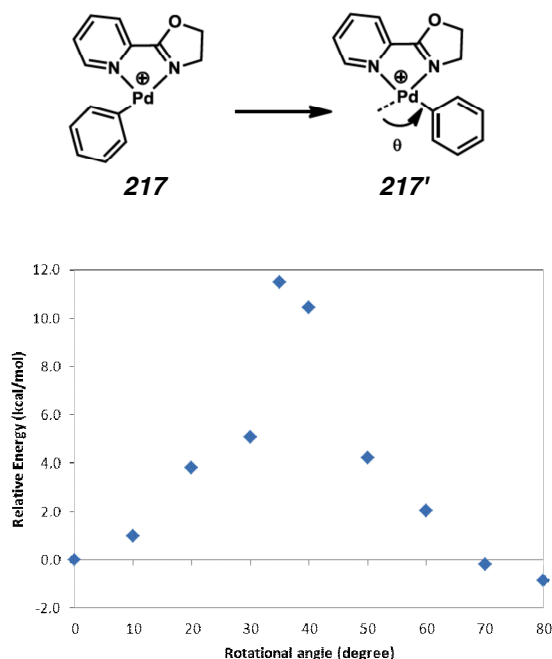
Houk attempted to compute the activation energies of transmetallation leading to

cis and *trans* cationic phenylpalladium(II) complexes (**217** and **217'**) with the (*S*)-*t*-

BuPyOx ligand. However, the geometry optimizations cannot locate the transmetallation

transition states. We then performed a scan of the forming Pd–C(phenyl) bond in the *cis*

and *trans* pathway (Table 4.11). In **237-ts**, the phenyl is *trans* to the oxazoline on the

ligand. In **238-ts**, the phenyl is *cis* to oxazoline. We fixed the forming Ph-C bond distance

in both structures to 2.20, 2.35, 2.40, 2.45, 2.50, 2.55 and 2.60 Å, respectively. In all

distances, the *cis* structure **238-ts** are at least 2.0 kcal/mol less stable than the *trans*

isomer **237-ts**. This indicates the formation of the *trans* product is favored in transmetallation. In the *cis* pathway, the phenyl is adjacent to the bulky *t*-Bu group on the ligand, and the transition state **238-ts** is destabilized by the steric repulsions between *t*-Bu and Ph.

Table 4.11 Scan of the forming Pd–C(phenyl) bond in pathways **237-ts** *and* **238-ts**

ᵃ　　　　**237-ts**　　　　　　　　**238-ts**
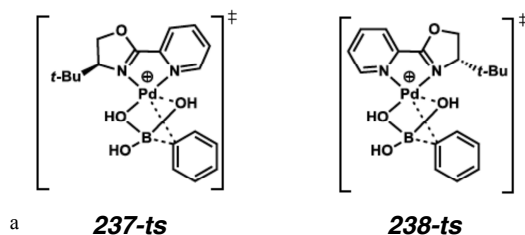
R_{Pd-C}	$E_{237\text{-ts}}$	$E_{238\text{-ts}}$	ΔE
2.20	5.6	9.5	3.9
2.35	8.3	11.3	3.0
2.40	8.8	11.9	3.0
2.45	9.5	12.5	3.0
2.50	10.1	13.1	3.0
2.55	10.8	13.6	2.7
2.60	11.6	14.0	2.4

ᵃThe values are energies in kcal/mol calculated at the BP86/6-31G(d)-SDD level without solvent corrections

4.2.7 Attempts to rationalize the importance of arylboronic acid additives

A small screen of alternative boron species was undertaken to explore the scope of the boron nucleophile beyond the known reactivity of arylboronic acids and their dehydrated forms, triarylboroxines (Table 4.12). Tetraarylborates (entry 1) were poor

substrates, and afforded trace product and rapid precipitation of palladium black. Potassium trifluoroborates also performed poorly (entry 2), though their efficacy could be increased by addition of additional equivalents of water (entry 3), though not by the presence of other proton sources, such as *ortho*-methylphenylboronic acid (entry 4). Additionally, an experiment was performed utilizing the cationic arylpalladium(II) species generated from the treatment of complex **235** with AgPF$_6$ under dilute conditions designed to mimic the catalytic reaction. Trace yield of the product was observed in the absence of boronic acid. Curiously, a comparable concentration of **235** in solution with enone and AgPF$_6$ produces high yield of ketone **35** in the presence of phenylboronic acid (Table 4.10, entry 1). Other phenyl sources, such as n-Bu$_3$SnPh or NaOSiMe$_2$Ph, produced no observable conjugate addition reaction, even at elevated temperature or in the presence of an unreactive boronic acid (entries 6–9). Presumably, these other organometallic phenyl reagents require additional activation to undergo transmetallation with palladium, such as fluoride additives in the case of dimethylphenyl sodium silanolate. Brief efforts to identify these conditions and additives yielded little more than trace conversion to the desired product.

Table 4.12 Alternative Boron Sources Screen

entry	phenyl source	boronic acid	H$_2$O (equiv.)	yield (%)	ee (%)
1	NaBPh$_4$	--	5	trace	--
2	KPhBF$_3$	--	5	19	91
3	KPhBF$_3$	--	25	46	90
4	KPhBF$_3$	*o*-methylphenyl	5	15	91
5[a]	(PyOx)Pd(Ph)(I)/AgPF$_6$	--	5	trace	--
6[b]	*n*-Bu$_3$SnPh	--	0	trace	--
7[b]	*n*-Bu$_3$SnPh	*o*-methylphenyl	0	trace	--
8[b]	NaOSiMe$_2$Ph	--	0	--	--
9[b]	NaOSiMe$_2$Ph	*o*-methylphenyl	0	--	--

Conditions: enone (0.25 mmol), phenyl source (0.50 mmol), NH$_4$PF$_6$ (0.075 mmol), H$_2$O (1.25 mmol), ClCH$_2$CH$_2$Cl (1 mL). [a]Reaction performed with Pd complex 29 (0.125 mmol), AgPF$_6$ (0.250 mmol), ClCH$_2$CH$_2$Cl (10 mL). [b]Reactions performed at 80 °C.

Next, Houk investigated if coordination of phenylboronic acid will activate the enone in the alkene insertion step (**220-ts**, Figure 4.3). Two different binding modes between the alkene insertion transition state **220-ts** and phenylboronic acid are considered in the calculations (Figure 4.7): the boronic acid acting as a hydrogen bonding donor (**239-ts-B**) and as a Lewis acid that the B atom is coordinated with the enone oxygen (**239-ts-C**). **239-ts-B** is 9.1 kcal/mol less stable than the uncoordinated **220-ts** in terms of Gibbs free energy. The structure of **239-ts-B** is shown in Figure 4.7. Geometry optimization of **239-ts-C** was not successful and always leading to dissociation of the B–O bond, indicating the interaction between B and O is not stabilizing. These results suggest that binding with boronic acid does not accelerate the alkene insertion, and are

not particularly surprising given that cationic organometallic palladium complexes are known to rapidly bind and insert olefins at ambient temperature. Furthermore, these calculations support our hypothesis that the boronic acid serves a secondary role in stabilizing the cationic palladium(II) intermediates along the hypothetical catalytic cycle, and prevent rapid disproportionation and formation of biphenyl as is observed with reactions seeking to use isolated arylpalladium(II) complex **235** as the only aryl source in the reaction medium (Table 4.10, entry 5).

*Figure 4.7 Activation free energies of alkene insertion with boronic acid coordination. Energies are with respect to the Pd(PyOx)Ph–enone complex **219***
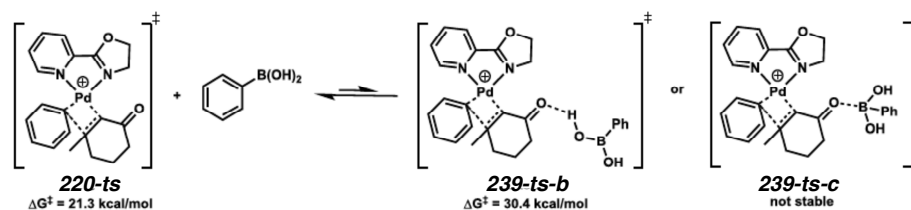
4.3 Summary and discussion

Several experimental results have been described that support the DFT-calculated mechanism for the Pd/PyOx-catalyzed asymmetric conjugate addition of arylboronic acids to cyclic enone (Figure 4.4); specifically, the role of the palladium catalyst has been addressed. Calculations and previous experimental work by Miyaura on palladium-catalyzed conjugate addition suggest that a transmetallation event occurs to transfer the aryl moiety from the boronic acid species to the palladium catalyst.[4] Houk's calculations indicated that the Pd/PyOx system operates under a similar manifold, and demonstrated a significant energy difference (transmetallation is favored by over 40 kcal/mol, Figure 4.4)

between the potential roles of the palladium catalyst, suggesting that the role of the palladium species is not simply that of a Lewis acid. Furthermore, it is difficult to rationalize the high degree of enantioselectivity imparted by the chiral palladium catalyst if it is assumed that the metal acts only as a Lewis acid and is not directly mediating the key C–C bond-forming step.[37] Finally, a number of Lewis- and π–acidic metal salts were substituted for palladium with no product observed, further indicating that palladium-catalyzed conjugate addition is likely not a Lewis acid-catalyzed process.[38]

While highly Lewis-acidic, the role of cationic palladium(II) is to provide a vacant coordination site for the enone substrate to approach the catalyst. The presence of a cationic intermediate is further supported by the observed rate acceleration of non-coordinating anionic additives such as PF_6^- and BF_4^- salts (Table 4.1). Conversely, the addition of coordinating anions, such as chloride, inhibited the reaction (Table 4.1, entry 1). This counterion effect was evident even from choice of palladium(II) precatalysts.[13] For instance, $Pd(MeCN)_2Cl_2$ was not a suitable precatalyst, nor were any palladium(II) halides. Additionally, $Pd(OAc)_2$ only afforded modest yield of conjugate adducts, whereas the less coordinating counterion present in $Pd(OCOCF_3)_2$ afforded complete conversion.

Satisfied that the palladium catalyst was not acting as a Lewis acid, we next sought to demonstrate the viability of the hypothesized arylpalladium(II) species as a catalyst (Table 4.10, entries 1–5). While serving as a suitable precatalyst under reaction conditions, arylpalladium(II) mixture **235** failed to facilitate the conjugate addition reaction when used in stoichiometric quantities in the presence of $AgPF_6$ (entry 5). We rationalize this outcome to be the result of the highly reactive nature of the quantitatively

generated arylpalladium(II) cation. Significant biphenyl formation– occurring even under dilute conditions representative of the catalytic reaction itself– suggest that alternative reaction pathways, such as disproportionation, readily out compete the desired insertion reaction. This reactive nature of the arylpalladium(II) cation led us to propose performing the stoichiometric reactions at low temperatures (Scheme 4.4). Successfully demonstrating that the key C–C bond could be generated, albeit in modest yield, from (PyOx)Pd(Ph)(I) (**235**) corroborates both the precise role of the arylpalladium(II) cation in the calculated mechanism as well as the transition state put forth in the calculations. However, the modest yield of this process and requisite cryogenic temperatures prompted, again, consideration of the role of the arylboronic acid.[39] Calculations suggest that the presence of boronic acids as Lewis basic entities may serve to stabilize these reactive intermediates under the reaction conditions (Figure 4.3, cationic arylpalladium **217**).[40] This suggestion is consistent with the successful use of arylpalladium(II) mixture **235** as a precatalyst in the presence of arylboronic acids (Table 4.10, entry 1). Calculations rule out the use of boronic acid further activating the enone, either as a hydrogen bond donor or Lewis acid (Figure 4.6).

Lastly, water (or another proton source) is required for efficient turnover of the reaction. Considerations of reaction scale (Scheme 4.2) and deuterium incorporation experiments (Figure 4.1) suggest that water is the likely protonation agent, despite numerous other protic sources in the heterogenous reaction mixture. Attempts to use other, miscible proton sources (MeOH, phenol, *t*-BuOH, etc.) typically resulted in 10–15% less enantioselectivity observed.[41] 2,2,2-Trifluoroethanol can be successfully substituted for water with minimal loss of enantioselectivity, however it affords no

supplementary benefit and water is the preferred additive for all reactions.[26] Water in combination with NH_4PF_6 serves to facilitate milder reaction conditions (Table 4.2), which in turn greatly increases the synthetic scope with respect to challenging arylboronic acid nucleophiles (Table 4.3). Synthetic yields were observed to double in many cases, greatly increasing the utility of these transformations. The functional group tolerance of the Pd/PyOx system is unprecedented for asymmetric conjugate addition; it encompasses a wide array of halides, carbonyl functional groups, protected phenols, acetamides, free hydroxyl groups, and even nitro groups. Many of these groups are incompatible with traditional rhodium- and copper-catalyzed conjugate additions due to the reactivity with the nucleophiles used or the strong coordination of the functional group to the metal catalyst.

The combined results described herein have allowed us to put forth the following catalytic cycle (Figure 4.8). The cationic catalyst, represented as (PyOx)Pd(X)(L) (**240**), undergoes transmetallation with an arylboronic acid to yield cationic (PyOx)Pd(Ar)(L) (**241**). Substrate coordination forms cationic arylpalladium(II) **242**, which undergoes rate and enantioselectivity-determining insertion of the aryl moiety into the enone π-system to afford C-bound palladium enolate **243**. Tautomerization to the O-bound palladium enolate (**244**), or direct protonolysis of the C-bound enolate (**243**), liberates the conjugate addition product (**35**) and regenerates a cationic palladium(II) species for reentry into the catalytic cycle.

Figure 4.8 Proposed catalytic cycle for Pd/PyOx-catalyzed conjugate addition of arylboronic acids to cyclic enones
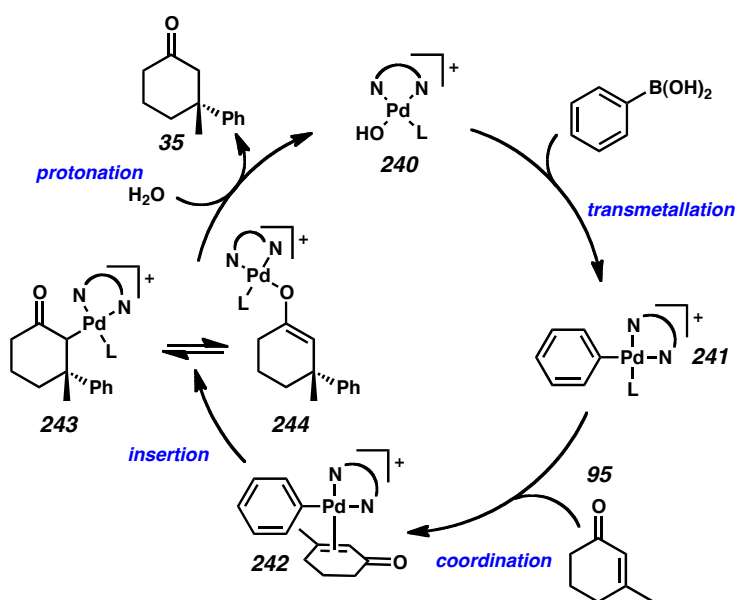
4.4 Conclusions

In conclusion, we have reported experimental and computational results that corroborate a single PyOx ligand/metal complex as the active catalytic species in the palladium-catalyzed asymmetric conjugate addition of arylboronic acids to enones for the construction of quaternary stereocenters. Houk has used computational models to rule out a suggested alternative mechanism in which the palladium catalyst is acting as a Lewis acid to activate the enone. The preferred mechanism involves formal transmetallation from boron to palladium, rate- and enantioselectivity-determining carbopalladation of the enone olefin by a cationic palladium species, and protonolysis of the resulting palladium-enolate. We have taken advantage of these mechanistic insights to develop a modified reaction system whereby the addition of water and ammonium hexafluorophosphate increase reaction rates, and can facilitate lower catalyst loadings. The modified conditions have opened the door to new substrate classes that were inaccessible by the

initially published reaction conditions. Furthermore, we have demonstrated that this operationally simple reaction is tolerant of ambient atmosphere and capable of producing enantioenriched, β-quaternary ketones on multi-gram scale. The steric and electronic effects of the boronic acid and enone substrates and the ligand on enantioselectivities were elucidated by a combined experimental and computational investigation. The enantioselectivity is mainly controlled by the steric repulsion of the *t*-Bu substituent of the oxazoline on the ligand and the $C_{\alpha'}$ position hydrogens of the cyclohexenone substrate in the alkene insertion transition state. Further investigations of both the scope of this transformation and its application toward natural product synthesis are current underway in our laboratories.

4.5 Experimental Procedures

4.5.1 Materials and Methods

Unless otherwise stated, reactions were performed with no extra precautions taken to exclude air or moisture. Air and moisture sensitive reactions were carried out under an atmosphere of argon using Schlenk and glovebox techniques. Diethyl ether, hexanes, benzene and toluene were dried and deoxygenated by passing through columns packed with activated alumina and Q5, respectively. Deionized water was purified with a Barnstead NANOpure Infinity UV/UF system. Dichloroethane was dried by stirring over CaH_2 and subsequent distillation, followed by deoxygenation by three freeze–pump–thaw cycles. Deuterated solvents were dried by distillation from CaH_2 (CD_2Cl_2) and deoxygenated by three freeze-pump-thaw cycles. Commercially available reagents were used as received from Sigma Aldrich unless otherwise stated. Enone substrates were

purchased from Sigma Aldrich (3-methylcyclohexenone, 2-cyclohexene-1-one, chromone) or prepared according to literature procedure.[42] Pyridinooxazoline ligands were synthesized according to literature procedures.[43] Iodobenzene was obtained from Sigma Aldrich and purified by distillation and deoxygenated by three freeze–pump–thaw cycles. $AgPF_6$ was obtained from ABCR and used without further purification. Reaction temperatures were controlled by an IKAmag temperature modulator. Thin-layer chromatography (TLC) was performed using E. Merck silica gel 60 F254 precoated plates (250 nm) and visualized by UV fluorescence quenching, potassium permanganate, or *p*-anisaldehyde staining. Silicycle Silia*Flash* P60 Academic Silica gel (particle size 40-63 nm) was used for flash chromatography. Analytical chiral HPLC was performed with an Agilent 1100 Series HPLC utilizing a Chiralcel OJ column (4.6 mm x 25 cm) obtained from Daicel Chemical Industries, Ltd with visualization at 254 nm and flow rate of 1 mL/min, unless otherwise stated. Analytical chiral SFC was performed with a JASCO 2000 series instrument utilizing Chiralpak (AD-H or AS-H) or Chiralcel (OD-H, OJ-H, or OB-H) columns (4.6 mm x 25 cm), or a Chiralpak IC column (4.6 mm x 10 cm) obtained from Daicel Chemical Industries, Ltd with visualization at 210 or 254 nm. ^{1}H and ^{13}C NMR spectra were recorded on a Varian Inova 500 (500 MHz and 125 MHz, respectively) and a Varian Mercury 300 spectrometer (300 MHz and 75 MHz, respectively). Data for ^{1}H NMR spectra are reported as follows: chemical shift (δ ppm) (multiplicity, coupling constant (Hz), integration). Data for ^{1}H NMR spectra are referenced to the centerline of $CHCl_3$ (δ 7.26), CD_2Cl_2 (δ 5.32), or $C_2D_4Cl_2$ (δ 3.72) as the internal standard and were reported in terms of chemical shift relative to Me_4Si (δ 0.00). Data for ^{13}C NMR spectra were referenced to the centerline of $CDCl_3$ (δ 77.0), CD_2Cl_2

(δ 53.8), or C₂D₄Cl₂ (δ 43.6)and were reported in terms of chemical shift relative to Me₄Si (δ 0.00). Infrared spectra were recorded on a Perkin Elmer Paragon 1000 Spectrometer and are reported in frequency of absorption (cm⁻¹). High resolution mass spectra (HRMS) were obtained on an Agilent 6200 Series TOF with an Agilent G1978A MultiMode source in electrospray ionization (ESI), atmospheric pressure chemical ionization (APCI) or mixed (MultiMode ESI/APCI) ionization mode. Optical rotations were measured on a Jasco P-2000 polarimeter using a 100 mm path-length cell at 589 nm.

4.5.2 Preparation of compounds

(*S*)-4-(*tert*-butyl)-2-(pyridin-2-yl)-4,5-dihydrooxazole (82).
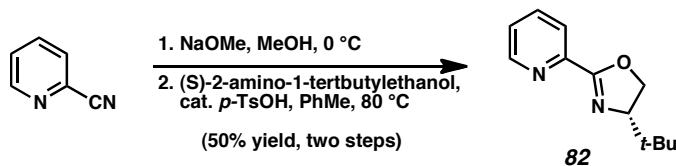
This route is amenable to smaller batches of ligand synthesis. Adapted from Brunner. H.; Obermann. U. *Chem. Ber*. **1989**, *122*, 499–507.

A flame-dried round bottom flask was charged with a stir bar and MeOH (110 mL). Sodium metal ingot (295 mg, 12.8 mmol, 0.1 equiv) was cut with a razor into small portions, washed in a beaker of hexanes and added in 5 portions over 5 min. The reaction mixture was stirred vigorously until no sodium metal remained, at which time it was cooled to 0 °C in an ice/water bath. At this time, 2-cyanopyridine (13.0 g, 125 mmol, 1.0 equv) was added dropwise, and the clear, colorless reaction mixture was allowed to warm to ambient temperature and stir. When all the starting material is consumed as indicated

by TLC analysis (50% EtOAc/Hexanes, *p*-anisaldehyde stain), the reaction was cooled to

0 °C in an ice/water bath and quenched by dropwise addition of glacial AcOH (1 mL).

The crude reaction mixture was concentrated *in vacuo*, redissolved in CH_2Cl_2 (100 mL)

and washed with brine (2 x 50 mL). The organic phase was dried ($MgSO_4$), concentrated

in vacuo, and dried under high vacuum for 1 h. The resulting crude methoxyimidate (light

yellow oil) was suitable for use in the next step without further purification. To a flame-

dried round bottom flask charged with a stir bar was added crude methoxyimidate (2.55

g, 18.7 mmol, 1.0 equiv), (*S*)-*tert*-leucinol (2.10 g, 17.9 mmol, 0.96 equiv) toluene (100

mL), and *p*-TsOH•H_2O (167 mg, 0.88 mmol, 5 mol %). The mixture was stirred at 80 °C

in an oil bath for 3 h, at which time the starting material was consumed as indicated by

TLC analysis (20% acetone/hexanes, *p*-anisaldehyde stain). The reaction was cooled to

ambient temperature and quenched with sat. aq. $NaHCO_3$ (60 mL). The reaction was

partitioned between EtOAc and water, and the aqueous phase extracted with EtOAc (3 x

50 mL). The combined organic extracts were washed with water (2 x 50 mL), brine (1 x

25 mL), dried ($MgSO_4$), and concentrated *in vacuo*. The crude mixture was purified by

flash column chromatography (eluent: 20% acetone/hexanes) to afford 1.85 g (9.06

mmol, 51%) (*S*)-*t*-BuPyOx as an off-white solid. R_f = 0.44 with 3:2 hexanes/acetone; mp

70.2 – 71.0 °C; ^1H NMR (500 MHz, $CDCl_3$) δ 8.71 (ddd, *J* = 4.8, 1.8, 0.9 Hz, 1H), 8.08

(dt, *J* = 7.9, 1.1 Hz, 1H), 7.77 (dt, *J* = 7.7, 1.7 Hz, 1H), 7.37 (ddd, *J* = 7.0, 4.5, 1.0 Hz,

1H), 4.45 (dd, *J* = 10.2, 8.7 Hz, 1H), 4.31 (t, *J* = 8.5 Hz, 1H), 4.12 (dd, *J* = 10.2, 8.5 Hz,

1H), 0.98 (s, 9H); ^{13}C NMR (125 MHz, $CDCl_3$) δ 162.4, 149.6, 147.0, 136.5, 125.4,

124.0, 76.5, 69.3, 34.0, 26.0; IR (Neat film, NaCl): 2981, 2960, 2863, 1641, 1587, 1466,

1442, 1358, 1273, 1097, 1038, 968 cm^{-1}; HRMS (MultiMode ESI/APCI) *m/z* calc'd for

C$_{12}$H$_{17}$N$_2$O [M+H]$^+$: 205.1335, found 205.1327; [α]$^{25}_D$ –90.5° (c 1.15, CHCl$_3$).

Representative General Procedure for the Enantioselective 1,4-Addition of Arylboronic Acids to Conjugate Acceptors.

A screw-top 1 dram vial was charged with a stir bar, Pd(OCOCF$_3$)$_2$ (4.2 mg, 0.0125 mmol, 5 mol %), (*S*)-*t*-BuPyOX (3.1 mg, 0.015 mmol, 6 mo l%), NH$_4$PF$_6$ (12.5 mg, 0.075 mmol, 30 mol %) and PhB(OH)$_2$ (61 mg, 0.50 mmol, 2.0 equiv). The solids were dissolved in dichloroethane (0.5 mL) and stirred for 2 min at ambient temperature, at which time a yellow color was observed. Not all solids were dissolved at this time. Conjugate acceptor substrate (0.25 mmol) and water (0.025 mL, 1.25 mmol, 5.0 equiv) were added. The walls of the vial were rinsed with an additional portion of dichloroethane (0.5 mL). The vial was capped with a Teflon/silicone septum and stirred at 40 °C in an oil bath for 12 h. Upon complete consumption of the starting material (monitored by TLC, 4:1 hexanes/EtOAc, *p*-anisaldehyde or iodine/silica gel stain) the reaction mixture was filtered through a pipet plug of silica gel, using CH$_2$Cl$_2$ as the eluent, and concentrated *in vacuo*. The crude residue was purified by column chromatography (gradient: 9:1 hexanes/EtOAc to 7:3 hexanes/EtOAc) to afford a colorless solid.

Representative General Procedure for Additive Screening for the Enantioselective 1,4-Addition of Arylboronic Acids to Conjugate Acceptors.

A screw-top 1 dram vial was charged with a stir bar, Pd(OCOCF$_3$)$_2$ (4.2 mg, 0.0125

mmol, 2.5 mol%), (*S*)-*t*-BuPyOX (3.1 mg, 0.015 mmol, 3 mol %), salt additive (0.15 mmol, 30 mol %) and PhB(OH)$_2$ (122 mg, 1.0 mmol, 2.0 equiv). The solids were dissolved in dichloroethane (1 mL) and stirred for 2 min at ambient temperature, at which time a yellow color was observed. Not all solids were dissolved at this time. Conjugate acceptor substrate (0.5 mmol) and water (0.025 mL, 1.25 mmol, 5.0 equiv) were added. The walls of the vial were rinsed with an additional portion of dichloroethane (1 mL). The vial was capped with a Teflon/silicone septum and stirred at the indicated temperature in an oil bath for 12 h. Upon complete consumption of the starting material (monitored by TLC, 4:1 hexanes/EtOAc, *p*-anisaldehyde or iodine/silica gel stain) the reaction mixture was filtered through a pipet plug of silica gel, using CH$_2$Cl$_2$ as the eluent, and concentrated *in vacuo*. The crude residue was purified by column chromatography (gradient: 9:1 hexanes/EtOAc to 7:3 hexanes/EtOAc) to afford a colorless solid.

General Procedure for the Synthesis of Racemic Products

Racemic products were synthesized in a manner analogous to the general procedure using PyOx synthesized from racemic *tert*-leucinol (3.1 mg, 0.015 mmol, 6 mol %) as a ligand.

Experimental Procedure for the Mercury Drop Experiment

This experiment was conducted following the general procedure for the enantioselective 1,4-addition of phenylboronic acid and 3-methylcyclohex-2-enone. Immediately following the addition of the conjugate acceptor substrate and water, mercury (501.5 mg, 37 μL, 2.50 mmol, 200 equiv. with respect to the catalyst) was added to the reaction.

Following completion, the reaction was filtered and the filtrate was concentrated under reduced pressure. The resulting yellow oil was purified by flash chromatography (9:1 hexanes/EtOAc) to afford 46.5 mg of (*R*)-3-phenyl-3-methylcyclohexanone **35** as a colorless oil (99% yield, 90% ee).

Experimental Procedure for the Deuteration Experiments

A flame-dried 1 dram vial with a septum-fitted screw-top was cycled into a glove box and charged with a stir bar, Pd(OCOCF$_3$)$_2$ (4.2 mg, 0.0125 mmol, 5 mol %), (*S*)-*t*-BuPyOX (3.1 mg, 0.015 mmol, 6 mol %), NH$_4$PF$_6$ (12.5 mg, 0.075 mmol, 30 mol %) and either PhB(OH)$_2$ (61 mg, 0.50 mmol, 2.0 equiv.) or triphenyl boroxine (103.9 mg, 0.33 mmol, 4 equiv.). The solids were dissolved in dry dichloroethane (0.5 mL) and stirred for 2 min at ambient temperature, at which time a yellow color was observed. Not all solids were dissolved at this time. Freshly distilled 3-methylcyclohexenone (0.25 mmol) was added. The walls of the vial were rinsed with an additional portion of dichloroethane (0.5 mL). The vial was capped with a Teflon/silicone septum and removed from the glove-box. Deuterium oxide (23 μL, 25.0 mg, 1.25 mmol, 5.0 equiv) was added and the reaction was stirred at 40 °C in an oil bath for 12 h. The reaction mixture was concentrated *in vacuo* and the crude residue was purified by column chromatography (gradient: 9:1 hexanes/EtOAc to 7:3 hexanes/EtOAc) to afford 44.2 mg of a colorless oil (94% yield, 92% ee) for phenylboronic acid and 46.8 mg (99% yield, 91% ee) for triphenyl boroxine, respectively. For the control experiment, ketone **3** was synthesized according to the general procedure and was then subjected to the above described conditions for the deuteration experiments.

General Procedure for Low Temperature NMR Experiments:

A J. Young NMR tube was charged with complex **235** (26 mg, 0.05 mmol, 1.0 equiv.), AgPF$_6$ (25 mg, 0.10 mmol, 2.0 equiv.), and either 3-methylcyclohexenone (5.5 mg, 5.7 μL, 0.05 mmol, 1.0 equiv.) or PPh$_3$ (26 mg, 0.10 mmol, 2.0 equiv). The NMR tube was attached to a vacuum transfer bridge and dry CD$_2$Cl$_2$ was condensed into the J. Young tube at –78 °C by trap-to-trap condensation. The J. Young tube was sealed and removed from the vacuum transfer bridge and maintained at –78 °C in a dry ice/*iso*-propanol bath. The NMR tube was quickly transferred to a pre-cooled (–60 °C) NMR probe. The sample was observed at 20 °C intervals before being quenched with 2,2,2-trifluoroethanol (17 μL) at 20 °C.

Attempts to React or Isomerize Complex 236

A solution of complex **236** (13 mg, 0.025 mmol, 1.0 equiv.) in dichloroethane (700 μL) was observed by ^{31}P NMR spectroscopy at 60 °C over the course of 2 h. No observable change in the ratio or intensity of the phosphorus signals was noted. Subsequently, 3-methylcyclohexenone (28 μL, 0.25 mmol, 1.0 equiv.) was added to the NMR sample tube. The sample was observed by ^{31}P NMR spectroscopy at 60 °C over the course of 2 h. No observable change in the ratio or intensity of the phosphorus signals was observed. No product ketone **35** was observed by LCMS or TLC analysis of the sample.

Procedure for Non-Linear Effect Experiments (Figure 4.2)

Stock solutions of both racemic *t*-BuPyOx and of (*S*)-*t*-BuPyOx were made (60 mg

ligand, 10 mL DCE) in separate 20 mL vials. Portions of each stock solution were transferred to a 4 mL vial by syringe and concentrated *in vacuo* to afford ligand mixtures of the desired enantiopurity. The vials with the ligand mixture were used in accordance with the general procedure to afford ketone **35** as a colorless oil. The various ligand mixtures were made as follows:

0% ee: 500 µL racemic *t*-BuPyOx (afforded ketone **35** in 0% ee)

20% ee: 400 µL racemic *t*-BuPyOx, 100 µL (*S*)- *t*-BuPyOx (afforded ketone **35** in 16% ee)

40% ee: 300 µL racemic *t*-BuPyOx, 200 µL (*S*)- *t*-BuPyOx (afforded ketone **35** in 34% ee)

60% ee: 200 µL racemic *t*-BuPyOx, 300 µL (*S*)- *t*-BuPyOx (afforded ketone **35** in 52% ee)

80% ee: 100 µL racemic *t*-BuPyOx, 400 µL (*S*)- *t*-BuPyOx (afforded ketone **35** in 68% ee)

100% ee: 500 µL (*S*)- *t*-BuPyOx (afforded ketone **35** in 92% ee)

4.5.3 Spectroscopic Data for Compounds
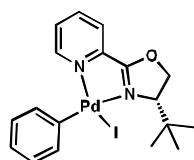
Synthesis of [PdIPh(PyOx)] (complex 235)

Pd(dba)₂ (288.0 mg, 0.50 mmol, 1.0 equiv) was dissolved in benzene (20 mL). *(S)-t-*BuPyOX (108.0 mg, 0.52 mmol, 1.05 equiv) and iodobenzene (83.0 µL, 0.75 mmol, 1.50 equiv) were added and the mixture was slowly heated to 50 °C and stirred overnight. Upon completion the crude product was filtered and the filtrate was concentrated under reduced pressure. The resulting brown oil was triturated with diethyl ether and washed several times with diethylether and hot hexanes. The resulting orange solid was dried *in vacuo* to yield 103 mg of the desired product (0.20 mmol, 40% yield). Two different

stereoisomers were visible in ^{1}H NMR in a 1:1.3 ratio. ^{1}H NMR (500 MHz, CDCl$_3$)

Major isomer: δ 0.63 (s, 9H), 3.90 (dd, J = 9.0, 3.2 Hz, 1H), 4.62 (t, J = 9.2 Hz, 1H), 4.82

(dd, J = 3.3, 9.3 Hz, 1H), 6.83 (t, J = 6.6 Hz, 1H), 6.89 (m, 2H), 7.28-7.33 (m, 2H), 7.62-

7.65 (m, 1H), 7.87 (d, J = 7.7 Hz, 1H), 8.05 (td, J = 7.8, 1.5 Hz, 1H), 9.39 (d, J = 5.1 Hz,

1H); Minor isomer: δ 1.09 (s, 9H), 4.37 (dd, J = 3.6, 9.2 Hz, 1H), 4.54 (t, J = 9.2 Hz,

1H), 4.79 (dd, J = 3.6, 9.2 Hz, 1H), 6.98 (dt, J = 7.1, 8.7 Hz, 1H), 7.06-7.11 (m, 2H),

7.43-7.48 (m, 2H), 7.50 (d, J = 4.5 Hz, 1H), 7.84 (d, J = 7.6 Hz, 1H), 8.00-8.03 (m, J =

7.8, 1H), 9.70 (d, J = 4.2 Hz, 1H); ^{13}C NMR (500 MHz, CDCl$_3$) Major isomer: δ 25.6,

35.0, 70.0, 73.3, 123.3, 124.3, 126.5, 129.0, 138.7, 138.8, 143.8, 144.0, 153.4, 168.6;

Minor isomer: δ 26.9, 35.4, 72.0, 73.5, 123.4, 124.4, 126.5, 128.8, 138.5, 138.7, 143.5,

144.9, 150.2, 166.6; IR (cm^{-1}) ν = 3050, 2961, 1636, 1587, 1560, 1490, 1467, 1405, 1395,

1368, 1297, 1251, 1209, 1159, 1094, 1062, 1018, 927, 791, 750, 732; Anal. Calc. for

C$_{18}$H$_{21}$ON$_2$IPd[1]: C, 41.11; H, 4.04; N, 5.42%. Found: C, 41.09; H, 3.91; N, 4.87%; ESI-

MS m/z = 436.8 ([M-Ph]$^+$)
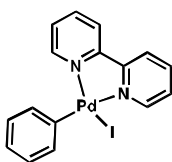
Synthesis of [PdIPh(bpy)] (complex S1)

Referring to a known procedure,[44] Pd(dba)$_2$ (115.0 mg, 0.20 mmol, 1.0 equiv) was

dissolved in benzene (5 mL). 2,2'-bipyridyl (40.3 mg, 0.26 mmol, 1.30 equiv) and

iodobenzene (32.0 _L, 0.286 mmol, 1.43 equiv) were added and the mixture was slowly

---

[1] Isolation of X-ray quality crystals shows 5 mol % contamination with (PyOx)Pd(I)$_2$.
This elemental analysis is consistent with that observed impurity, i.e. C, 42.00; H, 4.11;
N, 5.44 x 0.05 (C, 25.53; H, 2.86; N, 4.96) = C, 41.11; H, 4.04; N, 5.42.

heated to 50 °C and stirred overnight. Upon completion the crude product was filtered and the filtrate was concentrated under reduced pressure. The resulting orange oil was triturated with diethyl ether and washed several times with diethyl ether and hot hexanes. The resulting yellow solid was dried *in vacuo* to yield the title compound (41 mg, 0.09 mmol, 45% yield). All characterization data matches previously reported data.[44,45]
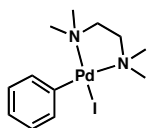
Synthesis of [PdIPh(TMEDA)] (complex S2)

Referring to a known procedure,[44] Pd(dba)$_2$ (80.0 mg, 0.14 mmol, 1.0 equiv) was dissolved in benzene (5 mL). Freshly distilled TMEDA (27.0 µL, 0.18 mmol, 1.30 equiv) and iodobenzene (22.0 _L, 0.20 mmol, 1.43 equiv) were added and the mixture was slowly heated to 50 °C and stirred overnight. Upon completion the crude product was filtered and the filtrate was concentrated under reduced pressure. The resulting orange oil was triturated with diethyl ether and washed several times with diethyl ether and hot hexanes. The resulting yellow solid was dried *in vacuo* to yield the title compound (30 mg, 0.07 mmol, 51% yield). All characterization data matches previously reported data.[44]
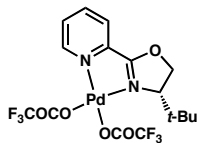
Synthesis of (PyOx)Pd(OCOCF$_3$)$_2$ (complex S3, thesis compound number 245)

Pd(MeCN)$_2$Cl$_2$ (362 mg, 1.40 mmol, 1 equiv.) and *(S)-t*-BuPyOX (321, 1.57 mmol, 1.12 equiv.) were dissolved in CH$_2$Cl$_2$ (6 mL) and stirred for 1 h at ambient temperature. The

reaction mixture was filtered through a plug of celite, and concentrated *in vacuo* until 1 mL of solution remained. The solution was triturated with hexanes to precipitate an orange powder. The powder was collected by filtration and dried under high vacuum to afford (PyOx)PdCl$_2$ as a pale orange solid (507 mg, 1.33 mmol, 95% yield). A portion of this solid (200 mg, 0.52 mmol, 1 equiv.) was dissolved in CH$_2$Cl$_2$ (10 mL) and Ag(OCOCF$_3$)$_2$ (290 mg, 1.09 mmol, 2.2 equiv.) was added at ambient temperature. The reaction was stirred for 1 h, filtered through a plug of celite and concentrated *in vacuo*, and was triturated with hexanes to afford a pale yellow solid (198 mg, 0.37 mmol, 72%). ^{1}H NMR (500 MHz, CD$_2$Cl$_2$) δ 8.26–8.18 (m, 2H), 7.87–7.80 (m, 1H), 7.75 (ddt, *J* = 7.8, 5.7, 1.5 Hz, 1H), 4.93 (dd, *J* = 9.5, 3.4 Hz, 1H), 4.86 (td, *J* = 9.4, 1.6 Hz, 1H), 3.92 (dt, *J* = 9.3, 2.7 Hz, 1H), 1.00 (d, *J* = 1.6 Hz, 9H), ^{13}C NMR (126 MHz, CD$_2$Cl$_2$) δ 171.9, 164.4 (q, J_{C-F} = 36 Hz), 164.3 (q, J_{C-F} = 37 Hz), 152.3, 145.9, 143.6, 131.7, 127.9, 116.3 (q, J_{C-F} = 295 Hz), 116.1 (q, J_{C-F} = 292 Hz), 76.5, 74.0, 36.8, 27.1; ^{19}F NMR (282 MHz, CD$_2$Cl$_2$) –74.7, -74.6; IR (Neat film, NaCl) ν = 2916, 1684, 1595, 1424, 1210, 1140 cm^{-1}; Anal. Calc. for C$_{16}$H$_{16}$O$_5$N$_2$F$_6$Pd: C, 35.80; H, 3.00; N, 5.22%. Found: C, 35.52; H, 3.29; N, 4.65%; HRMS (EI+) *m/z* calc'd for C$_{14}$H$_{16}$F$_3$N$_2$O$_3$Pd [M–(OCOCF$_3$)]$^+$: 423.0147, found 423.0163.
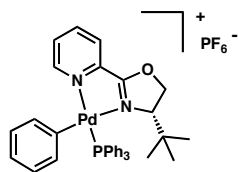
Synthesis of [PdPh(PPh$_3$)(PyOx)][PF$_6$] (complex 236)

Complex **29** (52.0 mg, 0.10 mmol, 1.0 equiv) and PPh$_3$ (25.0 mg, 0.10 mmol, 1.0 equiv) were dissolved in THF (10 mL) and the solution was cooled to –78 °C. A solution of

AgPF$_6$ (26.2 mg, 0.10 mmol, 1.0 equiv) in 10 mL of THF was added at –78 °C and the reaction was stirred for 30 min at this temperature. The reaction was allowed to come to ambient temperature and the resulting suspension was filtered. The solvent was removed under reduced pressure and the resulting yellow oil was dissolved in CH$_2$CL$_2$ and filtrated again. A white powder was precipitated from solution upon addition of diethyl ether and hexanes. The solid was washed with hexanes and dried *in vacuo* to yield the title compound (62 mg, 0.079 mmol, 79% yield). Two different stereoisomers were visible in ^{1}H NMR and ^{31}P NMR in a 1:1.35 ratio. ^{1}H NMR (500 MHz, CD$_2$Cl$_2$) Major isomer: δ 0.59 (s, 9H), 1.88 (dd, J = 8.9, 2.8 Hz, 1H), 4.25 (t, J = 9.2 Hz, 1H), 4.61 (dd, J = 2.6, 9.4 Hz, 1H), 6.48 (m, 1H), 6.60 (t, J = 8.0 Hz, 1H), 6.89 (t, J = 7.2 Hz, 1H), 6.98 (t, J = 7.1 Hz, 1H), 7.32 (t, J = 6.7 Hz, 2H), 7.55 (d, J = 7.7 Hz, 1H), 7.96 (d, J = 7.7 Hz, 1H), 8.10 (dt, J = 7.7, 1.2 Hz, 1H). Minor isomer: δ 0.63 (s, 9H), 3.68 (dd, J = 3.4, 8.9 Hz, 1H), 4.77 (t, J = 9.3 Hz, 1H), 4.90 (dd, J = 2.4, 11.9 Hz, 1H), 6.54 (m, 1H), 6.72 (m, 1H), 6.79 (m, 1H), 7.03 (d, J = 4.8 Hz, 1H), 7.16 (d, J = 4.8 Hz, 2H), 7.26 (m, 1H), 7.98 (m, 1H), 8.03 (dt, J = 7.7, 1.3 Hz, 1H); ^{13}C NMR (500 MHz, CD$_2$Cl$_2$) Major isomer: δ 25.6, 35.0, 70.0, 73.3, 123.3, 124.3, 126.5, 129.0, 138.7, 138.8, 143.8, 144.0, 153.4, 168.6. Minor isomer: δ 26.9, 35.4, 72.0, 73.5, 123.4, 124.4, 126.5, 128.8, 138.5, 138.7, 143.5, 144.9, 150.2, 166.6. ^{31}P NMR (161.8 MHz, CD$_2$Cl$_2$): δ 28.3 (major isomer), 33.5 (minor isomer), –166.5 (PF$_6^-$, septuplet, J = 712.9 Hz); IR (cm^{-1}) ν = 3050, 2961, 1636, 1587, 1560, 1490, 1467, 1405, 1395, 1368, 1297, 1251, 1209, 1159, 1094, 1062, 1018, 927, 791, 750, 732; Anal. Calc. for C$_{36}$H$_{36}$F$_6$N$_2$OP$_2$Pd: C, 54.39; H, 4.56; N, 3.52%. Found: C, 53.81; H, 4.94; N, 3.44%; HRMS (ESI+) *m/z* calc'd for C$_{36}$H$_{36}$N$_2$OPPd [M]$^+$: 649.1600, found 649.1598.
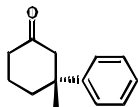
(*R*)-3-phenyl-3-methylcyclohexanone (35)

Synthesized according to the general procedure and purified by flash chromatography (9:1 hexanes/EtOAc) to afford a colorless oil (99% yield). $[\alpha]^{25}_D$ –56.1° (*c* 1.36, CHCl$_3$, 92% ee). All characterization data matches previously reported data.[46, 47, 48, 49, 50, 51, 52]
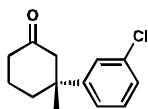
(*R*)-3-(3-chlorophenyl)-3-methylcyclohexanone (211a, Table 4.3)

Synthesized according to the general procedure and purified by flash chromatography (gradient: 100:0 hexanes/EtOAc to 95:5 hexanes/EtOAc) to afford a colorless oil (96% yield). $[\alpha]^{25}_D$ –56.7° (*c* 1.48, CHCl$_3$, 96% ee). All characterization data matches previously reported data.[42,46]
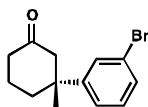
(*R*)-3-(3-bromophenyl)-3-methylcyclohexanone (211b, Table 4.3)

Synthesized according to the general procedure and purified by flash chromatography (gradient: 100:0 hexanes/EtOAc to 95:5 hexanes/EtOAc) to afford a colorless solid (84% yield). $[\alpha]^{25}_D$ –56.7° (*c* 0.68, CHCl$_3$, 84% ee). All characterization data matches previously reported data.[48]
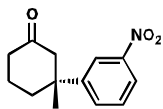
(*R*)-3-methyl-3-(3-nitrophenyl)cyclohexanone (211c, Table 3)

Synthesized according to the general procedure and purified by flash chromatography

(CH_2Cl_2) to afford a colorless solid (81% yield). $[\alpha]^{25}_D$ –61.5° (*c* 0.96, $CHCl_3$, 91% ee).

All characterization data matches previously reported data.[53]
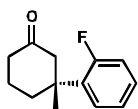
(*R*)-3-(2-fluorophenyl)-3-methylcyclohexanone (211d, Table 3)

Synthesized according to the general procedure and purified by flash chromatography

(gradient: 100:0 hexanes/EtOAc to 95:5 hexanes/EtOAc) to afford a colorless oil (70%

yield). $[\alpha]^{25}_D$ –41.0° (*c* 0.64, $CHCl_3$, 77% ee)All characterization data matches previously

reported data.[53]
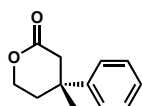
(*R*)-4-methyl-4-phenyltetrahydro-2H-pyran-2-one (Table 4.6, Entry 7)

Synthesized according to the general procedure and purified by flash chromatography

(gradient 100:0 hexanes/EtOAc to 90:10 hexanes/EtOAc) to afford a colorless solid (49%

yield). $[\alpha]^{25}_D$ –87.2 (*c* 0.99, $CHCl_3$, 57% ee). All characterization data matches

previously reported data.[54]
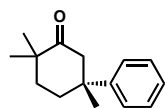
(*R*)-2,2,5-trimethyl-5-phenylcyclohexanone (Table 4.6, Entry 8, thesis comound 246)

Enone substrate was synthesized by known procedure.[55] Synthesized according to the

general procedure and purified by flash chromatography (gradient: 100:0 hexanes/EtOAc

to 90:10 hexanes/EtOAc) to afford a colorless oil (9% yield). ^{1}H NMR (500 MHz,

CDCl$_3$) δ 7.32 (d, *J* = 4.8 Hz, 4H), 7.24–7.16 (m, 1H), 2.92 (dd, *J* = 14.4, 1.5 Hz, 1H),

2.52 (dd, *J* = 14.4, 1.2 Hz, 1H), 2.18 (dddd, *J* = 14.0, 8.4, 4.1, 1.5 Hz, 1H), 1.97 (dddd, *J*

= 13.8, 8.5, 3.9, 1.2 Hz, 1H), 1.74–1.59 (m, 1H), 1.51 (ddd, *J* = 14.1, 8.6, 4.1 Hz, 1H),

1.29 (s, 3H), 1.15 (s, 3H), 1.06 (s, 3H); ^{13}C NMR (126 MHz, CDCl$_3$) δ 215.8, 147.8,

128.5, 128.4, 126.1, 125.5, 49.4, 44.1, 43.3, 36.4, 34.5, 29.6, 25.5, 25.1; IR (Neat film,

NaCl) ν = 2961, 2923, 2863, 1704, 1666, 1496, 1444, 1384, 1302, 1030 cm^{-1}; HRMS

(EI+) *m/z* calc'd for C$_{15}$H$_{21}$O [M+H]$^+$: 216.1514, found 216.1506; $[\alpha]^{25}_D$ –58.3° (*c* 0.48,

CHCl$_3$, 90% ee).
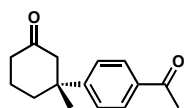
(*R*)-3-(4-acetylphenyl)-3-methylcyclohexanone (Table 4.7, Entry 9)

Synthesized according to the general procedure and purified by flash chromatography

(gradient: 95:5 hexanes/EtOAc to 85:15 hexanes/EtOAc) to afford colorless oil (99%

yield). $[\alpha]^{25}_D$ –58.9° (c 1.39, CHCl$_3$, 96% ee). All characterization data matches

previously reported data.[53]
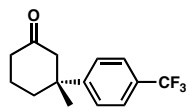
(*R*)-3-methyl-3-(4-(trifluoromethyl)phenyl)cyclohexanone (Table 4.7, Entry 10)

Synthesized according to the general procedure and purified by flash chromatography

(gradient: 95:5 hexanes/EtOAc to 85:15 hexanes/EtOAc) to afford colorless oil (99%

yield). $[\alpha]^{25}_{D}$ –58.5° (c 0.92, CHCl$_3$, 96% ee). All characterization data matches

previously reported data.[53]

Table 4.13 Chiral Assays

compound	product	HPLC conditions	retention time of major isomer (min)	retention time of minor isomer (min)	% ee
35		Chiralcel OJ-H 1% IPA/Hexanes isocratic 1 mL/min	15.3	19.6	92
211a (Table 3)		Chiralcel OJ-H 1% IPA/Hexanes isocratic 1 mL/min	17.2	20.4	96
211b (Table 3)		Chiralcel OJ-H 1% IPA/Hexanes isocratic 1 mL/min	14.7	16.9	85
211c (Table 3)		Chiralpak AD-H 1% IPA/Hexanes Isocratic 1mL/min	29.0	30.6	92
211d (Table 3)		Chiralcel OJ-H 1% IPA/Hexanes isocratic 1 mL/min	9.3	10.9	77
Table 6 Entry 7		Chiralcel OJ-H 5% IPA/Hexanes isocratic 1 mL/min	13.7	17.8	57
Table 6 Entry 8		Chiralcel OJ-H 1% IPA/Hexanes isocratic 1 mL/min	7.8	9.9	90
Table 7 Entry 9		Chiralpak AD-H 5% IPA/Hexanes isocratic 1 mL/min	30.4	29.5	96
Table 7 Entry 10		Chiralcel OJ-H 0.5% IPA/Hexanes isocratic 1 mL/min	35.0	41.1	96

4.6 Notes and Citations

(1)   (a) P. Perlmutter, in Conjugate Addition Reactions in Organic Synthesis, Tetrahedron Organic Chemistry Series 9; Pergamon, Oxford, **1992**; (b) K. Tomioka, Y. Nagaoka, in Comprehensive Asymmetric Catalysis, Vol. 3 (Eds: E. N. Jacobsen, A. Pfaltz, H. Yamamoto, Springer-Verlag, New York, **1999**; Chapter 31; (c) Gini, F.; Hessen, B.; Feringa, B. L.; Minnaard, A. J. *Chem. Commun.* **2007**, 710–712.

(2)   For reviews, see: (a) Harutyunyan, S. R.; den Hartog, T.; Geurts, K.; Minnaard, A. J.; Feringa, B. L. *Chem. Rev.* **2008**, *108*, 2824–2882. (b) Alexakis, A.; Backvall, J. E.; Krause, N.; Pamies, O.; Dieguez, M. *Chem. Rev.* **2008**, *108*, 2796–2893. (c) Lopez, F.; Minnarard, A. J.; Feringa, B. L. *Acc. Chem. Res.* **2007**, 40, 179–188. (d) Hayashi, T.; Yamasaki, K. *Chem. Rev.* **2003**, *103*, 2829–2844. (e) Feringa, B. L. *Acc. Chem. Res.* **2000**, *33*, 346–353. (f) Rossiter, B. E.; Swingle, N. M. *Chem. Rev.* **1992**, *92*, 771–806.

(3)   (a) Shintani, R.; Duan, W.-L.; Hayashi, T. *J. Am. Chem. Soc.* **2006**, *128*, 5628–5629. (b) Hayashi, T.; Takahashi, M.; Takaya, Y.; Ogasawara, M. *J. Am. Chem. Soc.* **2002**, *124*, 5052–5058. (c) Takaya, Y.; Ogasawara, M.; Hayashi, T. *J. Am. Chem. Soc.* **1998**, *120*, 5579–5580.

(4)   (a) Nishikata, T.; Yamamoto, Y.; Miyaura, N. *Angew. Chem., Int. Ed.* **2003**, *42*, 2768–2770. (b) Nishitaka, T.; Yamamoto, Y.; Miyaura, N. Chem. Lett. **2007**, 36, 1442–1443. (c) Nishitaka, T.; Kiyomura, S.; Yamamoto, Y.; Miyaura, N. Synlett **2008**, 2487–2490.

(5)   Gini, F.; Hessen, B.; Minnaard, A. J. Org. Lett. **2005**, 7, 5309–5312.

(6)   For reviews on the synthesis of quaternary stereocenters, see: (a) Denissova, I.;
        Barriault, L. *Tetrahedron* **2003**, *59*, 10105–10146. (b) Douglas, C. J.; Overman, L.
        E. *Proc. Natl. Acad. Sci. U.S.A.* **2004**, *101*, 5363–5267. (c) Christoffers, J.; Baro,
        A. *Adv. Synth. Catal.* **2005**, *347*, 1473–1482. (d) Trost, B. M.; Jiang, C. *Synthesis*
        2006, 369–396. (e) Mohr, J. T.; Stoltz, B. M. *Chem. Asian J.* **2007**, *21*, 1476–1491.
        (f) Cozzi, P. G.; Hilgraf, R.; Zimmermann, N. *Eur. J. Org. Chem.* **2007**,
        5969–5994. (g) For an excellent comprehensive review, see: Hawner, C.; Alexakis,
        A. *Chem. Commun.* **2010**, *46*, 7295–7306.

(7)   (a) Wu, J.; Mampreian D. M.; Hoveyda, A. H. *J. Am. Chem. Soc.* **2005**, *127*,
        4584–4585. (b) Hird, A. W.; Hoveyda, A. H. *J. Am. Chem. Soc.* **2005**, *127*,
        14988–14989. (c) Lee, K.-S.; Brown, M. K.; Hird, A. W.; Hoveyda, A. H. *J. Am.
        Chem. Soc.* **2006**, *128*, 7182–7184. (d) Brown, M. K.; May, T. L.; Baxter, C. A.;
        Hoveyda, A. H. *Angew. Chem., Int. Ed.* **2007**, *46*, 1097–1100. (e) Fillion, E.;
        Wilsily, A. *J. Am. Chem. Soc.* **2006**, *128*, 2774–2775. (f) Wilsily, A.; Fillion, E. *J.
        Org. Chem.* **2009**, *74*, 8583–8594. (g) Dumas, A. M.; Fillion, E. *Acc. Chem. Res.*
        2010, *43*, 440–454. (h) Wilsily, A.; Fillion, E. *Org. Lett.* **2008**, *10*, 2801–2804.

(8)   (a) Vaugnoux-d'Augustin, M.; Palais, L.; Alexakis, A. *Angew. Chem., Int. Ed.*
        2005, *44*, 1376–1378. (b) Vuagnoux-d'Augustin, M.; Alexakis, A. *Chem.–Eur. J.*
        2007, *13*, 9647–9662. (c) Palais, L.; Alexakis, A. *Chem.–Eur. J.* **2009**, *15*,
        10473–10485. (d) Fuchs, N.; d'Augustin, M.; Humam, M.; Alexakis, A.; Taras, R.;
        Gladiali, S. *Tetrahedron: Asymmetry* **2005**, *16*, 3143–3146. (e) Vuagnoux-
        d'Augustin, M.; Kehrli, S.; Alexakis, A. *Synlett*, **2007**, 2057–2060. (f) May, T. L.;

Brown, M. K.; Hoveyda, A. H. *Angew. Chem., Int. Ed.* **2008**, *47*, 7358–7362. (g) Ladjel, C.; Fuchs, N.; Zhao, J.; Bernardinelli, G. Alexakis, A. *Eur. J. Org. Chem.* **2009**, 4949–4955. (h) Palais, L.; Mikhel, I. S.; Bournaud, C.; Micouin, L.; Falciola, C. A.; Vuagnoux-d'Augustin, M.; Rosset, S.; Bernardinelli, G.; Alexakis, A. *Angew. Chem., Int. Ed.* **2007**, *46*, 7462–7465. (i) Hawner, C.; Li, K.; Cirriez, V.; Alexakis, A. *Angew. Chem., Int. Ed.* **2008**, *47*, 8211–8214. (j) Müller, D.; Hawner, C.; Tissot, M.; Palais, L.; Alexakis, A. *Synlett* **2010**, 1694–1698. (k) Hawner, C.; Müller, D.; Gremaud, L.; Felouat, A.; Woodward, S.; Alexakis, A. *Angew. Chem., Int. Ed.* **2010**, *49*, 7769–7772.

(9)   (a) Martin, D.; Kehrli, S.; d'Augustin, M.; Clavier, H.; Mauduit, M.; Alexakis, A. *J. Am. Chem. Soc.* **2006**, *128*, 8416–8417. (b) Kehrli, S.; Martin, D.; Rix, D.; Mauduit, M.; Alexakis, A. *Chem.–Eur. J.* **2010**, *16*, 9890–9904. (c) Hénon, H.; Mauduit, M.; Alexakis, A. *Angew. Chem., Int. Ed.* **2008**, *47*, 9122–9124. (d) Matsumoto, Y.; Yamada, K.-I.; Tomioka, K. *J. Org. Chem.* **2008**, *73*, 4578–4581.

(10)   (a) Shintani, R.; Tsutsumi, Y.; Nagaosa, M.; Nishimura, T.; Hayashi, T. *J. Am. Chem. Soc.* **2009**, *131*, 13588–13589. (b) Shintani, R.; Takeda, M.; Nishimura, T.; Hayashi, T. *Angew. Chem., Int. Ed.* **2010**, *49*, 3969–3971.

(11)   For excellent review articles, see: (a) Gutnov, A. *Eur. J. Org. Chem.* **2008**, 4547–4554. (b) Christoffers, J.; Koripelly, G.; Rosiak, A.; Rössle, M. *Synthesis* **2007**, 1279–1300.

(12)   Lin, S.; Lu, X. *Org. Lett.* **2010**, *12*, 2536–2539.

(13)   Kikushima, K.; Holder, J. C.; Gatti, M.; Stoltz, B. M. *J. Am. Chem. Soc.* **2011**, *133*, 6902–6905.

(14) PyOx ligand scaffolds are increasingly common in asymmetric catalysis, see: (a) Podhajsky, S. M.; Iwai, Y.; Cook-Sneathen, A.; Sigman, M. S. *Tetrahedron* **2011**, *67*, 4435–4441. (b) Aranda, C.; Cornejo, A.; Fraile, J. M.; García-Verdugo, E.; Gil, M. J.; Luis, S. V.; Mayoral, J. A.; Martínez-Merino, V.; Ochoa, Z. *Green Chem.* **2011**, *13*, 983–990. (d) Pathak, T. P.; Gligorich, K. M.; Welm, B. E.; Sigman, M. S. *J. Am. Chem. Soc.* **2010**, *132*, 7870–7871. (d) Jiang, F.; Wu, Z.; Zhang, W. *Tetrahedron Lett.* **2010**, *51*, 5124–5126. (e) Jensen, K. H.; Pathak, T. P.; Zhang, Y.; Sigman, M. S. *J. Am. Chem. Soc.* **2009**, *131*, 17074–17075. (f) He, W.; Yip, K.-T.; Zhu, N.-Y.; Yang, D. *Org. Lett.* **2009**, *11*, 5626–5628. (g) Dai, H.; Lu, X. *Tetrahedron Lett.* **2009**, *50*, 3478–3481. (h) Linder, D.; Buron, F.; Constant, S.; Lacour, J. *Eur. J. Org. Chem.* **2008**, 5778–5785. (i) Schiffner, J. A.; Machotta, A. B.; Oestreich, M. *Synlett* **2008**, 2271–2274. (j) Koskinen, A. M. P.; Oila, M. J.; Tois, J. E. *Lett. Org. Chem.* **2008**, *5*, 11–16. (k) Zhang, Y.; Sigman, M. S. *J. Am. Chem. Soc.* **2007**, *129*, 3076–3077. (l) Yoo, K. S.; Park, C. P.; Yoon, C. H.; Sakaguchi, S.; O'Neill, J.; Jung, K. W. *Org. Lett.* **2007**, *9*, 3933–3935. (m) Dhawan, R.; Dghaym, R. D.; St. Cyr, D. J.; Arndtsen, B. A. *Org. Lett.* **2006**, *8*, 3927–3930. (n) Xu, W.; Kong, A.; Lu, X. *J. Org. Chem.* **2006**, *71*, 3854–3858. (o) Malkov, A. V.; Stewart Liddon, A. J. P.; Ramírez-López, P.; Bendová, L.; Haigh, D.; Kocovsky, P. *Angew. Chem., Int. Ed.* **2006**, *45*, 1432–1435. (p) Abrunhosa, I.; Delain-Bioton, L.; Gaumont, A.-C.; Gulea, M.; Masson, S. *Tetrahedron* **2004**, *60*, 9263–9272. (q) Brunner, H.; Kagan, H. B.; Kreutzer, G. *Tetrahedron: Asymmetry* **2003**, *14*, 2177–2187. (r) Cornejo, A.; Fraile, J. M.; García, J. I.; Gil, M. J.; Herrerías, C. I.; Legarreta, G.; Martínez-Merino, V.; Mayoral, J. A. *J. Mol. Catal.*

A: Chem. **2003**, *196*, 101–108. (s) Zhang, Q.; Lu, X.; Han, X. *J. Org. Chem.* **2001**, *66*, 7676–7684. (t) Zhang, Q.; Lu, X. *J. Am. Chem. Soc.* **2000**, *122*, 7604–7605. (u) Perch, N. S.; Pei, T.; Widenhoefer, R. A. *J. Org. Chem.* **2000**, *65*, 3836–3845. (v) Bremberg, U.; Rahm, F.; Moberg, C. *Tetrahedron: Asymmetry* **1998**, *9*, 3437–3443. (w) Brunner, H.; Obermann, U.; Wimmer, P. *Organometallics* **1989**, *8*, 821–826.

(15) The ligand was prepared as described in the literature, see: Brunner, H.; Obermann, U. *Chem. Ber.* **1989**, *122*, 499–507.

(16) (a) Xu, Q.; Zhang, R.; Zhang, T.; Shi, M. *J. Org. Chem.* **2010**, *75*, 3935–3937; (b) Zhang, T.; Shi, M. *Chem.–Eur. J.* **2008**, *14*, 3759–3764; (c) Gottummukkala, A. L.; Matcha, K.; Lutz, M.; de Vries, J. G. ; Minnaard, A. J. *Chem.–Eur. J.* **2012**, *18*, 6907–6914.

(17) Holder, J. C., Marziale, A. N., Gatti, M.; Mao, B.; Stoltz, B. M. *Chem.–Eur. J.* **2013**, *19*, 74–77.

(18) We believe the small amount of deuterium incorporation at the methylene adjacent the enone occurs via substrate enolization during the extended reaction times under the mild reaction conditions.

(19) Duan, W.-L.; Iwamura, H.; Shintani, R.; Hayashi, T. *J. Am. Chem. Soc.* **2007**, *129*, 2130–2138.

(20) Guillaneux, D.; Zhao, S.-H.; Samuel, O.; Rainford, D.; Kagan, H. B. *J. Am. Chem. Soc.* **1994**, *116*, 9430–9439.

(21) (a) Inanaga, J.; Furuno, H.; Hayano, T. *Chem. Rev.* **2002**, *102*, 2211–2226. (b) Kagan, H. B. *Synlett* **2001**, 888–899. (c) Girard, C.; Kagan H. B. *Angew. Chem.,*

Int. Ed. **1998**, *37*, 2922–2959.

(22) For preparation and use of (PyOx)Pd(OCOCF$_3$)$_2$ see Experimental procedures.

(23) (a) Seymour, J. D.; Caprihan, A.; Altobelli, S. A.; Fukushima, E. *Physical Review Letters* **2000**, *84*, 266–269. (b) Antalek, B. *Concepts in Magnetic Resonance* **2002**, *14*, 225–258. (c) Price, W. S. *Diffusion Fundamentals* **2005**, *2*, 1–19.

(24) Nishitaka, T.; Yamamoto, Y.; Miyaura, N. *Organometallics* **2004**, *23*, 4317–4324.

(25) The catalyst itself is known to be soluble and not zero valent palladium nanoparticles due to exclusion by a mercury drop test, see ref 17. For examples of the mercury drop test, see: (a) Ines, B.; SanMartin, R.; Moure, M. J.; Dominguez, E. *Adv. Synth. Catal.* **2009**, *351*, 2124–2132. (b) Ogo, S.; Takebe, Y., Uehara, K., Yamazaki, T., Nakai, H., Watanabe, Y., Fukuzumi, S, *Organometallics* **2006**, *25*, 331–338.

(26) Attempts to study the reaction by NMR initially saw no reaction progress due to the inability to stir the immiscible reaction mixture in an NMR tube. Substitution of 2,2,2-trifluoroethanol for water as the super stoichiometric proton source facilitated the reaction to proceed in the absence of stirring with no detriment to the observed enantioselectivity, however the reaction was necessarily performed at sufficiently elevated temperature that observation of the initial rate was not tenable and, thus, kinetic study was abandoned.

(27) Lan, Y.; Houk, K. N. *J. Org. Chem.* **2011**, *76*, 4905–4909.

(28) For related computational studies on palladium-catalyzed conjugate additions of arylboronic acids to enones: (a) Nishikata, T.; Yamamoto, Y.; Gridnev, I. D.; Miyaura, N. *Organometallics* **2005**, *24*, 5025–5032. (b) Sieber, J. D.; Liu, S.;

Morken, J. P. *J. Am. Chem. Soc.* **2007**, *129*, 2214–2215. (c) Dang, L.; Lin, Z.; Marder, T. B. *Organometallics* **2008**, *27*, 4443–4454.

(29) (a) Becke, A. D. *J. Chem. Phys.* **1993**, *98*, 1372–1377. (b) Becke, A. D. *J. Chem. Phys.* **1993**, *98*, 5648–5652. (c) Perdew, J. P.; Chevary, J. A.; Vosko, S. H.; Jackson, K. A.; Pederson, M. R.; Singh, D. J.; Fiolhais, C. *Phys. Rev. B* **1992**, *46*, 6671–6687. (d) Perdew, J. P. *Phys. Rev. B* **1986**, *33*, 8822–8824.

(30) Gaussian 03, Revision C.02: Frisch, M. J et al. Gaussian, Inc., Wallingford CT, 2004.

(31) Here, it is assumed the isomeric trans and cis phenylpalladium complexes cannot undergo rapid isomerization before alkene insertion and thus the enantioselectivity is determined by the energy difference between **8-TS-A** and **8-TS-B**, since the transmetallation leading to the trans isomer is favored. If trans/cis isomerization is faster than alkene insertion, the enantioselectivity will be determined by the energy difference between **8-TS-A** and **8-TS-D** (98% ee).

(32) Other Lewis acids also proved incapable of catalyzing the reaction, including AlCl3 and Sn(OTf)2.

(33) These experiments were followed by NMR (^{1}H, ^{13}C, ^{31}P), however no discrete intermediates were successfully characterized.

(34) Attempts to separate the isomeric mixture of phenylpalladium iodide complexes failed by both conventional silica gel flash chromatography and preparatory HPLC.

(35) Optimization of the cis/trans isomerization transition state of the cationic phenyl palladium(II) complex failed to locate a TS. Scan of the reaction coordinate indicates the barrier of isomerization is higher than 10 kcal/mol with respect to the

cationic phenyl palladium complex **217**. This suggests the cis/trans isomerization via the dissociative mechanism via isomerization of the tri-coordinated complex **217** cannot occur. See Figure 4.7

(36) Computations indicated that alkene insertion to the minor isomer of phenyl palladium complex, in which the Ph is *cis* to the oxazoline, yields very low enantioselectivity. The chiral oxazoline is now *trans* to the enone, and thus the stereocontrol is diminished (see **1-TS-C** and **1-TS-D** in Figure 45).

(37) A similar argument about imparted enantioselectivity can be made to rule out the catalytic activity of palladium(0) nanoparticles. Additionally, a mercury(0) poisoning test has ruled out the activity of palladium(0) nanoparticles in the Pd/PyOx manifold. See ref. 17.

(38) Brønsted acid catalysis was also ruled out, as the substitution of trifluoroacetic acid for $Pd(OCOCF_3)_2$ proved unable to catalyze the reaction. Protic acids are not tenable catalysts in the absence of palladium salts.

(39) We have computed the effects of coordination with phenylboronic acid to activate the carbonyl on the enone in the alkene insertion step. No acceleration on alkene insertion was observed computationally with either Lewis acid or hydrogen bonding coordination.

(40) The suggestion of boronic acid stabilization of arylpalladium cationic intermediates is consistent with the observation that boron species lacking hydroxyl groups serve as poor substrates for the reaction. For example, greatly diminished yields (and high degrees of biphenyl formation) are observed with the use of $NaBPh_4$ or KF_3BPh as the phenyl donor species. See section 4.2.6.

(41) See Supporting Information of ref. 13 for details on the sensitivity of enantioselectivity of the Pd/PyOx system to polar, coordinating solvents. The addition of 5 equiv. of alcoholic co-solvent as a proton source is generally detrimental to the enantioselectivity and, occasionally, to the yield of the reaction.

(42) Shintani, R.; Yamagami, T.; Kimura, T.; Hayashi, T. *Org. Lett.* **2005**, *7*, 5317–5319.

(43) (a) i-PrPyOx: Frauenlob, R.; McCormack, M. M.; Walsh, C. M.; Bergin, E. *Org. Biomol. Chem.* **2011**, *9*, 6934–6937. (b) PhPyOx: Malkov, A. V.; Stewart-Liddon, A. J. P.; McGeoch, G. D.; Ramirez-Lopez, P.; Kocovsk, P. *Org. Biomol. Chem.* **2012**, *10*, 4864–4877. (c) i-BuPyOx: Brunner, H.; Obermann, U. *Chem. Ber.* **1989**, *122*, 499–507. (d) 4-OMePyOx, Jensen, K. H.; Webb, J. D.; Sigman, M. S. *J. Am. Chem. Soc.* **2010**, *132*, 17471–17482. (e) 4-CF3PyOx: Jensen, K. H.; Webb, J. D.; Sigman, M. S. *J. Am. Chem. Soc.* **2010**, *132*, 17471–17482. (f) 5-PhPyOx: Brunner, H.; Obermann, U. *Chem. Ber.* **1989**, *122*, 499–507. (g) *t*-BuQuinOx: He, W.; Yip, K-T.; Zhu, N-Y.; Yang, D. *Org. Lett.* **2009**, *11*, 5626–5628. (h) i-PrQuinOx: Zhang, Y.; Sigman, M. S. *J. Am. Chem. Soc.* **2007**, *129*, 3076–3077.

(44) Markies, B. A.; Canty, A. J.; de Graaf, W.; Boersma, J.; Janssen, M. D.; Hogerheide, M. P.; Smeets, W. J. J.; Spek, A. L.; van Koten, J. *J. Organomet. Chem.* **1994**, *482*, 191-199.

(45) Kirchberg, S.; Tani, S.; Ueda, K.; Yamaguchi, J.; Studer, A.; Itami, K. *Angew. Chem. Int. Ed.* **2011**, *50*, 2387–2391.

(46)   Shintani, R.; Tsutsumi, Y.; Nagaosa, M.; Nishimura, T.; Hayashi, T. *J. Am. Chem. Soc.* **2009**, *131*, 13588–13589.

(47)   Shintani, R.; Takeda, M.; Nishimura, T.; Hayashi, T. *Angew. Chem. Int. Ed.* **2010**, *49*, 3969–3971.

(48)   Hawner, C.; Müller, D.; Gremaud, L.; Felouat, A.; Woodward, S.; Alexakis, A. *Angew. Chem., Int. Ed.* **2010**, *49*, 7769–7772.

(49)   May, T. L.; Brown, M. K.; Hoveyda, A. H. *Angew. Chem., Int. Ed.* **2008**, *47*, 7358–7362.

(50)   Hawner, C.; Li, K.; Cirriez, V.; Alexakis, A. *Angew. Chem., Int. Ed.* **2008**, *47*, 8211–8214.

(51)   Palais, L.; Alexakis, A. *Chem.–Eur. J.* **2009**, *15*, 10473–10485.

(52)   Lin, S.; Lu, X. *Org. Lett.* **2010**, *12*, 2536–2539.

(53)   Kikushima, K.; Holder, J. C.; Gatti, M.; Stoltz, B. M. *J. Am. Chem. Soc.* **2011**, *133*, 6902–6905.

(54)   (a) Shintani, R.; Hayashi, T. *Org. Lett.* **2011**, *13*, 350–352. (b) Gottumukkala, A. L.; Matcha, K.; Lutz, M.; De Vries, J. G.; Minnaard, A. J. *Chem.–Eur. J.* **2012**, *18*, 6907–6914.

(55)   Vatéle, J.-M. *Tetrahedron* **2010**, *66*, 904–912.

Appendix 3

Spectra relevant to Chapter 4:
Mechanism and enantioselectivity in palladium-catalyzed conjugate
addition of arylboronic acids to β–substituted cyclic enones:
Insights from computation and experiment
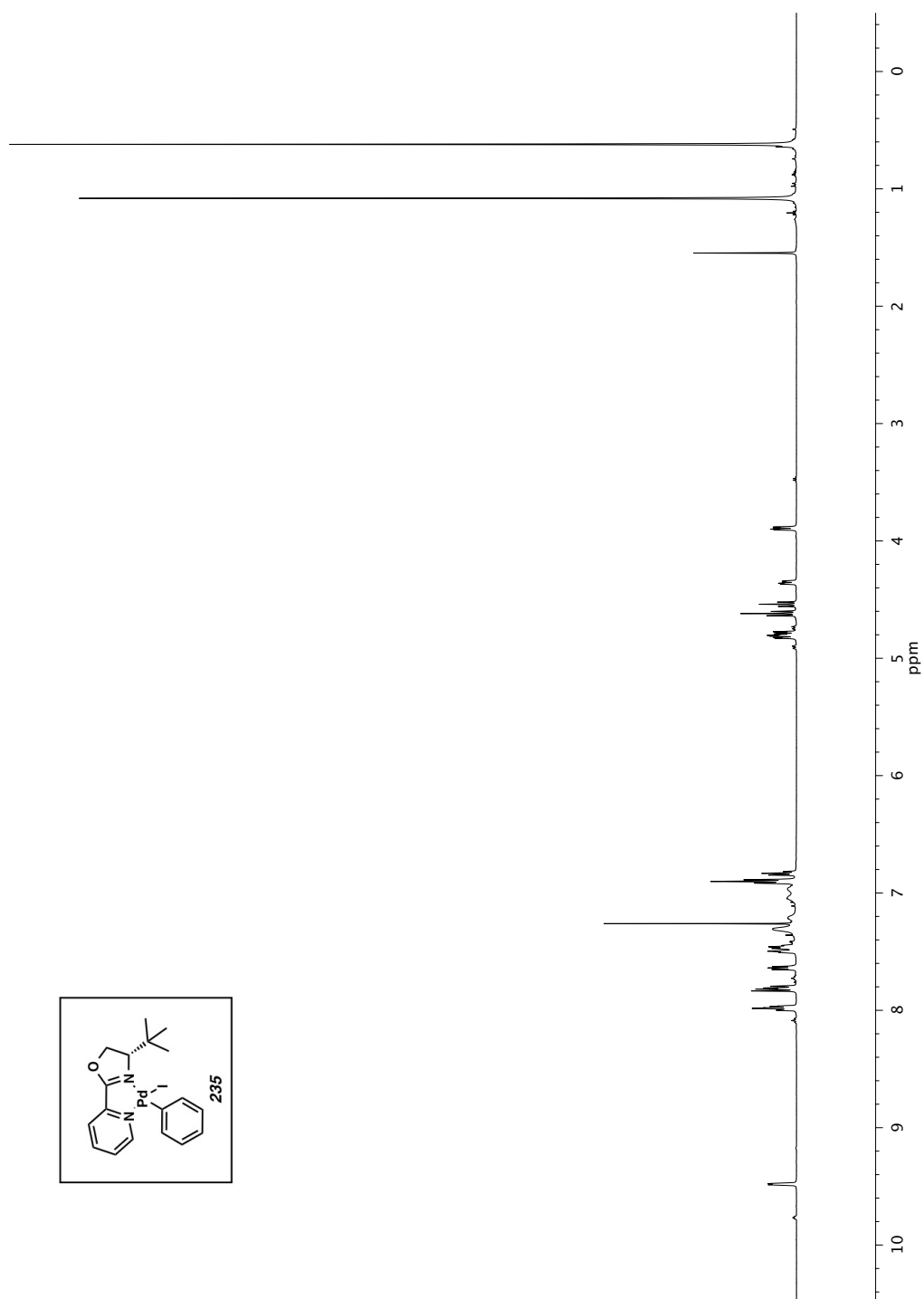
Figure A3.1 ^{1}H NMR (500 MHz, CDCl$_3$) of compound **235**
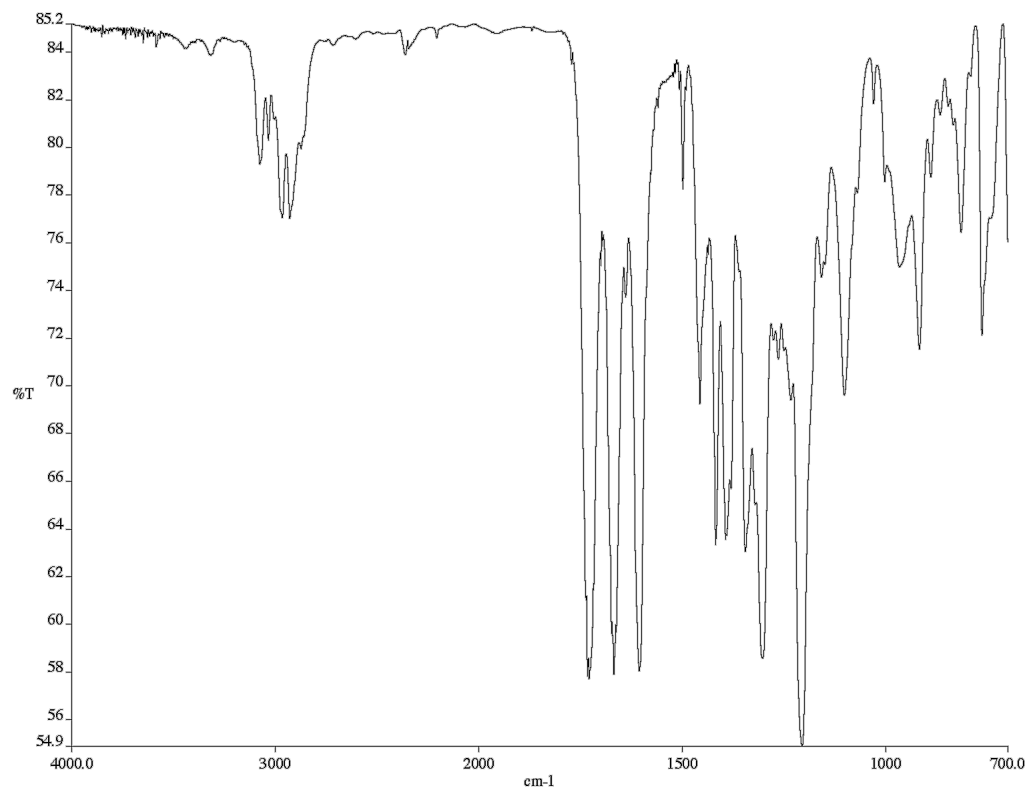
Figure A3.2 Infrared spectrum (Thin Film, NaCl) of compound **235**
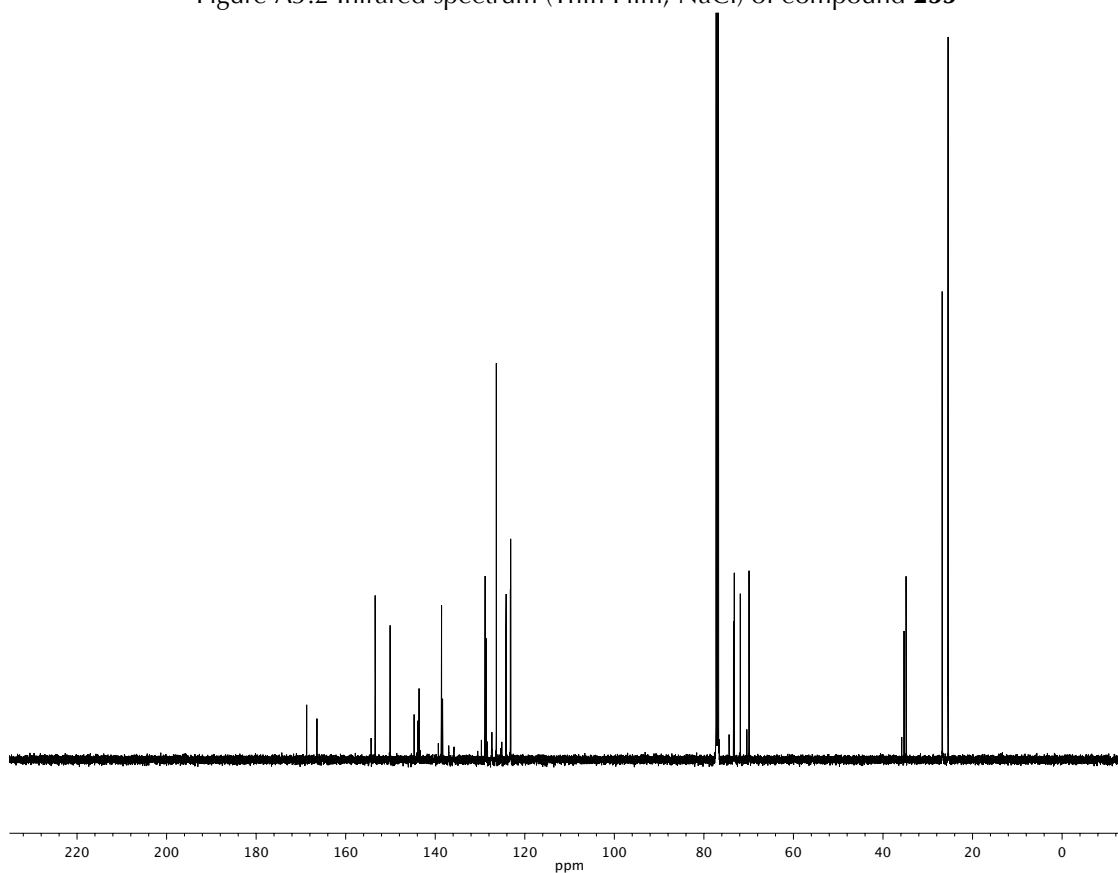
Figure A3.3 ^{13}C NMR (126 MHz, CDCl$_3$) of compound **235**
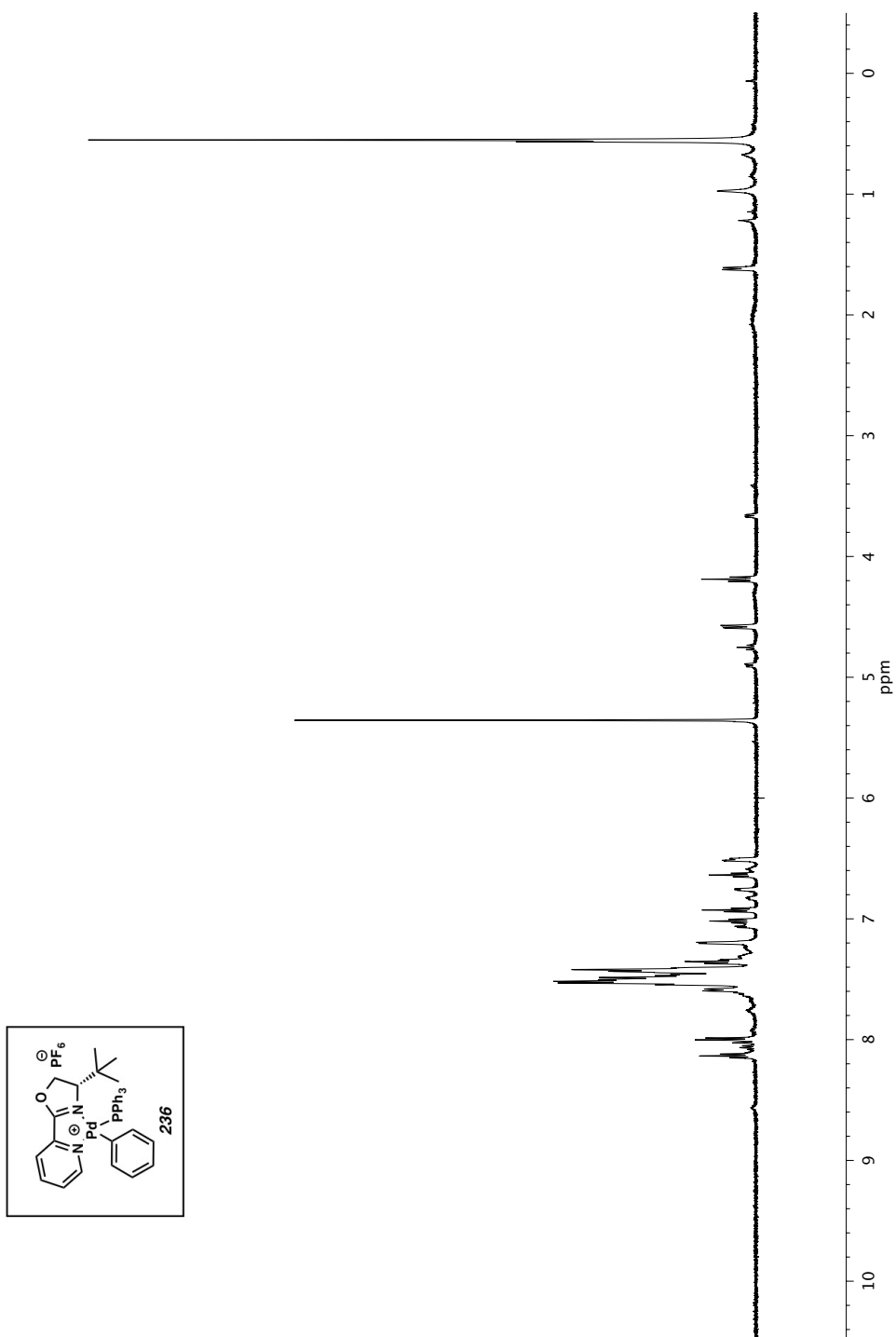
Figure A3.4 ^{1}H NMR (500 MHz, CDCl$_3$) of compound **236**
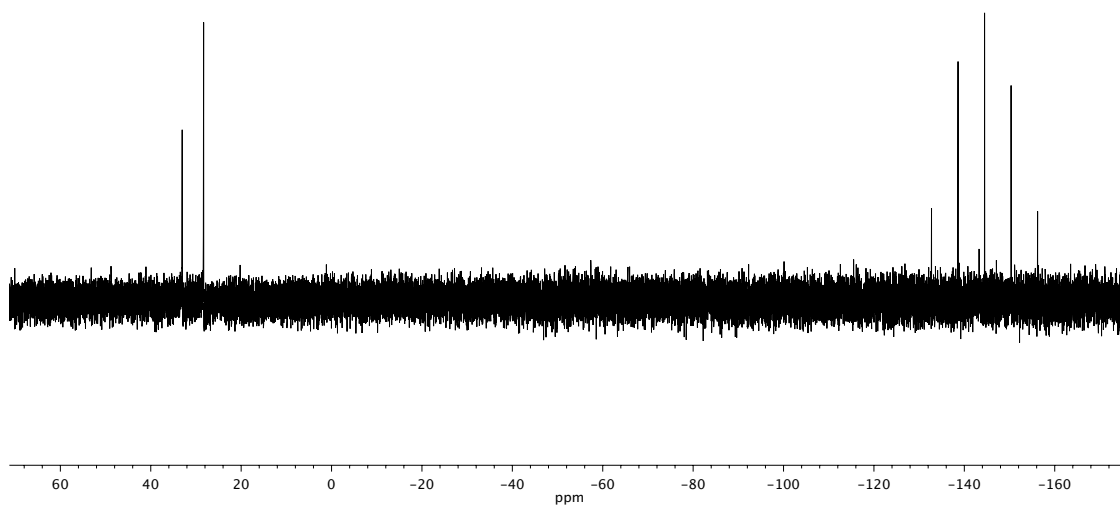
Figure A3.5 ^{31}P NMR (121 MHz, CDCl$_3$) of compound **236**
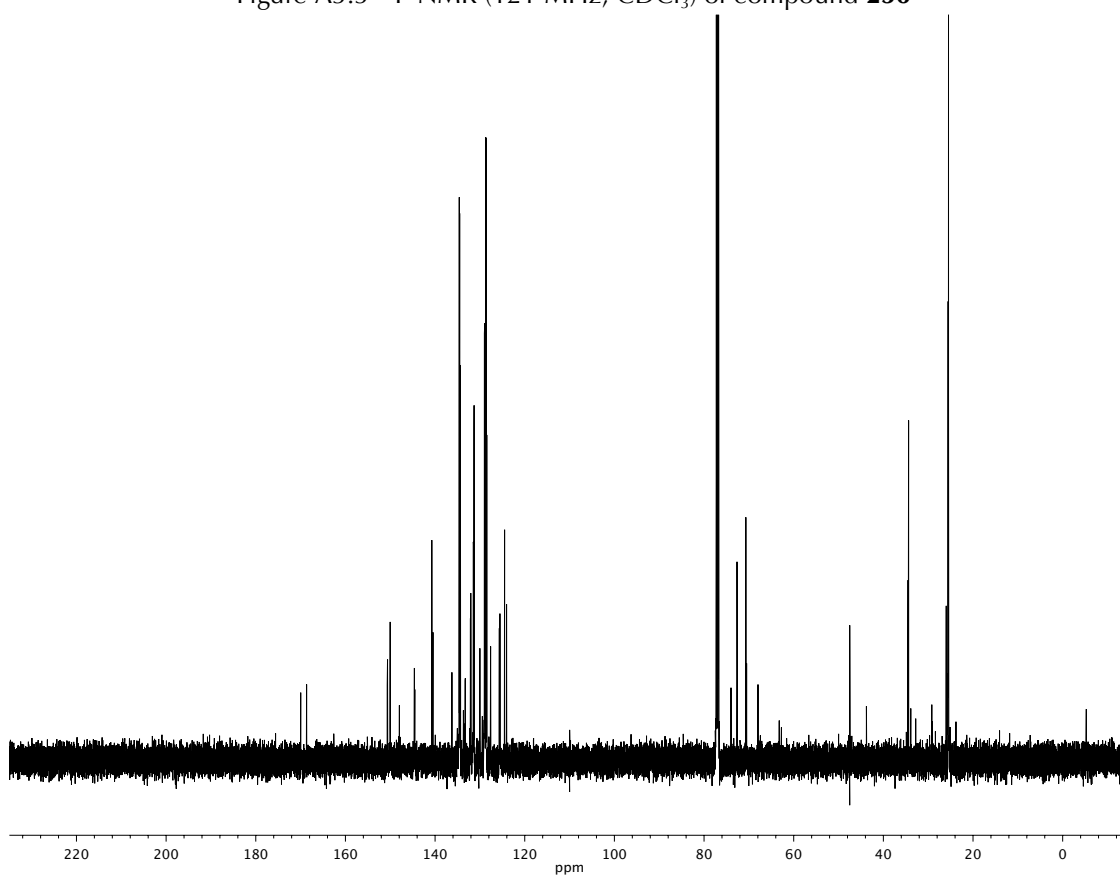
Figure A3.6 ^{13}C NMR (126 MHz, CDCl$_3$) of compound **236**
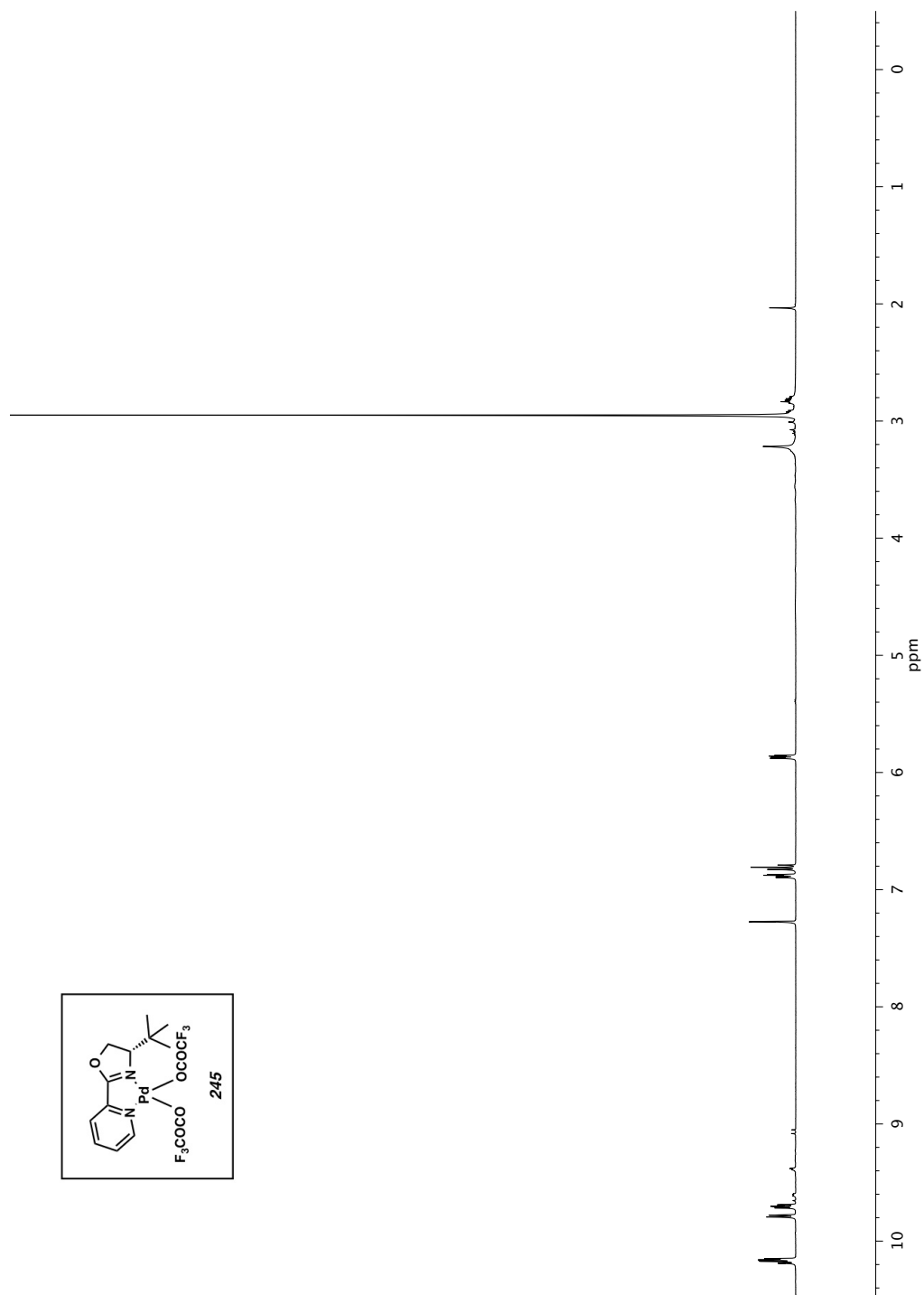
Figure A3.7 ^{1}H NMR (500 MHz, CDCl$_3$) of compound **245**
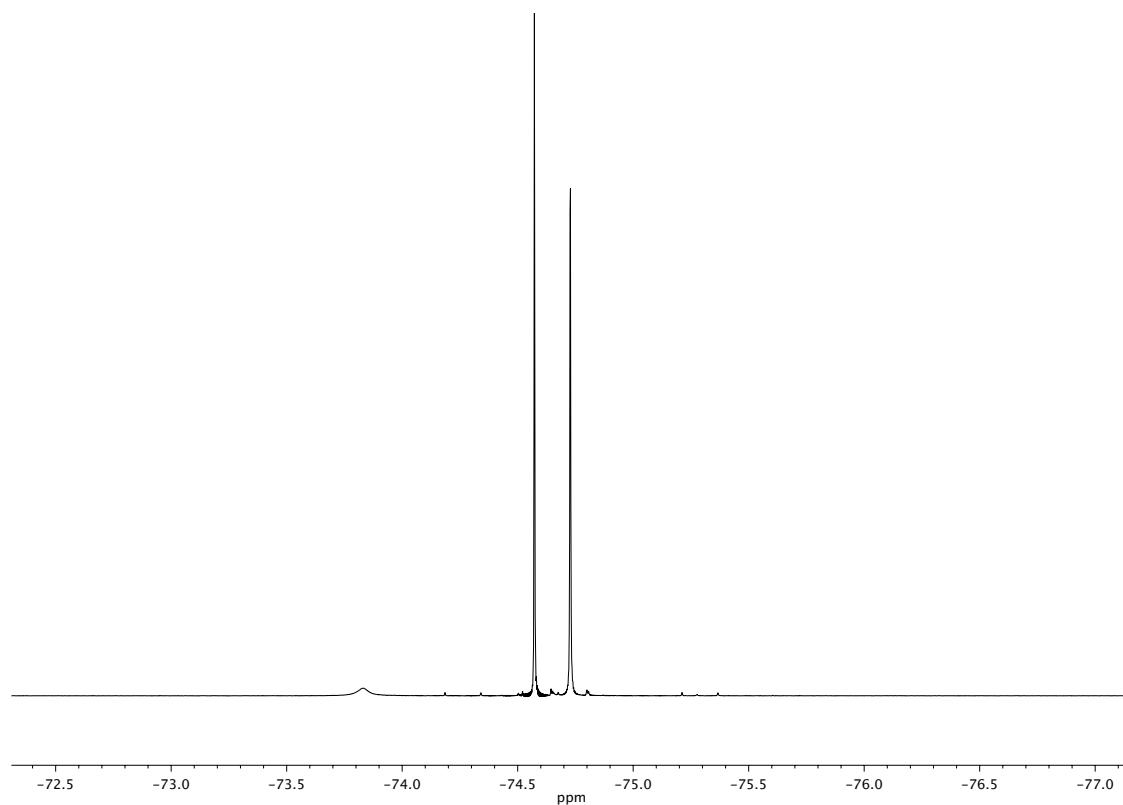
Figure A3.8 ^{19}F NMR (272 MHz, CDCl$_3$) of compound **245**
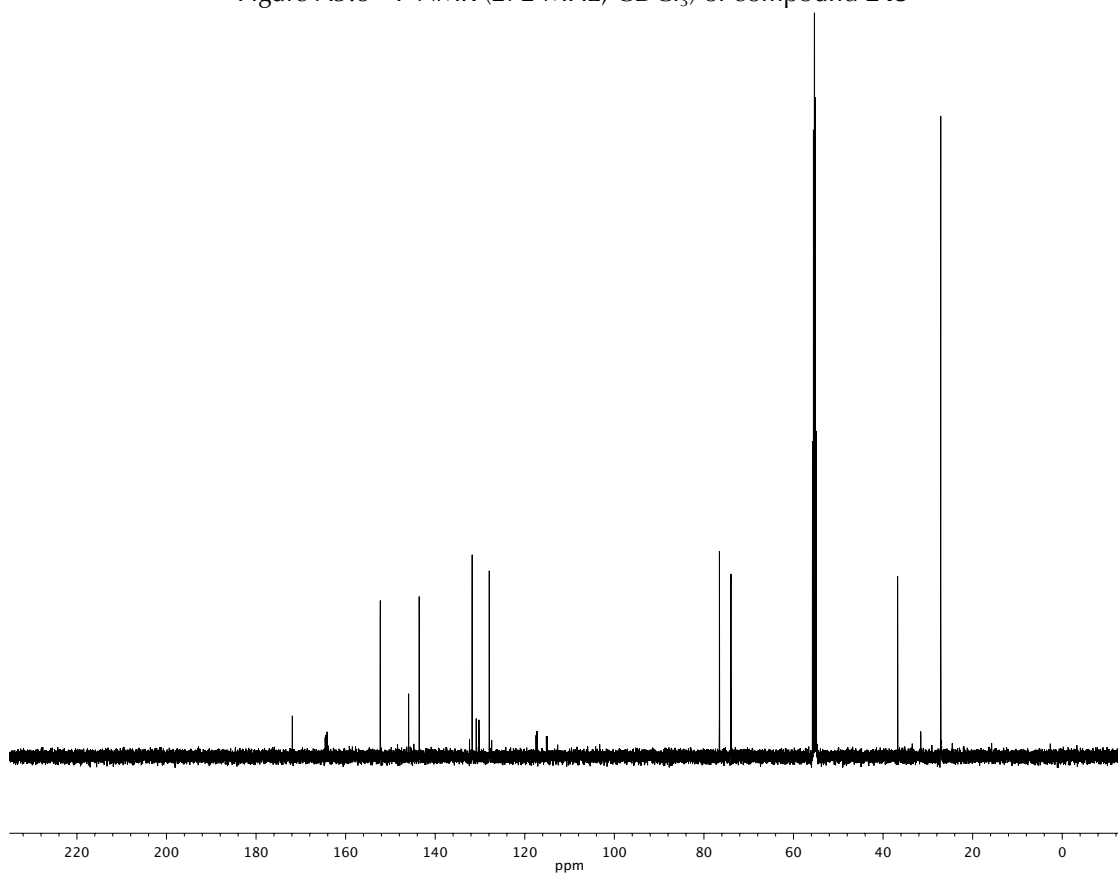
Figure A3.9 ^{13}C NMR (126 MHz, CDCl$_3$) of compound **245**
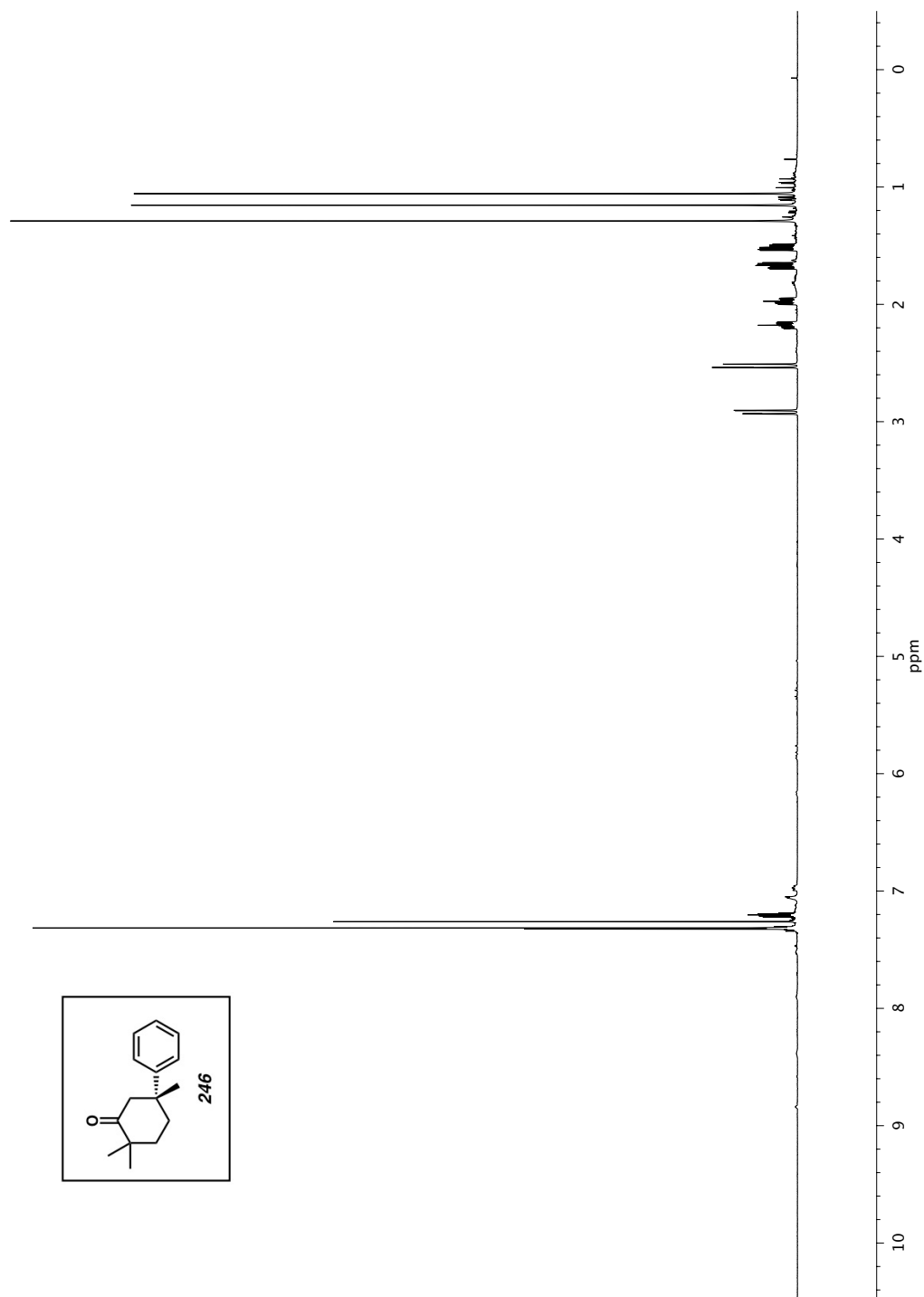
Figure A3.10 ^{1}H NMR (500 MHz, CDCl$_3$) of compound **246**
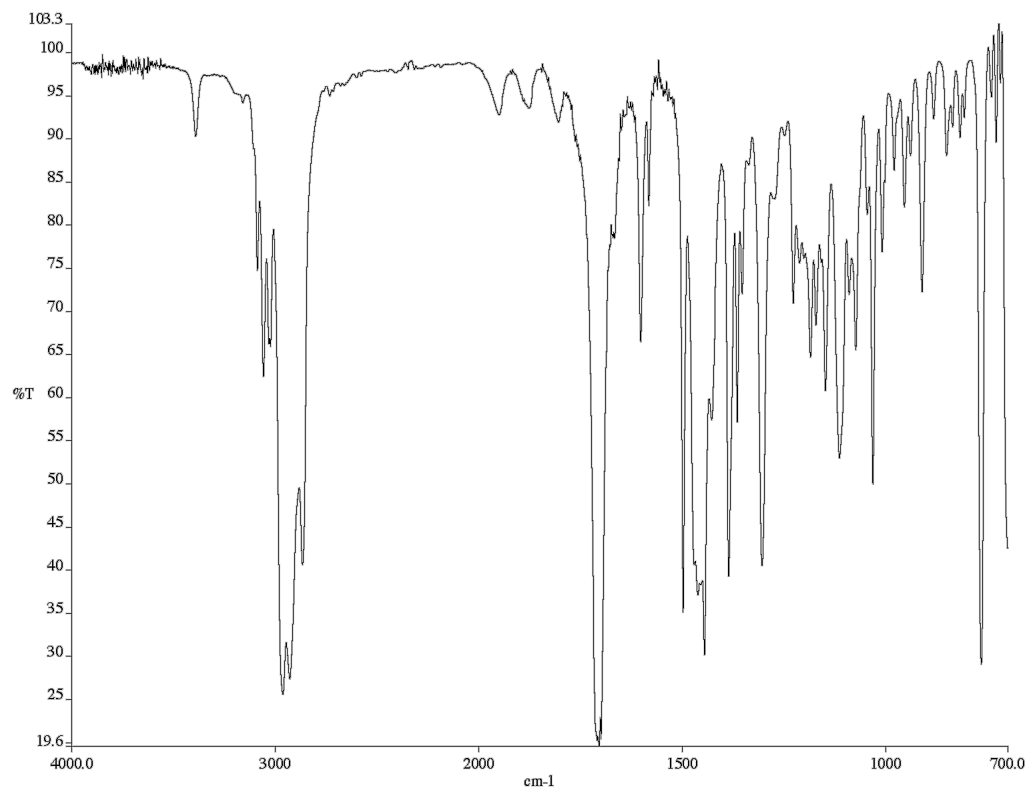
Figure A3.11 Infrared spectrum (Thin Film, NaCl) of compound **246**
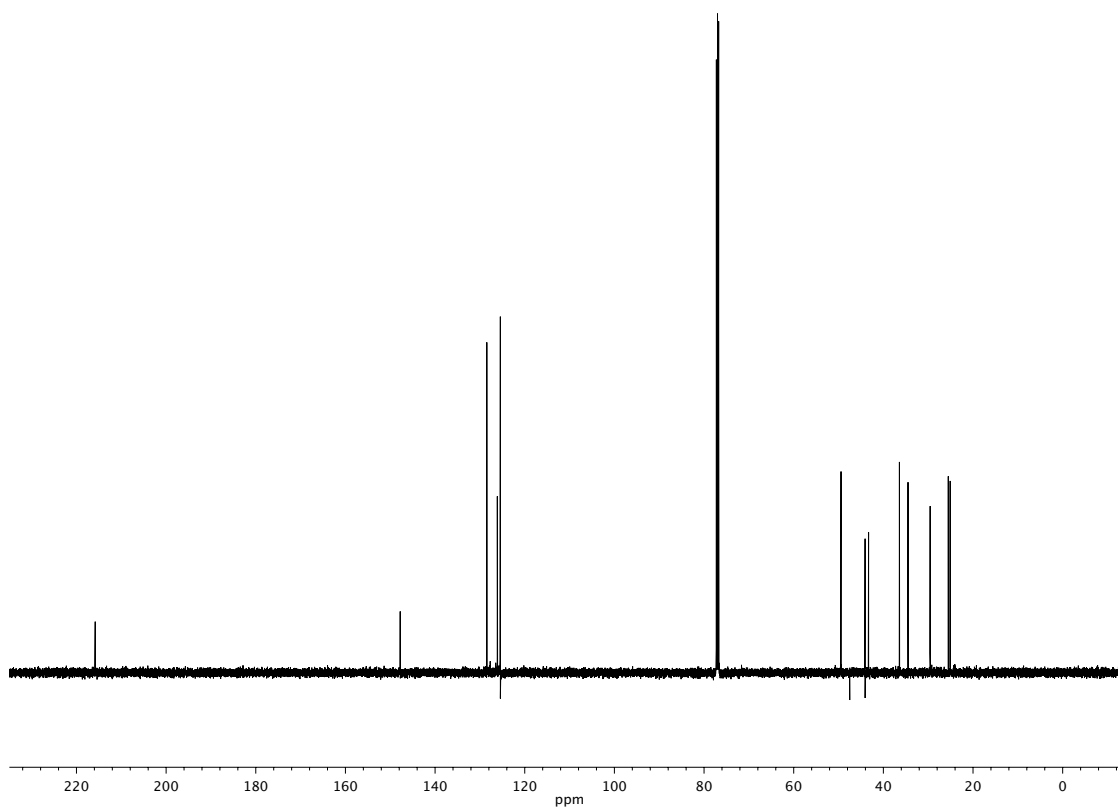
Figure A3.12 ^{13}C NMR (126 MHz, CDCl$_3$) of compound **246**

Figure A3.13 DOSY Spectrum Entry 1
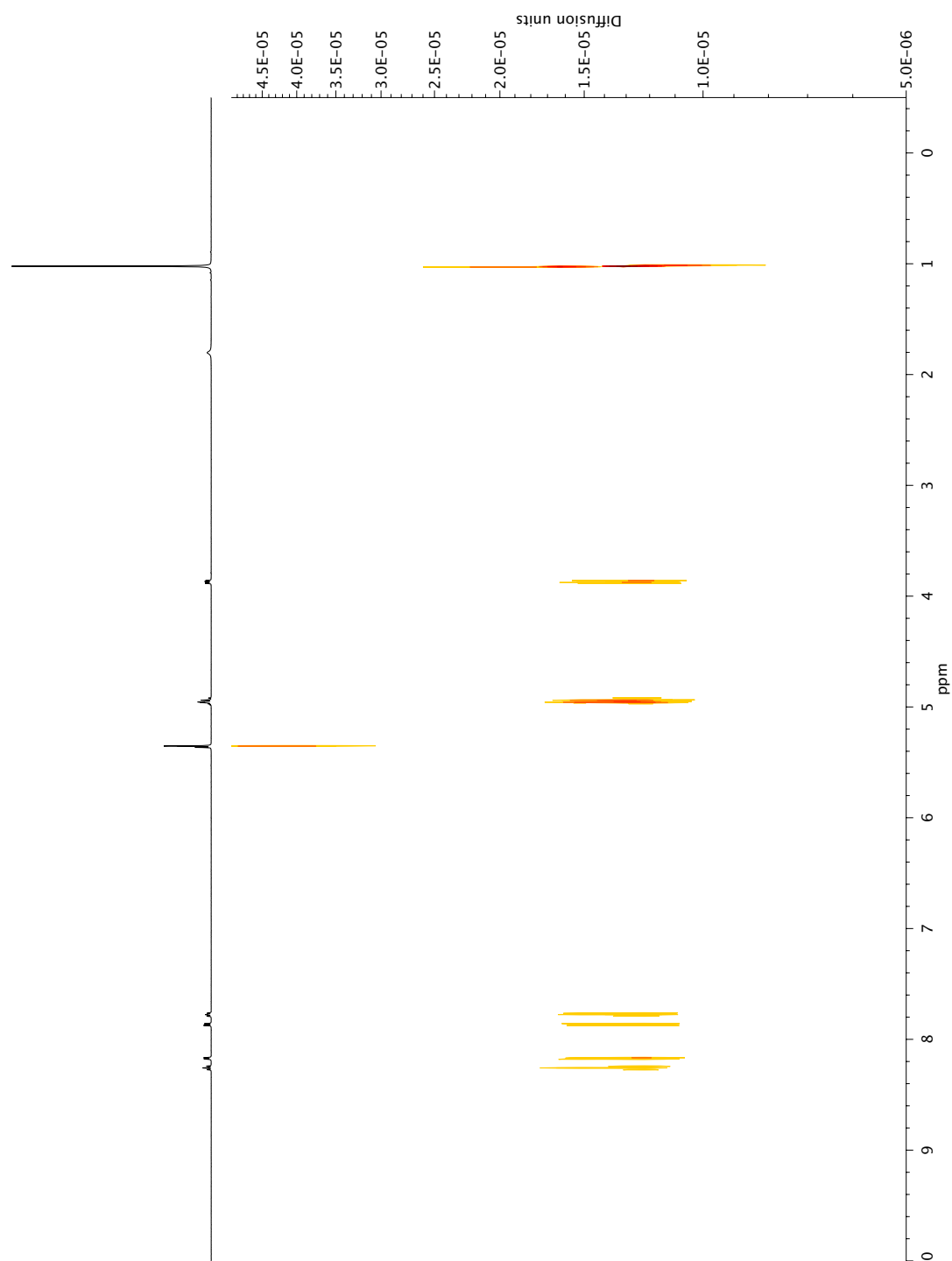
Figure A3.14 DOSY Spectrum Entry 2
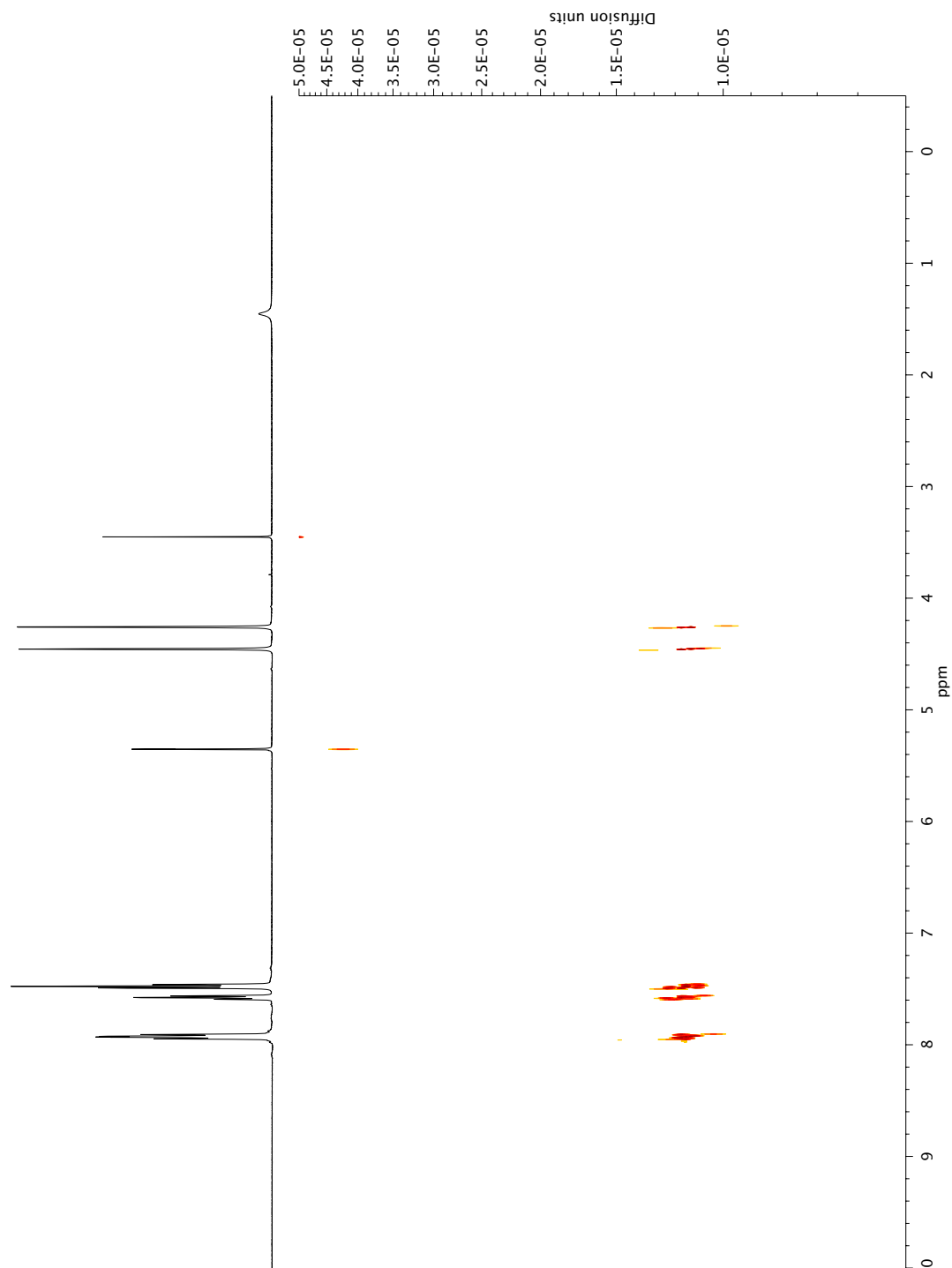
Figure A3.15 DOSY Spectrum Entry 3
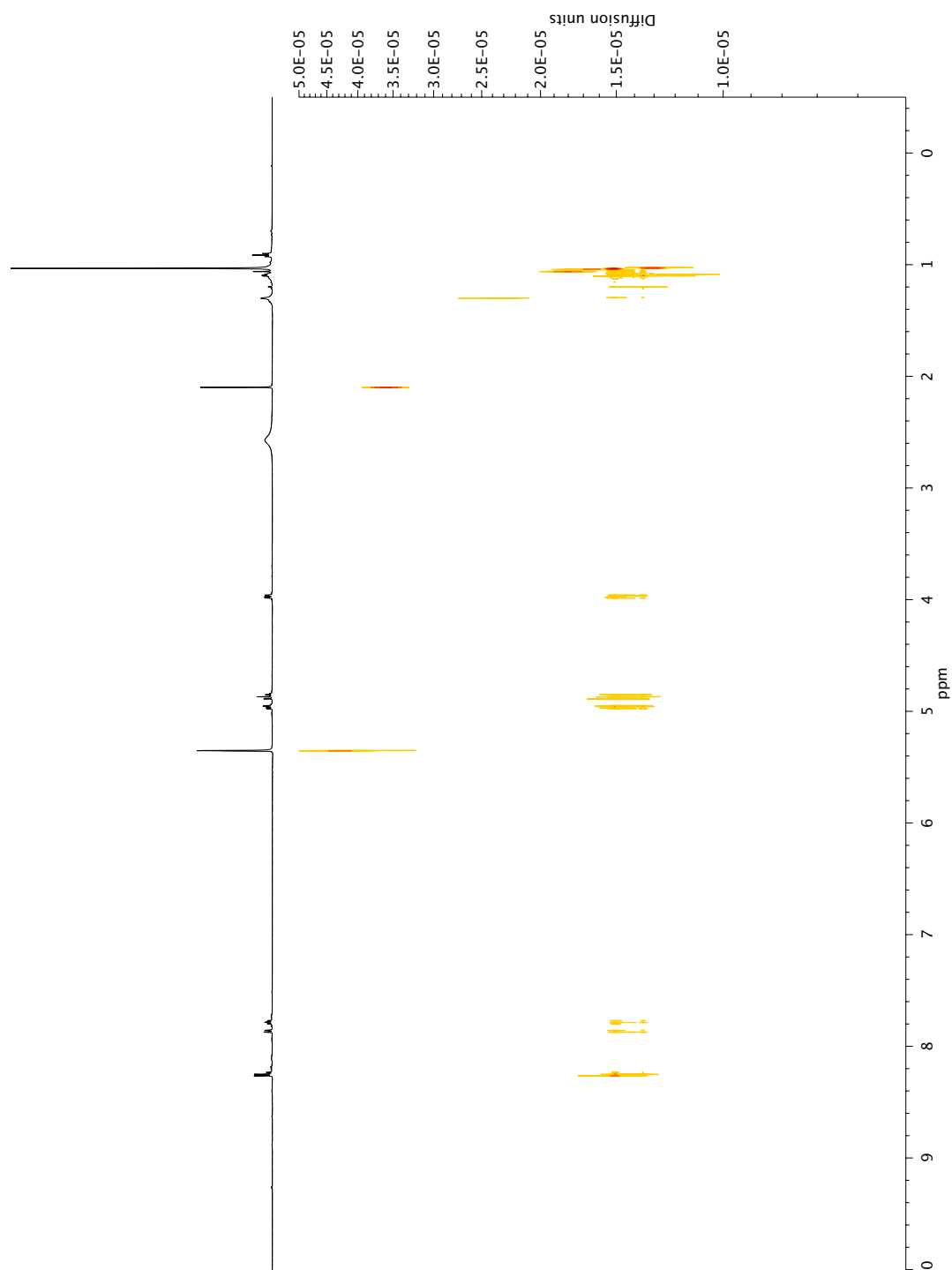
Appendix 4

X-ray structures relevant to Chapter 4:
Mechanism and enantioselectivity in palladium-catalyzed conjugate
addition of arylboronic acids to β–substituted cyclic enones:
Insights from computation and experiment

*Figure A4.1 X-ray Structure for Complex **235**, CCDC 953854*
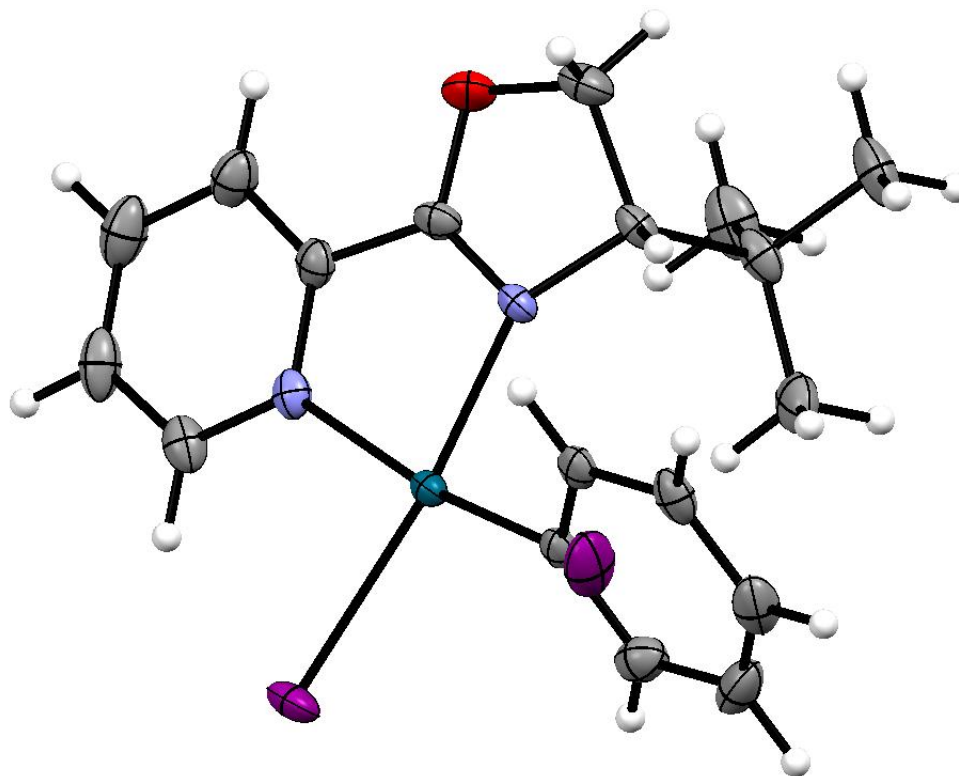
X-Ray Structure Determination

Low-temperature diffraction data (ϕ-and ω-scans) were collected on a Bruker Kappa four-circle diffractometer coupled to a Bruker APEX-II CCD detector with graphite-monochromated Mo Kα radiation (λ = 0.71073 Å) for the structure of compound anm02. The structure was solved by direct methods using SHELXS[i] and refined against F^2 on all data by full-matrix least squares with SHELXL-2013[ii] using established refinement techniques. [iii]   All non-hydrogen atoms were refined anisotropically. All hydrogen atoms were included into the model at geometrically calculated positions and refined using a riding model. The isotropic displacement parameters of all hydrogen atoms were fixed to 1.2 times the U value of the atoms they are linked to (1.5 times for methyl groups).

Compound anm02 crystallizes in the monoclinic space group C2 with one molecule in the asymmetric unit. The phenyl ligand is disordered with a partially occupied iodide ligand. A mixture of cis- and trans- isomers is identified in solution and the other position is probably also a mixture of phenyl and iodide. Refinement of a partially occupied phenyl ligand in the second position is not stable and the phenyl collides with a neighboring molecule. Because of this the second of the two iodide positions was refined fully occupied. The disordered iodine was refined with the help of similarity restraints on the Pd-I distance.

Table A4.1 Crystal data and structure refinement for anm02.

Identification code	anm02, CCDC 953854
Empirical formula	C17.80 H20.83 I1.03 N2 O Pd
Formula weight	516.47
Temperature	100(2) K
Wavelength	0.71073 Å
Crystal system	Monoclinic
Space group	C 2
Unit cell dimensions	a = 18.4571(12) Å α= 90°.
	b = 9.9004(6) Å β= 101.240(4)°.
	c = 10.5480(7) Å γ = 90°.
Volume	1890.5(2) Å^3
Z	4
Density (calculated)	1.815 Mg/m^3
Absorption coefficient	2.677 mm^{-1}
F(000)	1002
Crystal size	0.150 x 0.050 x 0.050 mm^3
Theta range for data collection	1.968 to 30.600°.
Index ranges	-26<=h<=26, -14<=k<=14, -15<=l<=15
Reflections collected	24103
Independent reflections	5762 [R(int) = 0.0380]
Completeness to theta = 25.242°	99.9 %
Absorption correction	Semi-empirical from equivalents
Max. and min. transmission	0.746 and 0.665
Refinement method	Full-matrix least-squares on F^2
Data / restraints / parameters	5762 / 2 / 221
Goodness-of-fit on F^2	1.027
Final R indices [I>2sigma(I)]	R1 = 0.0226, wR2 = 0.0403
R indices (all data)	R1 = 0.0269, wR2 = 0.0414
Absolute structure parameter	0.023(10)
Extinction coefficient	n/a
Largest diff. peak and hole	0.568 and -0.578 e.Å^{-3}

Table A4.2 Atomic coordinates (x 10^4) and equivalent isotropic displacement parameters ($Å^2x$ 10^3) for anm02. U(eq) is defined as one third of the trace of the orthogonalized U^{ij} tensor.

	x	y	z	U(eq)
I(1)	1111(1)	1537(1)	8477(1)	26(1)
Pd(1)	2229(1)	299(1)	7918(1)	15(1)
I(2A)	1528(8)	-1898(12)	7873(15)	39(4)
C(1)	1681(3)	-1422(6)	7810(6)	18(1)
C(2)	1048(2)	-1720(4)	6897(4)	27(1)
C(3)	736(2)	-3011(5)	6822(4)	33(1)
C(4)	1041(2)	-4014(4)	7665(5)	30(1)
C(5)	1653(2)	-3742(4)	8593(4)	24(1)
C(6)	1975(2)	-2458(4)	8672(4)	19(1)
N(1)	2975(2)	2025(3)	8127(3)	19(1)
C(7)	2837(2)	3340(4)	8273(4)	25(1)
C(8)	3397(3)	4273(4)	8546(4)	32(1)
C(9)	4114(3)	3889(5)	8663(4)	36(1)
C(10)	4270(2)	2532(4)	8515(4)	29(1)
C(11)	3682(2)	1648(4)	8243(3)	21(1)
C(12)	3766(2)	197(4)	8018(3)	20(1)
N(2)	3211(2)	-581(3)	7649(3)	16(1)
O(1)	4442(2)	-330(3)	8174(3)	29(1)
C(13)	4313(2)	-1793(4)	8025(4)	28(1)
C(14)	3507(2)	-1924(3)	7364(3)	18(1)
C(15)	3378(2)	-2221(4)	5897(3)	24(1)
C(16)	2554(2)	-2265(5)	5352(4)	34(1)
C(17)	3745(3)	-1142(4)	5188(4)	36(1)
C(18)	3710(3)	-3608(4)	5714(4)	36(1)

Table A4.3   Bond lengths [Å] and angles [°] for anm02.

I(1)-Pd(1)	2.5655(3)
Pd(1)-C(1)	1.973(6)
Pd(1)-N(2)	2.080(3)
Pd(1)-N(1)	2.178(3)
Pd(1)-I(2A)	2.526(10)
C(1)-C(2)	1.393(7)
C(1)-C(6)	1.407(7)
C(2)-C(3)	1.397(6)
C(2)-H(2)	0.9500
C(3)-C(4)	1.379(6)
C(3)-H(3)	0.9500
C(4)-C(5)	1.370(6)
C(4)-H(4)	0.9500
C(5)-C(6)	1.399(5)
C(5)-H(5)	0.9500
C(6)-H(6)	0.9500
N(1)-C(11)	1.341(5)
N(1)-C(7)	1.342(4)
C(7)-C(8)	1.373(6)
C(7)-H(7)	0.9500
C(8)-C(9)	1.360(7)
C(8)-H(8)	0.9500
C(9)-C(10)	1.389(7)
C(9)-H(9)	0.9500
C(10)-C(11)	1.380(5)
C(10)-H(10)	0.9500
C(11)-C(12)	1.470(6)
C(12)-N(2)	1.280(5)
C(12)-O(1)	1.332(4)
N(2)-C(14)	1.489(4)
O(1)-C(13)	1.471(5)
C(13)-C(14)	1.521(5)
C(13)-H(13A)	0.9900
C(13)-H(13B)	0.9900

C(14)-C(15)	1.548(5)
C(14)-H(14)	1.0000
C(15)-C(16)	1.519(6)
C(15)-C(18)	1.531(6)
C(15)-C(17)	1.534(6)
C(16)-H(16A)	0.9800
C(16)-H(16B)	0.9800
C(16)-H(16C)	0.9800
C(17)-H(17A)	0.9800
C(17)-H(17B)	0.9800
C(17)-H(17C)	0.9800
C(18)-H(18A)	0.9800
C(18)-H(18B)	0.9800
C(18)-H(18C)	0.9800
C(1)-Pd(1)-N(2)	94.67(18)
C(1)-Pd(1)-N(1)	171.83(18)
N(2)-Pd(1)-N(1)	78.00(11)
N(2)-Pd(1)-I(2A)	95.4(3)
N(1)-Pd(1)-I(2A)	171.3(4)
C(1)-Pd(1)-I(1)	89.97(16)
N(2)-Pd(1)-I(1)	173.14(8)
N(1)-Pd(1)-I(1)	97.02(8)
I(2A)-Pd(1)-I(1)	89.1(3)
C(2)-C(1)-C(6)	117.3(5)
C(2)-C(1)-Pd(1)	125.0(4)
C(6)-C(1)-Pd(1)	117.6(4)
C(1)-C(2)-C(3)	120.9(4)
C(1)-C(2)-H(2)	119.5
C(3)-C(2)-H(2)	119.5
C(4)-C(3)-C(2)	120.7(4)
C(4)-C(3)-H(3)	119.6
C(2)-C(3)-H(3)	119.6
C(5)-C(4)-C(3)	119.7(4)
C(5)-C(4)-H(4)	120.2
C(3)-C(4)-H(4)	120.2

C(4)-C(5)-C(6)	120.2(4)
C(4)-C(5)-H(5)	119.9
C(6)-C(5)-H(5)	119.9
C(5)-C(6)-C(1)	121.2(4)
C(5)-C(6)-H(6)	119.4
C(1)-C(6)-H(6)	119.4
C(11)-N(1)-C(7)	117.5(4)
C(11)-N(1)-Pd(1)	112.1(2)
C(7)-N(1)-Pd(1)	130.0(3)
N(1)-C(7)-C(8)	121.7(4)
N(1)-C(7)-H(7)	119.1
C(8)-C(7)-H(7)	119.1
C(9)-C(8)-C(7)	120.7(4)
C(9)-C(8)-H(8)	119.7
C(7)-C(8)-H(8)	119.7
C(8)-C(9)-C(10)	118.7(4)
C(8)-C(9)-H(9)	120.7
C(10)-C(9)-H(9)	120.7
C(11)-C(10)-C(9)	117.7(4)
C(11)-C(10)-H(10)	121.1
C(9)-C(10)-H(10)	121.1
N(1)-C(11)-C(10)	123.7(4)
N(1)-C(11)-C(12)	112.9(3)
C(10)-C(11)-C(12)	123.4(4)
N(2)-C(12)-O(1)	118.4(4)
N(2)-C(12)-C(11)	122.3(3)
O(1)-C(12)-C(11)	119.2(3)
C(12)-N(2)-C(14)	107.2(3)
C(12)-N(2)-Pd(1)	111.9(2)
C(14)-N(2)-Pd(1)	139.9(2)
C(12)-O(1)-C(13)	104.1(3)
O(1)-C(13)-C(14)	104.9(3)
O(1)-C(13)-H(13A)	110.8
C(14)-C(13)-H(13A)	110.8
O(1)-C(13)-H(13B)	110.8
C(14)-C(13)-H(13B)	110.8

H(13A)-C(13)-H(13B)	108.8
N(2)-C(14)-C(13)	101.3(3)
N(2)-C(14)-C(15)	112.3(3)
C(13)-C(14)-C(15)	114.8(3)
N(2)-C(14)-H(14)	109.4
C(13)-C(14)-H(14)	109.4
C(15)-C(14)-H(14)	109.4
C(16)-C(15)-C(18)	108.8(4)
C(16)-C(15)-C(17)	109.9(3)
C(18)-C(15)-C(17)	109.8(3)
C(16)-C(15)-C(14)	109.3(3)
C(18)-C(15)-C(14)	108.0(3)
C(17)-C(15)-C(14)	111.0(3)
C(15)-C(16)-H(16A)	109.5
C(15)-C(16)-H(16B)	109.5
H(16A)-C(16)-H(16B)	109.5
C(15)-C(16)-H(16C)	109.5
H(16A)-C(16)-H(16C)	109.5
H(16B)-C(16)-H(16C)	109.5
C(15)-C(17)-H(17A)	109.5
C(15)-C(17)-H(17B)	109.5
H(17A)-C(17)-H(17B)	109.5
C(15)-C(17)-H(17C)	109.5
H(17A)-C(17)-H(17C)	109.5
H(17B)-C(17)-H(17C)	109.5
C(15)-C(18)-H(18A)	109.5
C(15)-C(18)-H(18B)	109.5
H(18A)-C(18)-H(18B)	109.5
C(15)-C(18)-H(18C)	109.5
H(18A)-C(18)-H(18C)	109.5
H(18B)-C(18)-H(18C)	109.5

Symmetry transformations used to generate equivalent atoms:

Table A4.4. Anisotropic displacement parameters ($\mathring{A}^2$x 10^3) for anm02. The anisotropic displacement factor exponent takes the form: $-2\pi^2[\,h^2\,a^{*2}U^{11} + ... + 2\,h\,k\,a^*\,b^*\,U^{12}\,]$

	U^{11}	U^{22}	U^{33}	U^{23}	U^{13}	U^{12}
I(1)	21(1)	28(1)	29(1)	3(1)	8(1)	12(1)
Pd(1)	15(1)	15(1)	16(1)	0(1)	4(1)	4(1)
I(2A)	37(7)	32(8)	52(7)	-14(6)	20(5)	-17(5)
C(1)	17(3)	19(3)	21(2)	-4(2)	8(2)	0(2)
C(2)	21(2)	37(2)	24(2)	0(2)	5(2)	0(2)
C(3)	25(2)	47(3)	27(2)	-14(2)	7(2)	-14(2)
C(4)	30(2)	27(2)	41(2)	-10(2)	21(2)	-11(2)
C(5)	31(2)	22(2)	25(2)	-2(2)	17(2)	1(2)
C(6)	19(2)	22(2)	18(2)	-4(2)	9(2)	0(2)
N(1)	26(2)	17(2)	15(1)	0(1)	6(1)	0(1)
C(7)	37(2)	19(2)	19(2)	2(2)	7(2)	3(2)
C(8)	56(3)	18(2)	23(2)	-2(2)	11(2)	-8(2)
C(9)	49(3)	32(2)	28(2)	-5(2)	11(2)	-18(2)
C(10)	30(2)	31(2)	28(2)	-5(2)	9(2)	-10(2)
C(11)	24(2)	23(2)	17(2)	-4(2)	7(1)	-2(2)
C(12)	16(2)	25(2)	20(2)	2(2)	7(1)	3(2)
N(2)	17(1)	16(1)	18(1)	0(1)	6(1)	4(1)
O(1)	16(1)	35(2)	36(2)	-4(1)	7(1)	1(1)
C(13)	21(2)	31(2)	34(2)	2(2)	7(2)	9(2)
C(14)	22(2)	16(2)	19(2)	3(1)	10(1)	5(1)
C(15)	34(2)	21(2)	21(2)	2(2)	16(2)	6(2)
C(16)	41(2)	38(2)	21(2)	-10(2)	3(2)	4(2)
C(17)	58(3)	28(2)	29(2)	5(2)	25(2)	0(2)
C(18)	56(3)	27(2)	29(2)	-4(2)	21(2)	9(2)

Table A4.5   *Hydrogen coordinates (x 10^4) and isotropic displacement parameters ($Å^2$x 10 ^{3})*
for anm02.

	x	y	z	U(eq)
H(2)	825	-1036	6319	33
H(3)	310	-3199	6182	39
H(4)	827	-4891	7604	36
H(5)	1859	-4427	9185	29
H(6)	2401	-2283	9318	23
H(7)	2340	3634	8186	29
H(8)	3281	5196	8654	38
H(9)	4501	4536	8842	43
H(10)	4765	2224	8599	35
H(13A)	4403	-2247	8878	34
H(13B)	4640	-2197	7488	34
H(14)	3266	-2646	7802	22
H(16A)	2318	-2915	5844	50
H(16B)	2470	-2540	4443	50
H(16C)	2341	-1367	5418	50
H(17A)	3532	-255	5310	54
H(17B)	3660	-1356	4264	54
H(17C)	4277	-1124	5539	54
H(18A)	4238	-3603	6100	54
H(18B)	3645	-3809	4789	54
H(18C)	3460	-4299	6136	54

[i] Sheldrick, G. M. *Acta Cryst.* **1990**, A46, 467-473.
[ii] Sheldrick, G. M. *Acta Cryst.* **2008**, A64, 112-122.
[iii] Müller, P. *Crystallography Reviews* **2009**, *15*, 57-83.

CHAPTER 5

Development of a Scalable Synthesis of the (S)-4-(tert-butyl)-2-

(pyridin-2-yl)-4,5-dihydrooxazole ((S)–t-BuPyOx) Ligand[‡]

$0.43 per gram   Multi-Gram Scale
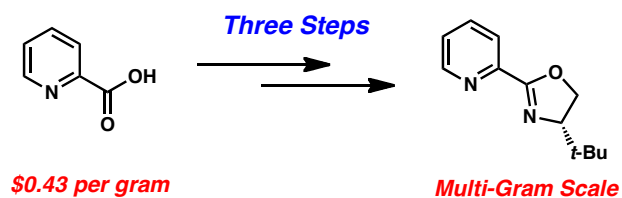
Abstract
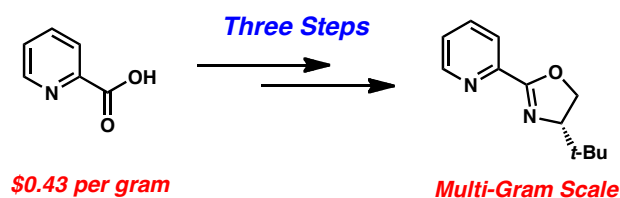
An efficient method for the synthesis of the (*S*)-4-(*tert*-butyl)-2-(pyridin-2-yl)-4,5-dihydrooxazole ((*S*)–*t*-BuPyOx) ligand has been developed. Inconsistent yields and tedious purification in known routes to (*S*)–*t*-BuPyOx suggested the need for an efficient, dependable, and scalable synthetic route. Furthermore, a route suitable for the synthesis of PyOx derivatives is desirable. Herein, we describe the development of a three-step route from inexpensive and commercially available 2-picolinic acid. This short procedure is amenable to multi-gram scale synthesis and provides the target ligand in 64% overall yield.

5.1 Introduction

Pyridinooxazoline (PyOx) ligands represent a growing class of bidentate dinitrogen ligands used in asymmetric catalysis.[1] Recently, our laboratory reported the catalytic asymmetric conjugate addition of arylboronic acids to cyclic, β,β'-disubstituted enones utilizing (*S*)–*t*-BuPyOx (**82**) as the chiral ligand (Figure 1).[2] This robust reaction is insensitive to oxygen atmosphere, highly tolerant of water,[3] and provides cyclic ketones bearing β-benzylic quaternary stereocenters in high yields and enantioselectivities. While the reaction itself proved to be amenable to multi-gram scale, the ligand is not yet commercially available and no reliable method for the large-scale synthesis of (*S*)–*t*-BuPyOx was known.[4] We sought to address this shortcoming by developing an efficient route starting from a cheap, commercially available precursor to pyridinooxazoline ligands (Scheme 5.1).

Scheme 5.1 Picolinic acid as a precursor for the synthesis of pyridinooxazoline ligands
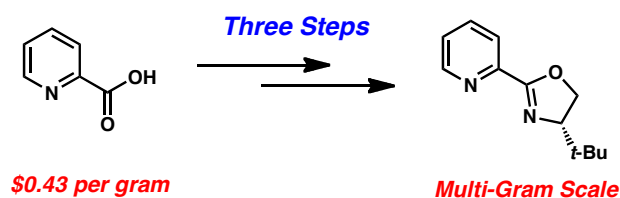
Three Steps

$0.43 per gram

Multi-Gram Scale

Inconsistent yields and tedious purification in known routes to (*S*)–*t*-BuPyOx suggested the need for an efficient, dependable, and scalable synthetic route. Furthermore, a route suitable for the synthesis of PyOx derivatives is desirable. Herein, we describe the development of a three-step route from inexpensive and commercially available 2-picolinic acid. This short procedure is amenable to multi-gram scale synthesis and provides the target ligand in 64% overall yield.

5.2 Results and Discussion

5.2.1 Revised Retrosynthetic Analysis of (S)-t-BuPyOx

Initially, (*S*)–*t*-BuPyOx (**82**) was synthesized by methanolysis of 2-cyanopyridine (**247**) to afford methoxyimidate **248**, and subsequent acid-catalyzed cyclization to afford the (*S*)–*t*-BuPyOx ligand (Figure 5.1).[5] We found the yields of this reaction sequence to be highly variable, and the purification by silica gel chromatography to be tedious. In the revised retrosynthesis, 2-picolinic acid (**250**) was identified as a comparably priced, commonly available surrogate for cyanopyridine **247**. Amidation of (*S*)-*tert*-leucinol (**251**) and picolinic acid (**250**) would generate amide **249**, which upon cyclization would generate the ligand framework.

Figure 5.1 Initial PyOx synthesis and revised plan
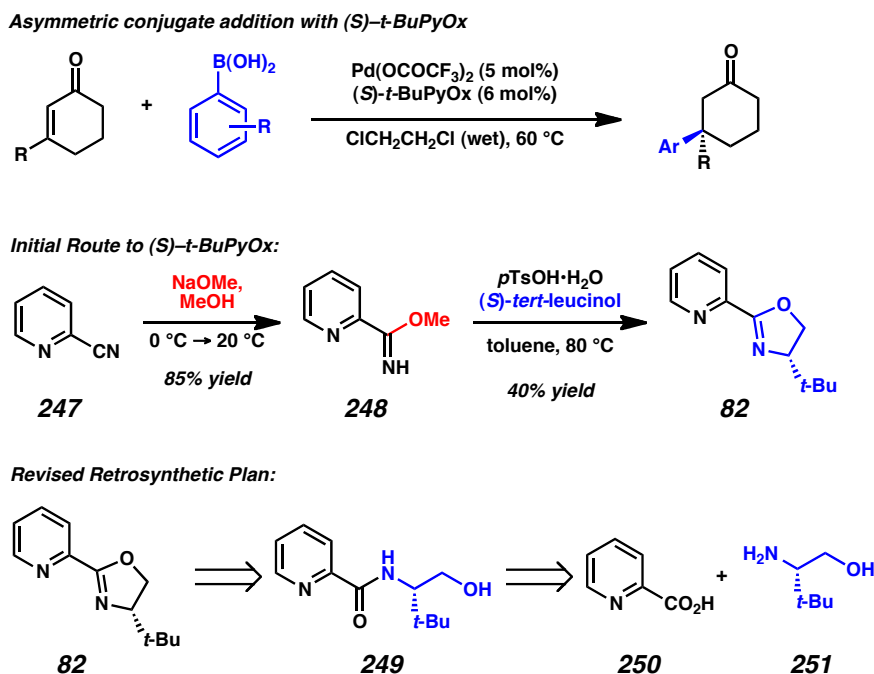
5.2.2 Amidation of 2-picolinic acid and (S)-tert-leucinol

Initial efforts focused on the amidation reaction between (*S*)-*tert*-leucinol and 2-picolinic acid (**250**) *via* acid chloride **252** (Table 5.1), which was generated *in situ* by treatment of acid **250** with a number of chlorinating agents. Oxalyl chloride (entries 1, 2) provided reasonable yields of amide **249**, however bis-acylation of (*S*)-*tert*-leucinol was observed as a common side product. Importantly, temperature control of this reaction (entry 2) allowed isolation of 75% of desired alcohol **249** in acceptable purity *without the use of column chromatography*. Use of diphenyl chlorophosphate (entries 3, 5-6) also resulted in noticeable quantities of over acylation product, as well as the generation of a small amount of phosphorylation of amide **249**. These results encouraged us to explore alternative activation strategies to generate the desired amide bond. Adapting a procedure from Sigman, activation of acid **250** by treatment with *iso*-butylchloroformate and *N*-methylmorpholine (anhydride **253**) facilitated the desired transformation with the highest overall yield, with amide **249** being isolated in 91% yield, albeit requiring column chromatography.[6]

Table 5.1 Amidation reactions of picolinic acid

entry	reagent	solvent 1 / 2	temp. (°C)	base	time (h)	yield (%)^b
1	(COCl)$_2$	THF/THF	50	Et$_3$N	1	55
2	(COCl)$_2$	THF/THF	0 → rt	Et$_3$N	7	75^c
3	DPCP	THF	0 → rt	Et$_3$N	6	72
4	SOCl$_2$	toluene/THF	rt	none	5	trace
5	DPCP	THF	50	none	2	30
6	DPCP	THF/THF	0 → rt	Et$_3$N	3	65^c
7	*i*-BuOCOCl, NMM	CH$_2$Cl$_2$/CH$_2$Cl$_2$	0 → rt	NMM	3	92

DPCP = diphenyl chlorophosphate, NMM = *N*-methylmorpholine. ^{a} Conditions: ^{b} Isolated yield. ^{c} Purification by flash chromatography not required.

5.2.3 Cyclization to form oxazoline ring

Satisfied with our ability to generate amide **249** on gram-scale with good yield, we turned our attention to the completion of the synthesis. The cyclization of amide **249** to (*S*)–*t*-BuPyOx (**82**) proved more challenging than anticipated. Activation of alcohol **249** as mesylate **254** (Table 5.2, entries 1-2) and tosylate **255** (entry 3) followed by *in situ* cyclization gave the desired product in low yield and incomplete conversion. This could potentially result from ligand hydrolysis under the reaction conditions.[7] As an alternative to *in situ* cyclization of an activated intermediate, alcohol **249** was reacted with thionyl chloride (entries 4–10) to yield chloride **256**, which was isolated as the hydrochloric acid salt and dried under vacuum. This compound proved to be bench stable and was spectroscopically unchanged after being left open to oxygen atmosphere and adventitious moisture for more than one week. Furthermore, chloride **256** proved to be a superior cyclization substrate. A series of bases were screened. Organic amine bases (entries 4-5) and sodium hydride (entry 6) provided inadequate conversion and low yields, whereas

hydroxide and alkoxide bases proved superior (entries 7-10). Finally, sodium methoxide was chosen to be optimal, as slower rates of hydrolysis of chloride **256** were observed when compared to the use of potassium hydroxide.

Table 5.2 Cyclization screen
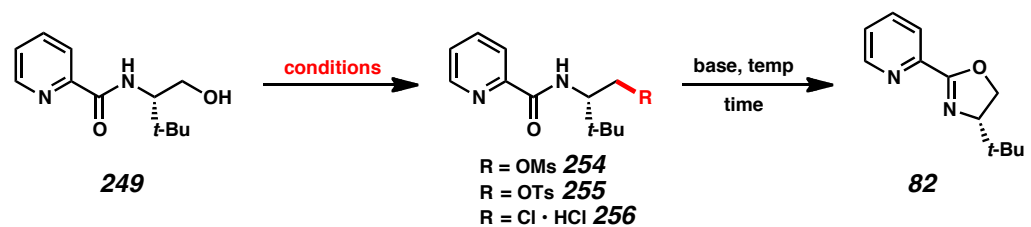
entry	conditions	R	base	temp (°C)	time (h)	yield (%)[a]
1	MsCl, Et$_3$N, CH$_2$Cl$_2$	OMs	Et$_3$N	0 → 40	12	N.D.[c]
2	MsCl, Et$_3$N, ClCH$_2$CH$_2$Cl	OMs	Et$_3$N	0 → 80	12	N.D.[c]
3	TsCl, DMAP, Et$_3$N, ClCH$_2$CH$_2$Cl	OTs	Et$_3$N	0 → 80	12	N.D.[c]
4	SOCl$_2$, CH$_2$Cl$_2$	Cl[b]	DABCO	rt	18	38
5	SOCl$_2$, CH$_2$Cl$_2$	Cl[b]	DBU	50	12	59
6	SOCl$_2$, CH$_2$Cl$_2$	Cl[b]	NaH, THF	0 → 50	18	60
7	SOCl$_2$, CH$_2$Cl$_2$	Cl[b]	5% KOH/EtOH	50	11	58
8	SOCl$_2$, CH$_2$Cl$_2$	Cl[b]	5% KOH/MeOH	50	11	62
9	SOCl$_2$, CH$_2$Cl$_2$	Cl[b]	25% NaOMe/MeOH	50	10	71
10	SOCl$_2$, CH$_2$Cl$_2$	Cl[b]	25% NaOMe/MeOH	50	3	72

MsCl = methanesulfonyl chloride, TsCl = 4-toluenesulfonyl chloride, DMAP = 4-dimethylaminopyridine, DABCO = 1,4-diazabicyclo[2.2.2]octane, DBU = 1,8-diazabicyclo[5.4.0]undec-7-ene. [a] isolated yield. [b]Intermediate **256** isolated as HCl salt and dried under high vacuum before use in cyclization reactions. [c]Incomplete conversion.

5.2.4 Attempts to purify the ligand by salt formation

Attempts to purify ligand **82** via salt formation failed due to instability of the generated products. Treatment with a number of carboxylic acids resulted in no salt formation, or a mixture of products as observed by ^{1}H NMR analysis (Table 5.3, entries 1–5). Treatment with stronger acids, such as HCl (entry 6), resulted in decomposition. While purification

via formation of the HBF$_4$ salt is successful (entry 7, **82b**), the salt is unstable in open air and decomposes to the amide alcohol **249**. Although salt formation is perhaps useful in the purification of the crude reaction mixture of **82**, further studies were suspended due to the instability of salt.

Table 5.3 Attempts to form HX salts of PyOx ligand

Entry	Acid	Scale	Solvent	Time	Result
1	maleic acid	5.1 mg	THF	8 h	peak shifted (mixture)
2	fumaric acid	5.1 mg	THF	8 h	not formed
3	malonic acid	5.1 mg	THF	8 h	peak shifted (mixture)
4	DL-malic acid	5.1 mg	THF	8 h	not formed
5	2-ethylhexanoic acid	5.1 mg	THF	8 h	not formed
6	HCl in ether	10 mg	ether	12 h	decomposed
7	HBF4 etherate	10 mg	ether	12 h	salt formed

5.2.5 Purification by conventional column chromatography

Purification by silica gel chromatography also proved challenging as up to 10% of crude ligand **82** was observed to decompose, even with the addition of triethylamine to the eluent. Finally, the use of neutral silica gel (American International Chemical ZEOprep ECO silica gel, 40–63 micron, $18/kg) allowed isolation of ligand **82** in high purity and with no observed decomposition.

5.3 Conclusion and completed synthesis of (*S*)-*t*-BuPyOx

In conclusion, we have developed a concise, highly efficient and scalable synthesis of the chiral ligand (*S*)–*t*-BuPyOx (**82**) (Figure 5.2). Efforts to further refine the synthesis by telescoping the procedure and removing chromatographic purifications are currently underway.

Figure 5.2 Scale-up synthesis of (S)–t-BuPyOx
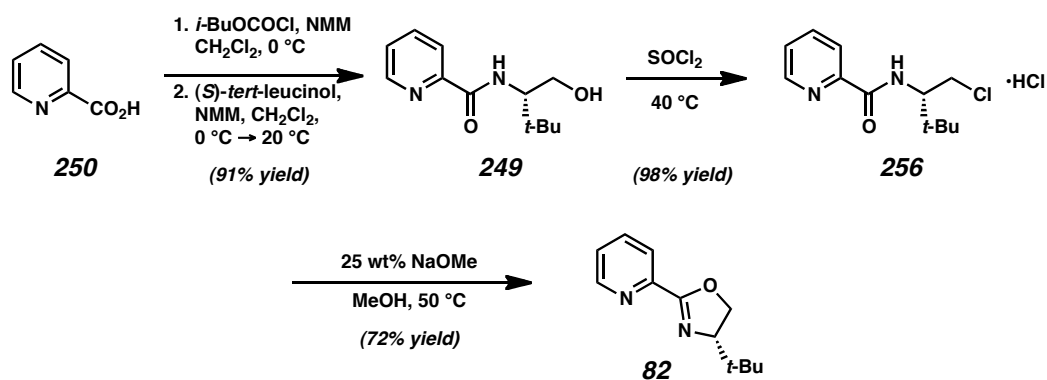
5.4 Experimental Procedures

5.4.1 Materials and Methods

All reactions were run under a nitrogen atmosphere. Solvents and reagents were obtained by commercial sources and used without further purification. Thin-layer chromatography (TLC) was visualized by UV fluorescence quenching, and *p*-anisaldehyde staining. American International Chemical ZEOprep® 60 ECO 40-63 micron silica gel was used for flash chromatography. Analytical chiral SFC was performed utilizing an OB-H column (4.6 mm x 25 cm) with visualization at 254 nm and flow rate of 5.0 mL/min, unless otherwise stated. ^{1}H and ^{13}C NMR spectra were recorded at 500 MHz and 125 MHz, respectively. Data for ^{1}H NMR spectra are referenced to the centerline of CHCl$_3$ (δ 7.26) as the internal standard and are reported in terms of chemical shift relative to Me$_4$Si (δ 0.00). Data for ^{13}C NMR spectra are referenced to the centerline of CDCl$_3$ (δ 77.16) and are reported in terms of chemical shift relative to Me$_4$Si (δ 0.00). Infrared spectra are reported in frequency of absorption (cm^{-1}).

5.4.2 Experimental Procedures

(*S*)–*tert*-leucine   (*S*)–*tert*-leucinol
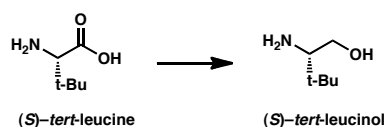
(*S*)-*tert*-Leucinol (251)

This procedure was adapted from: Krout, M. R.; Mohr, J. T.; Stoltz, B. M. *Org. Synth.* **2009**, *86*, 181. A 1000 mL separable flask equipped with a three-pitched curved blade, an internal thermometer, and a reflux condenser equipped with a two-tap Schlenk

adapter connected to a bubbler and a nitrogen/vacuum manifold was assembled hot and cooled under a steam of N$_2$. The flask was charged with (L)-*tert*-leucine (15.08 g, 115.0 mmol, 1.00 equiv, 99% ee) and THF (360 mL) under a positive pressure of nitrogen. The resulting slurry was cooled to 0 ºC in a dry ice-acetone bath and NaBH$_4$ (10.44 g, 276.0 mmol, 2.40 equiv) was added in one portion. A solution of I$_2$ (29.19 g, 115.0 mmol, 1.00 equiv) in THF (50 mL) was transferred dropwise over 2 hours by using a syringe pump. After the addition was complete, the cooling bath and the thermometer were removed and replaced by a condenser and the reaction was heat to reflux (80 ºC oil bath). After 20 h the reaction was allowed to cool to ambient temperature and methanol (150 mL) was added slowly, resulting in an almost clear solution. After stirring for 30 min the solution was quantitatively transferred to a 1000 mL round bottom flask with MeOH (100 mL) and concentrated on a rotary evaporator under reduced pressure (40 ºC) to a white semi-solid. The resulting material was dissolved in 20 wt% aqueous KOH (250 g) and stirred for 12 h at ambient temperature. The aqueous phase was extracted with CH$_2$Cl$_2$ (5 x 180 mL) and the combined organic extracts were dried over Na$_2$SO$_4$ (ca 25 g), filtered, and concentrated on a rotary evaporator under reduced pressure (40 ºC) and dried under vacuum to give crude (*S*)-*tert*-leucinol (14.00 g, quantitative yield) as a colorless oil. This material was used in the following step without further purification.

Alternative Route to (S)–t-BuPyOx*
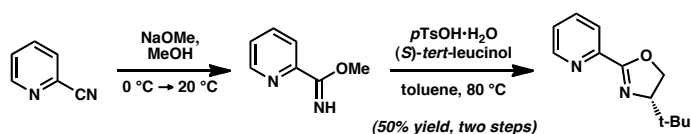
*This route is amenable to smaller batches of ligand synthesis.

Adapted from: Brunner. H.; Obermann. U. *Chem. Ber.* **1989**, *122*, 499–507.

A flame-dried round bottom flask was charged with a stir bar and MeOH (110 mL). Sodium metal ingot (295 mg, 12.8 mmol, 0.1 equiv) was cut with a razor into small pieces, washed in a beaker of hexanes, and added in five portions over 5 min. The reaction mixture was stirred vigorously until no sodium metal remained, at which time it was cooled to 0 °C in an ice/water bath. Subsequently, 2-cyanopyridine (13.0 g, 125 mmol, 1.0 equiv) was added drop wise, and the clear, colorless reaction mixture was allowed to warm to ambient temperature and stir. When all the starting material was consumed as indicated by TLC analysis (1:1 EtOAc/Hexanes, *p*-anisaldehyde stain), the reaction was cooled to 0 °C in an ice/water bath and quenched dropwise with glacial AcOH (1 mL). The crude reaction mixture was concentrated *in vacuo*, redissolved in CH_2Cl_2 (100 mL) and washed with brine (2 x 50 mL). The organic phase was dried ($MgSO_4$), concentrated *in vacuo*, and dried under high vacuum for 1 h. The resulting crude methoxyimidate (light yellow oil) was suitable for use in the next step without further purification.

To a flame-dried round bottom flask charged with a stir bar was added crude methoxyimidate (2.55 g, 18.7 mmol, 1.0 equiv), (*S*)–*tert*-leucinol (2.10 g, 17.9 mmol, 0.96 equiv), toluene (100 mL), and *p*-TsOH•H_2O (167 mg, 0.88 mmol, 5 mol%). The mixture was stirred at 80 °C in an oil bath for 3 h, at which time the starting material was consumed as indicated by TLC analysis (1:4 acetone/hexanes, *p*-anisaldehyde stain). The reaction was cooled to ambient temperature and quenched with sat. $NaHCO_3$ (60 mL). The reaction was partitioned with EtOAc and water, and the aqueous phase was extracted with EtOAc (3 x 50 mL). The combined organic extracts were washed with water (2 x

50mL), brine (1 x 25 mL), dried (MgSO$_4$) and concentrated *in vacuo*. The crude mixture

was purified by flash column chromatography using American International Chemical

ZEOprep® 60 ECO 40-63 micron silica gel (1:4 acetone/hexanes) to afford 1.85 g (9.06

mmol, 50%) (*S*)–*t*-BuPyOx as an off-white solid. Characterization data matches the data

previously reported in this document.
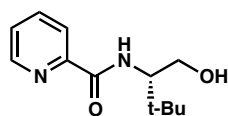
(*S*)-*N*-(1-hydroxy-3,3'-dimethylbutan-2-yl)picolinamide (249)

To a 200 mL round bottom flask was added 2-picolinic acid (2.46 g, 20.0 mmol, 1.00

equiv), 50 mL CH$_2$Cl$_2$, and *N*-methylmorpholine (3.03 g, 30.0 mmol, 1.50 equiv). The

reaction mixture was cooled to 0 °C in an ice bath and *iso*-butyl chloroformate (3.14 g,

23.0 mmol, 1.15 equiv) was added dropwise over 30 min. Following complete addition,

the reaction mixture was stirred for 30 min at 0 °C. In a separate flask, (*S*)-*tert*-leucinol

(2.58 g, 22.0 mmol, 1.10 equiv) was dissolved in CH$_2$Cl$_2$ (25 mL), and *N*-

methylmorpholine (2.43 g, 24.0 mmol, 1.20 equiv) was added. This solution was

transferred dropwise over the course of 1 h to the cooled reaction mixture using a syringe

pump. The cooling bath was removed and the reaction mixture was allowed to warm to

room temperature and stirred for 2 h. The mixture was quenched with an aqueous

solution of NH$_4$Cl (10 g in 50 mL H$_2$O) and the aqueous phase was extracted with CH$_2$Cl$_2$

(20 mL). The combined organic phase was dried over Na$_2$SO$_4$ (5 g), filtered, and

concentrated under reduced pressure. The residue was purified with flash silica gel

column chromatography (4:1 hexanes/acetone) to afford amide alcohol **249** as a white

solid (4.10 g, 92% yield). $R_f = 0.32$ with 3:2 hexanes/acetone; M.P. 79.6–79.9°C; ^{1}H

NMR (500 MHz, CDCl$_3$) δ 8.56 (ddd, *J* = 4.8, 1.8, 0.9 Hz, 1H), 8.32 (br d, *J* = 8.9 Hz, -

NH), 8.19 (dt, *J* = 7.8, 1.1 Hz, 1H), 7.85 (td, *J* = 7.7, 1.7 Hz, 1H), 7.43 (ddd, *J* = 7.6, 4.8,

1.2 Hz, 1H), 4.02–3.96 (m, 2H), 3.69 (m, 1H), 2.72 (br t, *J* = 6.5 Hz, -OH), 1.05 (s, 9H);

^{13}C NMR (125 MHz, CDCl$_3$) δ 165.6, 149.7, 148.2, 137.6, 126.4, 122.6, 63.7, 60.6, 33.9,

27.1; IR (Neat Film, NaCl): 3375, 2962, 1669, 1591, 1570, 1528, 1465, 1434, 1366,

1289, 1244, 1088, 1053, 998 cm^{-1}; HRMS (MultiMode ESI/APCI) *m/z* calc'd for

$C_{12}H_{19}N_2O_2$ [M+H]$^+$: 223.1447, found 223.1448; $[\alpha]^{25}_D$ –8.68° (*c* 1.17, CHCl$_3$, > 99% ee).
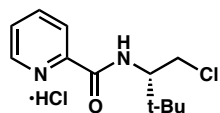
(*S*)-*N*-(1-chloro-3,3'-dimethylbutan-2-yl)picolinamide hydrochloride (256)

A 500 mL 3-neck round bottom flask was charged with a stir bar, amide alcohol **249**

(8.89 g, 40.0 mmol, 1.00 equiv) and toluene (140 mL). The resulting clear solution was

warmed to 60 °C. In a separate flask, SOCl$_2$ (9.25 g, 80.0 mmol, 2.00 equiv) was diluted

with toluene (20 mL). This solution was transferred slowly, dropwise, over 20 min to the

vigorously stirring reaction mixture at 60 °C. The reaction mixture was stirred at 60 °C

for 4 h, at which time the slurry was cooled to ambient temperature, concentrated on a

rotary evaporator under reduced pressure (40 °C, 40 mmHg), and dried under vacuum

(0.15 mmHg) to give a white powder of amide chloride hydrochloric salt **256** (10.80 g,

98% yield). This material was used in the following step without purification. ^{1}H NMR

(500 MHz, DMSO-d_6) δ 8.70 (ddd, *J* = 4.8, 2.0, 1.0 Hz, 1H), 8.66 (br d, *J* = 9.9 Hz, -NH),

8.10 (dt, *J* = 8.0, 1.0 Hz, 1H), 8.06 (td, *J* = 7.5, 1.4 Hz, 1H), 7.66 (ddd, *J* = 7.4, 4.8, 1.4

Hz, 1H), 4.08 (td, *J* = 9.9, 3.7 Hz, 1H), 3.97–3.90 (m, 2H), 0.93 (s, 9H); ^{13}C NMR (125

MHz, DMSO-*d₆*) δ 163.6, 149.0, 147.8, 138.1, 126.5, 122.0, 59.0, 44.9, 35.0, 26.3; IR

(Neat film, NaCl): 3368, 2963, 1680, 1520, 1465, 1434, 1369, 1285, 1239, 1087, 998 cm^{-1}; HRMS (MultiMode ESI/APCI) *m/z* calc'd for $C_{12}H_{18}ClN_2O$ [M+H]⁺: 241.1108, found

241.1092; [α]$^{25}_D$ +39.40° (*c* 0.96, MeOH, > 99% ee).
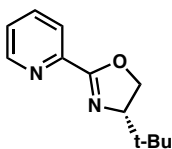
(*S*)-4-(*tert*-butyl)-2-(pyridin-2-yl)-4,5-dihydrooxazole (82)

A 500 mL 3-neck round bottom flask was charged with a stir bar, amide chloride

hydrochloric acid salt **256** (10.26 g, 37.0 mmol, 1.00 equiv) and MeOH (100 mL). To the

clear solution was added powdered NaOMe (9.99 g, 185.0 mmol, 5.00 equiv), and the

resulting mixture was heat to 55 °C in the oil bath. The slurry was stirred for 3 h until the

free amide chloride was fully consumed, according to TLC analysis (4:1

hexanes/acetone). After removing the oil bath, toluene (100 mL) was added and the

mixture was concentrated on a rotary evaporator (40 °C, 60 mmHg) to remove MeOH.

The residual mixture was extracted with H_2O (100 mL) and the aqueous phase was back

extracted with toluene (40 mL x 2). The combined organic extracts were dried over

Na_2SO_4 (10 g), filtered, and concentrated under reduced pressure. The residue was

purified by flash column chromatography using American International Chemical

ZEOprep® 60 ECO 40-63 micron silica gel (4:1 hexanes/acetone) to yield (*S*)-*t*-BuPyOx

(**82**) as a white solid (5.44 g, 72% yield). R$_f$ = 0.44 with 3:2 hexanes/acetone; M.P.

70.2–71.0 °C; ^{1}H NMR (500 MHz, CDCl₃) δ 8.71 (ddd, *J* = 4.8, 1.8, 0.9 Hz, 1H), 8.08

(dt, *J* = 7.9, 1.1 Hz, 1H), 7.77 (dt, *J* = 7.7, 1.7 Hz, 1H), 7.37 (ddd, *J* = 7.0, 4.5, 1.0 Hz,

1H), 4.45 (dd, *J* = 10.2, 8.7 Hz, 1H), 4.31 (t, *J* = 8.5 Hz, 1H), 4.12 (dd, *J* = 10.2, 8.5 Hz,

1H), 0.98 (s, 9H); ^{13}C NMR (125 MHz, CDCl$_3$) δ 162.4, 149.6, 147.0, 136.5, 125.4,

124.0, 76.5, 69.3, 34.0, 26.0; IR (Neat film, NaCl): 2981, 2960, 2863, 1641, 1587, 1466,

1442, 1358, 1273, 1097, 1038, 968 cm^{-1}; HRMS (MultiMode ESI/APCI) *m/z* calc'd for

C$_{12}$H$_{17}$ON$_2$ [M+H]$^+$: 205.1335, found 205.1327; $[\alpha]^{25}_D$ –90.5° (c 1.15, CHCl$_3$, > 99% ee).

5.5 Notes and Citations

(1)   (a) Podhajsky, S. M.; Iwai, Y.; Cook-Sneathen, A.; Sigman, M. S. *Tetrahedron* **2011**, *67*, 4435–4441. (b) Aranda, C.; Cornejo, A.; Fraile, J. M.; García-Verdugo, E.; Gil, M. J.; Luis, S. V.; Mayoral, J. A.; Martínez-Merino, V.; Ochoa, Z. *Green Chem.* **2011**, *13*, 983–990. (c) Pathak, T. P.; Gligorich, K. M.; Welm, B. E.; Sigman, M. S. *J. Am. Chem. Soc.* **2010**, *132*, 7870–7871. (d) Jiang, F.; Wu, Z.; Zhang, W. *Tetrahedron Lett.* **2010**, *51*, 5124–5126. (e) Jensen, K. H.; Pathak, T. P.; Zhang, Y.; Sigman, M. S. *J. Am. Chem. Soc.* **2009**, *131*, 17074–17075. (f) He, W.; Yip, K.-T.; Zhu, N.-Y.; Yang, D. *Org. Lett.* **2009**, *11*, 5626–5628. (g) Dai, H.; Lu, X. *Tetrahedron Lett.* **2009**, *50*, 3478–3481. (h) Linder, D.; Buron, F.; Constant, S.; Lacour, J. *Eur. J. Org. Chem.* **2008**, 5778–5785. (i) Schiffner, J. A.; Machotta, A. B.; Oestreich, M. *Synlett* **2008**, 2271–2274. (j) Koskinen, A. M. P.; Oila, M. J.; Tois, J. E. *Lett. Org Chem.* **2008**, *5*, 11–16. (k) Zhang, Y.; Sigman, M. S. *J. Am. Chem. Soc.* **2007**, *129*, 3076–3077. (l) Yoo, K. S.; Park, C. P.; Yoon, C. H.; Sakaguchi, S.; O'Neill, J.; Jung, K. W. *Org. Lett.* **2007**, *9*, 3933–3935. (m) Dhawan, R.; Dghaym, R. D.; St. Cyr, D. J.; Arndtsen, B. A. *Org. Lett.* **2006**, *8*, 3927–3930. (n) Xu, W.; Kong, A.; Lu, X. *J. Org. Chem.* **2006**, *71*, 3854–3858. (o) Malkov, A. V.; Stewart Liddon, A. J. P.; Ramírez-López, P.; Bendová, L.; Haigh, D.; Kocovsky, P. *Angew. Chem., Int. Ed.* **2006**, *45*, 1432–1435. (p) Abrunhosa, I.; Delain-Bioton, L.; Gaumont, A.-C.; Gulea, M.; Masson, S. *Tetrahedron* **2004**, *60*, 9263–9272. (q) Brunner, H.; Kagan, H. B.; Kreutzer, G. *Tetrahedron: Asymmetry*, **2003**, *14*, 2177–2187. (r) Cornejo, A.; Fraile, J. M.; García, J. I.; Gil, M. J.; Herrerías, C. I.; Legarreta, G.; Martínez-

Merino, V.; Mayoral, J. A. *J. Mol. Catal. A: Chem.* **2003**, *196*, 101–108.   (s)

Zhang, Q.; Lu, X.; Han, X. *J. Org. Chem.* **2001**, *66*, 7676–7684.   (t) Zhang, Q.;

Lu, X. *J. Am. Chem. Soc*. **2000**, *122*, 7604–7605.   (u) Perch, N. S.; Pei, T.;

Widenhoefer, R. A. *J. Org. Chem.* **2000**, *65*, 3836–3845.   (v) Bremberg, U.;

Rahm, F.; Moberg, C. *Tetrahedron: Asymmetry*, **1998,** *9*, 3437–3443.   (w)

Brunner, H.; Obermann, U.; Wimmer, P. *Organometallics* **1989**, *8*, 821–826.

(2)   Kikushima, K.; Holder, J. C.; Gatti, M.; Stoltz, B. M. *J. Am. Chem. Soc*. **2011**,

133, 6902–6905.

(3)   In fact, we have come to accept that the reaction requires a small amount of water

to run efficiently. Typically, 5 equiv. water are added to each reaction.

(4)   A number of syntheses are known, including: (a) Brunner. H.; Obermann. U.

Chem. Ber. **1989**, *122*, 499–507.   (b) Aranda, C.; Cornejo, A.; Gil, M. J.;

Martinez-Merino, V.; Ochoa, Z.; Fraile, J. M.; Mayoral, J. A.; Garcia-Verdugo,

E.; Luis, S. V. *Green Chemistry,* **2011**, *13*, 983–990.

(5)   This route, reported by our group in ref. 2, is adapted from the synthesis reported

in ref 4a.

(6)   Jensen, K. H.; Webb, J. D.; Sigman, M. S. *J. Am. Chem. Soc*. **2010**, *132*,

17471–17482. While Sigman and coworkers utilize these conditions to make

derivatives of PyOx ligands, such conditions are not reported for the synthesis of

t-BuPyOx.

(7)   Degradation experiments demonstrate that ligand **1** is susceptible to hydrolysis.

Exposure of *t*-BuPyOx to 3N HCl results in complete hydrolysis to amide **4** as

observed by 1H NMR.

APPENDIX 5

Spectra Relevant to Chapter 5:
: Development of a Scalable Synthesis of the (S)-4-(tert-butyl)-2-
(pyridin-2-yl)-4,5-dihydrooxazole ((S)–t-BuPyOx) Ligand
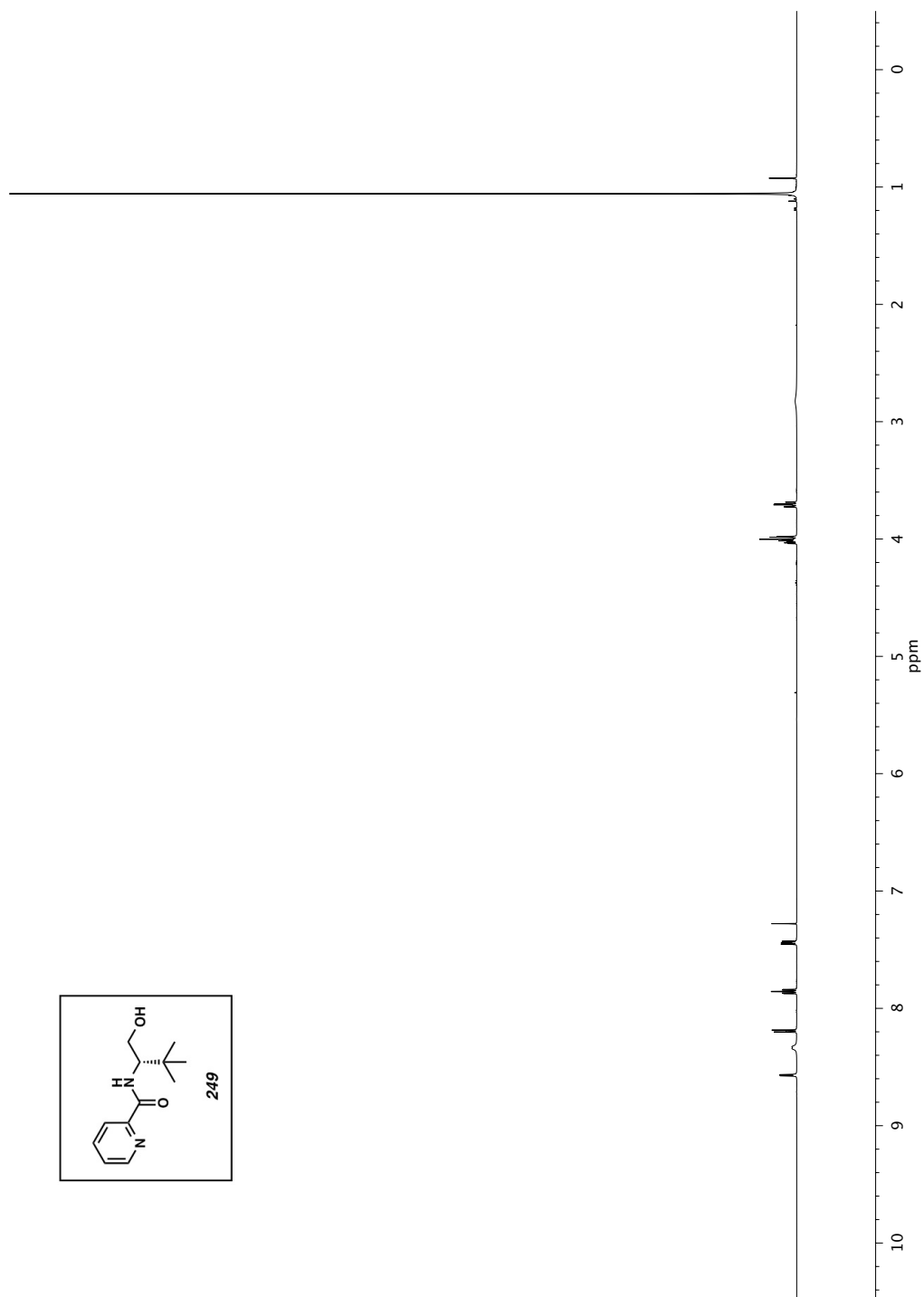
Figure A5.1 ^{1}H NMR (500 MHz, CDCl$_3$) of compound **249**
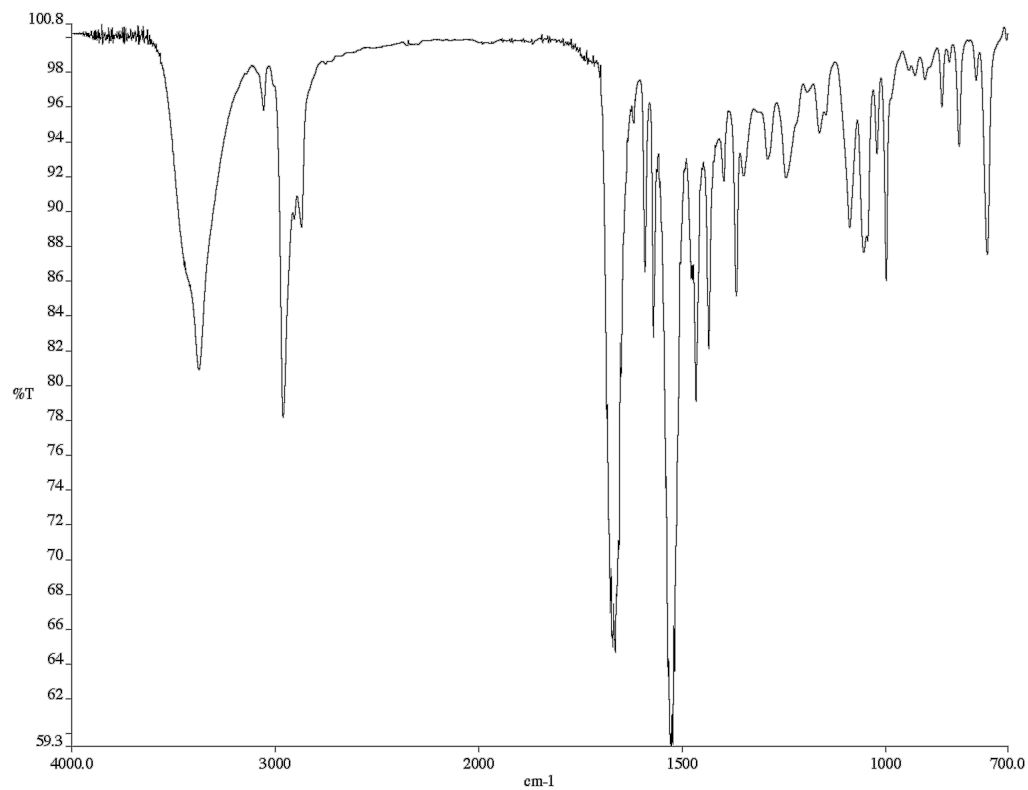
Figure A5.2 Infrared spectrum (Thin Film, NaCl) of compound **249**
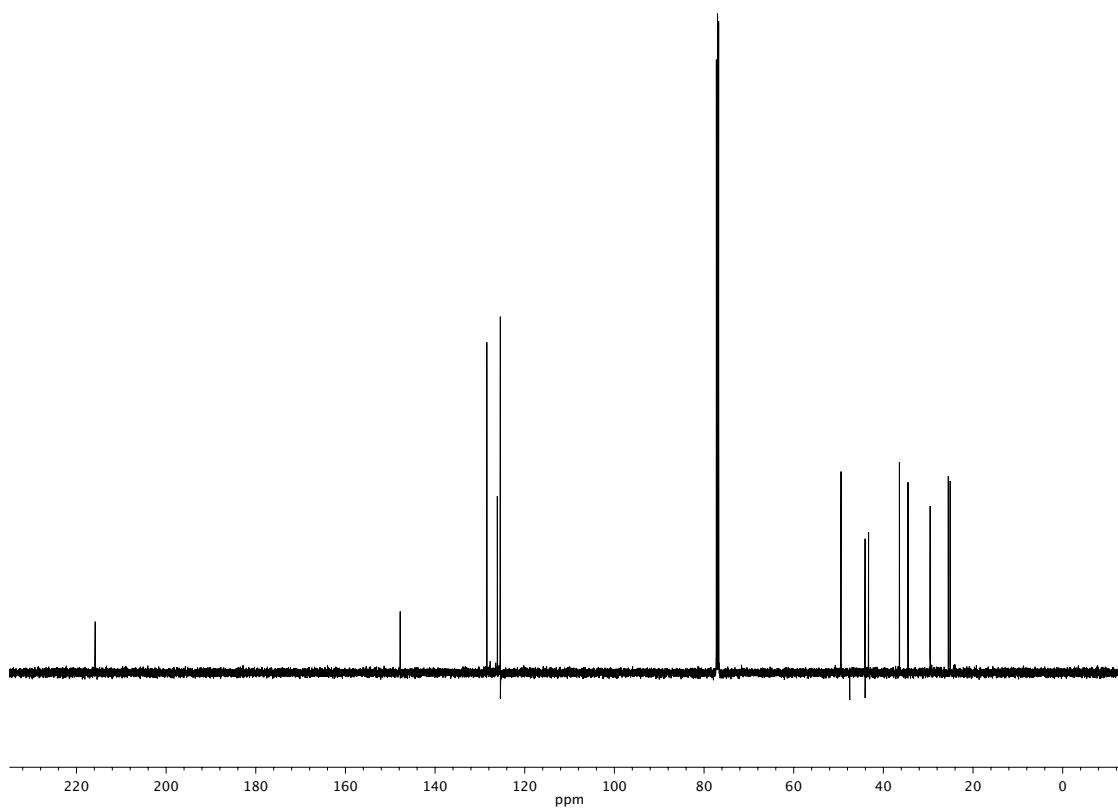
Figure A5.3 ^{13}C NMR (126 MHz, CDCl$_3$) of compound **249**
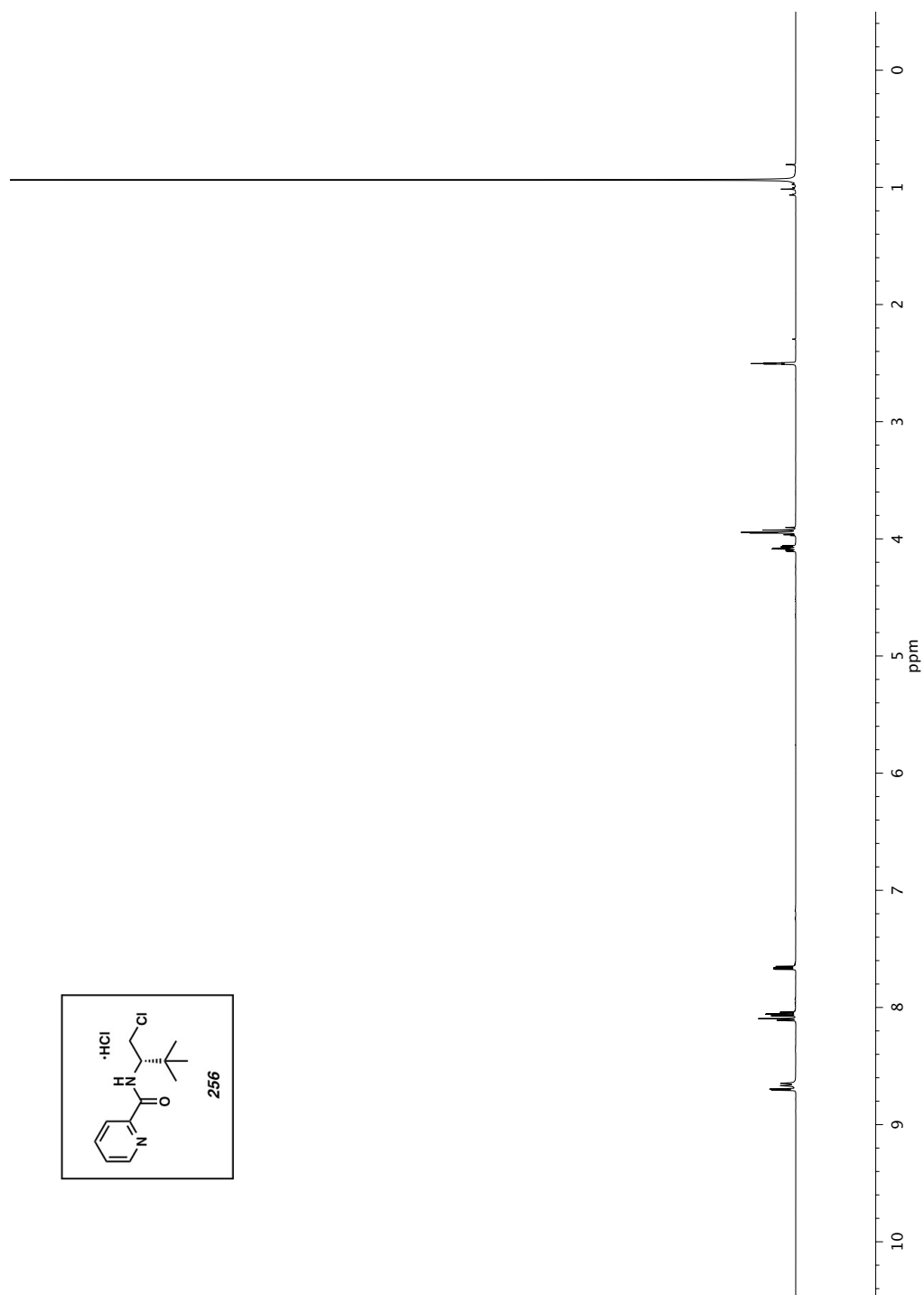
Figure A5.4 ^{1}H NMR (500 MHz, CDCl$_3$) of compound **256**
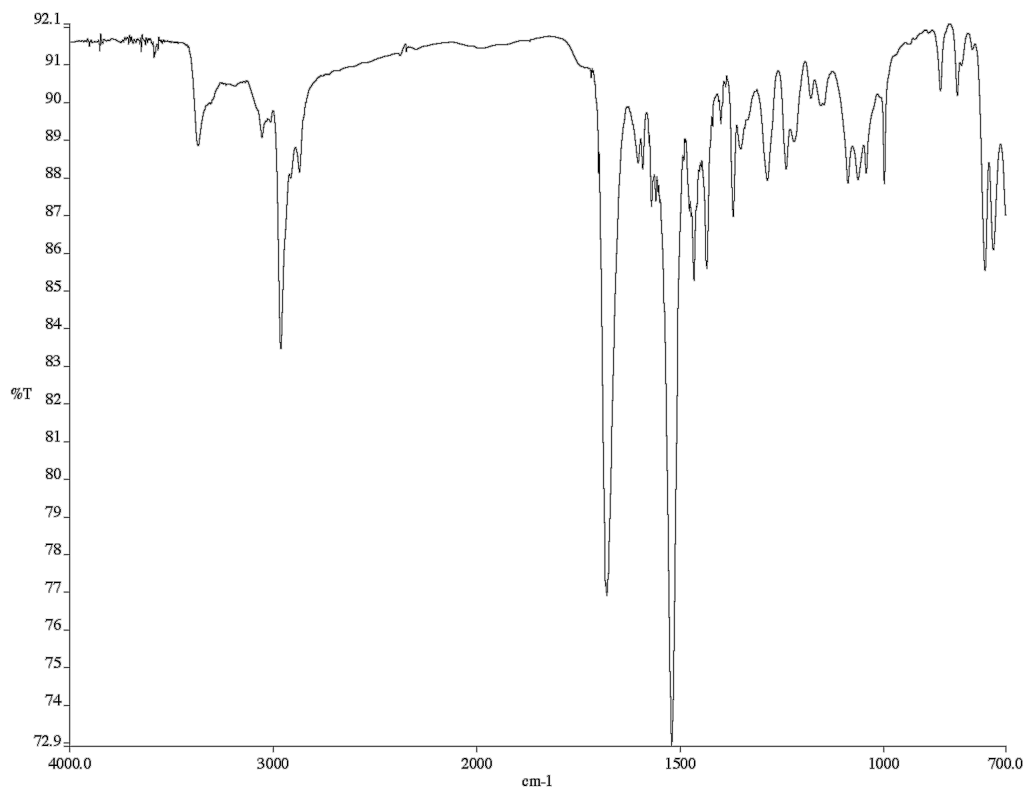
Figure A5.5 Infrared spectrum (Thin Film, NaCl) of compound **256**
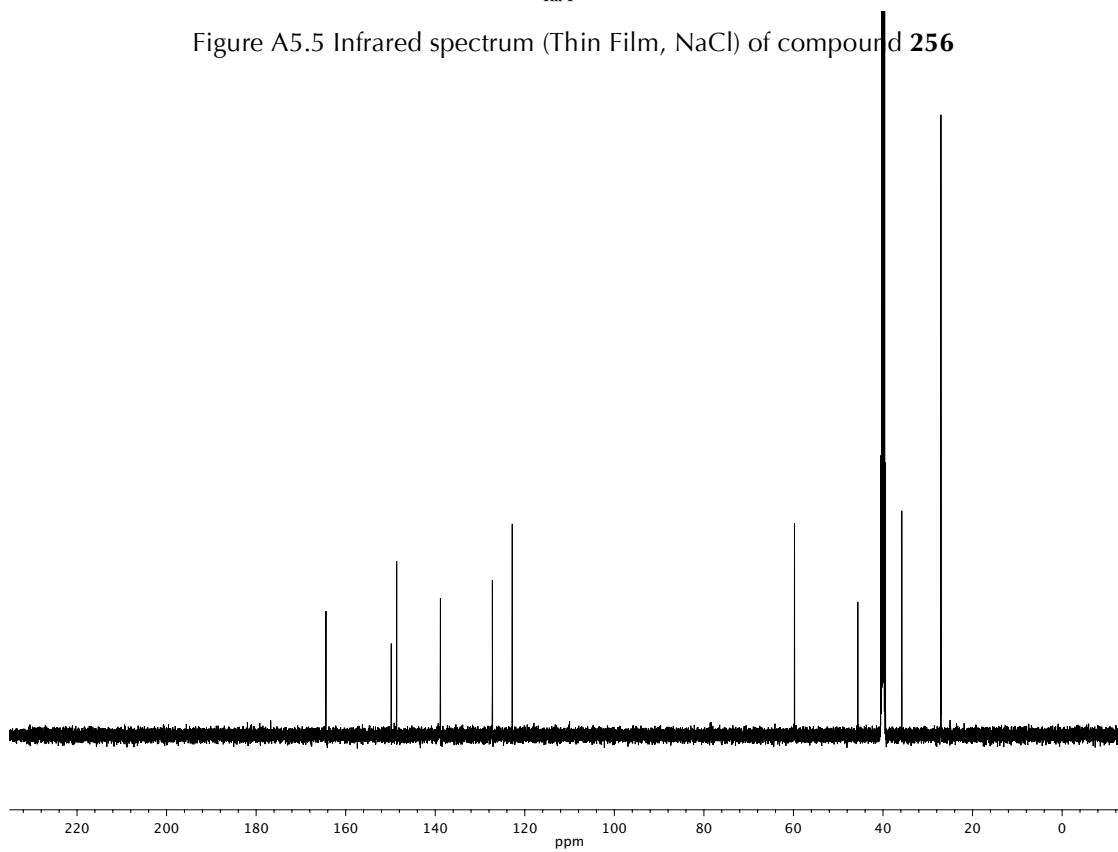
Figure A5.6 ^{13}C NMR (126 MHz, CDCl$_3$) of compound **256**
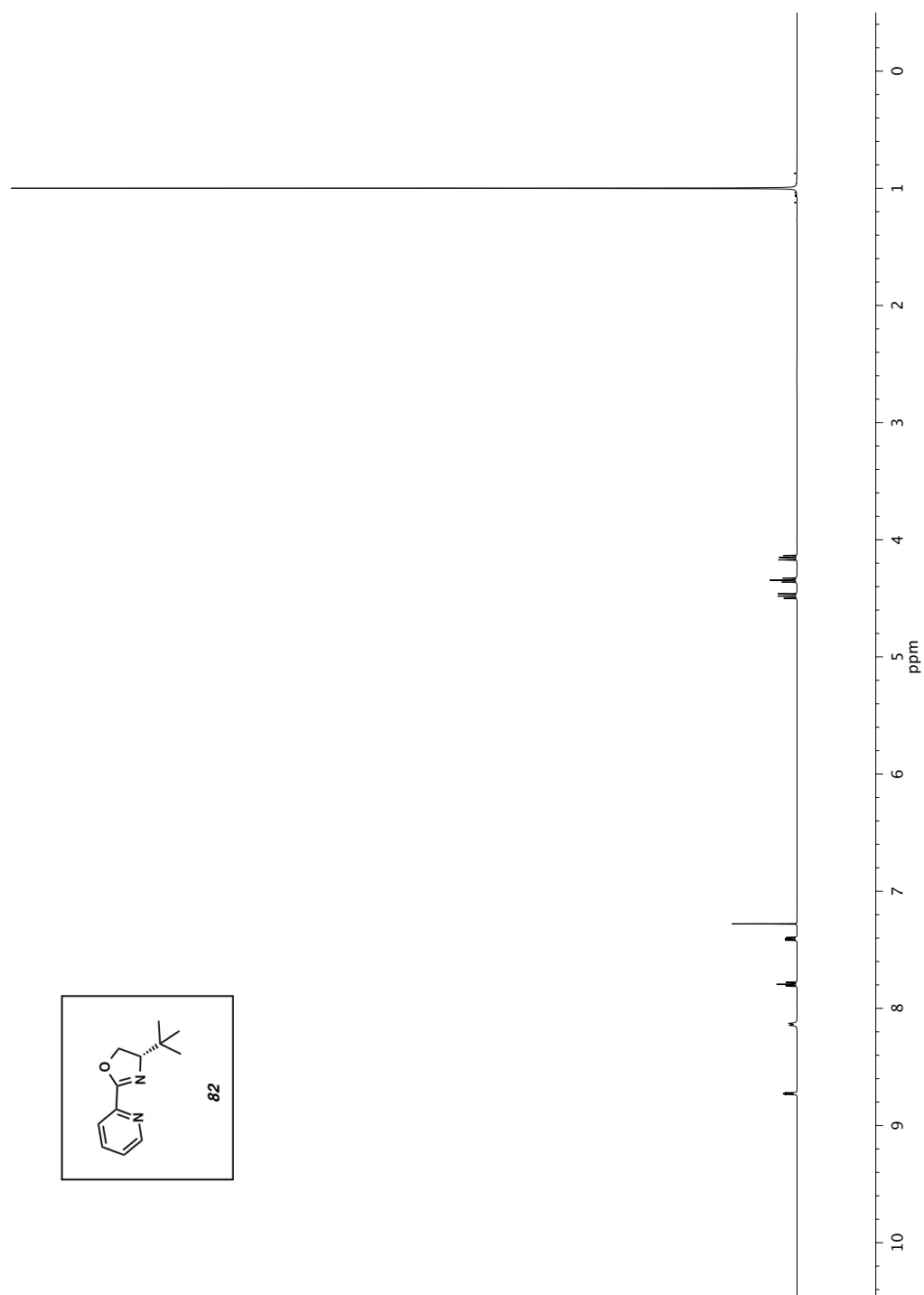
Figure A5.7 ^{1}H NMR (500 MHz, CDCl$_3$) of compound **82**
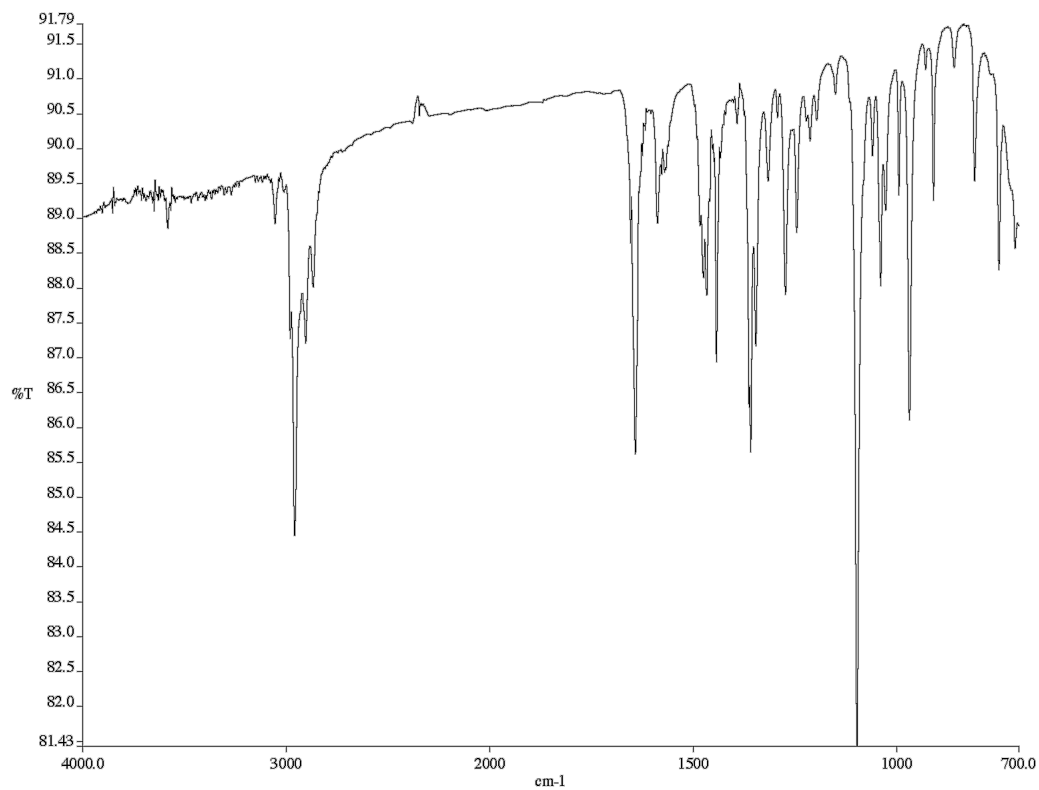
Figure A5.8 Infrared spectrum (Thin Film, NaCl) of compound **82**
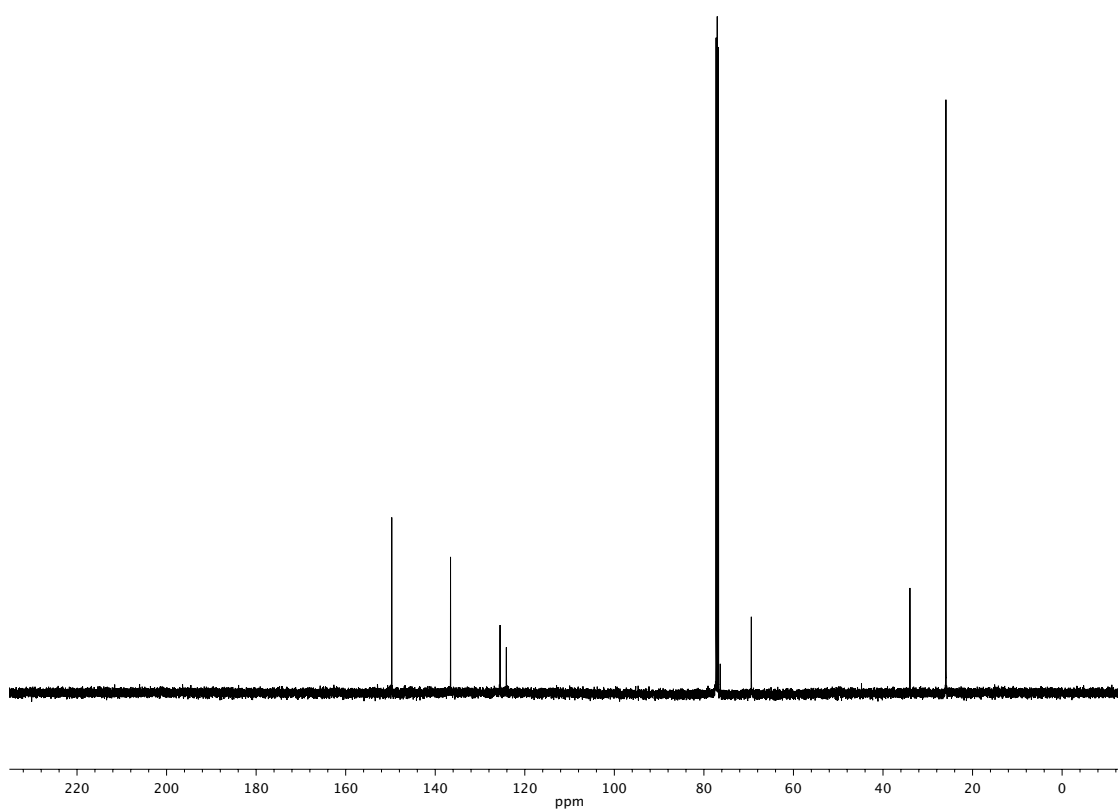
Figure A5.9 ^{13}C NMR (126 MHz, CDCl$_3$) of compound **82**
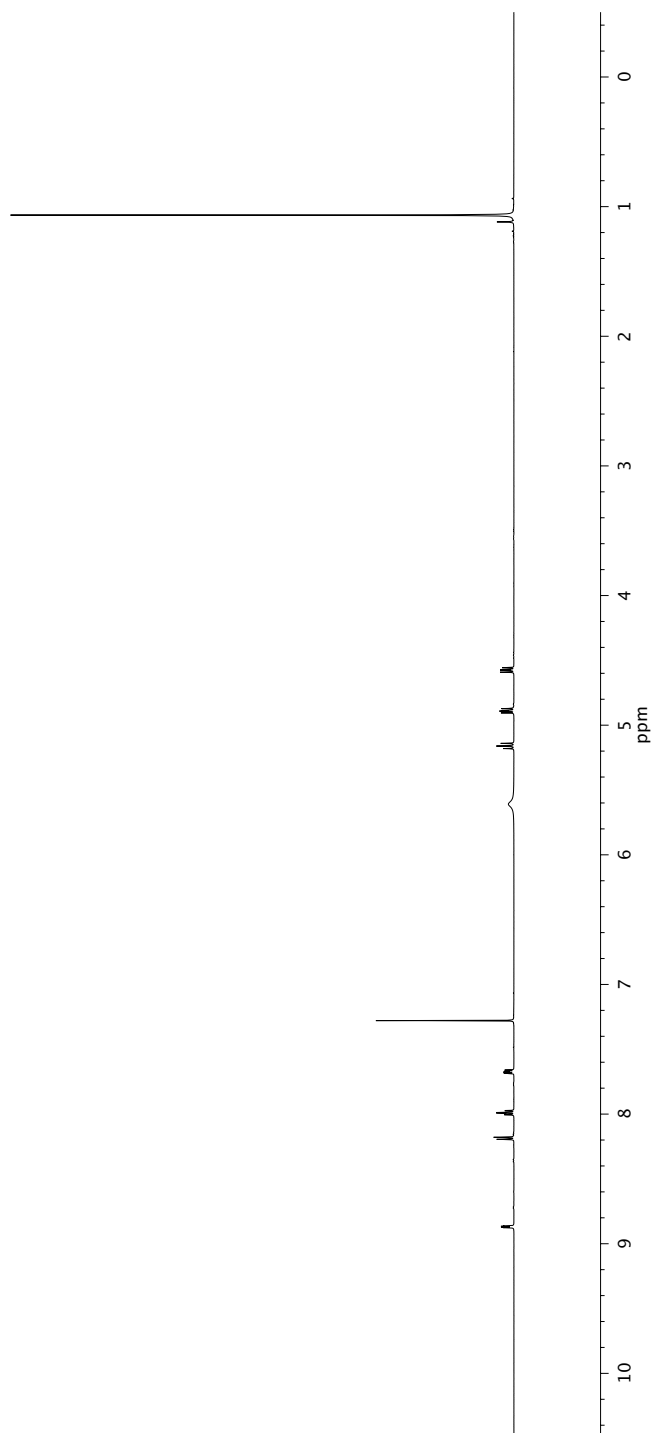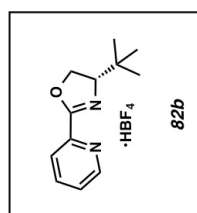
Figure A5.10 ^{1}H NMR (500 MHz, CDCl$_3$) of compound **82b**
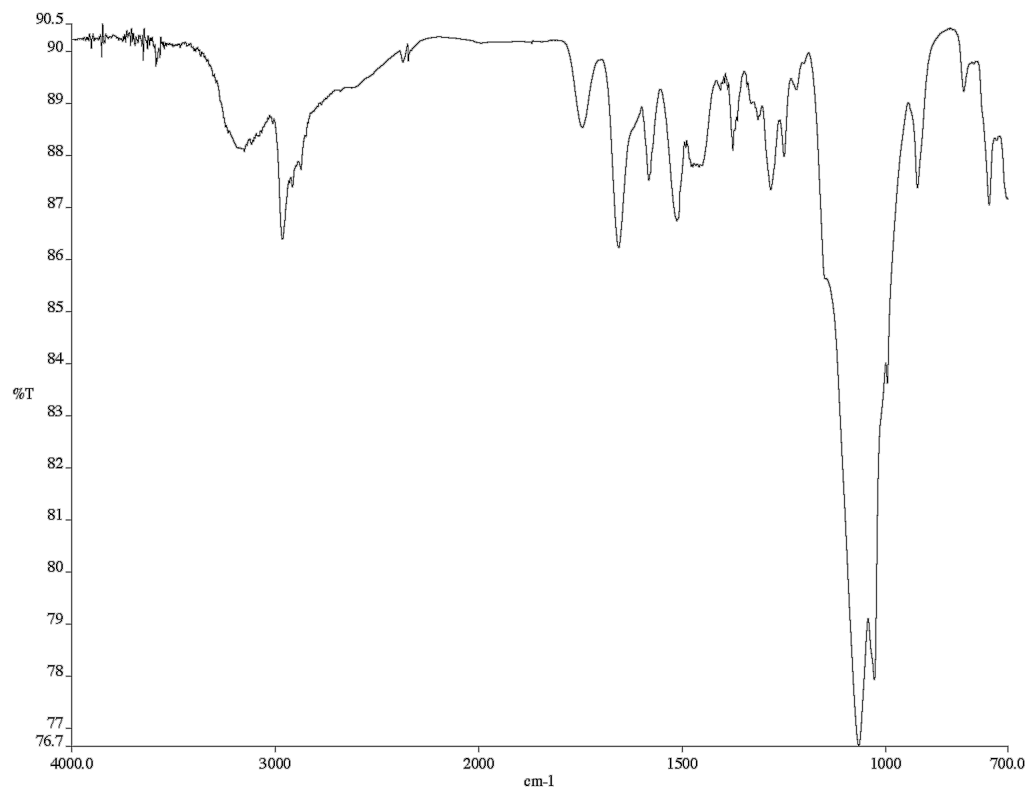
Figure A5.11 Infrared spectrum (Thin Film, NaCl) of compound **82b**
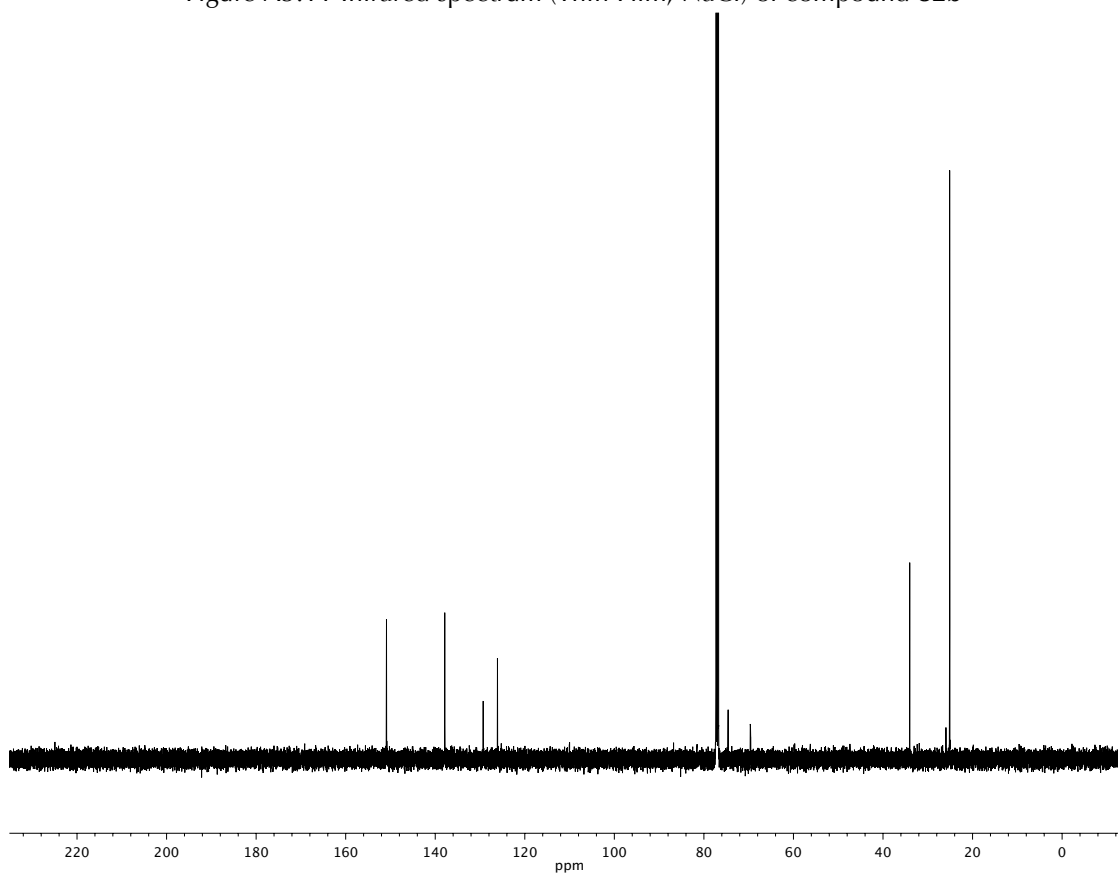
Figure A5.12 ^{13}C NMR (126 MHz, CDCl$_3$) of compound **82b**

CHAPTER 6

Progress toward the catalytic asymmetric total synthesis of

(+)−taiwaniaquinone H and other taiwaniaquinoid natural products‡

(+)-taiwaniaquinone H   **Asymmetric Conjugate Addition**

Abstract

(+)-taiwaniaquinone H   **Asymmetric Conjugate Addition**
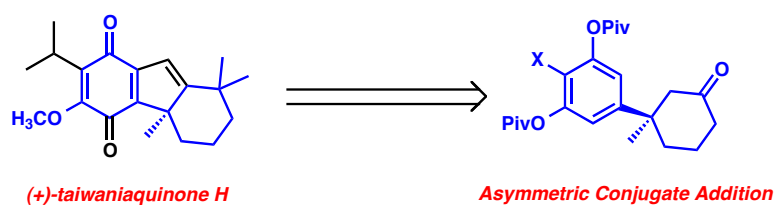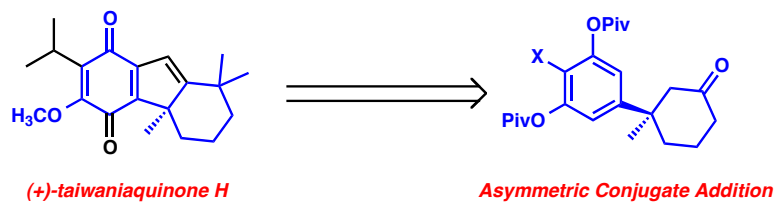
Work toward the catalytic, asymmetric total synthesis of (+)–taiwaniaquinone H is presented. This route features an expedient, highly convergent retrosynthetic analysis whereby 13 of the total 20 core scaffold carbon atoms are brought together by asymmetric palladium-catalyzed conjugate addition. The rational design of a highly enantioselective and high yielding conjugate addition substrate is discussed. Additionally, steps toward the synthesis of the B-ring are disclosed, including a highly surprising arene/ketone ene-type cyclization to afford a [3.2.1] bicyclic scaffold.

6.1 A biological and chemical introduction to the taiwaniaquinoids

6.1.1 Isolation and biological activity of taiwaniaquinoids

Isolated first in 1995, the taiwaniaquinoid family of natural products are a set of tricyclic diterpenoids obtained from the flowing sage *Salvia dichroantha Stapf* and the Taiwanese pine tree *Taiwania cryptomerioldes Hayata* (Figure 6.1).[12] Relatively little is known about the biological activity of these norditerpenoids, however, significant cytotoxicity is observed for many of the isolated natural products.[2] Furthermore, some have demonstrated aromatase inhibitory activity, which has potential therapeutic application in the treatment of carcinoma cancers.[3] Though their purported biological activity make these norditerpenoids an enticing target for natural product total synthesis, we were drawn to the unique architecture of these molecules. In particular, we thought that the challenge of installing the benzylic quaternary stereocenter would be well-suited to our recently developed asymmetric conjugate addition methodology. We believe that the high degree of oxidation on the C-ring will test the limitations of our methodology, and that the successful implementation of our strategy would yield a significant wealth of knowledge about the scope of the newly developed chemistry, specifically the tolerance for high degrees of substitution and oxidation on the arylboronic acid coupling partner. Finally, we were keen to demonstrate that we could synthesize tricyclic scaffolds from our aryl 1,4-addition products.

Unique to these diterpenoids is their [6.5.6]-*abeo*-abietane scaffold. Furthermore, much of the diversity comes from functionality of the central 5-membered B-ring, which can be found fully saturated (taiwaniaquinone G, Figure 6.2, **257**), unsaturated (taiwaniaquinone H **258**, dichroanone **259**, and dichroanal **260**), oxidized as a ketone (taiwaniaquinol B, **262**) or even with the full carbon count of a norditerpenoid (taiwaniaquinones A and F, **261**). Additionally, the oxidation state of the aromatic C-ring varies from quinone to quinol. Aside from these major factors, a number of structural motifs are highly conserved among all members of the class, including: *gem*-dimethyl functionality on the A-ring, benzylic quanternary stereocenter at the A/B-ring fusion, *iso*-propyl group on the C-ring, and high degree of oxygenation on the C-ring.

Figure 6.2 Taiwaniaquinoid natural products
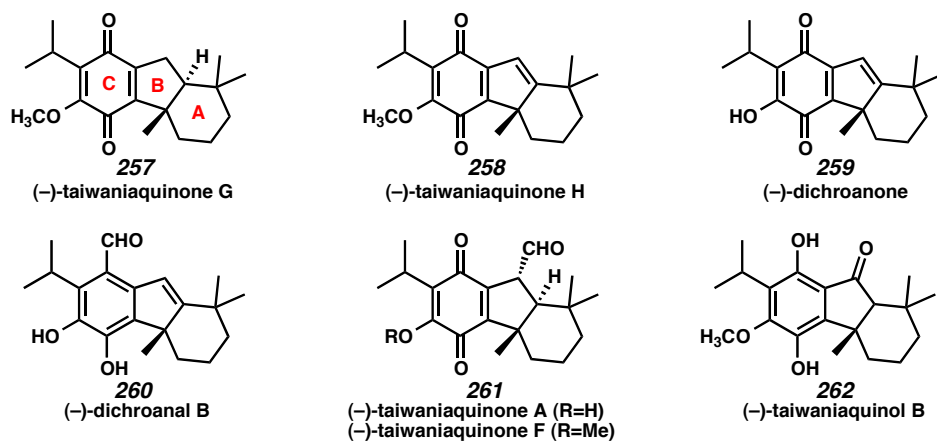
6.1.2 Previous Synthetic Work

No shortage of synthetic literature exists for the taiwaniaquinones. A number of total syntheses, semi-syntheses, and asymmetric total syntheses have been reported. Banerjee and coworkers reported the first synthesis of racemic dichroanal B (**260**), utilizing a reductive palladum-catalyzed 5-*exo*-trig cyclization.[4] A number of more efficient routes have been accomplished in more recent years (Figure 6.3). Notable strategies include acylation/alkylation reactions,[5] intramolecular aldol condensations,[6] cationic olefin cyclizations,[7] electrocyclizations,[8] Friedel-Crafts acylations,[9] and Heck cyclizations,[10] among others.[11] While significant work has been published regarding synthetic efforts toward these natural products, only three catalytic asymmetric approaches have been disclosed. Indeed, the installation of the benzylic quaternary stereocenter has proved to be the major challenge in these synthetic works.

Figure 6.3 Retrosynthetic disconnections of taiwaniaquinoids
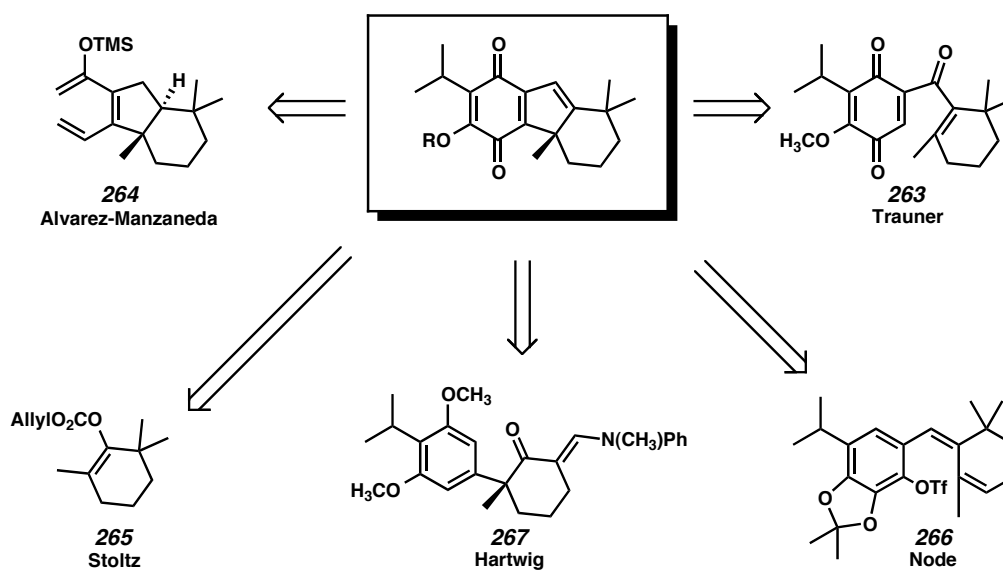
Trauner and coworkers reported a strategy centered around a Nazarov cyclization
of ketone **263** in 2006.[12] This is the most convergent approach to date, and demonstrates
the efficiency of a late-stage B-ring synthesis. However, the electrocyclization is racemic.
This approach benefited from the commercial availability of citral-derived aldehyde **269**,
and expedient the preparation of recorsinol **268**, which were combined *via* 1,2-addition.
Redox manipulations provided ketone **270**, which was the substrate for a TMSOTf-
catalyzed Nazarov cyclization. This approach installs the benzylic quaternary
stereocenter as the final bond in the tricyclic core, presumably reacting *via* cationic
intermediate **271** to afford cyclization product **272** upon hydrolytic work up. Trauner and
coworkers were able to quickly advance the core to taiwaniaquinol B (**262**) and
taiwaniaquione H (**258**) by deprotection and oxidation of the C-ring arene.

Scheme 6.1 Trauner synthesis of taiwaniaquinoids
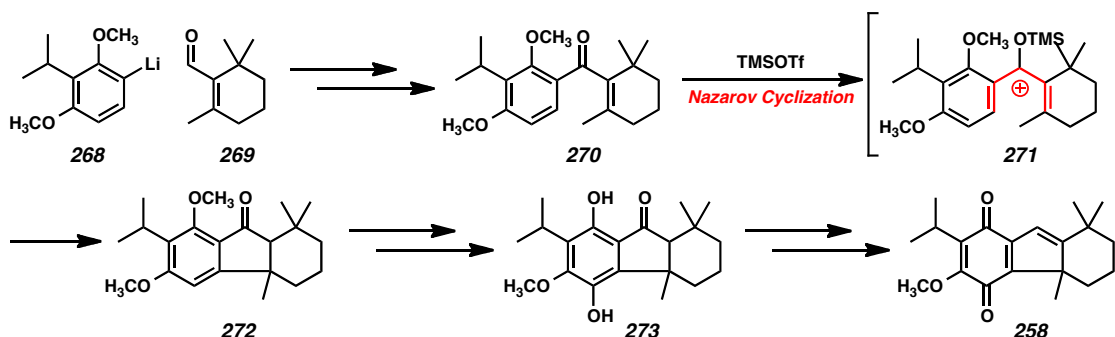
While Stoltz and McFadden reported the first catalytic, asymmetric total synthesis
of a taiwaniaquinoid natural product,[13] it was Node who first installed the benzylic
quaternary stereocenter in an asymmetric fashion, employing an enantioselective
intramolecular Heck.[14,10c] Working with a disconnection similar to that employed by

Trauner, Node begins with bromide **274** and citral-derivative **269**. Addition product of the aryl lithium of **274** affords alcohol **275**, which is advanced to the cyclization precursor (as an inconsequential mixture of olefin isomers) in a few steps. Triflate **276** serves as a precursor, whereby 5-*exo*-trig palladium migratory insertion affords diene **277**. Selective hydrogenation of the 1,2-*cis*-olefin and oxidation of the arene affords taiwaniaquinone H (**258**) in short order. This route effectively turns Trauner's synthetic disconnection into an asymmetric synthesis, however, significant functional group manipulations are required to adjust oxidation states and protecting groups to suit the chosen route.

Scheme 6.2 Node synthesis with asymmetric Heck
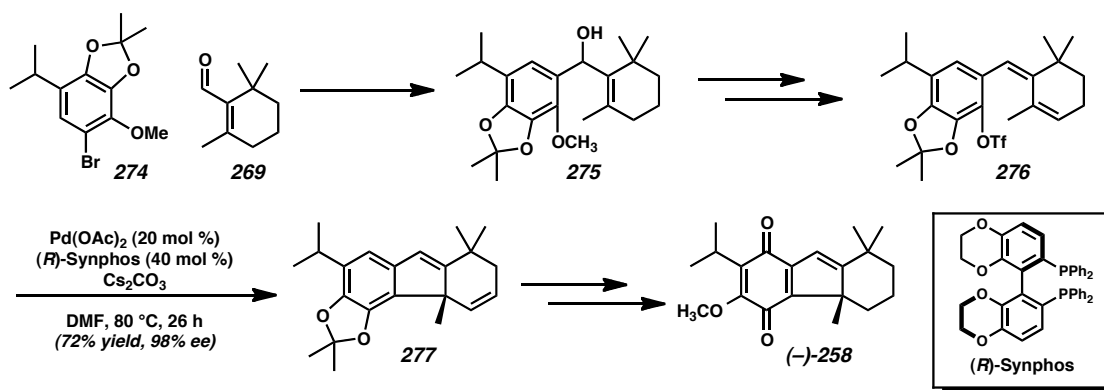
In what features the first truly *convergent*, catalytic, asymmetric synthesis of the quaternary stereocenter, Hartwig and coworkers utilized asymmetric α-arylation to directly furnish the benzylic quaternary stereocenter from two separate synthetic fragments in their syntheses of taiwaniaquinone H (**258**) and taiwaniaquinol B (Scheme 6.3, **262**).[15] Ketone **278** is treated with aryl bromide **279** in the presence of a catalyst derived from palladium(0) and (R)-difluorophos to afford arylated ketone **267** in 80%

yield and excellent enantioselectivity. Removal of the benzylidene blocking group, methylations, and Corey-Chaykovsky epoxidation affords epoxide **280** as a mixture of diastereomers. Lewis-acid mediated epoxy-keto rearrangement affords the corresponding aldehyde, which undergoes *in situ* nucleophilic attack by the electron-rich arene ring. Subsequent dehydration under the reaction conditions (or during the work up) affords styrenyl olefin product **281**. Deprotection of the flanking methoxy ethers on the C-ring and facile oxidation to the quinol and quinone readily affords (+)-taiwaniaquinone H (**258**). They are also able to furnish taiwaniaquinol B from the common intermediate, olefin **281**. Hartwig's route uniquely installs the benzylic quaternary stereocenter, and cleverly builds the tricyclic core scaffold. However, the necessary installation of the benzylidene blocking group (2 steps), and its subsequent removal (also 2 steps) reduces the efficiency of the α-arylation approach, although these steps are all reported in high chemical yield.

Scheme 6.3 Hartwig asymmetric α-arylation approach to taiwaniaquinoids
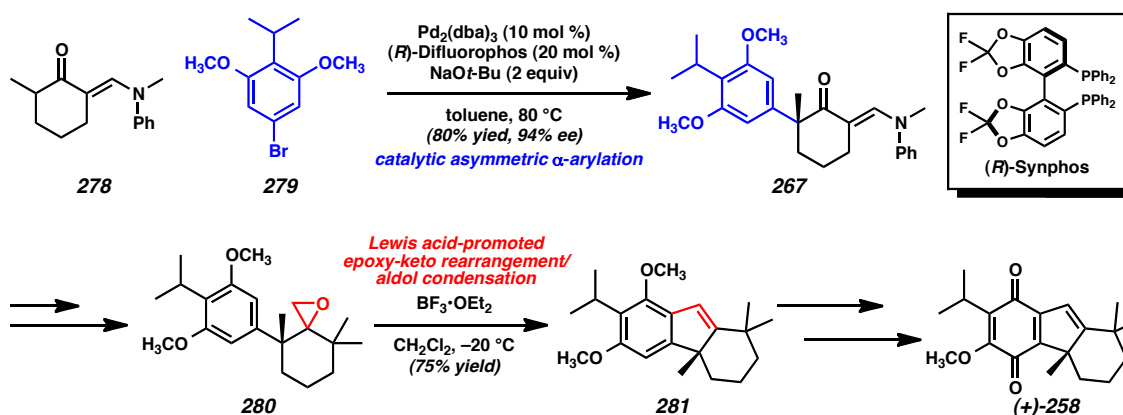
Thus far, considerable effort has been placed on the synthesis of the bond joining the A-ring and C-ring. The installation of this bond, and requisite completion of the benzylic quaternary stereocenter, are the most challenging aspects of synthesizing taiwaniaquinoid natural products.

6.2 Stoltz-McFadden Synthesis of dichroanone

6.2.1 Asymmetric quaternary center synthesis in the Stoltz laboratory

The Stoltz laboratory has developed a number of methodologies for the asymmetric synthesis of quaternary stereocenters. In 2009, Stoltz and corworkers reported the asymmetric addition of malonate derivatives to halo-oxindoles (**282**) catalyzed by a copper-(bis)oxazoline complex (Scheme 6.4a).[16] This process affords α-quaternary oxindoles (**283**) in high yields and good to excellent ee. The Stoltz laboratory has published considerable work in the field of asymmetric allylic alkylation,[17] including their 2004 discloser of the first asymmetric Tsuji-Trost reaction (Scheme 6.4b).[18] Allyl enol carbonate (**284**), or other allyl fragment-bearing precursors, undergo palladium-catalyzed decarboxylative allylic alkylation to afford α–quaternary ketones (**285**).

Scheme 6.4 Synthesis of quaternary stereocenters in Stoltz laboratory

(a) Enantioselective Alkylation of 3-Halooxindoles

282
X = Cl, Br

iPr$_2$NEt, CH$_2$Cl$_2$
3 Å molecular sieves
72 h –20 °C

283
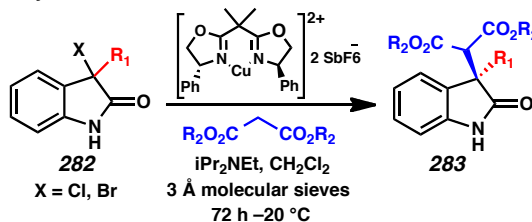
(b) Asymmetric Tsuji–Trost Decarboxylative Alkylation

Pd$_2$(dba)$_3$

toluene, 25 °C

284

285
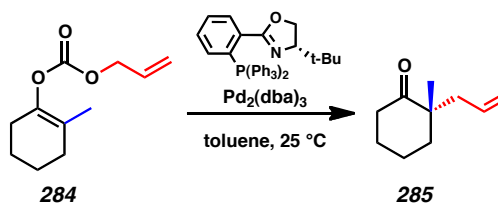
These methodologies for the asymmetric installation of quaternary stereocenters have been utilized as key steps in a number of synthetic efforts from the Stoltz laboratory. The catalytic, enantioselective decarboxylative allylic alkylation has been employed to install the key quaternary stereocenters in a number of natural product syntheses.[19] Cyanthiwigan F was constructed utilizing a double, asymmetric allylic alkylation from β-keto ester **286** to afford α-quaternary diketones **287** in 99% ee (Scheme 6.5a).[20] This compound was rapidly advanced to Cyanthiwigan F (**288**) in only 5 more steps. Vinylogous ester **289**, constructed through asymmetric allylic alkylation, served as a substrate for retro-aldol/aldol ring contraction to afford γ-quaternary acylcyclopentene **290**. This compound was advanced to presilphiperfolan-1-ol (**291**).[21] Most recently, application of the asymmetric addition of malonates to halooxindoles has been applied toward the synthesis of alkaloid natural products. Halooxindole **282** underwent asymmetric malonate addition to yield oxindole **283**, which has been advanced to a formal synthesis of two members of the communesin family of natural products (**292**).[22]

Scheme 6.5 Formation of asymmetric stereocenters in Stoltz total syntheses

(a) Double Catalytic Asymmetric Alkylation
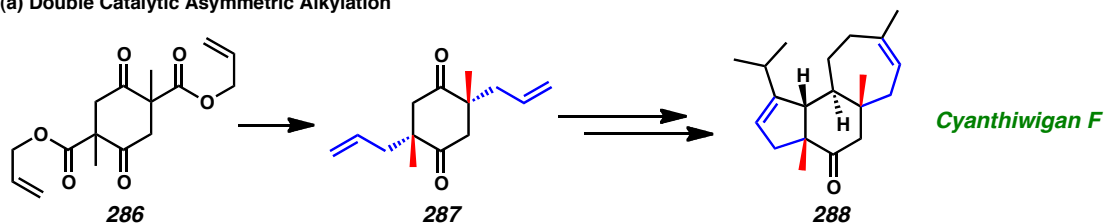
(b) Retro-Aldol/Aldol Functionaliation of Acylcyclopentenone
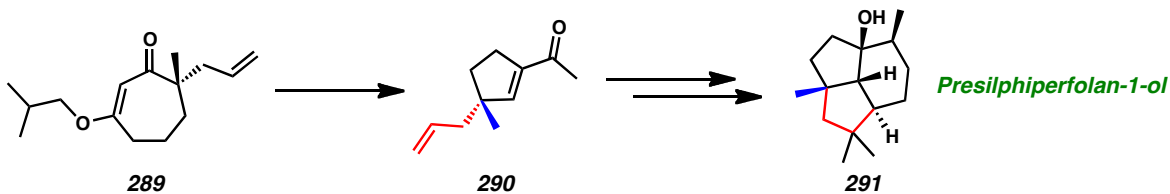
(c) Asymmetric Alkylation of Halooxindoles Toward Alkaloid Scaffolds
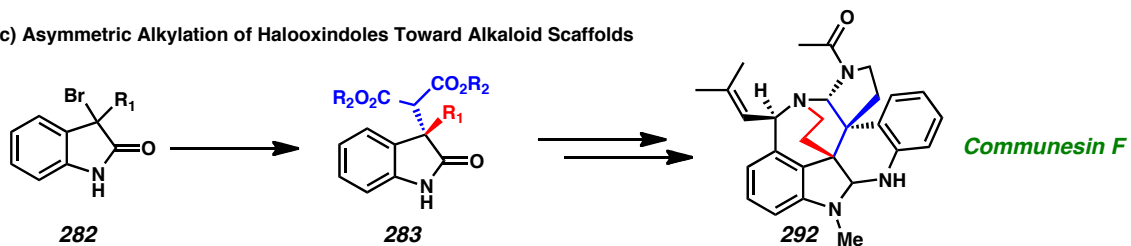
Stoltz and McFadden reported the first catalytic asymmetric total synthesis of (+)-dichroanone (**259**) in 2006.[13] Their retrosynthesis of (+)-dichroanone (Scheme 6.6, **259**) suggests linear sequencing, with formation of the quinone C-ring last. Bicyclic enone **293** is envisioned to form *via* Wacker-type oxidation and subsequent intramolecular aldol condensation of quaternary ketone **294**.

Scheme 6.6 Stoltz retrosynthetic analysis of dichroanone
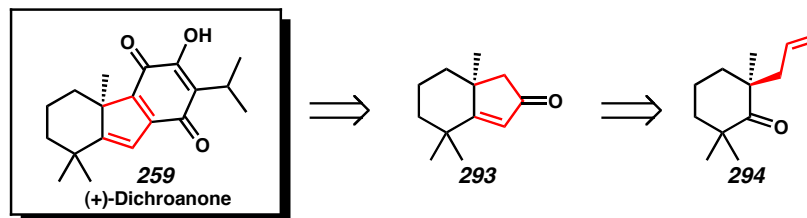
Synthesis of enone **293** was accomplished by allylic alkylation of enol carbonate **265** to afford ketone **295** (Scheme 6.7). Wacker oxidation gives diketone **286**, which undergoes aldol condensation to supply the desired enone **293** in 96% yield.

Scheme 6.7 McFadden and Stoltz synthesis of (+)-dichroanone
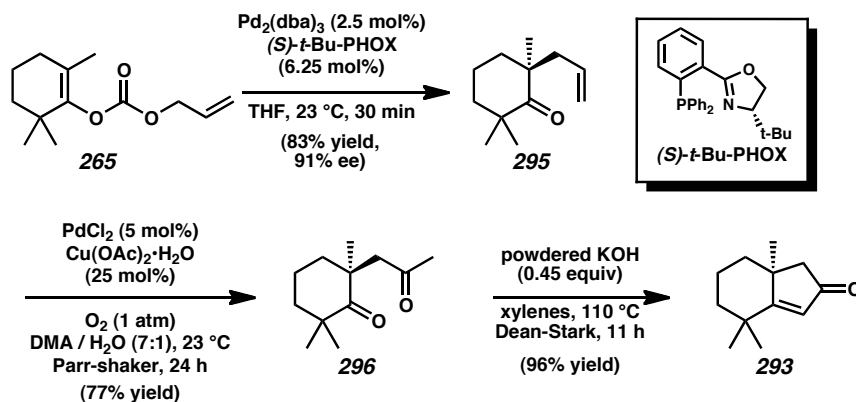
Completion of the synthesis is accomplished in short order from enone **293** (Scheme 6.8). 1,4-addition of methylvinyl ketone affords diketone **297** as an inconsequential mixture of diastereomers. Diketone **297** is also subjected to aldol condensation/dehydration to afford tricyclic enone **298**. Enol triflate formation (**299**) and subsequent Kumada-coupling and aromatization affords tricycle **300** in 65% yield. Titanium-promoted formylation affords aldehyde **301**, which undergoes Baeyer-Villager oxidation to phenol **302**. A carefully optimized, complex oxidation protocol furnishes the desired quinone, and completes the synthesis of (+)-dichroanone (**259**) in 35% yield.

Scheme 6.8 McFadden and Stoltz completion of (+)-dichroanone
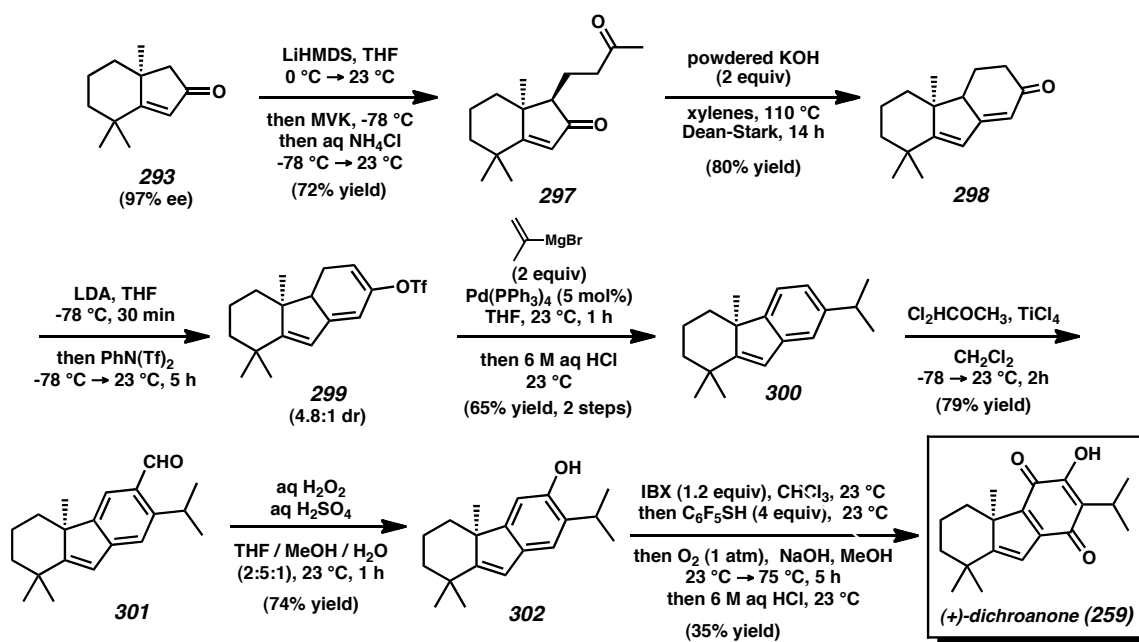
6.3 Toward the total synthesis of (+)-taiwaniaquinone H

6.3.1 Convergent Retrosynthetic Analysis

The Stoltz/McFadden synthesis of (+)-dichroanone was accomplished in a linear fashion, with sequential formation of the A, B, and finally C rings by a series of oxidations and aldol condensations. A more convergent retrosynthetic analysis can be employed (Figure 6.4), invoking β-aryl ketone **304** as the key intermediate. Cyclization of the B-ring would afford tricyclic enone **303**. Oxidation of this compound to the corresponding quinone is well-precedented, as seen in above examples of total syntheses of taiwaniaquinoids. Here, the major synthetic disconnection of β-aryl ketone **305** suggested asymmetric conjugate addition of an appropriate arylmetal reagent (**306**) to 3-methylcyclohexenone. This retrosynthetic analysis facilitates a highly convergent,

catalytic, enantioselective key step that joins together 13 of the 20 core carbons of the taiwaniaquinoid scaffold.

Figure 6.4 Comparative retrosynthetic analysis of dichroanone
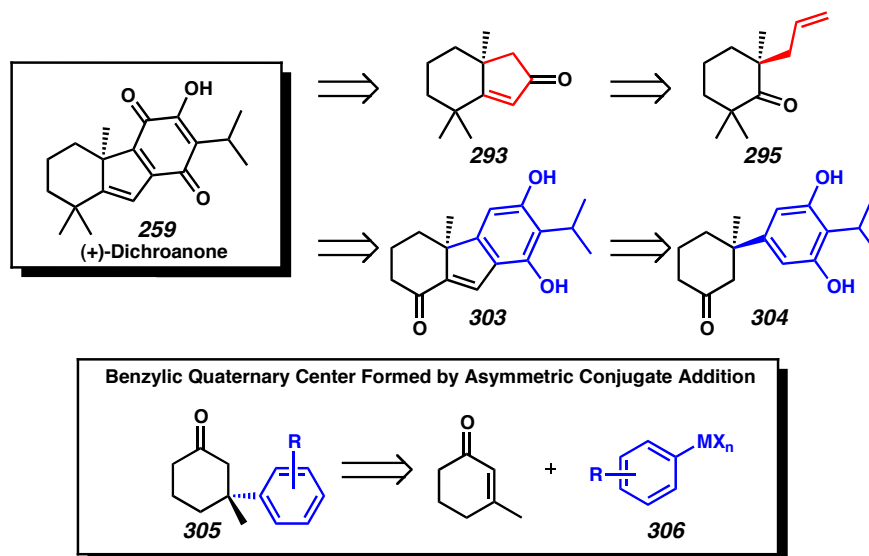
We envision quinone oxidation and *gem*-dimethyl installation to be the final two steps, thus tricyclic enone **307** is the key late-stage intermediate. *Para*-acylphenylboronic acid is a known asymmetric conjugate addition substrate that affords high yields and enantioselectivities, so it will be employed and derivatization of the acyl group (**308**) to the desired *iso*-propyl group (**307**) will be required. Aldol condensation from formyl equivalent **309** will afford the full tricyclic core. Finally, asymmetric conjugate addition will join the boronic acid (**310**) and enone (**95**) fragments. We will employ Hartwig borylation of arenes to generate the boronic acids for use in the asymmetric conjugate addition reaction from the C–H bond shown in arene **311**.

Scheme 6.9 Retrosynthetic analysis of (+)-taiwaniaquinone H
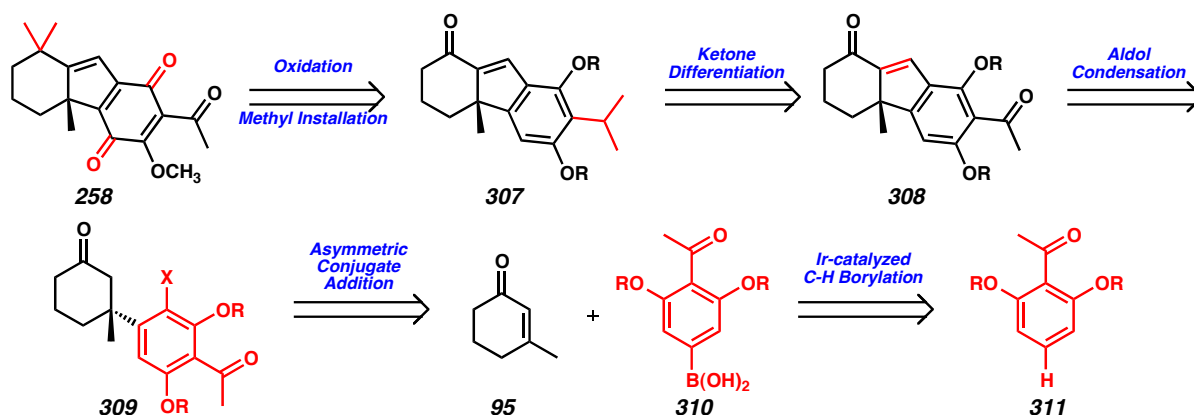
6.3.2 Model study

A model study was employed to ascertain whether the late-stage B-ring construction approach was synthetically tractable (Scheme 6.10). A boronic acid derived from dimethylresorcinol (**312**) was employed, however poor yields and virtually no enantioselectivity was observed in isolated ketone **313**. Protection of ketone **313** with neopentyl glycol afforded ketal **314**, which was treated with *N*-bromosuccinimide to afford aryl bromides **315**, as an intractable mixture of isomers. Lithium/bromine exchange and trapping with dimethylformamide afforded aldehyde **316**, which was separated from its isomer. Treatment with KOH afforded a mixture of aldol addition and condensation products **317**, demonstrating successful B-ring formation.

Scheme 6.10 Model study
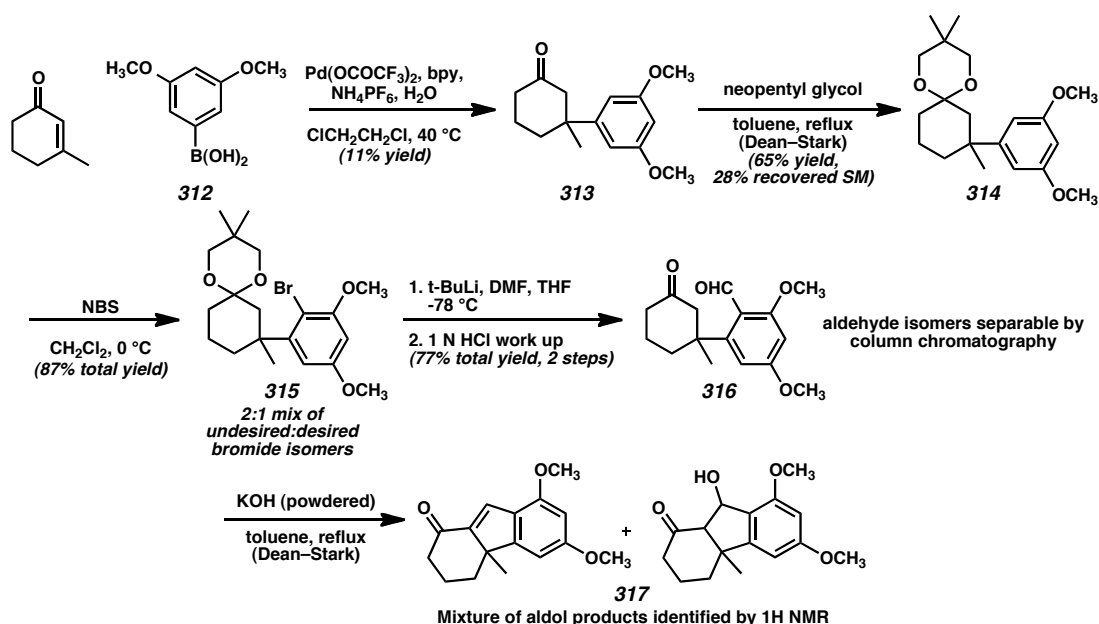
6.3.3 Identification of a suitable arylboronic acid for highly enantioselective asymmetric conjugate addition reaction with 3-methylcyclohexenone

The poor yield of the resorcinol-derived arylboronic acid, and low regioselectivity for the bromination step, prompted us to examine a more suitable arylboronic acid substrate. Early installation of the requisite *iso*-propyl group (ketone **318**) was unsuccessful in the conjugate addition chemistry. *Para*-electron-withdrawing substituents are highly enantioselective substrates, so we reasoned that use of a *p*-acylphenylboronic acid derivative would afford better results. However, ketone **319** also failed to react in appreciable yield. Finally, removing the methyl ethers and replacing them with pivaloyl esters produced the first quality result, affording ketone **320** in 59% yield and 80% ee. Applying the above logic, acetylphenyl ketone **321** was synthesized in 90% yield and 93% ee, sufficiently high yielding for practical use in the synthetic route.

Table 6.1 Identification of a suitable conjugate addition system
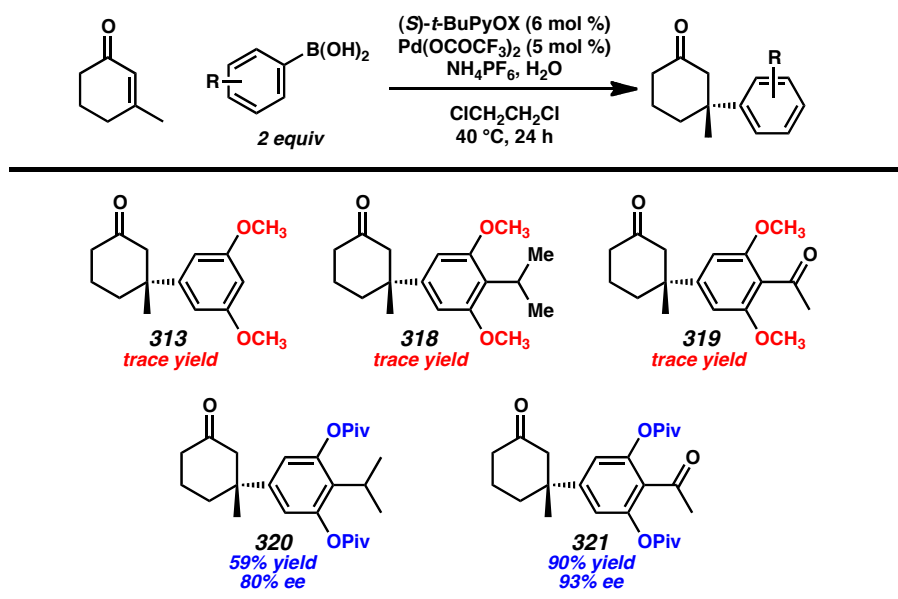
6.3.4 Toward the synthesis of the central B-ring: an unexpected sigmatropic rearrangement

With ketone **321** in hand, we turned our attention toward the installation of the B-ring. Deprotection of the aryl pivalates proved to be highly challenging. Indeed, attempts to drive monodeprotection to completion under a variety of conditions resulted in de-acyl phenol **322** (Scheme 6.11). However, we wished to remove both pivaloyl groups in a single chemical transformation. We were delighted to find that treatment with lithium ethylthioate in dimethylformamide resulted in rapid and clean double deprotection, affording what was initially assigned as diphenol **323**. Curiously, *N*-bromosuccinimide failed to react with our substrate, as it had in the model system. Switching to dibromo-dimethylhydantoin, we observed rapid bromination to what we believed was bromide **324**. Smooth methylation could be obtained with cesium carbonate and methyl iodide to afford methyl ether **325**. Conversely, a synthetic sequence starting with methylation to

afford phenol **326** could be employed. Mono-methyl ketone **326** underwent bromination

to bromide **327**, and subsequent methylation generated a structure matching what we had

assigned as dimethyl ether **325**. The dimethyl ether compound, however, did not undergo

bromination. Hence, we employed this stepwise approach.

Scheme 6.11 Synthesis of aryl halide cyclization precursor
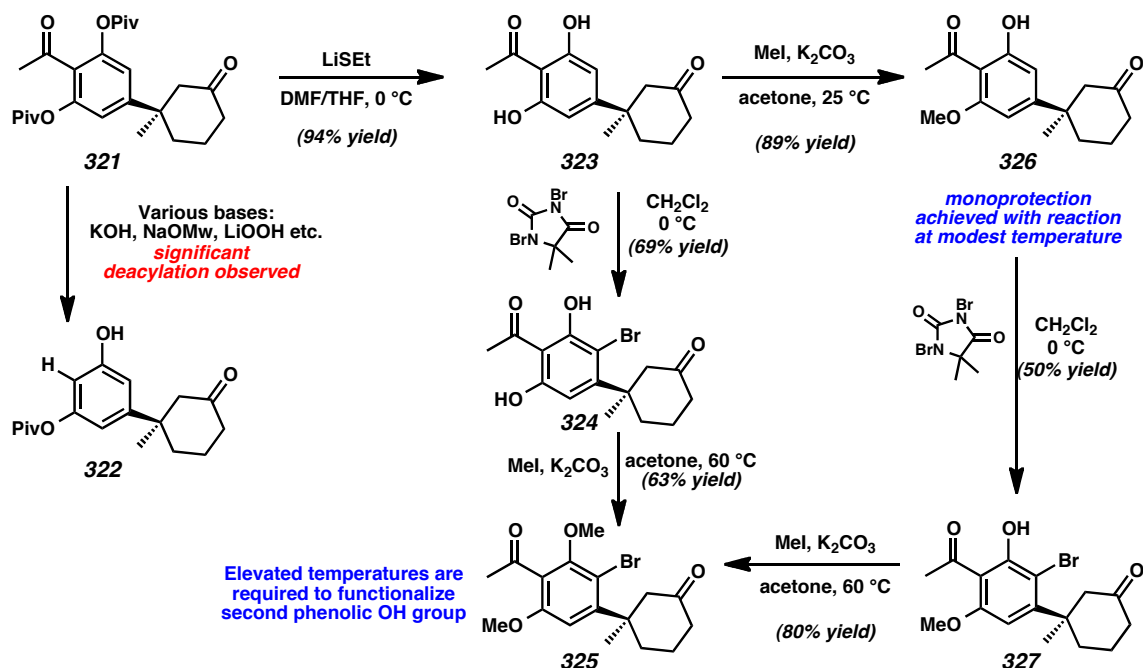
We had a number of plans developed to approach installation of the final B-ring

(Scheme 6.12). First, carbonylation of bromide **327** would afford carbonylated

intermediate **328**, which we envisioned would quickly undergo Dieckmann condensation

to afford diketone **329** (Scheme 6.12a). Second, as in the model system, lithium/halogen

exchange of bromide **325** for lithated arene **330** could lead to formylation by trapping

with dimethylformamide, and cyclization to key intermediate **331** (Scheme 6.12b).

Finally, we envisioned Lewis-acid mediated Nagata-type reactions, whereby coordination

of phenol **326** would generated metallo-ether **332** (Scheme 6.12c). This ether could undergo metallo-ene [3,3]-sigmatropic rearrangement to afford hydroxymethyl arene **333**. Unfortunately, preliminary results in all three reaction pathways were negative. We began to question our initial assignment of ketones **327**, **325**, and **326**.

Scheme 6.12 Synthetic plans to install the B-ring
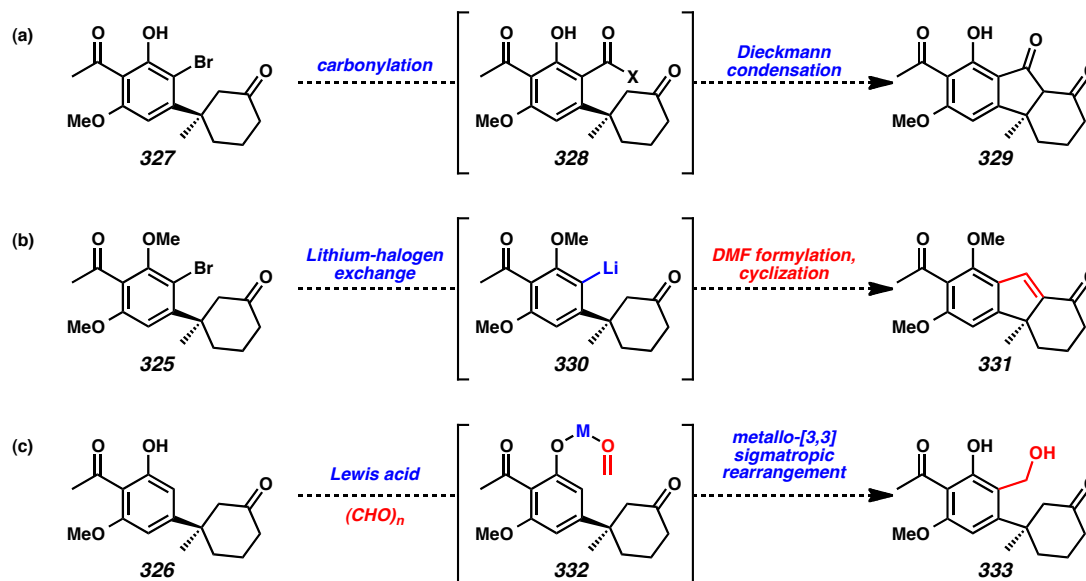
Despite high resolution mass spectrometry results suggesting the proper chemical formula, errant ^{13}C spectra suggested that we had isolated compounds isomeric to the desired ketones. To our great surprise we identified that our assignment of bromide **325** was actually [3,2,1]-bicycle **334** (Scheme 6.13). Likewise, all compounds generated from double-deprotection diphenol **323** contained the undersired bicyclic framework, due to formation of bicycle **335**. Curiously, smooth monodeprotection of ketone **321** to mono-phenol **336** was accomplished under standard ester cleavage conditions, and no cyclization was observed.

Scheme 6.13 Unexpected cyclization of phenolic intermediates
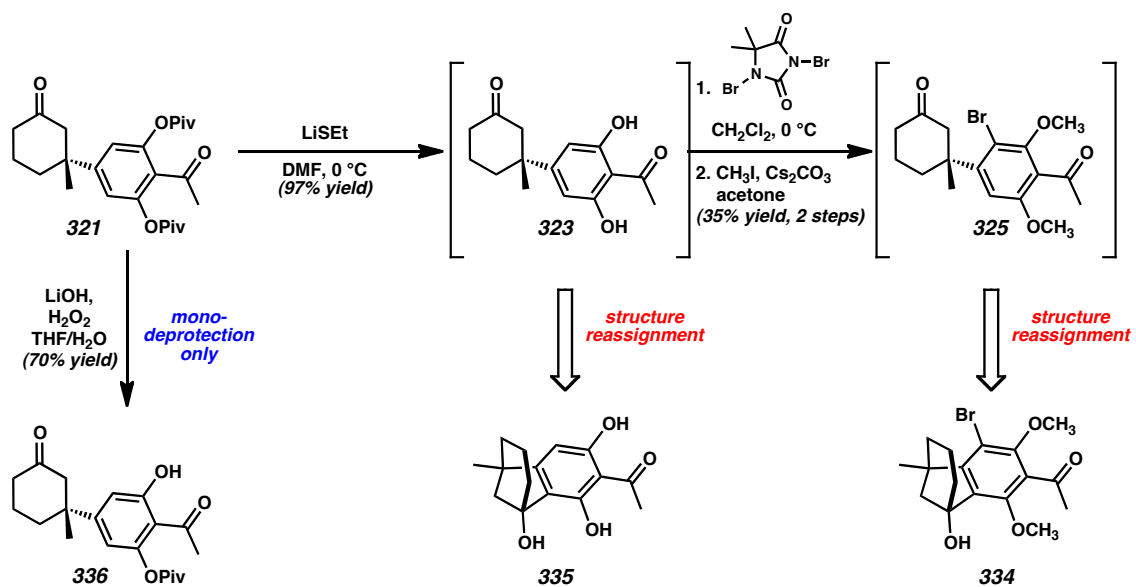
Single crystal x-ray diffraction confirmed our suspicions, elucidating the bicyclic structure of bromide **334** (Figure 6.5). This crystal structure also confirms our assignment of the absolute stereochemistry at the quaternary carbon. A cursory search of the literature shows that β-quaternary cyclohexanones with electron rich aryl rings as β-substituents have been observed to undergo this type of cyclization, though it is typically acid-catalyzed.

Figure 6.5 X-ray crystal structure of bicyclic bromide 334

334
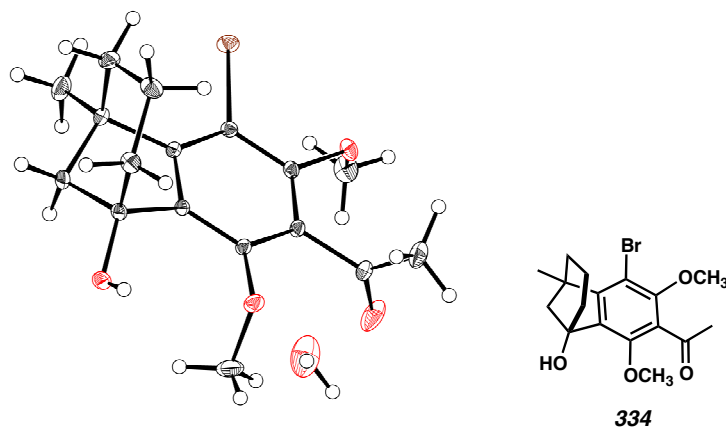
Strangely, none of the β-quaternary ketones we synthesized underwent this rearrangement, except those bearing the diphenol structure. We hypothesize that an ene-type sigmatropic rearrangement may be the operable mechanism (Scheme 6.14). Electron rich diphenol reaction intermediate **323** under goes ene reaction to afford ketone diene **337**, which quickly tautomerizes to rearomatize and afford bicyclic phenol **335**.

Scheme 6.14 Hypothetical mechanism for the cyclization of phenolic intermediates

323   **337**   **335**
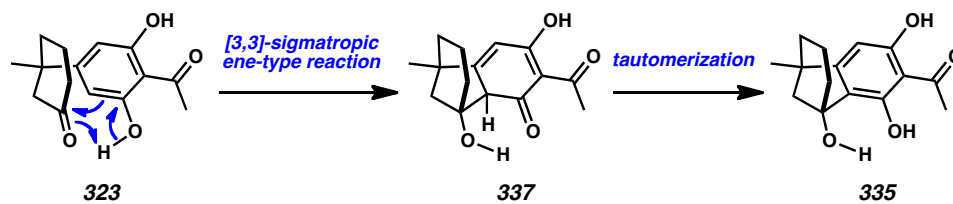
6.4 Experimental Procedures

Representative procedure for the synthesis of pivaloyl resorcinol derivatives
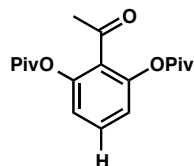
2-acetyl-1,3-phenylene bis(2,2-dimethylpropanoate) (339)

An oven-dred 1L round-bottom flask was charged with a magnetic stir bar, 2,6-dihydroxyacetophenone (10 g, 65.7 mmol, 1 equiv) and DMAP (800 mg, 6.57 mmol, 10 mol %). The flask was evacuated under vacuum and backfilled three times with argon gas. The solids were suspended in CH_2Cl_2 (450 mL), and NEt_3 (23 mL, 165 mmol, 2.5 equiv) was added, at which time the solution became homogenous and a transparent, pale yellow color was observed. The reaction solution was cooled to 0 °C in an ice/water bath and pivaloyl chloride (17 mL, 138 mmol, 2.1 equiv) was added *via* mechanical syringe pump addition over the course of 2 h. Slow addition is essential to maintain an internal temperature of less than 5 °C and minimize formation of side products. Upon complete addition, the ice/water bath was removed and the reaction mixture was allowed to warm to ambient temperature. After 1 h, the reaction was complete by TLC analysis (30% acetone/hexanes, stain *p*-anisaldehyde), and was quenched by the addition of sat. NH_4Cl (aq, 300 mL). The mixture was diluted with CH_2Cl_2 (400 mL) and transferred to a separatory funnel. The aqueous layer was extracted with CH_2Cl_2 (3 x 100 mL) and the combined organic extracts were washed with 1N HCl (3 x 100 mL) and brine (1 x 100 mL), dried over Mg_2SO_4 and concentrated *in vacuo*. The crude mixture was purified by

silica gel flash column chromatography (150 g silica gel, eluent: 20% acetone/hexanes) to afford the title compound as a white, crystalline solid (19.73 g, 94% yield). ^{1}H NMR (500 MHz, CDCl$_3$) δ 6.99 (d, J = 8.2 Hz, 2H), 2.45 (s, 3H), 1.32 (s, 18H); ^{13}C NMR (125 MHz, CDCl$_3$) δ 198.6, 176.3, 147.7, 130.3, 128.4, 119.9, 39.1, 31.5, 26.9; IR (Neat Film, NaCl): 3487, 3395, 2976, 2936, 2874, 1755, 1705, 1611, 1576, 1478, 1457, 1397, 1368, 1274, 1251, 1233, 1117, 1101 cm^{-1}; HRMS (MultiMode ESI/APCI) m/z calc'd for C$_{18}$H$_{23}$O$_5$ [M-H]$^-$: 319.1551, found 319.1542.
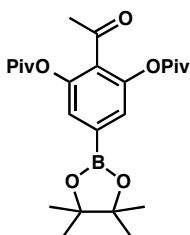
2-acetyl-5-(4,4,5,5-tetramethyl-1,3,2-dioxaborolan-2-yl)-1,3-phenylene bis(2,2-dimethylpropanoate) (340)

In a nitrogen-filled glovebox, a 500 mL round-bottom flask was charged with a stir bar, **339** (16.02 g, 50.0 mmol, 1.0 equiv), B$_2$Pin$_2$ (9.5 g, 37.5 mmol, 0.75 equiv), [Ir(cod)(OMe)]$_2$ (33 mg, 0.05 mmol, 0.1 mol %), and tetramethylphenanthroline (24 mg, 0.10 mmol, 0.2 mol %). The solids were suspended in THF (50 mL) and the flask was sealed with a rubber septum, secured with electrical tape, and removed from the glove box. The reaction mixture was placed under an argon gas atmosphere and stirred in an oil bath at 60 °C for 45 h, at which time the reaction was complete by TLC analysis (20% acetone/hexanes, p-anisaldehyde stain). The reaction mixture was cooled to ambient temperature and filtered through a silica gel plug (50 g silica gel, eluent: acetone), and

concentrated *in vacuo*. The crude reaction mixture was further purified by silica gel flash

chromatography (200 g silica gel, eluent: 20% acetone/hexanes) to afford the title

compound as an amorphous off-white solid (19.85 g, 89% yield). ^{1}H NMR (500 MHz,

CDCl$_3$) δ 7.38 (s, 2H), 2.43 (s, 3H), 1.33 (s, 12H), 1.32 (s, 18H); ^{13}C NMR (125 MHz,

CDCl$_3$) δ 198.6, 176.3, 147.1, 130.8, 125.8, 84.5, 39., 31.4, 27.0, 27.0, 24.8; IR (Neat

Film, NaCl): 3509, 2981, 2935, 1766, 1707, 1482, 1459, 1405, 1396, 1354, 1331, 1259,

1212, 1147 cm^{-1}; HRMS (MultiMode ESI/APCI) *m/z* calc'd for C$_{24}$H$_{39}$O$_7$BN [M+NH$_4$]$^+$:

463.2850, found 463.2852.
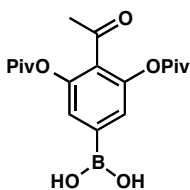
(4-acetyl-3,5-bis(pivaloyloxy)phenyl)boronic acid (341)

A 250 mL round bottom flask was charged with a stir bar and pinnacol boronate ester **340**

(8.65 g, 19.27 mmol, 1.0 equiv). The solid was dissolved in EtOAc (250 mL), and

diethanolamine (2.35 mL, 24.10 mmol, 1.25 equiv) was added with vigorous stirring. A

glass pipet was cut to have a wide bore, and this wide-bore pipet was used to add the

viscous diethanolamine. Upon addition of diethanolamine, a white precipitate forms. This

suspension was stirred a further 4 h at ambient temperature, at which time the mixture

was concentrated *in vacuo*. The crude white semi-solid was suspended in Et$_2$O (300 mL)

and stirred vigorously for 30 min. The suspension was then cooled to –20 °C in a freezer

overnight. The white solid was collected by vacuum filtration, and the compound was

washed with additional portions of Et$_2$O (3 x 50 mL). The collected white solid (7.38 g)

was suspended in 0.1 N HCl (200 mL) and stirred vigorously. CH_2Cl_2 (ca. 50 mL) was added until the solid fully dissolved. The biphasic mixture was stirred for 12 h with extreme vigor. The mixture was then subjected to continuous extraction with boiling CH_2Cl_2 (300 mL) for 6 h. The combined organic extracts were concentrated *in vacuo* and dried under high vacuum to afford the title compound as an off-white, flakey solid (6.45 g, 17.71 mmol, 92% yield over two steps). ^{1}H NMR (500 MHz, CDCl$_3$) δ 7.35 (s, 2H), 2.19 (s, 3H), 1.08 (s, 18H); ^{13}C NMR (125 MHz, acetone-d$_6$) δ 198.3, 176.5, 147.9, 130.9, 125.9, 39.32, 31.5, 27.1; IR (Neat Film, NaCl): 3446, 2975, 2359, 1751, 1700, 1653, 1635, 1558, 1540, 1480, 1456, 1407, 1340, 1247, 1100, 1038 cm^{-1}; HRMS (MultiMode ESI/APCI) *m/z* calc'd for $C_{18}H_{29}O_7BN$ [M+NH$_4$]$^+$: 381.2068, found 381.2061.
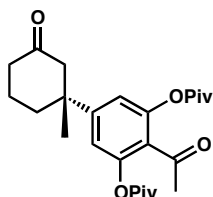
(*R*)-2-acetyl-5-(1-methyl-3-oxocyclohexyl)-1,3-phenylene bis(2,2-dimethylpropanoate) (321)

A 20 mL screw-top vial is charged with a stir bar, Pd(OCOCF$_3$)$_2$ (96 mg, 0.29 mmol, 2.5 mol %), (*S*)-*t*-BuPyOx (71 mg, 0.35 mmol, 3 mol %), NH$_4$PF$_6$ (570 mg, 3.45 mmol, 30 mol %), and the solids were dissolved in 1,2-dichloroethane (5 mL) and stirred at ambient temperature for 5 min. Not all solids dissolved at this time. A 100 mL round bottom flask was charged with a stir bar, boronic acid **341** (6.3 g, 17.29 mmol, 1.5 equiv), and NH$_4$PF$_6$ (570 mg, 3.45 mmol, 30 mol %), and suspended in 1,2-dichloroethane (40 mL) and

stirred at ambient temperature. The catalyst solution was filtered through a pipet plugged with a kimwipe and added to the suspension of boronic acid in one portion. 3-methylcyclohexen-2-one (1.30 mL, 11.53 mmol, 1 equiv) and water (1 mL, 57 mmol, 5 equiv) were added by syringe and the flask was stirred in an oil bath heat to 50 °C for 24 h. When the reaction was complete by TLC analysis (10% acetone/hexanes, *p*-anisaldehyde stain), the mixture was cooled to ambient temperature and filtered through a plug of silica gel (eluent: CH_2Cl_2) and concentrated *in vacuo*. The crude residue was purified by silica gel flash chromatography (200 g silica gel, eluent gradient: 5% acetone/hexanes to 10% acetone/hexanes) to afford the title compound as a colorless oil (3.37 g, 7.84 mmol, 68% yield). ^{1}H NMR (500 MHz, CDCl$_3$) δ 6.91 (s, 2H), 2.77 (d, *J* = 14.1 Hz, 1H), 2.42 (s, 4H), 2.33 (t, *J* = 6.8 Hz, 2H), 2.12 (s, 1H), 1.99–1.84 (m, 2H), 1.82–1.71 (m, 1H), 1.32 (s, 21H); ^{13}C NMR (125 MHz, CDCl$_3$) δ 210.3, 198.3, 176.3, 151.2, 147.9, 126.3, 117.4, 52.7, 42.9, 40.6, 39.1, 37.5, 31.4, 28.7, 27.0, 26.9, 26.8, 21.9; IR (Neat Film, NaCl): 3404, 2973, 2937, 2874, 1758, 1708, 1620, 1562, 1480, 1408, 1397, 1257, 1095 cm^{-1}; HRMS (MultiMode ESI/APCI) *m*/*z* calc'd for $C_{25}H_{34}O_6Na$ [M+Na]$^+$: 453.2248, found 453.2234; [α]$^{25}_D$ –36.1° (*c* 1.85, CHCl$_3$, 94% ee).
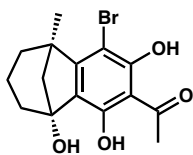
1-((5*R*,9*R*)-4-bromo-1,3,9-trihydroxy-5-methyl-6,7,8,9-tetrahydro-5*H*-5,9-methanobenzo[7]annulen-2-yl)ethanone (333)

A 50 mL, flame-dried, round bottom flask was charged with a stir bar, tricyclic compound **335** (110 mg, 0.419 mmol, 1 equiv) and dibromo-dimethylhydantoin (151 mg, 0.461 mmol, 1.1 equiv). The flask was evacuated under vacuum and back-filled with argon gas, and the solids were dissolved in CH_2Cl_2 (5 mL) and stirred at ambient temperature. After 30 min, an aliquot was partitioned between EtOAc (1 mL) and sat. $Na_2S_2O_3$ (aq, 1 mL), and the organic layer was subjected to LCMS analysis, where no starting material was observed. The red colored reaction was quenched by the addition of 20% $Na_2S_2O_3$ solution (aq, 20 mL) and stirred vigorously for 3 h, until the orange/red color was no longer observed. The mixture was partitioned between CH_2Cl_2 (20 mL) and water (20 mL) and transferred to a separatory funnel. 1N HCl was added until the aqueous layer was pH 3. The aqueous layer was extracted with CH_2Cl_2 (5 x 25 mL) and the combined organic extracts were dried over Na_2SO_4 and concentrated *in vacuo*. The crude residue was purified by silica gel column chromatography (12 g silica gel, eluent gradient: 10% EtOAc/hexanes to 25% EtOAc/hexanes) to afford the title compound as a yellow, semi-crystalline solid (92 mg, 0.273 mmol, 66% yield). ^1H NMR (500 MHz, CDCl$_3$) δ 13.37 (s, 1H), 9.10 (s, 1H), 2.74 (s, 3H), 2.55 (s, 1H), 2.22 (ddd, J = 9.7, 3.0, 2.2 Hz, 1H), 1.93 (ddd, J = 11.2, 6.2, 3.0 Hz, 1H), 1.75–1.64 (m, 4H), 1.61 (s, 3H), 1.35 (td, J = 13.0, 5.5 Hz, 1H), 0.96–0.80 (m, 1H); ^{13}C NMR (125 MHz, CDCl$_3$) δ 204.3, *203.6, 154.17*, 151.7, *120.1, 109.9*, 109.7, 97.7, 81.2, 58.9, 48.6, 34.3, 32.9, 32.8, 24.5, 21.4.; IR (Neat Film, NaCl): 3381, 2936, 2852, 1631, 1566, 1415, 1373, 1326, 1274, 1233 cm^{-1}; HRMS (MultiMode ESI/APCI) *m/z* calc'd for $C_{15}H_{16}BrO_4$ [M-H]$^-$: 339.0237, found 339.0230; $[\alpha]^{25}_D$ –20.8° (*c* 1.26, CHCl$_3$, 94% ee).
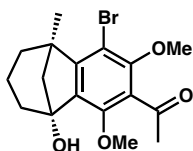
1-((5*R*,9*R*)-4-bromo-9-hydroxy-1,3-dimethoxy-5-methyl-6,7,8,9-tetrahydro-5*H*-5,9-methanobenzo[7]annulen-2-yl)ethanone (334)

A flame-dried 20 mL vial was charged with a stir bar, Bromo-diphenol **333** (92 mg, 0.270 mmol, 1 equiv), Cs_2CO_3 (194 mg, 0.595 mmol, 2.2 equiv), and acetone (5 mL). The vial was stirred under argon atmosphere at ambient temperature, and MeI (0.037 mL, 0.595 mmol, 2.2 equiv) was added in one portion. The yellow reaction slurry was stirred for 40 h at ambient temperature, at which time the color had faded to a white slurry and the reaction was determined to be complete by TLC analysis (20% EtOAc/hexanes, *p*-anisaldehyde stain). The reaction was quenched by the addition of sat. NH_4Cl solution (aq, 5 mL) and stirred for 12 h at ambient temperature. The reaction was diluted with EtOAc (10 mL) and water (10 mL), 1N HCl was added such that the pH was 2–3, and the mixture was transferred to a separatory funnel. The aqueous layer was extracted with EtOAc (3 x 10 mL) and the combined organic extracts were washed with water (2 x 10 mL) and brine (1 x 10 mL), dried over $MgSO_4$ and concentrated *in vacuo*. The crude residue was purified by silica gel flash chromatography (12 g silica gel, eluent gradient 10% EtOAc/hexanes to 20% EtOAC/hexanes) to afford the title compound as a clear oil that solidified to an amorphous white solid upon standing (62 mg, 63% yield). ^{1}H NMR (500 MHz, $CDCl_3$) d 3.81 (s, 3H), 3.80 (s, 3H), 2.56 (s, 3H), 2.24 (dt, *J* = 10.1, 2.5 Hz, 1H), 1.84–1.71 (m, 2H), 1.71–1.61 (m, 3H), 1.60 (s, 3H), 1.35 (td, *J* = 12.9, 5.8 Hz, 1H), 0.81–0.67 (m, 1H).^{13}C NMR (125 MHz, $CDCl_3$) d 201.6, 153.7, 150.9, 147.9, 135.8, 130.4, 108.8, 79.5, 63.8, 58.5, 47.9, 36.5, 33.0, 32.5, 24.9, 21.5.; IR (Neat Film, NaCl):

3429, 2938, 2853, 1704, 1642, 1590, 1450, 1382, 1323, 1237, 1120, 1077 cm^{-1}; HRMS (MultiMode ESI/APCI) *m/z* calc'd for $C_{17}H_{22}BrO_4$ [M+H]$^+$: 369.0696, found 369.0690; $[a]^{25}_D$ –5.8° (*c* 0.73, CHCl$_3$, 94% ee).

6.5 Notes and Citations

(1)   (a) Lin, W.-H.; Fang, J.-M.; Cheng, Y.-S. Phytochemistry **1995**, *40*, 871–873. (b) Lin, W.-H.; Fang, J.-M.; Cheng, Y.-S. P*hytochemistry* **1996**, *42*, 1657–1663. (c) Kawazoe, K.; Yamamoto, M.; Takaishi, Y.; Honda, G.; Fujita, T.; Sezik, E.; Yesilada, E. *Phytochemistry* **1999**, *50*, 493–497. (d) Ohtsu, H.; Iwamoto, M.; Ohishi, H.; Matsunaga, S.; Tanaka, R. *Tetrahedron Lett*. **1999**, *40*, 6419–6422. (e) Chang, C.-I.; Chien, S.-C.; Lee, S.-M.; Kuo, Y.-H. *Chem*. *Pharm*. *Bull*. **2003**, *51*, 1420–1422. (f) Chang, C.-I.; Chang, J.-Y.; Kuo, C.-C.; Pan, W.-Y.; Kuo, Y.-H. *Planta Med*. **2005**, *71*, 72–76.

(2)   For a review, see: Majetich, G.; Shimkus, J. M. *J*. *Nat*. *Prod*. **2010**, *73*, 284–298.

(3)   (a) Iwamoto, M.; Ohtsu, H.; Tokuda, H.; Nishino, H.; Matsunaga, S.; Tanaka, R. *Bioorg*. *Med*. *Chem*. **2001**, *9*, 1911–1921. (b) Minami, T.; Iwamoto, M.; Ohtsu, H.; Ohishi, H.; Tanaka, R.; Yoshitake, A. *Planta Med*. **2002**, *68*, 742–745. (c) Katoh, T.; Akagi, T.; Noguchi, C.; Kajimoto, T.; Node, M.; Tanaka, R.; Nishizawa, M.; Ohtsu, H.; Suzuki, N.; Saito, K. *Bioorg*. *Med*. *Chem*. **2007**, *15*, 2736–2748.

(4)   Banerjee, M.; Mukhopadhyay, R.; Achari, B.; Banerjee, A. K. *Org*. *Lett*. **2003**, *5*, 3931–3933.

(5)   (a) Fillion, E.; Fishlock, D. *J*. *Am*. *Chem*. *Soc*. **2005**, *127*, 13144–13145. (b) Tang, S.; Xu, Y.; He, J.; He, Y.; Zheng, J.; Pan, X.; She, X. *Org*. *Lett*. **2008**, *10*,

1855–1858.

(6)   Alvarez-Manzaneda, E.; Chahboun, R.; Alvarez, E.; Tapia, R.; Alvarez-Manzaneda, R. *Chem.Commun*. **2010**, *46*, 9244–9246.

(7)   (a) Li, S.; Chiu, P. *Tetrahedron Lett*. **2008**, *49*, 1741–1744. (b) Deng, J.; Li, R.; Luo, Y.; Li, J.; Zhou, S.; Li, Y.; Hu, J.; Li, A. *Org. Lett*. **2013**, *15*, 2022–2025.

(8)   (a) Alvarez-Manzaneda, E.; Chahboun, R.; Cabrera, E.; Alvarez, E.; Haidour, A.; Ramos, J. M.; Alvarez-Manzaneda, R.; Hmamouchi, M.; Es-Samti, H. *Chem. Commun*. **2009**, 592–594; (b) Alvarez-Manzaneda, E.; Chahboun, R.; Cabrera, E.; Alvarez, E.; Haidour, A.; Ramos, J. M.; Alvarez-Manzaneda, R.; Charrah, Y.; Es-Samti, H. *Org. Biomol. Chem*. **2009**, *7*, 5146–5155.

(9)   Alvarez-Manzaneda, E.; Chahboun, R.; Cabrera, E.; Alvarez, E.; Alvarez-Manzaneda, R.; Meneses, R.; Es-Samti, H.; Fernández, A. *J. Org. Chem*. **2009**, *74*, 3384–3388.

(10)   (a) Banerjee, M.; Mukhopadhyay, R.; Achari, B.; Banerjee, A. K. *J. Org. Chem*. **2006**, *71*, 2787–2796. (b) Planas, L.; Mogi, M.; Takita, H.; Kajimoto, T. *J. Org. Chem*. **2006**, *71*, 2896–2898. (c) Ozeki, M.; Satake, M.; Toizume, T.; Fukutome, S.; Arimitsu, K.; Hosoi, S.; Kajimoto, T.; Iwasaki, H.; Kojima, N.; Node, M.; Yamashita, M. *Tetrahedron* **2013**, *69*, 3841–3846.

(11)   Singh, R.; Parai, M. K.; Panda, G. *Org. Biomol. Chem*. **2009**, *7*, 1858–1867. (b) Tapia, R.; Guardia, J. J.; Alvarez, E.; Haidöur, A.; Ramos, J. M.; Alvarez-Manzaneda, R.; Chahboun, R.; Alvarez-Manzaneda, E. *J. Org. Chem*. **2012**, *77*, 573–584. (c) Thommen, C.; Jana, C. K.; Neuburger, M.; Gademann, K. *Org. Lett*. **2013**, *15*, 1390–1393.

(12)   Liang, G.; Xu, Y.; Seiple, I. B.; Trauner, D. *J. Am. Chem. Soc.* **2006**, *128*, 11022–11023.

(13)   McFadden, R. M.; Stoltz, B. M. *J. Am. Chem. Soc.* **2006**, *128*, 7738–7739.

(14)   Node, M.; Ozeki, M.; Planas, L.; Nakano, M.; Takita, H.; Mori, D.; Tamatani, S.; Kajimoto, T. *J. Org. Chem.* **2010**, *75*, 190–196.

(15)   Liao, X.; Stanley, L. M.; Hartwig, J. F. *J. Am. Chem. Soc.* **2011**, *133*, 2088–2091.

(16)   (a) Ma, S.; Han, X.; Krishnan, S.; Virgil, S. C.; Stoltz, B. M. *Angew. Chem. Int. Ed.* **2009**, *48*, 8037–8041. (b) Krishnan, S.; Stoltz, B. M. *Tetrahedron Lett.* **2007**, *48*, 7571–7573.

(17)   For an exhaustive review, see: Behenna, D. C.; Mohr, J. T.; Sherden, N. H.; Marinescu, S. C.; Harned, A. M.; Tani, K.; Seto, M.; Ma, S.; Novak, Z.; Krout, M. R.; McFadden, R. M.; Roizen, J. L.; Enquist, J. A., Jr.; White, D. E.; Levine, S. R.; Petrova, K. V.; Iwashita, A.; Virgil, S. C.; Stoltz, B. M. *Chem.–Eur. J.* **2011**, *17*, 14199–14223.

(18)   Behenna, D. C.; Stoltz, B. M. *J. Am. Chem. Soc.* **2004**, *126*, 15044–15045.

(19)   For a review, see: Hong, A. Y.; Stoltz, B. M. *Eur. J. Org. Chem.* **2013**, 2745–2759.

(20)   (a) Enquist, J. A., Jr.; Virgil, S. C.; Stoltz, B. M. *Chem.–Eur. J.* **2011**, *17*, 9957–9969. (b) Enquist, J. A., Jr.; Stoltz, B. M. *Nature* **2008**, *453*, 1228–1231.

(21)   Hong, A. Y.; Stoltz, B. M. *Angew. Chem. Int. Ed.* **2012**, *51*, 9674–9678.

(22)   Unpublished results: Han, S.; Stoltz, B. M. *Manuscript submitted*.

APPENDIX 6

Spectra relevant to Chapter 6:
Progress toward the catalytic asymmetric total synthesis of (+)-
taiwaniaquinone H and other taiwaniaquinoid natural products
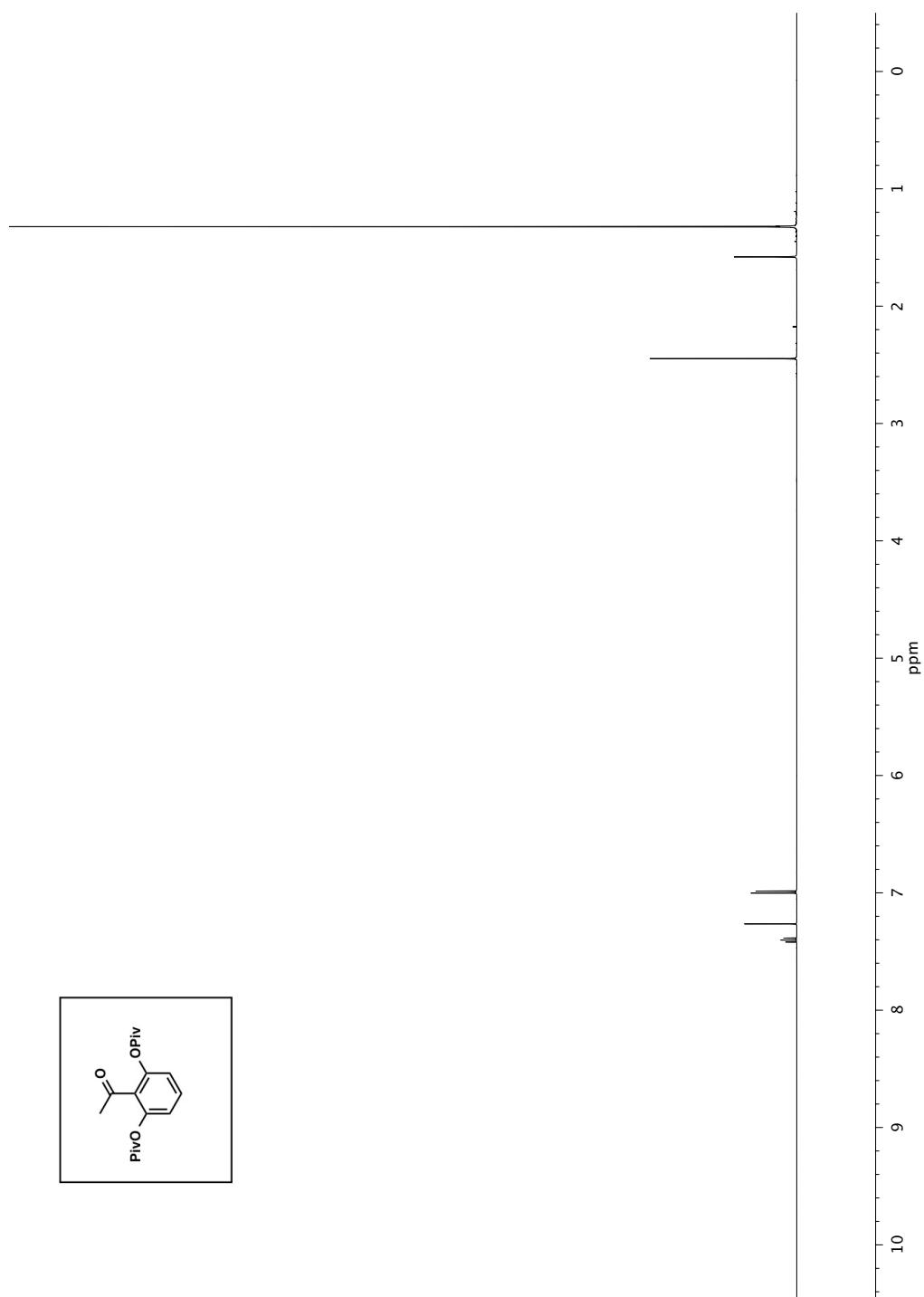
Figure A6.1 ^{1}H NMR (500 MHz, CDCl$_3$) of compound **339**
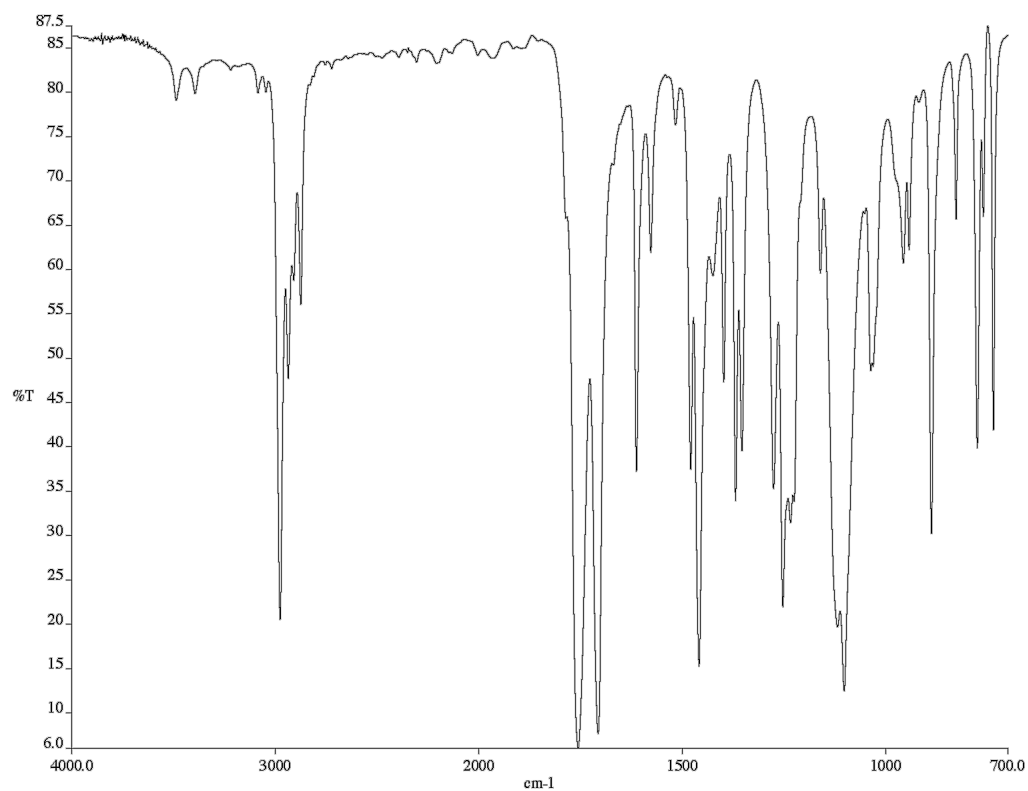
Figure A6.2 Infrared spectrum (Thin Film, NaCl) of compound **339**
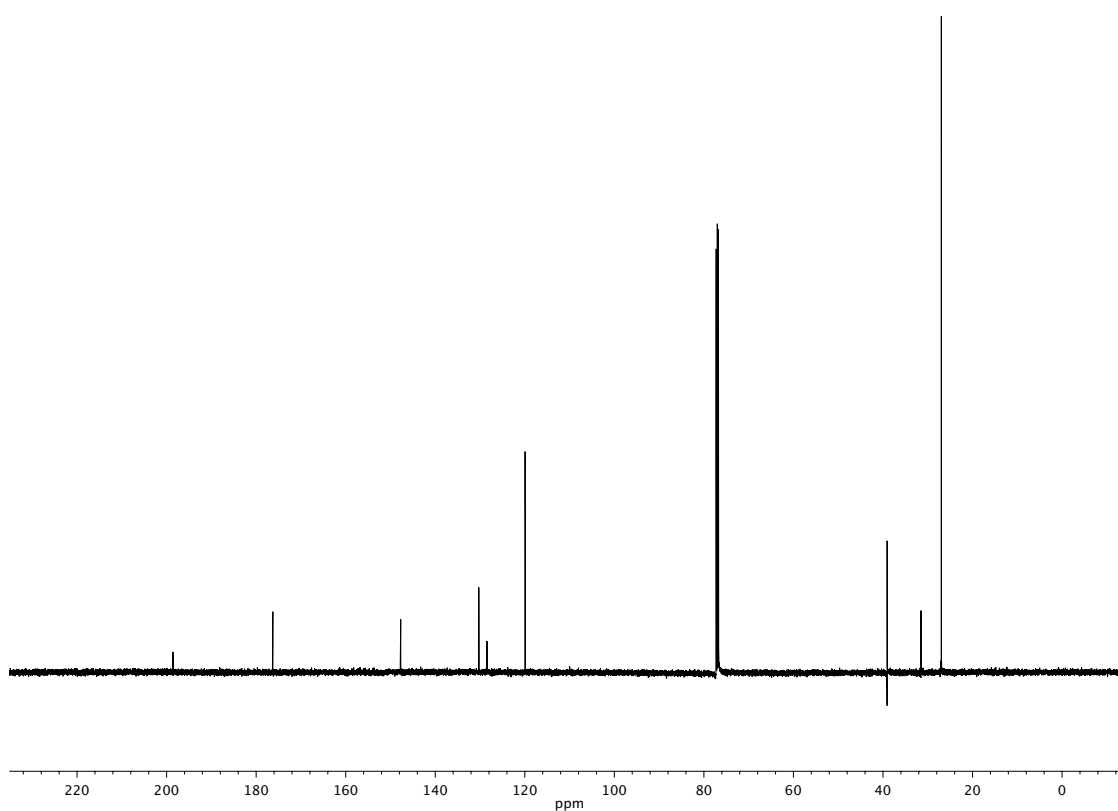
Figure A6.3 ^{13}C NMR (126 MHz, CDCl$_3$) of compound **339**
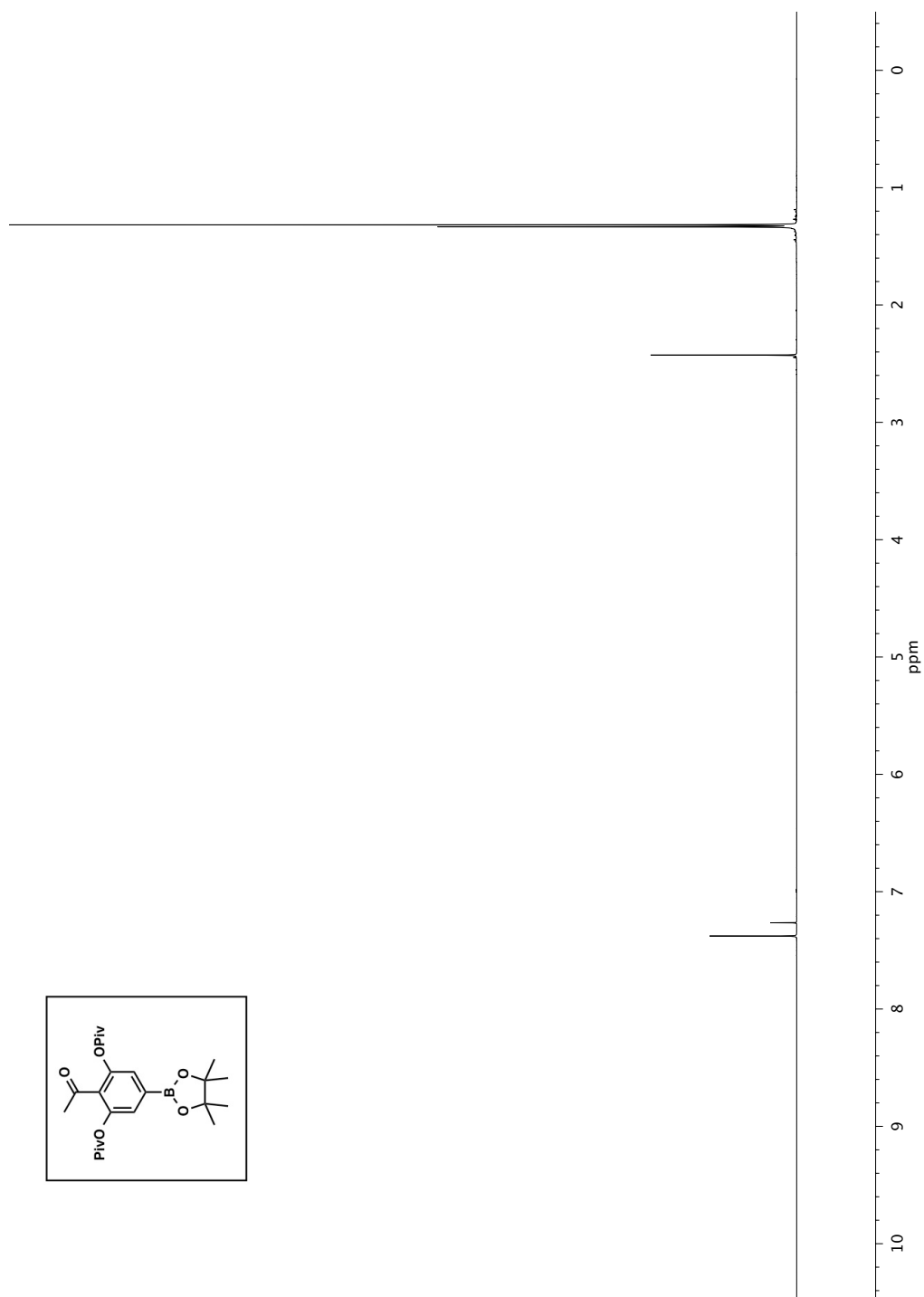
Figure A6.4 ^{1}H NMR (500 MHz, CDCl$_3$) of compound **340**
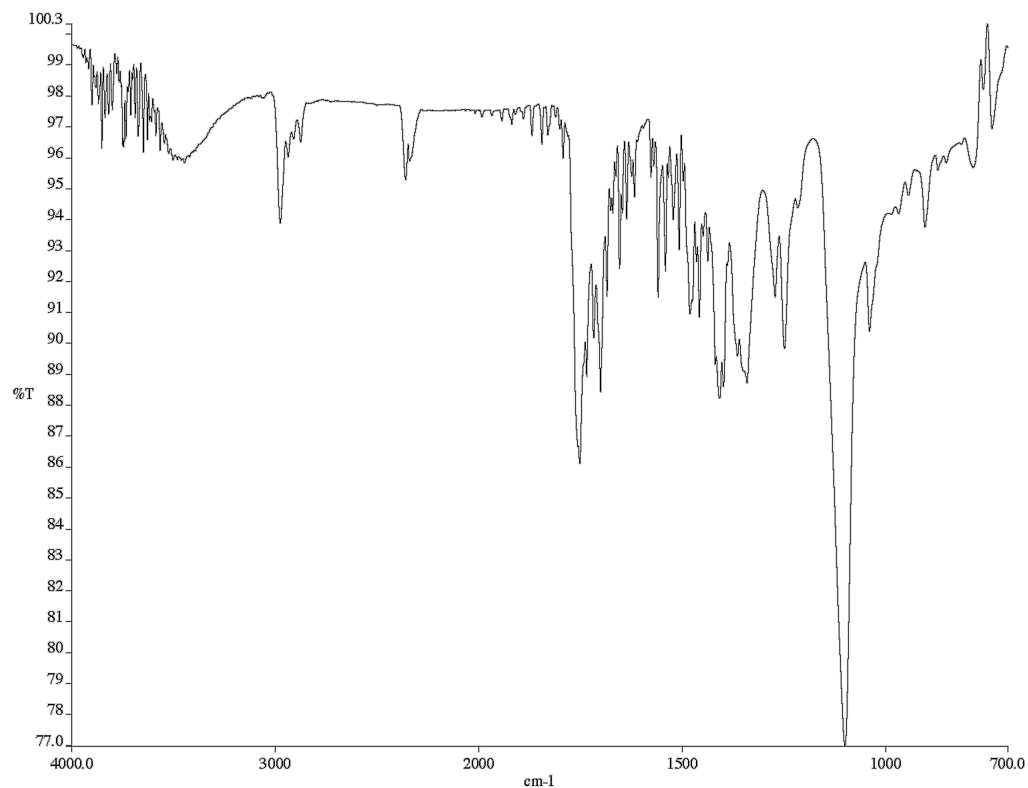
Figure A6.5 Infrared spectrum (Thin Film, NaCl) of compound **340**
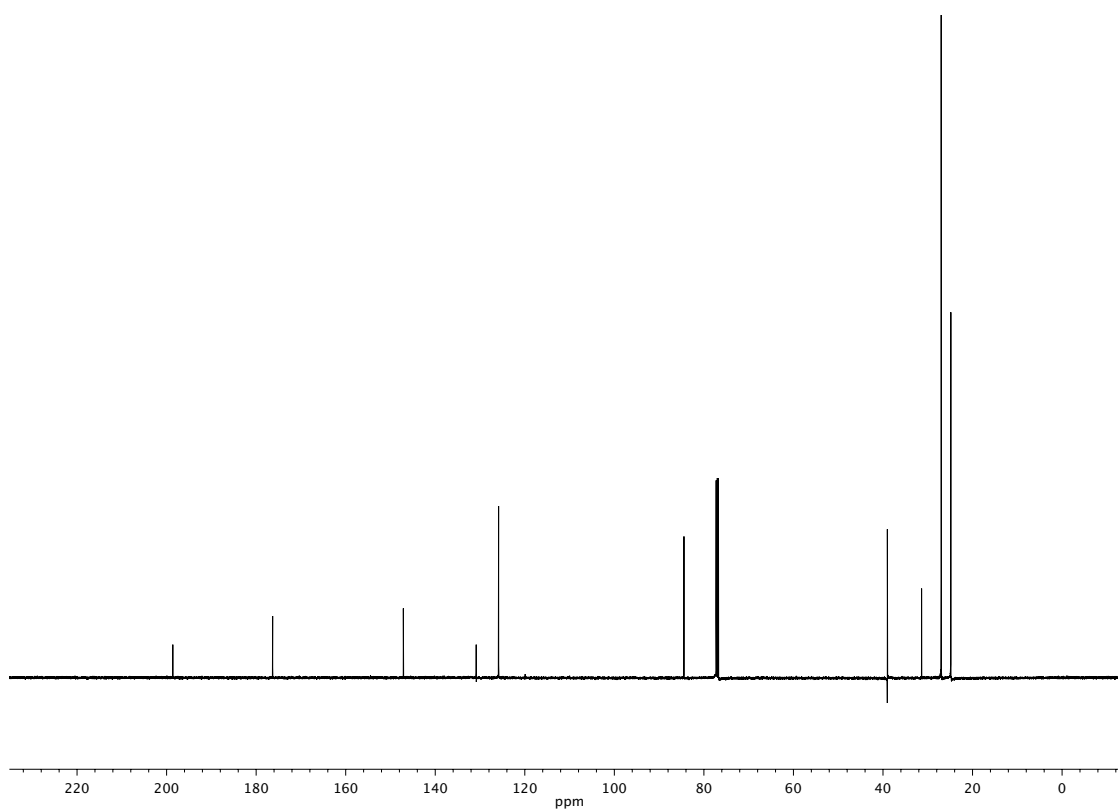
Figure A6.6 ^{13}C NMR (126 MHz, CDCl$_3$) of compound **340**
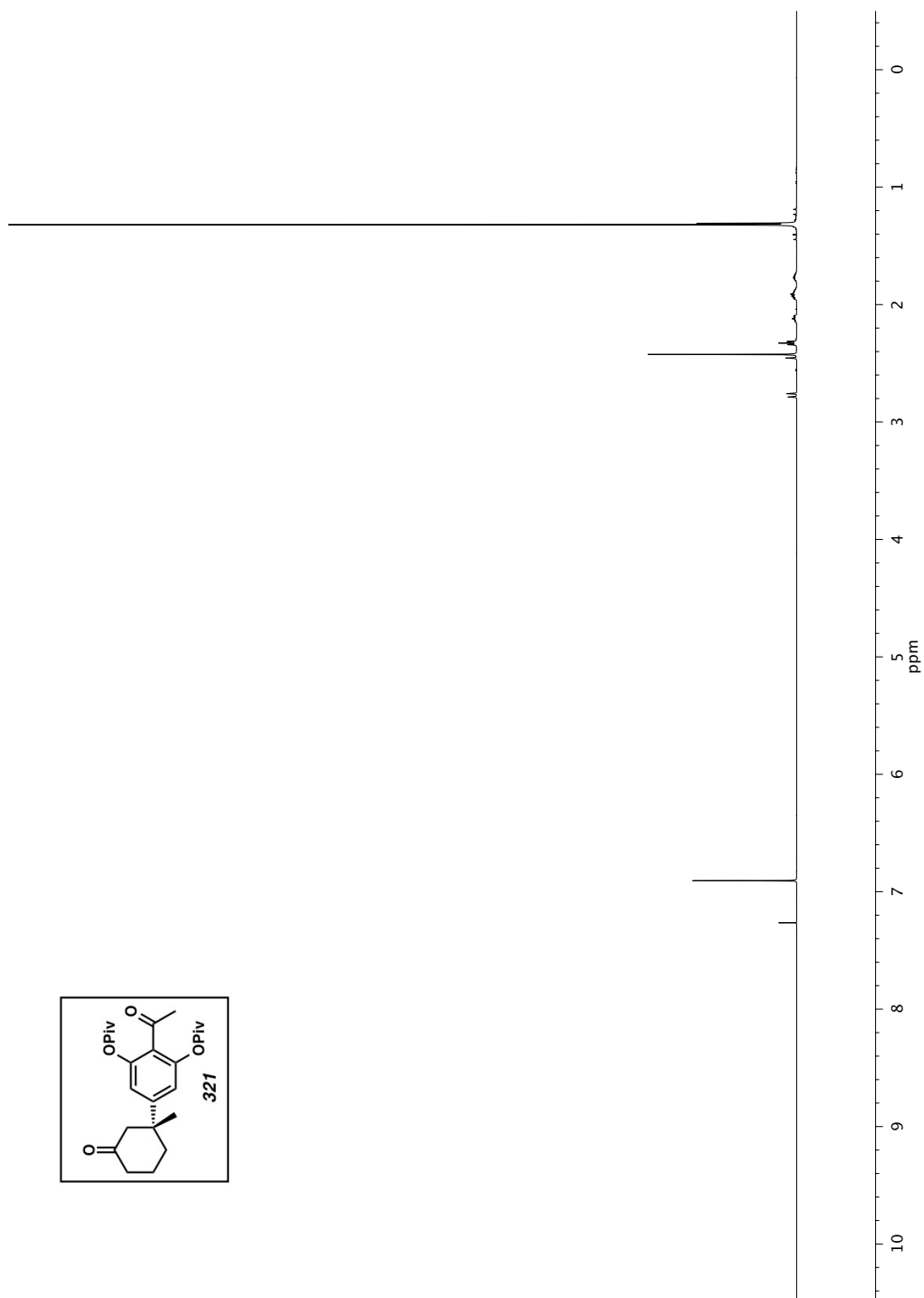
Figure A6.7 ^{1}H NMR (500 MHz, CDCl$_3$) of compound **321**
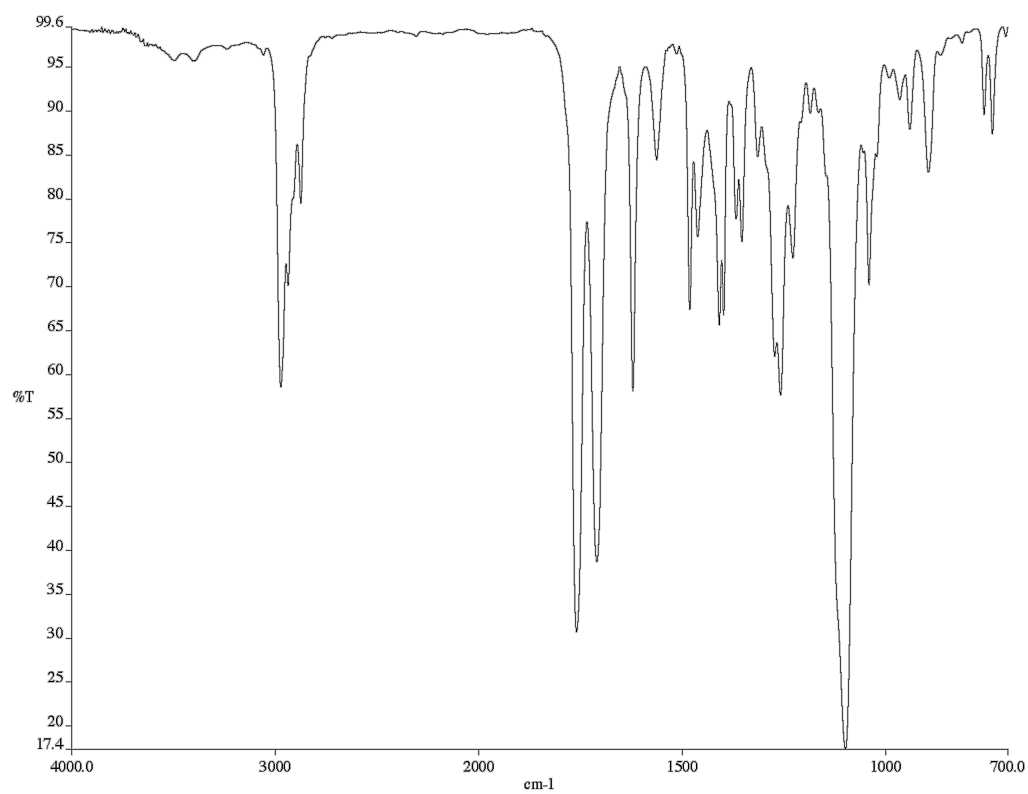
Figure A6.8 Infrared spectrum (Thin Film, NaCl) of compound **321**
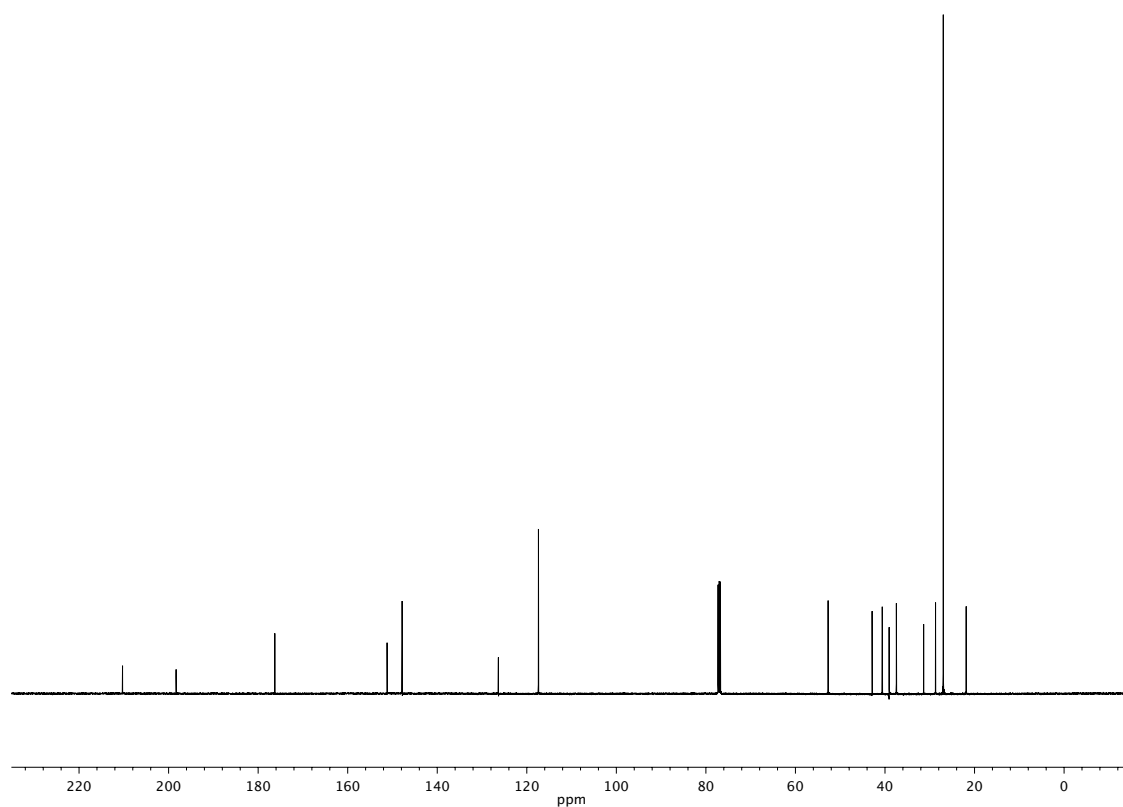
Figure A6.9 ^{13}C NMR (126 MHz, CDCl$_3$) of compound **321**
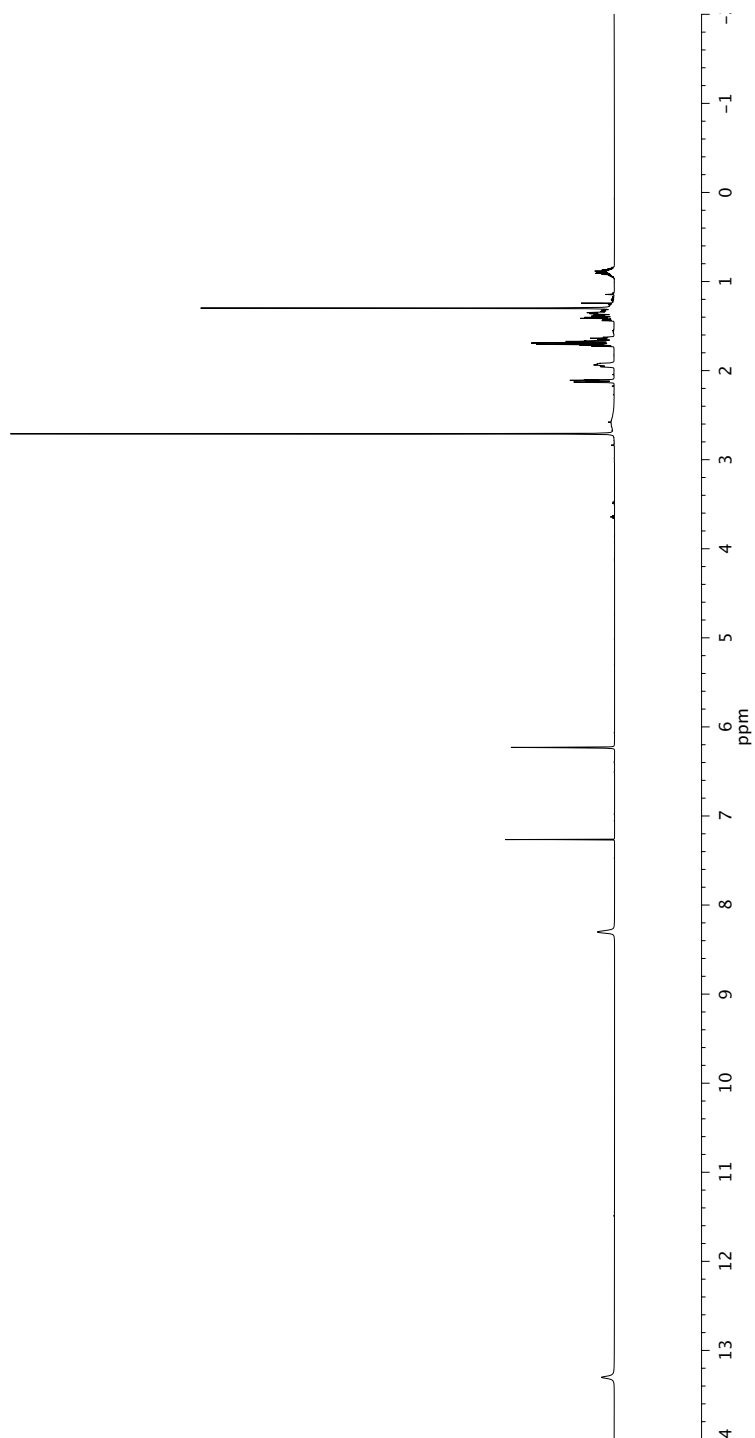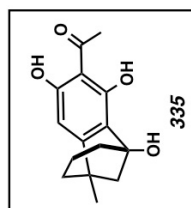
Figure A6.10 ^{1}H NMR (500 MHz, CDCl$_3$) of compound **335**
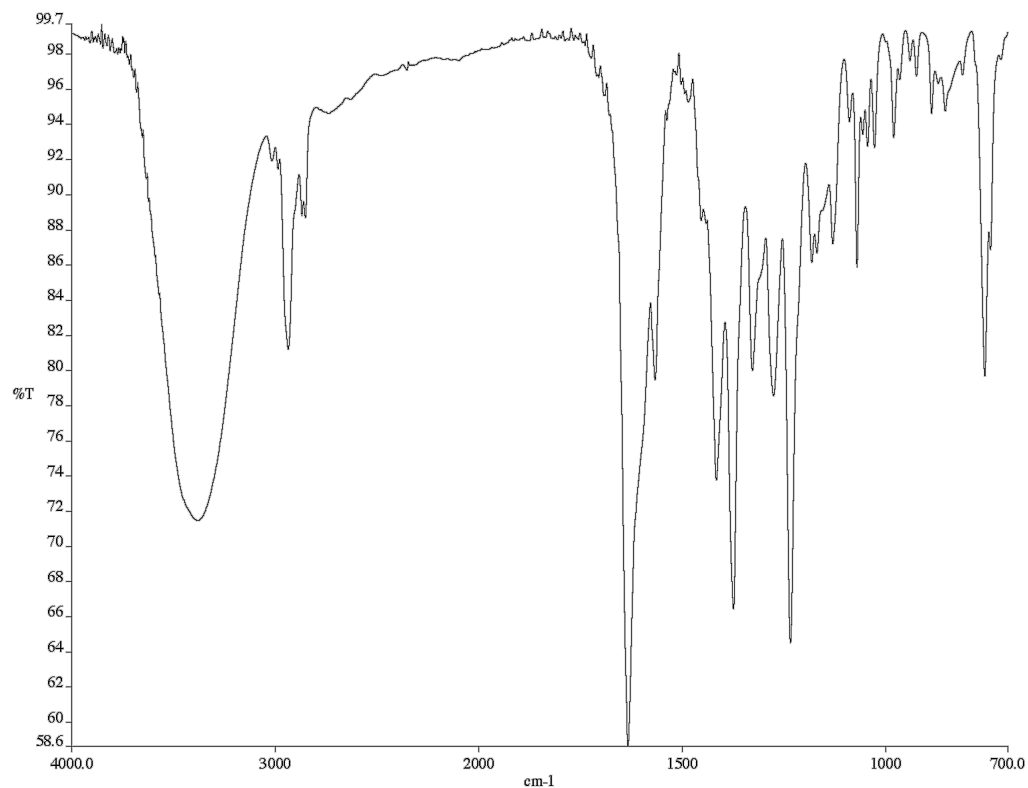
Figure A6.11 Infrared spectrum (Thin Film, NaCl) of compound **335**
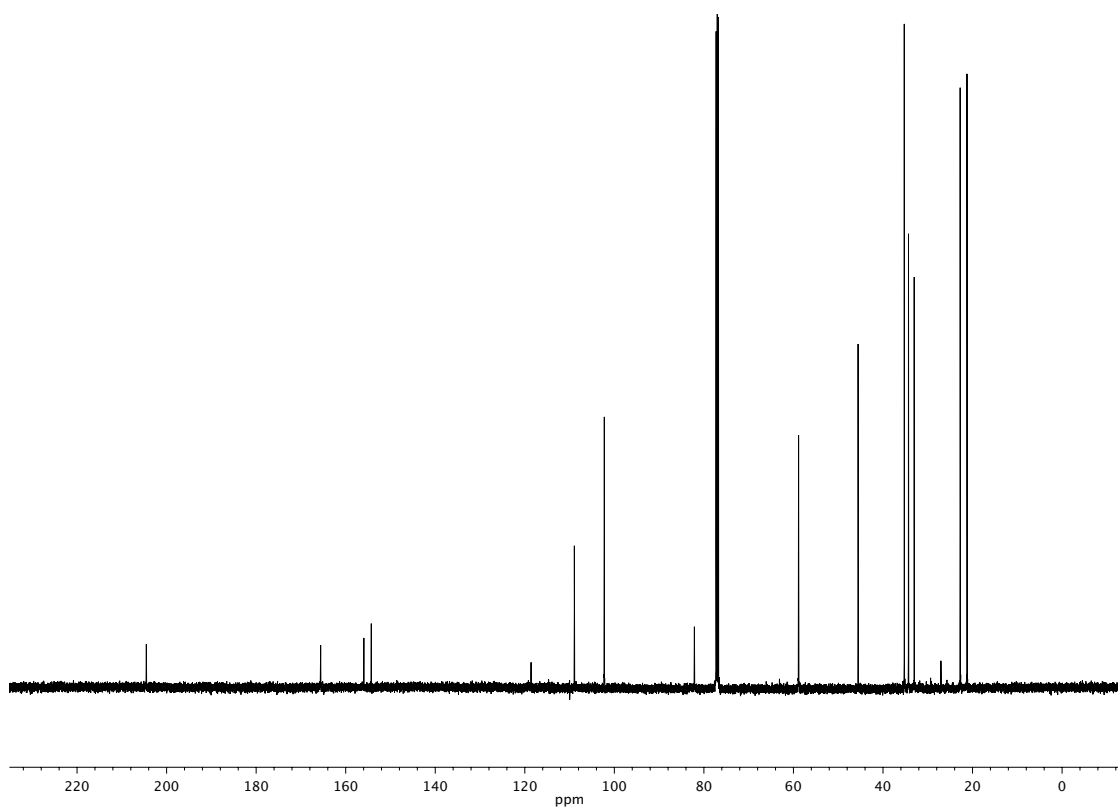
Figure A6.12 ^{13}C NMR (126 MHz, CDCl$_3$) of compound **335**
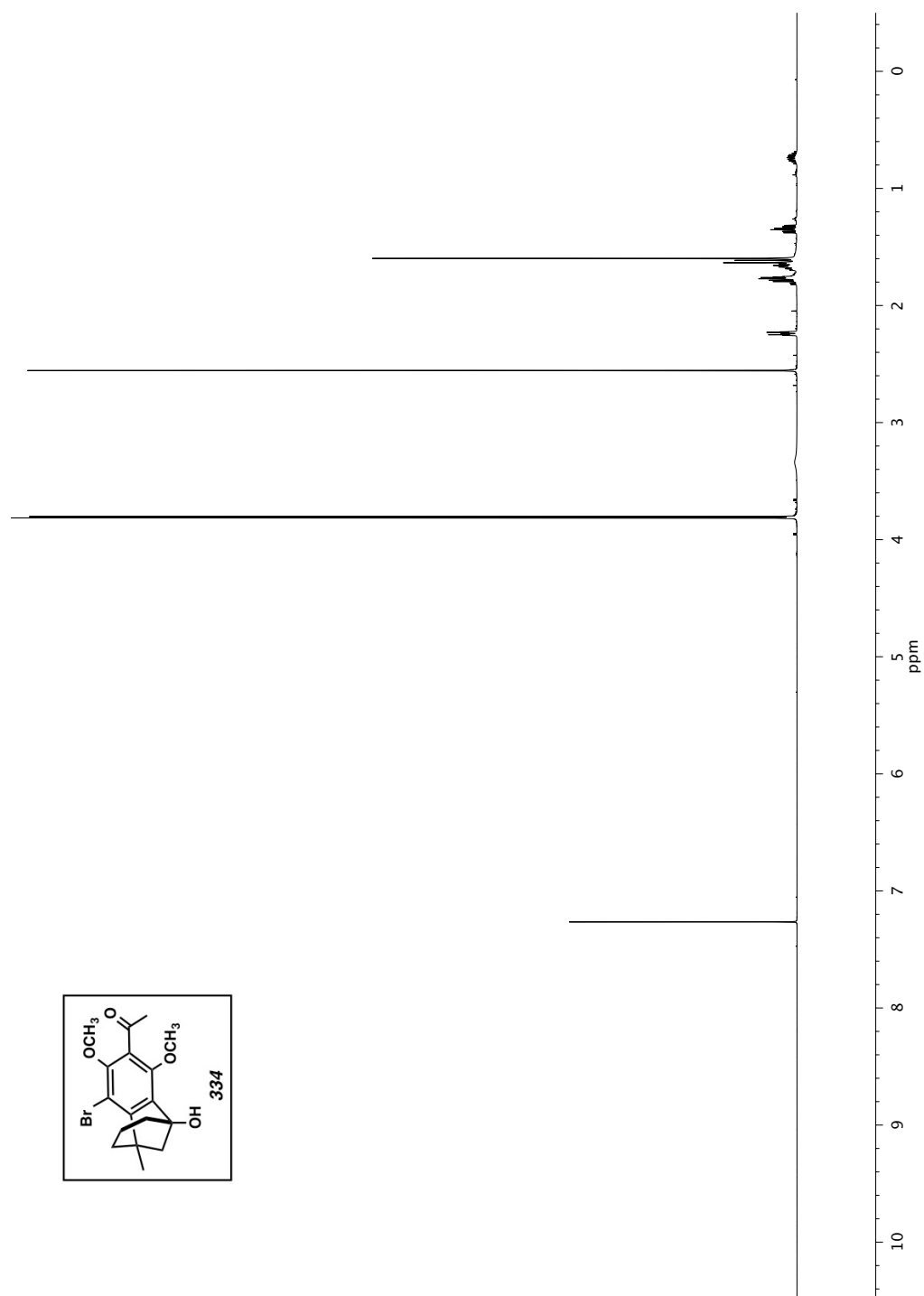
Figure A6.13 ^{1}H NMR (500 MHz, CDCl$_3$) of compound **334**
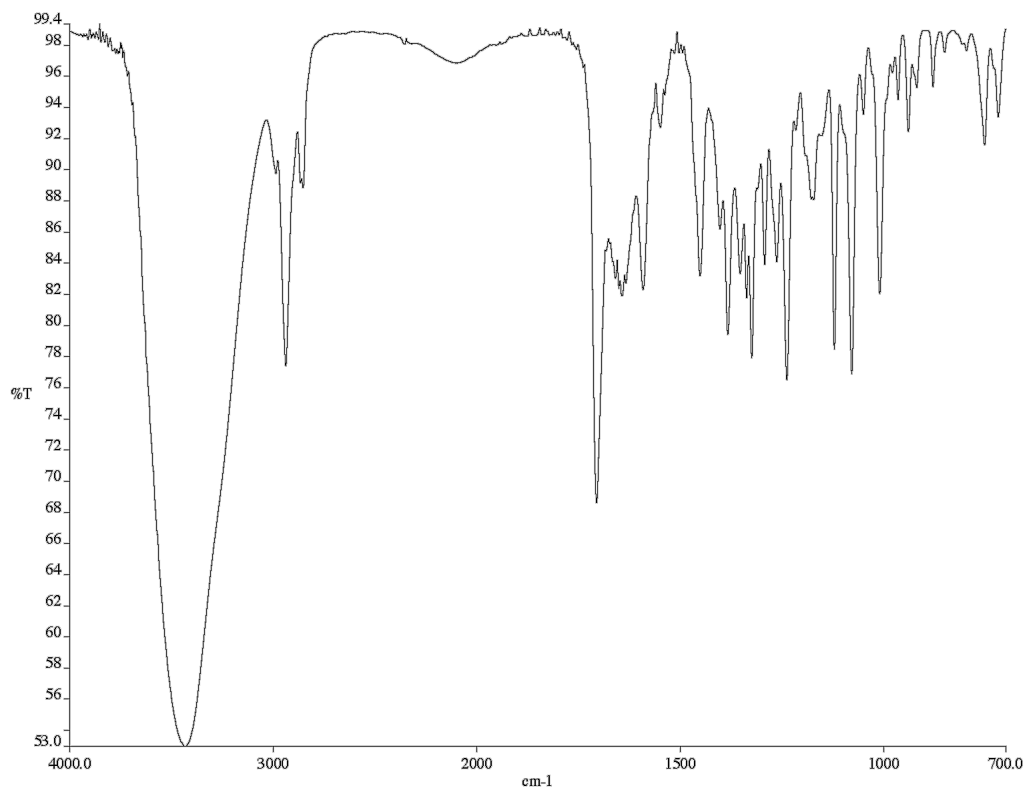
Figure A6.14 Infrared spectrum (Thin Film, NaCl) of compound **334**
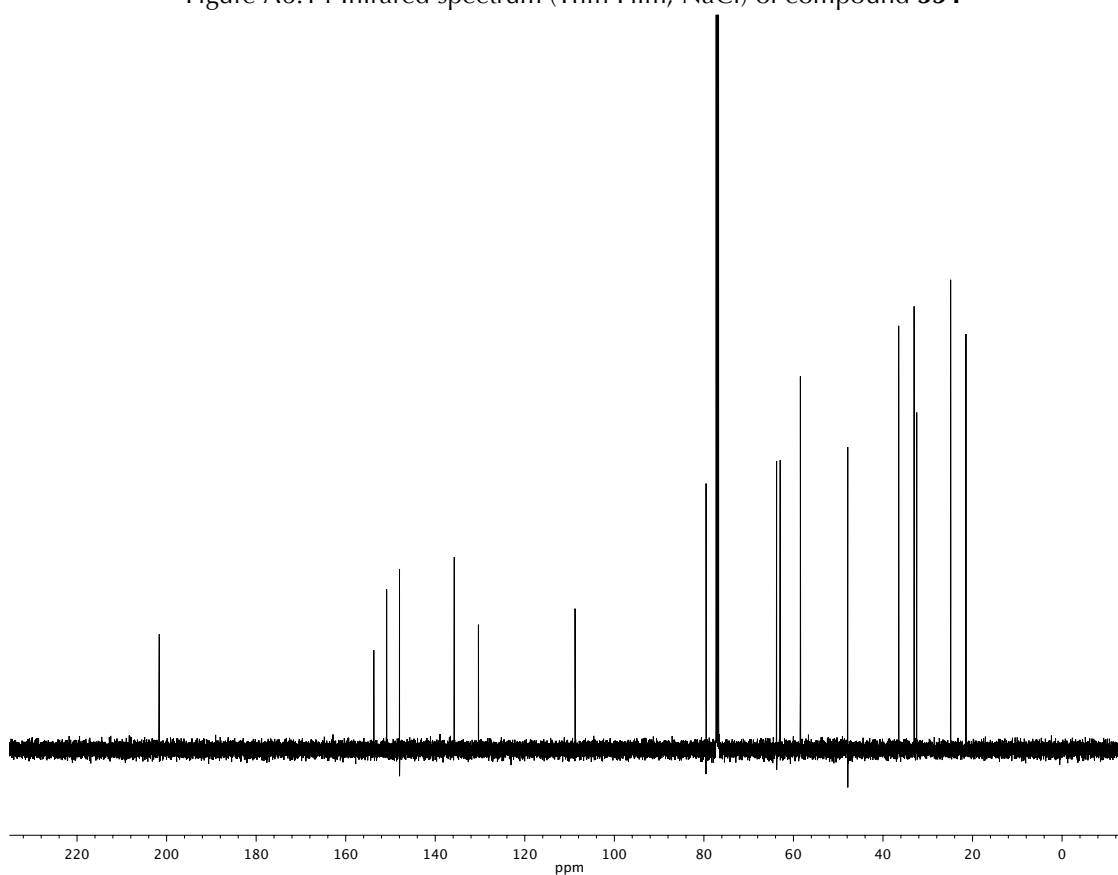
Figure A6.15 ^{13}C NMR (126 MHz, CDCl$_3$) of compound **334**
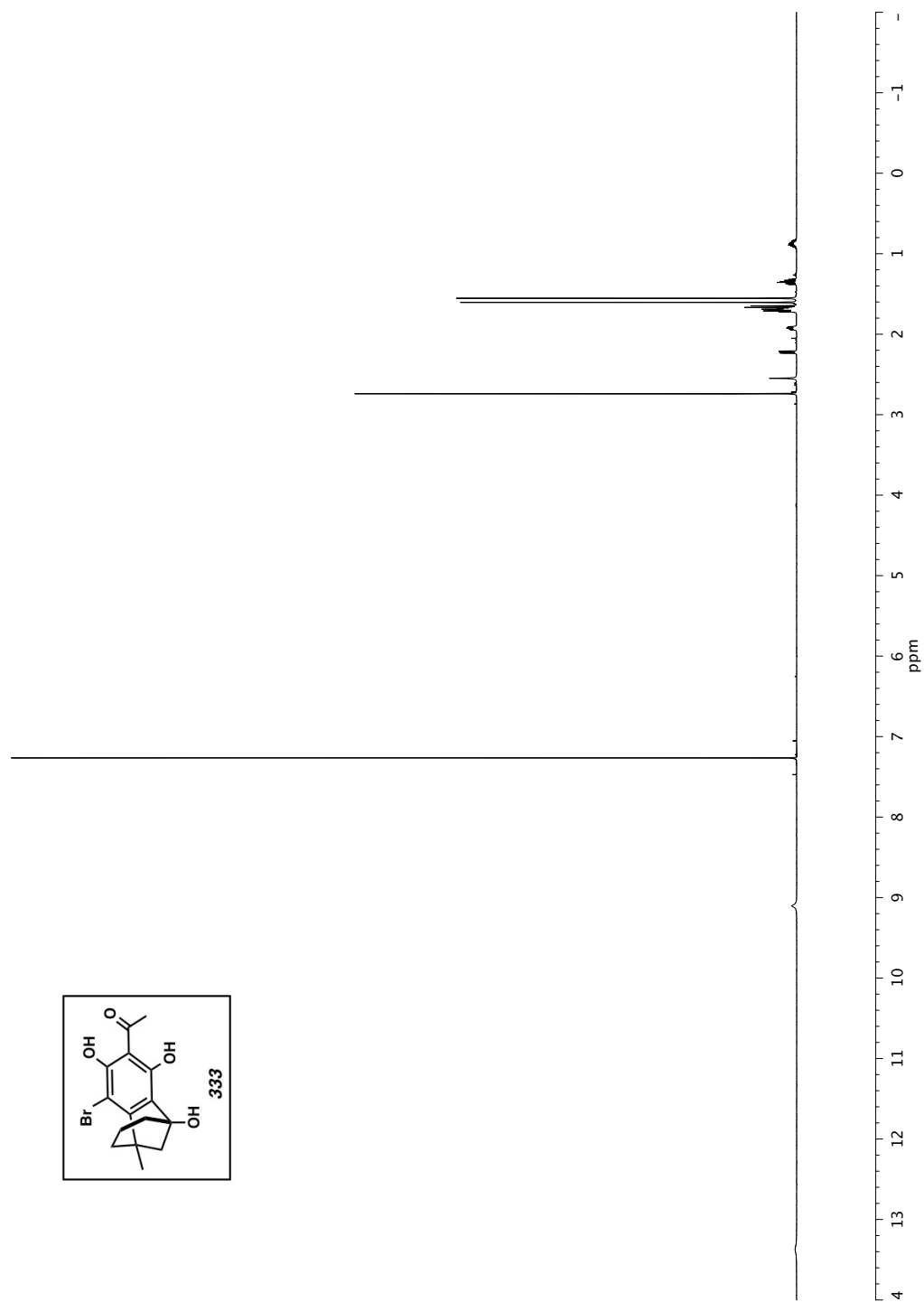
Figure A6.16 ^{1}H NMR (500 MHz, CDCl$_3$) of compound **333**
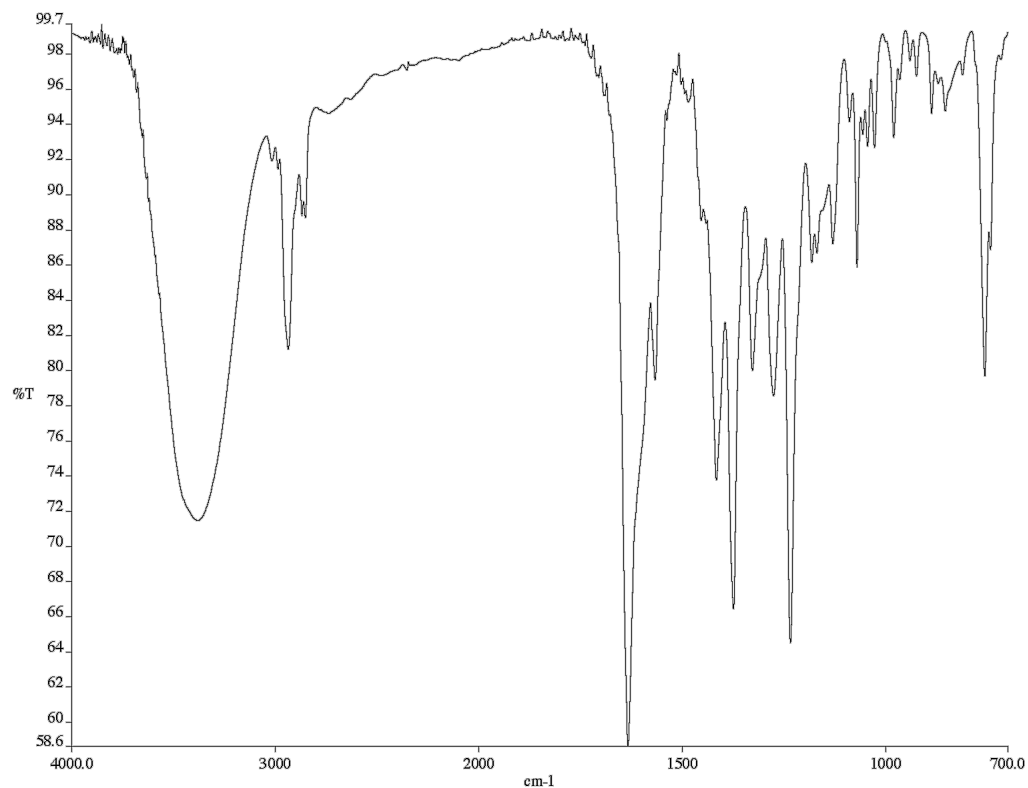
Figure A6.17 Infrared spectrum (Thin Film, NaCl) of compound **333**
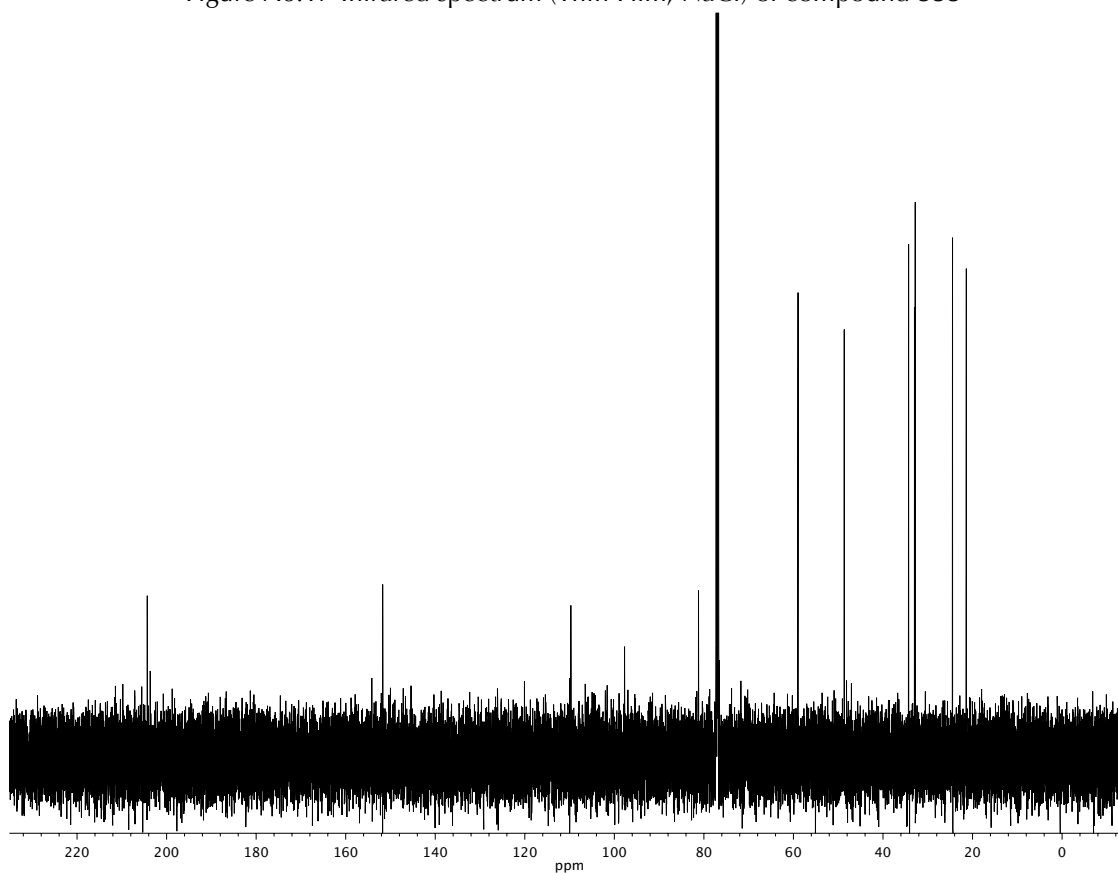
Figure A6.18 ^{13}C NMR (126 MHz, CDCl$_3$) of compound **333**

APPENDIX 7

X-ray structures relevant to Chapter 6:
Progress toward the catalytic asymmetric total synthesis of (+)-
taiwaniaquinone H and other taiwaniaquinoid natural products

*Figure A7.1 X-ray structure of compound **334***
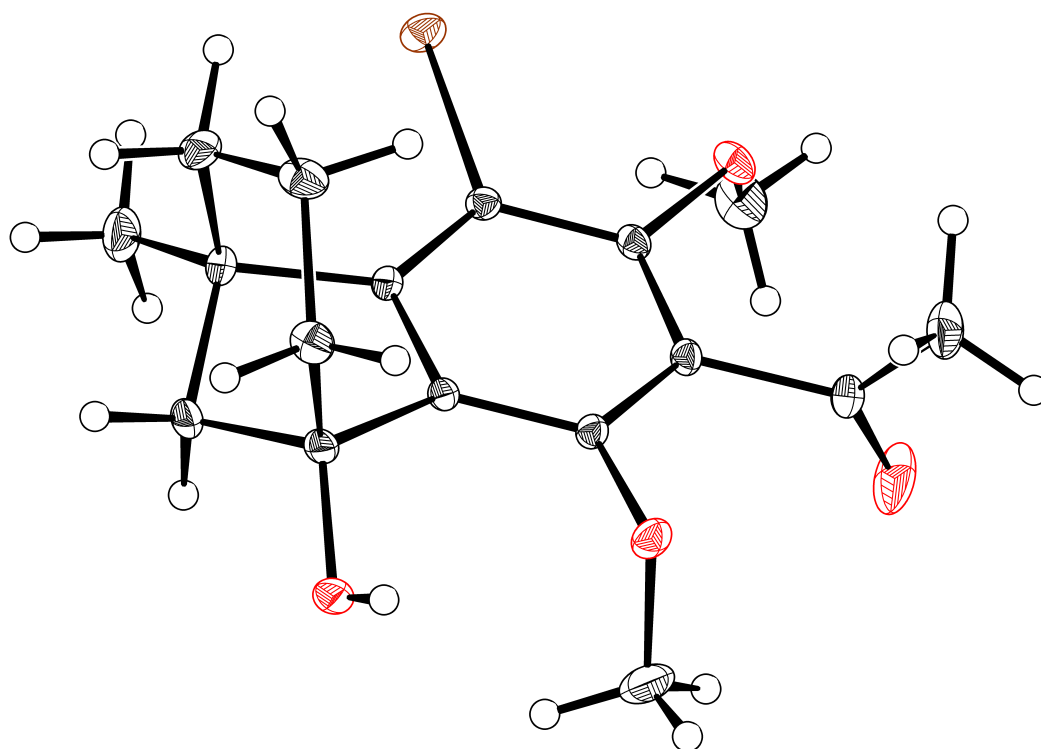
Table A7.1. Crystal data and structure refinement for a14105.

Identification code	a14105	
Empirical formula	C17 H23 Br O5	
Formula weight	387.26	
Temperature	100 K	
Wavelength	0.71073 Å	
Crystal system	Monoclinic	
Space group	C 1 2 1	
Unit cell dimensions	a = 18.8295(9) Å	a= 90°.
	b = 7.8451(4) Å	b= 95.208(2)°.
	c = 11.4443(5) Å	g = 90°.
Volume	1683.56(14) Å^3	
Z	4	
Density (calculated)	1.528 Mg/m^3	

Absorption coefficient	2.464 mm^{-1}
F(000)	800
Crystal size	0.43 x 0.42 x 0.29 mm^3
Theta range for data collection	1.787 to 48.826°.
Index ranges	-39<=h<=39, -16<=k<=16, -22<=l<=24
Reflections collected	78240
Independent reflections	16574 [R(int) = 0.0370]
Completeness to theta = 25.000°	99.8 %
Absorption correction	Analytical, multi-scan
Max. and min. transmission	0.5777 and 0.4462
Refinement method	Full-matrix least-squares on F^2
Data / restraints / parameters	16574 / 1 / 299
Goodness-of-fit on F^2	0.966
Final R indices [I>2sigma(I)]	R1 = 0.0256, wR2 = 0.0521
R indices (all data)	R1 = 0.0344, wR2 = 0.0538
Absolute structure parameter	0.0289(17)
Extinction coefficient	n/a
Largest diff. peak and hole	0.653 and -0.707 e.Å^{-3}

Table A7.2. Atomic coordinates (x 10^4) and equivalent isotropic displacement parameters ($\mathring{A}^2$x 10^3)for a14105. U(eq) is defined as one third of the trace of the orthogonalized U^{ij} tensor.

	x	y	z	U(eq)
Br(1)	2611(1)	10106(1)	9689(1)	15(1)
O(1)	3623(1)	7401(1)	8867(1)	14(1)
O(2)	3898(1)	5319(1)	6487(1)	32(1)
O(3)	2081(1)	4751(1)	5906(1)	15(1)
O(4)	746(1)	6695(1)	5256(1)	15(1)
C(1)	1792(1)	8548(1)	7722(1)	10(1)
C(2)	2444(1)	8611(1)	8398(1)	10(1)
C(3)	2985(1)	7448(1)	8188(1)	10(1)
C(4)	2858(1)	6206(1)	7328(1)	10(1)
C(5)	2190(1)	6066(1)	6697(1)	10(1)
C(6)	1663(1)	7235(1)	6896(1)	9(1)
C(7)	883(1)	7289(1)	6423(1)	11(1)
C(8)	433(1)	6312(1)	7261(1)	15(1)
C(9)	584(1)	6889(1)	8542(1)	17(1)
C(10)	655(1)	8831(1)	8680(1)	17(1)
C(11)	1110(1)	9610(1)	7757(1)	12(1)
C(12)	734(1)	9187(1)	6539(1)	13(1)
C(13)	4140(1)	8608(2)	8543(1)	21(1)
C(14)	3440(1)	4958(1)	7122(1)	14(1)
C(15)	3422(1)	3280(1)	7728(1)	21(1)
C(16)	2247(1)	5220(2)	4744(1)	23(1)
C(17)	1200(1)	11532(1)	7918(1)	21(1)
O(5)	4353(1)	8297(2)	5398(1)	43(1)

Table A7.3.   Bond lengths [Å] and angles [°] for a14105.

_____

Br(1)-C(2)	1.8906(8)
O(1)-C(3)	1.3713(9)
O(1)-C(13)	1.4310(12)
O(2)-C(14)	1.2111(12)
O(3)-C(5)	1.3751(10)
O(3)-C(16)	1.4412(14)
O(4)-H(4A)	0.70(4)
O(4)-C(7)	1.4158(11)
C(1)-C(2)	1.3921(11)
C(1)-C(6)	1.4044(11)
C(1)-C(11)	1.5333(11)
C(2)-C(3)	1.4041(11)
C(3)-C(4)	1.3893(12)
C(4)-C(5)	1.3969(11)
C(4)-C(14)	1.5033(12)
C(5)-C(6)	1.3859(11)
C(6)-C(7)	1.5183(10)
C(7)-C(8)	1.5397(13)
C(7)-C(12)	1.5231(12)
C(8)-H(8A)	0.98(2)
C(8)-H(8B)	0.949(19)
C(8)-C(9)	1.5366(14)
C(9)-H(9A)	1.035(18)
C(9)-H(9B)	1.01(2)
C(9)-C(10)	1.5357(16)
C(10)-H(10A)	0.98(2)
C(10)-H(10B)	0.906(18)
C(10)-C(11)	1.5458(13)
C(11)-C(12)	1.5417(13)
C(11)-C(17)	1.5262(13)
C(12)-H(12A)	0.993(18)
C(12)-H(12B)	0.961(15)
C(13)-H(13A)	0.92(2)
C(13)-H(13B)	0.98(2)

C(13)-H(13C)	0.932(18)
C(14)-C(15)	1.4899(15)
C(15)-H(15A)	0.97(3)
C(15)-H(15B)	0.95(2)
C(15)-H(15C)	1.00(2)
C(16)-H(16A)	1.02(2)
C(16)-H(16B)	0.97(2)
C(16)-H(16C)	0.84(3)
C(17)-H(17A)	0.96(2)
C(17)-H(17B)	0.93(2)
C(17)-H(17C)	1.19(2)
O(5)-H(5A)	0.83(4)
O(5)-H(5B)	0.93(8)
C(3)-O(1)-C(13)	114.67(7)
C(5)-O(3)-C(16)	112.54(9)
C(7)-O(4)-H(4A)	108(4)
C(2)-C(1)-C(6)	119.34(7)
C(2)-C(1)-C(11)	131.62(7)
C(6)-C(1)-C(11)	108.83(6)
C(1)-C(2)-Br(1)	122.18(6)
C(1)-C(2)-C(3)	119.90(7)
C(3)-C(2)-Br(1)	117.73(6)
O(1)-C(3)-C(2)	122.13(7)
O(1)-C(3)-C(4)	117.87(7)
C(4)-C(3)-C(2)	119.80(7)
C(3)-C(4)-C(5)	120.65(7)
C(3)-C(4)-C(14)	119.20(7)
C(5)-C(4)-C(14)	120.09(7)
O(3)-C(5)-C(4)	118.31(7)
O(3)-C(5)-C(6)	122.49(7)
C(6)-C(5)-C(4)	119.20(7)
C(1)-C(6)-C(7)	108.75(7)
C(5)-C(6)-C(1)	120.90(7)
C(5)-C(6)-C(7)	130.12(7)
O(4)-C(7)-C(6)	114.47(7)

O(4)-C(7)-C(8)	111.11(7)
O(4)-C(7)-C(12)	112.59(7)
C(6)-C(7)-C(8)	109.45(7)
C(6)-C(7)-C(12)	100.13(6)
C(12)-C(7)-C(8)	108.47(7)
C(7)-C(8)-H(8A)	110.3(9)
C(7)-C(8)-H(8B)	100.8(11)
H(8A)-C(8)-H(8B)	108.1(15)
C(9)-C(8)-C(7)	112.54(7)
C(9)-C(8)-H(8A)	111.3(9)
C(9)-C(8)-H(8B)	113.4(11)
C(8)-C(9)-H(9A)	112.7(10)
C(8)-C(9)-H(9B)	107.0(11)
H(9A)-C(9)-H(9B)	102.1(15)
C(10)-C(9)-C(8)	113.37(8)
C(10)-C(9)-H(9A)	107.8(11)
C(10)-C(9)-H(9B)	113.4(12)
C(9)-C(10)-H(10A)	108.4(13)
C(9)-C(10)-H(10B)	109.6(12)
C(9)-C(10)-C(11)	111.74(8)
H(10A)-C(10)-H(10B)	108.0(17)
C(11)-C(10)-H(10A)	110.9(12)
C(11)-C(10)-H(10B)	108.2(12)
C(1)-C(11)-C(10)	108.71(7)
C(1)-C(11)-C(12)	100.11(7)
C(12)-C(11)-C(10)	107.17(7)
C(17)-C(11)-C(1)	117.14(8)
C(17)-C(11)-C(10)	111.74(8)
C(17)-C(11)-C(12)	111.01(8)
C(7)-C(12)-C(11)	102.47(6)
C(7)-C(12)-H(12A)	110.7(10)
C(7)-C(12)-H(12B)	108.1(9)
C(11)-C(12)-H(12A)	111.6(10)
C(11)-C(12)-H(12B)	112.1(9)
H(12A)-C(12)-H(12B)	111.5(14)
O(1)-C(13)-H(13A)	108.7(14)

O(1)-C(13)-H(13B)	112.7(11)
O(1)-C(13)-H(13C)	109.0(12)
H(13A)-C(13)-H(13B)	105.4(18)
H(13A)-C(13)-H(13C)	106.8(17)
H(13B)-C(13)-H(13C)	113.8(16)
O(2)-C(14)-C(4)	120.71(9)
O(2)-C(14)-C(15)	122.24(9)
C(15)-C(14)-C(4)	117.05(8)
C(14)-C(15)-H(15A)	106.0(16)
C(14)-C(15)-H(15B)	108.4(13)
C(14)-C(15)-H(15C)	110.2(13)
H(15A)-C(15)-H(15B)	102(2)
H(15A)-C(15)-H(15C)	120(2)
H(15B)-C(15)-H(15C)	109.7(18)
O(3)-C(16)-H(16A)	112.2(11)
O(3)-C(16)-H(16B)	110.1(12)
O(3)-C(16)-H(16C)	102.7(17)
H(16A)-C(16)-H(16B)	111.1(18)
H(16A)-C(16)-H(16C)	110(2)
H(16B)-C(16)-H(16C)	110.8(19)
C(11)-C(17)-H(17A)	113.8(12)
C(11)-C(17)-H(17B)	105.1(16)
C(11)-C(17)-H(17C)	114.3(10)
H(17A)-C(17)-H(17B)	103.5(19)
H(17A)-C(17)-H(17C)	102.8(16)
H(17B)-C(17)-H(17C)	117.1(19)
H(5A)-O(5)-H(5B)	108(5)

_____

Symmetry transformations used to generate equivalent atoms:

Table A7.4.   Anisotropic displacement parameters ($Å^2$x 10^3) for a14105. The anisotropic displacement factor exponent takes the form: $-2\pi^2[h^2 a^{*2}U^{11} + ... + 2 h k a^* b^* U^{12}]$

	U^{11}	U^{22}	U^{33}	U^{23}	U^{13}	U^{12}
Br(1)	16(1)	16(1)	13(1)	-6(1)	0(1)	-2(1)
O(1)	9(1)	19(1)	15(1)	2(1)	-3(1)	-1(1)
O(2)	24(1)	30(1)	44(1)	12(1)	22(1)	12(1)
O(3)	15(1)	14(1)	14(1)	-5(1)	1(1)	1(1)
O(4)	12(1)	20(1)	11(1)	-3(1)	-2(1)	1(1)
C(1)	9(1)	10(1)	10(1)	0(1)	1(1)	1(1)
C(2)	10(1)	11(1)	9(1)	-1(1)	1(1)	-1(1)
C(3)	8(1)	12(1)	10(1)	1(1)	0(1)	0(1)
C(4)	8(1)	12(1)	12(1)	1(1)	1(1)	1(1)
C(5)	9(1)	11(1)	10(1)	-1(1)	1(1)	1(1)
C(6)	7(1)	12(1)	9(1)	0(1)	0(1)	1(1)
C(7)	8(1)	16(1)	10(1)	0(1)	0(1)	1(1)
C(8)	10(1)	20(1)	16(1)	2(1)	1(1)	-2(1)
C(9)	14(1)	25(1)	14(1)	4(1)	3(1)	-3(1)
C(10)	12(1)	25(1)	14(1)	-2(1)	4(1)	2(1)
C(11)	10(1)	13(1)	13(1)	0(1)	2(1)	4(1)
C(12)	10(1)	16(1)	13(1)	2(1)	0(1)	4(1)
C(13)	11(1)	26(1)	26(1)	1(1)	-1(1)	-6(1)
C(14)	10(1)	16(1)	16(1)	0(1)	2(1)	3(1)
C(15)	21(1)	15(1)	29(1)	4(1)	4(1)	6(1)
C(16)	22(1)	33(1)	15(1)	-8(1)	4(1)	1(1)
C(17)	22(1)	14(1)	26(1)	-3(1)	0(1)	6(1)
O(5)	34(1)	31(1)	66(1)	17(1)	12(1)	2(1)

Table A7.5.   *Hydrogen coordinates (x 10^4) and isotropic displacement parameters ($Å^2$x 10^3) for a14105.*

	x	y	z	U(eq)
H(4A)	730(20)	5810(50)	5270(40)	110(14)
H(8A)	504(8)	5090(30)	7183(13)	18(3)
H(8B)	-34(10)	6580(30)	6933(16)	24(4)
H(9A)	199(10)	6480(30)	9068(15)	23(4)
H(9B)	1018(11)	6250(30)	8880(17)	27(5)
H(10A)	863(11)	9080(30)	9475(18)	33(5)
H(10B)	216(9)	9320(20)	8589(16)	24(4)
H(12A)	213(9)	9400(20)	6506(16)	21(4)
H(12B)	947(8)	9770(20)	5920(13)	12(3)
H(13A)	4561(12)	8430(30)	9001(19)	37(5)
H(13B)	4005(10)	9790(30)	8697(17)	34(5)
H(13C)	4233(10)	8410(20)	7769(16)	23(4)
H(15A)	3716(14)	2520(40)	7310(20)	53(7)
H(15B)	2962(11)	2800(30)	7559(18)	34(5)
H(15C)	3523(11)	3430(30)	8598(19)	35(5)
H(16A)	2770(12)	5560(30)	4724(17)	36(6)
H(16B)	1930(11)	6120(30)	4436(18)	31(5)
H(16C)	2168(13)	4320(30)	4360(20)	43(6)
H(17A)	1378(10)	11860(30)	8703(18)	29(5)
H(17B)	737(13)	11970(30)	7840(20)	42(6)
H(17C)	1619(10)	12150(30)	7333(18)	32(5)
H(5A)	4075(17)	7470(50)	5340(30)	76(10)
H(5B)	4760(40)	8000(110)	5030(90)	114

Table A7.6. Torsion angles [°] for a14105.

_____

Br(1)-C(2)-C(3)-O(1)	-1.53(11)
Br(1)-C(2)-C(3)-C(4)	173.23(6)
O(1)-C(3)-C(4)-C(5)	172.81(7)
O(1)-C(3)-C(4)-C(14)	-4.40(12)
O(3)-C(5)-C(6)-C(1)	179.12(8)
O(3)-C(5)-C(6)-C(7)	5.42(14)
O(4)-C(7)-C(8)-C(9)	178.38(7)
O(4)-C(7)-C(12)-C(11)	-164.95(7)
C(1)-C(2)-C(3)-O(1)	-176.65(8)
C(1)-C(2)-C(3)-C(4)	-1.89(12)
C(1)-C(6)-C(7)-O(4)	150.32(7)
C(1)-C(6)-C(7)-C(8)	-84.20(8)
C(1)-C(6)-C(7)-C(12)	29.65(9)
C(1)-C(11)-C(12)-C(7)	40.37(8)
C(2)-C(1)-C(6)-C(5)	-3.86(12)
C(2)-C(1)-C(6)-C(7)	171.06(7)
C(2)-C(1)-C(11)-C(10)	-84.97(11)
C(2)-C(1)-C(11)-C(12)	162.89(9)
C(2)-C(1)-C(11)-C(17)	42.84(14)
C(2)-C(3)-C(4)-C(5)	-2.18(12)
C(2)-C(3)-C(4)-C(14)	-179.38(8)
C(3)-C(4)-C(5)-O(3)	-176.12(8)
C(3)-C(4)-C(5)-C(6)	3.18(12)
C(3)-C(4)-C(14)-O(2)	-84.34(12)
C(3)-C(4)-C(14)-C(15)	95.72(11)
C(4)-C(5)-C(6)-C(1)	-0.15(12)
C(4)-C(5)-C(6)-C(7)	-173.85(8)
C(5)-C(4)-C(14)-O(2)	98.44(12)
C(5)-C(4)-C(14)-C(15)	-81.50(11)
C(5)-C(6)-C(7)-O(4)	-35.38(12)
C(5)-C(6)-C(7)-C(8)	90.10(11)
C(5)-C(6)-C(7)-C(12)	-156.05(9)
C(6)-C(1)-C(2)-Br(1)	-170.04(6)
C(6)-C(1)-C(2)-C(3)	4.85(12)

C(6)-C(1)-C(11)-C(10)	89.61(8)
C(6)-C(1)-C(11)-C(12)	-22.54(9)
C(6)-C(1)-C(11)-C(17)	-142.58(9)
C(6)-C(7)-C(8)-C(9)	50.99(10)
C(6)-C(7)-C(12)-C(11)	-42.94(8)
C(7)-C(8)-C(9)-C(10)	42.10(11)
C(8)-C(7)-C(12)-C(11)	71.66(8)
C(8)-C(9)-C(10)-C(11)	-43.70(11)
C(9)-C(10)-C(11)-C(1)	-47.37(10)
C(9)-C(10)-C(11)-C(12)	60.01(9)
C(9)-C(10)-C(11)-C(17)	-178.18(8)
C(10)-C(11)-C(12)-C(7)	-72.96(8)
C(11)-C(1)-C(2)-Br(1)	4.07(13)
C(11)-C(1)-C(2)-C(3)	178.96(8)
C(11)-C(1)-C(6)-C(5)	-179.21(8)
C(11)-C(1)-C(6)-C(7)	-4.29(9)
C(12)-C(7)-C(8)-C(9)	-57.35(9)
C(13)-O(1)-C(3)-C(2)	-83.51(11)
C(13)-O(1)-C(3)-C(4)	101.63(10)
C(14)-C(4)-C(5)-O(3)	1.06(12)
C(14)-C(4)-C(5)-C(6)	-179.64(8)
C(16)-O(3)-C(5)-C(4)	-91.05(10)
C(16)-O(3)-C(5)-C(6)	89.68(10)
C(17)-C(11)-C(12)-C(7)	164.77(8)

_____

Symmetry transformations used to generate equivalent atoms:

Table A7.7. Hydrogen bonds for a14105 [Å and °].

D-H...A	d(D-H)	d(H...A)	d(D...A)	<(DHA)
O(4)-H(4A)...O(5)#1	0.70(4)	2.11(4)	2.7707(15)	158(5)
C(12)-H(12A)...O(2)#2	0.993(18)	2.577(18)	3.5655(12)	173.5(14)
C(13)-H(13B)...Br(1)	0.98(2)	2.963(19)	3.4746(12)	113.5(13)
C(16)-H(16B)...O(4)	0.97(2)	2.54(2)	3.1572(13)	121.7(15)
O(5)-H(5A)...O(2)	0.83(4)	2.18(4)	2.8176(15)	133(3)
O(5)-H(5B)...O(5)#3	0.93(8)	1.80(7)	2.678(3)	155(8)

Symmetry transformations used to generate equivalent atoms:

#1 -x+1/2,y-1/2,-z+1   #2 x-1/2,y+1/2,z   #3 -x+1,y,-z+1

APPENDIX 8

Progress Toward the Total Synthesis of Nanolobatolide

Abstract
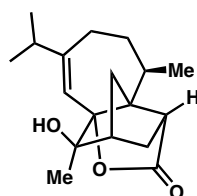
Nanolobatolide

Efforts toward the total synthesis of the bioactive terpenoid-derived product nanolobatolide are described. The investigation and application of various ring-expansion methodologies are detailed in the context of synthetic planning toward a key Diels–Alder reaction to generate the highly congested carbon scaffold of nanolobatolide. Synthetic efforts toward the key guaiane-derived intermediate revealed that substrates are prone to unselective deprotonation by strong bases and, therefore, traditional alkylation or cross-coupling strategies are not successful in promoting the desired reactions selectively. The application of a strategy based on a halogen-magnesium exchange reaction for the alkylation of bromo-enol phosphates is discussed as a potential method to circumvent undesired reactivity. Continued synthetic efforts and future plans aimed the completion of nanolobatolide are detailed.

A8.1 Background and synthetic approach

A8.1.1 Introduction and retrosynthetic analysis

Chronic diseases affecting quality of life have become a serious concern for modern society, as increased population longevity contributes to their increased frequency of occurrence. Therapies for maladies affecting cerebral function, such as Alzheimer's disease, present an unmet challenge in health science.[1] As such, the scientific community is interested in the study of neurodegeneration, and is particularly interested in the study of potential treatments for neurodegeneration. In particular, neuroprotective substances are a promising class of compounds. One such natural product, nanolobatolide (**A8-1**), has displayed promising neuroprotective properties in 6-hydroxy dopamine neurotoxicity studies.[2]

Nanolobatolide (**A8-1**) was isolated from the marine sponge *Sinularia nanolobata* in 2009 by Jyh-Horn Sheu and coworkers.[2] The compound possesses a unique 18 carbon molecular structure that is postulated to be terpenoid-related.[2] Its molecular architecture represents an interesting synthetic challenge due to its highly congested caged carbon core featuring a fused gamma lactone and norbornane-derived bicyclic system. Additionally, nanolobatolide contains six stereogenic centers, all of which are contiguous and one of which is an all-carbon quaternary center. Sheu and coworkers propose that the biosynthesis of nanolobatolide may hinge on the Diels–Alder reaction of guaiane-type precursor **A8-2** and a suitable acrylic acid derivative in an *endo* transition state geometry (Scheme A8.1). Subsequent oxidation and lactonization of Diels-Alder adduct **A8-3**

would provide nanolobatolide. Herein, we report progress toward the total synthesis of nanolobatolide.

Scheme A8.1 Proposed biosynthesis of nanolobatolide
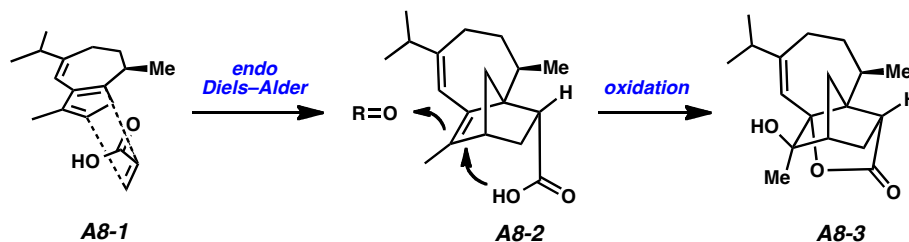
Synthetically, we sought to utilize a biomimetic approach for the preparation of **A8-1**, targeting guaiane **A8-2** for synthesis with the goal of subsequently utilizing the cyclopentadiene moiety as a diene for Diels–Alder reaction (Scheme A8.2). The cyclopentadiene motif found in guaiane **A8-2** is believed to be configurationally stable, based on synthetic efforts reported for similar guaiane-derived dienes.[3] We further envisioned synthesis of guaiane **A8-2** from cycloheptenone **A8-3**, itself ultimately derived from (–)-menthone (**A8-4**) via oxidative ring expansion.[4] Overall, this route would achieve the natural product synthesis rapidly, while providing opportunity to synthesize analogs for structure-activity relationship studies due to the short, highly flexible route.

Scheme A8.2 Retrosynthetic analysis of nanolobatolide
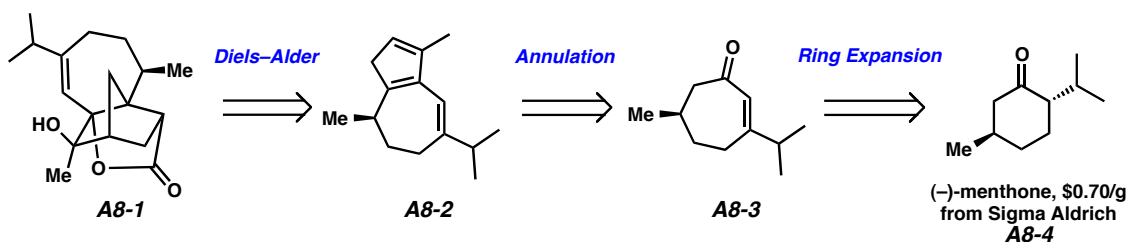
A8.2 Synthetic progress

A8.2.1 Synthesis of key enone intermediate

Initial investigations focused on the synthesis of enone **A8-3** via a reported 2-step ring expansion/oxidation protocol utilizing trimethylaluminum and trimethylsilyldiazomethane to generate a mixture of silyl enol ethers, followed by Saegusa-Ito oxidation to yield the desired enone (Scheme 5).[5] Though the product was obtained as described in the literature, yields were disappointingly low and the procedure proved difficult to scale efficiently. For example, performing this sequence 2 gram-scale (13.0 mmol) with (–)-menthone (**A8-4**) yielded only 4% of the desired enone product and 11% yield of the undesired isomer (**A8-7**). Additionally, the completely unselective nature of the initial ring expansion step yielded a 1:1 mixture of desired:undesired silyl enol ether isomers **A8-5** and **A8-6**. This represents a tremendous waste of material and further condemns this reaction as an unattractive first step in our synthetic sequence. After attempts to optimize the procedure proved futile, alternative preparative methods for enone **A8-3** were sought.

Scheme A8.3 Initial investigation into ring expansion methodology
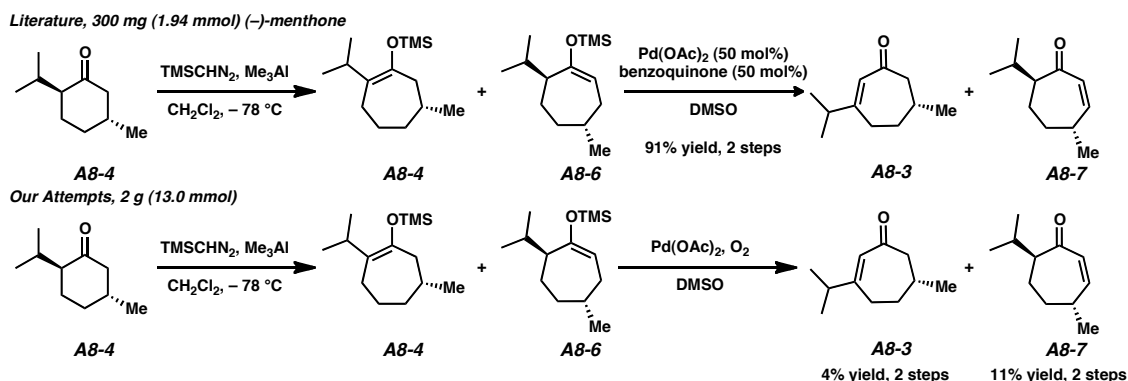
After searching the literature, a suitable surrogate route to enone **A8-3** was realized.[4] Beginning with ring expansion of (–)-menthone (**A8-4**) (Scheme 6), thermodynamic enolization and trapping with TMSCl yielded the silyl enol ether (**A8-8**). Initially, standard conditions in acetonitrile led to low conversion, however use of a pentane/acetonitrile biphase was found to drive the reaction toward completion. The resulting silyl enol ether (**A8-8**) was cyclopropanated under Simmons–Smith conditions to afford cyclopropane **A8-9**. The key step of this sequence is the iron(III) chloride-mediated reductive ring opening, which provides the desired enone (**A8-3**) after reflux in sodium acetate saturated methanol. We believe that this ring-opening step is the low-yielding step in our sequence, as formation of unusable cycloheptanone **A8-3a** is the major byproduct. Although the procedure was four steps, as opposed to only two, it proved reliable and scalable and could easily be performed on 20-gram scale (140 mmol), thus providing an ideal starting sequence for a total synthesis. Additionally, the use of (–)-menthone (**A8-4**) as a starting material provides a cheap ($ 0.70/gram from Sigma–Aldrich) and readily available source of enantioenriched material that allowed our

synthetic efforts to avoid tedious installation of the remote stereogenic methyl group found in the natural product.

Scheme A8.4 Synthesis of key enone intermediate
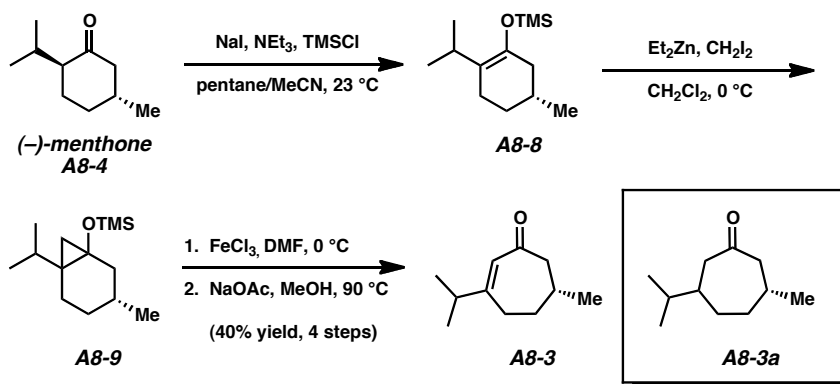
A8.2.2 Progress toward hypothesized biomimetic guaiane intermediate

Many approaches toward key guaiane **A8-2** have been examined with varying degrees of success. Initially, we tried to install the final three carbons of guaiane **A8-2** by the addition of isopropenyllithium to allyl enone **A8-10**. Treatment of enone **A8-3** with LDA and allyl iodide in DMPU/THF resulted in successful allylation to yield enone **A8-10** in 55% yield (Scheme 7). It should be noted that this alkylation was particularly difficult, and that reaction of the lithium enolate of enone **A8-3** with allyl bromide was sluggish, even at room temperature. Attempts to repeat this alkylation procedure without the use of freshly purified allyl iodide suffer from greatly diminished yields. The isopropenyl group was then added via treatment with isopropenyllithium. Though the reaction proceeded smoothly, resulting tertiary alcohol **A8-11** proved difficult to manipulate. Ring-closing metathesis of diene **A8-11** with the Grubbs-Hoveyda 3rd generation catalyst (**A8-12**) did not proceed to completion; we postulate that only the *syn*

diastereomers close. Furthermore, dehydration of alcohols **A8-13** proved difficult. Treatment of alcohols **A8-13** with trifluoroacetic acid yielded a complex mixture, while attempts at mesylation and base-mediated elimination also were unsuccessful.
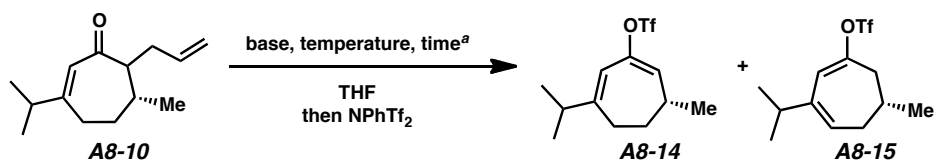
Scheme A8.5 Initial investigation into guaiane annulation strategy
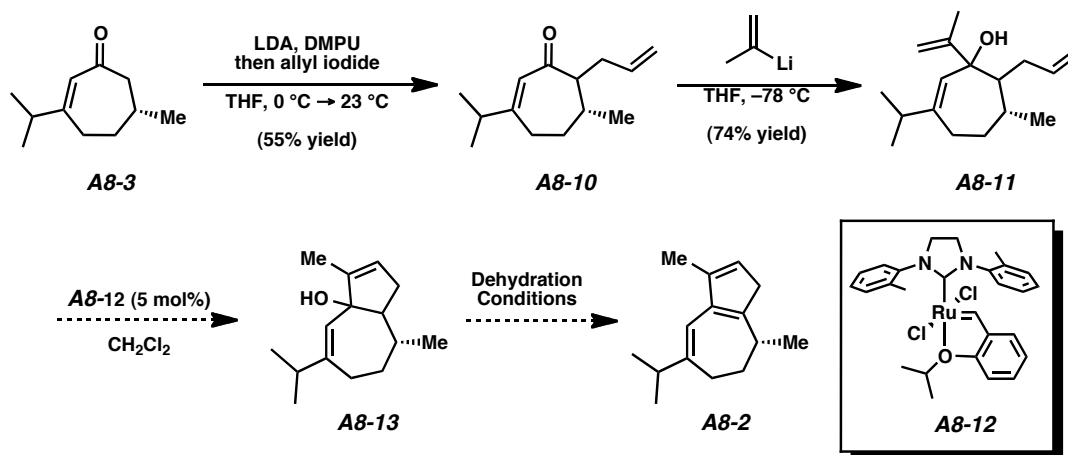
In revising our approach, we proposed that avoiding formation of alcohol **A8-13** would alleviate our problems. We chose to pursue a cross-coupling strategy from vinyl triflate **A8-14** that would allow for installation of the isopropenyl unit without formation of the unnecessary tertiary alcohol. Unfortunately, our initial attempt at enolization of enone **A8-10** and trapping with *N*-phenyltriflimide resulted in an inseparable mixture of dienyl triflate isomers **A8-14** and **A8-15** (Table A8.1, entry 1). A subsequent base screen on cycloheptenone **A8-10** demonstrated that base-driven elaboration of α-substituted cyclohexenones such as allylated enone **A8-10** results in the same inseparable mixtures of α and γ^1 deprotonated dienes **A8-14** and **A8-** 15 (entries 1–3) or no product isolated (entries 4-6). Attempts at thermodynamic enolizations of allyl enone **A8-10** resulted in a similar mixture of diene triflates (entries 7-8), with no quantifiable improvement in the

ratio of desired to undesired triflates realized. This result led us to believe enolization under either thermodynamic or kinetic control would not successfully furnish our desired product as a single isomer.

Table A8.1 *Base screen for selective enolization of enone* **A8-10**

entry	base	temperature (° C)	time (h)	result[b]
1	KHMDS	−78	0.5	isomer mix (1:1)
2	LHMDS	−78	0.5	isomer mix (1:1)
3	LDA	−78	0.5	isomer mix (1:1)
4	KO*t*-Bu	−78	0.5	no product
5	KH	0	0.5	no product
6	KH	50	4	no product
7	KHMDS[c]	0	2	isomer mix (1:1)
8	KHMDS[c]	23	2	isomer mix (1:1)

[a] Reaction conditions: base (1.2 equiv), THF (0.5 M), NPhTf$_2$ (1.2 equiv). [b] As determined by crude ^{1}H NMR. [c] 0.90 equiv base used.

With this disappointing finding at hand, we sought to find alternative means of generating a suitable cross coupling partner. Some investigations into Shapiro-type reactions were conducted, with hopes of generating vinyl iodide **A8-17** from hydrazones **A8-16**,[6] but predictably the base-mediated nature of these reactions proved ill-suited toward our system and no synthetically useful results were obtained (Scheme A8.6a). In fact, no successful iodination ever occurred from hydrazones **A8-16**, and only trace olefination was observed. Similarly, attempts to generate vinyl iodide **A8-17** *via* direct

treatment of allyl enone **A8-10** with hydrazine hydrate and iodine generated an

inseparable mixture of vinyl iodides **A8-17** and **A8-18** (Scheme A8.6b).[7]

Scheme A8.6 Attempts at selective iodination
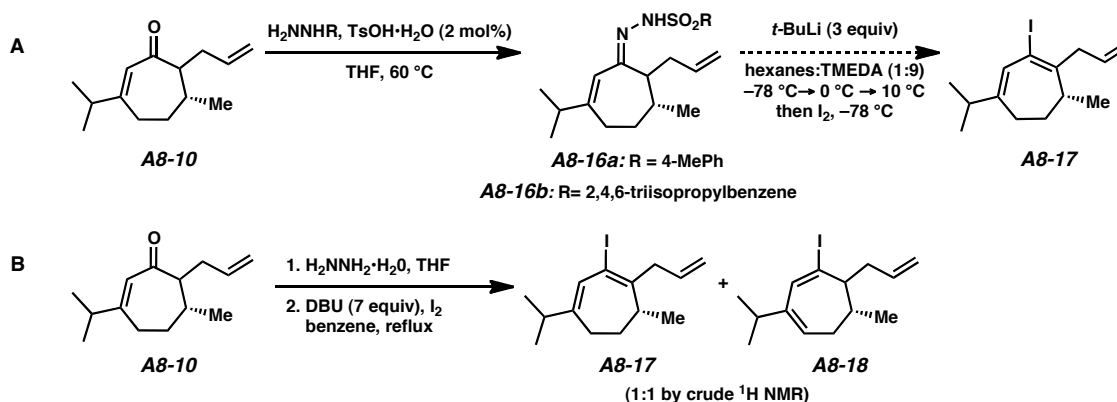
At this time, we became aware of work from the Barluenga group that utilized

hydrazones as direct substrates for cross-coupling reactions with aryl halides.[8] They

reported that treatment of *N*-tosylhydrazones with base, a palladium(0) source and Xphos

ligand **60** resulted in smooth cross coupling with a variety of aryl halides (Scheme 9).

With hydrazones **57** in hand, we envisioned extending their methodology toward the

installation of the isopropenyl unit of our system.

Scheme A8.7 Barluenga's cross-coupling of N-tosylhydrazones and aryl halides
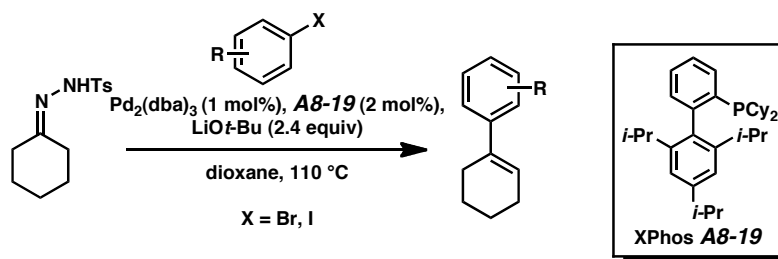
We attempted to utilize Barluenga's cross-coupling on our system. Using hydrazones **A8-16a** we found that, unfortunately, while the desired cross-coupling product was isolated (**A8-20**), a large quantity of diene **A8-21** was present as the major byproduct (Scheme A8.8). In fact, when isopropenyl bromide was used as the cross-coupling partner, only diene **A8-21** was obtained. Though discouraged, it was possible that the volatility of the bromide was the root of the reaction's failure.

Scheme A8.8 Attempted Barluenga couplings
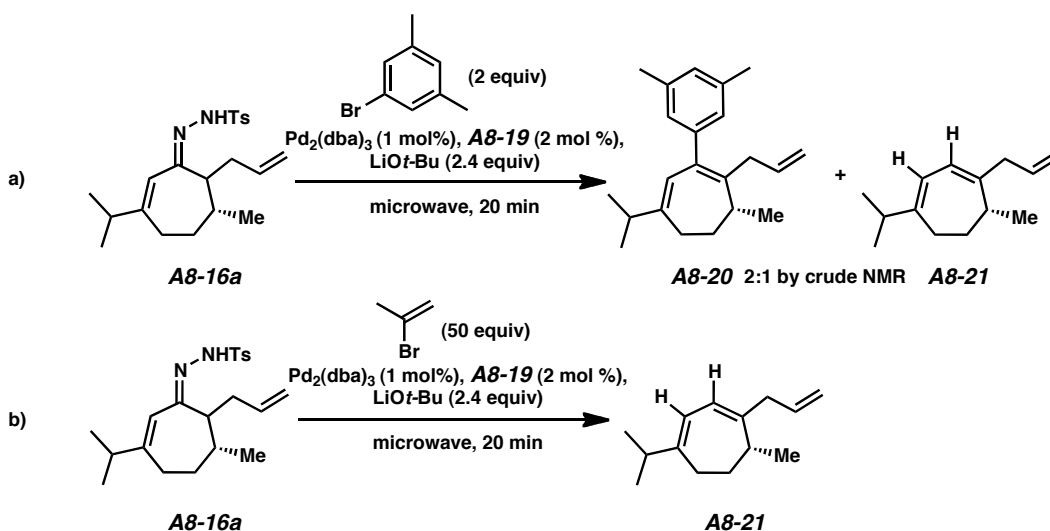
To probe the effect of substrate volatility, we proceeded to synthesize the less volatile, and potentially more active, alkene cross coupling partner **A8-24** (Scheme A8.9). Hydroboration of 1-phenylpropyne (**A8-22**) afforded boronic acid **A8-23**, which was treated with *N*-iodosuccinimide to readily afford b-iodostyrene **A8-24**.[9] To our dismay, cross coupling attempts with this alkenyl bromide were also unsuccessful, again yielding only diene **A8-21**.

*Scheme A8.9 Synthesis of iodide **A8-24** and application to synthesis*
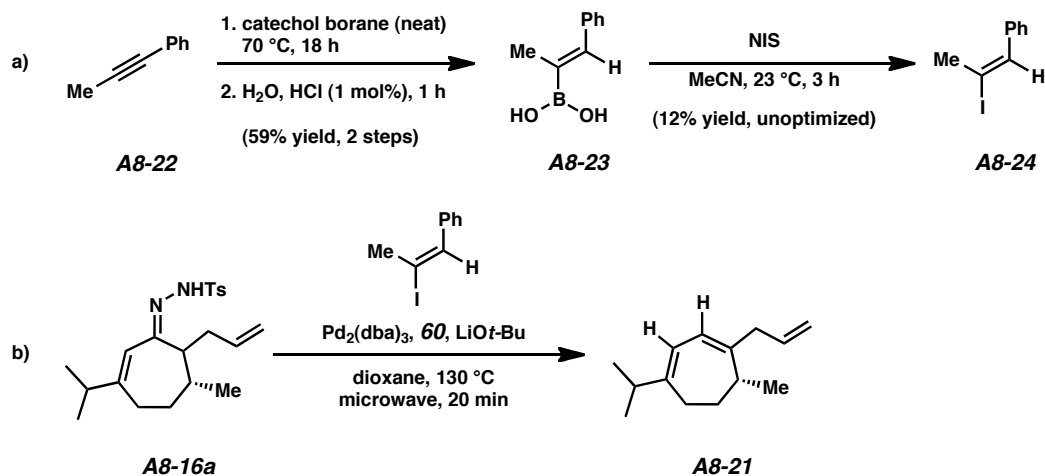
In light of these results, a route toward guaiane **A8-2** that provided an acidity bias to allow selective deprotonation was conceived (Scheme A8.10). Enone **A8-3** can be brominated (**A8-22**) and subsequently selectively enolized. This enolate can be trapped to yield enol phosphate **A8-23** as a single isomer.

*Scheme A8.10 Formation of bromo enol phosphate **A8-23***
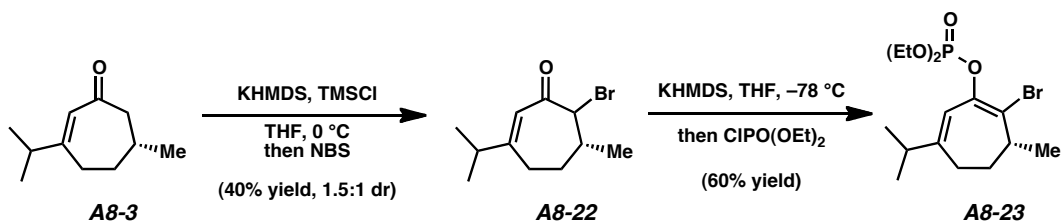
A8.2.3 Future Plans Toward the Completion of the Total Synthesis of Nanolobatolide

From this point on, we envision that organomagnesium reagent-mediated exchange would facilitate allylation to yield allylated enol phosphate **A8-24**,[10] thus circumventing the problems observed with the initial route. Allyl enol phosphate **A8-24** is itself an excellent substrate for Kumada cross-coupling (Scheme 13). Previous work from our group utilizes the inexpensive reagent iron(III) acetylacetonate for cross-coupling enol phosphates,[11] and we envision applying this reaction to enol phosphate **A8-24** with isopropenylmagnesium chloride will yield tetraene **A8-25**. Next, ring closing metathesis with the Grubbs–Hoveyda third generation catalyst (**A8-12**) will provide guaiane **A8-2**.

Scheme A8.11 Completion of guaiane intermediate
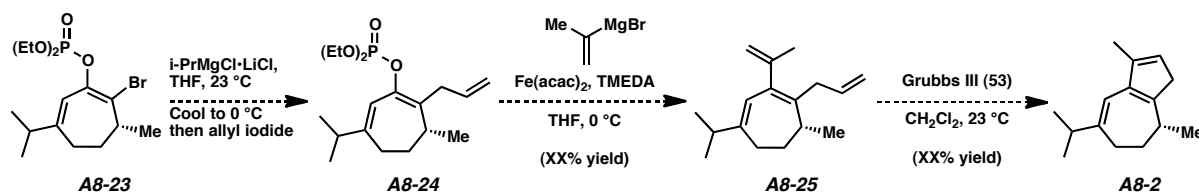
Completion of the synthesis will follow the previously described biosynthetic route. We believe that the stereogenic C(13) methyl group will provide adequate facial selectivity, with the acrylate approaching from the less sterically encumbered face (Scheme A8.12). To obtain the correct isomer, an endo-transition state is desired, which is well-known to be the favored transition state of intermolecular Diels–Alder reactions. In the unfortunate case that no facial selectivity is observed, we envision a number of

catalysts can be used to override or enhance substrate bias if necessary. For example, chiral lewis acids such as oxazaborolidine **A8-26** (CBS catalyst) are known to be excellent catalysts for Diels–Alder reactions and will provide a means of controlling facial bias.[12] Diels–Alder adduct **A8-3** will undergo epoxidation to yield epoxide **A8-27**, and ring-opening/lactonization will provide synthetic **A8-1** in only 11 total steps from commercial (–)-menthone (**A8-4**).

Scheme A8.12 Plan for completion of the synthesis
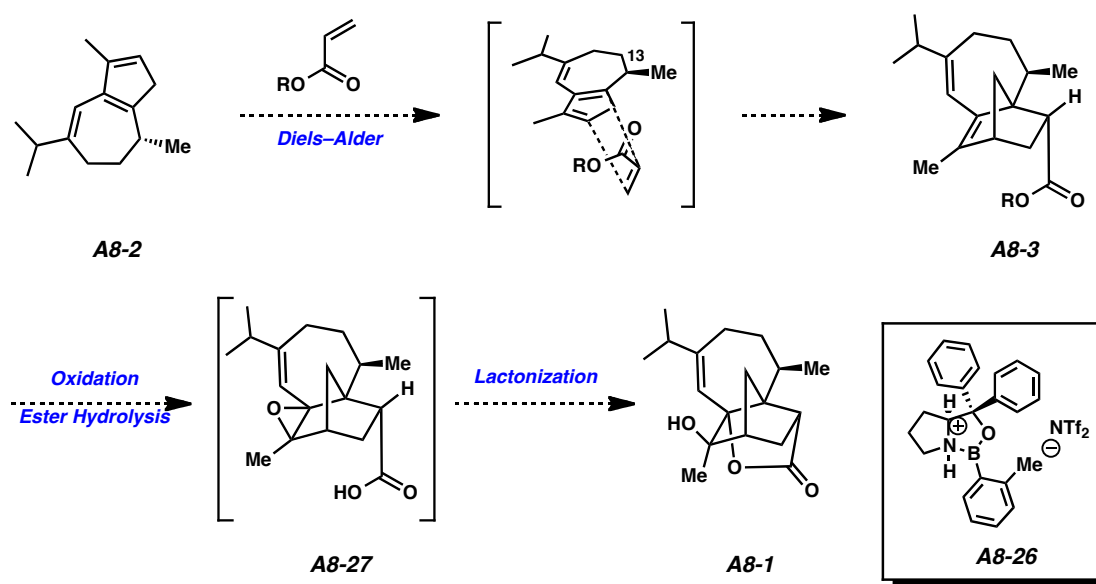
A8.3 Chen synthesis of ent-nanolobatolide

Efforts toward the total synthesis of nanolobatolide were abandoned following the publication of a nearly identical route from Chen and coworkers.[13] Their route features many of the transformations we proposed for the synthesis of nanolobatolide, including the synthesis of enone **A8-3**, as we have described herein. They transiently synthesize

guaiane **A8-2** *in situ* and complete the synthesis by the Diels-Alder/oxidation cascade as we had planned.

A8.4 Notes and citations

(1)   (a) Meek, P. D.; McKeithan, K.; Schumock, G. T. *Pharmacotherapy* **1998**, *18*, 68. (b) Brookmeyer, R.; Johnson, E.; Ziegler-Graham, K.; Arrighi, H. M. *Alzheimer's and Dementia* **2007**, *3*, 186.

(2)   Tseng, Y.-J.; Wen, Z.-H.; Dai, C.-F.; Chiang, M. Y.; Sheu, J.-H. *Org. Lett.* **2009**, *11*, 5030.

(3)   Brocksom, T. J.; Brocksom, U.; Fredericoa, D. *Tetrahedron Lett.* **2004**, *45*, 9289.

(4)   Ito, Y.; Fujii, S.; Nakatuska, M.; Kawamoto, F.; Saegusa, T. *Org. Synth.* **1979**, *59*, 113.

(5)   Yang, S.; Hungerhoff, B.; Metz, P. *Tetrahedron Lett.* **1998**, *39*, 2097.

(6)   (a) Chamberlain, A. R.; Liotta, E. L.; Bond, T. F. *Org. Synth.* **1983**, *61*, 141. (b) Chamberlain, A. R.; Bond, T. F. *J. Org. Chem.* **1978**, *43*, 154.

(7)   Brossard, D.; Kihel, L. E.; Khalid, M.; Rault, S. *Synlett* **2010**, *2*, 0215.

(8)   (a) Barluenga, J.; Moriel, P.; Valdes, C.; Aznar, F. *Angew. Chem., Int. Ed.* **2007**, *46*, 5587. (b) Barluenga, J.; Tomas-Gamasa, M.; Moriel, P.; Aznar, F.; Valdes, C. *Chem.–Eur. J.* **2008**, *14*, 4792. (c) Barluenga, J.; Escribano, M.; Aznar, F.; Valdes, C. *Angew. Chem., Int. Ed.* **2010**, *49*, 6856.

(9)   (a) Brown, H. C.; Gupta, S. K. *J. Am. Chem. Soc.* **1972**, *94*, 4370. (b) Petasis, N. A.; Zavialov, I. A. *Tetrahedron Lett.* **1996**, *37*, 567.

(10)   Piller, F. M.; Bresser, T.; Fischer, M. K. R.; Knochel, P. *J. Org. Chem.* **2010**, *75*, 4365–4375.
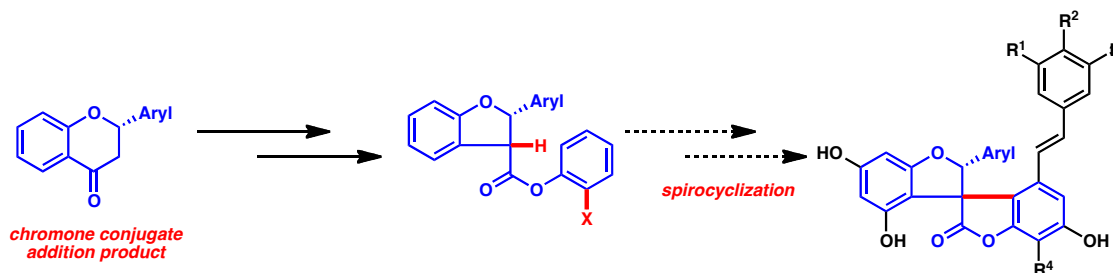
(11)   Stoltz group, Andrew McClory postdoctoral report.

(12)   Corey, E. J.; Shibata, T.; Lee, T. W. *J. Am. Chem. Soc.* **2002**, *124*, 3808.

(13)   Cheng, H. M.; Tian, W.; Peixoto, P. A.; Dhudshia, B.; Chen, D. Y.-K. *Angew. Chem. Int. Ed.* **2011**, *50*, 4165–4168.

APPENDIX 9

Progress toward the total synthesis of yuccaol natural products[✠]

Abstract

Progress toward the natural products yuccaol A–E is presented. The synthetic route utilizes chiral flavanone products that can be produced in high enantioselectivity *via* asymmetric conjugate addition of arylboronic acids to chromone electrophiles. Several strategies for the spirocyclization of the yuccaol core are discussed, and an amended proposal for a new synthetic approach is disclosed. Finally, synthetic methods for the construction of the highly oxygenated chromone scaffold and stilbene moiety are presented.

A9.1 Background and Introduction

The molecules that comprise the Yuccaol class of natural products are extracted from the plant *Yucca Schidigera*, found in the Mojave Desert in areas of California, south Nevada, and western Arizona. These natural products have been found to have antioxidant, radical scavenging, and platelet inhibitory effects as well as anti-inflammatory activity.[1] To date, no syntheses of any of these five natural products Yuccaols A-E have been reported (Figure A9.1). We undertook a model study targeting the core (outlined in blue), to see if we could quickly synthesize the scaffold.

The synthesis of these compounds would also facilitate accurate total structural assignment. The members of this class are diastereomeric pairs that differ in stereochemistry about the spirocyclic ring junction. It is unknown which absolute stereochemistry corresponds to A or B (**A9-1**), and likewise which of the A/B diastereomers is the direct stereochemical analog of the C/D pairing (**A9-2**). The E member of this family has no isolated diastereomeric relative, though it stands to reason that this highly oxygenated natural product also has a diastereomeric partner differing at the absolute stereochemistry of the spirocyclic ring fusion.

Figure A9.1 Yuccaol natural product family

Yuccaol A/B (A9-1) R1=R2=R3=R4=H, Aryl = *p*-phenol
Yuccaol C/D (A9-2) R1=R3= OH, R2= OMe. R4= H. Aryl = *p*-phenol
Yuccaol E (A9-3) R1=R2=R3= OH, R4= OMe, Aryl = *p*-phenol
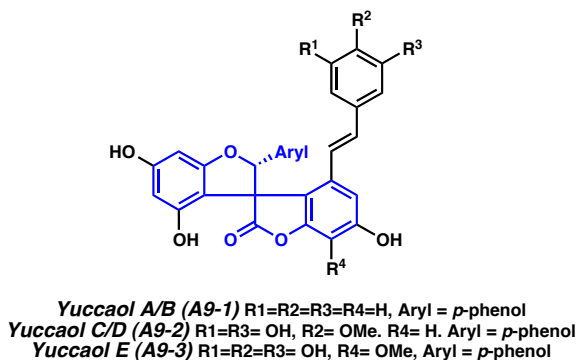
A9.2 Retrosynthetic analysis

We were drawn to target the yuccaol core (**A9-4**) because we believed we could rapidly access the structure from a skeletal rearrangement of flavanone **A9-7**, the product of an asymmetric conjugate addition of an appropriate arylboronic acid to chromone (**A9-8**). We envisioned late-stage spirocyclization, from aryl ether **A9-5**, and likewise imagined that a variety of ethers could be employed by saponification and esterification of methyl ester **A9-6**. Ring contraction compound **A9-6** was the product of a relatively well-precedented ring contraction of flavanones, and seemed an ideal mechanism by which to access the 6-5 ring framework of the yuccaols. It should be noted that an early alternative retrosynthetic analysis involved direct α-arylation of flavanone **A9-7**, however this route was plagued by consistent competitive retro-oxa-Michael reaction of the enolate of **A9-7** and, combined with the uncertainty involved in the ring contraction step of this α-arylated ketone, this route was abandoned.

Scheme A9.1 Retrosynthetic analysis of yuccaol natural products
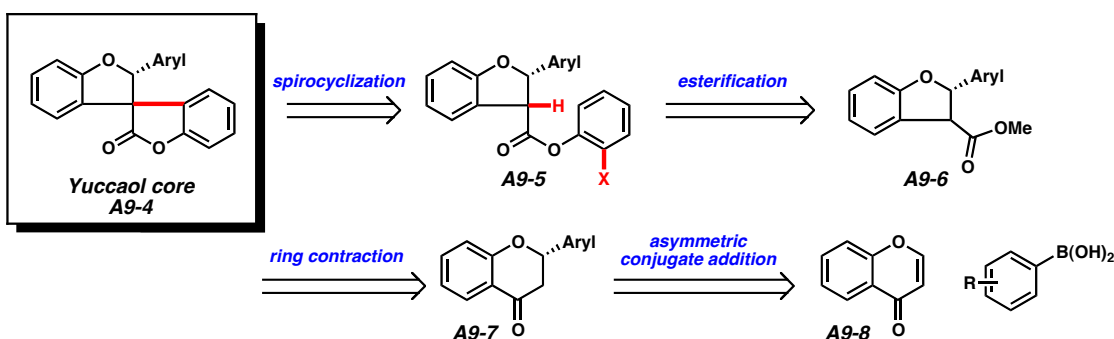
We envisioned two major routes to the spirocyclic core (**A9-4**, Scheme A9.2). First, we imagined an electron-rich aromatic ring might be able to cyclize onto an iodonium ion or similar transient electrophile formed on ring contraction product **A9-9**. Second, we considered intramolecular arylation of ester **A9-10** with its pendant *ortho*-halo aryl ether. Aryl halide **A9-10** would also serve as a suitable precursor for a radical cyclization were either of these routes to fail.

Scheme A9.2 Spirocyclization strategies
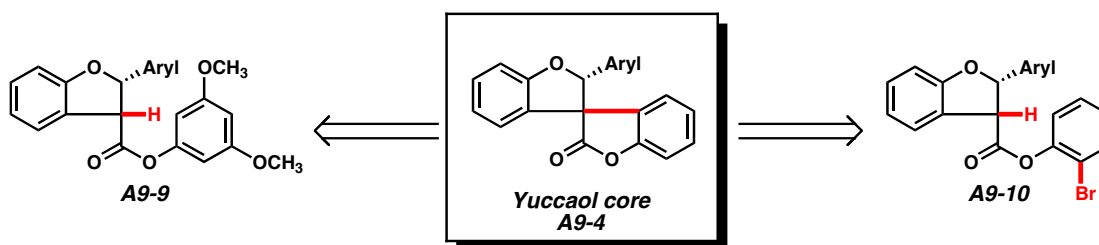
A9.3 Ring Contraction Approach

We first undertook optimization of the ring contraction from flavanone **A9-7** to methyl ester **A9-6** (Table A9.1). Ample literature precedent suggested the use of iodobenzene oxidants, however our trials with iodobenzene bis(trifluoroacetate) (entry 1) afforded poor conversion.[2] Likewise, iodobenzenediacetate afforded modest yield of the desired ring contraction product (entry 2). We found that iodosobenzene, however, was an optimal reagent for the transformation. Unfortunately, the reaction appeared to be sensitive to scale of operation, although extensive exploration of concentrations and reagent stoichiometry was not undertaken.

Table A9.1 Ring contraction optimization
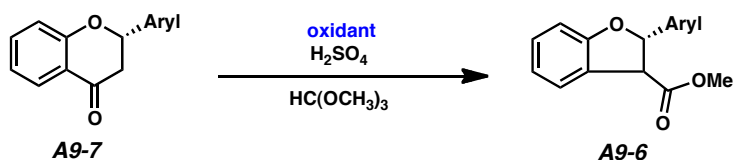
Trial	Reagent(s)	Yield
Lit	TTN·3H$_2$O, Trimethyl Orthoformate (TMOF), HClO$_4$	76%[9], 75%[6]
Lit	PhI(OAc)$_2$, TMOF, conc H$_2$SO$_4$	66%[9], 40%[7]
Lit	Pb(OAc)$_4$, TMOF, conc H$_2$SO$_4$	33%[9], 80%[8]
1	PhI(O$_2$CCF$_3$)$_2$, TMOF, HCOOH, H$_2$SO$_4$ (2eq)	6%
2	PhI(OAc)$_2$, TMOF, H$_2$SO$_4$ (2eq)	32% (1mmol)
3	*Iodosobenzene, TMOF, H$_2$SO$_4$ (2eq)*	*71% (.5mmol)*
		47% (1mmol)
		32% (4mmol)

We next set out to prepare the aryl ether cyclization substrates. Facile hydrolysis of methyl ester **A9-6** in 95% yield afforded carboxylic acid **A9-11**, which was isolated in high purity by simple acid/base extraction. EDC-mediated coupling with a variety of phenols afforded aryl ethers **A9-12–A9-14**, in modest to good yields.

Scheme A9.3 Synthesis of aryl ether intermediates
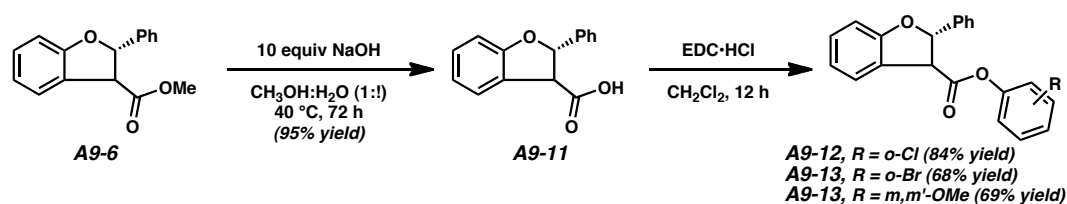
A9.4 Oxidative cyclization routes

Attempts to cyclize aryl ether **A9-14** by treatment with base and iodine resulted in no productive reaction. We had envisioned formation of iodonium ion **A9-16** and intramolecular cyclization to afford spirocycle **A9-15** via putative intermediate **A9-17** (Scheme A9.4). Unfortunately, the only observed product was benzofuran **A9-19**, leading us to hypothesize that iodinated intermediate **A9-18** was the intermediate adduct formed, and that the tertiary iodide was insufficiently reactive in the desired S_n2 process. Similar trials

Scheme A9.4 Attempts at oxidative cyclizations to form the yuccaol core
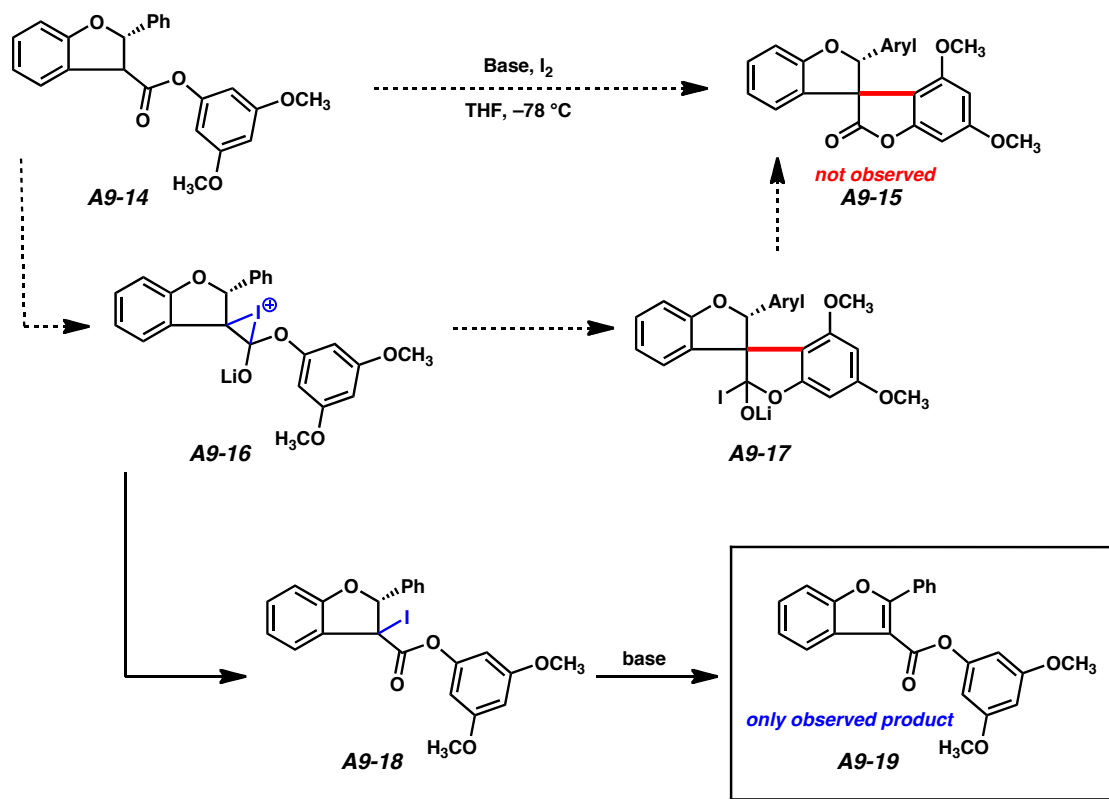
Perhaps taking advantage of hypothetical iodine **A9-18**, we could invoke a Kornblum-type process mediated by Ag+ to abstract the halide and promote intramolecular cyclization to **A9-15** (Scheme A9.5a). Alternatively, the undesired benzofuran **A9-19** could be used for an oxidative cyclization, however, this route destroys the stereochemistry set by the key conjugate addition reaction, and is therefore not optimal (Scheme A9.5b).

Scheme A9.5 Hypothetical routes to key intermediate
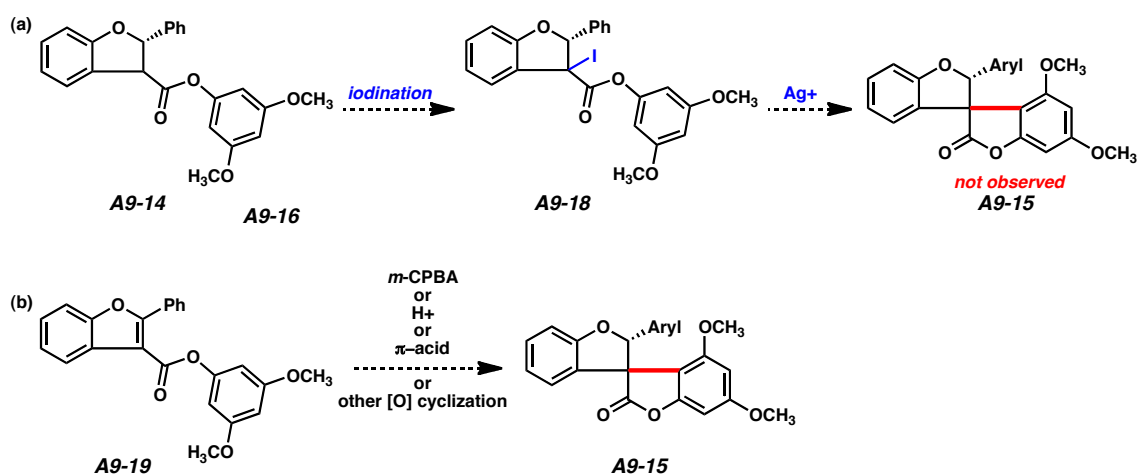
A9.5 Arylation route attempts

A screen of arylation conditions demonstrates difficulty in successfully cyclizing **A9-13** to the yuccaol core (**A9-15**, Table A9.2).[3] Mass hits failed to provide isolable material, and the formation of isomeric benzofuran **A9-22** is a likely undesired byproduct. This benzofuran hypothetically results from Pd-catalyzed reduction of the arylbromide and oxidative aromatization to afford the isomer **A9-22**. At this point in time, we considered an alternative approach may be required, as the harsh conditions of arylation and oxidation both readily furnished undesired side reactions.

Table A9.2 Screen of arylation conditions
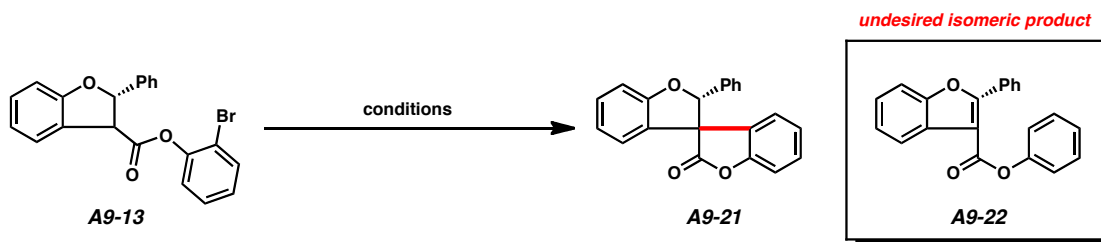
Trial	Reagent(s)	Scale	Result
1	Pd(OAc)$_2$, JohnPhos, KHMDS	10 mg	Mass Hit
2	Pd(OAc)$_2$, JohnPhos, KHMDS	10 mg	Mass Hit
3	Pd(NHC)(Acac)Cl, KHMDS	20 mg	No productive reaction
4	Pd(NHC)(Biphenyl)Cl, KHMDS	20 mg	No productive reaction
5	Pd$_2$dba$_3$, P(tBu)$_3$, KHMDS	20 mg	No productive reaction
6	Pd$_2$dba$_3$, JohnPhos, KHMDS	20 mg	No productive reaction
7	Pd$_2$dba$_3$, SPhos, KHMDS	20 mg	No productive reaction
8	Pd(OAc)$_2$, P(tBu)$_3$, KHMDS	20 mg	No productive reaction
9	Pd(OAc)$_2$, JohnPhos, KHMDS	20 mg	No productive reaction
10	Pd(OAc)$_2$, SPhos, KHMDS	20 mg	No productive reaction

A9.6 Toward a radical cyclization approach

We envisioned a 5-*endo*-trig radical cyclization from silyl enol ether **A9-20** to afford desired spiro-benzofuran **A9-21** (Scheme A9.6). Admittedly, the base-sensitive and oxidation-prone nature of **A9-20** provides many alternative pathways for undesired reactivity, however we believe that a radical approach may be our best chance at observing clean formation of the yuccaol core from ring contraction product **A9-13**.

Scheme A9.6 Radical cyclization approach
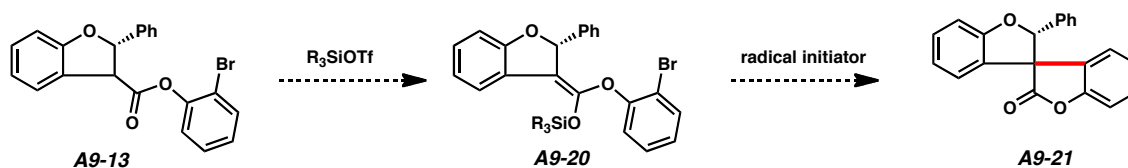
## A9.7 Synthesis of fully-oxygenated framework of yuccaol A/B

The high degree of oxidation found in the yuccaols requires early installation of a large number of hydroxy groups. We envision a fully oxygenated intermediate (**A9-23**) being broken into two halves, the flavanone **A9-24** and the stilbene **A9-25** (Scheme A9.7). Flavanone **A9-24** can be synthesized by asymmetric conjugate addition of arylboronic acid **A9-27** to chromone **A9-26**. Stilbene **A9-25** can be synthesized by Heck reaction, and those intermediates will be derived from aldehyde **A9-29** and iodobenzene **A9-30**.

Scheme A9.7 Retrosynthesis of yuccaol A/B
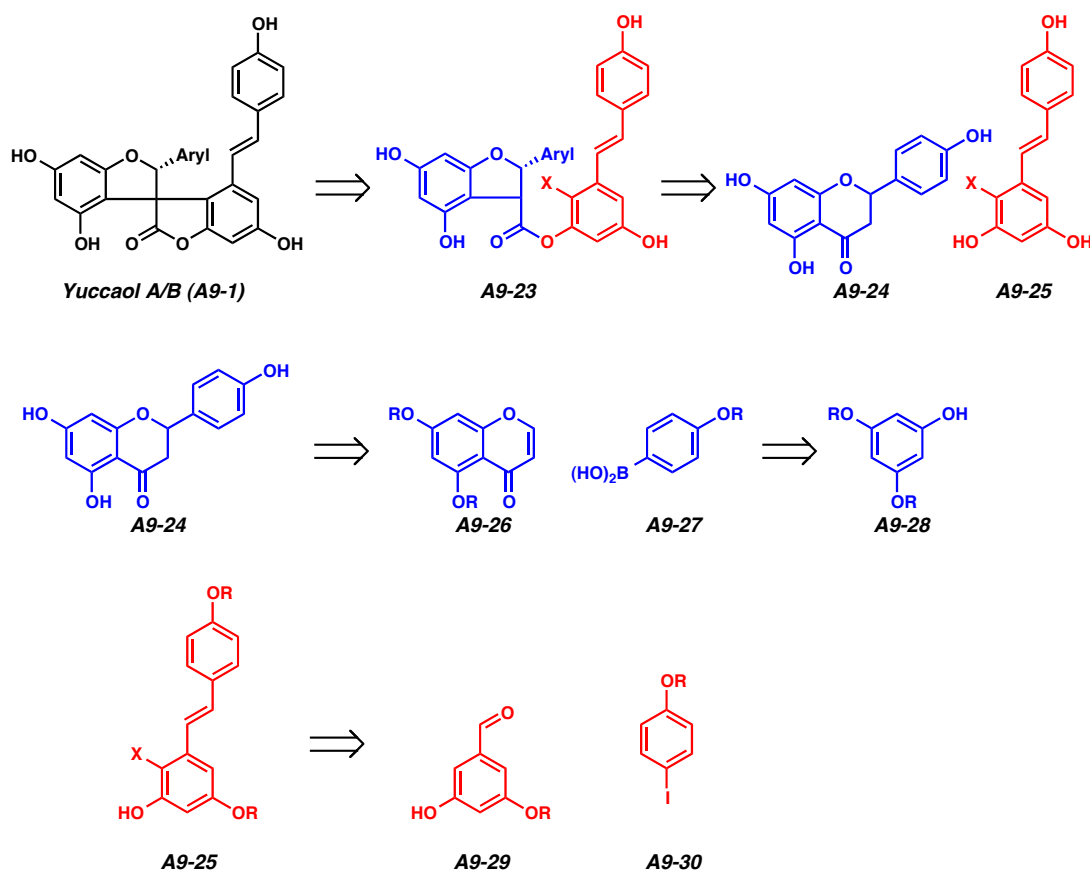
Synthesis of flavanone **A9-26** proceeded smoothly from triphenol **A9-28**,[4] however we found that unprotected chromone **A9-26** did not react in conjugate addition reactions. A suitable protecting group scheme will need to be found. Methoxy groups make sense, however, concern with their removal and the reactivity of electron-rich substrates in conjugate addition reactions makes them less attractive.

Scheme A9.8 Synthesis of chromone intermediate
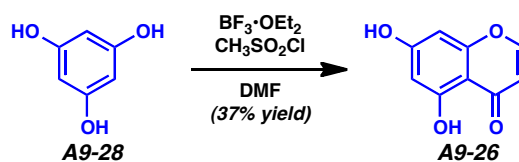
Synthesis of the requisite stilbene fragment **A9-25** was less straightforward. A three-step sequence starting from aldehyde **A9-29** produced styrene **A9-31** in poor yield (Scheme A9.9), as a mix of mono- and bis-methylated isomers that were not easily separated. Treatment of the mixture with iodide **A9-30** resulted in isolation of the desired Heck product for only the bis-methylated styrene, poising the question of how to selectively remove one of three methyl groups chemoselectively.

Scheme A9.9 Synthesis of stilbene moiety
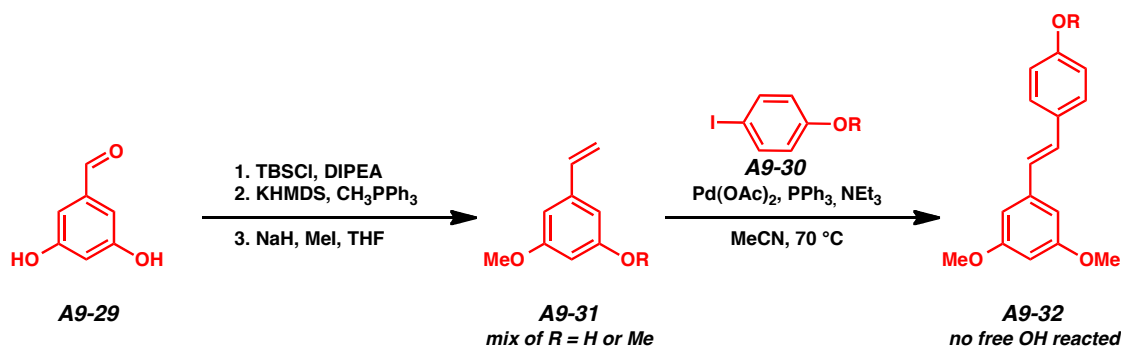
A9.8 Conclusion and outlook

We have presented a reasonable route toward the yuccaol natural products. The key step, the synthesis of the key spirocyclic stereocenter, remains to be demonstrated. Currently, the preferred route is a radical cyclization. Finally, fully oxygenated pieces have been synthesized, however, an optimal protecting group scheme and substrates for the key conjugate addition need to be identified.

A9.9 Notebook references for compounds

See notebooks for Emmett D. Goodman (EDG), specifically notebook II. Racemic flavanone used as starting material for majority of the studies, purchased from Sigma-Aldrich.

– Ring contraction product **A9-6**: EDG-II-077, EDG-II-085, EDG-II-153

– Saponification product **A9-11:** EDG-II-097, EDG-II-105, EDG-II-121

– Aryl ethers **A9-12, A9-13, A9-14:** EDG-II-131, EDG-II-165, EDG-II-167, EDG-II-189, EDG-II-191

– Benzofuran side reaction **A9-22**: EDG-II-135

– Chromone **A9-26**: EDG-II-155

– Stilbene synthetic intermediates: JCH-XI

A9.10 Notes and Citations

(1)   (a) Wenzig, E.; Oleszek, W.; Stochmal, A.; Kunert, O.; Bauer, R. *J. Agric. Food Chem.* **2008**, *56*, 8885–8890. (b) Marzoco, S.; Piacente, S.; Pizza, C.; Oleszek, W.; Stochmal, A.; Pinto, A.; Sorrentino, R.; Autore, G. *Life Sciences.* **2004**, *75(12)*, pp 1491-1501.

(2)   Khanna, M. S.; Singh, O. V.; Garg, C. H. P.; Kapoor, R. P. *Synth. Commun.* **1993**, 23, 585–590. (b) Khanna, M. S. *O. P. P. I. Briefs.* **1994**, 26, 125–127. (c) Prakash, O.; Tanwar, M. P. *Bull. Chem. Soc. Jpn.* **1995**, 68, 1168–1171. (d) Nemeth, I.; Kiss-Szikszai, A.; Illyes, T. Z.; Mandi, A.; Komaromi, I.; Kurtan, T.; Antus, S. *Z. Naturforsch.* **2012**, 67b, 1289–1296.

(3)   (a) Hama, T.; Hartwig, J. F. Org. Lett. **2008,** *10*, pp 1549-1552. (b) Garcia-Fortanet, J.; Buchwald, S. L. *Angew. Chem. Int. Ed.* **2008**, *47*, 8108–8111.

(4)   (a) Zheng, S.; Shen, Z. *Tet. Lett.* **2010**, *51*, 2883–2887. (b) Guo, W.; Biao, Y. *Eur. Joc.* **2008**, *18*, 3156–3163.

APPENDIX 10

The development of novel NHC-based ligand scaffolds for use in

heteroaromatic conjugate addition reactions

Abstract
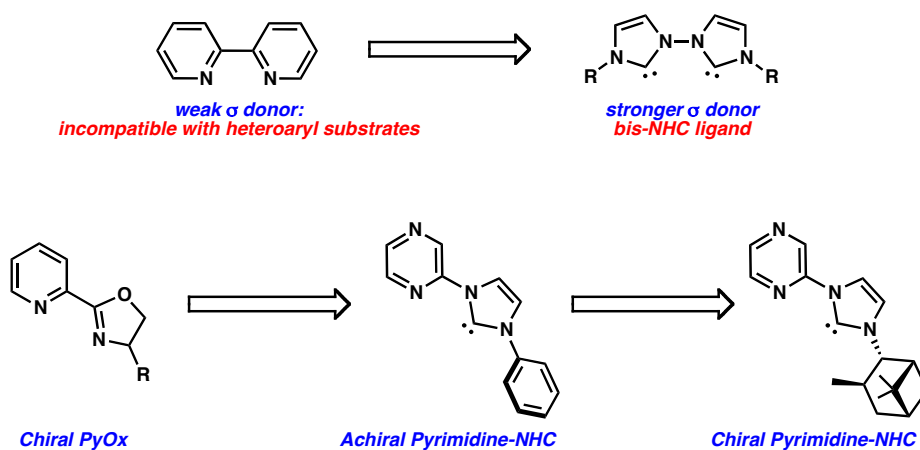
Efforts toward the asymmetric conjugate addition of heteroaromatic boronic acids are discussed. Pyridine-derived ligands were observed to be incompatible with Lewis basic functionality, such as pyridylboronic acids. Synthesis and evaluation of a number of mono- and bis-NHC ligands was undertaken to evaluate these ligands for catalytic activity in palladium-catalyzed conjugate addition reactions. Low conversions were observed with these ligands, prompting the synthesis and evaluation of mixed pyridine-NHC and pyrimidine-NHC ligands. These ligands have bite angles analogous to bipyridine and may lead to superior function in palladium-catalyzed conjugate addition reactions.

A10.1 Introduction and background

Palladium-catalyzed asymmetric conjugate addition has been achieved with a number of ligand scaffold designs. Our efforts with bipyridine (bpy) and pyridinooxazoline (PyOx) ligands were unsuccessful in reacting heteroarylboronic acids (Scheme A10.1). A number of heteroarylboronic acids were screened, and all failed to afford appreciable conversion to the conjugate addition adducts with the exception of 4-dibenzofuranboronic acid. Heteroarylboronic acids with Lewis basic functionalities, such as 3-pyridylboronic acid and 3-thiopheneboronic acid, were observed to chelate the palladium complex, and may out compete the relatively weak σ donor atoms of bpy or PyOx, knocking these ligands off the metal and leaving the metal unreactive and coordinatively saturated. The observations led us to consider alternative ligand scaffolds, in hope that we could identify a scaffold compatible with these highly Lewis basic heteroarylboronic acids.
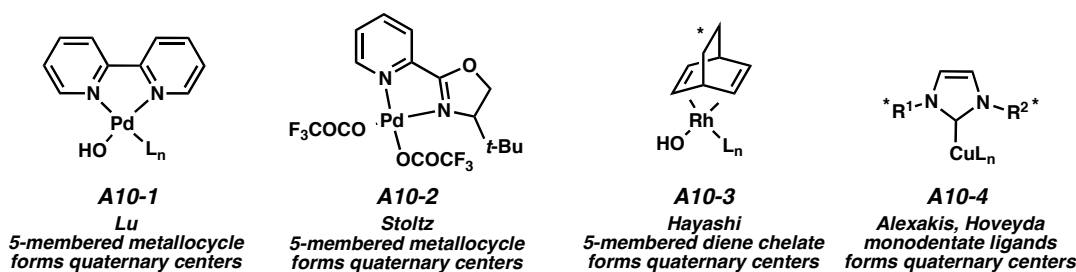
Scheme A10.1 Failed reactions with bpy and PyOx ligands
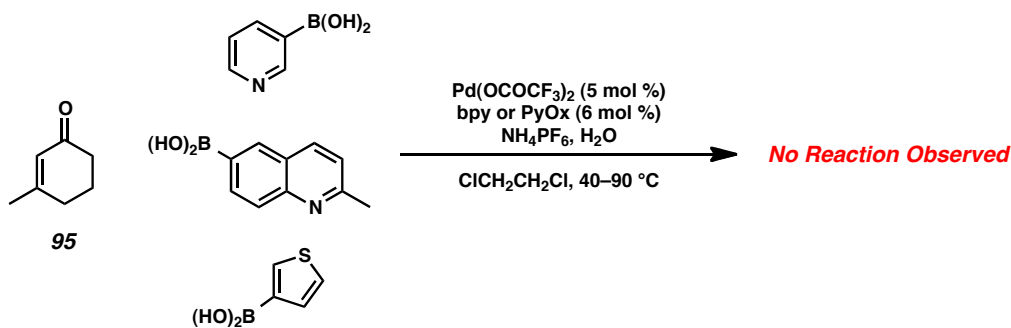
Early on, we noticed that bulky, di- and triarylphosphine ligands were incapable of catalyzing the synthesis of quaternary stereocenters *via* reaction with methylcyclohexenone (**95**). Presumably, the steric demands of the transition state- olefin

insertion into the arylpalladium bond- are prohibitively high in energy for systems involving bulky, sterically demanding ligands. There are several known systems capable of catalyzing conjugate addition reactions that form quaternary stereocenters (Figure A10.1), including Lu's (bpy)Pd complexes (**A10-1**), our own (PyOx)Pd manifold (**A10-2**), Hayashi's chiral diene systems (**A10-3**) and the monodentate Cu-NHCs popularized by Alexakis and Hoveyda (**A10-4**). Analysis of these systems reveals a number of similarities, particularly in the rhodium and palladium manifolds, 1) a five-membered chelate of the metal center; 2) a small bite angle; 3) no large groups projecting around the metal center from the ligand. The Alexakis and Hoveyda model, based on monodentate copper/NHCs, is the only catalytic system that does not involve bidentate ligands. However, it demonstrates that monomeric NHC ligands may be functional with palladium metal centers, too.

Figure A10.1 Known catalytic systems for conjugate addition forging quaternary centers

A10-1
Lu
5-membered metallocycle forms quaternary centers

A10-2
Stoltz
5-membered metallocycle forms quaternary centers

A10-3
Hayashi
5-membered diene chelate forms quaternary centers

A10-4
Alexakis, Hoveyda
monodentate ligands forms quaternary centers

Taking these complexes as starting points, we began to devise an approach toward NHC ligands that would incorporate the key features of the catalyst scaffolds. Namely, we set out to test monodentate NHCs, bis NHCs, and mixed NHC/pyridine bidentate ligands for competency in catalyzing conjugate addition reactions with both
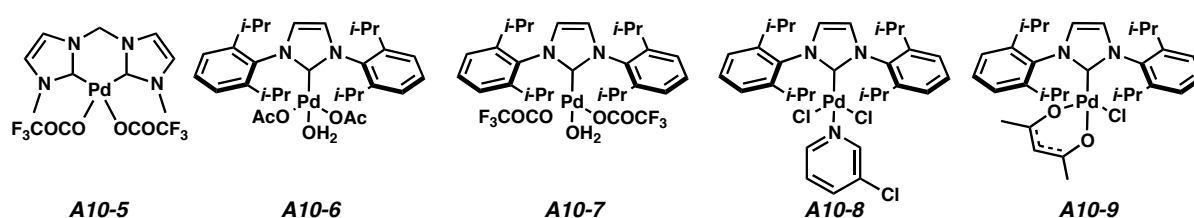
phenylboronic acid and heteroarylboronic acids. In particular, we hoped to combine the narrow bite angle of bpy ligand derivatives with the superior σ donating ability of NHC ligands.

A10.2 Results

A10.2.1 Synthesis of NHC complexes

A variety of NHC complexes were synthesized. See citations for appropriate preparative references. Most of these were monodentate NHC ligands, as they were easiest to prepare. Hermann's bis NHC **A10-5**,[1] derived from *N*-methylimidazole and dibromomethane, was the only bis-NHC completed at the time of this writing. Sigman's palladium(II) acetate derivative NHCs (**A10-6**) was synthesized according to his published procedures.[2] We made an analog of this complex with trifluoroacetate, **A10-7**. These aquo complexes are known to affect the oxidation of alcohols to ketones and aldehydes under basic conditions. The PEPPSI-iPr catalyst (**A10-8**) and well-known α-arylation catalyst **A10-9** were the final complexes synthesized.

Figure A10.2 Palladium NHC complexes synthesized

A10-5   **A10-6**   **A10-7**   **A10-8**   **A10-9**

A10.2.2 Reactions with cyclohexenone

We first tested these complexes as catalysts in the conjugate addition reaction of phenylboronic acid to cyclohexenone and 3-methylcyclohexenone (Table A10.1).

Catalyst **A10-5** featured good conversion with cyclohexenone and chromone, albeit conversion took several days, though no reaction was observed with methylcyclohexenone. Catalyst **A10-6**, however, demonstrated almost no productive reaction with any of the three substrates screened, however, biphenyl production was observed. Catalyst **A10-7** provided a similar reaction profile to bis-NHC **A10-6**, although it catalyzed reactions much slower. Finally, chloride anion containing catalysts **A10-8** and **A10-9** produced no observable reactions. Observation of competent reactivity with phenylboronic acid led us to consider a screen involving heteroarylboronic acids.

Table A10.1 Reactions of NHC complexes with phenylboronic acid

catalyst	R = H	R = CH$_3$	chromone
A10-5	good conversion	no conversion biphenl observed	good conversion
A10-6	trace product, biphenyl observed	no product biphenyl observed	trace product biphenyl observed
A10-7	modest conversion much slower than A10-5	no product biphenyl observed	modest conversion biphenyl observed
A10-8	no reaction	no reaction	no reaction
A10-9	no reaction	no reaction	no reaction

Next, we employed the same catalysts in the conjugate addition reaction of 3-pyridylboronic acid to cyclohexenone and 3-methylcyclohexenone. Surprisingly, complex **A10-5** gave no conversion with either enone. Complex **A10-6**, on the other hand, indicated trace conversion by TLC, and peaks on the LCMS suggested Heck product **A10-11** was forming. Trifluoroacetate analog **A10-7** reacted similarly in low conversion, and 2 mg of the Heck adduct was isolated by column chromatography. Significant proteodeborylation and biaryl formation was observed, as well. We postulate

that these reactions may perform better in polar solvents, where the coordination complex of the pyridine substrate and the metal catalyst would be less stabilized. Highly polar solvents, however, often promote oxidative Heck reactivity. Continuing the trend observed with phenylboronic acid, chloride anion complexes **A10-8** and **A10-9** promoted no reactivity whatsoever.

Table A10.2 Reactions of NHC complexes with 3-pyridylboronic acid

catalyst	R = H	R = CH₃	comment
A10-5	no conversion	no conversion	most successful catalyst with phenylboronic acid surprisingly unreactive
A10-6	trace conversion to **A10-11** by LCMS	no conversion	low reactivity, probably would benefit from more polar solvent
A10-7	low conversion to **A10-11** 2 mg isolated	no conversion	low reactivity, probably would benefit from more polar solvent
A10-8	no conversion	no conversion	chloride anions hinder reactivity, as predicted
A10-9	no conversion	no conversion	chloride anions hinder reactivity, as predicted

A10.3 Future Directions

We believe that NHC ligands with bite angles more closely related to bpy would show significant activity in palladium-catalyzed conjugate addition (Figure A10.3). As was observed with diamine ligands, bite angle is exceedingly important to high reactivity, and we imagine a similar bite angle would accelerate NHC/palladium-catalyzed 1,4-addition reactions.

Figure A10.3 Conceptual NHC design with bite angle analogous to bpy
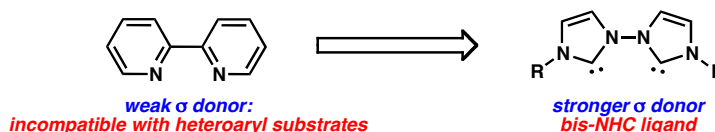
A number of ligands are known that feature bis-NHC moieties based on the bpy and phenanthroline scaffolds (Figure A10.4). The Crabtree group's "bitz" ligand (**A10-12**),[3] and the Bertrand group's "i-bitz" (**A10-13**) are bpy-derived bis-NHCs bearing analogous bite angles.[4] The Kunz group has a scaffold related to 1,10-phenanthroline with a bidentate NHC chelate (**A10-14**).[5]

Figure A10.4 Known bis-NHC ligands with smaller bite angles
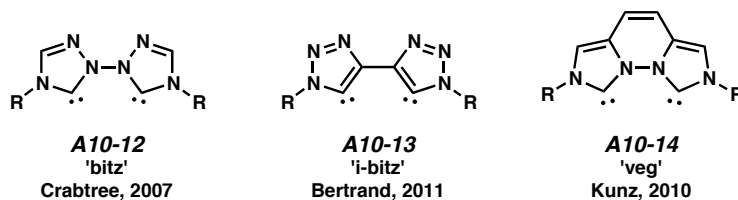
Furthermore, a number of *N*-NHC bidentate ligands are known, whereby the pyridine chelate from the PyOx scaffold is conserved, and the oxazoline is replaced with an NHC chelate (Figure A10.5). These ligands are particularly attractive because of the success we have seen with the C_1 symmetric PyOx ligands. The Monkowius group's 1,10-phentanthroline-derived *N*-NHC bidentate ligand (**A10-15**),[6] and Strassner's pyrimidine-derived NHC (**A10-16)** are both interesting ligands to test.[7] Some progress toward the synthesis of the Strassner ligand has been performed (see notebook cross reference at end of this chapter).

Figure A.10.5 Bidentate N-NHC ligands

A10-15
Monkowius, 2012

A10-16
Strassner, 2009
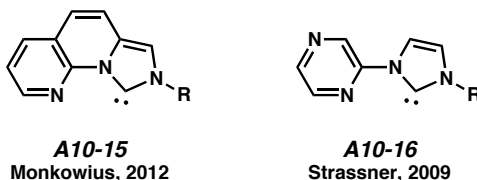
Furthermore, the use of bidentate *N*-NHC ligands would immediately posit analogous chiral C_1 ligands (Figure A10.6). Though pyrimidine/NHC ligands are generally aryl substituted on the NHC nitrogen atom (e.g., **A10-18**), we have postulated the isopino-campheylamine-derived NHC (**A10-19**) based on its steric similarity to the *t*-BuPyOx ligand (**A10-17**, R = (*S*)-*t*-Bu) currently used for the conjugate addition methodology.

Figure A.10.6 Logical extension to chiral NHC ligands

| **A10-17** | **A10-18** | **A10-19** |
| **Chiral PyOx** | **Achiral Pyrimidine-NHC** | **Chiral Pyrimidine-NHC** |
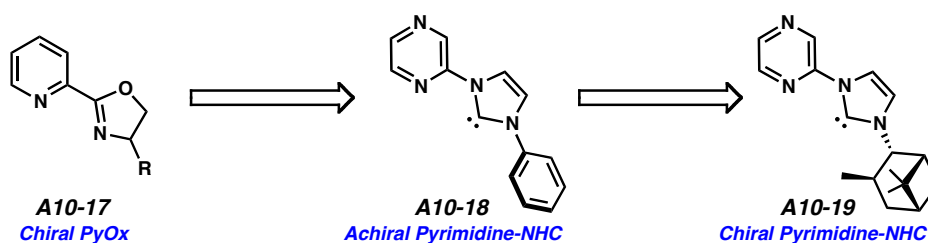
Synthesis of the ligand requires mono-aryl imidazole (**A10-20**) and 2-chloropyrimidine (Scheme A10.2, **A10-21**), which are heated neat to afford imidazolium salt **A10-22**. This salt is ligated to silver(I) in the absence of light and transmetallated to Pd(nbd)Cl$_2$ to afford dichloride **A10-23**. As chloride anions are incompatible with the conjugate addition methodology, this species would need to be further refined, to either a trifluoroacetate (**A10-24**) or dicationic (**A10-25**) analog via halogen abstraction or other ligand exchange. We posit that **A10-24** and **A10-25** would be excellent catalysts for palladium-catalyzed 1,4-addition reactions.

Scheme A10.2 Synthesis of idealized trifluoroacetate complex

A10-24, X = OCOCF$_3$
A10-25, X = PF$_6$
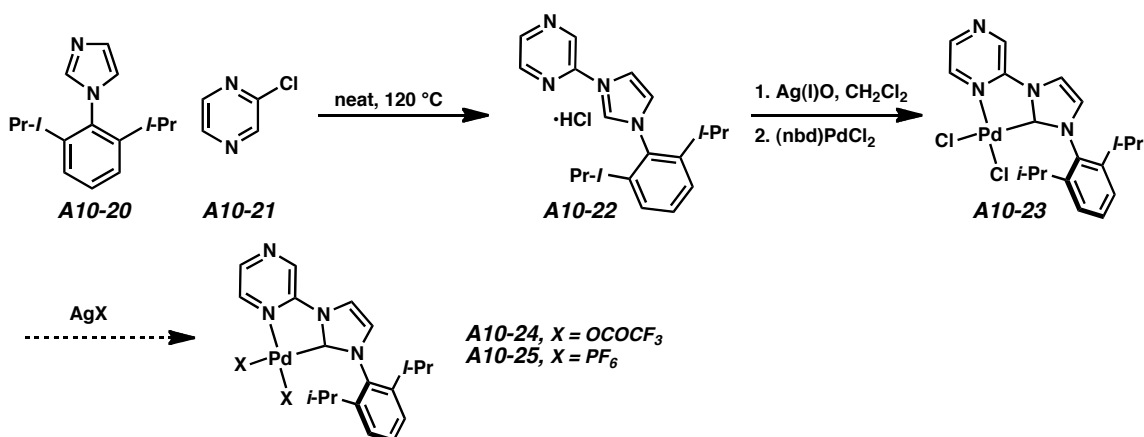
A10.4 Conclusions

Progress toward the design of a palladium-catalyzed conjugate addition system capable of tolerating heteroarylboronic acids is presented. Suggestions for future directions and ligand designs have been made.

A10.5 Notebook references for compounds and tables in Appendix 10

A10-5 bis-NHC: JCH-XI-075, JCH-XI-079, JCH-XI-081, JCH-XI-097

A10–6 Sigman mono-DIPP NHCs: JCH-XI-103, JCH-XI-127, JCH-XI-151, JCH-XI-155, JCH-XI-163, JCH-XI-165

A10-7: trfluoroacetate analog JCH-XI-167

A10-14: JCH-XI-291, JCH-XI-295, JCH-XI-297, JCH-XI-299

A10.6 Notes and Citations

(1)   (a) Strassner, T.; Muehlhofer, M.; Zeller, A.; Herdtwreck, E.; Hermann, W. A. *J.*
        Organometl. Chem. **2004**, 1418–1424. (b) Muehlhofer, M.; Strassner, T.;
        Herdtweck, E.; Hermann, W. A. *J. Organomet. Chem.* **2002**, 121–126. (c)
        Slootweg, J. C.; Chen, P. *Organometallics* **2006**, *25*, 5863–5869.

(2)   (a) Jensen, D. A.; Schultz, M. J.; Mueller, J. A.; Sigman, M. S. *Angew. Chem. Int.*
        Ed. **2003**, *42*, 3810–3813. (b) Jensen, D. R.; Sigman, M. S. *Org. Lett.* **2003**, *5*,
        63–65.

(3)   (a) Poyatos, M.; McNamara, W.; Incarvito, C.; Peris, E.; Crabtree, R. H. *Chem.*
        Commun. **2007**, 2267–2269. (b) Poyatos, M.; McNamara, W.; Incarvito, C.; Clot,
        E.; Peris, E.; Crabtree, R. H. *Organometallics* **2004**, *23*, 1253–1263.

(4)   (a) Guisado-Barrios, G.; Boufard, J.; Donnadieu, B.; Bertrand, G.
        Organometallics, **2011**, *30*, 6017–6021.

(5)   (a) Gierz, V.; Urbanaite, A.; Seyboldt, A.; Kunz, D. *Organometallics*, **2012**, *31*,
        7532–7538. (b) Gierz, V.; Maichle-Mossmer, C.; Kunz, D. *Organometallics*,
        2012, *31*, 739–747.

(6)   Kriechbaum, M.; List, M.; Berger, R. J. F.; Patzchke, M.; Monkowius, U.
        Chem.–Eur. J. **2012**, *18*, 5506–5509.

(7)   (a) Liu, J.; Chen, J.; Zhao, J.; Zhao, Y.; Li, L.; Zhang, H. *Synthesis* **2003**, *17*,
        2661–2666. (b) Meyer, D.; Taige, M. A.; Zeller, A.; Hohlfeld, K.; Ahrens, S.;
        Strassner, T. *Organometallics* **2009**, *28*, 2142–2149.

APPENDIX 11

Progress toward the development of a novel reductive Heck reaction[‡]

[‡] This work was performed in conjunction with Dr. Wen-Bo "Boger" Liu, who spent considerable time investigating conventional reductive Heck reductants. See his notebooks (WBL) for full details.

Abstract
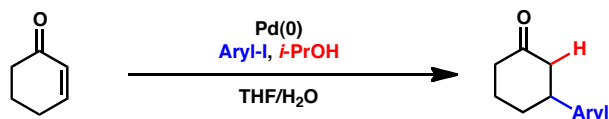
Efforts toward the rational design of a new reaction manifold for a reductive Heck catalytic cycle are presented. This catalytic cycle differs from a typical palladium-catalyzed conjugate addition in that the reactive arylpalladium(II) intermediate is formed *via* oxidative addition. Thus, a reduction event is required to regenerate the palladium(0) catalyst. Herein, we describe efforts toward the use of *iso*-propanol as the stoichiometric reductant. Modest conversions to the desired adducts are reported, however significant side products are observed. Attempts to render the transformation enantioselective by employing the ligand (*R, R*)-Me-DuPhos are reported. Finally, attempts to generalize the reaction for use with heteroaryl reagents are discussed.

A11.1 Introduction and background

A11.1 Historical perspective

      Reductive Heck reactions are attractive alternatives to conventional conjugate addition reactions. There are numerous situations where one might be better served by the reductive Heck reaction, such as a situation where the desired aryl congener is not stable as a boronic acid, or is overly prone to proteodeborylation or other undesired side reaction. Furthermore, the elevated temperatures and phosphine ligands typically employed in reductive Heck reactions are more likely to accommodate heteroaryl reagents, as opposed to the mild temperatures and diamine ligands scaffolds that are typically employed in conjugate addition reactions. In the conventional diamine-palladium-catalyzed conjugate addition reaction, heteroaryl reagents or other Lewis basic moieties are able to out compete the ligand for metal chelation, effectively sequestering the catalyst off-cycle. However, conventional reductive Heck reactions employ harsh conditions and elevated temperatures (Scheme A11.1), utilizing formic acid and triethylamine as reductants to add aryl halides (**A11-2**) to enones (**A11-1**) to form β−arylated ketones (**A11-3**).

Scheme A11.1 Typical reductive Heck reaction conditions
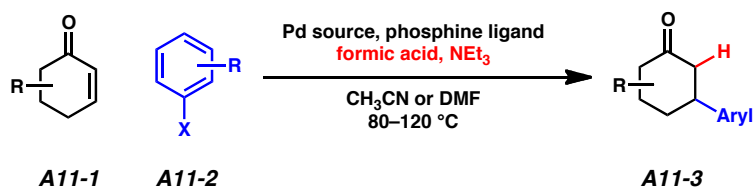
A11.1.2 Proposed catalytic cycle

Our group has spent considerable time investigating this processes, with hopes of synthesizing β-heteroaryl ketone products in an asymmetric fashion. This catalytic cycle starts with palladium(0), and forms the active arylpalldium(II) intermediate (akin to that of the conjugate addition catalytic cycle) *via* oxidative addition. Thu**s,** a reduction event (hence *reductive* Heck reaction) is required to regenerate the palladium(0) catalyst.

Recently, we began to pursue an alternative reduction mechanism, whereby the stoichiometric reductant was actually an alcohol cosolvent. In this manifold, the cosolvent (shown as *iso*-propanol, Figure A11.1) undergoes β-hydride elimination to form a palladium(II) hydride (**A11-11**) which undergoes reductive proton loss to regenerate the palladium(0) catalyst (**A11-4**). As in the conventional Heck reaction, this catalyst undergoes oxidative addition to form arylpalladium(II) **A11-5**, however we envision silver-mediated halogen abstraction enabling the quantitative generation of *cationic* arylpalladium(II) **A11-6**, which undergoes addition to the enone olefin to generate palladium enolate **A11-8**. This enolate acts as the requisite base, deprotonating the alcoholic cosolvent to liberate arylated product **A11-9** and form palladium alkoxide **A11-10**, which is primed for reduction to regenerate the catalyst.

Figure A11.1 Proposed catalytic cycle for new reductive Heck reaction
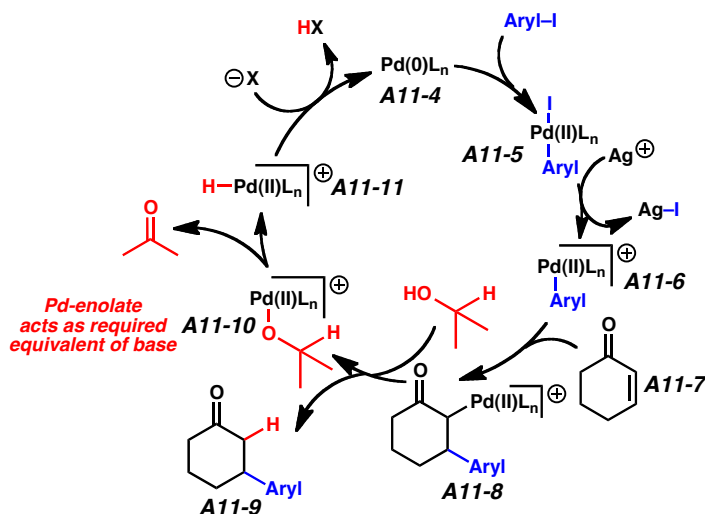
A11.2 Results

A11.2.1 Identification of an operable reductive Heck reaction

A small solvent screen was undertaken to determine if the reaction was operable as proposed. Ironically, the use of 1,2-dichloroethane was found to be unproductive, as heating with silver salts resulted in displacement of the chlorides. THF (Table A11.1, entries 1-2) and CH$_2$Cl$_2$ (entries 3–4) were screened with either water or *iso*-propanol as cosolvent. Water was utilized as a control, to see if conversion to the desired product was detected, and to assay the validity of our hypothesis for the silver additive in promoting the desired 1,4-addition reaction. THF proved a superior solvent to CH$_2$Cl$_2$, and upon scale-up 20-35% yield of the desired adduct **A11-13** could be isolated via the method described in entry 2. However, significant side product **A11-14** was also observed, accounting for a majority of the mass balance. It should be noted that reactions tried using phenyl triflate, instead of iodobenzene and without silver salts, were unsuccessful.

It appears that using non-coordinating counterions alone without the silver, such as triflate, is insufficient to catalyze the reaction. Additionally, we suggest screening additional silver salts. In particular, those with basic counterions (such as acetate, or trifluoroacetate) may assist in reaction turnover, and increase conversion.

Table A11.1 Solvent and cosolvent screen

entry	solvent	cosolvent	conversion	comment
1	THF	H_2O	trace	mix of *A11-13, A11-14*
2	THF	*i*-PrOH	>90%	mix of *A11-13, A11-14*
3	CH_2Cl_2	H_2O	trace	majority *A11-13*
4	CH_2Cl_2	*i*-PrOH	trace	majority *A11-13*

Attempts to induce enantioselectivity by replacing dppbz with (*R,R*)-Me-DuPhos failed to generate any conjugate addition product (Scheme A11.2). (*R,R*)-Me-DuPhos is known to induce asymmetry in palladium-catalyzed conjugate addition reactions in THF/H_2O mixtures. Curiously, only Heck reaction product **A11-14** was observed in our attempts. Of course, further attempts with similar chiral ligands (e.g., Dipamp) should be pursued.

Scheme A11.2 Attempt to induce asymmetry with chiral ligand
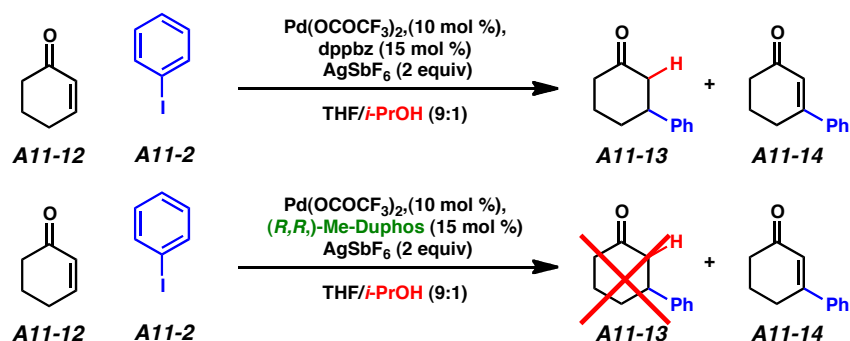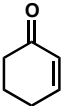
We made brief attempts to apply the reaction toward the synthesis of β-heteroaryl

ketones (**A11-16**), however the incompatibility of silver(I) salts with heteroatom ligands

appears prohibitive to the desired reactivity. For example, use of 3-bromoquinoline

provided no conversion, and only proteodehalogenation and some dimerization was

observed (Table A11.2).

Table A11.2 Bromoquinoline screen
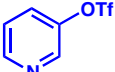
entry	solvent	cosolvent	conversion	comment
1	THF	H$_2$O	trace	mostly H-quinoline, dimer
2	THF	*i*-PrOH	trace	mostly H-quinoline, dimer
3	CH$_2$Cl$_2$	H$_2$O	trace	mostly H-quinoline, dimer
4	CH$_2$Cl$_2$	*i*-PrOH	trace	mostly H-quinoline, dimer

Likewise, the use of 3-pyridyltriflate failed to produce successful reactions (Table A11.3). Again, some proteodetriflation and dimerization signals were observed by LCMS, but not productive conversion was detected. Again, the incompatibility of silver salts with heteroaryl substrates may be prohibitive.

Table A11.3 Pyridine triflate screen
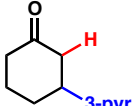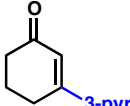
entry	solvent	cosolvent	conversion	comment
1	THF	H_2O	trace	mostly H-pyr, dimer
2	THF	*i*-PrOH	trace	mostly H-pyr, dimer
3	CH_2Cl_2	H_2O	trace	mostly H-pyr, dimer
4	CH_2Cl_2	*i*-PrOH	trace	mostly H-pyr, dimer

A11.3 Conclusion and future directions

The two most pressing tasks are 1) to demonstrate the compatibility of this reaction with chiral ligands and 2) to try milder methods of halogen abstraction from the putative arylpalladium(II) halogen intermediate.
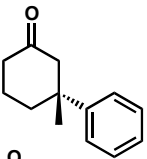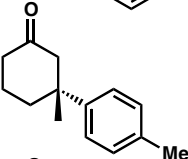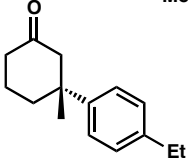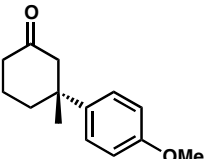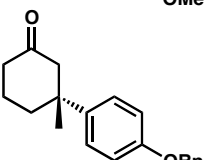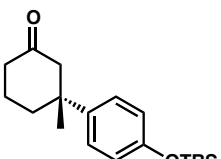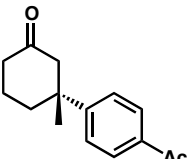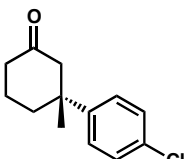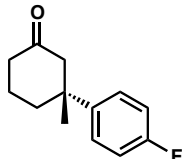
Regarding the search for a compatible chiral ligand, bidentate phosphines forming 5-membered chelates should be examined. A rigid structure and narrow bite angle, as is helpful in other conjugate addition systems, may be desirable.
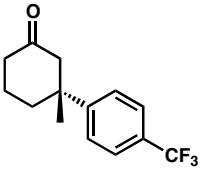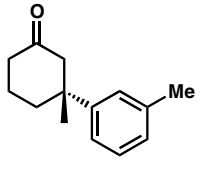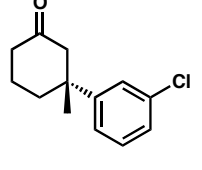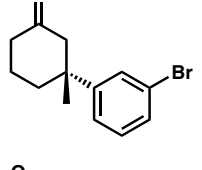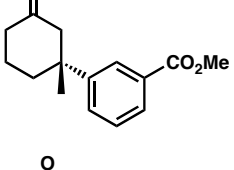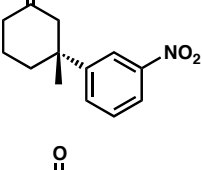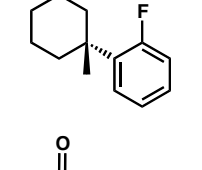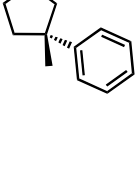
The second goal, mild halogen abstraction, is considerably broader in scope. The mildest method, conceivably, would entail the use of aryltriflates with additives such as hexafluorophosphate or hexalfuoroantimonate salts. Though, to date, these approaches have been non-productive. The use of silver, however, is not compatible with heteroaryl substrates. Additionally, significant deposits of metal mirrors were observed in these cases.
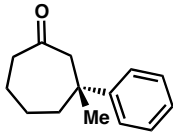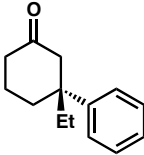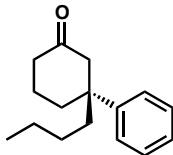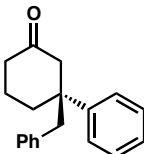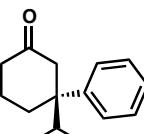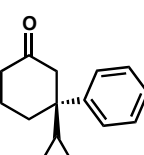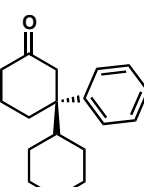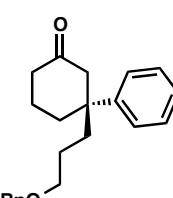
APPENDIX 12

Notebook cross-reference for new compounds

Table A12.1 Compounds from Chapter 2

Compound	product	Notebook reference	NMR and IR data files
35		KIX-II-031b	kix-c6M3Ph1
127		KIX-II-057b KIX-II-051b	kix-c6MePhpMe-1
128		KIX-II-075a KIX-II-079a	kix-c6MePhpEt2
129		KIX-II-095 KIX-II-051a	kix-c6MePhpOMe-1
130		KIX-II-119c KIX-II-151c	kix-c6-MePhpOBn-1
131		KIX-II-101b	kix-c6MePhpOTBS-3
132		KIX-II-103b KIX-II-105d	kix-c6MePhpAc
133		KIX-II-037b KIX-II-043b	kix-c6MePhpCl
134		KIX-II-053 KIX-II-043a	kix-c6MePhpF-1

Compound	product	Notebook reference	NMR and IR data files
89		KIX-II-101a KIX-II-105a	kix-c6MePhpCF3-1
135		KIX-II-057c KIX-II-051f	kix-c6MePhmMe
136		KIX-II-057d KIX-II-051e	kix-c6MePhmCl-1
90		KIX-II-117b KIX-II-151d	kix-c6MePhmBr-2
88		KIX-II-119a KIX-II-151b	kix-c6MePhpCOOMe
137		KIX-II-079c KIX-II-153d	kix-c6MePhmNO2
134a		KIX-II-153b KIX-II-143	kix-c6MePhoF JCH-c6MePhoF
52		KIX-II-073 KIX-II-077	kix-c5MePh-1

entry	product	Notebook reference	NMR and IR data files
83		KIX-II-091c KIX-II-087	kix-c7MePh-1
138		KIX-II-155a KIX-II-089a	kix-c6EtPh
139		KIX-II-099c	kix-c6BuPh
140		KIX-II-139a KIX-II-141a	kix-c6BnPh-1
141		KIX-II-155b KIX-II-089b	kix-c6iPrPh-1
142		KIX-II-113a KIX-II-111a	kix-c6cPrPh-1
86		KIX-II-155c KIX-II-175	kix-c6cHexPh
88		KIX-II-141b KIX-II-139b	kix-c6C3ObnPh-1
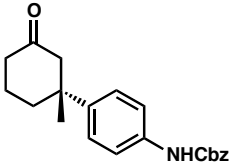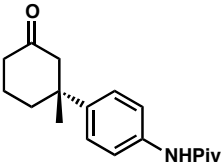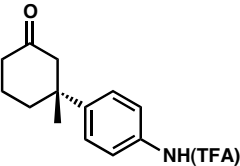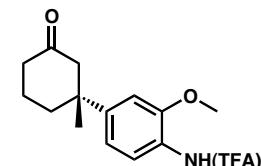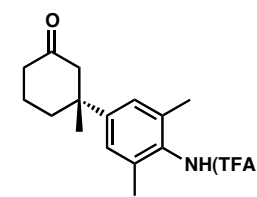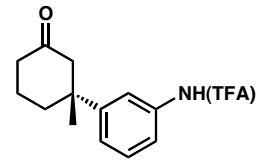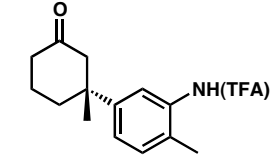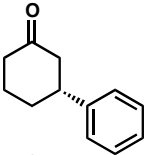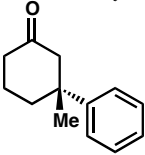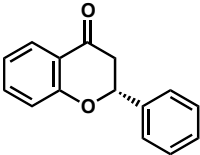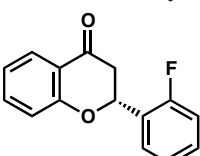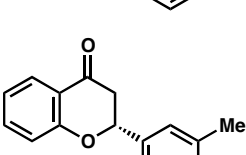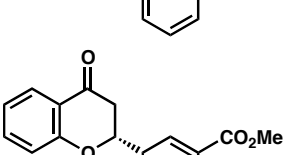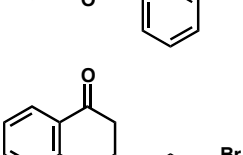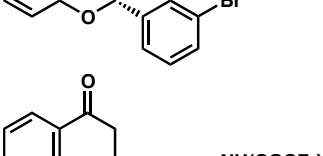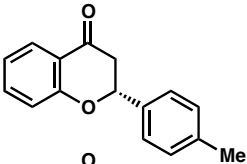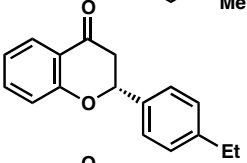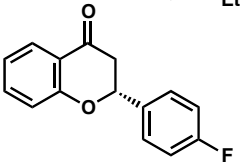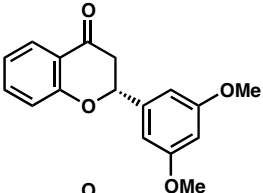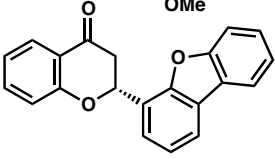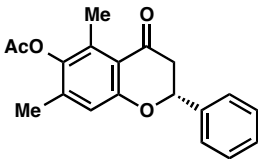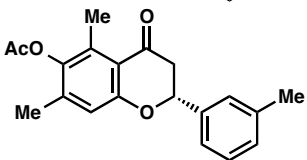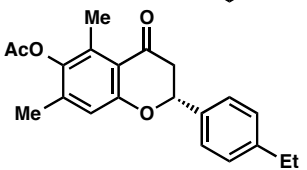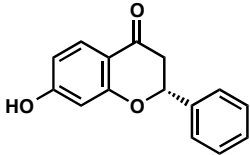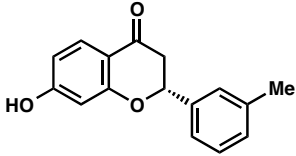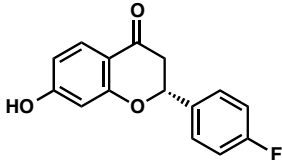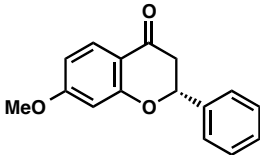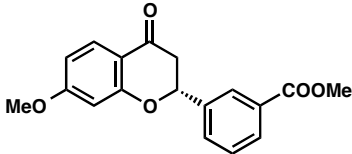
Compound	product	Notebook reference	NMR and IR data files
160		MG-III-0225	MG-III-0225
161		MG-III-227	MG-III-227
162		MG-II-071	MG-II-071
163		MG-III-251	MG-III-251
164		MG-II-127 MG-II-131	MG_2_127_Fr1
165		MG-II-093	MG-II-093
166		MG-II-237	MG-II-237

Table A12.2 Compounds from Chapter 3

Compound	product	Notebook reference	NMR and IR data files
25		JCH-VIII-301	JCH-VIII-301 JCH-c6HPh
35		KIX-II-031b	kix-c6MePh-1
84		AM-I-01	AM-1-01
174		JCH-VII-039 JCH-VII-047	JCH-VII-chromone-2F
175		JCH-VII-095 JCH-VII-075	JCH-VII-095 JCH-VII-075
176		AM-I-11	AM-i-11 AM-i-11_1H_pure
177		JCH-VIII-087 JCH-VII-049	JCH-cheomone-3Br
178		AM-i-15	AM-i-15_finalcharac_2

Compound	product	Notebook reference	NMR and IR data files
180		AM-i-02 JCH-VII-093	AM-i-02 JCH-VII-093
181		JCH-VII-087 JCH-VII-059	JCH-VII-087 JCH-VII-059
182		AM-i-03 JCH-VII-063	AM-i-03 JCH-VII-063
183		AM-i-07 JCH-VIII-073	AM_07_1H_pure
184		AM-I-29	AM-i-29_Y AM-i-29_13C
185		AM-i-30	AM-i-40 AM-i-40_13C
186		AM-i-23 JCH-VIII-097	AM-i-23
187		AM-i-24	AM-i-24_full

Compound	product	Notebook reference	NMR and IR data files
188		MG-III-181	AM-MG-III-181
189		AM-i-42	AM-i-42 AM-i-42_13C
190		AM-i-34	AM-i-34 AM-i-34_13C
191		JCH-VII-089 AM-i-33	AM-i-33 AM-i-33_13C
192		AM-I-41	AM-i-41 AM-i-41_13C
194		AM-i-30	AM-i-30_X AM-i-30
195		MG-III-179	AM-MG-iii-179
85		AM-i-53	AM-i-53_full
196		AM-i-22 MG-III-157	AM_MG-iii-157 AM-i-22

Compound	product	Notebook reference	NMR and IR data files
196		AM-i-26	AM-i-26_full
197		AM-i-27	AM-i-27_full
198		AM-i-59	AM-i-59_1H
199		AM-i-21 MG-iii-155	AM-i-27_F_3
200		AM-i-48	AM-i-48 AM-i-48_13C
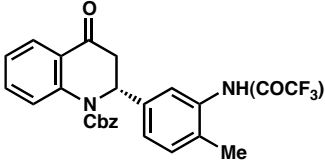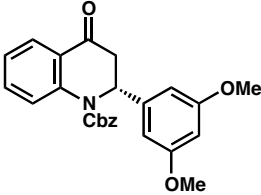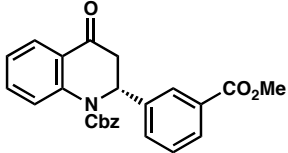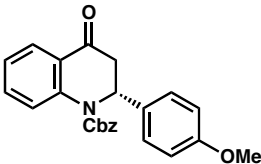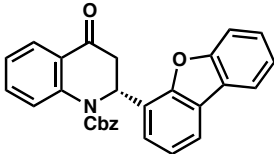
Compound	product	Notebook reference	NMR and IR data files
202		JCH-VIII-277	JCH-VIII-277-again quinolone-3Me4NHTFA
204		JCH-VIII-261	JCH-VIII-261 quinolone-3-5-OMe
205		JCH-VIII-259	JCH-VIII-259 quinolone-3-CO2Me
208		JCH-VIII-299	JCH-VIII-299
209		JCH-VIII-297	JCH-VIII-297 quinolone-DBF

Table A12.3 Compounds from Chapter 4
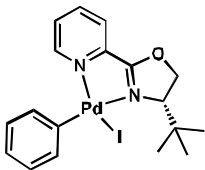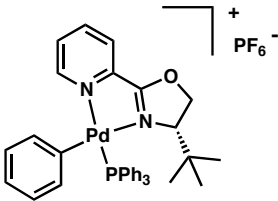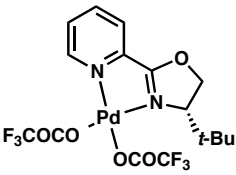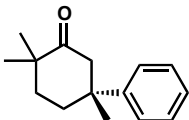
Compound	product	Notebook reference	NMR and IR data files
235		AM-i-38 AM-i-43 AM-i-140	AM-i-43_13C
236		JCH-XII--083 AM-i-145	AM-i-145_full
245		AM-i-119 MG-III-205	MG-III-205 AM-PyOXPdOTFA2
246		JCH-VII-101	JCH-dimethyl-ACA-pdt JCH-dimethyl-c6MePh

Table A12.4 Compounds from Chapter 5
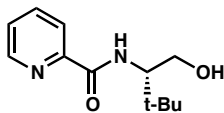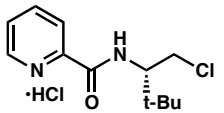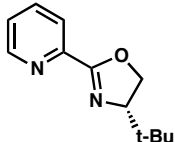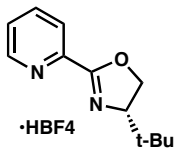
Compound	product	Notebook reference	NMR and IR data files
249		HS-II-211	HS-II-211-amide-OH
256		HS-II-207 HS-II-213	HS-II-207-amide-Cl-HCl
82		HS-II-205 HS-II-213	HS-II-PyOx
82b		HS-II-127	PyOx-HBF4-HS-II-127

Table A12.5 Compounds from Chapter 6

Compound	product	Notebook reference	NMR and IR data files
339		JCH-V-125	JCH-X-bispiv_13C
340		JCH-X-165 JCH-V-131	JCH-X-165 JCH-X-165Bpin
341		JCH-X-167 JCH-V-135	JCH-X-167
321		JCH-X-169	JCH-X-169A
336		JCH-X-183	JCH-X-183A
335		JCH-X-189	JCH-X-189A
334		JCH-X-215	JCH-X-215-A

Comprehensive Bibliography

Abrunhosa, I.; Delain-Bioton, L.; Gaumont, A.-C.; Gulea, M.; Masson, S. *Tetrahedron* **2004**, *60*, 9263–9272.

Albeniz, A. C.; Marta Catalina, N.; Espinet, P.; Redon, R. *Organometallics* **1999**, *18*, 5571–5576.

Alexakis, A.; Backvall, J. E.; Krause, N.; Pamies, O.; Dieguez, M. *Chem. Rev.* **2008**, *108, 2796–2893*.

Alvarez-Manzaneda, E.; Chahboun, R.; Alvarez, E.; Tapia, R.; Alvarez-Manzaneda, R. *Chem.Commun.* **2010**, *46*, 9244–9246.

Alvarez-Manzaneda, E.; Chahboun, R.; Cabrera, E.; Alvarez, E.; Alvarez-Manzaneda, R.; Meneses, R.; Es-Samti, H.; Fernández, A. *J. Org. Chem.* **2009**, *74*, 3384–3388.

Alvarez-Manzaneda, E.; Chahboun, R.; Cabrera, E.; Alvarez, E.; Haidour, A.; Ramos, J. M.; Alvarez-Manzaneda, R.; Hmamouchi, M.; Es-Samti, H. *Chem. Commun.* **2009**, 592–594.

Alvarez-Manzaneda, E.; Chahboun, R.; Cabrera, E.; Alvarez, E.; Haidour, A.; Ramos, J. M.; Alvarez-Manzaneda, R.; Charrah, Y.; Es-Samti, H. *Org. Biomol. Chem.* **2009**, *7*, 5146–5155.

Alexakis, A.; Benhaim, C. *Eur. J. Org. Chem.* **2002**, 3221–3236.

Andersen, O. M.; Markham, K. R. in *Flavonoids: Chemistry, Biochemistry and Applications*, Taylor & Francis, London, **2006**.

Antalek, B. *Concepts in Magnetic Resonance* **2002**, *14*, 225–258.

Aranda, C.; Cornejo, A.; Gil, M. J.; Martinez-Merino, V.; Ochoa, Z.; Fraile, J. M.; Mayoral, J. A.; Garcia-Verdugo, E.; Luis, S. V. *Green Chemistry,* **2011**, *13*, 983–990.

Banerjee, M.; Mukhopadhyay, R.; Achari, B.; Banerjee, A. K. *J. Org. Chem.* **2006**, *71*, 2787–2796.

Banerjee, M.; Mukhopadhyay, R.; Achari, B.; Banerjee, A. K. *Org. Lett.* **2003**, *5*, 3931–3933.

Barluenga, J.; Escribano, M.; Aznar, F.; Valdes, C. *Angew. Chem., Int. Ed.* **2010**, *49*, 6856.

Barluenga, J.; Moriel, P.; Valdes, C.; Aznar, F. *Angew. Chem., Int. Ed.* **2007**, *46*, 5587.

Barluenga, J.; Tomas-Gamasa, M.; Moriel, P.; Aznar, F.; Valdes, C. *Chem.–Eur. J.* **2008**, *14*, 4792.

Becke, A. D. *J. Chem. Phys.* **1993**, *98*, 1372–1377.

Becke, A. D. *J. Chem. Phys.* **1993**, *98*, 5648–5652.

Bedford, R. B.; Betham, M.; Charmant, J. P. H.; Haddow, M. F.; Guy Orpen, A.; Pilarski, L. T. *Organometallics* **2007**, *26*, 6346–6353.

Behenna, D. C.; Mohr, J. T.; Sherden, N. H.; Marinescu, S. C.; Harned, A. M.; Tani, K.; Seto, M.; Ma, S.; Novak, Z.; Krout, M. R.; McFadden, R. M.; Roizen, J. L.; Enquist, J. A., Jr.; White, D. E.; Levine, S. R.; Petrova, K. V.; Iwashita, A.; Virgil, S. C.; Stoltz, B. M. *Chem.–Eur. J.* **2011**, *17*, 14199–14223.

Behenna, D. C.; Stoltz, B. M. *J. Am. Chem. Soc.* **2004**, *126*, 15044–15045.

Biddle, M. M.; Lin, M.; Scheidt, K. A. *J. Am. Chem. Soc.* **2007**, *129*, 3830–3831.

Bremberg, U.; Rahm, F.; Moberg, C. *Tetrahedron: Asymmetry*, **1998,** *9*, 3437–3443.

Brocksom, T. J.; Brocksom, U.; Fredericoa, D. *Tetrahedron Lett.* **2004**, *45*, 9289.

Brookmeyer, R.; Johnson, E.; Ziegler-Graham, K.; Arrighi, H. M. *Alzheimer's and Dementia* **2007**, *3*, 186.

Brossard, D.; Kihel, L. E.; Khalid, M.; Rault, S. *Synlett* **2010**, *2*, 0215.

Brown, H. C.; Gupta, S. K. *J. Am. Chem. Soc.* **1972**, *94*, 4370.

Brown, M. K.; Degrado, S. J.; Hoveyda, A. H. *Angew. Chem. Int. Ed.* **2005**, *44*, 5306–5310.

Brown, M. K.; May, T. L.; Baxter, C. A.; Hoveyda, A. H. *Angew. Chem., Int. Ed.* **2007**, *46*, 1097–1100.

Brunner, H.; Kagan, H. B.; Kreutzer, G. *Tetrahedron: Asymmetry*, **2003**, *14*, 2177–2187.

Brunner. H.; Obermann. U. *Chem. Ber.* **1989**, *122*, 499–507.

Brunner, H.; Obermann, U.; Wimmer, P. *Organometallics* **1989**, *8*, 821–826.

Banerjee, M.; Mukhopadhyay, R.; Achari, B.; Banerjee, A. K. *Org. Lett.* **2003**, *5*, 3931–3933.

Cacchi, S.; Misiti, D.; Palmieri, G. *Tetrahedron* **1981**, *37*, 2941–2946.

Cacchi, S.; La Torre, F.; Misiti, D.; Palmieri, G. *Tetrahedron Lett*. **1979**, *20*, 4591–4595.

Campbell, A. N.; Stahl, S. S. *Acc. Chem. Res*. **2012**, *45*, 851–863.

Carrow, B. P.; Hartwig, J. F. *J. Am. Chem. Soc*. **2011**, *133*, 2116–2119.

Chamberlain, A. R.; Bond, T. F. *J. Org. Chem*. **1978**, *43*, 154.

Chamberlain, A. R.; Liotta, E. L.; Bond, T. F. *Org. Synth*. **1983**, *61*, 141.

Chang, C.-I.; Chang, J.-Y.; Kuo, C.-C.; Pan, W.-Y.; Kuo, Y.-H. *Planta Med*. **2005**, *71*, 72–76.

Chang, C.-I.; Chien, S.-C.; Lee, S.-M.; Kuo, Y.-H. *Chem. Pharm. Bull*. **2003**, *51*, 1420–1422.

Chang, L. C.; Kinghorn, A. D. in *Bioactive Compounds from Natural Sources: Isolation, Characterisation and Biological Properties* (Ed: Tringali, C.), Taylor & Francis, London, **2001**, ch. 5.

Chen, J.; Chen, J.; Lang, F.; Zhang, X.; Cun, L.; Zhu, J.; Deng, J.; Liao, J. *J. Am. Chem. Soc*. **2010**, *132*, 4552–4553.

Cheng, H. M.; Tian, W.; Peixoto, P. A.; Dhudshia, B.; Chen, D. Y.-K. *Angew. Chem. Int. Ed*. **2011**, *50*, 4165–4168.

Cho, C. S.; Motofusa, S.-I.; Ohe, K.; Uemura, S. *Bull. Chem. Soc. Jpn*. **1996**, *69*, 2341–2348.

Cho, C. S.; Motofusa, S.-I.; Ohe, K.; Uemura, S.; Shim, S. C. *J. Org. Chem.* **1995**, *60*, 883–888.

Cho, C. S.; Motofusa, S.-I.; Uemura, S. *Tetrahedron Letters* **1994**, *35*, 1739–1742.

Christoffers, J.; Baro, A. *Adv. Synth. Catal.* **2005**, *347*, 1473–1482.

Corey, E. J.; Shibata, T.; Lee, T. W. *J. Am. Chem. Soc.* **2002**, *124*, 3808.

Cornejo, A.; Fraile, J. M.; García, J. I.; Gil, M. J.; Herrerías, C. I.; Legarreta, G.; Martínez-Merino, V.; Mayoral, J. A. *J. Mol. Catal. A: Chem.* **2003**, *196*, 101–108.

Cozzi, P. G.; Hilgraf, R.; Zimmermann, N. *Eur. J. Org. Chem.* **2007**, 5969–5994.

Culkin, D. A.; Hartwig, J. F. *J. Am. Chem. Soc.* **2001**, *123*, 5816–5817.

Dai, H.; Lu, X. *Tetrahedron Lett.* **2009**, *50*, 3478–3481.

Dang, L.; Lin, Z.; Marder, T. B. *Organometallics* **2008**, *27*, 4443–4454.

Dauzonne, D.; Monneret, C. *Synthesis* **1997**, 1305–*1308*.

Deng, J.; Li, R.; Luo, Y.; Li, J.; Zhou, S.; Li, Y.; Hu, J.; Li, A. *Org. Lett.* **2013**, *15*, 2022–2025.

Denissova, I.; Barriault, L. *Tetrahedron* **2003**, *59*, 10105–10146.

Denmark, S. E.; Amishiro, N. *J. Org. Chem.* **2003**, *68*, 6997.

Dhawan, R.; Dghaym, R. D.; St. Cyr, D. J.; Arndtsen, B. A. *Org. Lett.* **2006**, *8*, 3927–3930.

Dittmer, C.; Taabe, G.; Hintermann, L. *Eur. J. Org. Chem.* **2007**, 5886–5898.

Douglas, C. J.; Overman, L. E. *Proc. Natl. Acad. Sci. U.S.A.* **2004**, *101*, 5363–5267.

Duan, W.-L.; Iwamura, H.; Shintani, R.; Hayashi, T. *J. Am. Chem. Soc.* **2007**, *129*, 2130–2138.

Dumas, A. M.; Fillion, E. *Acc. Chem. Res.* **2010**, *43*, 440–454.

Enquist, J. A., Jr.; Virgil, S. C.; Stoltz, B. M. *Chem.–Eur. J.* **2011**, *17*, 9957–9969.

Enquist, J. A., Jr.; Stoltz, B. M. *Nature* **2008**, *453*, 1228–1231.

Frauenlob, R.; McCormack, M. M.; Walsh, C. M.; Bergin, E. *Org. Biomol. Chem.* **2011**, *9*, 6934–6937.

Feringa, B. L. *Acc. Chem. Res.* **2000**, *33*, 346–353.

Fillion, E.; Fishlock, D. *J. Am. Chem. Soc.* **2005**, *127*, 13144–13145.

Fillion, E.; Wilsily, A. *J. Am. Chem. Soc.* **2006**, *128*, 2774–2775.

Fischer, C.; Defieber, C.; Suzuki, T.; Carreira, E. M. *J. Am. Chem. Soc.* **2004**, *126*, 1628.

Fuchs, N.; d'Augustin, M.; Humam, M.; Alexakis, A.; Taras, R.; Gladiali, S. *Tetrahedron: Asymmetry* **2005**, *16*, 3143–3146.

Gierz, V.; Urbanaite, A.; Seyboldt, A.; Kunz, D. *Organometallics*, **2012**, *31*, 7532–7538.

Gierz, V.; Maichle-Mossmer, C.; Kunz, D. *Organometallics,* **2012**, *31*, 739–747.

Gini, F.; Hessen, B.; Feringa, B. L.; Minnaard, A. J. *Chem. Commun.* **2007**, 710.

Gini, F.; Hessen, B.; Minnaard, A. J. *Org. Lett.* **2005**, *7*, 5309–5312.

Girard, C.; Kagan H. B. *Angew. Chem., Int. Ed.* **1998**, *37*, 2922–2959.

Gottumukkala, A. L.; Matcha, K.; Lutz, M.; de Vries, J. G.; Minnaard, A. J. *Chem. Eur. J.* **2012**, *18*, 6907–6914.

Gottumukkala, A. L.; Suljagic, J.; Matcha, K.; de Vries, J. G.; Minnaard, A. J. *Chem. Sus. Chem.* **2013**, *6*, 1636–1639.

Guillaneux, D.; Zhao, S.-H.; Samuel, O.; Rainford, D.; Kagan, H. B. *J. Am. Chem. Soc.* **1994**, *116*, 9430–9439.

Guisado-Barrios, G.; Boufard, J.; Donnadieu, B.; Bertrand, G. *Organometallics*, **2011**, *30*, 6017–6021.

Gutnov, A. *Eur. J. Org. Chem.* **2008**, 4547–4554

Han, F.; Chen, G.; Zhang, X.; Liao, J. *Eur. J. Org. Chem.* **2011**, 2928–2931.

Harborne, J. B. in *The Flavonoids: Advances in Research Since 1980*, Chapman and Hall, New York, **1988**.

Harborne, J. B.; Williams, C. A. *Nat. Prod. Rep.* **1995**, *12*, 639–642.

Hahn, B. T.; Tewes, F.; Fröhlich, R.; Glorius, F. *Angew Chem., Int. Ed.* **2010**, *49*, 1143.

Harutyunyan, S. R.; Hartog, den, T.; Geurts, K.; Minnaard, A. J.; Feringa, B. L. *Chem. Rev.* **2008**, *108*, 2824–2852.

Hawner, C.; Alexakis, A. *Chem. Commun.* **2010**, *46*, 7295–7306.

Hawner, C.; Li, K.; Cirriez, V.; Alexakis, A. *Angew. Chem. Int. Ed.* **2008**, *47*, 8211–8214.

Hawner, C.; Muller, D.; Gremaud, L.; Fellouat, A.; Woodward, S.; Alexakis, A. *Angew. Chem. Int. Ed.* **2010**, *49*, 7769–7772.

Hayashi, T.; Takahashi, M.; Takaya, Y.; Ogasawara, M. *J. Am. Chem. Soc.* **2002**, *124*, 5052–5058.

Hayashi, T.; Ueyama, K.; Tokunaga, N.; Yoshida, K. *J. Am. Chem. Soc.* **2003**, *125*, 11508.

Hayashi, T.; Yamasaki, K. *Chem. Rev.* **2003**, *103*, 2829–2844.

He, P.; Lu, Y.; Dong, C.-G.; Hu, Q.-S. *Org. Lett.* **2007**, *9*, 343–346.

He, W.; Yip, K.-T.; Zhu, N.-Y.; Yang, D. *Org. Lett.* **2009**, *11*, 5626–5628.

Hénon, H.; Mauduit, M.; Alexakis, A. *Angew. Chem., Int. Ed.* **2008**, *47*, 9122–9124.

Hird, A. W.; Hoveyda, A. H. *J. Am. Chem. Soc.* **2005**, *127*, 14988–14989.

Hodgetts, K. J.; Maragkou, K. I.; Wallace, T. W.; Wooton, R. C. R. *Tetrahedron* **2001**, *57*, 6793–6804.

Holder, J. C.; Marziale, A. N.; Gatti, M.; Mao, B.; Stoltz, B. M. *Chem. Eur. J.* **2013**, *19*, 74–77.

Holder, J. C.; Zou, L.; Marziale, A. N.; Liu, P.; Lan, Y.; Gatti, M.; Kikushima, K.; Houk, K. N.; Stoltz, B. M. *J. Am. Chem. Soc.* **2013**, *135*, 14996–15007.

Hong, A. Y.; Stoltz, B. M. *Angew. Chem. Int. Ed.* **2012**, *51*, 9674–9678.

Hong, A. Y.; Stoltz, B. M. *Eur. J. Org. Chem.* **2013**, 2745–2759.

Huang, S.-H.; Wu, T.-M.; Tasi, F.-Y. *Appl. Organometal. Chem.* **2010**, *24*, 619–624.

Huang, Z.; Dong, G. *J. Am. Chem. Soc.* **2013**, *135*, 17747–17750.

Inanaga, J.; Furuno, H.; Hayano, T. *Chem. Rev.* **2002**, *102*, 2211–2226.

Inés, B.; San Martin, R.; Moure, M. J.; Domínguez, E. *Adv. Synth. Catal.* **2009**, *351*, 2124-2132.

Ito, Y.; Fujii, S.; Nakatuska, M.; Kawamoto, F.; Saegusa, T. *Org. Synth.* **1979**, *59*, 113.

Iwamoto, M.; Ohtsu, H.; Tokuda, H.; Nishino, H.; Matsunaga, S.; Tanaka, R. *Bioorg. Med. Chem.* **2001**, *9*, 1911–1921.

Jaen, J. C.; Wise, L. D.; Heffner, T. G.; Pugsley, T. A.; Meltzer L. T. *J. Med. Chem.* **1991**, *34*, 248–256.

Jensen, D. A.; Schultz, M. J.; Mueller, J. A.; Sigman, M. S. *Angew. Chem. Int. Ed.* **2003**, *42*, 3810–3813.

Jensen, D. R.; Sigman, M. S. *Org. Lett.* **2003**, *5*, 63–65.

Jensen, K. H.; Pathak, T. P.; Zhang, Y.; Sigman, M. S. *J. Am. Chem. Soc.* **2009**, *131*, 17074–17075.

Jensen, K. H.; Webb, J. D.; Sigman, M. S. *J. Am. Chem. Soc.* **2010**, *132*, 17471–17482.

Jiang, F.; Wu, Z.; Zhang, W. *Tetrahedron Lett.* **2010**, *51*, 5124–5126.

Jordan-Hore, J. A.; Sanderson, J. N.; Lee, A.-L. *Org. Lett.* **2012**, *14*, 2508–2511.

Kagan, H. B. *Synlett* **2001**, 888–899.

Katoh, T.; Akagi, T.; Noguchi, C.; Kajimoto, T.; Node, M.; Tanaka, R.; Nishizawa, M.; Ohtsu, H.; Suzuki, N.; Saito, K. *Bioorg. Med. Chem.* **2007**, *15*, 2736–2748.

Kawazoe, K.; Yamamoto, M.; Takaishi, Y.; Honda, G.; Fujita, T.; Sezik, E.; Yesilada, E. *Phytochemistry* **1999**, *50*, 493–497.

Kehrli, S.; Martin, D.; Rix, D.; Mauduit, M.; Alexakis, A. *Chem.–Eur. J.* **2010**, *16*, 9890–9904.

Kikushima, K.; Holder, J. C.; Gatti, M.; Stoltz, B. M. *J. Am. Chem. Soc.* **2011**, *133*, 6902–6905.

Kim, S.; Koh, J. S. *J. Chem. Soc., Chem. Commun.* **1992**, *18*, 1377.

Kirchberg, S.; Tani, S.; Ueda, K.; Yamaguchi, J.; Studer, A.; Itami, K. *Angew. Chem. Int. Ed.* **2011**, *50*, 2387–2391.

Klier, L.; Bresser, T.; Nigst, T. A.; Karaghiosoff, K.; Knochel, P. *J. Am. Chem. Soc.* **2012**, *134*, 13584–13587.

Korenaga, T.; Hayashi, K.; Akaki, Y.; Maenishi, R.; Sakai, T. *Org. Lett.* **2011**, *13*, 2022–2025.

Koskinen, A. M. P.; Oila, M. J.; Tois, J. E. *Lett. Org Chem.* **2008**, *5*, 11–16.

Krause, N.; Hoffmann-Röder, A. *Synthesis* **2001**, *2*, 171–196.

Kriechbaum, M.; List, M.; Berger, R. J. F.; Patzchke, M.; Monkowius, U. *Chem.–Eur. J.* **2012**, *18*, 5506–5509.

Krishnan, S.; Stoltz, B. M. *Tetrahedron Lett.* **2007**, *48*, 7571–7573.

Krout, M. R.; Mohr, J. T.; Stoltz, B. M. *Org. Synth.* **2009**, *86*, 181

Kuriyama, M.; Nagai, K.; Yamada, K.-I.; Miwa, Y.; Taga, T.; Tomioka, K. *J. Am. Chem. Soc.* **2002**, *124*, 8932–8939.

Ladjel, C.; Fuchs, N.; Zhao, J.; Bernardinelli, G. Alexakis, A. *Eur. J. Org. Chem.* **2009**, 4949–4955.

Lan, Y.; Houk, K. N. *J. Org. Chem.* **2011**, *76*, 4905–4909.

Larock, R. C.; Yum, E. K.; Yang, H. *Tetrahedron* **1994**, *50*, 305–321.

Lee, K.-S.; Brown, M. K.; Hird, A. W.; Hoveyda, A. H. *J. Am. Chem. Soc.* **2006**, *128*, 7182–7184.

Li, S.; Chiu, P. *Tetrahedron Lett.* **2008**, *49*, 1741–1744.

Liao, X.; Stanley, L. M.; Hartwig, J. F. *J. Am. Chem. Soc.* **2011**, *133*, 2088–2091.

Liang, G.; Xu, Y.; Seiple, I. B.; Trauner, D. *J. Am. Chem. Soc.* **2006**, *128*, 11022–11023.

Lin, W.-H.; Fang, J.-M.; Cheng, Y.-S. Phytochemistry **1995**, *40*, 871–873.

Lin, W.-H.; Fang, J.-M.; Cheng, Y.-S. P*hytochemistry* **1996**, *42*, 1657–1663.

Linder, D.; Buron, F.; Constant, S.; Lacour, J. *Eur. J. Org. Chem.* **2008**, 5778–5785.

Lin, S.; Lu, X. *Org. Lett.* **2010**, *12*, 2536–2539.

Lin, S.; Lu, X. *Tetrahedron Letters* **2006**, *47*, 7167–7170.

Liu, J.; Chen, J.; Zhao, J.; Zhao, Y.; Li, L.; Zhang, H. *Synthesis* **2003**, *17*, 2661–2666.

Lopez, F.; Minnarard, A. J.; Feringa, B. L. *Acc. Chem. Res.* **2007**, *40*, 179–188.

Lu, X.; Lin, S. *J. Org. Chem.* **2005**, *70*, 9651–9653.

Ma, S.; Han, X.; Krishnan, S.; Virgil, S. C.; Stoltz, B. M. *Angew. Chem. Int. Ed.* **2009**, *48*, 8037–8041.

Majetich, G.; Shimkus, J. M. *J. Nat. Prod.* **2010**, *73*, 284–298.

Malkov, A. V.; Stewart Liddon, A. J. P.; Ramírez-López, P.; Bendová, L.; Haigh, D.; Kocovsky, P. *Angew. Chem., Int. Ed.* **2006**, *45*, 1432–1435.

Markies, B. A.; Canty, A. J.; de Graaf, W.; Boersma, J.; Janssen, M. D.; Hogerheide, M. P.; Smeets, W. J. J.; Spek, A. L.; van Koten, J. *J. Organomet. Chem.* **1994**, *482*, 191–199.

Martin, D.; Kehrli, S.; d'Augustin, M.; Clavier, H.; Mauduit, M.; Alexakis, A. *J. Am. Chem. Soc.* **2006**, *128*, 8416–8417.

Martin, N. J. A.; List, B. *J. Am. Chem. Soc.* **2006**, *128*, 13368.

Matsumoto, Y.; Yamada, K.-I.; Tomioka, K. J. Org. Chem. **2008**, 73, 4578–4581.

Mauleón, P.; Carretero, J. C. *Chem. Commun.* **2005**, 4961.

May, T. L.; Brown, M. K.; Hoveyda, A. H. *Angew. Chem. Int. Ed.* **2008**, *47*, 7358–7362.

McFadden, R. M.; Stoltz, B. M. *J. Am. Chem. Soc.* **2006**, *128*, 7738–7739.

Mecking, S. *Coord. Chem. Rev.* **2000**, *203*, 325–351.

Meek, P. D.; McKeithan, K.; Schumock, G. T. *Pharmacotherapy* **1998**, *18*, 68.

Meyer, D.; Taige, M. A.; Zeller, A.; Hohlfeld, K.; Ahrens, S.; Strassner, T. *Organometallics* **2009**, *28*, 2142–2149.

Minami, T.; Iwamoto, M.; Ohtsu, H.; Ohishi, H.; Tanaka, R.; Yoshitake, A. *Planta Med.* **2002**, *68*, 742–745.

Miyaura, N. *Top. Curr. Chem.* **2002**, *219*, 11.

Mohr, J. T.; Stoltz, B. M. *Chem. Asian J.* **2007**, *21*, 1476–1491.

Mori, S.; Nambo, M.; Chi, L.-C.; Bouffard, J.; Itami, K. *Org. Lett.* **2008**, *10*, 4609–4612.

Morimoto, M.; Tanimoto, K.; Nakano, S.; Ozaki, T.; Nakano, A.; Komai, K. *J. Agric. Food Chem.* **2003,** *51,* 389.

Moritani, Y.; Appella, D. H.; Jurkauskas, V.; Buchwald, S. L. *J. Am. Chem. Soc.* **2000**, *122*, 6797.

Muehlhofer, M.; Strassner, T.; Herdtweck, E.; Hermann, W. A. *J. Organomet. Chem.* **2002**, 121–126.

Müller, D.; Hawner, C.; Tissot, M.; Palais, L.; Alexakis, A. *Synlett* **2010**, 1694–1698.

Mullick, A. B.; Jeletic, M. S.; Powers, A. R.; Ghiviriga, I.; Abboud, K. A.; Viege, A. S. *Polyhedron* **2013**, *52*, 810–819.

Nishitaka, T.; Kiyomura, S.; Yamamoto, Y.; Miyaura, N. *Synlett* **2008**, 2487–2490.

Nishikata, T.; Kobayashi, Y.; Kobayashi, K.; Yamamoto, Y.; Miyaura, N. *Synlett* **2007**, *19*, 3055–3057.

Nishikata, T.; Yamamoto, Y.; Gridnev, I. D.; Miyaura, N. *Organometallics*, **2005**, *24*, 5025–5032.

Nishikata, T.; Yamamoto, Y.; Miyaura, N. *Adv. Synth. Catal.* **2007**, *349*, 1759–1764.

Nishikata, T.; Yamamoto, Y.; Miyaura, N. *Angew. Chem., Int Ed.* **2003**, *42*, 2768–2770.

Nishikata, T.; Yamamoto, Y.; Miyaura, N. *Chem. Commun.* **2004**, 1822–1823.

Nishikata, T.; Yamamoto, Y.; Miyaura, N. *Chem. Lett.* **2005**, *34*, 720–721.

Nishikata, T.; Yamamoto, Y.; Miyaura, N. *Chem. Lett.* **2007**, *36*,1442–1443.

Nishikata, T.; Yamamoto, Y.; Miyaura, N. *Organometallics* **2004**, *23*, 4317–4324.

Nishikata, T.; Yamamoto, Y.; Miyaura, N. *Tetrahedron Lett*. **2007**, *48*, 4007–4010.

Nishimura, T.; Katoh, T.; Takatsu, K.; Shintani, R.; Hayashi, T. *J. Am. Chem. Soc.* **2007**, *129*, 14158–14159.

Node, M.; Ozeki, M.; Planas, L.; Nakano, M.; Takita, H.; Mori, D.; Tamatani, S.; Kajimoto, T. *J. Org. Chem.* **2010**, *75*, 190–196.

Ogo, S.; Takebe, Y.; Uehara, K.; Yamazaki, T.; Nakai, H.; Watanabe, Y.; Fukuzumi, S.*Organometallics*, **2006**, *25*, 331-338.

Ohtsu, H.; Iwamoto, M.; Ohishi, H.; Matsunaga, S.; Tanaka, R. *Tetrahedron Lett*. **1999**, *40*, 6419–6422.

Ohe, T.; Uemura, S. *Tetrahedron Lett*. **2002**, *43*, 1269–1271.

Ohe, T.; Wkita, T.; Motofua, S.-I.; Cho, C. S.; Ohe, K.; Uemura, S. *Bull. Chem. Soc. Jpn.* **2000**, *73*, 2149–2155.

Otomaru, Y.; Okamoto, K.; Shintani, R.; Hayashi, T. *J. Org. Chem.* **2005**, *70*, 2503.

Ozeki, M.; Satake, M.; Toizume, T.; Fukutome, S.; Arimitsu, K.; Hosoi, S.; Kajimoto, T.; Iwasaki, H.; Kojima, N.; Node, M.; Yamashita, M. *Tetrahedron* **2013**, *69*, 3841–3846.

Palais, L.; Alexakis, A. *Chem.–Eur. J*. **2009**, *15*, 10473–*10485*.

Palais, L.; Mikhel, I. S.; Bournaud, C.; Micouin, L.; Falciola, C. A.; Vuagnoux-
d'Augustin, M.; Rosset, S.; Bernardinelli, G.; Alexakis, A. *Angew. Chem., Int. Ed.*
2007, *46*, 7462–7465.

Paquin, J.-F.; Defieber, C.; Stephenson, C. R. J.; Carreira, E. M. *J. Am. Chem. Soc.* **2005**,
127, 10850.

Pathak, T. P.; Gligorich, K. M.; Welm, B. E.; Sigman, M. S. *J. Am. Chem. Soc.* **2010**,
132, 7870–7871.

Perch, N. S.; Pei, T.; Widenhoefer, R. A. *J. Org. Chem.* **2000**, *65*, 3836–3845.

Perdew, J. P. *Phys. Rev. B* **1986**, *33*, 8822–8824.

Perdew, J. P.; Chevary, J. A.; Vosko, S. H.; Jackson, K. A.; Pederson, M. R.; Singh, D.
J.; Fiolhais, C. *Phys. Rev. B* **1992**, *46*, 6671–6687.

Perlmutter, P. in *Conjugate Addition Reactions in Organic Synthesis*, Tetrahedron
Organic Chemistry Series 9; Pergamon, Oxford, **1992**.

Petasis, N. A.; Zavialov, I. A. *Tetrahedron Lett.* **1996**, *37*, 567.

Pfeiffer, P.; Oberlin, H.; Konermann, E. *Chemische Berichte*, **1925**, *58*, 1947–1958.

Piers, E.; Banville, J.; Lau, C. K.; Nagakura, I. *Can. J. Chem.* **1982**, *60*, 2965.

Piller, F. M.; Bresser, T.; Fischer, M. K. R.; Knochel, P. *J. Org. Chem.* **2010**, *75*,
4365–4375.

Planas, L.; Mogi, M.; Takita, H.; Kajimoto, T. *J. Org. Chem.* **2006**, *71*, 2896–2898.

Podhajsky, S. M.; Iwai, Y.; Cook-Sneathen, A.; Sigman, M. S. *Tetrahedron* **2011**, *67*, 4435–4441.

Poláckóvá, V.; Bariak, V.; Sebesta, R.; Toma, S. *Chem. Pap.* **2011**, *65*, 338–344.

Price, W. S. *Diffusion Fundamentals* **2005**, *2*, 1–19.

Poyatos, M.; McNamara, W.; Incarvito, C.; Clot, E.; Peris, E.; Crabtree, R. H. *Organometallics* **2004**, *23*, 1253–1263.

Poyatos, M.; McNamara, W.; Incarvito, C.; Peris, E.; Crabtree, R. H. *Chem. Commun.* **2007**, 2267–2269.

Rossiter, B. E.; Swingle, N. M. *Chem. Rev.* **1992**, *92*, 771–806.

Schiffner, J. A.; Machotta, A. B.; Oestreich, M. *Synlett* **2008**, 2271–2274.

Seymour, J. D.; Caprihan, A.; Altobelli, S. A.; Fukushima, E. *Physical Review Letters* **2000**, *84*, 266–269.

Shimizu, H.; Holder, J. C.; Stoltz, B. M. *Beilstein J. Org. Chem.* **2013**, *9*, 1637–1642.

Shintani, R.; Duan, W.-L.; Hayashi, T. *J. Am. Chem. Soc.* **2006**, *128*, 5628–5629.

Shintani, R.; Hayashi, T. *Org. Lett.* **2011**, *13*, 350–352.

Shintani, R.; Takeda, M.; Nishimura, T.; Hayashi, T. *Angew. Chem. Int. Ed.* **2010**, *49*, 3969–3971.

Shintani, R.; Tsutsumi, Y.; Nagaosa, M.; Nishimura, T.; Hayashi, T. *J. Am. Chem. Soc.* **2009**, *131*, 13588–13589.

Shintani, R.; Ueyama, K.; Yamada, I.; Hayashi, T. *Org. Lett.* **2004**, *6*, 3425.

Shintani, R.; Yamagami, T.; Kimura, T.; Hayashi, T. *Org. Lett.* **2005**, *7*, 5317–5319.

Sieber, J. D.; Liu, S.; Morken, J. P. *J. Am. Chem. Soc.* **2007**, *129*, 2214–2215.

Sibi, M. P.; Manyem, S. *Tetrahedron* **2000**, *56*, 8033–8061.

Singh, R.; Parai, M. K.; Panda, G. *Org. Biomol. Chem.* **2009**, *7*, 1858–1867.

Slootweg, J. C.; Chen, P. *Organometallics* **2006**, *25*, 5863–5869.

Stahl, S. S. *Science* **2005**, *309*, 1824–1826.

Strassner, T.; Muehlhofer, M.; Zeller, A.; Herdtwreck, E.; Hermann, W. A. *J. Organometl. Chem.* **2004**, 1418–1424.

Suzuma, Y.; Hayashi, S.; Yamamoto, T.; Oe, Y.; Ohta, T.; Ito, Y. *Tetrahedron: Asymmetry* **2009**, *20*, 2751–2758.

Suzuma, Y.; Yamamoto, T.; Ohta, T.; Ito, Y. *Chem. Lett.* **2007**, *36*, 470–471.

Tanaka, Y.; Kanai, M.; Shibasaki, M. *J. Am. Chem. Soc.* **2010**, *132*, 8862.

Takaya, Y.; Ogasawara, M.; Hayashi, T. *J. Am. Chem. Soc.* **1998**, *120*, 5579–5580.

Takaya, Y.; Ogasawara, M.; Hayashi, T.; Sakai, M.; Miyaura, N. *J. Am. Chem. Soc.* **1998**, *120*, 5579.

Tapia, R.; Guardia, J. J.; Alvarez, E.; Haidöur, A.; Ramos, J. M.; Alvarez-Manzaneda, R.; Chahboun, R.; Alvarez-Manzaneda, E. *J. Org. Chem.* **2012**, *77*, 573–584.

Tang, S.; Xu, Y.; He, J.; He, Y.; Zheng, J.; Pan, X.; She, X. *Org. Lett.* **2008**, *10*, 1855–1858.

Thommen, C.; Jana, C. K.; Neuburger, M.; Gademann, K. *Org. Lett.* **2013**, *15*, 1390–1393.

Tomioka, K.; Nagaoka, Y. in *Comprehensive Asymmetric Catalysis*, Vol. 3 (Eds: Jacobsen, E. J.; Pfaltz, A.; Yamamoto, H. Springer-Verlag, New York, **1999**; Chapter 31.

Trost, B. M.; Jiang, C. *Synthesis* **2006**, 369–396.

Tseng, Y.-J.; Wen, Z.-H.; Dai, C.-F.; Chiang, M. Y.; Sheu, J.-H. *Org. Lett.* **2009**, *11*, 5030.

Ullah, E.; Appel, B.; Fischer, C.; Langer, P. *Tetrahedron*, **2006**, *62*, 9694.

Vatéle, J.-M. *Tetrahedron* **2010**, *66*, 904–912.

Vuagnoux-d'Augustin, M.; Alexakis, A. *Chem.–Eur. J.* **2007**, *13*, 9647–9662.

Vuagnoux-d'Augustin, M.; Kehrli, S.; Alexakis, A. *Synlett*, **2007**, 2057–2060.

Vaugnoux-d'Augustin, M.; Palais, L.; Alexakis, A. *Angew. Chem., Int. Ed.* **2005**, *44*, 1376–1378

Wang, H.; Li, Y.; Zhang, R.; Jin, K.; Zhao, D.; Duan, C. *J. Org. Chem.* **2012**, *77*, 4849–4853.

Wang, L. J.; Liu, H.; Dong, Fu, X.; Feng, X. M. *Angew. Chem. Int. Ed.* **2008**, *47*, 8670–8673.

Wang, X.; Reisinger, C. M.; List, B. *J. Am. Chem. Soc.* **2008**, *130*, 6070.

Walker, S. E.; Boehnke, J.; Glen, P. E.; Levey, S.; Patrick, L.; Jordan-Hore, J. A.; Lee, A.-L. *Org. Lett.* **2013**, *15*, 1886–1889.

Wilsily, A.; Fillion, E. *J. Org. Chem.* **2009**, *74*, 8583–8594.

Wilsily, A.; Fillion, E. Org. Lett. **2008**, 10, 2801–2804.

Wu, J.; Mampreian D. M.; Hoveyda, A. H. *J. Am. Chem. Soc.* **2005**, *127*, 4584–4585.

Xia, Y.; Yang, Z.-Y.; Xia, P.; Bastow, K. F.; Tachibana, Y.; Kuo, S.-C.; Hamel, E.; Hackl, T.; Lee, K.-H. *J. Med. Chem.* **1998**, *41*, 1155–1162.

Xu, Q.; Zhang, R.; Zhang, T.; Shi, M. *J. Org. Chem.* **2010**, *75*, 3935–3937.

Xu, W.; Kong, A.; Lu, X. *J. Org. Chem.* **2006**, *71*, 3854–3858.

Yamamoto, T.; Iizuka, M.; Takenaka, H.; Ohta, T.; Ito, Y. *Journal of Organometallic Chemistry* **2009**, *694*, 1325–1332.

Yang, S.; Hungerhoff, B.; Metz, P. *Tetrahedron Lett.* **1998**, *39*, 2097.

Yamamoto, Y.; Nishikata, T.; Miyaura, N. *Pure Appl. Chem.* **2008**, *80*, 807–817.

Yeh, M. C.; Knochel, P.; Butler, W. M.; Berk, S. C. *Tetrahedron Lett.* **1988**, *29*, 6693.

Yoo, K. S.; Park, C. P.; Yoon, C. H.; Sakaguchi, S.; O'Neill, J.; Jung, K. W. *Org. Lett.* **2007**, *9*, 3933–3935.

Zhang, Q.; Lu, X.; Han, X. *J. Org. Chem.* **2001**, *66*, 7676–7684. (t) Zhang, Q.; Lu, X. *J. Am. Chem. Soc.* **2000**, *122*, 7604–7605.

Zhang, S.-X.; Feng, J.; Kuo, S.-C.; Brossi, A.; Hamel, E.; Tropsha, A.; Lee, K.-H. *J. Med. Chem.* **2000**, *43*, 167–176.

Zhang, T.; Shi, M. *Chem. Eur.–J.* **2008**, *14*, 3759–3764.

Zhang, X.; Chen, J.; Han, F.; Cun, L.; Liao, J. *Eur. J. Org. Chem.* **2011**, 1443–1446.

Zhang, Y.; Sigman, M. S. *J. Am. Chem. Soc.* **2007**, *129*, 3076–3077.

ABOUT THE AUTHOR

Jeffrey Clinton Holder was born in Tampa, Florida on 15 December 1986. He is the eldest child of Clinton D. Holder and Joanne D. Beaudet. His younger sister, Allison Elizabeth, practices medicine in Miami, where she lives with her fiancé, Matthew Williams. Jeff spent his formative years in St. Petersburg, Florida, where he augmented his time as a Lego architect by enjoying the fantastic year-round weather while playing baseball and swimming. He attended the International Baccalaureate program at historic St. Petersburg High School, where he was an active member of the Men of Key service club, pursued a number of musical interests playing guitar and bass, and worked as a martial arts instructor.

In the fall of 2005, Jeff matriculated at Harvard University, where he would purchase his first winter coat. He entered university with plans to major in chemistry before moving on to medical school, however, his habit of repeatedly fainting at the sight of blood averted these early career plans. He was led to research by a conversation with Professor Daniel E. Kahne, who was kind enough to offer Jeff an opportunity to do summer research. That summer, Jeff spent what little time he could find in between 2006 World Cup Matches transfecting *E. coli* and making buffer solutions for a graduate student studying the mechanism of action of β-lactam antibiotics. He was first drawn to organic synthesis while working with the late Ahimindra Jain on modifications to the Corey synthesis of (–)-Oseltamivir ("Tamiflu"). He would take his interest in synthetic chemistry back to the Kahne laboratory, where he would work on the semi-synthesis of a number of Rifampicin derivatives and degradation products, and later to Professor E. J. Corey's laboratory, where he toiled to make a farnesol-derived steroid precursor for a year without success.

In the fall of 2009, Jeff moved to Pasadena, California, where he began doctoral research with Professor Brian M. Stoltz at the California Institute of Technology. His doctoral research involves the development of a novel palladium-catalyzed 1,4-addition and its application toward the total synthesis of taiwaniaquinoid natural products. During his time at Caltech, Jeff's research interests drifted significantly toward the synthesis and study of organometallic complexes and organotransition-metal catalyzed reactions. He will move to Berkeley, California, in July 2014 and begin postdoctoral studies in the laboratory of Professor John F. Hartwig to pursue those interests.